

SECTION 14SAFETY ANALYSISTABLE OF CONTENTS

<u>Section</u>	<u>Title</u>	<u>Page</u>
14.0	INTRODUCTION	14.1-1
14.1	CORE AND COOLANT BOUNDARY PROTECTION ANALYSIS	14.1-1
14.1.1	<u>Uncontrolled Rod Cluster Control Assembly Bank Withdrawal from a Subcritical Condition</u>	14.1-1
14.1.1.1	Identification of Causes and Accident Description	14.1-1
14.1.1.2	Analysis of Effects and Consequences	14.1-2
14.1.2	<u>Uncontrolled Rod Cluster Control Assembly Bank Withdrawal at Power</u>	14.1-4
14.1.2.1	Identification of Causes and Accident Description	14.1-4
14.1.2.2	Analysis of Effects and Consequences, Method of Analysis	14.1-6
14.1.3	<u>Rod Cluster Control Assembly Misalignment</u>	14.1-7
14.1.3.1	Identification of Causes and Accident Description	14.1-7
14.1.3.2	Analysis of Effects and Consequences, Method of Analysis	14.1-8
14.1.3.3	Conclusions	14.1-10
14.1.4	<u>Uncontrolled Boron Dilution</u>	14.1-10
14.1.4.1	Identification of Causes and Accident Description	14.1-10
14.1.4.2	Method of Analysis and Results	14.1-11
14.1.4.3	Conclusions	14.1-13
14.1.5	<u>Partial Loss of Forced Reactor Coolant Flow</u>	14.1-13
14.1.5.1	Identification of Causes and Accident Description	14.1-13
14.1.5.2	Analysis of Effects and Consequences	14.1-14
14.1.6	<u>Startup of an Inactive Reactor Coolant Loop</u>	14.1-15
14.1.6.1	Identification of Causes and Accident Description	14.1-15
14.1.6.2	Analysis of Effects and Consequences	14.1-16
14.1.7	<u>Loss of External Electrical Load and/or Turbine Trip</u>	14.1-17
14.1.7.1	Identification of Causes and Accident Description	14.1-17
14.1.7.2	Analysis of Effects and Consequences	14.1-17
14.1.7.3	Conclusions	14.1-19

TABLE OF CONTENTS (CONT'D)

<u>Section</u>	<u>Title</u>	<u>Page</u>
14.1.8	<u>Loss of Normal Feedwater</u>	14.1-20
14.1.8.1	Identification of Causes and Accident Description	14.1-20
14.1.8.2	Analysis of Effects and Consequences	14.1-21
14.1.8.3	Conclusions	14.1-24
14.1.9	<u>Excessive Heat Removal Due to Feedwater System Malfunctions</u>	14.1-24
14.1.9.1	Identification of Causes and Accident Description	14.1-24
14.1.9.2	Analysis of Effects and Consequences	14.1-24
14.1.10	<u>Excessive Load Increase Incident</u>	14.1-26
14.1.10.1	Identification of Causes and Accident Description	14.1-26
14.1.10.2	Analysis of Effects and Consequences	14.1-27
14.1.10.3	Conclusions	14.1-28
14.1.11	<u>Loss of Offsite Power to the Station Auxiliaries (Station Blackout)</u>	14.1-28
14.1.11.1	Identification of Causes and Accident Description	14.1-28
14.1.11.2	Analysis of Effects and Consequences	14.1-29
14.1.12	<u>Turbine-Generator Accidents Missiles</u>	14.1-30
14.1.12.1	Probability of Missile Generation and Ejection (P1)	14.1-31
14.1.12.2	Probability of Missile Strike (P2)	14.1-32
14.1.12.3	Probability of Damage (P3)	14.1-32
14.1.12.4	Probability Evaluation (P4)	14.1-32
14.1.12.5	Turbine Overspeed Protection	14.1-32
14.1.13	<u>Accidental Depressurization of the Main Steam System</u>	14.1-33
14.1.14	<u>External Environmental Causes</u>	14.1-33
14.1.14.1	Identification of Causes	14.1-33
14.1.14.2	Analysis of Effects and Consequences	14.1-33
14.1.15	<u>Accidental Depressurization of the Reactor Coolant System</u>	14.1-34
14.1.15.1	Identification of Causes and Accident Description	14.1-34
14.1.15.2	Analysis of Effects and Consequences	14.1-35
14.1.15.3	Conclusions	14.1-36
14.1.16	<u>Spurious Operation of the Safety Injection System at Power</u>	14.1-36
14.1.16.1	Identification of Causes	14.1-36
14.1.16.2	Analysis of Effects and Consequences	14.1-37
14.1.16.2.1	Pressurizer Safety Valve (PSV) Operability Assessment	14.1-38
14.1.16.2.2	Power Operated Relief Valve Operability Assessment	14.1-39
14.1.16.2.3	Piping Analysis	14.1-40
14.1.16.3	Results	14.1-40
14.1.16.4	Conclusions	14.1-40
14.2	STANDBY SAFEGUARDS ANALYSIS	14.2-1
14.2.1	<u>Fuel Handling Accident</u>	14.2-1

TABLE OF CONTENTS (CONT'D)

<u>Section</u>	<u>Title</u>	<u>Page</u>
14.2.1.1	Accident Description	14.2-1
14.2.1.2	Radiological Consequence Analysis Methods, Assumptions and Results	14.2-3
14.2.2	<u>Accidental Release of Waste Liquid</u>	14.2-4
14.2.3	<u>Accidental Release of Waste Gases</u>	14.2-4
14.2.4	<u>Steam Generator Tube Rupture</u>	14.2-4
14.2.4.1	Accident Description	14.2-4
14.2.4.2	Analysis of Effects and Consequences	14.2-6
14.2.4.2.1	Method of Analysis	14.2-6
14.2.4.2.2	Environmental Consequences of Tube Rupture	14.2-7
14.2.4.2.3	Recovery Procedure	14.2-8
14.2.4.2.4	Results	14.2-9
14.2.4.3	Conclusions	14.2-10
14.2.5	<u>Major Secondary System Line Break</u>	14.2-10
14.2.5.1	Major Line Break	14.2-10
14.2.5.1.1	Identification of Causes and Accident Description	14.2-10
14.2.5.1.2	Analysis of Effects and Consequences	14.2-12
14.2.5.1.3	Results	14.2-14
14.2.5.1.4	Conclusions	14.2-18
14.2.5.1.5	Steam System Piping Failure at Full Power	14.2-18
14.2.5.1.5.1	Identification of Causes and Accident Description	14.2-18
14.2.5.1.5.2	Analysis of Effects and Consequences	14.2-18
14.2.5.1.5.3	Results	14.2-19
14.2.5.1.5.4	Conclusions	14.2-20
14.2.5.2	Major Rupture of a Main Feedwater Pipe	14.2-20
14.2.5.2.1	Identification of Causes and Accident Description	14.2-20
14.2.5.2.2	Analysis of Effects and Consequences	14.2-21
14.2.6	<u>Rupture of a Control Rod Drive Mechanism</u> <u>Housing Rod Cluster Control Assembly</u> <u>Ejection</u>	14.2-24
14.2.6.1	Identification of Causes and Accident Description	14.2-24
14.2.6.1.1	Design Precautions and Protection	14.2-24
14.2.6.1.2	Limiting Criteria	14.2-27
14.2.6.2	Analysis of Effects and Consequences	14.2-27
14.2.6.2.1	Calculation of Basic Parameters	14.2-29
14.2.6.2.2	Results	14.2-31
14.2.6.3	Conclusions - Thermal Analysis	14.2-32
14.2.6.4	Radiological Consequences	14.2-33
14.2.7	<u>Single Reactor Coolant Pump Locked Rotor</u>	14.2-35

TABLE OF CONTENTS (CONT'D)

<u>Section</u>	<u>Title</u>	<u>Page</u>
14.2.7.1	Identification of Causes and Accident Description	14.2-35
14.2.7.2	Analysis of Effects and Consequences	14.2-36
14.2.7.2.1	Method of Analysis	14.2-36
14.2.7.2.2	Locked Rotor Results	14.2-38
14.2.8	<u>Inadvertent Loading of a Fuel Assembly into an Improper Position</u>	14.2-40
14.2.8.1	Identification of Causes and Accident Description	14.2-40
14.2.8.2	Analysis of Effects and Consequences	14.2-41
14.2.8.2.1	Method of Analysis	14.2-41
14.2.8.2.2	Results	14.2-41
14.2.8.3	Conclusions	14.2-42
14.2.9	<u>Complete Loss of Forced Reactor Coolant Flow</u>	14.2-42
14.2.9.1	Accident Description	14.2-42
14.2.9.2	Method of Analysis	14.2-43
14.2.9.3	Results	14.2-44
14.2.9.4	Conclusions	14.2-44
14.2.10	<u>Single RCCA Withdrawal at Full Power</u>	14.2-44
14.2.10.1	Accident Description	14.2-44
14.2.10.2	Method of Analysis	14.2-45
14.2.10.3	Results	14.2-45
14.2.10.4	Conclusions	14.2-46
14.2.11	<u>Minor Secondary System Pipe Breaks</u>	14.2-46
14.2.11.1	Identification of Causes and Accident Description	14.2-46
14.2.11.2	Analysis of Effects and Consequences	14.2-46
14.2.11.3	Conclusions	14.2-46
14.3	LOSS-OF-COOLANT ACCIDENT	14.3-1
14.3.1	<u>Loss of Reactor Coolant from Small Ruptured Pipes or From Cracks in Large Pipes Which Actuates Emergency Core Cooling System (ECCS)</u>	14.3-2
14.3.2	<u>Major Reactor Coolant System Pipe Breaks (Loss of Coolant Accident)</u>	14.3-5
14.3.2.1	General	14.3-6
14.3.2.2	Method of Analysis	14.3-8
14.3.2.3	Analysis Assumptions	14.3-10
14.3.2.4	Design Basis Accident	14.3-10
14.3.2.5	Post Analysis of Record Evaluations	14.3-12
14.3.2.6	Conclusions	14.3-13

TABLE OF CONTENTS (CONT'D)

<u>Section</u>	<u>Title</u>	<u>Page</u>
14.3.3	<u>Core and Internals Integrity Analysis</u>	14.3-14
14.3.3.1	Internals Evaluation	14.3-14
14.3.3.2	Design Criteria	14.3-14
14.3.3.3	Dynamic System Analysis of Reactor Internals Under Loss of Coolant Accident (LOCA)	14.3-15
14.3.4	<u>Containment Evaluation</u>	14.3-20
14.3.4.1	Design Bases	14.3-20
14.3.4.2	LOCA Mass and Energy Release	14.3-21
14.3.4.2.1	LOCA Mass and Energy Release Safety Analysis	14.3-21
14.3.4.2.2	MAAP-DBA Code	14.3-32
14.3.4.3	Pressure Transient Results	14.3-39
14.3.4.4	Post-DBA Hydrogen Generation	14.3-40
14.3.4.5	Analysis of Containment Subcompartments	14.3-41
14.3.5	<u>Radiological Consequences</u>	14.3-44
14.3.5.1	Fission Product Cleanup	14.3-45
14.3.5.2	Release Pathways for DBA Case	14.3-51
14.3.6	<u>Summary of Loss-of-Coolant Accident Effects on the Reactor Coolant System, the Containment and on Offsite Doses</u>	14.3-58

TABLE OF CONTENTS (CONT'D)

<u>Section</u>	<u>Title</u>	<u>Page</u>
14B	<u>RADIATION SOURCES</u>	14B-1
14B.1	<u>ACTIVITIES IN THE CORE</u>	14B-1
14B.2	<u>ACTIVITIES IN THE FUEL ROD GAP FOR NON-LOCA EVENTS</u>	14B-1
14B.3	<u>FUEL HANDLING SOURCES</u>	14B-2
14B.4	<u>REACTOR COOLANT FISSION PRODUCT ACTIVITIES</u>	14B-3
14B.4.1	<u>Reactor Coolant and Secondary System</u>	
	<u>Equilibrium Activities</u>	14B-4
14B.4.2	<u>Reactor Coolant System Iodine Spiking</u>	14B-4
14B.5	<u>TRITIUM PRODUCTION WITHIN A LIGHT WATER REACTOR</u>	
		14B-5
14B.5.1	<u>General - Overall Sources</u>	14B-5
14B.5.2	<u>Specific Individual Sources of</u>	
	<u>Tritium-Light Water Reactors</u>	14B-5
14B.5.2.1	<u>Ternary Fissions - Clad Diffusion</u>	14B-5
14B.5.2.2	<u>Tritium Produced from Boron Reactions</u>	14B-6
14B.5.2.3	<u>Tritium Produced from Lithium Reactions</u>	14B-7
14B.5.2.4	<u>Control Rod Sources</u>	14B-7
14B.5.2.5	<u>Tritium Production from Deuterium Reactions</u>	14B-7
14B.5.2.6	<u>Total Tritium Sources</u>	14B-7
14B.6	<u>WASTE GAS SYSTEM DECAY TANK RUPTURE ACTIVITY RELEASE</u>	14B-8
14B.7	<u>WASTE GAS SYSTEM LINE RUPTURE ACTIVITY RELEASE</u>	14B-8
14B.8	<u>DOSE MODELS FOR DESIGN BASIS ACCIDENT</u>	14B-8
14B.8.1	<u>Assumptions</u>	14B-8
14B.8.2	<u>Updated Dose Calculation Models</u>	14B-9
14B.9	<u>CONTAINMENT LEAKAGE MODEL - DBA CASE</u>	14B-9
14B.9.1	<u>Radioiodine and Other Aerosol</u>	14B-9
14B.9.2	<u>Noble Gases and Organic Iodine</u>	14B-10
14B.9.3	<u>ESF Leakage and RWST Back-leakage</u>	14B-11
14C	<u>HEAT TRANSFER COEFFICIENTS USED IN THE</u>	
	<u>LOCTA-R2 CORE THERMAL ANALYSIS</u>	14C-1
14C.1	<u>TIME OF BREAK UNTIL OCCURRENCE OF DNB</u>	14C-1
14C.2	<u>FROM DNB UNTIL TIME OF UNCOVERING (STEAM COOLING PERIOD)</u>	14C-1
14C.3	<u>DURING UNCOVERING (STEAM COOLING PERIOD)</u>	14C-2
14C.4	<u>VERIFICATION OF CORRELATIONS USED DURING STEAM COOLING PERIOD</u>	14C-3

TABLE OF CONTENTS (CONT'D)

<u>Section</u>	<u>Title</u>	<u>Page</u>
14C.5	RECOVERY PHASE OF THE ACCIDENT	14C-4
14D	<u>CONDITION I - NORMAL OPERATION AND OPERATIONAL TRANSIENTS</u>	14D-1
14D.1	(DELETED)	
14D.2	OPTIMIZATION OF CONTROL SYSTEMS	14D-1
14D.3	INITIAL POWER CONDITIONS ASSUMED IN ACCIDENT ANALYSES	14D-1
14D.3.1	<u>Power Rating</u>	14D-1
14D.3.2	<u>Initial Conditions</u>	14D-1
14D.3.3	<u>Power Distribution</u>	14D-2
14D.4	TRIP POINTS AND TIME DELAYS TO TRIP ASSUMED IN ACCIDENT ANALYSES	14D-3
14D.5	(DELETED)	
14D.6	ROD CLUSTER CONTROL ASSEMBLY INSERTION CHARACTERISTIC	14D-3
14D.7	REACTIVITY COEFFICIENTS	14D-4
14D.8	FISSION PRODUCT INVENTORIES	14D-5
14D.9	RESIDUAL DECAY HEAT	14D-5
14D.9.1	<u>Fission Product Decay</u>	14D-6
14D.9.2	<u>Decay of U-238 Capture Products</u>	14D-6
14D.9.3	<u>Residual Fissions</u>	14D-7
14D.9.4	<u>Distribution of Decay Heat Following Loss-of-Coolant Accident</u>	14D-7
14D.10	COMPUTER CODES UTILIZED	14D-7
14D.10.1	<u>FACTRAN</u>	14D-8
14D.10.2	<u>(DELETED)</u>	
14D.10.3	<u>(DELETED)</u>	
14D.10.4	<u>LOFTRAN</u>	14D-8
14D.10.5	<u>LEOPARD</u>	14D-9
14D.10.6	<u>TURTLE</u>	14D-9
14D.10.6.1	Advanced Nodal Code (ANC)	14D-9
14D.10.6.2	Phoenix-P	14D-9
14D.10.6.3	NEXUS/PARAGON	14D-9
14D.10.7	<u>TWINKLE</u>	14D-10
14D.10.8	<u>(DELETED)</u>	
14D.10.9	<u>(DELETED)</u>	
14D.10.10	<u>VIPRE</u>	14D-10

LIST OF TABLES

<u>Table</u>	<u>Title</u>
14.0-1	List of Conditions
14.1-1	(Deleted)
14.1-1A	Postulated Control Room Accident Dose, REM
14.1-1B	Beaver Valley Power Station BVPS-1 Exclusion Area Boundary and Low Population Dose (TEDE)
14.1-2	Time Sequence of Events for Condition II Events
14.1-3	Parameters Used in Control Room Habitability Analysis of the Loss of AC Powered Auxiliaries Accident
14.2-1	(Deleted)
14.2-2	Time Sequence of Events for Condition IV Events
14.2-3	Parameters Used in the Analysis of the Rod Cluster Control Assembly Ejection Accident
14.2-4a	Summary of Results for Locked Rotor Transients
14.2-4b	Parameters Used in Radiological Analysis of the Locked Rotor Accident
14.2-5	Time Sequence of Events for Condition III Events
14.2-6	Parameters Used in Radiological Analysis of the Fuel Handling Accident
14.2-6a	Core Activity of Noble Gases and Halogens
14.2-7	(Deleted)
14.2-8	(Deleted)
14.2-9	Parameters Used in Radiological Analysis of the Steam Generator Tube Rupture Accident
14.2-10	Parameters Used in Main Steam Line Break Analysis
14.2-11	(Deleted)
14.2-12	Parameters Used in Radiological Analysis of the RCCA Ejection Accident



LIST OF TABLES (CONT'D)

<u>Table</u>	<u>Title</u>
14.3-1a	(Deleted)
14.3-1b	(Deleted)
14.3-1c	(Deleted)
14.3-1d	(Deleted)
14.3-1e	Small Break LOCA Time Sequence of Events
14.3-1f	Small Break LOCA Fuel Cladding Data
14.3-1g	Peak Clad Temperature Including All Penalties and Benefits Small Break LOCA
14.3.2-1	Plant Operating Range Analyzed by the Best-Estimate Large-Break LOCA Analysis for Beaver Valley Unit 1
14.3.2-2	Large Break LOCA Containment Data
14.3.2-2a	Maximum Containment Spray Flow Rate
14.3.2-3	Large Break Containment - Heat Sink Data Structural Heat Sinks
14.3.2-4	Beaver Valley Unit 1 Best Estimate Large Break LOCA Total Minimum Injected SI Flow High Head Safety Injection (HHSI) and Low Head Safety Injection (LHSI) from Two Intact Loops
14.3.2-5	Beaver Valley Unit 1 Best-Estimate Large Break LOCA Results
14.3.2-6	Peak Clad Temperature Including All Penalties and Benefits Best Estimate Large Break LOCA (ASTRUM)
14.3.2-7a	Large Break LOCA Mass & Energy Releases from BCL Vessel Side Used for COCO Calculations
14.3.2-7b	Large Break LOCA Mass & Energy Releases from RCP Side Used for COCO Calculations
14.3.2-8	Sequence of Events for the Limiting Case
14.3.2-9	(Deleted)
14.3.2-10	(Deleted)
14.3-2	(Deleted)
14.3-2a	(Deleted)
14.3-2b	Plant Parameters Used In Small Break LOCA
14.3-3	(Deleted)
14.3-3a	(Deleted)

LIST OF TABLES (CONT'D)

<u>Table</u>	<u>Title</u>
14.3-3b	(Deleted)
14.3.4-1	System Parameters Initial Conditions for Thermal Uprate
14.3.4-2	Safety Injection Flow Minimum Safeguards
14.3.4-3	Safety Injection Flow Maximum Safeguards
14.3.4-4	Double-Ended Hot-Leg Break Blowdown Mass and Energy Releases
14.3.4-5	Double-Ended Pump Suction Break Blowdown Mass and Energy Releases (Same for all DEPS Runs)
14.3.4-6	Double-Ended Pump Suction Break Minimum Safeguards Reflood Mass and Energy Releases
14.3.4-7	Double-Ended Pump Suction Break – Minimum Safeguards Principle Parameters During Reflood
14.3.4-8	Double-Ended Pump Suction Break Minimum Safeguards Post-Reflood Mass and Energy Releases
14.3.4-9	Double-Ended Pump Suction Break Maximum Safeguards Mass and Energy Releases
14.3.4-10	Double-Ended Pump Suction Break – Maximum Safeguards Principle Parameters During Reflood
14.3.4-11	Double-Ended Pump Suction Break Maximum Safeguards Post-Reflood Mass and Energy Releases
14.3.4-12	LOCA Mass and Energy Release Analysis ANS 1979 Core Decay Heat Power Fraction
14.3.4-13	Double-Ended Hot-Leg Break Mass Balance
14.3.4-14	Double-Ended Pump Suction Break Mass Balance Minimum Safeguards
14.3.4-15	Double-Ended Pump Suction Break Mass Balance Maximum Safeguards
14.3.4-16	Double-Ended Hot-Leg Break Energy Balance
14.3.4-17	Double-Ended Pump Suction Break Energy Balance Minimum Safeguards
14.3.4-18	Double-Ended Pump Suction Break Energy Balance – Maximum Safeguards
14.3-4	(Deleted)

LIST OF TABLES (CONT'D)

<u>Table</u>	<u>Title</u>
14.3-4a	(Deleted)
14.3-4b	(Deleted)
14.3-4c	(Deleted)
14.3-5	(Deleted)
14.3-5a	Key Input Data to MAAP-DBA (Peak Pressure Calculations)
14.3-5b	Physical Constants for Containment and Coolant System Materials
14.3-6	Beaver Valley MAAP-DBA Parameter File Summary of Junction Flow Areas
14.3-7	Beaver Valley MAAP-DBA Parameter File Summary of Containment Nominal Volumes and Metal Heat Sinks
14.3-8	Beaver Valley MAAP-DBA Parameter File Summary of Containment Concrete Heat Sinks
14.3-8a	(Deleted)
14.3-8b	(Deleted)
14.3-9	(Deleted)
14.3-10	Parameters Used in Control Room Habitability Analysis of the Small Line Break Accident
14.3-11	(Deleted)
14.3-12	Containment Thermodynamic Data - Loss of Coolant Accident
14.3-13	(Deleted)
14.3-14a	Parameters Used in Evaluating the Radiological Consequences of a Loss-of-Coolant Accident
14.3-15	(Deleted)
14.3-16	MAAP-DBA Containment Peak Pressure, Results for a Design Basis Large Break LOCA Beaver Valley – BVPS-1
14.3-17	(Deleted)
14.3-17A	BVPS-1 Double-Ended Hot-Leg Break Sequence of Events
14.3-17B	BVPS-1 Double-Ended Pump Suction Break Minimum Safeguards Sequence of Events

LIST OF TABLES (CONT'D)

<u>Table</u>	<u>Title</u>
14.3-17C	BVPS-1 Double-Ended Pump Suction Break Maximum Safeguards Sequence of Events
14.3-18	(Deleted)
14.3-19	(Deleted)
14.3-20	Steam Generator Cubicle Mass And Energy Inflow Rates for DER of Hot Leg
14.3-21	Steam Generator Cubicle IA Mass and Energy Inflow Rates for SER of Hot Leg
14.3-22	Mass and Energy Release Rates for DER of Surge Line in Pressurizer Subcompartment
14.3-23	Mass and Energy Release Rates for DER of Spray Line in Pressurizer Subcompartment Superstructure (Above El. 767 ft-10 inches)
14.3-24	(Deleted)
14.3-25	(Deleted)
14.3-26	(Deleted)
14.3-27	(Deleted)
14.3-28	(Deleted)
14.3-29	(Deleted)
14.3-30	(Deleted)
14.3-31	(Deleted)
14.3-32	Containment Subcompartment Free Volume and Vent Areas

LIST OF TABLES (CONT'D)

<u>Table</u>	<u>Title</u>
14B-1	(Deleted)
14B-1A	Equilibrium Core Inventory Based on a Core Power of 2918 MWT and an 18 Month Fuel Cycle
14B-2	Core Temperature Distribution
14B-3	(Deleted)
14B-4	(Deleted)
14B-5	Parameters Used in the Calculation of Reactor Coolant Activities
14B-6	Design Reactor Coolant Noble Gas and Iodine Activities
14B-7	Parameters Used in the Calculation of Tritium Sources
14B-8	Tritium Production in the Reactor Coolant Curies Per Year
14B-9	(Deleted)
14B-10	(Deleted)
14B-11	Thyroid Dose Conversion Factors

LIST OF TABLES (CONT'D)

<u>Table</u>	<u>Title</u>
14B-12	Summary of Two-Region Spray Model Expressions
14B-13	(Deleted)
14B-14	(Deleted)
14B-15	Primary and Secondary Coolant Technical Specification Iodine and Noble Gas Concentrations
14B-15a	(Deleted)
14B-16	RCS Iodine Spike Activities
14D-1	Nuclear Steam Supply System Power Ratings Used in Analysis
14D-2	Summary of Initial Conditions and Computer Codes Used
14D-3	Trip Points and Time Delays to Trip Assumed in Accident Analyses
14D-4	(Deleted)

LIST OF FIGURES

<u>Figure</u>	<u>Title</u>
14.1-1	Uncontrolled Rod Withdrawal from a Subcritical Condition, Nuclear Power Versus Time
14.1-2	Uncontrolled Rod Withdrawal from a Subcritical Condition, Core Heat Flux Versus Time
14.1-3	Uncontrolled Rod Withdrawal from a Subcritical Condition, Core Heat Flux Versus Time
14.1-4	Transient Response for Uncontrolled Rod Withdrawal from Full Power Terminated by High Neutron Flux Trip
14.1-5	Transient Response for Uncontrolled Rod Withdrawal from Full Power Terminated by High Neutron Flux Trip
14.1-6	Transient Response for Uncontrolled Rod Withdrawal from Full Power Terminated by Overtemperature Delta-T Trip
14.1-7	Transient Response for Uncontrolled Rod Withdrawal from Full Power Terminated by Overtemperature Delta-T Trip
14.1-8	Effect of Reactivity Insertion Rate on Minimum DNBR for a Rod Withdrawal Accident from 100% Power
14.1-9	Effect of Reactivity Insertion Rate on Minimum DNBR for a Rod Withdrawal Accident from 60% Power
14.1-10	Effect of Reactivity Insertion Rate on Minimum DNBR for a Rod Withdrawal Accident from 10% Power
14.1-11	Transient Response to Dropped Rod Cluster Control Assembly

LIST OF FIGURES (CONT'D)

<u>Figure</u>	<u>Title</u>
14.1-12	(Deleted)
14.1-13	Reactor Vessel and Faulted Loop Flow Transients for Partial Loss of Flow - One Pump Coasting Down
14.1-14	Nuclear Power and RCS Pressure Transients for Partial Loss of Flow - One Pump Coasting Down
14.1-15	Average Channel and Hot Channel Heat Flux Transients for Partial Loss of Flow - One Pump Coasting Down
14.1-16	DNBR Versus Time for Partial Loss of Flow - One Pump Coasting Down
14.1-17	(Deleted)
14.1-18	(Deleted)
14.1-19	(Deleted)
14.1-20	(Deleted)
14.1-21	(Deleted)
14.1-22	(Deleted)
14.1-23	Loss of Load Accident with Pressurizer Spray and Power-Operated Relief Valves
14.1-24	Loss of Load Accident with Pressurizer Spray and Power-Operated Relief Valves
14.1-25	Loss of Load Accident with Pressurizer Spray and Power-Operated Relief Valves
14.1-26	Loss of Load Accident with Pressurizer Spray and Power-Operated Relief Valves



LIST OF FIGURES (CONT'D)

<u>Figure</u>	<u>Title</u>
14.1-27	Loss of Load Accident without Pressurizer Spray and Power-Operated Relief Valves
14.1-28	Loss of Load Accident without Pressurizer Spray and Power-Operated Relief Valves
14.1-29	Loss of Load Accident without Pressurizer Spray and Power-Operated Relief Valves
14.1-30	Loss of Load Accident without Pressurizer Spray and Power-Operated Relief Valves
14.1-31	Nuclear Power and Core Heat Flux Transients for Loss of Normal Feedwater
14.1-31A	Reactor Coolant Temperature and Steam Generator Pressure Transients for Loss of Normal Feedwater
14.1-31B	Pressurizer Pressure and Water Volume Transients for Loss of Normal Feedwater
14.1-31C	Vessel Mass Flow Rate and Pressurizer Insurge Transient for Loss of Normal Feedwater
14.1-31D	Core Reactivity Transient and Feedline Flow Transient for Loss of Normal Feedwater
14.1-31E	Nuclear Power and Core Heat Flux Transients for Loss of AC Power
14.1-31F	Reactor Coolant Temperature and Steam Generator Pressure Transients for Loss of AC Power
14.1-31G	Pressurizer Pressure and Water Volume Transients for Loss of AC Power
14.1-31H	Vessel Mass Flow Rate and Pressurizer Insurge Transients for Loss of AC Power
14.1-31I	Core Reactivity Transient and Feedline Flow Transient for Loss of AC Power
14.1-32A	Nuclear Power, Core Heat Flux, and Pressurizer Pressure Transients for Feedwater Control Valve Malfunction at Full Power, Automatic Rod Control

LIST OF FIGURES (CONT'D)

<u>Figure</u>	<u>Title</u>
14.1-32B	Loop Delta-T, Core Average Temperature and DNBR Transients for Feedwater Control Valve Malfunction at Full Power, Automatic Rod Control
14.1-33	Excessive Load Increase without Rod Control, Beginning of Life
14.1-34	Excessive Load Increase without Rod Control, Beginning of Life
14.1-35	Excessive Load Increase without Rod Control, End of Life
14.1-36	Excessive Load Increase without Rod Control, End of Life
14.1-37	Excessive Load Increase with Rod Control, Beginning of Life
14.1-38	Excessive Load Increase with Rod Control, Beginning of Life

LIST OF FIGURES (CONT'D)

<u>Figure</u>	<u>Title</u>
14.1-39	(Deleted)
14.1-40	(Deleted)
14.1-41	Variation of Keff with Core Temperatures
14.1-42	Safety Injection flow vs RCS Pressure
14.1-43	(Deleted)
14.1-44	Nuclear Power Transient for Accidental RCS Depressurization
14.1-45	Pressurizer Pressure and Core Average Temperature Transients for Accidental RCS Depressurization
14.1-46	DNBR Transient for Accidental RCS Depressurization
14.1-47	Spurious Actuation of Safety Injection System at Power
14.1-48	Spurious Actuation of Safety Injection System at Power
14.2-1	(Deleted)
14.2-2	(Deleted)
14.2-3	Steam Generator Tube Rupture Old/New Equilibrium Break Flow
14.2-4	Variation of Reactivity with Power at Constant Core Average Temperature
14.2-5	Core Average Temperature Transient for Steam Line Break at Exit of Steam Generator with Offsite Power
14.2-6	RCS Pressure Transient for Steam Line Break at Exit of Steam Generator with Offsite Power

LIST OF FIGURES (CONT'D)

<u>Figure</u>	<u>Title</u>
14.2-7	Core Heat Flux Transient for Steam Line Break at Exit of Steam Generator with Offsite Power
14.2-8	Core Reactivity Transient for Steam Line Break at Exit of Steam Generator with Offsite Power
14.2-9	Integrated Safety Injection Flow Rate of Borated Water for Steam Line Break at Exit of Steam Generator with Offsite Power
14.2-10A	Nuclear Power and Total Reactivity Transients for Feedwater Pipe Rupture With Offsite Power Available
14.2-10B	Feedline Break Flow and Pressurizer Relief Transients for Major Rupture of a Main Feedwater Pipe with Offsite Power Available
14.2-10C	Pressurizer Pressure and Pressurizer Water Volume Transients for Major Rupture of a Main Feedwater Pipe with Offsite Power Available
14.2-10D	Loop Temperatures for Major Rupture of a Main Feedwater Pipe with Offsite Power Available
14.2-10E	Steam Generator Pressure and Core Heat Flux Transients for Major Rupture of a Main Feedwater Pipe with Offsite Power Available
14.2-10F	Nuclear Power and Total Reactivity for Major Rupture of a Main Feedwater Pipe without Offsite Power Available
14.2-10G	Feedline Break Flow and Pressurizer Relief Transients for Major Rupture of a Main Feedwater Pipe without Offsite Power Available
14.2-10H	Pressurizer Pressure and Pressurizer Water Volume Transients for Major Rupture of a Main Feedwater Pipe without Offsite Power Available
14.2-10I	Loop Temperatures for Major Rupture of a Main Feedwater Pipe without Offsite Power Available

LIST OF FIGURES (CONT'D)

<u>Figure</u>	<u>Title</u>
14.2-10J	Steam Generator Pressure and Core Heat Flux Transients for Major Rupture of a Main Feedwater Pipe without Offsite Power Available
14.2-11	Nuclear Power Transient BOL-HFP Ejection Accident
14.2-12	Peak Fuel and Clad Average Temperature Versus Time BOL-HFP Ejection Accident
14.2-13	Nuclear Power Transient EOL-HZP Ejection Accident
14.2-14	Peak Fuel and Clad Average Temperature Versus Time, EOL-HZP Ejection Accident
14.2-15	Reactor Vessel and Faulted Loop Flow Transients for Three Loop Operation, One Locked Rotor
14.2-16	Nuclear Power and Reactor Coolant System Pressure for Three Loop Operation - One Locked Rotor
14.2-17	Average Channel and Hot Channel Heat Flux Transients for Three Loop Operation, One Locked Rotor
14.2-18	Maximum Clad and Fuel Centerline Temperatures at Hot Spot for Three Loop Operation, One Locked Rotor
14.2-19	Steam System Piping Failure at Power - 0.60 Ft. <sup>2</sup> Break - Nuclear Power and Core Heat Flux Transients
14.2-20	Steam System Piping Failure at Power - 0.60 Ft. <sup>2</sup> Break - Pressurizer Pressure and Water Volume Transients
14.2-21	Steam System Piping Failure at Power - 0.60 Ft. <sup>2</sup> Break - Core Inlet Temperature Transient and DNR Ratio versus Time
14.2-22	Steam System Piping Failure at Power - 0.60 Ft. <sup>2</sup> Break - Steam Generator Pressure and Steam Mass Flow Transients
14.2-23	(Deleted)
14.2-24	(Deleted)
14.2-25	Interchange Between Region 1 and Region 3 Assembly

LIST OF FIGURES (CONT'D)

<u>Figure</u>	<u>Title</u>
14.2-26	Interchange Between Region 1 and Region 2 Assembly, Burnable Poison Rods Being Retained by the Region 2 Assembly
14.2-27	Interchange Between Region 1 and Region 2 Assembly, Burnable Poison Rods Being Transferred to Region 1 Assembly
14.2-28	Enrichment Error: A Region 2 Assembly Loaded into the Core Central Position
14.2-29	Loading A Region 2 Assembly into a Region 1 Position Near Core Periphery
14.2-30	Core Flow Coastdown vs Time for Three Loops in Operation, Complete Loss of Flow, Frequency Decay
14.2-31	Nuclear Power Transient and Pressurizer Pressure Transients for Three Loops in Operation, Three Loops Coasting Down, Complete Loss of Flow
14.2-32	Average Channel and Hot Channel Heat Flux Transients for Three Loops in Operation, Complete Loss of Flow, Frequency Decay
14.2-33	DNBR Versus Time for Three Loops in Operation, Three Pumps Coasting Down, Complete Loss of Flow
14.2-34	Containment Pressure - Peak Pressure Analysis, MSLB (30% Power) 1.4 ft <sup>2</sup> DER, MSCV SAF
14.2-35	Containment Atmos. Temp. - Peak Temperature Analysis, MSLB (30% Power) 1.4 ft <sup>2</sup> DER, MSCV SAF
14.2-36	Containment Liner Temp. - Peak Temperature Analysis, MSLB (30% Power) 1.4 ft <sup>2</sup> DER, MSCV SAF

LIST OF FIGURES (CONT'D)

<u>Figure</u>	<u>Title</u>
14.3-1A	(Deleted)
14.3-1B	(Deleted)
14.3-1C	(Deleted)
14.3.1-2	2.75-Inch Break RCS Pressure
14.3.1-3	2.75-Inch Break Core Mixture Level
14.3.1-4	2.75-Inch Break Peak Clad Temperature
14.3.1-5	Steam Flow (2.75-Inch)
14.3.1-6	2.75-Inch Break Rod Film Heat Transfer Coefficient
14.3.1-7	2.75-Inch Hot Spot Fluid Temperature
14.3.1-8	Core Power Transient
14.3.1-9A	2-Inch Break RCS Pressure
14.3.1-9B	2.25-Inch Break RCS Pressure
14.3.1-9C	2.5-Inch Break RCS Pressure
14.3.1-9D	3-Inch Break RCS Pressure
14.3.1-9E	3.25-Inch Break RCS Pressure
14.3.1-9F	4-Inch Break RCS Pressure
14.3.1-9G	6-Inch Break RCS Pressure
14.3.1-10A	2-Inch Break Core Mixture Level
14.3.1-10B	2.25-Inch Break Core Mixture Level
14.3.1-10C	2.5-Inch Break Core Mixture Level
14.3.1-10D	3-Inch Break Core Mixture Level
14.3.1-10E	3.25-Inch Break Core Mixture Level
14.3.1-10F	4-Inch Break Core Mixture Level

LIST OF FIGURES (CONT'D)

<u>Figure</u>	<u>Title</u>
14.3.1-10G	6-Inch Break Core Mixture Level
14.3.1-11A	2-Inch Break Peak Clad Temperature Transient
14.3.1-11B	2.25-Inch Break Peak Clad Temperature Transient
14.3.1-11C	2.5-Inch Break Peak Clad Temperature
14.3.1-11D	3-Inch Break Peak Clad Temperature
14.3.1-11E	3.25-Inch Break Peak Clad Temperature
14.3.1-11F	4-Inch Break Peak Clad Temperature
14.3.1-11G	6-Inch Break Peak Clad Temperature
14.3.2-1	(Deleted)
14.3.2-1A	Limiting Case Cladding Temperature at the PCT Elevation
14.3.2-1B	Limiting Case Vessel Side Break Flow
14.3.2-1C	Limiting Case Broken and Intact Loop Pump Void Fraction
14.3.2-1D	Limiting Case Hot Assembly Top of Core Vapor Flow
14.3.2-1E	Limiting Case Pressurizer Pressure
14.3.2-1F	Limiting PCT Lower Plenum Collapsed Liquid Level
14.3.2-1G	Limiting Case Vessel Fluid Mass
14.3.2-1H	Limiting Case Loop 2 Accumulator Flow
14.3.2-1I	Safety Injection Flow for the Limiting PCT Case
14.3.2-1J	Limiting Case Core Average Channel Collapsed Liquid Level
14.3.2-1K	Limiting Case Loop 2 Downcomer Collapsed Liquid Level
14.3.2-1L	Peak Clad Temperature Elevation for the Hot Rod for the Limiting PCT Case
14.3.2-2	Beaver Valley Unit 1 BELOCA Analysis Axial Power Shape Operating Space Envelope
14.3.2-3	WCOBRA/TRAC Assumed Backpressure versus Calculated Containment Backpressure



LIST OF FIGURES (CONT'D)

<u>Figure</u>	<u>Title</u>
14.3.2-4	(Deleted)
14.3.2-5	(Deleted)
14.3.2-6	(Deleted)
14.3.2-7	(Deleted)
14.3.2-8	(Deleted)
14.3.2-9	(Deleted)
14.3.2-10	(Deleted)
14.3.2-11	(Deleted)
14.3.2-12	(Deleted)
14.3.2-13	(Deleted)
14.3.2-14	(Deleted)
14.3.2-15	(Deleted)
14.3.2-16	(Deleted)
14.3-2	(Deleted)
14.3-3	(Deleted)
14.3-4	(Deleted)
14.3-5	(Deleted)
14.3-6	(Deleted)
14.3-7	(Deleted)
14.3-8	(Deleted)
14.3-9A	(Deleted)
14.3-9B	(Deleted)
14.3-9C	(Deleted)
14.3-9D	(Deleted)
14.3-10A	(Deleted)
14.3-10B	(Deleted)
14.3-10C	(Deleted)
14.3-10D	(Deleted)
14.3-11A	(Deleted)
14.3-11B	(Deleted)

LIST OF FIGURES (CONT'D)

<u>Figure</u>	<u>Title</u>
14.3-11C	(Deleted)
14.3-11D	(Deleted)
14.3-12A through 14.3-44	(Deleted)
14.3-45	MAAP-DBA Containment Nodalization
14.3-46	MAAP-DBA Containment Nodalization (Plan View)
14.3-47	MAAP-DBA Node and Junction Arrangement
14.3-48 through 14.3-53	(Deleted)
14.3-54	(Deleted)
14.3-55	(Deleted)
14.3-55A	(Deleted)
14.3-56	Containment Pressure & Temperature Time-History for the DEHL Break Case
14.3-56A	Containment Pressure & Temperature Time-History for the DEPS Minimum SI Break Case
14.3-56B	Containment Pressure & Temperature Time-History for the DEPS Maximum SI Break Case
14.3-57	(Deleted)
14.3-58	(Deleted)
14.3-59	(Deleted)
14.3-60	(Deleted)
14.3-61	(Deleted)
14.3-61A	(Deleted)

LIST OF FIGURES (CONT'D)

<u>Figure</u>	<u>Title</u>
14.3-61B	(Deleted)
14.3-61C	(Deleted)
14.3-62 through 14.3-76	(Deleted)
14.3-77A	(Deleted)
14.3-77B	(Deleted)
14.3-78A	(Deleted)
14.3-78B	(Deleted)
14.3-79	(Deleted)
14.3-80	(Deleted)
14.3-81	(Deleted)
14.3-82	Free Volumes and Vent Areas for Steam Generator and Pressurizer Cubicle
14.3-83	(Deleted)
14.3-84	(Deleted)
14.3-85	(Deleted)
14.3-86	Differential Pressure Vs Time Steam Generator Cubicle A Hot Leg DER
14.3-87	Differential Pressure Vs Time Steam Generator Cubicle B Hot Leg DER
14.3-88	Differential Pressure Vs Time Steam Generator Cubicle C Hot Leg DER

LIST OF FIGURES (CONT'D)

<u>Figure</u>	<u>Title</u>
14.3-89	Pressurizer Nodal Configuration and Node, S-Junction Model Spray Line Break in Node 3
14.3-90	Pressure Differential Vs Time Pressurizer Cubicle (2 Node Model)
14.3-91	Nodal Configuration For Pressurizer Subcompartments (Middle Node 1 & Lower Node 2)
14.3-92	Pressure Differential Vs Time Pressurizer Cubicle (2 Node Model)
14.3-93	(Deleted)
14.3-94	(Deleted)
14.3-95	(Deleted)
14.3-96	(Deleted)
14.3-97	Thrust Force As a Function of Time After a Cold Leg DER
14.3-98	Jet Forces on Typical Steam Generator Cubicle
14.3-99	Typical Steam Generator Cubicle Configuration
14.3-100	Aerosol Removal Rates Within Sprayed Region
14.3-101	Aerosol Removal Rates Within Unsprayed Region

LIST OF FIGURES (CONT'D)

<u>Figure</u>	<u>Title</u>
14B-1	Loss of Coolant Accident Release Pathways
14C-1	Predicted Versus Measured Total Heat Transfer Coefficient - Blowdown Heat Transfer Test
14C-2	Predicted Versus Measured Total Heat Transfer Coefficient - Steam in Turbulent Flow
14D-1	Illustration of Overtemperature and Overpower $\Delta T$ Protection
14D-2	Negative Reactivity Insertion Vs Time on Reactor Trip
14D-3	Normalized RCCA Reactivity Worth Vs Rod Insertion
14D-4	Normalized RCCA Bank Reactivity Worth Vs Time After Trip
14D-5	Doppler Power Coefficient Used in Accident Analysis
14D-6	Residual Decay Heat
14D-7	Fuel Rod Cross Section
14E-1A	(Deleted)
14E-1B	(Deleted)
14E-1C	(Deleted)
14E-2A	(Deleted)
14E-2B	(Deleted)
14E-2C	(Deleted)
14E-3A	(Deleted)
14E-3B	(Deleted)
14E-3C	(Deleted)

LIST OF FIGURES (CONT'D)

<u>Figure</u>	<u>Title</u>	
14E-4A	(Deleted)	
14E-4B	(Deleted)	
14E-4C	(Deleted)	
14E-5A	(Deleted)	
14E-5B	(Deleted)	
14E-5C	(Deleted)	
14E-6A	(Deleted)	
14E-6B	(Deleted)	
14E-6C	(Deleted)	
14E-7A	(Deleted)	
14E-7B	(Deleted)	
14E-7C	(Deleted)	
14E-8A	(Deleted)	
14E-8B	(Deleted)	
14E-8C	(Deleted)	
14E-9A	(Deleted)	
14E-9B	(Deleted)	
14E-9C	(Deleted)	
14E-10A	(Deleted)	
14E-10B	(Deleted)	
14E-10C	(Deleted)	

LIST OF FIGURES (CONT'D)

<u>Figure</u>	<u>Title</u>	
14E-11A	(Deleted)	
14E-11B	(Deleted)	
14E-11C	(Deleted)	
14E-12A	(Deleted)	
14E-12B	(Deleted)	
14E-12C	(Deleted)	
14E-13A	(Deleted)	
14E-13B	(Deleted)	
14E-13C	(Deleted)	
14E-14A	(Deleted)	
14E-14B	(Deleted)	
14E-14C	(Deleted)	
14E-15A	(Deleted)	
14E-15B	(Deleted)	
14E-15C	(Deleted)	
14E-16	(Deleted)	
14E-17	(Deleted)	

SECTION 14SAFETY ANALYSIS

## 14.0 INTRODUCTION

Condition I occurrences are those which are expected frequently or regularly in the course of power operation, refueling, maintenance, or maneuvering of the plant. As such, Condition I occurrences are accommodated with margin between any plant parameter and the value of that parameter which would require either automatic or manual protective action. Inasmuch as Condition I occurrences occur frequently or regularly, they must be considered from the point of view of affecting the consequences of fault conditions (Conditions II, III, and IV). In this regard, analysis of each fault condition described is generally based on a conservative set of initial conditions corresponding to the most adverse set of conditions which can occur during Condition I operation. Refer to Table 14.0-1 for a typical list of Condition I Events.

## 14.1 CORE AND COOLANT BOUNDARY PROTECTION ANALYSIS

14.1.1 Uncontrolled Rod Cluster Control Assembly Bank Withdrawal from a Subcritical Condition

## 14.1.1.1 Identification of Causes and Accident Description

A rod cluster control assembly (RCCA) withdrawal accident is defined as an uncontrolled addition of reactivity to the reactor core caused by withdrawal of RCCAs resulting in a power excursion. Such a transient could be caused by a malfunction of the reactor control or control rod drive systems. This could occur with the reactor either subcritical, hot zero power or at power. The "at power" case is discussed in Section 14.1.2.

Although the reactor is normally brought to power from a subcritical condition by means of rod cluster control assembly withdrawal, initial startup procedures with a clean core call for boron dilution. The maximum rate of reactivity increase in the case of boron dilution is less than that assumed in this analysis (Section 14.1.4, Uncontrolled Boron Dilution.)

The rod cluster control assembly drive mechanisms are wired into preselected bank configurations which are not altered during reactor life. These circuits prevent the RCCAs from being withdrawn in other than their respective banks. Power supplied to the banks is controlled such that no more than two banks can be withdrawn at the same time. The rod cluster control assembly drive mechanisms are of the magnetic latch type and coil actuation is sequenced to provide variable speed travel. The maximum reactivity insertion rate analyzed in the detailed plant analysis is that occurring with the simultaneous withdrawal of the combination of the two control banks having the maximum combined worth at maximum speed.

This event is classified as an ANS Condition II incident. The neutron flux response to a continuous reactivity insertion is characterized by a very fast rise terminated by the reactivity feedback effect of the negative Doppler coefficient. This self limitation of the power burst is of primary importance since it limits the power to a tolerable level during the delay time for protection action. Should a continuous rod cluster control assembly withdrawal accident occur,



the transient will be terminated by the following automatic features of the Reactor Protection System:

1. Source Range High Neutron Flux Reactor Trip - actuated when either of two independent source range channels indicates a neutron flux level above a preselected manually adjustable setpoint. This trip function may be manually bypassed when either intermediate range flux channel indicates a flux level above a specified level. It is automatically reinstated when both intermediate range channels indicate a flux level below a specified level.
2. Intermediate Range High Neutron Flux Reactor Trip - actuated when either of two independent intermediate range channels indicates a flux level above a preselected manually adjustable setpoint. This trip function may be manually bypassed when two of the four power range channels are reading above approximately 10 percent of full power and is automatically reinstated when three of the four channels indicate a power below this value.
3. Power Range High Neutron Flux Reactor Trip (Low Setting) - actuated when two out of the four power range channels indicate a power level above approximately 25 percent of full power. This trip function may be manually bypassed when two of the four power range channels indicate a power level above approximately 10 percent of full power and is automatically reinstated when three of the four channels indicate a power level below this value.
4. Power Range High Neutron Flux Reactor Trip (High Setting) - actuated when two out of the four power range channels indicate a power level above a preset setpoint. This trip function is always active.
5. High Neutron Flux Rate Trip - Actuated when the positive rate of change of neutron flux on two out of four nuclear power range channels indicate a rate above the preset setpoint. This trip function is always active.

In addition, control rod stops on high intermediate range flux level (one of two) and high power range flux level (one out of four) serve to discontinue rod withdrawal and prevent the need to actuate the intermediate range flux level trip and the power range flux level trip, respectively.

#### 14.1.1.2 Analysis of Effects and Consequences

##### Method of Analysis

The analysis of the uncontrolled RCCA bank withdrawal from subcritical accident is performed in three stages: 1) an average core nuclear power transient calculation; 2) an average core heat transfer calculation; and 3) the departure from nucleate boiling ratio (DNBR) calculation. The average core nuclear calculation is performed using a spatial neutron kinetics code, TWINKLE (Reference 10), to determine the average power generation with time including the various total core feedback effects, i.e., Doppler reactivity and moderator reactivity. The average heat flux and temperature transients are determined by performing a fuel rod transient heat transfer calculation in FACTRAN (Reference 2). The average heat flux is next used in VIPRE (Reference 21, described in FSAR Section 3) for the transient DNBR calculation.

In order to give conservative results for a startup accident, the following assumptions are made concerning the initial reactor conditions:

1. Since the magnitude of the power peak reached during the initial part of the transient for any given rate of reactivity insertion is strongly dependent on the Doppler coefficient conservative values (low absolute magnitude) as a function of power are used. The magnitude does not correlate directly to Figure 14D-5 because the TWINKLE code, on which the neutronics analysis is based, is a thermal diffusion code rather than a point kinetics approximation.
2. Contribution of the moderator reactivity coefficient is negligible during the initial part of the transient because the heat transfer time between the fuel and the moderator is much longer than the neutron flux response time. However, after the initial neutron flux peak, the succeeding rate of power increase is affected by the moderator reactivity coefficient. A conservative value (+5 pcm/°F) is used in the analysis to yield the maximum peak heat flux.
3. The reactor is assumed to be at hot zero power. This assumption is more conservative than that of a lower initial system temperature. The higher initial system temperature yields a larger fuel-water heat transfer coefficient, larger specific heats, and a less negative (smaller absolute magnitude) Doppler coefficient, all of which tend to reduce the Doppler feedback effect, thereby increasing the neutron flux peak. The initial effective multiplication factor is assumed to be 1.0 since this results in maximum neutron flux peaking. Studies made with various initial values for effective multiplication factors have shown that a larger neutron flux peak occurs for larger initial values. Since  $k = 1.0$  is the upper limit to the subcritical region, it is the value used in the analysis.
4. Reactor trip is assumed to be initiated by power range high neutron flux (low setting). The most adverse combination of instrument and setpoint errors, as well as delays for trip signal actuation and rod cluster control assembly release, is taken into account. A 10 percent increase is assumed for power range flux trip setpoint raising it from the nominal value of 25 percent to 35 percent. Previous results, however, show that rise in the neutron flux is so rapid that the effect of errors in the trip setpoint on the actual time at which the rods are released is negligible. In addition, the reactor trip insertion characteristic is based on the assumption that the highest worth rod cluster control assembly is stuck in its fully withdrawn position. See Section 14D.5 for rod cluster control assembly insertion characteristics.
5. The maximum positive reactivity insertion rate assumed is greater than that for the simultaneous withdrawal of the combination of the two control banks having the greatest combined worth at maximum speed (48.125 inches/minute). Control rod drive mechanism design is discussed in Section 3.2.3.
6. The most limiting axial and radial power shapes, associated with having the two highest combined worth sequential control banks in their highest worth position, is assumed in the departure from nucleate boiling (DNB) analysis.
7. The initial power level was assumed to be below the power level expected for any shutdown condition ( $10E-09$  of nominal power). The combination of highest reactivity insertion rate and lowest initial power produces the highest peak heat flux.

8. Two RCPs are assumed to be in operation. This lowest initial flow minimizes the resulting DNBR.

### Results

Figures 14.1-1, 14.1-2 and 14.1-3 show the transient behavior for the uncontrolled RCCA bank withdrawal with the accident terminated by reactor trip at 35 percent nominal power. This insertion rate is greater than that for the two highest worth control banks, both assumed to be in their highest incremental worth region.

Figure 14.1-1 shows the neutron flux transient. The neutron flux overshoots the full power nominal value but this occurs for only a very short time period. Hence, the energy release and the fuel temperature increases are relatively small. The thermal flux response, of interest for DNB considerations, is shown on Figure 14.1-2. The beneficial effect of the inherent thermal lag in the fuel is evidenced by a peak heat flux less than the full power nominal value. There is a large margin to DNB during the transient since the rod surface heat flux remains below the design value, and there is a high degree of subcooling at all times in the core. Figure 14.1-3 shows the response of the hot spot fuel and cladding temperature. The hot spot fuel average temperature increases to a value lower than the nominal full power hot spot value. The minimum DNBR at all times remains above the safety analysis limit value.

The calculated sequence of events for this accident is shown in Table 14.1-2. With the reactor tripped, the plant returns to a stable condition. The plant may subsequently be cooled down further by following normal plant shutdown procedures.

### Conclusions

In the event of a rod cluster control assembly withdrawal accident from the subcritical condition, the core and the Reactor Coolant System are not adversely affected, since the combination of thermal power and the coolant temperature result in a Departure from Nucleate Boiling Ratio (DNBR) which is always greater than the limit value. Thus, the DNB design basis as described in FSAR Section 3 is met.

#### 14.1.2 Uncontrolled Rod Cluster Control Assembly Bank Withdrawal at Power

##### 14.1.2.1 Identification of Causes and Accident Description

Uncontrolled rod cluster control assembly bank withdrawal at power results in an increase in the core heat flux. Since the heat extraction from the steam generator lags behind the core power generation until the steam generator pressure reaches the relief or safety valve setpoint, there is a net increase in the reactor coolant temperature. Unless terminated by manual or automatic action, the power mismatch and resultant coolant temperature rise would eventually result in a violation of the DNB design basis. Therefore, in order to avert damage to the cladding the Reactor Protection System is designed to terminate the transient to ensure the DNBR safety analysis acceptance criteria are met.

The automatic features of the Reactor Protection System which prevent core damage following the postulated accident include the following:

1. Power range neutron flux instrumentation actuates a reactor trip if two out of four channels exceed an overpower setpoint.
2. Reactor trip is actuated if any two out of three  $\Delta T$  channels exceed an overtemperature  $\Delta T$  setpoint. This setpoint is automatically varied with axial power imbalance, coolant temperature and pressure to protect against violating the DNB design basis.
3. Reactor trip is actuated if any two out of three  $\Delta T$  channels exceed an overpower  $\Delta T$  setpoint.
4. A high pressurizer pressure reactor trip actuated from any two out of three pressure channels which is set at a fixed point. This set pressure is less than the set pressure for the pressurizer safety valves.
5. A high pressurizer water level reactor trip actuated from any two out of three level channels which is set at a fixed point.
6. A positive neutron flux rate reactor trip actuates if any two-out-of-four channels reach a fixed setpoint.

In addition to the above listed reactor trips, there are the following rod cluster control assembly withdrawal blocks:

1. High neutron flux (one out of four)
2. Overpower  $\Delta T$  (two out of three)
3. Overtemperature  $\Delta T$  (two out of three)

The manner in which the combination of overpower and overtemperature  $\Delta T$  trips provide protection over the full range of Reactor Coolant System conditions is described in Section 7. This includes a plot (Figure 14D-1) illustrating allowable reactor coolant loop average temperature and  $\Delta T$  for the design power distribution and flow as a function of primary coolant pressure. The boundaries of operation defined by the overpower  $\Delta T$  trip and the overtemperature  $\Delta T$  trip are represented as "protection lines" on this diagram. The protection lines are drawn to include all adverse instrumentation and setpoint errors so that under nominal conditions trip would occur well within the area bounded by these lines. The utility of this diagram is in the fact that the limit imposed by any given DNBR can be represented as a line. The DNBR lines represent the locus of conditions for which the DNBR equals the safety analysis limit. All points below and to the left of a DNBR line for a given pressure have a DNBR greater than the safety analysis limit. The diagram shows that the DNB design basis is met for all cases if the area enclosed with the maximum protection lines is not traversed by the applicable DNBR line at any point.

The area of permissible operation (power, pressure, and temperature) is bounded by the combination of reactor trips: high neutron flux (fixed setpoint); high pressure (fixed setpoint); low pressure (fixed setpoint); overpower and overtemperature  $\Delta T$  (variable setpoints).

#### 14.1.2.2 Analysis of Effects and Consequences, Method of Analysis

This transient is analyzed by the LOFTRAN<sup>(3)</sup> code. This code simulates the neutron kinetics, Reactor Coolant System, pressurizer, pressurizer relief and safety valves, pressurizer spray, steam generator and steam generator safety valves. The code computes plant variables including temperatures, pressures, and power level. The core limits as illustrated in Figure 14D-1 are used as input to LOFTRAN to determine the minimum DNBR during the transient. The core limits are calculated as described in Section 3.4.2.3.1.

In order to obtain conservative values of DNBR the following assumptions are made:

1. This accident is analyzed with the Revised Thermal Design Procedure<sup>(13)</sup>. Therefore, initial reactor power, pressure, and RCS temperatures are assumed to be at their nominal values. Uncertainties in initial conditions are included in the limit DNBR.
2. Reactivity Coefficients - Two cases are analyzed:
  - a. Minimum Reactivity Feedback - A +5 pcm/°F moderator temperature coefficient of reactivity is assumed corresponding to the beginning of core life. A variable Doppler power coefficient with core power is used in the analysis. A conservatively small (in absolute magnitude) value is assumed.
  - b. Maximum Reactivity Feedback - A conservatively large positive moderator density coefficient and large (in absolute magnitude) negative Doppler power coefficient are assumed.
3. The reactor trip on high neutron flux is assumed to be actuated at a conservative value of 116 percent of nominal full power. The  $\Delta T$  trips include all adverse instrumentation and setpoint errors, while the delays for the trip signal actuation are assumed at their maximum values.
4. The rod control cluster assembly trip insertion characteristic is based on the assumption that the highest worth assembly is stuck in its fully withdrawn position.
5. The maximum reactivity insertion rate assumed is greater than that for the simultaneous withdrawal of the combination of the two control banks having the maximum combined worth at maximum speed.

#### Results

Figures 14.1-4 and 14.1-5 show the response of neutron flux, pressure, average coolant temperature, and DNBR to a rapid rod withdrawal incident starting from full power. Reactor trip on high neutron flux occurs after the start of the accident. Since this is rapid with respect to the thermal time constants of the plant, small changes in  $T_{avg}$  and pressure result and a large margin to the DNBR limit is maintained.

The response of neutron flux, pressure, average coolant temperature, and DNBR to a slow rod control assembly withdrawal from full power is shown in Figures 14.1-6 and 14.1-7. Reactor trip on overtemperature  $\Delta T$  occurs after a longer period and the rise in temperature and pressure is consequently larger than for the rapid rod cluster control assembly withdrawal.

Figure 14.1-8 shows the minimum DNBR as a function of reactivity insertion rate from initial full power operation for the minimum and maximum reactivity feedback. It can be seen that two reactor trip channels provide protection over the whole range of reactivity rates. These are the high neutron flux and overtemperature  $\Delta T$  trip channels. The DNBR safety analysis acceptance criteria are met.

Figures 14.1-9 and 14.1-10 show the minimum DNBR as a function of reactivity insertion rate for rod cluster control assembly withdrawal incidents starting at 60 and 10 percent power, respectively. The results are similar to the 100 percent power case, except as the initial power is decreased, the range over which the overtemperature  $\Delta T$  trip is effective is increased. The DNBR safety analysis acceptance criteria are met for both cases.

### Conclusions

The high neutron flux and overtemperature  $\Delta T$  trip channels provide adequate protection over the entire range of possible reactivity insertion rates, i.e., the DNBR safety analysis acceptance criteria are met. The DNBR predictions shown on Figures 14.1-8, 14.1-9 and 14.1-10 apply to the hottest channel in the core and are the minimum values for any point in the core.

#### 14.1.3 Rod Cluster Control Assembly Misalignment

##### 14.1.3.1 Identification of Causes and Accident Description

Rod cluster control assembly misalignment accidents include:

1. A dropped full-length assembly
2. A dropped full-length assembly bank
3. Statically misaligned full length assembly.

Each rod cluster control assembly has a position indication system channel which displays position of the assembly. The displays of assembly positions are grouped for the operator's convenience. Fully inserted assemblies are further indicated by a rod bottom light. Group demand position is also indicated. The full length assemblies are always moved in preselected banks and the banks are always moved in the same preselected sequence.

A dropped assembly or assembly banks are detected by:

1. Sudden drop in the core power level is seen by the Nuclear Instrument System
2. Asymmetric power distribution as seen on out of core neutron detectors or core exit thermocouples

3. Rod bottom light(s)
4. Rod deviation alarm
5. Rod position indication.

Misaligned assemblies are detected by:

1. Asymmetric power distribution as seen on out of core neutron detectors or core exit thermocouples
2. Rod deviation alarm
3. Rod position indicators
  - a. Analog rod position indicators.
  - b. In-plant computer points for rod position.

The resolution of the rod position indication system channel is  $\pm 5$  percent of span ( $\pm 7.2$  inches). Deviation of any assembly from its group by twice this distance (10 percent of span, or 14.4 inches) will not cause power distributions worse than the design limits. The deviation alarm alerts the operator to rod deviation with respect to group demand position in excess of 5 percent of span. If the rod deviation alarm is not operable, the operator is required to log the rod cluster control assembly positions in a prescribed time sequence to confirm alignment.

If one or more rod position indication system channels should be out of service, detailed operating instructions shall be followed to assure the alignment of the non-indicated RCCAs. The operator is also required to take action as required by the Technical Specifications.

#### 14.1.3.2 Analysis of Effects and Consequences, Method of Analysis

Steady state power distributions for the RCCA misalignment have been analyzed in three dimensions using an updated version of the Advanced Nodal Code (ANC)<sup>(23)</sup>. The lattice code used for the generation of macroscopic group constants in ANC is PHOENIX-P<sup>(24)</sup> or NEXUS/PARAGON<sup>(25, 26)</sup>. The peaking factors calculated by ANC were then used by the VIPRE<sup>(21)</sup> to calculate DNBR.

For the transient response to a dropped RCCA or RCCA bank the LOFTRAN<sup>(3)</sup> code is used. The code simulates the neutron kinetics, Reactor Coolant System, pressurizer, pressurizer relief and safety valves, pressurizer spray, steam generator, and steam generator safety valves. The code computes pertinent plant variables including temperatures, pressures, and power level.

#### Results

A dropped rod cluster control assembly typically results in a reactivity insertion of -0.15 percent  $\Delta k/k$ . Analyses have shown that with the core power distribution which exists following the drop of a single rod cluster control assembly, the reactor may be returned to full power with the full power Reactor Coolant System temperature without the DNBR going below the safety analysis limit. This is verified for each fuel reload.

Extensive analyses were performed to show that the minimum DNBR occurs near the end of the transient when the system has essentially returned to a new steady state equilibrium condition. Without automatic rod control, the system will return to a new equilibrium condition at a reduced primary temperature as a result of the moderator reactivity feedback. As typical of PWR uncontrolled response, the return of power is monotonic and therefore, power overshoot is not a condition for this case.

A power overshoot after a dropped rod cluster assembly incident can only result from the action of the automatic rod controller.

For a given PWR system, the power overshoot is essentially a function of the rod controller characteristics. Large power overshoots can result if the rod controller is essentially designed to restore primary system coolant temperature or secondary system steam pressure. The Westinghouse design uses a dual controller which limits the power overshoot to a maximum of two percent. The essential feature of the Westinghouse rod controller is that it terminates rod withdrawal well before the primary coolant average temperature is restored to an equilibrium condition. This not only minimizes the power overshoot but also ensures extra margin to DNB.

Sensitivity studies have confirmed that the maximum power overshoot occurs for the following conditions:

1. Minimum moderator reactivity feedback corresponding to beginning of core life conditions
2. Maximum reactivity worth of the control bank.

Figure 14.1-11 illustrates a typical dropped rod transient for the following limiting conditions:

1. Initial Power: 100.6 percent of rated power
2. Zero Moderator Reactivity Coefficient
3. Control Bank Reactivity Worth: 12 pcm/step
4. Dropped Rod Cluster Control Assembly Reactivity Worth: 0.25 percent  $\Delta k/k$ .

A dropped rod cluster control assembly group typically results in a reactivity insertion of -1.2 percent  $\Delta k/k$ . The core is not adversely affected during the insertion period, since power is decreasing rapidly. The transient will proceed as described above; however, the return to power will be less due to the greater worth of an entire bank. Following plant stabilization, normal rod retrieval or shutdown procedures may subsequently be followed to further cool the plant.



The most severe misalignment situations with respect to DNBR at significant power levels arise from cases in which group D is fully inserted with one assembly fully withdrawn; a 12 foot misalignment error. Multiple independent alarms, including a bank insertion limit alarm, alert the operator well before the postulated conditions are approached. The group can be inserted to its insertion limit with any one assembly fully withdrawn without the DNBR falling below the safety analysis limit.

The insertion limits in the Technical Specifications may vary from time to time depending on a number of limiting criteria. It is preferable, therefore, to analyze the misaligned assembly case at full power for a position of the control group as deeply inserted as the criteria on minimum DNBR and power peaking factor will allow. The full power insertion limits on control group D must then be chosen to be above that position and will usually be dictated by other criteria. Detailed results will vary from cycle to cycle depending on fuel arrangements.

DNB calculations have not been performed specifically for assemblies missing from other banks, however, power shape calculations have been done as required for the rod cluster control assembly ejection analysis. Inspection of the power shapes shows that the DNB and peak kW/ft situation is less severe than the group D case discussed above assuming insertion limits on the other groups.

#### 14.1.3.3 Conclusions

It is shown that in all cases of dropped single assemblies or dropped banks, the DNBR remains greater than the safety analysis limit value at power and consequently do not cause core damage.

For all cases of any group inserted to its rod insertion limit with any single rod cluster control assembly in that group fully withdrawn, the DNBR remains greater than the safety analysis limit. Thus, rod misalignments do not result in core damage.

#### 14.1.4 Uncontrolled Boron Dilution

##### 14.1.4.1 Identification of Causes and Accident Description

Reactivity can be added to the core by feeding primary grade water into the Reactor Coolant System via the reactor makeup portion of the Chemical and Volume Control System. Boron dilution is a manual operation under strict administrative controls with procedures calling for a limit on the rate and duration of dilution. A boric acid blend system is provided to permit the operator to match the boron concentration of reactor coolant makeup water during normal charging to that in the Reactor Coolant System. The Chemical and Volume Control System is designed to limit, even under various postulated failure modes, the potential rate of dilution to a value which, after indication through alarms and instrumentation, provides the operator sufficient time to correct the situation in a safe and orderly manner.

The opening of the primary water makeup control valve provides makeup to the Reactor Coolant System which can dilute the reactor coolant. Inadvertent dilution from this source can be readily terminated by closing the control valve. In order for makeup water to be added to the Reactor Coolant System at pressure, at least one charging pump must be running in addition to a primary makeup water pump.

The rate of addition of unborated water makeup to the Reactor Coolant System when it is not at pressure is limited by the capacity of the primary water supply pumps. The maximum addition rate in this case is 300 gpm with both primary water supply pumps running. The 300 gpm reactor makeup water delivery rate is based on a pressure drop calculation comparing the pump curves with the system resistance curve. This is the maximum delivery based on the unit piping layout. Normally, only one charging pump is operating.

The boric acid from the boric acid tank is blended with primary grade water in the blender and the composition is determined by the preset flow rates of boric acid and primary grade water on the control board.

In order to dilute, two separate operations are required:

1. The operator must switch from the automatic makeup mode to the dilute mode
2. The makeup switch must be placed to START.

Omitting either step would prevent dilution.

Information on the status of the reactor coolant makeup is continuously available to the operator. Lights are provided on the control board to indicate the operating condition of the pumps in the Chemical and Volume Control System. Alarms are actuated to warn the operator if boric acid or demineralized water flow rates deviate from preset values as a result of system malfunction.

#### 14.1.4.2 Method of Analysis and Results

Boron dilution during refueling, hot shutdown, cold shutdown, startup, and power operation are considered in this analysis. Table 14.1-2 contains the time sequence of events for this accident.

##### Dilution During Hot Shutdown, Cold Shutdown and Refueling

The primary means for a significant boron dilution is through the injection of unborated water into the Reactor Coolant System. Inadvertent boron dilution is prevented by administrative controls which isolate the primary grade water system from the Chemical and Volume Control System, except during planned boron dilution or makeup activities. Thus, unborated water cannot be injected into the Reactor Coolant System inadvertently making an unplanned boron dilution at these conditions highly improbable. The source of unborated water to the charging pumps is isolated and the low head safety injection pumps cannot be aligned to the primary grade water supply. This precludes an inadvertent boron dilution event in these modes of operation.

The primary grade water system isolation valves may be opened when directed by the control room during this mode of operation only for a planned boron dilution or makeup activity. The primary grade water system isolation valves will be verified to be locked, sealed or otherwise

secured in the closed position within 15 minutes after the planned boron dilution or makeup activity is completed. During planned boron dilution events, operator attention will be focused on the boron dilution process and any inappropriate blender operation is unlikely and will be readily identified.

The operator has prompt and definite indication of any boron dilution from the audible count rate supplied by the source range detectors. High count rate is alarmed in the reactor containment and the control room. In addition, a high source range flux level is alarmed in the control room. The count rate increase is proportional to the subcritical multiplication factor.

#### Dilution During Startup

In the Startup Mode, the plant is being taken from one long term mode of operation, Hot Standby, to another, Power. Typically, the plant is maintained in the Startup Mode only for the purpose of startup testing at the beginning of each cycle. During this mode of operation rod control is in manual. All normal actions required to change power level, either up or down, require operator initiation. Conditions assumed for the analysis are:

1. A maximum dilution flow of 231 gpm.
2. A minimum RCS water volume of 7504 cubic feet. This active volume includes the reactor vessel volume, reactor coolant loop piping volumes and the primary steam generator volume. Specifically excluded are the pressurizer and pressurizer surge line volumes.
3. The initial boron concentration is assumed to be 1800 ppm, which is a conservative maximum value for the critical concentration at the condition of hot zero power, rods to the insertion limits and no Xenon.
4. The critical boron concentration following reactor trip is assumed to be 1500 ppm, corresponding to the hot zero power, all rods inserted (minus the most reactive RCCA), no Xenon condition. The 300 ppm change from the initial condition noted above is a conservative minimum value.

This mode of operation is a transitory operational mode in which the operator intentionally dilutes and withdraws control rods to take the plant critical. During this mode, the plant is in manual control with the operator required to maintain a high awareness of the plant status. For a normal approach to criticality, the operator must manually initiate a limited dilution and subsequently manually withdraw the control rods, a process that takes several hours. Once critical, the power escalation must be sufficiently slow to allow the operator to manually block the source range reactor trip after receiving P-6 from the intermediate range. Too fast a power escalation (due to an unknown dilution) would result in reaching P-6 unexpectedly, leaving insufficient time to manually block the source range reactor trip. Failure to perform this manual action results in a reactor trip and immediate shutdown of the reactor. From initiation of the event, there are greater than 15 minutes available for operator action prior to return to criticality.

#### Dilution at Power

In the Power Mode, the plant may be operated in either automatic or manual rod control. The conditions assumed for the analysis of an inadvertent boron dilution transient are:

1. A maximum dilution flow of 231 gpm.

2. A minimum RCS water volume of 7504 cubic feet. This active volume includes the reactor vessel volume, reactor coolant loop piping volumes and the primary steam generator volume. Specifically excluded are the pressurizer and pressurizer surge line volumes.
3. The initial boron concentration is assumed to be 1800 ppm, which is a conservative maximum value for the critical concentration at the condition of hot full power, rods to the insertion limits, and no Xenon.
4. The critical boron concentration following reactor trip is assumed to be 1500 ppm, corresponding to the hot zero power, all rods inserted (minus the most reactive RCCA), no Xenon condition. The 300 ppm change from the initial condition noted above is a conservative minimum value.

With the reactor in automatic rod control, the power and temperature increase from boron dilution results in insertion of the control rods and a decrease in the available shutdown margin. The rod insertion limit alarms (LOW and LOW-LOW settings) alert the operator more than 15 minutes prior to criticality. This is the amount of time available for the operator to determine the cause of the dilution, isolate the reactor water makeup source, and initiate boration before the available shutdown margin is lost.

With the reactor in manual control and no operator action taken to terminate the transient, the power and temperature rise will cause the reactor to reach the Power Range High Neutron Flux trip setpoint resulting in a reactor trip. The boron dilution transient in this case is essentially the equivalent to an uncontrolled RCCA bank withdrawal at power. The maximum reactivity insertion rate for a boron dilution is conservatively estimated to be 2.8 pcm/sec, which is within the range of insertion rates analyzed. Thus, the effects of dilution prior to reactor trip are bounded by the Uncontrolled RCCA Bank Withdrawal at Power analysis (FSAR Section 14.1.2). Following reactor trip there are at least 15 minutes prior to criticality. This is the amount of time available for the operator to determine the cause of the dilution, isolate the reactor water makeup source, and initiate boration before the available shutdown margin is lost.

#### 14.1.4.3 Conclusions

Because of the procedure involved in the dilution process, an inadvertent dilution is considered to be highly unlikely. Nevertheless, if an unintentional dilution of boron in the reactor coolant does occur, numerous alarms and indications are available to alert the operator to the condition. Furthermore, the maximum reactivity addition due to the dilution is slow enough to allow the operator to determine the cause and take corrective action before shutdown margin is lost. Dilution during hot shutdown, cold shutdown and refueling has been precluded through administrative control of valves in the possible dilution flow paths.

#### 14.1.5 Partial Loss of Forced Reactor Coolant Flow

##### 14.1.5.1 Identification of Causes and Accident Description

A partial loss-of-coolant flow accident can result from a mechanical or electrical failure in a reactor coolant pump, or from a fault in the power supply to the pump. Each RCP is supplied by a separate bus. If the reactor is at power at the time of the accident, the immediate effect of loss-of-coolant flow is a rapid increase in the coolant temperature. This increase could result in DNB with subsequent fuel damage if the reactor is not tripped promptly.

This event is classified as an ANS Condition II incident. The necessary protection against a partial loss-of-coolant flow accident is provided by the low primary coolant flow reactor trip which is actuated by two out of three low flow signals in any reactor coolant loop. Above approximately 30 percent power (Permissive 8), low flow in any loop will actuate a reactor trip. Between approximately 10 percent power (Permissive P-7) and the power level corresponding to Permissive P-8 low flow in any two loops will actuate a reactor trip. Above P-7, two or more RCP circuit breakers opening will actuate a reactor trip which serves as a backup to the low flow trip.

Normal power for the pumps is supplied through buses connected to the main generator. Each pump is on a separate bus. When a generator trip occurs, the pumps are automatically transferred to a bus supplied from external power lines, and the pumps will continue to supply coolant flow to the core. Following any turbine trip where there are no electrical faults which require tripping the generator from the network, the generator remains connected to the network for approximately 30 seconds. The reactor coolant pumps remain connected to the generator thus ensuring full flow for approximately 30 seconds after the reactor trip before any transfer is made.

#### 14.1.5.2 Analysis of Effects and Consequences

##### Method of Analysis

The loss of one reactor coolant pump with three loops in operation has been analyzed. The analysis is performed to bound operation with steam generator tube plugging levels up to 22 percent (maximum loop-to-loop plugging difference of 10 percent) with a maximum loop-to-loop flow asymmetry of 5 percent.

This transient is analyzed by three digital computer codes: 1) the LOFTRAN Code (Reference 3) is used to calculate the loop and core flow during the transient, the time of reactor trip based on the calculated flows, the nuclear power transient, and the primary system pressure and temperature transients; 2) the FACTRAN Code (Reference 2) is then used to calculate the heat flux transient based on the nuclear power and flow from LOFTRAN; and 3) the VIPRE Code (Reference 21) is used to calculate the departure from nucleate boiling ratio (DNBR) during the transient based on the heat flux determined by FACTRAN and the flow determined by LOFTRAN. The DNBR transient presented represents the minimum of the typical or thimble cell. This transient is analyzed with the revised thermal design procedure as described in WCAP 11397-P-A (Reference 13).

##### Initial Conditions

Initial core power is assumed to be at its nominal value consistent with steady-state, full-power operation. RCS pressure is at its nominal value and the RCS vessel average temperature is at its nominal value plus a 4.5°F bias. Uncertainties in initial conditions are included in the limit DNBR as described in WCAP-11397-P-A.

##### Reactivity Coefficients

A conservatively large absolute value of the Doppler-only power coefficient is used (See Table 14D-2). The total integrated Doppler reactivity from 0 to 100 percent is assumed to be  $0.016\Delta k$ .

The lowest absolute magnitude of the moderator temperature coefficient ( $0.0 \Delta k/F$ ) is assumed since this results in the maximum hot-spot heat flux during the initial part of the transient when the minimum DNBR is reached.

### Flow Coastdown

The flow coastdown analysis is based on a momentum balance around each reactor coolant loop and across the reactor core. This momentum balance is combined with the continuity equation, a pump momentum balance and the pump characteristics and is based on high estimates of system pressure losses.

### Results

Figures 14.1-13, 14.1-14, 14.1-15, and 14.1-16 show the transient response for the loss of a reactor coolant pump with three loops in operation. Figure 14.1-16 shows the DNBR versus time. The results of the partial loss of flow transient confirms that the minimum DNBR acceptance criterion is met.

Since DNB does not occur, the ability of the primary coolant to remove heat from the fuel rod is not greatly reduced. Thus, the average fuel and clad temperatures do not increase significantly above their respective initial values.

The calculated sequence of events for the case analyzed is shown in Table 14.1-2. The affected reactor coolant pump will continue to coast down and the core flow will reach a new equilibrium value associated with the two remaining operating pumps. With the reactor tripped, a stable plant condition will eventually be attained. Normal plant shutdown may then proceed.

### Conclusions

The analysis shows that the DNBR acceptance criterion is met. Thus, the DNB design basis as described in Section 3 is met and there will be no cladding damage and no release of fission products to the Reactor Coolant System.

#### 14.1.6 Startup of an Inactive Reactor Coolant Loop

##### 14.1.6.1 Identification of Causes and Accident Description

The plant can be operated in Modes 5 or 6 with an inactive loop in either of two ways. The reactor coolant pump in the inactive loop can be turned off and the plant operated with the loop isolation valves in the normal fully open position. In this case, there is reverse flow through the inactive loop when a reactor coolant pump in any unisolated loop is operated. The plant can also be operated with the loop isolation valves of a loop closed in order to perform maintenance. In this case, there is no flow from the reactor vessel and active loops to the inactive loop. The plant operates much as if it were a plant without that loop. With the isolation valves closed, the boron concentration of the isolated section of the loop may deviate from the boron concentration of the active loops. The plant may isolate a loop only while the plant is shutdown. Analysis has not been conducted for power operation with a loop isolation valve closed.

Inadvertent opening of an isolated loop is prevented by (1) requiring that any loop isolation valve movement follow strict procedural criteria, and (2) loop isolation valve operators have their power removed while a loop is isolated.

Procedures require that 1) the boron concentration of the isolated loop be verified, and 2) the isolated loop drained and refilled from the Refueling Water Storage Tank or Reactor Coolant System prior to opening the loop isolation valves, returning the loop to service. An isolated loop will be returned to service within 4 hours of the completion of the refilling to ensure that there is no unacceptable boron stratification in the isolated loop.

Interlocks are provided to prevent starting a reactor coolant pump unless:

1. The cold leg loop stop valve in the same loop is fully closed, or
2. Both the hot leg loop stop valve and cold leg loop stop valve are fully open.

The interlocks are a part of the Reactor Protection System and include the following redundancy:

1. Two independent limit switches to indicate that a valve is fully open.
2. Two independent limit switches to indicate that a valve is fully closed.

The interlocks meet the IEEE 279-1971 criteria and, therefore, cannot be negated by a single failure.

#### 14.1.6.2 Analysis of Effects and Consequences

Procedures require that the isolated loop water boron concentration be verified prior to opening loop isolation valves. Procedures also require an isolated loop to be drained and refilled with water supplied from the Refueling Water Storage Tank or Reactor Coolant System, and that either the hot or cold leg isolation valves be open within 4 hours of draining and refilling the isolated loop. This prevents several potential concerns. A potential single failure of the blender if the Chemical and Volume Control System was used to fill an isolated loop could lead to unborated primary grade water being injected. Using water from the Refueling Water Storage Tank or Reactor Coolant System ensures that the boron concentration of the isolated loop is sufficient to prevent a dilution of the boron concentration in the active reactor coolant loops which would reduce the shutdown margin to below those values used in safety analyses. Thus, when the isolated loop is returned to service, no single failure could cause an isolated loop to be filled with unborated water. Opening the loop isolation valves within 4 hours of the refill prevents any boron concentration stratification concerns.

#### Conclusions

Procedures and interlocks prevent inadvertent opening of loop isolation valves and require that the startup of an isolated loop be performed in a controlled manner. This virtually eliminates any sudden positive reactivity addition from boron dilution. Thus, the core cannot be adversely affected by the startup of an isolated loop and fuel design limits are not exceeded.

### 14.1.7 Loss of External Electrical Load and/or Turbine Trip

#### 14.1.7.1 Identification of Causes and Accident Description

Major load loss on the plant can result from loss of external electrical load or from a turbine trip. For either case offsite power is available for the continued operation of the plant components such as the reactor coolant pumps. The case of loss of all AC power (station blackout) is analyzed in Section 14.1.11.

For a turbine trip, the reactor would be tripped directly (above P-9) from a signal derived from the turbine autostop oil pressure (Westinghouse Turbine) and turbine stop valves. Below P-9 such a direct reactor trip would not be generated, and the unit would be expected to respond without challenges to RCS pressure, provided sufficient secondary steam dump capacity is available. The automatic steam dump system would accommodate the excess steam generation. Reactor coolant temperatures and pressure do not significantly increase if the steam dump system and pressurizer pressure control system are functioning properly. If the turbine condenser was not available, the excess steam generation would be dumped to atmosphere. Additionally, main feedwater flow would be lost if the turbine condenser was not available. For this situation feedwater flow would be maintained by the auxiliary feedwater system.

In the event the steam dump valves fail to open following a large loss of load, the steam generator safety valves may lift and the reactor may be tripped by the high pressurizer pressure signal, the high pressurizer water level signal or the overtemperature  $\Delta T$  signal. The steam generator shell side pressure and reactor coolant temperatures will increase rapidly. The pressurizer safety valves and steam generator safety valves are, however, sized to protect the Reactor Coolant System and steam generator against overpressure for all load losses without assuming the operation of the steam dump system, pressurizer spray, pressurizer power operated relief valves, automatic rod cluster control assembly control nor direct reactor trip on turbine trip.

The steam generator safety valves are sized to maintain secondary pressure below 110 percent of the steam system design pressure. The pressurizer safety valve capacity is sized based on a complete loss of heat sink with the plant initially operating at the maximum calculated turbine load along with operation of the steam generator safety valves. The pressurizer safety valves are then able to maintain the Reactor Coolant System pressure within 110 percent of the Reactor Coolant System design pressure without direct or immediate reactor trip action.

A more complete discussion of overpressure protection can be found in Reference 6.

#### 14.1.7.2 Analysis of Effects and Consequences

Two cases have been considered -- one to demonstrate the adequacy of the pressure relieving devices and the other to demonstrate that the Departure from Nucleate Boiling Ratio (DNBR) limit is not violated. In the pressure case, the initial reactor power and RCS temperatures are assumed to be at their maximum values consistent with steady-state full power operation including allowances for calibration and instrument errors. For the DNB case, the initial reactor power and RCS temperatures are assumed to be at their nominal full power values consistent with the Revised Thermal Design Procedure (RTDP) which is discussed in Reference 13.



The total loss of load transients are analyzed by employing the detailed digital computer program LOFTRAN which is described in Section 14D. The program simulates the neutron kinetics, Reactor Coolant System, pressurizer, pressurizer relief and safety valves, pressurizer spray, steam generator, and steam generator safety valves. The program computes pertinent plant variables including temperatures, pressures, and power level.

Assumptions are:

1. Initial Operating Conditions - In the pressure case, the initial reactor power and RCS temperatures are assumed to be at their maximum values consistent with steady-state full power operation including allowances for calibration and instrument errors. The initial RCS pressure is assumed to be at a minimum value consistent with steady-state full power operation including allowances for calibration and instrument errors. The RCS flow rate assumed is the Thermal Design Flow (TDF).

For the DNB case, the initial reactor power and RCS temperatures are assumed to be at their nominal full power values. The initial RCS pressure is assumed to be at its nominal full power value. The RCS flow rate assumed is the Minimum Measured Flow (MMF). This is consistent with the Revised Thermal Design Procedure (RTDP) which is discussed in Reference 13.

2. Moderator and Doppler Coefficients of Reactivity - The total loss of load is analyzed with a conservatively small (absolute value) Doppler power coefficient. The moderator temperature coefficient assumed is 0 pcm/°F, which bounds part power conditions with a positive moderator temperature coefficient of 0 pcm/°F.
3. Reactor Control - from the standpoint of the maximum pressures attained it is conservative to assume that the reactor is in manual control.
4. Steam Release - no credit is taken for the operation of the steam dump system or steam generator power operated relief valves. The steam generator pressure rises to the safety valve setpoint where steam release through the safety valves limits secondary steam pressure.
5. Pressurizer Spray, Power Operated Relief Valves, and Safety Valves – Full credit is taken for the effect of pressurizer spray, power operated relief valves and safety valves in reducing or limiting the pressure for the DNB case. This case is analyzed to demonstrate that the DNBR limit is met and, for this case, minimizing RCS pressure is conservative. Thus, a -3% allowance for safety valve setpoint tolerance is modeled.

When calculating the peak RCS pressure, no credit is taken for the effect of pressurizer spray and power operated relief valves in reducing or limiting the coolant pressure. The pressurizer safety valves are modeled including the effects of pressurizer safety valve loop seals using the methodology described in Reference 22, and a +3% allowance for safety valve tolerance is also employed, which maximizes the RCS pressure.

6. Feedwater Flow - Main feedwater flow to the steam generators is assumed to be lost at the time of turbine trip. No credit is taken for auxiliary feedwater flow.

Eventually, however, auxiliary feedwater flow would be initiated and a stabilized plant condition would be reached.

7. Reactor Trip – Only the overtemperature  $\Delta T$ , high pressurizer pressure, and low-low steam generator water level reactor trips are assumed operable for the purposes of this analysis. No credit is taken for a reactor trip on high pressurizer level, or for the direct reactor trip on turbine trip.

### Results

The transient responses for a turbine trip from full power operation are presented for two cases: one case with pressurizer pressure control and one case without pressure control.

In the case with pressurizer pressure control, pressurizer sprays and pressurizer PORVs are modeled. This case is analyzed to demonstrate that the DNBR limit is met and, for this case, minimizing RCS pressure is conservative. The transient responses for this case are shown in Figures 14.1-23 through 14.1-26. No credit is taken for the steam dump system. The reactor is tripped by the Overtemperature  $\Delta T$  trip signal. The minimum departure from nucleate boiling ratio (DNBR) remains well above the applicable limit value. Pressurizer relief valves prevent overpressurization of the primary system. Pressurizer safety valves do not actuate for this case. The steam generator safety valves actuate to maintain the secondary system pressure below 110 percent of the design value.

The total loss of steam load accident is also analyzed assuming BVPS-1 to be initially operating at 100.6 percent of full power with no credit taken for the pressurizer spray, pressurizer PORVs or steam dump. In this case, the reactor is tripped on the high pressurizer pressure signal. The transient responses for this case are shown in Figures 14.1-27 through 14.1-30. The nuclear power and core heat flux remain essentially constant until the reactor is tripped. In this case, the pressurizer safety valves are actuated and maintain the primary system pressures below 110 percent of the design value. The steam generator safety valves also actuate to maintain the secondary system pressure below 110 percent of the design value.

Section 14.1.8 presents additional results of analysis for a complete loss of heat sink including loss of main feedwater. This report shows the overpressure protection that is afforded by the pressurizer and steam generator safety valves.

#### 14.1.7.3 Conclusions

Results of the analyses, including those in Section 14.1.8, show that the plant design is such that a total loss of external electrical load without a direct or immediate reactor trip presents no hazard to the integrity of the Reactor Coolant System or the main steam system. Pressure relieving devices incorporated in the two systems are adequate to limit the maximum pressures to less than 110% of the design limits.

The integrity of the core is maintained by operation of the Reactor Protection System, i.e., the DNBR will be maintained within the DNBR acceptance criteria. Thus there will be no cladding damage and no release of fission products to the Reactor Coolant System.

### 14.1.8 Loss of Normal Feedwater

#### 14.1.8.1 Identification of Causes and Accident Description

A loss of normal feedwater (from pump failures, valve malfunctions, or loss of offsite AC power) results in a reduction in capability of the secondary system to remove the heat generated in the reactor core. If the reactor were not tripped during this accident, core damage would possibly occur from a sudden loss of heat sink. If an alternate supply of feedwater were not supplied to the plant, residual heat following reactor trip would heat the primary system water to the point where water relief from the pressurizer occurs. Significant loss of water from the Reactor Coolant System could conceivably lead to core damage. Since the plant is tripped well before the steam generator heat transfer capability is reduced, the primary system variables never approach a DNB condition.

The following provide the necessary protection against a loss of normal feedwater:

1. Reactor trip on low-low water level in any steam generator
2. Turbine trip-Reactor trip on loss of feedwater in any two-out-of-three feedwater loops via the Anticipated Transient Without Scram (ATWS) Mitigating System Actuation Circuitry (AMSAC).
3. Two motor driven auxiliary feedwater pumps which are started on:
  - a. Either no bus loss of power, or diesel generator loading sequence signal coincident with any of the following:
    - (1) Low-low level in two out of three steam generators
    - (2) Both main feed pumps stopped and either control switch for main feed pump FW-P-1A in close and after close position or control switch for main feed pump FW-P-1B in close and after close position
    - (3) Safety injection signal
  - b. Manual Actuation
  - c. Loss of feedwater in any two-out-of-three feedwater loops via the Anticipated Transient Without Scram (ATWS) Mitigating System Actuation Circuitry (AMSAC).

4. One turbine driven auxiliary feedwater pump which is started on:
  - a. Low-low level in any steam generator
  - b. Undervoltage on any two reactor coolant pump buses.
  - c. Manual actuation.
  - d. Loss of feedwater in any two-out-of-three feedwater loops via the Anticipated Transient Without Scram (ATWS) Mitigating System Actuation Circuitry (AMSAC).
  - e. Safety injection signal.

The motor driven auxiliary feedwater pumps are supplied by the diesels if a loss of offsite power occurs and the turbine-driven pump utilizes steam from the secondary system. Both type pumps are designed to start within one minute even if a loss of all AC power occurs simultaneously with loss of normal feedwater. The turbine exhausts the secondary steam to the atmosphere. The auxiliary pumps take suction from the primary demineralized water storage tank for delivery to the steam generators.

The analysis shows that following a loss of normal feedwater, the auxiliary feedwater system is capable of removing the stored and residual heat thus preventing either overpressurization of the Reactor Coolant System or loss of water from the reactor core.

#### 14.1.8.2 Analysis of Effects and Consequences

##### Method of Analysis

A detailed analysis using the LOFTRAN<sup>(3)</sup> code is performed in order to obtain the plant transient following a loss of normal feedwater. The simulation describes the plant thermal kinetics, Reactor Coolant System (RCS) including natural circulation, pressurizer, steam generators and feedwater system. The digital program computes pertinent variables including the steam generator level, pressurizer water level, and reactor coolant average temperature.

Major assumptions are:

1. The plant is initially operating at 100.6% of the NSSS power (100.6% of 2910 MWt). After a reactor trip, a maximum reactor coolant pump heat of 15 MWt is included in the analysis. The RCPs are assumed to continuously operate throughout the transient providing a constant reactor coolant volumetric flow equal to the Thermal Design Flow (TDF) value. Although not assumed in the analysis, the reactor coolant pumps could be manually tripped at some later time in the transient to reduce the heat addition to the RCS caused by the operation of the pumps.
2. The direction of conservatism for both initial reactor vessel average coolant temperature and pressurizer pressure is not consistent from analysis to analysis. As such, cases are considered with the initial temperature and pressure uncertainties applied in each direction. The initial average temperature and pressure uncertainty is assumed to be +8.5°F and -9.5°F, which includes 3.5°F for loop-to-loop average temperature variation. The initial pressurizer pressure

uncertainty is conservatively assumed to be  $\pm 40$  psi. The worst loss of normal feedwater case is with the temperature uncertainties added to the nominal value and the pressure uncertainty subtracted from the nominal value (i.e., 588.5°F and 2210 psia).

3. Reactor trip occurs on steam generator low-low water level at 5% of the narrow range span.
4. It is assumed that two motor driven AFW pumps are available to supply a minimum of 489 gpm, split equally to all three steam generators, 60 seconds following a low-low steam generator water level signal. (The worst single failure, which is modeled in the analysis, is the loss of the turbine driven AFW pump.) The AFW line purge volume is conservatively assumed to be 168 ft<sup>3</sup>, and the initial AFW enthalpy is assumed to be 90.77 BTU/lbm.
5. The pressurizer sprays and PORVs are assumed operable, maximizing the pressurizer water volume. If these control systems did not operate, the pressurizer safety valves would prevent the RCS pressure from exceeding the RCS design pressure limit during this transient. The pressurizer heaters are modeled to exacerbate the heat-up and volumetric expansion of the water in the pressurizer.
6. Secondary system steam relief is achieved through the self-actuated main steam safety valves. Note that steam relief will, in fact, be through the steam generator atmospheric relief valves or condenser dump valves for most cases of loss of normal feedwater. Since these valves and controls are not safety grade, however, they have been assumed unavailable.
7. The main steam safety valves are modeled assuming a 3% tolerance and an accumulation model that assumes the valves are wide open once the pressure exceeds the setpoint (plus tolerance) by 5 psi.
8. Core residual heat generation is based on the 1979 version of ANS 5.1 (Reference 11). ANSI/ANS-5.1-1979 is a conservative representation of the decay energy release rates. Long term operation at the initial power level preceding the trip is assumed.
9. Steam generator tube plugging levels of both 0% and 22% are analyzed. The worst loss of normal feedwater case resulted from the case that assumed 0% steam generator tube plugging.

The loss of normal feedwater analysis is performed to demonstrate the adequacy of the Reactor Protection System (RPS) and engineered safeguards systems (for example, the Auxiliary Feedwater System [AFWS]) in removing long term decay heat and preventing excessive heatup of the RCS with possible resultant RCS overpressurization or loss of RCS water. As such, the assumptions used in this analysis are designed to minimize the energy removal capability of the system and to maximize the possibility of water relief from the coolant system by maximizing the coolant system expansion, as noted in the assumptions listed previously.

For the loss of normal feedwater transient, the reactor coolant volumetric flow remains at its normal value, and the reactor trips via the low-low steam generator level trip. The reactor coolant pumps may be manually tripped at some later time to reduce heat addition to the RCS.

Normal reactor control systems are not required to function. The RPS is required to function following a loss of normal feedwater as analyzed here. The AFWS is required to deliver a minimum auxiliary feedwater flow rate. No single active failure will prevent operation of any system required to function.

### Results

Figures 14.1-31 through 14.1-31D show plant parameters following a loss of normal feedwater.

Following the reactor and turbine trip from full load, the water level in the steam generators will fall due to the reduction of steam generator void fraction and because steam flow through the safety valves continues to dissipate the stored and generated heat. One minute following the initiation of the low-low level trip, the auxiliary feedwater pump is automatically started, reducing the rate of water level decrease.

The capacity of the auxiliary feedwater pump is such that the water level in the steam generators being fed does not recede below the lowest level at which sufficient heat transfer area is available to dissipate core residual heat without water relief from the Reactor Coolant System relief or safety valves.

The calculated sequence of events for this accident is listed in Table 14.1-2. As shown in Figures 14.1-31 through 14.1-31D, the plant approaches a stabilized condition following reactor trip and auxiliary feedwater initiation. Plant procedures may be followed to further cool down the plant.

### 14.1.8.3 Conclusions

Results of the analysis show that a loss of normal feedwater does not adversely affect the core, the Reactor Coolant System, or the steam system since the auxiliary feedwater capacity is such that the reactor coolant water is not relieved from the pressurizer relief or safety valves.

### 14.1.9 Excessive Heat Removal Due to Feedwater System Malfunctions

#### 14.1.9.1 Identification of Causes and Accident Description

Reductions in feedwater temperature or additions of excessive feedwater are means of increasing core power above full power. Such transients are attenuated by the thermal capacity of the secondary plant and of the Reactor Coolant System. The overpower - overtemperature protection (neutron power, overtemperature and overpower  $\Delta T$  trips) prevents any power increase which could result in the violation of the DNBR safety analysis acceptance criteria.

One example of excess heat removal from the primary system is the transient associated with the accidental opening of the feedwater bypass valve which diverts flow around the low pressure feedwater heaters. In the event of an accidental opening of the bypass valve, there is a sudden reduction in feedwater inlet temperature to the steam generators. The increased subcooling will create a greater load demand on the Reactor Coolant System.

Another example of excessive feedwater flow would be a full opening of a feedwater control valve due to a feedwater control system malfunction or an operator error. At power this excess flow causes a greater load demand on the Reactor Coolant System due to increased subcooling in the steam generator. With the plant at no-load conditions the addition of cold feedwater may cause a decrease in Reactor Coolant System temperature and thus a reactivity insertion due to the effects of the negative moderator coefficient of reactivity. Continuous addition of excessive feedwater is prevented by the steam generator high-high water level trip.

#### 14.1.9.2 Analysis of Effects and Consequences

##### Method of Analysis

The excessive heat removal due to a feedwater system malfunction transient is analyzed using the detailed digital computer code LOFTRAN<sup>(3)</sup>. This code simulates neutron kinetics, thermal-hydraulic conditions, a pressurizer, steam generators, reactor coolant pumps, and control and protection systems. LOFTRAN computes pertinent plant variables including temperatures, pressures, and power level.

The system is analyzed to evaluate plant behavior in the event of a feedwater system malfunction. Feedwater temperature reduction due to the opening of a feedwater heater bypass valve resulting in feedwater flow bypassing a portion of the feedwater heaters is considered.

Excessive feedwater addition due to a control system malfunction or operator error that allows one feedwater control valve to open fully is considered. The following cases are considered:

- A. Accidental full opening of one feedwater control valve at zero power with the reactor critical and in manual rod control.
- B. Accidental full opening of one feedwater control valve at full power. The full power cases are analyzed with the reactor in both manual and automatic rod control.
- C. Accidental opening of the feedwater bypass valve at full power resulting in a sudden reduction in feedwater temperature. This case is analyzed in manual and automatic rod control.

The feedwater malfunction event was analyzed with the following assumptions:

1. For the feedwater malfunction event that results in an increase in feedwater flow to one steam generator at zero power conditions, a step increase in flow to one steam generator from zero to 187 percent of the nominal full load value for one steam generator is assumed.
2. For the cases analyzed at zero power conditions, a conservatively low feedwater temperature of 32°F is assumed.
3. For the feedwater malfunction event that results in an increase in feedwater flow to one steam generator at full power conditions, a step increase in flow to one steam generator from the nominal full power flow rate to 136.8 percent of the nominal full load value for one steam generator is assumed.
4. In all cases analyzed, no credit is taken for the heat capacity of the Reactor Coolant System thick metal and steam generator thick metal in attenuating the resulting plant cooldown.
5. In all feedwater flow increase cases analyzed, the resulting feedwater flow is terminated by the steam generator high-high water level signal which closes all feedwater control valves and trips the main feedwater pumps and the turbine.
6. For the feedwater malfunction cases that result in a sudden decrease in feedwater temperature, it is assumed that the final feedwater temperature will be 300°F.
7. For the feedwater temperature decrease cases analyzed, the resulting feedwater flow is terminated by the low pressurizer pressure SI signal, which closes the feedwater control valves and trips the main feedwater pumps. Reactor Trip, (and a subsequent Turbine Trip) are provided by the Overpower  $\Delta T$  (OP $\Delta T$ ) Trip function.



## Results

Opening of a low pressure heater bypass valve causes a reduction in feedwater temperature which increases the thermal load on the primary system. This increased thermal load would result in a transient very similar to the feedwater flow increase case discussed in detail in this section. The primary difference between the two events is that the reactor trip for the feedwater temperature reduction case comes from the OP $\Delta$ T Trip function rather than the High-High Steam Generator Water Level Trip function. A feedwater temperature reduction of 155°F (455°F to 300°F) was explicitly analyzed, and all acceptance criteria satisfied. Due to the similarity of these two events, however, the results of this analysis are not presented.

The accidental full opening of one feedwater control valve at zero power conditions with manual rod control, is less limiting than the accidental full opening of one feedwater control valve at hot full power. Therefore, the results of these cases are not presented. It should be noted that if the incident occurs with the unit just critical at no load, the reactor may be tripped by the power range high neutron flux trip (low setting) set at approximately 25 percent.

The limiting full power case is the accidental full opening of one feedwater control valve with the reactor in automatic rod control. The continuous addition of cold feedwater is prevented by closure of all feedwater control valves, a trip of the feedwater pumps, and closure of the feedwater isolation valves on steam generator high level. A turbine trip and reactor trip are actuated when the steam generator reaches the high-high water level setpoint.

Transient results, shown on Figures 14.1-32A and 14.1-32B, show the core heat flux, pressurizer pressure,  $T_{avg}$ , DNBR, as well as the increase in nuclear power and loop  $\Delta T$  associated with the increased thermal load on the reactor. The DNBR decreases due to the increased power, but the DNBR does not drop below the safety analysis limit value.

## Conclusions

Results show that the consequences of excess load increases due to opening the low pressure heater bypass valve do not violate any Condition II acceptance criterion. DNB ratios encountered for excessive feedwater addition at power, or at no load, satisfy the DNBR safety analysis acceptance criterion.

### 14.1.10 Excessive Load Increase Incident

#### 14.1.10.1 Identification of Causes and Accident Description

An excessive load increase incident is defined as a rapid increase in the steam flow that causes a power mismatch between the reactor core power and the steam generator load demand. The RCS is designed to accommodate a 10 percent step load increase or a 5 percent per minute ramp load increase in the range of 15 to 100 percent full power. Any loading rate in excess of these values may cause a reactor trip actuated by the reactor protection system.

This accident could result from either an administrative violation such as excessive loading by the operator or an equipment malfunction in the steam dump control or turbine speed control.

During power operation, steam dump to the condenser is controlled by reactor coolant conditions signals; i.e., high reactor coolant temperature indicates a need for steam dump. A single controller malfunction does not cause steam dump; an interlock is provided which blocks the opening of the valves unless a large turbine load decrease or a turbine trip has occurred.

Protection against an excessive load increase accident is provided by the following reactor protection system signals:

1. Overpower  $\Delta T$
2. Overtemperature  $\Delta T$
3. Power range high neutron flux.
4. Low Pressurizer Pressure

#### 14.1.10.2 Analysis of Effects and Consequences

##### Method of Analysis

At beginning of life the core has the least negative moderator temperature coefficient of reactivity and therefore the least inherent transient capability. At end of life the moderator temperature coefficient of reactivity has its highest absolute value. This results in the largest amount of reactivity feedback due to changes in coolant temperature.

A conservative limit on the turbine valve opening is assumed and all cases are studied without credit being taken for pressurizer heaters. The revised thermal design procedure (RTDP)<sup>(13)</sup> is used. Therefore, uncertainties in initial conditions are included in the DNBR limit, and initial operating conditions are assumed to be at nominal values, consistent with steady state full power operation.

Given the non-limiting nature of this event with respect to the DNBR safety analysis criterion, an explicit analysis was not performed as part of the 9.4% plant power uprating. Instead, an evaluation of this event was performed. The evaluation model consists of the generation of statepoints based on generic conservative data. These statepoints are then compared to the core thermal limits to ensure that the DNBR limit is not violated. A total of three cases are included in this evaluation. These are:

- Reactor in manual rod control with BOL (minimum moderator) reactivity feedback;
- Reactor in manual rod control with EOL (maximum moderator) reactivity feedback;
- Reactor in automatic rod control

### 14.1.10.3 Conclusions

It has been demonstrated that for an excessive load increase the DNBR safety analysis acceptance criteria are met.

### 14.1.11 Loss of Offsite Power to the Station Auxiliaries

#### 14.1.11.1 Identification of Causes and Accident Description

In the event of a complete loss of offsite power and a turbine trip there will be a loss of power to the plant auxiliaries, i.e., the reactor coolant pumps, condensate pumps, etc.

The loss of power may be caused by a complete loss of the offsite grid accompanied by a turbine generator trip at BVPS-1.

This transient is more severe than the turbine trip event analyzed in Section 14.1.7 because for this case the decrease in heat removal by the secondary system is accompanied by a flow coastdown which further reduces the capacity of the primary coolant to remove heat from the core.

The events following a loss of a-c power with turbine and reactor trip are described in the sequence listed below:

1. Plant vital instruments are supplied by emergency power sources.
2. As the steam system pressure rises following the trip, the steam system power operated relief valves are automatically opened to the atmosphere. Steam dump to the condenser is assumed not to be available. If the steam flow rate through the power relief valves is not available, the steam generator self-actuated safety valves may lift to dissipate the sensible heat of the fuel and coolant plus the residual heat produced in the reactor. Refer to Section 10.3.1 for steam discharge capability following a design basis tornado generated missile impact.
3. As the no load temperature is approached, the steam system power relief valves (or the self-actuated safety valves, if the power relief valves are not available) are used to dissipate the residual heat and to maintain the plant at the hot shutdown condition.
4. The emergency diesel generators started on loss of voltage on the plant emergency buses begin to supply plant vital loads.

The auxiliary feedwater system is started automatically as discussed in the loss of normal feedwater analysis. The steam driven auxiliary feedwater pump utilizes steam from the secondary system and exhausts to the atmosphere. The motor driven auxiliary feedwater pumps are supplied by power from the diesel generators. The pumps take suction directly from the primary plant demineralized water storage tank for delivery to the steam generators.

Upon the loss of power to the reactor coolant pumps, coolant flow necessary for core cooling and the removal of residual heat is maintained by natural circulation in the reactor coolant loops.

A loss of offsite power to the station auxiliaries is a more limiting event than the turbine trip initiated decrease in secondary heat removal without loss of AC power, which was analyzed in Section 14.1.7. However, a loss of AC power to the BVPS-1 auxiliaries as postulated previously results in a loss of normal feedwater since the condensate pumps lose their power supply.

Following the reactor coolant pump coastdown caused by the loss of AC power, the natural circulation capability of the Reactor Coolant System will remove residual and decay heat from the core, aided by auxiliary feedwater in the secondary system. An analysis is presented here to show that the natural circulation flow in the Reactor Coolant System following a loss of AC power event is sufficient to remove residual heat from the core.

#### 14.1.11.2 Analysis of Effects and Consequences

##### Method of Analysis

A detailed analysis using the LOFTRAN<sup>(3)</sup> code is done to obtain the natural circulation flow following a station blackout. The simulation describes the plant thermal kinetics, Reactor Coolant System including natural circulation, pressurizer, steam generators and Feedwater System. The digital program computes pertinent variables including the steam generator level, pressurizer water level, and reactor coolant average temperature.

The assumptions used in the analysis are identical to those for the loss of normal feedwater event (Section 14.1.8), except for the assumptions that power to the reactor coolant pumps is lost at the time of reactor trip, and the worst case loss-of-offsite-power-to-the-station-auxiliaries exists, i.e., when the uncertainties are subtracted from the nominal values of temperature and pressure, (viz., 570°F and 2210 psia, respectively). A heat transfer coefficient in the steam generator associated with Reactor Coolant System natural circulation following reactor coolant pump coastdown is assumed.

##### Radiological Dose Consequences

An analysis of the radiation doses in the common control room from a loss of AC power to station auxiliaries was performed. Table 14.1-3 tabulates significant analysis parameters. Tables 14.1-1A and 14.1-1B tabulates analysis results.

The transport models associated with the Locked Rotor Accident (LRA) and the Loss of AC Powered Auxiliaries (LACP) are similar with the exception that the LRA results in fuel damage and associated release of gap activity, whereas the LACP has no fuel damage, and the maximum release is associated with Technical Specification concentrations. The parameter values presented in Table 14.1-3 are those applicable to the LACP with the exception of the failed fuel percentage. No separate dose assessment is performed for the LACP. The dose consequences are estimated as less than that calculated for the LRA. The dose acceptance criteria utilized for the site boundary was the most limiting set forth in RG 1.183 of 2.5 rem TEDE and is the same as the LRA. The dose acceptance criteria utilized for the control room is 5 rem TEDE per 10CFR50.67. Since the RCS Technical Specification activity is significantly smaller than the gap activity associated with failed fuel, it is concluded that the dose consequences of the LRA bound that of the LACP. See Section 14.2.7 for a discussion of the environmental releases and dose consequences following a LRA.

## Results

The transient response of the Reactor Coolant System following a loss of AC power is shown in Figures 14.1-31E through 14.1-31I. The calculated sequence of events for this event is listed in Table 14.1-2.

The first few seconds of the transient will closely resemble a simulation of the complete loss of flow incident (Section 14.2.9), i.e., core damage due to rapidly increasing core temperatures is prevented by promptly tripping the reactor. After the reactor trip, stored and residual heat must be removed to prevent damage to either the Reactor Coolant System or the core.

## Conclusions

Results of the "Complete Loss of Forced Reactor Coolant Flow" analysis (Section 14.2.9) and the "Loss of Normal Feedwater" analysis (Section 14.1.8) show that for a loss of all a-c power no adverse conditions occur in the reactor core. The DNBR safety analysis acceptance criteria are met. The Reactor Coolant System is not overpressurized and no water relief will occur through the pressurizer relief or safety valves. Thus, there will be no cladding damage and no release of fission products to the Reactor Coolant System.

### 14.1.12 Turbine Missiles

Postulated turbine missiles have been evaluated by considering the probabilities of missile generation and of impact to safety-related items.

The probability (P4) of damage to plant structures, systems, and components important to safety is:

$$P4 = P1 \times P2 \times P3$$

where:

P1 = the probability of generation and ejection of a high energy missile,

P2 = the probability that a missile strikes a critical plant region, given its generation and ejection, and

P3 = the probability that the missile strike damages its target in a manner leading to unacceptable consequences. Unacceptable consequences are defined here as the loss of the capacity to maintain the integrity of the reactor coolant pressure boundary, to shut down the plant, maintain it in a safe shutdown condition, and/or limit offsite radiation exposures.

#### 14.1.12.1 Probability of Missile Generation and Ejection (P1)

A turbine missile can be caused by brittle fracture of a rotating turbine part at or near turbine operating speed, or by ductile fracture upon runaway after extensive, highly improbable, control system failures.

The probabilities of such failures are, however, significantly reduced by the effects of inservice testing and inspection frequencies. Reduced probability of missile generation and ejection is the approach used by BVPS-1 for ensuring that the probability of unacceptable damage to essential structures, systems, and components is sufficiently low.

The turbine manufacturer has performed an analysis of turbine reliability, which considers known and likely failure mechanisms and expresses such failure probability in terms of the intervals between inservice inspection and test. Consequently, the rated-speed missile generation probability is related to disk design parameters, material properties, and the inservice volumetric (ultrasonic) disk inspection interval. Further, the overspeed missile generation probability is related to the turbine governor and overspeed protection system's sensing and tripping characteristics, the design and arrangement of main steam control and stop valves and the reheat steam intercept and stop valves, and the inservice testing and inspection intervals for system components and valves. Inspection and test methods, which meet the necessary safety objectives, are provided in Section 10.3.

Probability of Missile Generation and Ejection (P1) is the sum of the following terms:

$$P1 = P(R) + P(O)$$

where:

P(R) = probability of external turbine missile generation at rated speed and speeds up to 120% of rated speed

P(O) = probability of external turbine missile generation at design overspeed

Values for P(R) and P(O) are provided by the turbine and NSSS vendors and are specific for each turbine rotor and associated discs. Different values are provided as a function of Low Pressure turbine rotor operating hours. Note that each value used for P(R) and P(O) is the sum of the probabilities for each Low Pressure turbine rotor currently in use at BVPS-1. This value is provided as a function of turbine valve testing interval. The P1 values are for the total unit considering all rotors and both design and overspeed conditions.

#### 14.1.12.2 Probability of Missile Strike (P2)

In the event of missile ejection, the probability of a strike on a plant region (P2) is a function of the energy and direction of an ejected missile and of the orientation of the turbine with respect to the plant region. A favorably oriented turbine is one in which there are no safety-related systems, structures or components located in the missile strike zone. Conversely, an unfavorably oriented turbine is one in which the plant regions located in the missile strike zone contain safety-related structures, systems and components. Because the Unit 1 Containment, Auxiliary Building, and Safety Equipment Building are located in the missile strike zone, BVPS Unit 1 is an unfavorably oriented turbine.

#### 14.1.12.3 Probability of Damage (P3)

The probability of damage (P3) is a function of the energy of the missile, its angle of impact upon the affected structure, and the ability of that structure to prevent unacceptable damage to the essential systems it protects.

#### 14.1.12.4 Probability Evaluation (P4)

The probability of unacceptable damage to safety-related structures, systems and components by turbine disc fragments must be less than or equal to the plant safety objective of  $10^{-7}$  per year. This is accomplished by a sufficiently frequent turbine testing and inspection schedule, which ensures that the probability of turbine missile generation (P1) is maintained at  $10^{-5}$  per year or less. A calculation was performed which determined values for P(1) as a function of turbine operating time between inspections using the vendor supplied values for P(R) and P(O). The results of the calculation determined the maximum allowable interval between turbine inspections to maintain P1 less than or equal to  $10^{-5}$ . Turbine inspections, as described in Section 10.3.3.5, will be performed prior to exceeding the maximum allowable interval.

The combined probability of strike and damage (P2 x P3) is assumed to be  $10^{-2}$  per year or less. This conservatively considers the unfavorable orientation of the turbine generator. The use of the value  $10^{-2}$  for the combined probability (P2 x P3) is in accordance with NRC guidance on this topic.

#### 14.1.12.5 Turbine Overspeed Protection

The turbine speed control system has adequate redundancy to ensure that the turbine does not attain destructive overspeed. The standard control system includes three separate speed sensors mounted on the turbine stub shaft located in the turbine front pedestal as follows:

1. Mechanical overspeed trip weight (spring loaded bolt)
2. Electro-magnetic pickup for main speed governing channel
3. Electro-magnetic pickup for overspeed protective controller. This pickup uses the same toothed wheel as Item 2 above.

An overspeed protection controller is provided and is activated in the event turbine speed exceeds 103 percent of rated speed (1,800 rpm).

During a full load drop, both the governor and the interceptor valves close. The governor valves remain closed until the speed is decreased to rated speed (1,800 rpm). The interceptor valves are modulated and reopened when speed decreases to below 103 percent of rated speed to remove entrapped steam in the reheat system. If speed again increases above 103 percent, they reclose and continue to modulate until speed remains below 103 percent of 1,800 rpm.

Should the turbine exceed approximately 111 percent of rated speed, all the steam admission valves will be tripped closed by both the mechanical overspeed weight and the backup electrical trip. Thus, the turbine is tripped by redundant trip systems from independent speed sensors to assure utmost safety.

#### 14.1.13 Accidental Depressurization of the Main Steam System

The results of an accidental depressurization of the main steam system are always bounded by the results of a major secondary steam line break, as presented in Section 14.2. The Condition III/IV major secondary steam line break is analyzed to Condition II acceptance criteria to bound the Condition II accidental depressurization of the main steam system event.

#### 14.1.14 External Environmental Events

##### 14.1.14.1 Identification of Causes

The natural occurrences considered to have an abnormal effect on the unit are tornado, severe earthquake, or flooding.

The probability of occurrence and a description of the events are given in Sections 2.2.2.5 for tornado, Section 2.5 and 2.6 for earthquake, and Section 2.3 for flooding.

##### 14.1.14.2 Analysis of Effects and Consequences

Safety-related (Q.A. Category I) equipment or structures designated in Table B.1-1 of Appendix B will be designed to withstand the natural occurrences described above without impairment of their function or loss of safety.

For tornado protection, safety-related equipment will be housed in and protected by structures that will be designed to withstand the effects of tornado forces. The tornado criteria are given in Section 2.7 and the design of structures to withstand tornadoes is discussed in the same section.

All safety-related equipment, along with the structures that support that equipment, will be designed to withstand the DBE. Appendix B describes the seismic analysis and design of Seismic Category I equipment and piping. The seismic analysis of Seismic Category I structures and the design of such structures is also discussed in Appendix B.



The Probable Maximum Flood Level for the BVPS-1 is El. 730 ft above mean sea level, and the plant is able to achieve safe shutdown at this condition. Following is a brief discussion of specific safety-related areas:

1. The intake structure is a floodproof and Seismic Category I structure. No detrimental effect will be experienced by the enclosed equipment during the Probable Maximum Flood.
2. The river water valve pit is floodproof to Elev. 721 ft. Above 721 ft the valve pit will flood; however, equipment in it is not required to be functional beyond the Standard Project Flood elevation of 705 ft.
3. The containment area is located at a Grade El. 735. Where the containment extends below grade, there is a waterproof membrane installed below contiguous structures and below approximately El. 730 in other areas.
4. The primary auxiliary building basement floor is at El. 722 ft-6 inches. The charging pumps at El. 722 ft-6 inches are enclosed in watertight cubicles.
5. All safety-related equipment in the main steam, cable vault, safeguard structures, and fuel building are located above El. 730 ft. Those portions of the structure below El. 730 ft with the exception of the fuel pool are allowed to flood.
6. The turbine building basement level is El. 693 ft. The building is designed to flood when the flood exceeds El. 707 ft-6 inches. The floor mat is constructed so that it will not float and cause damage to any systems for flooding up to that level.
7. The cooling tower pump house is flood protected to El. 705 ft; however, for water levels above El. 705 ft, the pump house will flood but plant safety will not be affected.
8. The service building is located at El. 713 ft-6 inches and is protected from flooding up to El. 730 ft.

#### 14.1.15 Accidental Depressurization of the Reactor Coolant System

##### 14.1.15.1 Identification of Causes and Accident Description

The most severe core conditions resulting from an accidental depressurization of the Reactor Coolant System are associated with an inadvertent opening of a pressurizer relief valve. To conservatively bound this scenario, the Westinghouse methodology models the failure of a pressurizer safety valve since a safety valve is sized to relieve approximately twice the steam flowrate of a relief valve and will allow a much more rapid depressurization upon opening. This yields the most-severe core conditions resulting from an accidental depressurization of the RCS. Initially the event results in a rapidly decreasing Reactor Coolant System pressure which could reach hot leg saturation conditions without reactor protection system intervention. At that time, the pressure decrease is slowed considerably. The pressure continues to decrease, however, throughout the transient. The effect of the pressure decrease would be to increase power via the moderator density feedback but the reactor control system (if in the automatic mode) functions to maintain the power essentially constant throughout the initial stage of the transient. The average coolant temperature decreases slowly, but the pressurizer level increases until reactor trip.

The reactor will be tripped by the following reactor protection system signals:

1. Low Pressurizer Pressure
2. Overtemperature  $\Delta T$

#### 14.1.15.2 Analysis of Effects and Consequences

##### Methods of Analysis

The accidental depressurization transient is analyzed by employing the detailed digital computer code LOFTRAN. The code simulates the neutron kinetics, Reactor Coolant System, Pressurizer, pressurizer relief and safety valves, pressurizer spray, steam generator, and steam generator safety valves. The code computes pertinent plant variables including temperatures, pressures, and power level. In calculating the DNBR the following conservative assumptions are made:

1. Initial conditions of nominal core power, pressure, and reactor coolant temperatures at full power are assumed consistent with the Revised Thermal Design Procedure (Reference 13). This results in the minimum initial margin to DNB (See Appendix 14D).
2. A negative MDC (corresponding to a positive MTC) is assumed. This provides a conservatively high amount of positive reactivity due to changes in the moderator density. The spatial effect of void due to local or subcooled boiling is not considered in the analysis with respect to reactivity feedback or core power shape.
3. A least negative Doppler only power coefficient of reactivity is assumed in order to limit the amount of negative feedback as power increases due to moderator density feedback.

It should also be noted that in the analysis power peaking factors are kept constant at the design values while, in fact, the core feedback effects would result in considerable flattening of the power distribution. This would significantly increase the calculated DNBR; however, no credit is taken for this effect.

##### Results

The system response to an inadvertent opening of a pressurizer relief valve is shown in Figures 14.1-44, 14.1-45 and 14.1-46. Figure 14.1-44 illustrates the nuclear power transient following the depressurization. Nuclear power is maintained at the initial value until reactor trip occurs on low pressurizer pressure. The pressure decay transient following the accident is given in Figure 14.1-45. Pressure drops more rapidly after core heat generation is reduced via the trip, and then slows once saturation temperature is reached in the hot leg. The DNBR remains above the limit value throughout the transient.

Following reactor trip, RCS pressure will continue to fall until flow through the inadvertently opened valve is terminated. Automatic actuation of the safety injection system may occur if the pressure falls to the low pressurizer pressure safety injection setpoint. The RCS pressure will stabilize following operator action to terminate flow to the inadvertently opened valve; normal operating procedures may then be followed. The operating procedures would call for operator action to control RCS boron concentration and pressurization level using the chemical and volume control system (CVCS) and to maintain steam generator level through control of the main or auxiliary feedwater system. Any action required of the operator to stabilize BVPS-1 will be in a time frame in excess of ten minutes following reactor trip. The calculated sequence of events for the inadvertent opening of a pressurizer relief valve incident is shown in Table 14.1-2.

#### 14.1.15.3 Conclusions

The pressurizer low pressure and the overtemperature  $\Delta T$  reactor protection system signals provide adequate protection against this accident, and the DNBR safety analysis acceptance criteria are met. Thus, no cladding damage or release of fission products to the Reactor Coolant System is predicted for this event.

#### 14.1.16 Spurious Operation of the Safety Injection System at Power

##### 14.1.16.1 Identification of Causes

Spurious Safety Injection System (SIS) operation at power could be caused by operator error or a false electrical actuating signal. A spurious signal in any of the following channels could cause this incident.

1. High containment pressure
2. Low pressurizer pressure
3. Low steam line pressure.

Following the actuation signal, the suction of the coolant charging pumps is diverted from the volume control tank to the refueling water storage tank. The boron injection tank outlet valves then automatically open. Refueling water then flows from the charging pumps, through the boron injection tank, to the cold leg injection lines. The low head safety injection pumps also start automatically, but provide no flow when the Reactor Coolant System is at normal pressure. The passive injection system and the low head system also provide no flow at normal Reactor Coolant System pressure.

An SIS signal normally results in a reactor trip followed by a turbine trip. However, it cannot be assumed that any single fault that actuates the SIS will also produce a reactor trip. Therefore, two different courses of events are considered:

1. Case A Trip occurs at the same time spurious injection starts
2. Case B The reactor protection system produces a trip later in the transient.

For Case A the operator should determine if the spurious signal was transient or steady state in nature, i.e., an occasional occurrence or a definite fault. The operator must also determine if the safety injection system must be defeated for repair. For the former case the operator would stop the safety injection and bring the plant to the hot shutdown conditions. If the safety injection system must be disabled for repair, boration should continue and the plant brought to cold shutdown.

For Case B the reactor protection system does not produce an immediate trip and the reactor experiences a negative reactivity excursion causing a decrease in reactor power. The power unbalance causes a drop in  $T_{avg}$  and consequent coolant shrinkage.

Pressurizer pressure and level drop. Load will decrease due to the effect of reduced steam pressure on load if the electro-hydraulic governor fully opens the turbine governor valve. If automatic rod control is used, these effects will be lessened until the rods have moved out of the core. The transient is eventually terminated by the reactor protection system low pressure trip or by manual trip. The time to trip is affected by initial operating conditions including core burnup history which affects initial boron concentration, rate of change of boron concentration, Doppler and moderator coefficients.

Recovery from this incident for Case B is made in the same manner described for Case A. The only difference is the lower  $T_{avg}$  and pressure associated with the power unbalance during the transient. The time at which reactor trip occurs is of no concern for this accident. At lighter loads coolant contraction will be slower resulting in a longer time to trip. This event is classified as Condition II (i.e., an incident of moderate frequency).

It is also necessary to assess the effect of the event on the pressurizer safety valve (PSV) operability. Should the transient result in pressurizer overfill prior to the passing of an acceptable amount of time, which allows the operator to diagnose and terminate the event, water could be passed through the pressurizer safety valves. If the number of water relief events is excessive, and/or the fluid temperature during relief is too low, the potential for damage to the PSVs exists. Such damage, potentially leading to the failure of a valve to reclose, must be avoided to preclude the event from progressing to a Condition III Small Break LOCA. As such, separate cases are considered for an assessment of the PSV operability. These cases are discussed in Section 14.1.16.2.1.

Also discussed in Section 14.1.16.2.1 is the operability of the power operated relief valves (PORVs) and the PSV and PORV inlet and discharge piping for a pressurizer overfill event.

#### 14.1.16.2 Analysis of Effects and Consequences

Based on precedent, this event does not lead to a serious challenge to the DNB design basis. The decrease in core power and RCS average temperature more than offset the decrease in RCS pressure, such that the minimum calculated DNBR occurs at the start of the transient. As such, no explicit reanalysis of the event has been performed to address DNB concerns. The discussion in this section is representative of a typical DNBR analysis of the Spurious Operation of the Safety Injection System at Power event, except for Section 14.1.16.2.1, which discusses the PSV operability/pressurizer overfill case.

### Method of Analysis

The spurious operation of the SIS system is analyzed by employing the detailed digital computer program LOFTRAN<sup>(3)</sup>. The code simulates the neutron kinetics, Reactor Coolant System, pressurizer, pressurizer relief and safety valves, and the effect of the safety injection system. The program computes pertinent plant variables including temperatures, pressures, and power level.

Because of the power and temperature reduction during the transient, operating conditions do not approach the core limits. Analysis of several cases shows the results are relatively independent of time to trip.

A typical transient, representing conditions at beginning of core life, is presented. Results at end of life are similar except that moderator feedback effects result in a slower transient.

The assumptions are:

1. Initial Operating Conditions - The initial reactor power and Reactor Coolant System temperatures are assumed at their maximum values consistent with the steady state full power operation including allowances for calibration and instrument errors.
2. Moderator and Doppler Coefficients of Reactivity - A low beginning of life moderator temperature coefficient was used. A low (absolute value) Doppler power coefficient was assumed.
3. Reactor Control - The reactor was assumed to be in manual control.
4. Pressurizer Heaters - Pressurizer heaters were assumed to be nonoperable in order to increase the rate of pressure drop.
5. Boron Injection - At the start of the transient two charging pumps inject borated water into the cold legs of each loop.
6. Turbine Load - Turbine load was assumed constant until the electro-hydraulic governor drives the throttle valve wide open. Then the turbine load drops as steam pressure drops.
7. Reactor Trip - Reactor trip was initiated very conservatively by low pressure at 1775 psia.

#### 14.1.16.2.1 Pressurizer Safety Valve Operability Assessment

Since the potential for overfilling the pressurizer exists during a Spurious Operation of the Safety Injection System at Power event, water could be discharged from the pressurizer. Under certain conditions, the BVPS-1 Technical Specifications allow the pressurizer PORVS to be blocked. Should the event occur when the PORVS are blocked, water could be discharged through the pressurizer safety valves (PSVs). The PSVs are not designed to pass water, so some additional cases are considered to address PSV operability concerns.

These additional cases are similar to those discussed earlier, with the following exceptions:

1. The initial reactor coolant average temperature is assumed to be 9.5°F below its nominal value, and the initial pressurizer pressure is assumed to be 40 psi below its nominal value;
2. Reactor trip is assumed to occur from the SI signal coincident with the start of the transient. This assumption exacerbates the pressurizer water volume transient;
3. The initial pressurizer water level is assumed to be at its nominal, full power level plus 7% span to account for uncertainties;
4. The pressurizer sprays are modeled at their full capacity. Operation of the pressurizer sprays tends to fill the pressurizer faster;
5. Operation of the pressurizer heaters will tend to fill the pressurizer faster, but operation of the heaters will also result in more favorable fluid conditions at the time of filling. Thus, cases are evaluated both with and without the pressurizer heaters;
6. A large (absolute value) Doppler power coefficient is assumed.

Both cases (i.e., with and without pressurizer heaters) were analyzed. Both predicted pressurizer overflow and four PSV openings prior to ten minutes. The water relief temperature for the case without pressurizer heaters is slightly lower than the case with heaters assumed. An assessment of the resulting fluid conditions was conducted, and it was concluded that PSV operability was maintained. The fluid conditions do not challenge the integrity of the PSVs.

#### 14.1.16.2.2 PORV Operability Assessment

Control systems are not assumed to operate unless their operation could give worse results. Loss of offsite power is not assumed because this would result in loss of RCP pump heat, which would be a benefit. A single failure is not assumed in the overflow analysis since no credit is taken for protection. However, the failure of a block valve to close is a valid single failure, which is the reason for the need to qualify the PORVs and associated piping. If the block valve fails to close, the PORV is required to close and therefore these valves need to be qualified to operate for this event.

The pressurizer PORVs close automatically upon loss of power to the solenoid or instrument air. The pressurizer PORVs receive a non-Class 1E automatic closure signal to close when the high pressure signal to open the valve is re-set. The pressurizer PORVs also receive a Class 1E automatic close signal during low RCS pressure conditions initiated from the safety related pressurizer pressure instrument loops. Upstream of each PORV is a motor-operated block valve, powered by safety buses, that serves as a backup isolation valve for each PORV. The block valves are powered from a power source, i.e., 480 volts AC power, which is diverse from the 125 volt DC powered PORVs.

#### 14.1.16.2.3 Piping Analysis

The LOFTRAN computer code was used to analyze the pressurizer overflow and water flow through the PSVs and PORVs in the event of inadvertent SI actuation during power operation. Operability of the PSVs and PORVs was evaluated based on the water relief temperatures, flowrates through the PSVs and PORVs, and valve open/close cycles. It was determined that, due to fluid conditions and limited number of cycles on water relief, the PSVs and PORVs will not fail and will reseal properly such that there is no adverse affect on the RCS pressure boundary.

Input from the Spurious SI overflow analysis was used in the development of the fluid transient forcing functions; these forcing functions were used as input into a pipe stress analysis of pressurizer PSV and PORV piping.

Forcing functions were developed using RELAP5/MOD computer code and PSVs and PORVs discharging water. The pipe stress analysis of PSV and PORV inlet and discharge piping was performed using NUPIPE-SWPC computer code. The pipe stresses, pipe support loads, valve accelerations, and pressurizer nozzle, pressurizer relief tank nozzle, and safety valve nozzle and flange loads were generated. The acceptance criteria for all commodities were considered to be consistent with existing design basis limits. The calculated pipe stress associated with water solid discharge events were determined to be acceptable.

The calculated pipe support loads for the water solid events were bounded by the existing design basis loads in the piping regions upstream and downstream of the PORVs and PSVs and in the discharge piping to the pressurizer relief tank. Therefore, the pipe support loads and loads on structures transmitted by the pipe supports were concluded to be acceptable. Since the calculated loads for the water solid events were bounded by the existing design basis loads, the pressurizer PORV and PSV nozzle loads, pressurizer belly support loads, and pressurizer relief tank nozzle loads were determined to be acceptable.

#### 14.1.16.3 Results

The transient response is shown in Figures 14.1-47 and 14.1-48. Nuclear power starts decreasing immediately due to boron injection, but steam flow does not decrease until 50 seconds into the transient when the turbine throttle valve goes wide open. The mismatch between load and nuclear power causes  $T_{avg}$ , pressurizer water level, and pressurizer pressure to drop. The low pressure trip setpoint is reached at 116 seconds and rods start moving into the core at 118 seconds. The calculated sequence of events is shown in Table 14.1-2.

After trip, pressures and temperatures slowly rise since the turbine is tripped and the reactor is producing some power due to delayed neutron fission and decay heat.

#### 14.1.16.4 Conclusions

Results of the analysis show that spurious safety injection with or without immediate reactor trip presents no hazard to the integrity of the Reactor Coolant System.

DNB ratio is never less than the initial value. Thus, there will be no cladding damage and no release of fission products to the Reactor Coolant System.

If the reactor does not trip immediately, the low pressure reactor trip will be actuated. This trips the turbine and prevents excess cooldown thereby expediting recovery from the incident.



References to Section 14.1

1. Deleted by Revision 23.
2. H. G. Hargrove, "FACTRAN - A Fortran IV Code for Thermal Transients in UO<sub>2</sub> Fuel Rod," WCAP-7908-A, December 1989.
3. Burnett, T. W. T., et al., "LOFTRAN Code Description," WCAP-7907-P-A (Proprietary), WCAP-7907-A (Non-Proprietary), April 1984.
4. S. Altomare, R. F. Barry, "The TURTLE 24.0 Diffusion Depletion Code," WCAP-7758, Westinghouse Electric Corporation (September 1971).
5. F. M. Bordelon, "Calculation of Flow Coastdown After Loss of Reactor Coolant Pump (PHOENIX Code)," WCAP-7969, Westinghouse Electric Corporation (September 1972).
6. M. A. Mangan, "Overpressure Protection for Westinghouse Pressurized Water Reactors," WCAP-7769, Westinghouse Electric Corporation (October 1971).
7. J. M. Geets, R. Salvatori, "Long Term Transient Analysis Program for PWR's (BLKOUT Code)," WCAP-7898, Westinghouse Electric Corporation (June 1972).
8. Deleted by Revision 23.
9. J. Shefcheck, "Application of the THINC Program to PWR Design," WCAP-7359-L, (August 1969), Westinghouse Electric Corporation (Proprietary), and WCAP-7838, Westinghouse Electric Corporation (January 1972).
10. D. H. Risher, Jr., R. F. Barry, "TWINKLE - A Multi-Dimensional Neutron Kinetics Computer Code," WCAP-7979, Westinghouse Electric Corporation (November 1972).
11. ANSI/ANS-5.1-1979, "American National Standard for Decay Heat Power in Light Water Reactors," August 1979.
12. Deleted by Revision 20.
13. Friedland, A. J., Ray, S., "Revised Thermal Design Procedure," WCAP-11397-P-A, April 1989.
14. "Westinghouse Revised Thermal Design Procedure Instrument Uncertainty Methodology for FirstEnergy Nuclear Operating Company Beaver Valley Unit 1," WCAP-15264, Revision 3.
15. "Westinghouse Setpoint Methodology for Protection Systems Beaver Valley Power Station - Unit 1," WCAP-11419, Revision 2.

## References to Section 14.1 (Continued)

16. Hochreiter, L. E., Cheulemer, H., "Application of THINC IV Program to PWR Design," WCAP-8054-P-A, February 1989.
17. Friedland, A. J., Ray, S., "Improved THINC IV Modeling for PWR Core Design," WCAP-12330-A, September 1991.
18. Deleted by Revision 23.
19. Deleted by Revision 23.
20. Deleted by Revision 23.
21. Sung, Y. X., et. al., "VIPRE-01 Modeling and Qualification for Pressurized Water Reactor Non-LOCA Thermal-Hydraulic Safety Analysis," WCAP-14565-P-A (Proprietary), and WCAP-15306-NP-A (Non-Proprietary), October 1999.
22. Barrett, G. O., et. al., "Pressurizer Safety Valve Set Pressure Shift," WCAP-12910, Revision 0 (Proprietary), May 1993.
23. Y. S. LIU, et., al., "ANC: A Westinghouse Advanced Nodal Computer Code," WCAP-10965-P-A, Westinghouse Electric Corporation (September 1986).
24. T. Q. Nguyen, et., al., "Qualification of the PHOENIX-P/ANC Nuclear Design System for Pressurized Water Reactor Cores," WCAP-11596-P-A, Westinghouse Electric Corporation (June 1988)
25. Ouisloumen, M. et al., "Qualification of the Two-Dimensional Transport Code PARAGON," WCAP-16045-P-A, Westinghouse, 2004.
26. Zhang, B. et al., "Qualification of the NEXUS Nuclear Data Methodology," WCAP-16045-P-A, Addendum 1, Westinghouse 2005.

## 14.2 STANDBY SAFEGUARDS ANALYSIS

### 14.2.1 Fuel Handling Accident

This section discusses the design features which preclude a serious accident during fuel handling, and then verifies that the consequences of the worst case assumptions meet 10 CFR 50.67 limits and NUREG-0800 (SRP 15.0.1) guidelines.

The following representative fuel handling accidents are evaluated during the course of design to ensure that no hazards are created:

1. A fuel assembly becomes stuck inside the reactor vessel, in the penetration valve in the transfer carriage, or the transfer carriage itself becomes stuck. In this case, the criterion is to ensure cooling of the fuel.
2. A fuel assembly is dropped onto the floor (or onto other assemblies which may be present) of the refueling cavity or spent fuel pool. In this case, assuming that 137 fuel rods are ruptured, the criterion is to ensure that the offsite dose is acceptable as described above.

#### 14.2.1.1 Accident Description

The possibility of a fuel handling incident is very remote because of the many administrative controls and physical limitations imposed on fuel handling operations. All refueling operations are conducted in accordance with prescribed procedures under direct surveillance of a supervisor technically trained in nuclear safety.

The fuel handling manipulators and hoists are designed so that fuel cannot be raised above a position which provides adequate shield water depth for the safety of operating personnel. This safety feature applies to handling facilities in both the containment and in the spent fuel pool area.

In the spent fuel pool, the design of storage racks and manipulation facilities is such that:

1. Fuel at rest is positioned by positive restraints in an oversafe ( $k_{\text{eff}} \leq 0.95$ ), always subcritical, geometrical array, with no credit taken for boric acid in the water.
2. Only one fuel assembly can be manipulated at a time.
3. A minimum boron concentration of 400 ppm will maintain  $k_{\text{eff}} \leq 0.95$  for fuel assembly misplacement. Misplacement of a new fuel assembly of 5.0 weight percent enrichment in a Region 2/Region 3 location, surrounded by locations filled with fuel of the highest permissible reactivity, could cause  $k_{\text{eff}}$  to exceed 0.95 without soluble boron.
4. Crane facilities do not permit the handling of heavy objects, such as a spent fuel shipping container, above the fuel racks.

Adequate cooling of fuel during underwater handling is provided by convective heat transfer to the surrounding water. The fuel assembly is immersed continuously while in the refueling cavity or spent fuel pool. There is no danger of overheating of the fuel. Even if a spent fuel assembly becomes stuck in the transfer tube, the fuel assembly is completely immersed and natural convection will maintain adequate cooling to remove the decay heat.

If an accident were to damage the fuel pool cooling system (Section 9.5), the heat of the spent fuel would have to be removed by evaporation of the spent fuel pool water. This would require intermittent makeup of the spent fuel pool water through the use of the connection from the refueling water storage tank or temporary lines from the fire protection system. Alternatively forced cooling could be supplied by the installation of temporary pump(s) and hoses. The rate of increase of fuel pool water temperature depends primarily on the number of freshly discharged fuel assemblies in the pool and their time after reactor shutdown when cooling is lost.

Radioactivity and clarity of the water are controlled by means of an ion exchanger and filter in the fuel pool purification system (Section 9.5). Any radioactivity escaping into the atmosphere above the pool is carried off by the supplementary leak collection and release system (Section 6.6).

If the spent fuel assembly or rod cluster control assembly were to come loose from the manipulator crane or spent fuel hoists, the item would be seen clearly through the water and retrieved remotely.

The motions of the cranes which move the fuel assemblies are limited to a low maximum speed. Caution is exercised during fuel handling to prevent the fuel assembly from striking another fuel assembly or structures in the containment or fuel building.

The fuel handling equipment suspends the fuel assembly in the vertical position during fuel movements except when the fuel is moved through the fuel transfer tube.

The design of the fuel assembly is such that the fuel rods are restrained by grid clips which provide a total restraining force of approximately 60 lb on each fuel rod. If the fuel rods are in contact with the bottom plate of the fuel assembly, any force transmitted to the fuel rods is limited due to the restraining force of the grid clips. The force transmitted to the fuel rods during fuel handling is not sufficient to breach the fuel rod cladding. If the fuel rods are in contact with the bottom plate of the assembly, the rods would have to slide against the 60 lb friction force. This would absorb the shock and thus limit the force on the individual fuel rods.

After the reactor is shutdown, the fuel rods contract during the subsequent cooldown and would not be in contact with the bottom plate of the assembly.

Considerable deformation would have to occur before the rod would make contact with the top plate and apply any appreciable load on the fuel rod. Based on the above, it is unlikely that any damage would occur to the individual fuel rods during handling. If one assembly is lowered on top of another, no damage to the fuel rods would occur that would breach the integrity of the cladding.

All these safety features make the probability of a fuel handling accident very low. The worst case, which is hypothesized with respect to the release of fission products to the environment, is a fuel handling accident in the fuel handling building.

#### 14.2.1.2 Radiological Consequence Analysis Methods, Assumptions and Results

The fuel handling accident is classified as an ANS Condition IV event; i.e., faults that are not expected to occur but are postulated because their consequences include the potential for the release of significant amounts of radioactive material.

This DBA is described in NRC Regulatory Guide 1.183 (Reference 33) and NUREG-0800 Chapter 15, Section 15.0.1. The parameters and assumptions used to perform the radiological consequence analysis are summarized in Tables 14.2-6 and 14.2-6a. The dose calculation methodology is provided in Appendix 14B.

The accident occurs while moving a fuel assembly in either the fuel building fuel storage pool or in the reactor building containment cavity or transfer canal. The assembly is dropped, resulting in rupture of 137 fuel rods (in the dropped assembly plus other assemblies that may be struck) and release of radioactive iodine and noble gas into the pool water. The extent of damage has been determined by performing an analysis using the limiting drop conditions and considering the weight of the dropped fuel assembly (plus any attached handling grapples), the height of the drop, and the compression, torsion, and shear stresses on the irradiated fuel rods. Damage to adjacent assemblies has been considered.

All of the fuel gap activity associated with the damaged rods is assumed to be released. A radial peaking factor of 1.75 is applied to the core average gap activity. The activity (consisting of noble gases, halogens, and alkali metals) is released in a "puff" to the fuel pool or reactor cavity.

The radioiodine released from the fuel gap is assumed to be 95% CsI, 4.85% elemental, and 0.15% organic. Due to the acidic nature of the water in the reactor cavity (pH less than 7), the CsI will immediately disassociate, thus changing the chemical form of iodine in the water to 99.85% elemental and 0.15% organic. The minimum depth of water in the fuel pool and reactor cavity is 23 ft over the top of the damaged fuel assembly. Therefore, per RG 1.183, the pool provides an overall effective decontamination factor for elemental and organic iodines of 200. Per RG 1.183, the chemical form of the iodines above the reactor cavity is 57% elemental and 43% organic.

Noble gas and unscrubbed iodines rise to the water surface whereas all of the alkali metals released from gap are retained in the reactor cavity water. Since the fuel pool area and containment are assumed to be open, and there is no means of isolating the accident release, all of the airborne activity resulting from the FHA is exhausted out of the building in a period of 2 hours. The analysis assumes that during refueling, the ventilation is operational above the spent fuel pool area.

The exhaust flows from the containment and Fuel Pool Area may be directed out of the SLCRS release point. However, since the containment and fuel buildings are "open," releases could also occur from anywhere along the containment wall (e.g., via the equipment or personnel hatch) or via the fuel building normal operation release point, i.e., the ventilation vent. Because

the location of the release is unknown, the worst case dispersion factor (identified for purposes of assessment as that associated with the BVPS-1 ventilation vent to the BVPS-1 CR intake) is used without taking any credit for SLCRS flows or filtration.

The environmental radioactivity release is transported to the dose receptor points assuming dispersion due to diffusion and local meteorological conditions with no consideration given to radioactive decay during transport or to gravitational settling. To establish dose consequences to control room personnel, no credit is taken for initiation of the control room emergency ventilation system following a FHA. Subsequent to a BVPS-1 FHA, following termination of the environmental release, the control room is purged, at T=2 hours, at a rate of 16,200 cfm for a period of 30 minutes.

The dose analysis results are presented in Tables [14.1-1A](#) and [14.1-1B](#).

These postulated fuel handling accident doses are within the limits provided in 10 CFR 50.67 of 25 rem TEDE for the EAB and LPZ, and 5 rem TEDE for the control room. Additionally, the accident doses are within the more restrictive criteria provided in NUREG-0800 Section 15.0.1 of 6.3 rem TEDE for the EAB and LPZ.

#### 14.2.2 Accidental Release of Waste Liquid

Section 14.2.2 and 14.2.3 have been moved to Chapter 11.

#### 14.2.3 Accidental Release of Waste Gases

Section 14.2.2 and 14.2.3 have been moved to Chapter 11.

#### 14.2.4 Steam Generator Tube Rupture

##### 14.2.4.1 Accident Description

The accident examined is the complete severance of a single steam generator tube. The accident is assumed to take place at power with the reactor coolant contaminated with fission products corresponding to continuous operation with a limited amount of defective fuel rods. The accident leads to an increase in contamination of the secondary system due to leakage of radioactive coolant from the reactor coolant system. In the event of a coincident loss of offsite power, or failure of the condenser dump system, discharge of activity to the atmosphere takes place via the steam generator safety and/or atmospheric dump valves.

Because the steam generator tube material is Alloy 690 and is a highly ductile material, it is considered that the assumption of a complete severance is conservative. The more probable mode of tube failure would be one or more minor leaks. Activity in the steam and power conversion system is subject to continual surveillance, the maximum value of this activity is given in the Technical Specifications.

The operator is expected to determine that a steam generator tube rupture has occurred, identify the steam generator with the ruptured tube, and isolate it as promptly as possible to minimize contamination of the secondary system and ensure termination of radioactive release to the atmosphere from the ruptured unit. The recovery procedure can be carried out on a time scale that ensures that break flow to the secondary system is terminated before water level in the affected steam generator rises into the main steam pipe. Sufficient indications and controls are provided to enable the operator to carry out these functions satisfactorily.

Assuming normal operation of the various plant control systems, the following events occur after a tube rupture:

1. Pressurizer low pressure and low level alarms are actuated and charging pump flow increases in an attempt to maintain pressurizer level. On the secondary side there is a steam flow/feedwater flow mismatch before trip as feedwater flow to the affected steam generator is reduced to the additional break flow which is now being supplied to that unit.
2. Continued loss of reactor coolant inventory leads to a reactor trip signal generated by low pressurizer pressure. Resultant plant cooldown following reactor trip leads to a rapid change of pressurizer level, and the safety injection signal, initiated by low pressurizer pressure, follows soon after the reactor trip. The safety injection signal (SIS) automatically terminates normal feedwater supply and initiates auxiliary feedwater addition.
3. The steam generator blowdown liquid monitor and the condenser air ejector vent monitor will alarm indicating a sharp increase in radioactivity in the secondary system. Upon reaching a high-high radiation level, the condenser air ejector vent monitor will automatically divert the condenser air ejector discharge to containment.
4. The reactor trip automatically trips the turbine and if off-site power is available the steam dump valves open permitting steam dump to the condenser. In the event of a coincident station blackout, the steam dump valves would remain closed or be automatically closed to protect the condenser. The steam generator pressure would rapidly increase resulting in steam discharge to the atmosphere through the steam generator safety and/or atmospheric dump valves.
5. Following reactor trip, the continued action of auxiliary feedwater supply and borated safety injection flow (supplied from the refueling water storage tank) provide a heat sink which absorbs some of the decay heat. Thus, steam bypass to the condenser, or in the case of loss of offsite power, steam relief to atmosphere, is attenuated during the time period in which the recovery procedure leading to isolation is being carried out.
6. Safety injection flow results in increasing pressurizer water level. The time after trip at which the operator can clearly see returning level in the pressurizer is dependent upon the amount of operating auxiliary equipment.

#### 14.2.4.2 Analysis of Effects and Consequences

##### 14.2.4.2.1 Method of Analysis

In estimating the mass transfer from the Reactor Coolant System through the broken tube, the following assumptions are made:

1. Reactor trip occurs automatically as a result of low pressurizer pressure.
2. Following the initiation of the SIS, two centrifugal charging pumps are actuated and continue to deliver flow until safety injection is procedurally terminated.
3. After reactor trip, the break flow reaches equilibrium at the point where incoming safety injection flow is balanced by outgoing break flow as shown in Figure 14.2-3. The resultant break flow persists from plant trip until after cooldown and depressurization.
4. The steam generators are controlled at the safety valve setting rather than the atmospheric dump valve setting.
5. The operator identifies the accident type and terminates break flow from the ruptured steam generator.

The reactor coolant mass transfer analysis assumes that the operator actions can be performed and that the ruptured steam generator can be isolated within 30 minutes of accident initiation.

In order to confirm that the operators are capable of carrying out their actions satisfactorily, a steam generator tube rupture operational response analysis is performed to evaluate reactor coolant mass transfer and margin to steam generator overflow. The operational response reactor coolant mass transfer analysis demonstrates that the licensing basis reactor coolant mass transfer data assuming break flow termination at 30 minutes is more limiting than the operational response reactor coolant mass transfer analysis data that considers the tube rupture transient from break initiation to break flow termination. The time allowed for the operational response is >30 minutes. However, the operational response reactor coolant mass transfer analysis confirms that the 30 minute assumptions of the licensing basis analysis remain conservative with respect to providing reactor coolant mass transfer data that is conservative for use in environmental consequence analysis.

The licensing basis thermal hydraulic analysis model used to determine the post accident releases and associated dose consequences at the site boundary and control room for the SGTR is a simplified model that was common industry practice prior to 1980. The model predicts conservative environmental releases and utilizes an assumed termination time of 30 minutes for the break flow and releases from the ruptured steam generator. This analysis is considered to be the BVPS-1 licensing basis.

The environmental releases based on an operational response thermal hydraulic model which reflects a more realistic transient and takes into consideration simulator based operator action times was also evaluated. The operational response thermal hydraulic model utilized simulator



based operator action times, addressed single failure considerations and included margin for steam generator overfill. It was determined that the site boundary and control room doses using the licensing basis thermal hydraulic analysis bound the dose estimates developed utilizing the thermal hydraulic input data based on the operational response case. Although, the times exceed the 30 minutes used in dose analysis, the licensing basis dose analysis is bounding.

#### 14.2.4.2.2 Environmental Consequences of Tube Rupture

The site boundary and control room doses due to airborne activity releases following a BVPS-1 licensing basis SGTR are calculated by computer code PERC2<sup>(34)</sup>. The analysis is performed at a core power level of 2918 MWt and with Alternative Source Term (AST) methodology as outlined in Regulatory Guide 1.183<sup>(33)</sup>. PERC2 is a multiple compartment activity transport code which calculates the Committed Effective Dose Equivalent (CEDE) from Inhalation and the Deep Dose Equivalent (DDE) from submersion due to halogens and noble gases at offsite locations and in the control room. The Total Effective Dose Equivalent (TEDE) is the sum of CEDE and DDE. The dose calculation model is described in Appendix 14B and is consistent with the regulatory guidance.

The worst 2-hour period dose at the Exclusion Area Boundary (EAB), the dose at the Low Population Zone (LPZ) for the duration of the release, and the 0 to 30-day dose to an operator in the control room due to inhalation and submersion are calculated based on postulated airborne radioactivity releases. The atmospheric dispersion factors from various activity release paths to the control room intakes are calculated using the latest version of the "Atmospheric Relative Concentrations in Building Wakes" (ARCON96) methodology<sup>(35)</sup> and are presented in Table 2.2-12a. Table 14.2-9 lists the key assumptions/parameters utilized to develop the radiological consequences following a SGTR.

The acceptance criteria for the EAB and LPZ doses for a SGTR are based on 10 CFR Part 50 paragraph 50.67<sup>(36)</sup> and Section 4.4 Table 6 of Regulatory Guide 1.183<sup>(33)</sup>.

The SGTR results in a reactor trip and a simultaneous loss of offsite power at 225 seconds after the event. Due to the tube rupture, primary coolant with elevated iodine concentrations (due to a pre-accident or a concurrent iodine spike) flows into the ruptured steam generator, and the associated activities are released to the environment via secondary side steam releases. Before the reactor trip, the activities are released from the air ejector. After the reactor trip the steam release is via the MSSVs/ADVs. The primary coolant activities (with the iodine spike) in the intact steam generators at the maximum allowable primary-to-secondary leakage value, are also released to the environment via secondary steam releases. The steam release from the intact steam generator continues until initiation of shutdown cooling 24 hours after the accident.

Since there is no postulated fuel damage associated with this accident, the main radiation source is the activity in the primary coolant system and the two iodine spiking cases addressed, i.e., a) a pre-accident iodine spike and, b) a concurrent iodine spike.

- a. Pre-accident spike - the initial primary coolant iodine activity is assumed to be 21  $\mu\text{Ci/gm}$  of DE I-131.

- b. Concurrent spike - the initial primary coolant iodine activity is assumed to be 0.35  $\mu\text{Ci/gm}$  DE I-131. Immediately following the accident, the iodine appearance rate from the fuel to the primary coolant is assumed to increase to 335 times the equilibrium appearance rate corresponding to the 0.35  $\mu\text{Ci/gm}$  DE I-131 coolant concentration. In accordance with the current design basis, the duration of the assumed spike is 4 hours.

The initial secondary side liquid and steam activity is relatively small and its contribution to the total dose is small compared to that contributed by the rupture flow. However, the release of the secondary side liquid activity and the resultant doses are included in the analysis. The initial secondary side iodine activity is assumed to be at the 0.1  $\mu\text{Ci/gm}$  DE I-131.

The most limiting atmospheric dispersion factors for each of the release points relative to the two control room intakes (identified for purposes of assessment as the BVPS-1 MSSVs/ADVs to the BVPS-1 control room intake, and the BVPS-1 Air Ejector to the BVPS-1 Intake) are selected to determine a bounding control room dose. No credit is taken for initiation of the control room emergency ventilation system following a SGTR. Following termination of the environmental release, the control room is purged for a period of 30 minutes.

#### 14.2.4.2.3 Recovery Procedure

Immediately, apparent symptoms of a tube rupture accident, such as falling pressurizer pressure and level and increase charging pump flow, are also symptoms of small steam line breaks and loss of coolant accidents (LOCA). It is therefore, important for the operator to determine that the accident is a rupture of a steam generator tube in order that he may carry out the correct recovery procedure. The accident under discussion is uniquely identified by a condenser air ejector radiation alarm and/or a steam generator blowdown radiation alarm and the operator will proceed with the following recovery procedures only if at least one of these alarms is received. In the event of a relatively large rupture, it will be clear soon after trip that the level in one steam generator is rising more rapidly than in the other. This too is a unique indication of a tube rupture accident.

The steam generator tube rupture recovery sequence consists of the following major operator actions:

1. Identification of the steam generator with failed tubes. This is accomplished by monitoring high activity in the corresponding steam generator blowdown line, main steamline, or water sample; and/or monitoring an uncontrolled increase in steam generator water level.
2. Isolation of the steam generator with failed tubes. This is accomplished by isolating steam flow from and stopping feedwater flow to the affected steam generators.
3. Cooldown of the RCS fluid to approximately 50°F below no load temperature to ensure subcooling in the RCS intact loops at the ruptured steam generator pressure.

4. Controlled depressurization of the RCS until pressurizer level has been restored and RCS pressure is equal to the ruptured steam generator pressure.
5. Termination of safety injection flow with normal charging and letdown flow established to provide normal RCS inventory control. RCS pressure and charging flow are adjusted to maintain pressurizer level and prevent leakage through the failed tube.
6. Prepare for cooldown to cold shutdown. A series of operator actions should be performed to prepare the plant for cooldown to cold shutdown conditions. The operator must also select the best post-SGTR cooldown method based on an evaluation of the plant status.

With offsite power unavailable, the principle systems/components affected are the steam dump system, reactor coolant pumps (RCPs), and RCS pressure control.

Sufficient instrumentation and controls are provided to ensure that necessary recovery actions can be completed with offsite power unavailable. Although the recovery method is the same with or without offsite power available, the equipment used may be different.

Since neither the condenser steam dump valves or the condenser would be available with offsite power unavailable, the RCS is cooled using the atmospheric steam dump valves and the Residual Heat Release Valve on the intact steam generators. RCPs trip on a loss of offsite power and a gradual transition to natural circulation flow ensues. With RCPs stopped, normal pressurizer spray would not be available. Consequently, RCS pressure must be controlled using pressurizer PORVs or auxiliary spray.

The objectives of the above recovery procedure are to limit the release of radioactive effluents from the ruptured steam generator, stop primary-to-secondary leakage to prevent steam generator overfill, and restore reactor coolant inventory to ensure adequate core cooling and plant pressure control.

There is ample time available to carry out the above recovery procedure that maintains margin to overfill in the affected steam generator. The steam generator secondary side and the main steam line volume up to the main steam isolation valve are both credited in the Steam Generator Overfill Analysis. The available time scale is improved by the termination of auxiliary feedwater flow to the ruptured steam generator and the regulation of pressurizer water level with only one charging pump operating. Normal operator vigilance, therefore, assures that excessive water level will not be attained. In addition, the main steam piping and supports are capable of withstanding the analyzed condition due to water intrusion into the affected main steam line as described in Section 10.3.1.1.

#### 14.2.4.2.4 Results

Figure 14.2-3 illustrates the flow rate that would result through the ruptured steam generator tube. The previous assumptions lead to a conservative estimate for the total amount of reactor coolant transferred to the secondary side of the ruptured steam generator.

AST methodology requires that the worst case dose to an individual located at any point on the boundary at the EAB, for any 2-hr period following the onset of the accident, be reported as the EAB dose. The major source for the SGTR is the flashed portion of the RCS break flow which is terminated before time equals 2 hours. Therefore the worst 2-hour window dose for both the

pre-accident and concurrent iodine spike case occurs during time equals 0 hours to time equals 2 hours after the accident.

The calculated doses are provided in Table 14.1-1B and within the regulatory limits of 25 rem TEDE and 2.5 rem TEDE specified in 10CFR50.67<sup>(36)</sup> for the pre-accident and concurrent iodine spike, respectively. The control room dose is within the regulatory limit of 5 rem TEDE specified in 10CFR50.67, and is presented in Table 14.1-1A.

#### 14.2.4.3 Conclusions

A steam generator tube rupture will cause no subsequent damage to the Reactor Coolant System or the reactor core. An orderly recovery from the accident can be completed even assuming simultaneous loss of offsite power. The SGTR accident, an ANS Condition IV event, will transfer radioactive reactor coolant to the shell side of the SG as a result of the ruptured tube, and ultimately, into the atmosphere. The resulting offsite radiation doses will stay within the allowable guidelines and there was margin available, so no SG overfilling occurred.

#### 14.2.5 Major Secondary System Line Break

##### 14.2.5.1 Major Steam Line Break

###### 14.2.5.1.1 Identification of Causes and Accident Description

The steam release arising from a main steam line break would result in an initial increase in steam flow which decreases during the accident as the steam pressure falls. The energy removal from the Reactor Coolant System causes a reduction of coolant temperature and pressure. In the presence of a negative moderator temperature coefficient, the cooldown results in a reduction of core shutdown margin. If the most reactive rod cluster control assembly is assumed stuck in its fully withdrawn position after reactor trip, there is an increased possibility that the core will become critical and return to power. A return to power following a main steam line break is a potential problem mainly because of the high power peaking factors which exist assuming the most reactive rod cluster control assembly to be stuck in its fully withdrawn position. The core is ultimately shut down by the boric acid injection delivered by the safety injection system.

The analysis of a main steam line break is performed to demonstrate that the following criteria are satisfied:

1. Assuming a stuck rod cluster control assembly, with or without offsite power, and assuming a single failure in the engineered safeguards, there is no consequential damage to the primary system and the core remains in place and intact.
2. Energy release to containment from the worst steam pipe break does not cause failure of the containment structure.
3. Radiation doses are not expected to exceed the regulatory guidelines.

Although DNB and possible clad perforation following a steam line break are not necessarily unacceptable, the following analysis, in fact, shows that the DNB design basis is met for any break assuming the most reactive assembly stuck in its fully withdrawn position.

The following functions provide the necessary protection against a steam line break:

1. Safety injection system actuation from any of the following:
  - a. Two-out-of-three low pressurizer pressure.
  - b. Two-out-of-three low steamline pressure in any one loop.
  - c. Two-out-of-three high containment pressure.
2. The overpower reactor trips (neutron flux and  $\Delta T$ ) and the reactor trip occurring in conjunction with receipt of the safety injection signal.
3. Redundant isolation of the main feedwater lines: Sustained high feedwater flow would cause additional cooldown. Therefore, in addition to normal control action which will close the main feedwater control valves, a safety injection signal will rapidly close all feedwater control and feedwater isolation valves, trip the main feedwater pumps and close the feedwater pump discharge valves. (Main feedwater pump discharge valves are not credited for feedwater isolation in the safety analyses.)
4. Trip of the fast acting steam line trip valves (designed to close in 5 seconds after receipt of the signal) on:
  - a. Two-out-of-three low steam line pressure in any loop (above Permissive P-11).
  - b. Intermediate high-high containment pressure.
  - c. Two-out-of-three high steam line pressure rate in any loop (below Permissive P-11).

Fast-acting trip valves are provided in each steam line that will fully close within 8 seconds of a low pressure signal from a large break in the steam line. In addition, a normally closed 2 inch bypass valve is provided around each trip valve. For breaks downstream of the trip valves, closure of all valves would terminate the blowdown. For any break, in any location, no more than one steam generator would completely blowdown even if one of the isolation valves fails to close or a bypass valve is open. A description of steam line isolation is included in Section 10.

Steam flow is measured by monitoring dynamic head in nozzles inside the steam pipes. The nozzles which are of considerably smaller diameter than the main steam pipe are located inside the containment near the steam generators and also serve to limit the maximum steam flow for any break further downstream.

#### 14.2.5.1.2 Analysis of Effects and Consequences

##### Method of Analysis

The analysis of the main steam line break has been performed to determine:

1. The core heat flux and reactor coolant system temperature and pressure resulting from the cooldown following the steam line break. The LOFTRAN<sup>(11)</sup> code has been used.
2. The thermal and hydraulic behavior of the core following a steam line break. A detailed thermal and hydraulic digital-computer calculation has been used to determine if DNB occurs for the core conditions computed in Item 1 above.

The steam line break releases activity by two modes. The activity released is the steam generator equilibrium activity and that which leaks from the primary system during depressurization and cooldown. The steam generator equilibrium activity is derived from computer program "IONEXCHANGER" described in Section 14.2.2.2.

The following conditions were assumed to exist at the time of a main steam line break accident:

1. End of life shutdown margin at no load, equilibrium xenon conditions, and the most reactive assembly stuck in its fully withdrawn position: Operation of the control rod banks during core burnup is restricted in such a way that addition of positive reactivity in a steam line break accident will not lead to a more adverse condition than the case analyzed. The value of shutdown margin used is 1.77 percent.
2. The negative moderator coefficient corresponding to the end of life rodded core with the most reactive rod in the fully withdrawn position. The variation of the coefficient with temperature and pressure has been included. The  $k_{\text{eff}}$  versus temperature at 1,050 psia corresponding to the negative moderator temperature coefficient used plus the Doppler temperature effect, is shown in Figure 14.1-41. The effect of power generation in the core on overall reactivity is shown in Figure 14.2-4.

The core properties associated with the sector nearest the affected steam generator and those associated with the remaining sector were conservatively combined to obtain average core properties for reactivity feedback calculations. Further, it was conservatively assumed that the core power distribution was uniform. These two conditions cause underprediction of the reactivity feedback in the high power region near the stuck rod. These core analyses considered the Doppler reactivity from the high fuel temperature near the stuck RCCA, moderator feedback from the high water enthalpy near the stuck RCCA, power redistribution and nonuniform core inlet temperature effects. For cases in which steam generation occurs in the high flux regions of the core, the effect of void formation was also included.

3. Minimum capability for injection of the boric acid solution in the RWST, corresponding to the most restrictive single failure in the safety injection system. This corresponds to the flow delivered by one safety injection pump delivering its full flow to the cold leg header. The safety injection flow rates as a function of RCS pressure are shown on Figure 14.1-42. No credit has been taken for the low concentration boric acid which must be swept from the safety injection lines downstream of the boron injection tank isolation valves prior to the delivery of the boric acid solution to the reactor coolant loops.
4. Several combinations of break sizes and initial plant conditions have been considered in determining the core power and Reactor Coolant System transients:
  - a. Hot zero power conditions were modeled with, and without, offsite power available
  - b. Cases were modeled assuming the Model 54F replacement steam generators. Only one break size, 1.4 ft<sup>2</sup>, was analyzed because the 54F SGs are equipped with a flow restrictor built into the steam exit nozzle
  - c. Separate cases were analyzed assuming unisolatable steam paths that could potentially occur after receiving a steam line isolation signal and achieving full closure of the MSIVs. The piping for the atmospheric dump, valves, the residual heat release valve supply line, and the supply line for the turbine-driven auxiliary feedwater pump all branch off the main steam line, upstream of the MSIVs and, therefore, cannot be isolated by a steam line isolation signal.
5. Power peaking factors corresponding to one stuck rod cluster control assembly and non-uniform core inlet coolant temperatures are determined at the end of core life. The coldest core inlet temperatures are assumed to occur in the sector with the stuck rod. The power peaking factors account for the effect of the local void in the region of the stuck control assembly during the return to power phase following the steam line break. This void, in conjunction with the large negative moderator coefficient, partially offsets the effect of the stuck assembly. The power peaking factors depend upon the core power, temperature, pressure and flow, and thus are different for each case studied.

All the cases above assume initial hot shutdown conditions at time zero since this represents the most pessimistic initial condition. Should the reactor be just critical or operating at power at the time of a steam line break, the reactor will be tripped by the normal overpower protection system when power level reaches a trip point. Following a trip at power, the reactor coolant system contains more stored energy than at no load, the average coolant temperature is higher than at no load and there is appreciable energy stored in the fuel. Thus, the additional stored energy is removed via the cooldown caused by the steam line break before the no load conditions of Reactor Coolant System temperature and shutdown margin assumed in the analyses are reached. After the additional stored energy has been removed, the cooldown and reactivity insertions proceed in the same manner as in the analysis which assumes no load condition at time zero.

However, since the initial steam generator water inventory is greatest at no load, the magnitude and duration of the Reactor Coolant System cooldown are less for steam line breaks occurring at power.

6. In computing the steam flow during a steam line break, the Moody Curve<sup>(2)</sup> for  $f/D = 0$  is used.
7. Perfect moisture separation in the steam generator is assumed, which leads to conservative results because, in fact, considerable water would be discharged. Water carryover would reduce the magnitude of the temperature decrease in the core and the pressure increase in the containment.

#### 14.2.5.1.3 Results

The results presented are a conservative indication of the events which would occur assuming a steam line break since it is postulated that all of the conditions described above occur simultaneously.

#### Core Power and Reactor Coolant System Transient

The break assumed is the largest that can occur anywhere inside the containment (i.e., the complete severance of a pipe). The analysis further assumes the plant at initial no load conditions with the Westinghouse Model 54F replacement steam generators, and the additional steam release paths following steam line isolation described in Section 14.2.5.1.2, paragraph 4c. Also, offsite power is assumed available so that full reactor coolant flow exists. Should the core be critical at near zero power when the rupture occurs, the initiation of safety injection by low steam line pressure will trip the reactor. Major steam release from more than one steam generator will be prevented by automatic trip of the fast action trip valves in the steam lines by low steam line pressure. Even if one valve were to fail, the valves on the other two steam generators will trip shut, limiting the steam release from the unaffected steam generators. The steam line trip valves are designed to be fully closed in less than 5 seconds with no flow through them. With the high flow existing during a steam line break, the valves will close considerably faster. Figures 14.2-5, 14.2-6, and 14.2-7 show, respectively, the core average temperature, the reactor coolant system pressure, and the core heat flux transients following a main steam line break inside the containment.

As shown in Figure 14.2-8 the core attains criticality with the rod cluster control assemblies inserted (with the design shutdown assuming one stuck assembly) before boron solution enters the reactor coolant system from the safety injection system. The delay time consists of the time to receive and actuate the safety injection signal and the time to completely open valve trains in the safety injection lines. The safety injection pumps are then ready to deliver flow. At this stage, a further delay of time is incurred before boron solution can be injected to the reactor coolant system due to low concentration solution being swept from the safety injection lines. A peak core power well below the nominal full power is attained.



The calculation assumes the boric acid is mixed with and diluted by the water flowing in the reactor coolant system prior to entering the reactor core. The concentration after mixing depends upon the relative flow rates in the reactor coolant system and in the safety injection system. The variation of mass flow rate in the reactor coolant system due to water density changes is included in the calculation as is the variation of flow rate from the safety injection system and the accumulators due to changes in the reactor coolant system pressure. The safety injection system flow calculation includes the line losses in the system as well as the pump head curve.

The accumulators provide an additional source of borated water after the RCS pressure decreases to below 575 psia. The integrated flow rate of borated water from both the accumulators and the safety injection system for each of the four cases can be found in Figure 14.2-9.

It should be noted that following a steam line break only one steam generator blows down completely. Thus, the remaining steam generators are still available for dissipation of decay heat after the initial transient is over. In the case of loss of offsite power, this heat is removed by the atmospheric dump or safety valves which have been sized to cover this condition.

As mentioned, the results presented in Figures 14.2-5, 14.2-6, 14.2-7, 14.2-8, and 14.2-9, as well as the time sequence of events in Table 14.2-2, correspond to the limiting case assuming operation with the Westinghouse Model 54F replacement steam generators.

### Radiological Consequences

The site boundary and control room doses due to airborne activity releases following a MSLB are calculated by computer code PERC2<sup>(34)</sup>. The analysis is performed at a core power level of 2918 MWt and with Alternative Source Term (AST) methodology as outlined in Regulatory Guide 1.183<sup>(33)</sup>. PERC2 is a multiple compartment activity transport code which calculates the Committed Effective Dose Equivalent (CEDE) from Inhalation and the Deep Dose Equivalent (DDE) from submersion due to halogens and noble gases at offsite locations and in the control room. The Total Effective Dose Equivalent (TEDE) is the sum of CEDE and DDE. The dose calculation model is described in Appendix 14B and is consistent with the regulatory guidance.

The worst 2-hour period dose at the Exclusion Area Boundary (EAB), the dose at the Low Population Zone (LPZ) for the duration of the release, and the 0 to 30-day dose to an operator in the control room due to inhalation and submersion are calculated based on postulated airborne radioactivity releases. The atmospheric dispersion factors from various activity release paths to the control room intakes are calculated using the latest version of the "Atmospheric Relative Concentrations in Building Wakes" (ARCON96) methodology<sup>(35)</sup> and are presented in Table 2.2-12a. Table 14.2-10 lists the key assumptions/parameters utilized to develop the radiological consequences following a MSLB.

The acceptance criteria for the EAB and LPZ doses for a MSLB are based on 10 CFR Part 50 paragraph 50.67<sup>(36)</sup> and Section 4.4 Table 6 of Regulatory Guide 1.183<sup>(33)</sup>

The radiological model conservatively assumes immediate dry-out of the faulted SG following a MSLB resulting in the instantaneous release of all of the SG contents, which are assumed at maximum Technical Specification concentrations. Based on an assumption of a simultaneous Loss of Offsite Power, the condenser is unavailable, and environmental steam releases via the MSSVs/ADVs from the intact steam generators are used to cool down the reactor until the Residual Heat Removal (RHR) system starts shutdown cooling. The elevated iodine activity in the RCS due to a postulated pre-accident or concurrent iodine spike, as well as the noble gas (at Technical Specification concentrations), leak into the faulted and intact steam generators, and are released to the environment from the break point, and from the MSSVs/ADVs, respectively.

The steam releases from the intact SGs continue until shutdown cooling is initiated via operation of the RHR system resulting in the termination of environmental releases via this pathway. The releases from the faulted SG due to primary to secondary leakage continues until the RHR System is brought to the primary coolant temperature of 212°F).

Since there is no postulated fuel damage associated with this accident, the primary radiation source is the activity in the reactor coolant system. Two iodine spiking cases are addressed: a pre-accident iodine spike and a concurrent iodine spike.

- a. Pre-accident spike - initial primary coolant iodine activity is assumed to be at 21  $\mu\text{Ci/gm}$  of DE I-131.
- b. Concurrent spike - the initial primary coolant iodine activity is assumed to be at 0.35 $\mu\text{Ci/gm}$  DE I-131. Immediately following the accident the iodine appearance rate from the fuel to the primary coolant is assumed to increase to 500 times the equilibrium appearance rate corresponding to the 0.35  $\mu\text{Ci/gm}$  DE I-131 coolant concentration. In accordance with the current design basis, the duration of the assumed spike is four hours.

The initial secondary coolant iodine activity is assumed to be 0.1  $\mu\text{Ci/gm}$  DE I-131.

Following a MSLB, the primary and secondary reactor coolant activity is released to the environment via two pathways; i.e., the main steam line break location and the MSSVs/ADVs. The most limiting atmospheric dispersion factors for each of the release points relative to the two control room intakes (identified for purposes of assessment as the BVPS-1 MSSVs/ADVs to the BVPS-1 control room intake, and the BVPS-1 main steam line break location to the BVPS-1 Intake) are selected to determine a bounding control room dose.

The control room emergency ventilation system is manually initiated and a pressurized control room is available after the accident. Following termination of the environmental release, the control room is purged, for a period of 30 minutes.

### Results

AST methodology requires that the worst case dose to an individual located at any point on the boundary at the EAB, for any 2-hr period following the onset of the accident be reported as the EAB dose.

The calculated doses presented in Table 14.1-1B are within the regulatory limits of 25 rem TEDE and 2.5 rem TEDE specified in 10CFR50.67<sup>(36)</sup> for the pre-accident and concurrent iodine spike, respectively. The control room dose is within the regulatory limit of 5 rem TEDE specified in 10CFR50.67, and is presented in Table 14.1-1A.

### Containment Structure Pressure and Temperature Transients

Main Steam Line Break (MSLB) analyses have been performed to determine the containment pressure and temperature transients. The containment transient analysis code MAAP-DBA was used to evaluate containment pressure and temperature response resulting from a main steam line break. A spectrum of break sizes and power levels provided by Westinghouse were analyzed in conjunction with single active failure (SAF) considerations. Four SAFs are assumed to produce the worst containment transient conditions for the MSLB. These SAFs are:

1. Failure of one train of Quench Spray
2. Failure of one emergency diesel generator (resulting in the loss of one train each of SI, QS, RS, and RW)
3. Failure of a main steam non-return valve
4. Failure of a main feedwater isolation valve

A matrix of runs combining power level, break size, SAF consideration and initial containment conditions was performed to determine the limiting combinations that produce peak pressures and peak temperatures inside containment following a main steam line break.

The major assumptions used in calculating the MSLB pressure and temperature profiles were:

1. Steam generators are isolated by controls upon sensing the break.
2. The main steam non-return valve (NRV) functions instantaneously to isolate the faulted steam generator break from reverse steam flow. The NRV is considered to be functional for any MSLB scenario where the SAF is either a feedwater isolation valve or an emergency 4KV bus.
3. All auxiliary feedwater pumps are operational.
4. Full power feedwater is at approximately 455°F.

The MSLB peak pressure and temperature transients are based on either double-ended circumferential or longitudinal split main steam line breaks. The worst case break for peak pressure occurs when the plant is operating at 30% power level, double-ended break with the SAF of the main steamline non return valve. This limiting break possesses the combination of loop steam generator pressure transient, main feedwater flow rate characteristic and the feedwater isolation delay that produces the maximum peak pressure and temperature. The worst case break for peak containment temperature occurs when the plant is operating at 30% power level, 1.4 ft<sup>2</sup> double-ended break with the SAF of the main steamline non-return valve. The resulting MSLB containment peak pressure, and peak temperature profiles are shown on Figures 14.2-34 and 14.2-35. The liner plate temperatures profiles are shown in Figures 14.2-36.

Figure 14.2-35 shows a peak containment air temperature, which briefly exceeds the containment liner design temperature of 280°F. Figure 14.2-36 provides the results of the transient analysis showing that the containment liner remains at or below the 280°F design.

#### 14.2.5.1.4 Conclusions

The analysis has shown that the criteria stated earlier in this section are satisfied.

Although an MSLB is an ANS Condition IV event, it has been evaluated against the more restrictive DNB requirements of ANS Condition II, which assumes fuel failure does not occur.

#### 14.2.5.1.5 Steam System Piping Failure at Full Power

##### 14.2.5.1.5.1 Identification of Causes and Accident Description

A rupture in the main steam system piping from an at-power condition creates an increased steam load, which extracts an increased amount of heat from the RCS via the steam generators. This results in a reduction in RCS temperature and pressure. In the presence of a strong negative moderator temperature coefficient, typical of end-of-cycle life conditions, the colder core inlet coolant temperature causes the core power to increase from its initial level due to the positive reactivity insertion. The power approaches a level equal to the total steam flow.

Depending on the break size, a reactor trip may occur due to overpower conditions or as a result of a steam line break protection function actuation.

The steam system piping failure accident analysis described in subsection 14.2.5.1 is performed assuming a hot zero power initial condition with the control rods inserted in the core, except for the most reactive rod in the fully withdrawn position, out of the core. That condition could occur while the reactor is at hot shutdown at the minimum required shutdown margin or after the plant has been tripped manually or by the reactor protection system following a steam line break from an at-power condition. For an at-power break, the analysis of subsection 14.2.5.1 represents the limiting condition with respect to core protection for the time period following reactor trip. The purpose of this section is to describe the analysis of a steam system piping failure occurring from an at-power initial condition, to demonstrate that core protection is maintained prior to and immediately following reactor trip.

Depending on the size of the break, this event is classified as either an ANS Condition III (infrequent fault) or Condition IV (limiting fault), as defined in subsection 14.0.1.

##### 14.2.5.1.5.2 Analysis of Effects and Consequences

#### Method of Analysis

The analysis of the steam line rupture is performed in the following stages:

1. The LOFTRAN code (Reference 11) is used to calculate the nuclear power, core heat flux, and RCS temperature and pressure transients resulting from the cooldown following the steam line break.

2. The core radial and axial peaking factors are determined using the thermal-hydraulic conditions from the transient analysis as input to the nuclear core models. The VIPRE code (Reference 38) is then used to calculate the DNBR for the limiting time during the transient.

This accident is analyzed with the Revised Thermal Design Procedure as described in Reference 39. Plant characteristics and initial conditions are discussed in subsection 14.2.5.1.2.

The following assumptions are made in the transient analysis:

1. Initial Conditions – The initial core power, reactor coolant temperature, and RCS pressure are assumed to be at their nominal full-power values. The full power condition is more limiting than part-power in terms of DNBR. The RCS Minimum Measured Flow is used. Uncertainties in initial conditions are included in the DNBR limit as described in Reference 39. Initial conditions are summarized in Section 14.2.5.1.2.
2. Break size – A spectrum of break sizes is analyzed. Small breaks do not result in a reactor trip. Intermediate size breaks result in a reactor trip on Overpower  $\Delta T$ . Larger break sizes result in a reactor trip as a consequence of the lead-lag compensated Low Steam Pressure Safety Injection actuation.
3. Break flow – In computing the steam flow during a steam line break, the Moody curve<sup>(2)</sup> for  $fL/D = 0$  is used.
4. Reactivity Coefficients – The analysis assumes maximum moderator reactivity feedback and minimum Doppler power feedback to maximize the power increase following the break.
5. Protection System – The protection system features that mitigate the effects of a steam line break are described in subsection 14.2.5.1. This analysis only considers the initial phase of the transient initiated from an at-power condition. Protection in this phase of the transient is provided by a reactor trip, if necessary.

Subsection 14.2.5.1 presents the analysis of the bounding transient following reactor trip, where other protection system features are actuated to mitigate the effects of the steam line break.

6. Control Systems – The results of the analysis would not be more severe as a result of control system actuation, therefore their effects have been ignored in the analysis. Control system are not credited in mitigating the effects of the transient.

#### 14.2.5.1.5.3 Results

A spectrum of steam line break sizes was analyzed from 0.1 ft<sup>2</sup> to 1.4 ft<sup>2</sup>. The results show that for small break sizes up to 0.3 ft<sup>2</sup> a reactor trip is not generated. In this case, the event is similar to an excessive load increase event as described in subsection 14.1.10. The core reaches a new equilibrium condition at a higher power equivalent to the increased steam release. For break sizes of 0.4 ft<sup>2</sup> to 0.6 ft<sup>2</sup> the power increase results in a reactor trip on overpower  $\Delta T$ . For break sizes of 0.7 ft<sup>2</sup> and larger a reactor trip is generated within a few seconds of the break on the lead-lag compensated Low Steam Pressure Safety Injection actuation signal.

The limiting case for demonstrating DNB protection is the 0.6 ft<sup>2</sup> break, the largest break size that results in a trip on overpower  $\Delta T$ . The time sequence of events for this case is shown on Table 14.2-2. Figures 14.2-19, 14.2-20, 14.2-21, and 14.2-22 show the transient response.

#### 14.2.5.1.5.4 Conclusions

A detailed DNB analysis is performed as part of each cycle-specific reload safety evaluation, using radial and axial core peaking factors which are dependent on the cycle-specific loading pattern. The analysis concludes that the DNB design basis is met for the limiting case. Although DNB and possible clad perforation following a steam pipe rupture are not necessarily unacceptable and not precluded by the criteria, the above analysis, in fact, shows that the minimum DNBR remains above the limit value for any rupture occurring from an at-power condition prior to and immediately following a reactor trip.

#### 14.2.5.2 Main Feedwater Line Break

##### 14.2.5.2.1 Identification of Causes and Accident Description

A major feedwater line break is defined as a break in a feedwater pipe large enough to prevent the addition of sufficient feedwater to the steam generators to maintain shell-side fluid inventory in the steam generators. If the break is postulated in a feedline between the check valve and the steam generator, fluid from the steam generator may also be discharged through the break. Further, a break in this location could preclude the subsequent addition of auxiliary feedwater to the affected steam generator. (A break upstream of the feedline check valve would affect the nuclear steam supply system only as a loss of feedwater. This case is covered by the evaluation in Section 14.1.8.)

Depending upon the size of the break and the plant operating conditions at the time of the break, the break could cause either a reactor coolant system cooldown (by excessive energy discharge through the break), or a reactor coolant system heatup. Potential reactor coolant system cooldown resulting from a secondary pipe break is evaluated in Section 14.2.5.1. Therefore, only the reactor coolant system heatup effects are evaluated for a feedwater line break.

A feedwater line break reduces the ability to remove heat generated by the core from the reactor coolant system because of the following reasons:

1. Feedwater to the steam generators is reduced. Since feedwater is subcooled, its loss may cause reactor coolant temperatures to increase prior to reactor trip.
2. Liquid in the steam generator may be discharged through the break, and would then not be available for decay heat removal after trip.
3. The break may be large enough to prevent the addition of any main feedwater after trip.

An auxiliary feedwater system is provided to assure that adequate feedwater will be available such that:

1. No substantial overpressurization of the reactor coolant system shall occur.
2. Liquid in the reactor coolant system shall be sufficient to cover the reactor core at all times.

The following provides the necessary protection against a main feedwater line break:

1. A reactor trip on any of the following conditions:
  - a. High pressurizer pressure
  - b. Overtemperature delta-T
  - c. Low-low steam generator water level in any steam generator
  - d. Safety injection signals from either of the following:
    - 1) Low steam line pressure
    - 2) High containment pressure

(Refer to Section 7 for a description of the actuation system.)
2. An auxiliary feedwater system to provide an assured source of feedwater to the steam generators for decay heat removal. (Refer to Section 10 for description of the auxiliary feedwater system.)

#### 14.2.5.2.2 Analysis of Effects and Consequences

##### Method of Analysis

A detailed analysis using the LOFTRAN<sup>(11)</sup> code is performed in order to determine the plant transient following a feedwater line break. The code describes the plant thermal kinetics, Reactor Coolant System including natural circulation, Pressurizer, steam generators and Feedwater System, and computes pertinent variables including the pressurizer pressure, pressurizer water level, and reactor coolant average temperature.

Major assumptions are:

1. The plant is initially operating at 100.6 percent of the uprated thermal power (2910 MWt).
2. Initial reactor coolant average temperature is 8.5°F above the nominal value and the initial pressurizer pressure is 40 psi below its nominal value.
3. No credit is taken for the pressurizer spray.

4. No credit is taken for the high pressurizer pressure reactor trip.
5. Main feedwater to all steam generators is assumed to stop at the time the break occurs.
6. A conservative feedwater line break discharge quality is assumed, which minimizes the heat removal capability of the affected steam generator.
7. Reactor trip is assumed to be actuated when the low-low steam generator level trip setpoint (minus uncertainties) is reached in the faulted steam generator.
8. The worst possible break area is assumed. This assumption maximizes the blowdown discharge rate following the time of trip, and thereby maximizes the resultant heatup of the reactor coolant.
9. No credit is taken for heat energy deposited in Reactor Coolant System metal during the Reactor Coolant System heatup.
10. No credit is taken for charging or letdown.
11. Initial pressurizer level is at the nominal programmed value plus 7 percent; initial steam generator water level is at the nominal value plus 10 percent in the faulted steam generator and at the nominal value minus 10 percent in the intact steam generators.
12. Steam generator heat transfer area is assumed to decrease as the shell-side liquid inventory decreases.
13. Core residual heat generation is assumed based upon ANSI/ANS-5.1-1979 (Reference 19), a conservative representation of the decay energy release rate.
14. Auxiliary feedwater is assumed to initiate 60 seconds after reactor trip, with a feed rate of 250 gpm split equally between the two intact steam generators, before the faulted steam generator is isolated. Operator action, 15 minutes after reactor trip, is credited to isolate the faulted steam generator, providing 400 gpm of auxiliary feedwater flow split equally between the two intact steam generators. Approximately 700 seconds after auxiliary feedwater is initiated, the feedlines are purged and the relatively cold (120°F) auxiliary feedwater enters the unaffected steam generators.
15. The analysis assumes operation with the full Westinghouse Model 54F replacement steam generators.



Receipt of a low-low steam generator narrow range level signal in at least two steam generators starts the motor-driven auxiliary feedwater pumps, which then deliver auxiliary feedwater flow to the steam generators. The turbine-driven auxiliary feedwater pump is started if the low-low steam generator water signal is generated in at least one steam generator. Similarly, receipt of a low steam line pressure signal in at least one steam line initiates a steam line isolation signal which closes the main steam line isolation valves in all steam lines. This signal also gives a safety injection signal which initiates flow of borated water into the Reactor Coolant System. The amount of safety injection flow is a function of Reactor Coolant System pressure.

Emergency operating procedures following a secondary system line break call for the following actions to be taken.

1. Isolate feedwater flow spilling out from the break in the feedwater line and align the system so that the water level in the intact steam generators recovers.
2. Stop high head safety injection and initiate charging flow.

Isolating feedwater flow through the break allows additional auxiliary feedwater flow to be diverted to the intact steam generators.

Subsequent to recovery of level in the intact steam generators, operating procedures will be followed in cooling the plant to hot shutdown conditions.

The Reactor Protection System is required to function following a feedwater line break as analyzed here. No single active failure will prevent operation of this system.

The engineered safety systems assumed to function are the Auxiliary Feedwater System and the Safety Injection System. The turbine-driven auxiliary feedwater pump has been assumed to fail. The motor-driven pumps deliver 400 gpm to two intact steam generators after isolation of the faulted steam generator. Only one train of safety injection has been assumed to be available.

### Results

Calculated parameters following a major feedwater line break are shown in the figures described below. Results for the case with offsite power available are presented in Figures 14.2-10A, 14.2-10B, 14.2-10C, 14.2-10D, and 14.2-10E. Results for the case where offsite power is lost are presented in Figures 14.2-10F, 14.2-10G, 14.2-10H, 14.2-10I, and 14.2-10J. The calculated sequences of events for both cases analyzed are listed in Table 14.2-2.

The system response following the feedwater line break is similar for both cases analyzed. Results presented in Figures 14.2-10C and 14.2-10E (with offsite power available) and Figures 14.2-10H and 14.2-10J (without offsite power available) show that pressures in the Reactor Coolant System and Main Steam System remain below 110 percent of their respective design pressures. Addition of the safety injection flow aids in cooling down the primary system and helps to ensure sufficient fluid to keep the core covered with water.

The reactor core remains covered with water throughout the transient, water relieved due to thermal expansion is limited by the heat removal capability of the Auxiliary Feedwater System, and makeup is provided by the high head safety injection pumps.

### Conclusion

Results of the analysis show that for the postulated feedwater line break, the assumed Auxiliary Feedwater System capacity is adequate to remove decay heat, to prevent overpressurizing the Reactor Coolant System, and to prevent uncovering the reactor core. All applicable acceptance criteria are therefore met for this ANS Condition IV event.

## 14.2.6 Rupture of a Control Rod Drive Mechanism Housing Rod Cluster Control Assembly Ejection

### 14.2.6.1 Identification of Causes and Accident Description

This accident is defined as the mechanical failure of a control rod mechanism pressure housing resulting in the ejection of a rod cluster control assembly and drive shaft. The consequence of this mechanical failure is a rapid reactivity insertion together with an adverse core power distribution, possibly leading to localized fuel rod damage.

#### 14.2.6.1.1 Design Precautions and Protection

Certain features in the BVPS-1 pressurized water reactor are intended to preclude the possibility of a rod ejection accident, or to limit the consequences if the accident were to occur. These include a sound, conservative mechanical design of the rod housings, together with a thorough quality control (testing) program during assembly, and a nuclear design which lessens the potential ejection worth of rod cluster control assembly and minimizes the number of assemblies inserted at power.

### Mechanical Design

The mechanical design is discussed in Section 4.2. Mechanical design and quality control procedures intended to preclude the possibility of a rod cluster control assembly drive mechanism housing failure sufficient to allow a rod cluster control assembly to be rapidly ejected from the core are listed below:

1. Each full length control rod drive mechanism housing is completely assembled and shop tested at 3,750 psi.
2. The mechanism housings are inspected, completely assembled and leak tested as they are attached to the head adapters in the reactor vessel head.
3. Stress levels in the mechanism are not affected by anticipated system transients at power, or by the thermal movement of the coolant loops. Moments induced by the design earthquake can be accepted within the allowable primary working stress range specified by the ASME Code, Section III, for Class 1 components.

4. The pressure housing is a single length of forged Type-304LN stainless steel. This material exhibits excellent notch toughness at all temperatures which will be encountered.

A significant margin of strength in the elastic range together with the large energy absorption capability in the plastic range gives additional assurance that gross failure of the housing will not occur. The joint between the mechanism housing and head adapter is threaded and sealed by a canopy weld.

### Nuclear Design

Even if a rupture of a rod cluster control assembly drive mechanism housing is postulated, the operation of plant utilizing chemical shim is such that the severity of an ejected rod cluster control assembly is inherently limited. In general, the reactor is operated with the rod cluster control assemblies inserted only far enough to permit load flow. Reactivity changes caused by core depletion and xenon transients are compensated by boron changes. Further, the location and grouping of control rod banks are selected during the nuclear design to lessen the severity of a rod cluster control assembly ejection accident. Therefore, should a rod cluster control assembly be ejected from its normal position during high power operation, only minor reactivity excursion, at worst, could be expected to occur.

However, it may be occasionally desirable to operate with larger than normal insertions. For this reason, a rod insertion limit is defined as a function of power level. Operation with the rod cluster control assemblies above this limit guarantees adequate shutdown capability and acceptable power distribution. The position of all rod cluster control assemblies is continuously indicated in the control room. An alarm will occur if a bank of rod cluster control assemblies approaches its insertion limit or if one assembly deviates from its bank. There are low and low-low level insertion monitors with visual and audio signals. Operating instructions require boration at low level alarm and emergency boration at the low-low alarm.

### Reactor Protection

The reactor protection in the event of a rod ejection accident has been described in Reference 3. The protection for this accident is provided by the power range high neutron flux trip (high and low setting) and high rate of neutron flux increase trip. These protection functions are described in detail in Section 7.2.

### Effects on Adjacent Housings

Disregarding the remote possibility of the occurrence of a rod cluster control assembly mechanism housing failure, investigations have shown that failure of a housing due to either longitudinal or circumferential cracking is not expected to cause damage to adjacent housings leading to increased severity of the initial accident.

A control rod drive mechanism assembly is shown in Figure 3.2-17. This assembly consists of a steel tube surrounded by a continuous stack of copper wire coils. The assembly is held together by two end plates, an outer sleeve and four axial tie rods.

### Effect of Longitudinal Failures

If a longitudinal failure of the rod travel portion of the CRDM housing should occur, the region of the position indicator assembly opposite the break would be stressed by the reactor coolant pressure of 2,250 psia. The most probable leakage path would be provided by the radial deformation of the position indicator coil assembly, resulting in the growth of axial flow passages between the rod travel housing and the steel tube.

If failure of the position indicator coil assembly should occur, the resulting free radial jet from the failed housing could cause it to bend and contact adjacent housings. If the adjacent housings were on the periphery, they might bend outward from their bases. The housing material is quite ductile; plastic hinging without cracking would be expected. Housings adjacent to a failed housing, in locations other than the periphery, would not be bent because of the rigidity of multiple adjacent housings.

### Effect of Circumferential Failures

If circumferential failure of a rod travel portion of the CRDM housing should occur, the broken-off section of the housing would be ejected vertically because the driving force is vertical and the position indicator coil stack assembly and the drive shaft would tend to guide the broken-off piece upwards during its travel. Travel is limited by the missile shield, thereby limiting the projectile acceleration. When the projectile reached the missile shield it would partially penetrate the shield and dissipate its kinetic energy. The water jet from the break would continue to push the broken-off piece against the missile shield.

If the broken-off piece of the rod travel housing were short enough to clear the break when fully ejected, it would rebound after impact with the missile shield. The top end plates of the position indication coil stack assemblies would prevent the broken piece from directly hitting the rod travel portion of a second drive mechanism. Even if a direct hit by the rebounding piece were to occur, the low kinetic energy of the rebounding projectile would not be expected to cause significant damage.

### Possible Consequences

From the above discussion, the probability of damage to an adjacent housing must be considered remote. However, even if damage is postulated, it cannot lead to a more severe transient since RCCA's are inserted in the core in symmetric patterns, and control rods immediately adjacent to worst ejected rods are not in the core when the reactor is critical. Damage to an adjacent housing could, at worst, cause the RCCA not to fall on receiving a trip signal; however, this is already taken into account in the analysis by assuming a stuck rod adjacent to the ejected rod.

The considerations given above lead to the conclusion that failure of a control rod housing, due either to longitudinal or circumferential cracking, would not cause damage to adjacent housings that would increase the severity of the initial accident.

#### 14.2.6.1.2 Limiting Criteria

This event is classified as an ANS Condition IV incident. Due to the extremely low probability of a rod cluster control assembly ejection accident, some fuel damage could be considered an acceptable consequence.

Comprehensive studies of the threshold of fuel failure and of the threshold of significant conversion of the fuel thermal energy to mechanical energy, have been carried out as part of the SPERT project by the Idaho Nuclear Corporation.<sup>(4)</sup> Extensive tests of UO<sub>2</sub> zirconium clad fuel rods representative of those in pressurized water reactor type cores have demonstrated failure thresholds in the range of 240 to 257 cal/gm. However, other rods of a slightly different design have exhibited failures as low as 225 cal/gm. These results differ significantly from the TREAT<sup>(5)</sup> results, which indicated a failure threshold of 280 cal/gm. Limited results have indicated that this threshold decreases by about 10 percent with fuel burnup. The clad failure mechanism appears to be melting for zero burnup rods and brittle fracture for irradiated rods. Also important is the conversion ratio of thermal to mechanical energy. This ratio becomes marginally detectable above 300 cal/gm for unirradiated rods and 200 cal/gm for irradiated rods; catastrophic failure, (large fuel dispersal, large pressure rise) even for irradiated rods, did not occur below 300 cal/gm.

In view of the above experimental results, criteria are applied to ensure that there is little or no possibility of fuel dispersal in the coolant, gross lattice distortion or severe shock waves.

These criteria are:

1. Average fuel pellet enthalpy at the hot spot below 225 cal/gm for unirradiated fuel and 200 cal/gm for irradiated fuel.
2. Peak reactor coolant pressure less than that which would cause stresses to exceed the faulted condition stress limits.
3. Fuel melting will be limited to less than 10 percent of the fuel volume at the hot spot even if the average fuel pellet enthalpy is below the limits of criterion 1 above.

#### 14.2.6.2 Analysis of Effects and Consequences

##### Method of Analysis

The analysis of the RCCA ejection accident is performed in two stages, first an average core channel calculation and then a hot spot heat transfer calculation. The average core power calculation is performed using spatial neutron kinetics methods to determine the average power generation with time including the various total core feedback effects, i.e., Doppler reactivity and moderator reactivity. Enthalpy and temperature transients in the hot spot are then determined by multiplying the average core energy generation by the hot channel factor and performing a fuel rod transient heat transfer calculation. The power distribution calculated without feedback is pessimistically assumed to persist throughout the transient. A detailed discussion of the method of analysis can be found in Reference 6.

### Average Core Analysis

The spatial kinetics computer code TWINKLE<sup>(7)</sup> (described in Section 14D.10.7) is used for the average core transient analysis. This code solves the two group neutron diffusion theory kinetic equations in one, two or three spatial dimensions (rectangular coordinates) for six delayed neutron groups and up to 2,000 spatial points. The computer code includes a detailed multiregion, transient fuel-clad-coolant heat transfer model, for calculation of pointwise Doppler and moderator feedback effects. In this analysis, the code is used primarily as a one dimensional axial kinetics code since it allows a more realistic representation of the spatial effects of axial moderator feedback and rod cluster control assembly movement and the elimination of axial feedback weighting factors. However, since the radial dimension is missing, it is still necessary to employ very conservative methods (described below) of calculating the ejected rod worth and hot channel factor.

### Hot Spot Analysis

The average core energy addition, calculated as described above, is multiplied by the appropriate hot channel factors, and the hot spot analysis is performed using a detailed fuel and clad transient heat transfer computer code, FACTRAN<sup>(8)</sup>. This computer code calculates the transient temperature distribution in a cross section of a metal clad UO<sub>2</sub> fuel rod, and the heat flux at the surface of the rod, using as input the nuclear power versus time and the local coolant conditions. The local coolant conditions before the start of the transient are input to the code. This consists of the system pressure, flow rate and bulk coolant temperature and corresponding density appropriate to the power level. Due to the excellent heat transfer, the fuel and clad temperature is not particularly sensitive to these parameters. The zirconium-water reaction is explicitly represented, and all material properties are represented as functions of temperature. A parabolic radial power distribution is used within the fuel rod.

FACTRAN uses the Dittus-Boelter or Jens-Lottes correlation to determine the film heat transfers before DNB, and the Bishop-Sandberg-Tong correlation<sup>(9)</sup> to determine the film boiling coefficient after DNB.

The Dittus-Boelter correlation is used to compute the forced convection heat transfer coefficient before DNB. At the same time, the Jens-Lottes correlation is used to compute the surface temperature to support local boiling. The code automatically switches to this mode of heat transfer when the surface temperature reaches the local boiling surface temperature. The DNB heat flux is not calculated; instead, the code is forced into DNB by specifying a conservative DNB heat flux.

After DNB, the computer code automatically computes water properties at the film temperature for input to the film boiling heat transfer correlation. In the correlation, the film temperature is defined as the average between the clad surface and bulk coolant temperatures. The metal-water exothermic reaction is taken into account by conservatively using the Baker-Just parabolic rate equation to compute the amount of reacted material and adding the heat generation as a source term in the clad. The gap heat transfer coefficient may be calculated by the code; however, it is adjusted in order to force the full power steady state temperature distribution to agree with that predicted by design fuel transfer codes presently used by Westinghouse. The transient gap heat transfer coefficient is conservatively assumed to increase linearly from its initial value to 10,000 BTU/hr-ft<sup>2</sup> in one half second, even though more detailed calculations indicate gap closure is not expected. This leads to conservatively high clad temperatures while not significantly affecting the fuel centerline temperature.

For full power cases, the design initial hot channel factor ( $F(T,Q)$ ) is input to the code. The hot channel factor during the transient is assumed to increase from the steady state design value to the maximum transient value in 0.1 seconds, and remain at the maximum for the duration of the transient. This is conservative, since detailed spatial kinetics models show that the hot channel factor decreases shortly after the nuclear power peak due to power flattening caused by preferential feedback in the hot channel<sup>(6)</sup>. Further description of FACTRAN appears in Section 14D.10.1.

### System Overpressure Analysis

Because safety limits for fuel damage specified earlier are not exceeded, there is little likelihood of fuel dispersal into the coolant. The pressure surge may therefore be calculated on the basis of conventional heat transfer from the fuel and prompt heat generation in the coolant.

The pressure surge is calculated by first performing the fuel heat transfer calculation to determine the average and hot spot heat flux versus time. Using this heat flux data, a THINC calculation is conducted to determine the volume surge. Finally, the volume surge is simulated in a plant transient computer code. This code calculates the pressure transient taking into account fluid transport in the system, heat transfer to the steam generators, and the action of the pressurizer spray and pressure relief valves. No credit is taken for the possible pressure reduction caused by the assumed failure<sup>(6)</sup> of the control rod pressure housing.

#### 14.2.6.2.1 Calculation of Basic Parameters

Input parameters for the analysis are conservatively selected on the basis of values calculated for this type of core. The more important parameters are discussed below. Table 14.2-3 presents the parameters used in this analysis.

### Ejected Rod Worths and Hot Channel Factors

The values for ejected rod worths and hot channel factors are calculated using a synthesis of one dimensional and two dimensional calculations. Standard nuclear design codes are used in the analysis. No credit is taken for the flux flattening effects of reactivity feedback. The calculation is performed for the maximum allowed bank insertion at a given power level, as determined by the rod insertion limits. Adverse Xenon distributions are considered in the calculation.

The total transient hot channel factor,  $F(T,Q)$ , is then obtained by combining the axial and radial factors.

The method of analysis employed assumes the hot channel factor is constant at its peak value for the duration of the hot spot transient analysis and is therefore not affected by scram time. The peak value is determined by a steady-state analysis without regard to the beneficial effects of feedback.

Appropriate margins are added to the results to allow for calculational uncertainties, including an allowance for nuclear power peaking due to densification.

### Reactivity Feedback Weighting Factors

The largest temperature rises, and hence the largest reactivity feedbacks occur in channels where the power is higher than average. Since the weight of a region is dependent on flux, these regions have high weights. This means that the reactivity feedback is larger than that indicated by a simple channel analysis. Physics calculations are carried out for temperature changes with a flat temperature distribution, and with a large number of axial and radial temperature distributions. Reactivity changes are compared and effective weighting factors determined. These weighting factors take the form of multipliers which when applied to single channel feedbacks correct them to effective whole core feedbacks for the appropriate flux shape. In this analysis, since a one dimensional (axial) spatial kinetics method is employed, the axial weighting is not used. In addition, no weighting is applied to the moderator feedback. A conservative radial weighting factor is applied to the transient fuel temperature to obtain an effective fuel temperature as a function of time accounting for the missing spatial dimension. These weighting factors are shown to be conservative compared to three dimensional analysis.<sup>(6)</sup>

### Moderator and Doppler Coefficient

The critical boron concentrations at the beginning of life and end of life were adjusted in the nuclear code in order to obtain moderator density coefficient curves which are conservative compared to actual design conditions for the plant. As discussed above, no weighting factor is applied to these results.

The Doppler reactivity defect is determined as a function of power level using the one dimensional steady state computer code with a Doppler weighting factor of 1.0. The resulting curve is conservative compared to design predictions for this plant. The Doppler weighting factor should be larger than 1.0, just to make the present calculation agree with design predictions before ejection. This weighting factor will increase under accident conditions, as discussed above. The transient weighting factor used in the analysis is presented in Table 14.2-3.

### Delayed Neutron Fraction

Calculations of the effective delayed neutron fraction ( $\beta_{\text{eff}}$ ) typically yield values of 0.70 percent at beginning of life and 0.50 percent at end of life for the first cycle. The accident is sensitive to  $\beta_{\text{eff}}$  if the ejected rod worth is nearly equal to or greater than  $\beta_{\text{eff}}$  as in zero power transients. In order to allow for future fuel cycles, pessimistic estimates of  $\beta_{\text{eff}}$  of 0.55 percent at beginning of cycle and 0.47 percent at end of cycle were used in the analysis.

### Trip Reactivity Insertion

The trip reactivity insertion is assumed to be 4 percent from hot full power and 2 percent from hot zero power including the effect of one stuck rod. These values are reduced by the ejected rod reactivity. The shutdown reactivity was simulated by dropping a rod of the required depth into the core. The start of rod motion occurred 0.5 seconds after the high neutron flux trip point is reached. This delay is assumed to consist of 0.2 second for the instrument channel to produce a signal, 0.15 second for the trip breaker to open and 0.15 second for the coil to



release the rods. The analyses presented are applicable for a rod insertion time of 2.7 seconds from coil release to entrance to the dash pot. The choice of such a conservative insertion rate means that there is over 1 second after the trip point is reached before significant shutdown reactivity is inserted into the core. This is a particularly significant conservatism for hot full power accidents.

The rod insertion versus time is described in Section 14D.5.

#### 14.2.6.2.2 Results

The values of the parameters used in the analysis, as well as the results of the analysis, are presented in Table 14.2-3 and discussed below.

##### Beginning of Cycle, Full Power

Control bank D was assumed to be inserted to its insertion limit. The worst ejected rod worth and hot channel factor were .20 percent  $\Delta k$  and 7.11 respectively. The peak fuel enthalpy was 313.4 Btu/lb (174.1 cal/gm). The peak hot spot fuel center temperature exceeded the beginning of life melt temperature of 4,900°F. However, melting was restricted to less than 10 percent of the pellet.

##### Beginning of Cycle, Zero Power

For this condition, control bank D was assumed to be fully inserted and B and C were at their insertion limits. The worst ejected rod is located in control bank D and has a worth of 0.7 percent  $\Delta k$  and a hot channel factor of 10.0. The peak fuel enthalpy reached 173.9 Btu/lb (96.6 cal/gm). The peak fuel centerline temperature was 2,868°F.

##### End of Cycle, Full Power

Control bank D was assumed to be inserted to its insertion limit. The ejected rod worth and hot channel factors were 0.21 percent  $\Delta k$  and 7.6 respectively. This resulted in a peak fuel enthalpy of 300.9 Btu/lb (167.2 cal/gm). The peak hot spot fuel centerline temperature exceeded the end of life melt 4,800°F. However, melting was restricted to less than 10 percent of the pellet. The variation in melt temperature with burnup is discussed in Section 3.4.1.2.

##### End of Cycle, Zero Power

The ejected rod worth and hot channel factor for this case were obtained assuming control bank D to be fully inserted and bank B and C at their insertion limits. The results were 1.0 percent  $\Delta k$  and 25.0 respectively. The peak fuel enthalpy and fuel center temperatures were 304.4 Btu/lb (169.1 cal/gm) and 4,420°F, respectively.

A summary of the cases presented above is given in Table 14.2-3. The nuclear power and hot spot fuel and clad temperature transients for the worst cases (BOL full power and EOL zero power) are presented in Figures 14.2-11, 14.2-12, 14.2-13, and 14.2-14.

The calculated sequence of events for the rod ejection accidents, as shown in Figure 14.2-11, 14.2-12, 14.2-13 and 14.2-14, are presented in Table 14.2-2. For all cases, reactor trip occurs very early in the transient, after which the nuclear power excursion is terminated. The reactor will remain subcritical following reactor trip.

#### Fission Product Release

It is assumed that fission products are released from the gaps of all rods entering DNB. This gap activity is postulated because it is conservatively assumed that any rod entering DNB is experiencing clad rupture, although no actual clad failure is expected to occur. In all cases considered, less than 10 percent of the rods experience such assumed damage based on a detailed 3 dimensional THINC analysis. Although limited fuel melting at the hot spot was predicted for the full power cases, in practice melting is not expected since the analysis is conservatively assumed that the hot spots before and after ejection were coincident.

#### Pressure Surge

A detailed calculation of the pressure surge for an ejection worth 1 dollar at BOL, hot full power, indicates the peak pressure does not exceed that which would cause stress to exceed the faulted condition stress limits.<sup>(6)</sup> Since the severity of the present analysis does not exceed this "worst case" analysis, the accident for this plant will not result in an excessive pressure rise or further damage to the Reactor Coolant System.

#### Lattice Deformations

A large temperature gradient will exist in the region of the hot spot. Since the fuel rods are free to move in the vertical direction, differential expansion between separate rods cannot produce distortion. However, the temperature gradients across individual rods may produce a force tending to bow the midpoint of the rods toward the hot spot. Physics calculations indicate that the net result of this would be a negative reactivity insertion. In practice, no significant bowing is anticipated, since the structural rigidity of the core is more than sufficient to withstand the forces produced. Boiling in the hot spot region would produce a net flow away from that region. However, the heat from the fuel is released to the water relatively slowly, and it is considered inconceivable that cross flow will be sufficient to produce significant lattice forces. Even if massive and rapid boiling, sufficient to distort the lattice, is hypothetically postulated, the large void fraction in the hot spot region would produce a reduction in the total core moderator to fuel ratio, and a large reduction in this ratio at the hot spot. The net effect would therefore, be a negative feedback. It can be concluded that no conceivable mechanism exists for a net positive feedback resulting from lattice deformation. In fact, a small negative feedback may result. The effect is conservatively ignored in the analyses.

#### 14.2.6.3 Conclusions - Thermal Analysis

Reference 6 shows limiting hot channel factors for a given reactivity insertion which meet the limiting criteria of Section 14.2.6.1.2. The peak hot channel factors obtained for the RCCA incidents in Section 14.2.6.2.3 are all below the limiting hot channel factors and thus meet all of ANS Condition IV acceptance criteria.

Even on a pessimistic basis, the analyses indicated that the described fuel and clad limits are not exceeded. It is concluded that there is no danger of sudden fuel dispersal into the coolant. Since the peak pressure does not exceed that which would cause stresses to exceed the faulted condition stress limits, it is concluded that there is no danger of further consequential damage to the primary circuit. The analyses have demonstrated that upper limit on fission product release as a result of a number of fuel rods entering DNB amounts to 10 percent.

#### 14.2.6.4 Radiological Consequences

The site boundary and control room doses due to airborne activity releases following a RCCA ejection accident are calculated by computer code PERC2<sup>(34)</sup>. The analysis is performed at a core power level of 2918 MWt and with the Alternative Source Term (AST) methodology. The guidance provided in Regulatory Guide 1.183<sup>(33)</sup> is followed in the radiological assessment. PERC2 is a multiple compartment activity transport code which calculates the Committed Effective Dose Equivalent (CEDE) from Inhalation and the Deep Dose Equivalent (DDE) from submersion due to halogens, noble gases and other nuclides at the offsite locations and in the control room. The Total Effective Dose Equivalent (TEDE) is the sum of CEDE and DDE. The dose calculation model is described in Appendix 14B and is consistent with the regulatory guidance.

The worst 2-hour period dose at the Exclusion Area Boundary (EAB), the dose at the Low Population Zone (LPZ) for the duration of the release, and the 0 to 30-day dose to an operator in the control room due to inhalation and submersion are calculated based on postulated airborne radioactivity releases. The atmospheric dispersion factors from various activity release paths to the control room intakes are calculated using the latest version of the "Atmospheric Relative Concentrations in Building Wakes" (ARCON96) methodology<sup>(35)</sup> and are presented in Table 2.2-12a and Table 2.2-12b. Table 14.2-12 lists the key assumptions/parameters utilized to develop the radiological consequences following the RCCA ejection accident. The analysis is intended to cover a RCCA ejection in either unit of BVPS, so the bounding parameters are listed in the Table.

The acceptance criteria for the EAB and LPZ doses for a RCCA ejection event are based on 10 CFR Part 50 paragraph 50.67<sup>(36)</sup> and Section 4.4 Table 6 of Regulatory Guide 1.183<sup>(33)</sup>:

In accordance with guidance provided in RG 1.183, two independent release paths to the environment are analyzed:

Scenario 1: The failed/melted fuel resulting from a postulated RCCA ejection is released into the RCS, which is released in its entirety into the containment via the ruptured control rod drive mechanism housing, is mixed in the free volume of the containment, and then released at containment technical specification leak rate. Environmental releases are assumed to occur via the containment wall.

Scenario 2: The failed/melted fuel resulting from a postulated RCCA ejection is released into the RCS which is then transmitted to the secondary side via steam generator tube leakage. The condenser is assumed to be unavailable due to a loss of offsite power. Environmental releases occur from the steam generators via the MSSVs and the ADVs.

For the RCCA ejection event, less than 10% of the fuel rods are damaged due to thermal transients. The analysis also conservatively assumes that 0.25% of the core fuel melts. To account for differences in power level across the core, a design radial peaking factor of 1.75 was applied in determining the inventory of the damaged rods. The equilibrium fuel cycle core inventory at a power level of 2918 MWt, calculated by SCALE4.3-ORIGEN-S computer code<sup>(37)</sup> and listed in Table 14B-1a, is used to calculate the offsite and control room doses.

In accordance with Regulatory Guide 1.183, the gap activity is assumed to be composed of 10% of the core noble gas and 10% of the core halogens associated with the percentage of fuel that has failed. Depending on the release pathway, the composition of the melted fuel is varied. For the containment leakage pathway, the melted fuel activity released is assumed to be composed of 100% of the core noble gas and 25% of the core halogens associated with the percentage of fuel that has melted. For the Secondary System Release pathway the melted fuel activity released is composed of 100% of the core noble gas and 50% of the core halogens associated with the percentage of fuel that has melted.

The chemical composition of the iodine in the gap/melted fuel is assumed to be 95% CsI, 4.85% elemental and 0.15% organic. However, because the sump pH is not controlled following a RCCA ejection, it is conservatively assumed that the iodine released via the containment leakage pathway has the same composition as the iodine released via the secondary system release pathway; i.e., it is assumed that for both scenarios, 97% of all halogens available for release to the environment are elemental, while the remaining 3% is organic.

#### Scenario 1: Transport from the Containment

The failed/melted fuel activity released due to a RCCA ejection into the RCS is assumed to be instantaneously released into the containment where it mixes homogeneously in the containment free volume. The containment is assumed to leak at the Technical Specification leak rate of  $0.001 \text{ day}^{-1}$  for the first 24 hours and at half that value for the remaining 29 days after the event. Except for decay, no credit is taken for depleting the halogen (or noble gas) concentrations airborne in the containment. No credit is taken for processing the containment leakage via the safety related ventilation exhaust and filtration system that services the areas contiguous to containment; i.e., the Supplementary Leak Collection and Release System (SLCRS) filters. To ensure bounding values, the atmospheric dispersion factors utilized for the containment release path reflects the worst value between the containment wall release point and the SLCRS release point for each time period.

#### Scenario 2: Transport from the Secondary System

The failed or melted fuel activity released due to a RCCA ejection into the RCS is assumed to be instantaneously and homogeneously mixed in the reactor coolant system and transmitted to the secondary side via primary to secondary steam generator (SG) tube leakage assumed to be at the Technical Specification value of 150 gpd (at STP) from each steam generator (450 gpd total). The primary to secondary leakage terminates at 2500 seconds after the event when primary pressure is below secondary pressure. At BVPS, the SG tubes remain covered for the duration of the event; therefore, per Regulatory Guide 1.183, the gap/fuel iodines have a partition coefficient of 100 in the SG. The gap noble gases are released freely to the environment without retention in the SG. The condenser is assumed unavailable due to a

coincident loss of offsite power. Consequently, the radioactivity release resulting from a RCCA ejection is discharged to the environment from the steam generators via the MSSVs and the ADVs. The SG releases continue until shutdown cooling is initiated via operation of the RHR system and environmental releases are terminated.

Per the regulatory requirement, the 2-hour EAB dose must reflect the worst case 2-hour activity release period following the RCCA ejection event.

The activity associated with the release of secondary steam/liquid, and primary to secondary leakage of normal operation RCS, (both at Technical Specification levels) via the MSSVs/ADVs are insignificant compared to the failed fuel release, and are therefore not included in this assessment.

The calculated doses are provided in Table 14.1-1B following a RCCA ejection event in an atmospheric containment are all within the regulatory limit of 6.3 rem TEDE specified in 10 CFR 50.67<sup>(36)</sup>. The control room doses following a RCCA ejection are presented in Table 14.1-1A.

#### 14.2.7 Single Reactor Coolant Pump Locked Rotor

##### 14.2.7.1 Identification of Causes and Accident Description

The accident postulated is an instantaneous seizure of a reactor coolant pump rotor. Flow through the affected reactor coolant loop is rapidly reduced, leading to an initiation of a reactor trip on a low flow signal.

Following initiation of the reactor trip heat stored in the fuel rods continues to be transferred to the coolant causing the coolant to expand. At the same time, heat transfer to the shell side of the steam generators is reduced, first because the reduced flow results in a decreased tube side film coefficient and then because the reactor coolant in the tubes cools down while the shell side temperature increases (turbine steam flow is reduced to zero upon plant trip). The rapid expansion of the coolant in the reactor core, combined with reduced heat transfer in the steam generators causes an insurge into the pressurizer and a pressure increase throughout the Reactor Coolant System. The insurge into the pressurizer compresses the steam volume, actuates the automatic spray system, opens the power operated relief valves, and opens the pressurizer safety valves, in that sequence. The three power operated relief valves are designed for reliable operation and would be expected to function properly during the accident. However, for conservatism, their pressure reducing effect as well as the pressure reducing effect of the spray is not included in the analysis. This event is classified as an ANS Condition IV incident.

#### 14.2.7.2 Analysis of Effects and Consequences

##### 14.2.7.2.1 Method of Analysis

Two locked rotor cases are analyzed; they are:

1. Peak RCS pressure resulting from a locked rotor in one-of three loops
2. Number of rods-in-DNB resulting from a locked rotor in one-of three loops

The first case is aimed at maximizing the RCS pressure transient. This is done using the Standard Thermal Design Procedure. Thermal Design Flow is assumed. Initial core power, reactor coolant temperature and pressure are assumed to be at their maximum values consistent with full-power conditions including allowances for calibration and instrument errors (i.e., initial power includes a 0.6% power calorimetric uncertainty, initial pressure includes a +40 psi uncertainty and initial RCS vessel average temperature includes a +8.5°F uncertainty). These assumptions result in a conservative calculation of the coolant insurge into the pressurizer, which in turn results in a maximum calculated peak RCS pressure. The pressure response shown in Figure 14.2-16 is the pressure response at the point in the RCS having the maximum pressure (e.g., RCP outlet).

The peak pressure case is analyzed using two digital computer codes. The LOFTRAN Code (Reference 11) is used to calculate the resulting loop and core flow transients following the pump seizure, the time of reactor trip based on the loop flow transients, the nuclear power following reactor trip, and the peak RCS pressure. The thermal behavior of the fuel located at the core hot spot is calculated using the FACTRAN Code, (Reference 8) which uses the core flow and nuclear power calculated by LOFTRAN. The FACTRAN Code includes a film boiling heat transfer coefficient.

The second case is an evaluation of DNB in the core during the transient. This case is analyzed using the Revised Thermal Design Procedure (Reference 28). Initial core power is assumed to be at its nominal value consistent with steady-state, full-power operation. RCS pressure is at its nominal value and RCS vessel average temperature is at its nominal value plus a 4.5°F bias. Uncertainties in initial conditions are included in the limit DNBR as described in Reference 28.

The rods-in-DNB case is analyzed using two digital computer codes, LOFTRAN and VIPRE. The LOFTRAN Code (Reference 11) is used in the same manner as in the peak pressure case described above. The VIPRE Code (References 38) is used to calculate the core heat flux and DNBR during the transient based on the nuclear power and core flow from LOFTRAN.

The analysis for the peak RCS pressure case assumes a zero moderator temperature coefficient (MTC) and a conservatively large (absolute value) of the Doppler-only power coefficient; the analysis for the rods-in-DNB case assumes an MTC of -3 pcm/°F. The negative reactivity from control rod insertion/scram for both cases is based on 4.0%  $\Delta k/k$  trip reactivity from hot full power.

In both cases the analysis is performed to bound operation with steam generator tube plugging levels up to 22% (maximum loop-to-loop plugging difference of 10%) with a maximum loop-to-loop flow asymmetry of 5%.

### Evaluation of the Pressure Transient

After pump seizure, the neutron flux is rapidly reduced by control rod insertion effect. Rod motion is assumed to begin one second after the flow in the affected loop reaches 87 percent of nominal flow. The time delay of 1.0 second used in connection with the low flow reactor trip is a very conservative allowance for the total time delay between the time the flow reaches 87 percent of nominal and the time the rods begin moving into the core. This total includes individual delays associated with the following: flow sensors/transmitters, solid state protection system input relays, solid state protection system, voltage drop on reactor trip breaker undervoltage and control rod gripper release. No credit is taken for the pressure reducing effect of the pressurizer relief valves, pressurizer spray, steam dump or controlled feedwater flow after plant trip.

Although these operations are expected to occur and would result in a lower peak pressure, an additional degree of conservatism is provided by ignoring their effect.

The pressurizer safety valves are actuated at 2,580 psia and their capacity for steam relief is as stated in Table 4.1-8. An additional delay (1.05 seconds) is included to account for the water filled loop seals and the pilot.

### Evaluation of the Effects of DNB in the Core During the Accident

For this accident, DNB is assumed to occur in the core and, therefore, an evaluation of the consequences with respect to fuel rod thermal transients is performed. Results obtained from analysis of this "hot spot" condition represent the upper limit with respect to clad temperature and zirconium water reaction.

In the evaluation, the rod power at the hot spot is conservatively assumed to be 2.52 times the average rod power (i.e.,  $F(Q) = 2.52$ ) at the initial core power level. The number of rods in DNB was conservatively calculated to not exceed 0 percent of the total rods in the core, i.e., no fuel rods are calculated to experience a DNBR less than the limit value.

### Film Boiling Coefficient

The film boiling coefficient is calculated in the FACTRAN code using the Bishop-Sandberg-Tong film boiling correlation. The fluid properties are evaluated at film temperature (average between wall and bulk temperatures). The program calculates the film coefficient at every time step based upon the actual heat transfer conditions at the time. The neutron flux, system pressure, bulk density and mass flow rate as a function of time are used as program input.

For this analysis, the initial values of the pressure and the bulk density are used throughout the transient since they are the most conservative with respect to clad temperature response. For conservatism, DNB was assumed to start at the beginning of the accident.

### Fuel Clad Gap Coefficient

The magnitude and time dependence of the heat transfer coefficient between fuel and cladding (gap coefficient) has a pronounced influence on the thermal results. The larger the value of the gap coefficient, the more heat is transferred between pellet and clad. Based on investigations on the effect of the gap coefficient upon the maximum clad temperature during the transient, the gap coefficient was assumed to increase from steady state value consistent with the initial fuel temperature to 10,000 Btu/hr-ft<sup>2</sup>°F at the initiation of the transient. This assumption causes energy stored in the fuel to be released to the clad at the initiation of the transient and maximizes the clad temperature during the transient.

### Zirconium-Steam Reaction

The zirconium-steam reaction can become significant above 1,800°F (clad temperature). The Baker-Just parabolic rate equation shown below is used to define the rate of the zirconium steam reaction.

$$\frac{d(w^2)}{dt} = 33.3 \times 10^6 \exp\left(\frac{-45,500}{1.986T}\right)$$

where:

w = amount reacted (mg/cm<sup>2</sup>)  
 t = time (sec)  
 T = temperature (K)  
 The reaction heat is 1,510 cal/gm

The effect of zirconium-steam reaction is included in the calculation of the "hot spot" cladding temperature transient.

#### 14.2.7.2.2 Locked Rotor Results

The transient results without offsite power available are shown in Figures 14.2-15, 14.2-16, 14.2-17, and 14.2-18. The results of these calculations are also summarized in Table 14.2-4a. The peak Reactor Coolant System pressure reached during the transient is less than that which would cause stresses to exceed the faulted condition stress limits. Also, the peak clad surface temperature is considerably less than 2375°F (the limit associated with Optimized ZIRLO™ cladding). It should also be noted that the clad temperature was conservatively calculated assuming that DNB occurs at the initiation of the transient.

The calculated sequence of events is shown on Table 14.2-4a. With the reactor tripped, a stable plant will eventually be attained. Normal plant shutdown may then proceed.

### Conclusions

1. Since the peak Reactor Coolant System pressure reached during any of the transients is less than that which would cause stresses to exceed the faulted condition stress limits, the integrity of the primary coolant system is not endangered.



2. Since the peak clad surface temperature calculated for the hot spot during the worst transient remains considerably less than 2375°F and the amount of Zirconium-water reaction is small and the core will remain in place and intact with no consequential loss of core cooling capability.

### Radiological Consequences

The site boundary and control room doses due to airborne activity releases following a Locked Rotor Accident (LRA) are calculated by computer code PERC2<sup>(34)</sup>. The analysis is performed at a core power level of 2918 MWt and with the Alternative Source Term (AST) methodology. The guidance provided in Regulatory Guide 1.183<sup>(33)</sup> is followed in the radiological assessment. PERC2 is a multiple compartment activity transport code which calculates the Committed Effective Dose Equivalent (CEDE) from Inhalation and the Deep Dose Equivalent (DDE) from submersion due to halogens, noble gases and other nuclides at the offsite locations and in the control room. The Total Effective Dose Equivalent (TEDE) is the sum of CEDE and DDE. The dose calculation model is described in Appendix 14B and is consistent with the regulatory guidance.

The worst 2-hour period dose at the Exclusion Area Boundary (EAB), the dose at the Low Population Zone (LPZ) for the duration of the release, and the 0 to 30-day dose to an operator in the control room due to inhalation and submersion are calculated based on postulated airborne radioactivity releases. The atmospheric dispersion factors from various activity release paths to the control room intakes are calculated using the latest version of the "Atmospheric Relative Concentrations in Building Wakes" (ARCON96) methodology<sup>(35)</sup> and are presented in Table 2.2-12a and Table 2.2-12b. Table 14.2-4b lists the key assumptions/parameters utilized to develop the radiological consequences following the LRA. The analysis is intended to cover a LRA in either unit of BVPS, so the bounding parameters are listed in the Table.

The acceptance criteria for the EAB and LPZ doses for a LRA are based on 10 CFR Part 50 paragraph 50.67<sup>(36)</sup> and Section 4.4 Table 6 of Regulatory Guide 1.183<sup>(33)</sup>:

A BVPS LRA results in less than 20% failed fuel and a release of the associated gap activity (note that the BVPS-1 thermal-hydraulic analysis discussed in Section 14.2.7.2.1 demonstrates a result of 0% failed fuel and the BVPS-2 result of 20% failed fuel is bounding for dose analyses). The gap activity (consisting of noble gases, halogens and alkali metals) are instantaneously and homogeneously mixed in the reactor coolant system and transmitted to the secondary side via primary to secondary steam generator tube leakage assumed to be at the value of 450 gpd at STP. There is no fuel melting assumed.

A radial peaking factor of 1.75 is applied to the activity release. The chemical form of the iodines in the gap are assumed to be 95% CsI, 4.85% elemental and 0.15% organic. At BVPS, the SG tubes remain submerged for the duration of the event; therefore, the gap iodines are assumed to have a partition coefficient of 100 in the SG. The iodine releases from the SG are assumed to be 97% elemental and 3% organic. The gap noble gases are assumed to be released freely to the environment without retention in the SG, whereas the particulates are carried over in accordance with the design basis SG moisture carryover fraction.

The condenser is assumed unavailable due to a coincident loss of offsite power. Consequently, the radioactivity release resulting from a LRA is discharged to the environment from the steam generators via the MSSVs and the ADVs. The SG releases continue for 8 hours, at which time

shutdown cooling is initiated via operation of the RHR system, and environmental releases are terminated.

The activity associated with the release of secondary steam and liquid, and primary to secondary leakage of normal operation RCS, (both at Technical Specification activity limits) via the MSSVs/ADVs is insignificant compared to the failed fuel release, and are therefore not included in this assessment.

#### Accident Specific Control Room Model Assumptions

The control room is conservatively assumed to remain in the normal operation mode. The most limiting atmospheric dispersion factors between the MSSVs/ADVs at each unit relative to the two control room intakes (identified for purposes of assessment as the BVPS-1 MSSVs/ADVs to the BVPS-1 control room intake) is selected to determine a bounding control room dose.

#### Results

AST methodology requires that the worst case dose to an individual located at any point on the boundary at the EAB, for any 2-hour period following the onset of the accident be reported as the EAB dose. Regardless of the starting point of the worst 2 hour window, the 0-2 hour EAB X/Q is utilized.

The calculated doses in Table 14.1-1B remain within the regulatory limit of 2.5 rem TEDE specified in 10CFR50.67<sup>(36)</sup>. The control room dose is within the regulatory limit of 5 rem TEDE specified in 10CFR50.67, and is presented in Table 14.1-1A.

### 14.2.8 Inadvertent Loading of a Fuel Assembly into an Improper Position

#### 14.2.8.1 Identification of Causes and Accident Description

Fuel and core loading errors, such as can arise from the inadvertent loading of one or more fuel assemblies into improper positions, loading a fuel rod during manufacture with one or more pellets of the wrong enrichment, or the loading of a full fuel assembly during manufacture with pellets of the wrong enrichment, will lead to increased heat fluxes if the error results in placing fuel in core positions calling for fuel of lesser enrichment. Also included among possible core loading errors is the inadvertent loading of one or more fuel assemblies requiring burnable poison rods into a new core without burnable poison rods.

Any error in enrichment, beyond the normal manufacturing tolerances, can cause power shapes which are more peaked than those calculated with the correct enrichments. The incore system of moveable flux detectors which is used to verify power shapes at the start of life is capable of revealing any assembly enrichment error or loading error which causes power shapes to be peaked in excess of the design value.

To reduce the probability of core loading errors, each fuel assembly is marked with an identification number and loaded in accordance with a core loading diagram. After core loading, the identification numbers are verified for every assembly in the core.

The power distortion due to any combination of misplaced fuel assemblies would significantly raise peaking factors and would be readily observable with in-core flux monitors. In addition to the flux monitors, thermocouples are located at the outlet of about one-third of the fuel assemblies in the core. There is a high probability that these thermocouples would also indicate any abnormally high coolant enthalpy rise. In-core flux measurements are taken during the startup subsequent to every refueling operation.

#### 14.2.8.2 Analysis of Effects and Consequences

##### 14.2.8.2.1 Method of Analysis

Steady state power distribution in the x-y plane of the core are calculated using the TURTLE<sup>(12)</sup> code based on macroscopic cross section calculated by the LEOPARD<sup>(13)</sup> code. A discrete representation is used wherein each individual fuel rod is described by a mesh interval. The power distributions in the x-y plane for a correctly loaded core are also given in Section 3 based on enrichments given in that section.

For each core loading error case analyzed, the percent deviations from detector readings for a normally loaded core are shown at all in-core detector locations (Figures 14.2-25, 14.2-26, 14.2-27, 14.2-28 and 14.2-29).

##### 14.2.8.2.2 Results (Historical Information)

The following core loading error cases have been analyzed:

###### Case A:

Case in which a Region 1 fuel assembly is interchanged with a Region 3 assembly. The particular case considered was the interchange of two adjacent assemblies near the periphery of the core (Figure 14.2-25).

###### Case B:

Case in which a Region 1 fuel assembly is interchanged with a neighboring Region 2 fuel assembly. Two analyses have been performed for this case (Figures 14.2-26 and 14.2-27). In Case B-1, the interchange is assumed to take place with the burnable poison rods transferred with the Region 2 assembly mistakenly loaded into Region 1.

In Case B-2, the interchange is assumed to take place closer to core center and with burnable poison rods located in the correct Region 2 position, but in a Region 1 assembly mistakenly loaded into the Region 2 position.

###### Case C:

Enrichment error: Case in which a Region 2 fuel assembly is loaded in the core central position (Figure 14.2-28).

Case D:

Case in which a Region 2 fuel assembly instead of a Region 1 assembly is loaded near the core periphery (see Figure 14.2-29).

#### 14.2.8.3 Conclusions

Fuel assembly enrichment errors would be prevented by administrative procedures implemented in fabrication.

In the event that a single pin or pellet has a higher enrichment than the nominal value, the consequences in terms of reduced DNBR and increased fuel and clad temperatures will be limited to the incorrectly loaded pin or pins.

Fuel assembly loading errors are prevented by administrative procedures implemented during core loading. In the unlikely event that a loading error occurs, analyses in this section confirm that resulting power distribution effects will either be readily detected by the in-core moveable detector system or will cause a sufficiently small perturbation to be acceptable within the uncertainties allowed between nominal and design power shapes.

#### 14.2.9 Complete Loss of Forced Reactor Coolant Flow

##### 14.2.9.1 Accident Description

A complete loss of forced reactor coolant flow may result from a simultaneous loss of electrical power supply or a reduction in power supply frequency to all reactor coolant pumps. If the reactor is at power at the time of the accident, the immediate effect of loss-of-coolant flow is a rapid increase in the coolant temperature. This increase could result in DNB with subsequent fuel damage if the reactor were not tripped promptly. This event is classified as an ANS Condition III incident. The following provide necessary protection against a loss-of-coolant flow accident:

1. Undervoltage or underfrequency on reactor coolant pump power supply busses
2. Low reactor coolant loop flow
3. Overpower  $\Delta T$  reactor trip function.

The reactor trip on reactor coolant pump bus undervoltage is provided to protect against conditions which can cause a loss of voltage to all reactor coolant pumps, i.e., station blackout. However, due to the possibility of a common mode failure in the cabinets containing the circuitry, the undervoltage and underfrequency reactor trip functions may not be available. The undervoltage and underfrequency trip functions are blocked below approximately 10 percent power (Permissive P-7). If the undervoltage and underfrequency reactor trips were not available, the low reactor coolant flow trip is available to provide the reactor trip function. Reactor protection system diversity is provided by the overpower  $\Delta T$  reactor trip function.

The reactor trip on reactor coolant pump underfrequency is provided to open the reactor coolant pump breaker and trip the reactor for an underfrequency condition, resulting from frequency disturbances on the major power grid. The trip disengages the reactor coolant pumps from the power grid so that the pump kinetic energy is available for full coastdown. If the maximum grid frequency decay rate is less than approximately 5 Hz/sec., this trip function will protect the core from underfrequency events without requiring tripping of the reactor coolant pump breakers. Reference 17 provides analyses of grid frequency disturbances and the resulting nuclear steam supply system protection requirements which are generally applicable.

The reactor trip on low primary coolant loop flow is provided to protect against loss of flow conditions which affect only one reactor coolant loop. It also serves as a backup to the undervoltage and underfrequency trips. This function is generated by two out of three low flow signals per reactor coolant loop. Above approximately 30 percent power (Permissive 8), low flow in any loop will actuate a reactor trip. Between approximately 10 percent power and 30 percent power (Permissive 7 and Permissive 8), low flow in any two loops will actuate a reactor trip.

Normal power for the reactor coolant pumps is supplied through busses from a transformer connected to the generator. Each pump is on a separate bus. When generator trip occurs, the busses are automatically transferred to a transformer supplied from external power lines, and the pumps will continue to supply coolant flow to the core. Following any turbine trip, where there are no electrical faults which require tripping the generator from the network, the generator remains connected to the network for approximately 30 seconds. The reactor coolant pumps remain connected to the generator thus ensuring full flow for 30 seconds after the reactor trip before any transfer is made.

#### 14.2.9.2 Method of Analysis

The complete loss of flow transient has been analyzed for a loss of all three reactor coolant pumps with three loops in operation. The analysis assumes a common mode failure which results in the unavailability of the undervoltage and underfrequency reactor trips. Thus, the low reactor coolant loop flow reactor trip is the primary reactor trip function for the complete loss of flow analysis. These transients are analyzed using three digital computer codes: LOFTRAN, FACTRAN and VIPRE. First, the LOFTRAN Code (Reference 11) is used to calculate the loop and core flow during the transient, the time of reactor trip based on the calculated flows, the nuclear power transient, and the primary system pressure and temperature transients. The FACTRAN Code (Reference 8) is then used to calculate the heat flux transient based on the nuclear power and flow from LOFTRAN. The VIPRE Code (Reference 38) is used to calculate the DNBR during the transient based on the heat flux from FACTRAN and the flow from LOFTRAN. The DNBR transient presented is the minimum of the typical or thimble cell.

The complete loss of flow event results in a loss of forced reactor coolant flow to all loops. Hence, the modeling of initial asymmetric loop-to-loop flow variations is not necessary in the analysis for this event.

Initial core power is assumed to be at its nominal value consistent with steady-state, full-power operation. RCS pressure is at its nominal value and the RCS vessel average temperature is at its nominal value plus a 4.5°F bias. Uncertainties in initial conditions are included in the limit DNBR as described in WCAP-11397-A.

### 14.2.9.3 Results

Figures 14.2-30, 14.2-31, 14.2-32, and 14.2-33 show the transient response for the more limiting case; the frequency decay complete loss of flow event with three loops in operation. The reactor is assumed to be tripped on a low reactor coolant loop flow signal. Figure 14.2-33 shows the minimum DNBR versus time.

Since DNBR limit is not violated, the ability of the primary coolant to remove heat from the fuel rod is not greatly reduced. Thus, the average fuel and clad temperatures do not increase significantly above their respective initial values.

The calculated sequence of events for the case analyzed is shown in Table 14.2-5. A frequency decay of 5 Hz/sec is modeled to occur resulting in a reactor trip on a low reactor coolant loop flow signal. With the reactor tripped, a stable plant condition will eventually be attained and natural circulation flow will be established. Normal plant shutdown may then proceed.

### 14.2.9.4 Conclusions

The analysis performed has demonstrated that for the complete loss of forced reactor coolant flow, the minimum DNBR acceptance criterion is met. Thus, the DNB design basis as described in Section 3, is met. There is no fuel clad damage or release of fission products to the Reactor Coolant System. Although this event is classified ANS Condition III, it has been evaluated against the more restrictive DNB requirements of ANS Condition II, which assumes fuel failure does not occur.

## 14.2.10 Single RCCA Withdrawal at Full Power

### 14.2.10.1 Accident Description

No single electrical or mechanical failure in the rod control system could cause the accidental withdrawal of a single rod cluster control assembly from the inserted bank at full power operation. The operator could deliberately withdraw a single rod cluster control assembly in the control bank. This feature is necessary in order to retrieve an assembly should one be accidentally dropped. In the extremely unlikely event of simultaneous electrical failures which could result in single rod cluster control assembly withdrawal, rod deviation and rod control urgent failure would be displayed on the plant annunciator, and the rod position indicators and in-plant computer points for rod position would indicate the relative positions of the assemblies in the bank. The urgent failure alarm also inhibits automatic rod motion in the group in which it occurs. Withdrawal of a single rod cluster control assembly by operator action, whether deliberate or by a combination of errors, would result in activation of the same alarm and the same visual indications.

Each bank of rod cluster control assemblies in the system is divided into two groups of four mechanisms each. The rods comprising a group operate in parallel through multiplexing thyristors. The two groups in a bank move sequentially such that the first group is always within one step of the second group in the bank. A definite schedule of actuation and deactuation of the stationary gripper, movable gripper and lift coils of a mechanism is required to withdraw the rod cluster control assembly attached to the mechanism. Since the four stationary gripper,

movable gripper and lift coils associated with the four rod cluster control assemblies of a rod group are driven in parallel, any single failure which would cause rod withdrawal would affect a minimum of one group, or four rod cluster control assemblies. Mechanical failures are in the direction of insertion, or immobility.

In the unlikely event of multiple failures which result in continuous withdrawal of a single rod cluster control assembly, it is not possible, in all cases, to provide assurances of automatic reactor trip such that core safety limits are not violated. Withdrawal of a single rod cluster control assembly results in both positive reactivity insertion tending to increase core power, and an increase in local power density in the core area "covered" by the rod cluster control assembly.

#### 14.2.10.2 Method of Analysis

Power distributions within the core are calculated by the TURTLE<sup>(12)</sup> code based on macroscopic cross section generated by LEOPARD<sup>(13)</sup>. The peaking factors calculated by TURTLE are then used by THINC to calculate the minimum DNB for the event. The case analyzed was the worst rod withdrawn from bank D inserted at the insertion limit, with the reactor initially at full power.  $F(\Delta H)$  for this case was 1.71 including appropriate allowances for calculational uncertainties.

#### 14.2.10.3 Results

Two cases have been considered as follows:

1. If the reactor is in the manual control mode, continuous withdrawal of a single rod cluster control assembly results in both an increase in core power and coolant temperature, and an increase in the local hot channel factor in the area of the failed rod cluster control assembly. In terms of the overall system response, this case is similar to those presented in Section 14.1.7; however, the increased local power peaking in the area of the withdrawn rod cluster control assembly results in lower minimum DNBR's than for the withdrawn bank cases. Depending on initial bank insertion and location of the withdrawn rod cluster control assembly, automatic reactor trip may not occur sufficiently fast to prevent the minimum core DNB ratio from falling below the design limit. Evaluation of this case at the power and coolant conditions at which the overtemperature  $\Delta T$  trip would be expected to trip the plant shows that an upper limit for the number of rods within a DNBR less than the design limit is 5 percent.
2. If the reactor is in automatic control mode, withdrawal of a single rod cluster control assembly will result in the immobility of the other rod cluster control assemblies in the controlling bank. The transient will then proceed in the same manner as Case 1 described above. For such cases as above, a trip will ultimately ensue, although not sufficiently fast in all cases to prevent violation of the DNBR safety analysis acceptance criteria.

#### 14.2.10.4 Conclusions

For the case of one rod cluster control assembly fully withdrawn with the reactor in the automatic or manual control mode and initially operating at full power with Bank D at the insertion limit, an upper bound on the number of fuel rods experiencing DNBR less than the design limit is 5 percent of the total fuel rods in the core.

For both cases discussed, the indicators and alarms mentioned would function to alert the operator to the malfunction before DNB could occur. For case 1 discussed above the insertion limit alarms (low and low-low alarms) would also serve in this regard.

#### 14.2.11 Minor Secondary System Pipe Breaks

##### 14.2.11.1 Identification of Causes and Accident Description

Included in this grouping are breaks of secondary system lines which would result in steam release rates equivalent to a 6 inch diameter break or smaller.

##### 14.2.11.2 Analysis of Effects and Consequences

Minor secondary system pipe breaks must be accommodated with the failure of only a small fraction of the fuel elements in the reactor. Since the results of analysis presented in Section 14.2.5 for a major secondary system pipe break also meet this criteria, separate analysis for minor secondary system pipe breaks is not required.

The analysis of the more probable accidental opening of a secondary system steam dump, relief or safety valve is presented in Section 14.1.13. These analyses are illustrative of a pipe break equivalent in size to a single valve opening.

##### 14.2.11.3 Conclusions

The analysis presented in Section 14.2.5 demonstrates that the consequences of a minor secondary system pipe break are acceptable since a DNBR of less than the design value does not occur even for a more critical major secondary system pipe break.



References to Section 14.2

1. Deleted by Revision 23
2. F. S. Moody, Transactions of the American Society of Mechanical Engineers, "Journal of Heat Transfer", (February 1965), Figure 3, page 134.
3. T. W. T. Burnett, "Reactor Protection System Diversity in Westinghouse Pressurized Water Reactor," WCAP-7306, Westinghouse Electric Corporation (April 1969).
4. T. G. Taxelius, ed. "Annual Report-Spert Project, October 1968 September 1969", IN-1370, Idaho Nuclear Corporation (June 1970).
5. R. C. Liimatainen and F. J. Testa, "Studies in TREAT of Zircaloy-2-Clad UO-Core Simulated Fuel Elements", January - June 1966, ANL-7225, 177, Argonne National Laboratory (November 1966).
6. D. H. Risher, Jr., "An Evaluation of the Rod Ejection Accident in Westinghouse Pressurized Water Reactors Using Spatial Kinetics Methods," WCAP-7588, Revision 1-A, Westinghouse Electric Corporation (January 1975).
7. D. H. Risher, Jr., R. F. Barry, "TWINKLE - A Multi-Dimensional Neutron Kinetics Computer Code", WCAP-7979-P-A (Proprietary), Westinghouse Electric Corporation (January 1975).
8. H. G. Hargrove, "FACTRAN - A Fortran IV Code for Thermal Transients in a UO<sub>2</sub> Fuel Rod," WCAP-7908-A, December 1989.
9. A. A. Bishop, R. O. Sandberg and L. S. Tong, "Forced Convection Heat Transfer at High Pressure After the Critical Heat Flux," 65-HT-31, American Society of Mechanical Engineers (August 1965).
10. F. M. Bordelon, "Calculation of Flow Coastdown After Loss of Reactor Coolant Pump (PHOENIX Code)," WCAP-7969, Westinghouse Electric Corporation (September 1972).
11. T. W. T. Burnett, et. al., "LOFTRAN Code Description," WCAP-7907-P-A (Proprietary), WCAP-7907-A (Non-Proprietary), April 1984.
12. S. Altomare and R. F. Barry, "The TURTLE 24.0 Diffusion Depletion Code," WCAP-7758, Westinghouse Electric Corporation (September 1971).
13. R. F. Barry, "LEOPARD - A Spectrum Dependent Non-Spatial Depletion Code for the IBM-7094," WCAP-3269-26, Westinghouse Electric Corporation (September 1963).
14. "RADIOISOTOPE, A Computer Program for Calculating Residual Activities in a Closed System After One or More Decay Periods," RP-1, Stone & Webster Engineering Corporation (November 1972).
15. "ACTIVITY, A Computer Program for Calculating Fission Product Activity in Fuel, Coolant, and Selected Tanks for a Nuclear Power Plant," RP-3, Stone & Webster Engineering Corporation (January 1973).

References to Section 14.2 (CONT'D)

16. "IONEXCHANGER, A Computer Program for Determining Gamma Activities in Ion Exchangers or Tanks as a Function of Time for Constant Feed Activity," RP-2, Stone & Webster Engineering Corporation (December 1972).
17. M. S. Baldwin, M. M. Merrian, H. S. Schenkle, and D. J. Van De Walle, "An Evaluation of Loss of Flow Accidents Caused by Power System Frequency Transients in Westinghouse PWRs," WCAP-8424, Revision 1, June 1975.
18. Deleted by Revision 23
19. ANSI/ANS-5.1-1979, "American National Standard for Decay Heat Power in Light Water Reactors," August 1979.
20. Deleted by Revision 23
21. Deleted by Revision 23
22. Deleted by Revision 23
23. Deleted by Revision 23
24. Deleted by Revision 20.
25. Deleted by Revision 23
26. Deleted by Revision 23
27. USNRC, "Standard Review Plan for the Review of Safety Analysis Reports for Nuclear Power Plants." NUREG-0800.
28. Friedland, A. J. and Ray, S., "Revised Thermal Design Procedure," WCAP-11397-P-A (Proprietary) and WCAP-11398-A (non-Proprietary), April 1989.
29. Sung, Y. X., et. al., "VIPRE-01 Modeling and Qualification for Pressurized Water Reactor Non-LOCA Thermal-Hydraulic Safety Analysis," WCAP-14565-P-A (Proprietary) and WCAP-15306-NP-A (Non-Proprietary), October 1999.
30. Deleted by Revision 26
31. "Westinghouse Revised Thermal Design Procedure Instrument Uncertainty Methodology for FirstEnergy Nuclear Operating Company Beaver Valley Unit 1," WCAP-15264, Revision 3.
32. "Westinghouse Setpoint Methodology for Protection Systems Beaver Valley Power Station - Unit 1," WCAP-11419, Revision 2.
33. USNRC Regulatory Guide 1.183, "Alternative Radiological Source Terms for Evaluating Design Basis Accidents at Nuclear Power Reactors."

References to Section 14.2 (CONT'D)

34. S&W Computer Code, PERC2, "Passive Evolutionary Regulatory Consequence Code," NU-226, V00, L01.
35. Industry Computer Code ARCON96, "Atmospheric Relative Concentrations in Building Wakes" developed by PNL (S&W Program EN-292, V00, L00).
36. Code of Federal Regulations, Title 10, Part 50.67, "Accident Source Term."
37. Industry Computer Code SCALE 4.3, "Modular Code System for Performing Standardized Computer Analyses for Licensing Evaluation for Workstations And Personal Computers," Control Module SAS2H, Version 3.1, developed by ORNL (S&W Program NU-230, V04, L03).
38. Sung, Y. X., et. al., "VIPRE-01 Modeling and Qualification for Pressurized Water Reactor Non-LOCA Thermal-Hydraulic Safety Analysis," WCAP-14565-P-A (Proprietary) and WCAP-15306-NP-A (Non-Proprietary), October 1999.
39. Friedland, A. J. and Ray, S., "Revised Thermal Design Procedure," WCAP-11397-P-A (Proprietary), WCAP-11397-A (Non-Proprietary), April 1989.

### 14.3 LOSS OF COOLANT ACCIDENT

Section 14.3 presents the analyses and evaluations of Loss-of-Coolant Accidents (LOCA).

Section 14.3.1 discusses the loss of reactor coolant from small ruptured pipes or from cracks in large pipes which actuates the Emergency Core Cooling System. This type of fault is classified as a Condition III occurrence. By definition, Condition III occurrences are faults which may occur very infrequently during the life of the plant. They will be accommodated with the failure of only a small fraction of the fuel rods although sufficient fuel damage might occur to preclude resumption of the operation for a considerable outage time. The release of radioactivity will not be sufficient to interrupt or restrict public use of those areas beyond the exclusion radius. A Condition III fault will not, by itself, generate a Condition IV fault or result in a consequential loss of function of the Reactor Coolant System or containment barriers.

Section 14.3.2 discusses the major reactor coolant system pipe ruptures up to and including the double-ended rupture of the largest pipe in the Reactor Coolant System. This type of accident has been classified as a Condition IV occurrence. Condition IV occurrences are faults which are not expected to take place, but are postulated because their consequences would include the potential for the release of significant amounts of radioactive material. These are the most drastic occurrences which must be designed against and represent limiting design cases. Condition IV faults are not to cause a fission product release to the environment resulting in an undue risk to public health and safety in excess of guideline values of 10CFR Part 50.67. A single Condition IV fault is not to cause a consequential loss of required functions of systems needed to cope with the fault including those of the Emergency Core Cooling System and the containment.

Section 14.3.3 presents an analysis of the core and reactor internals integrity following the LOCA.

Section 14.3.4 presents the Containment evaluation in response to a LOCA.

The analysis of doses resulting from the LOCA appears in Section 14.3.5. Core activities that form a basis for these calculations are presented in Appendix 14B.

Sections 5 and 6 also include discussions of the systems contributing to limiting of radioactivity releases from the containment during a LOCA.

#### 14.3.1 Loss of Reactor Coolant from Small Ruptured Pipes or From Cracks in Large Pipes Which Actuates Emergency Core Cooling System

##### Identification of Causes and Accident Description

A loss of coolant accident is defined as a rupture of the Reactor Coolant System piping or of any line connected to the system. See Section 4 for a more detailed description of the loss of reactor coolant accident boundary limits. Ruptures of small cross section will cause expulsion of the coolant at a rate which can be accommodated by the charging pumps which could maintain an operational water level in the pressurizer permitting the operator to execute an orderly shutdown. The coolant which would be released to the containment contains the fission products existing in it.

The maximum break size for which the normal makeup system can maintain the pressurizer level is obtained by comparing the calculated flow from the Reactor Coolant System through the postulated break against the charging pump makeup flow at normal Reactor Coolant System pressure, i.e., 2,250 psia. A makeup flow rate from one centrifugal charging pump is typically adequate to sustain pressurizer level at 2,250 psia for a break through a 0.375 inch diameter hole. (This break results in a loss of approximately 17.5 lb per second.) As part of the normal makeup system, a second charging pump is available to provide additional makeup flow to help maintain pressurizer level and pressure.

Should a larger break occur, depressurization of the Reactor Coolant System causes fluid to flow to the Reactor Coolant System from the pressurizer resulting in a pressure and level decrease in the pressurizer. Reactor trip occurs when the pressurizer low pressure trip setpoint is reached. The Safety Injection System is actuated when the appropriate setpoint is reached. The consequences of the accident are limited in two ways:

1. Reactor trip and borated water injection complement void formation in causing rapid reduction of nuclear power to a residual level corresponding to the delayed fission and fission product decay.
2. Injection of borated water ensures sufficient flooding of the core to prevent excessive clad temperatures.

Before the break occurs, the plant is in an equilibrium condition, i.e., the heat generated in the core is being removed via the secondary system. During blowdown, heat from decay, hot internals and the vessel continues to be transferred to the Reactor Coolant System. The heat transfer between the Reactor Coolant System and the secondary system may be in either direction depending on the relative temperatures. In the case of continued heat addition to the secondary system, pressure increases and steam dump may occur. Make-up to the secondary side is automatically provided by the auxiliary feedwater pumps.

The low pressurizer pressure safety injection signal stops normal feedwater flow by closing the main feedwater line isolation valves and initiates emergency feedwater flow by starting auxiliary feedwater pumps.

The secondary flow aids in the reduction of Reactor Coolant System pressure. When the Reactor Coolant System depressurizes, the accumulators begin to inject water into the reactor coolant loops. The reactor coolant pumps are assumed to be tripped at the initiation of the accident and effects of pump coastdown are included in the blowdown analyses.

### Analysis of Effects and Consequences

For breaks less than 1.0 ft<sup>2</sup>, the NOTRUMP<sup>(1)</sup> digital computer code is employed to calculate the transient depressurization of the Reactor Coolant System as well as to describe the mass and enthalpy of flow through the break.

NOTE: The reporting requirements of 10 CFR 50.46 for licensees to assess and report the effect of changes to or errors in the evaluation model used in the LOCA analysis are discussed in Section 14.3.2.5.

### Small Break LOCA Evaluation Model

For loss-of-coolant accidents due to small breaks less than 1 square foot, the NOTRUMP<sup>(1,2,115)</sup> computer code is used to calculate the transient depressurization of the Reactor Coolant System as well as to describe the mass and enthalpy of flow through the break. The NOTRUMP computer code is a state-of-the-art one-dimensional general network code consisting of a number of advanced features. Among these features are the calculation of thermal non-equilibrium in all fluid volumes, flow regime-dependent drift flux calculations with counter-current flooding limitations, mixture level tracking logic in multiple-stacked fluid nodes and regime-dependent heat transfer correlations. The NOTRUMP small break LOCA emergency core cooling system (ECCS) evaluation model was developed to determine the Reactor Coolant System response to design basis small break LOCAs and to address the NRC concerns expressed in NUREG-0611, "Generic Evaluation of Feedwater Transients and Small Break Loss-of-Coolant Accidents in Westinghouse-Designed Operating Plants."

In NOTRUMP, the Reactor Coolant System is nodalized into volumes interconnected by flowpaths. The broken loop is modeled explicitly, with the intact loops lumped into a second loop. The transient behavior of the system is determined from the governing conservation equations of mass, energy, and momentum applied throughout the system. A detailed description of the NOTRUMP code is provided in References 1, 2, and 115.

The use of NOTRUMP in the analysis involves, among other things, the representation of the reactor core as heated control volumes with an associated bubble rise model to permit a transient mixture height calculation. The multinode capability of the program enables an explicit and detailed spatial representation of various system components. In particular, it enables a proper calculation of the behavior of the loop seal during a loss-of-coolant accident.

Safety injection flow rate to the Reactor Coolant System as a function of the system pressure is used as part of the input. The Safety Injection System (SIS) was assumed to be delivering to the Reactor Coolant System 27 seconds after the generation of a safety injection signal. The 27 second delay includes time required for signal processing, diesel startup and loading of the safety injection pumps onto the emergency buses, as well as the pump acceleration and valve delays.

Minimum Safeguards Emergency Core Cooling System capability and operability has been assumed in these analyses. NOTRUMP evaluation model analyses are performed assuming loss of offsite power coincident with reactor trip, and a limiting single active failure (i.e., loss of one ECCS train on a failure to start of one diesel generator). Diesel generator failure is presumed to render inoperable one motor driven auxiliary feedwater pump which results in one motor driven auxiliary feedwater pump being credited in the analyses. The turbine-driven auxiliary feedwater pump is not credited in the analysis.

Peak clad temperature analyses are performed with the LOCTA IV<sup>(4)</sup> code which uses the RCS pressure, fuel rod power history, steam flow past the uncovered part of the core and mixture height history calculated by the NOTRUMP code.

A summation of the plant parameters used in the small break LOCA analysis is provided in Table 14.3-2b.

The Small Break LOCA analysis was performed at the Extended Power Uprate (EPU) conditions (reactor core power of 2900 MWt), and using the Model 54F Replacement Steam Generators (RSG).

The NOTRUMP<sup>(1)</sup> evaluation model assumes that the Auxiliary Feedwater (AFW) actuates on the low pressurizer pressure SI signal.

### Results

A full spectrum of breaks was analyzed at the beginning-of-life (BOL) fuel rod conditions to determine the limiting break size for peak clad temperature (PCT) and transient oxidation. The limiting PCT and oxidation cases were each analyzed to determine the limiting time-in-life. A break spectrum of 1.5-, 2-, 2.25-, 2.75-, 2.5-, 3-, 3.25-, 4-, and 6-inch breaks was considered. The 1.5-inch case was found to be non-limiting in NOTRUMP and therefore peak clad temperature (PCT) information was not calculated. The 2.75-inch break was found to be limiting for PCT at a limiting time-in-life of 8,000 MWD/MTU, using ZIRLO<sup>®</sup> fuel with annular pellets modeled. A summary of the results can be found in Table 14.3-1E and Table 14.3-1F.

Note: The Small Break LOCA analysis was performed with ZIRLO<sup>®</sup> cladding. However, Reference 124 concluded that the LOCA ZIRLO<sup>®</sup> models are acceptable for application to Optimized ZIRLO<sup>™</sup> cladding in the Small Break analysis, and that no additional calculations are necessary for evaluating the use of Optimized ZIRLO<sup>™</sup> cladding provided that plant specific ZIRLO<sup>®</sup> calculations were previously performed.

For the AOR, the limiting maximum local oxidation case was the 2.5-inch break case. The limiting transient oxidation occurs at the burst elevation and includes both outside and post-rupture inside oxidation. Pre-existing (pre-transient) oxidation was also considered and the sum of the pre-transient and transient oxidation remains below 17 percent at all times in life.

Figures 14.3.1-9A, 14.3.1-9B, 14.3.1-9C, 14.3.1-9D, 14.3.1-9E, 14.3.1-9F, and 14.3.1-9G present the Reactor Coolant System pressure transient for the 2-, 2.25-, 2.5-, 3-, 3.25-, 4- and 6-inch breaks, respectively. Figures 14.3.1-10A, 14.3.1-10B, 14.3.1-10C, 14.3.1-10D, 14.3.1-10E, 14.3.1-10F, and 14.3.1-10G present the volume history (mixture height) plots for the breaks. The peak clad temperatures for all cases are less than the peak clad temperature of the 2.75-inch break. The peak clad temperatures are given in Figures 14.3.1-11A, 14.3.1-11B, 14.3.1-11C, 14.3.1-11D, 14.3.1-11E, 14.3.1-11F, and 14.3.1-11G.

During the earlier part of the small break transient, the effect of the break flow is not strong enough to overcome the flow maintained by the reactor coolant pumps through the core as they are coasting down following reactor trip. Therefore, upward flow through the core is maintained. The resultant heat transfer cools the fuel rod and clad to very near the coolant temperatures as long as the core remains covered by a two-phase mixture.

For the AOR, the limiting maximum hot spot clad temperature calculated is for a 2.75 inch break. Figure 14.3.1-2 shows the RCS pressure response transient, and Figure 14.3.1-3 provides the core mixture height, each for the limiting PCT break case. The peak clad temperature transient is shown in Figure 14.3.1-4 for the limiting PCT break size. The steam flow rate for the limiting PCT break is shown in Figure 14.3-5. When the mixture level drops below the top of the core, the steam flow computed by NOTRUMP provides cooling to the upper portion of the core. The heat transfer coefficients for this phase of the transient are given in



Figure 14.3.1-6. The hot spot fluid temperature for the limiting PCT break is shown in Figure 14.3.1-7.

The core power (dimensionless) transient following the accident (relative to reactor scram time) is shown in Figure 14.3.1-8.

The reactor shutdown time (4.7 seconds) is equal to the reactor trip signal time (2.0 seconds) plus 2.7 seconds for rod insertion. During this rod insertion period the reactor is conservatively assumed to operate at rated power.

#### Post Analysis of Record Evaluations

In addition to the analyses presented in this section, evaluations and assessments may be performed as needed to address computer code errors and emergent issues, or to support plant changes. The issues or changes are evaluated, and the impact on the PCT is determined. The resultant increase or decrease in PCT is applied to the analysis of record PCT. The PCTs, including all penalties and benefits, are presented in Table 14.3-1g for the small break LOCA. The resultant PCT is demonstrated to be less than the 10 CFR 50.46(b) requirement of 2200 °F.

As discussed in Section 14.3.2.5, 10 CFR 50.46 requires that licensees assess and report the effect of changes to or errors in the evaluation model used in the LOCA analyses. The requirements discussed in Section 14.3.2.5 are also applicable to the small break LOCA analysis.

#### Conclusions

Analyses presented in this section show that the Emergency Core Cooling System provides sufficient core flooding to meet the required limits of 10 CFR 50.46(b)(1), (2), and (3). Hence, adequate protection is afforded by the Emergency Core Cooling System in the event of a small break loss-of-coolant accident.

#### 14.3.2 Major Reactor Coolant System Pipe Breaks (Loss of Coolant Accident)

For the purpose of ECCS analyses, Westinghouse defines a large break loss-of-coolant accident (LOCA) as a rupture 1.0 ft<sup>2</sup> or larger of the reactor coolant system piping including the double ended rupture of the largest pipe in the reactor coolant system or of any line connected to that system. Should a major break occur, rapid depressurization of the Reactor Coolant System (RCS) to a pressure nearly equal to the containment pressure occurs in approximately 40 seconds, with a nearly complete loss of system inventory. Rapid voiding in the core shuts down reactor power. A safety injection (SI) system signal is actuated when the low pressurizer pressure setpoint is reached. These countermeasures will limit the consequences of the accident in two ways:

- 1) Borated water injection complements void formation in causing rapid reduction of power to a residual level corresponding to fission product decay heat. An average RCS/sump mixed boron concentration is calculated to ensure that the post-LOCA core remains subcritical. However, no credit is taken for the insertion of control rods to shut down the reactor in the large break analysis.
- 2) Injection of borated water provides heat transfer from the core and prevents excessive cladding temperatures.

Before the break occurs, the reactor is assumed to be in a full power equilibrium condition, i.e., the heat generated in the core is being removed through the steam generator secondary system. At the beginning of the blowdown phase, the entire RCS contains sub-cooled liquid which transfers heat from the core by forced convection with some fully developed nucleate boiling. During blowdown, heat from fission product decay, hot internals and the vessel, continues to be transferred to the reactor coolant. After the break develops, the time to departure from nucleate boiling is calculated. Thereafter, the core heat transfer is unstable, with both nucleate boiling and film boiling occurring. As the core becomes voided, both transition boiling and forced convection are considered as the dominant core heat transfer mechanisms. Heat transfer due to radiation is also considered.

The heat transfer between the RCS and the secondary system may be in either direction, depending on the relative temperatures. In the case of the large break LOCA, the primary pressure rapidly decreases below the secondary system pressure, and the steam generators are an additional heat source. In the Beaver Valley Power Station Unit 1 Large Break LOCA analysis using the WCOBRA/TRAC methodology, the steam generator secondary is conservatively assumed to be isolated (main feedwater and steam line) at the initiation of the event to maximize the secondary side heat load.

#### 14.3.2.1 General

When the Final Acceptance Criteria (FAC) governing the Loss-Of-Coolant Accident (LOCA) for Light Water Reactors was issued in Appendix K of 10 CFR 50.46, both the Nuclear Regulatory Commission (NRC) and the industry recognized that the stipulations of Appendix K were highly conservative. That is, using the then accepted analysis methods, the performance of the Emergency Core Cooling System (ECCS) would be conservatively underestimated, resulting in predicted Peak Cladding Temperatures (PCTs) much higher than expected. At that time, however, the degree of conservatism in the analysis could not be quantified. As a result, the NRC began a large-scale confirmatory research program with the following objectives:

- 1) Identify, through separate effects and integral effects experiments, the degree of conservatism in those models permitted in the Appendix K rule. In this fashion, those areas in which a purposely prescriptive approach was used in the Appendix K rule could be quantified with additional data so that a less prescriptive future approach might be allowed.
- 2) Develop improved thermal-hydraulic computer codes and models so that more accurate and realistic accident analysis calculations could be performed. The purpose of this research was to develop an accurate predictive capability so that the uncertainties in the ECCS performance and the degree of conservatism with respect to the Appendix K limits could be quantified.

Since that time, the NRC and the nuclear industry have sponsored reactor safety research programs directed at meeting the above two objectives. The overall results have quantified the conservatism in the Appendix K rule for LOCA analyses and confirmed that some relaxation of the rule can be made without a loss in safety to the public. It was also found that some plants were being restricted in operating flexibility by the overly conservative Appendix K requirements. In recognition of the Appendix K conservatism that was being quantified by the research programs, the NRC adopted an interim approach for evaluation methods. This interim approach

is described in SECY-83-472. The SECY-83-472 approach retained those features of Appendix K that were legal requirements, but permitted applicants to use best-estimate thermal-hydraulic models in their ECCS evaluation model. Thus, SECY-83-472 represented an important step in basing licensing decisions on realistic calculations, as opposed to those calculations prescribed by Appendix K.

In 1998, the NRC Staff amended the requirements of 10 CFR 50.46 and Appendix K, "ECCS Evaluation Models," to permit the use of a realistic evaluation model to analyze the performance of the ECCS during a hypothetical LOCA. This decision was based on an improved understanding of LOCA thermal-hydraulic phenomena gained by extensive research programs. Under the amended rules, best-estimate thermal-hydraulic models may be used in place of models with Appendix K features. The rule change also requires, as part of the LOCA analysis, an assessment of the uncertainty of the best-estimate calculations. It further requires that this analysis uncertainty be included when comparing the results of the calculations to the prescribed acceptance criteria of 10 CFR 50.46. Further guidance for the use of best-estimate codes is provided in Regulatory Guide 1.157.

To demonstrate use of the revised ECCS rule, the NRC and its consultants developed a method called the Code Scaling, Applicability, and Uncertainty (CSAU) evaluation methodology (NUREG/CR-5249). This method outlined an approach for defining and qualifying a best-estimate thermal-hydraulic code and quantifying the uncertainties in a LOCA analysis.

A LOCA evaluation methodology for three- and four-loop Pressurized Water Reactor (PWR) plants based on the revised 10 CFR 50.46 rules was developed by Westinghouse with the support of EPRI and Consolidated Edison and has been approved by the NRC (WCAP-12945-P-A).

Westinghouse subsequently developed an alternative uncertainty methodology called ASTRUM, which stands for Automated Statistical Treatment of Uncertainty Method (WCAP-16009-P-A). This method is still based on the CQD methodology and follows the steps in the CSAU methodology (NUREG/CR-5249). However, the uncertainty analysis (Element 3 in the CSAU) is replaced by a technique based on order statistics. The ASTRUM methodology replaces the response surface technique with a statistical sampling method where the uncertainty parameters are simultaneously sampled for each case. The ASTRUM methodology has received NRC approval for referencing in licensing applications in WCAP-16009-P-A (WCAP-16009-P-A).

The three 10 CFR 50.46 criteria (peak cladding temperature, maximum local oxidation, and core-wide oxidation) are satisfied by running a sufficient number of WCOBRA/TRAC calculations (sample size). In particular, the statistical theory predicts that 124 calculations are required to simultaneously bound the 95<sup>th</sup> percentile values of three parameters with a 95-percent confidence level.

This analysis is in accordance with the applicability limits and usage conditions defined in Section 13-3 of WCAP-16009-P-A, as applicable to the ASTRUM methodology. Section 13-3 of WCAP-16009-P-A was found to acceptably disposition each of the identified conditions and limitations related to WCOBRA/TRAC and the CQD uncertainty approach per Section 4.0 of the ASTRUM Final Safety Evaluation Report appended to this topical report.

#### 14.3.2.2 Method of Analysis

The methods used in the application of WCOBRA/TRAC to the large break LOCA with ASTRUM are described in WCAP-12945-P-A and WCAP-16009-P-A. A detailed assessment of the computer code WCOBRA/TRAC was made through comparisons to experimental data. These assessments were used to develop quantitative estimates of the ability of the code to predict key physical phenomena in a PWR large break LOCA. Modeling of a PWR introduces additional uncertainties which are identified and quantified in the plant-specific analysis. WCOBRA/TRAC MOD7A was used for the execution of ASTRUM for Beaver Valley Unit 1 (WCAP-16009-P-A).

WCOBRA/TRAC combines two-fluid, three-field, multi-dimensional fluid equations used in the vessel with one-dimensional drift-flux equations used in the loops to allow a complete and detailed simulation of a PWR. This best-estimate computer code contains the following features:

- 1) Ability to model transient three-dimensional flows in different geometries inside the vessel
- 2) Ability to model thermal and mechanical non-equilibrium between phases
- 3) Ability to mechanistically represent interfacial heat, mass, and momentum transfer in different flow regimes
- 4) Ability to represent important reactor components such as fuel rods, steam generators, reactor coolant pumps, etc.

A typical calculation using WCOBRA/TRAC begins with the establishment of a steady-state, initial condition with all loops intact. The input parameters and initial conditions for this steady-state calculation are discussed in the next section.

Following the establishment of an acceptable steady-state condition, the transient calculation is initiated by introducing a break into one of the loops. The evolution of the transient through blowdown, refill, and reflood is calculated continuously, using the same computer code (WCOBRA/TRAC) and the same modeling assumptions. Containment pressure is modeled with the BREAK component using a time dependent pressure table. Containment pressure is calculated using the COCO code (WCAP-8326) and mass and energy releases from the WCOBRA/TRAC calculation.

The final step of the best-estimate methodology, in which all uncertainties of the LOCA parameters are accounted for to estimate a PCT, Local Maximum Oxidation (LMO), and Core-Wide Oxidation (CWO) at 95-percent probability (and 95-percent confidence level), is described in the following sections.

1) Plant Model Development:

In this step, a WCOBRA/TRAC model of the plant is developed. A high level of nodding detail is used in order to provide an accurate simulation of the transient. However, specific guidelines are followed to ensure that the model is consistent with models used in the code validation. This results in a high level of consistency among plant models, except for specific areas dictated by hardware differences, such as in the upper plenum of the reactor vessel or the ECCS injection configuration.

2) Determination of Plant Operating Conditions:

In this step, the expected or desired operating range of the plant to which the analysis applies is established. The parameters considered are based on a "key LOCA parameters" list that was developed as part of the methodology. A set of these parameters, at mostly nominal values, is chosen for input as initial conditions to the plant model. A transient is run utilizing these parameters and is known as the "initial transient." Next, several confirmatory runs are made, which vary a subset of the key LOCA parameters over their expected operating range in one-at-a-time sensitivities. Because certain parameters are not included in the uncertainty analysis, these parameters are set at their bounding condition. This analysis is commonly referred to as the confirmatory analysis. The most limiting input conditions, based on these confirmatory runs, are then combined into the model that will represent the limiting state for the plant, which is the starting point for the assessment of uncertainties.

3) Assessment of Uncertainty:

The ASTRUM methodology is based on order statistics. The technical basis of the order statistics is described in Section 11 of WCAP-16009-P-A. The determination of the PCT uncertainty, LMO uncertainty, and CWO uncertainty relies on a statistical sampling technique. According to the statistical theory, 124 WCOBRA/TRAC calculations are necessary to assess against the three 10 CFR 50.46 criteria (PCT, LMO, and CWO).

The uncertainty contributors are sampled randomly from their respective distributions for each of the WCOBRA/TRAC calculations. The list of uncertainty parameters, which are randomly sampled for each time in the cycle, break type (split or double-ended guillotine), and break size for the split break are also sampled as uncertainty contributors within the ASTRUM methodology.

Results from the 124 calculations are tallied by ranking the PCT from highest to lowest. A similar procedure is repeated for LMO and CWO. The highest rank of PCT, LMO, and CWO will bound 95 percent of their respective populations with 95-percent confidence level.

4) Plant Operating Range:

The plant operating range over which the uncertainty evaluation applies is defined. Depending on the results obtained in the above uncertainty evaluation, this range may be the desired range or may be narrower for some parameters to gain additional margin.

#### 14.3.2.3 Analysis Assumptions

The expected PCT and its uncertainty developed are valid for a range of plant operating conditions. The range of variation of the operating parameters has been accounted for in the uncertainty evaluation. Table 14.3.2-1 summarizes the operating ranges for Beaver Valley Unit 1 as defined for the proposed operating conditions, which are supported by the Best-Estimate LBLOCA analysis. Tables 14.3.2-2, 14.3.2-3, and 14.3.2-7 summarize the LBLOCA containment data used for calculating containment pressure. If operation is maintained within these ranges, the LBLOCA results developed in this report are considered to be valid. Note that some of these parameters vary over their range during normal operation within a fuel cycle (e.g., accumulator temperature) and other parameters are typically fixed during normal operation within a fuel cycle (full-power Tavg).

For the Best-Estimate large break LOCA analysis, one ECCS train (including one High Head Safety Injection (HHSI) pump and one Low Head Safety Injection (LHSI) pump) starts and delivers flow through the injection lines. The accumulator and safety injection flows from the broken loop were assumed to be spilled to containment. Both emergency diesel generators (EDGs) are assumed to start in the modeling of the containment spray pumps. Modeling full containment heat removal systems operation is required by Branch Technical Position CSB 6-1 and is conservative for the large break LOCA.

To minimize delivery to the reactor, the HHSI and LHSI branch line chosen to spill is selected as the one with the minimum resistance.

The Large Break LOCA analysis was performed with ZIRLO® cladding. However, Reference 124 concluded that the LOCA ZIRLO® models are acceptable for application to Optimized ZIRLO™ cladding in the Large Break analysis, and that no additional calculations are necessary for evaluating the use of Optimized ZIRLO™ cladding provided that plant specific ZIRLO® calculations were previously performed.

#### 14.3.2.4 Design Basis Accident

The Beaver Valley Unit 1 PCT/LMO/CWO-limiting transient is a double-ended guillotine break (discharge coefficient = 0.9920 and break area multiplier = 2.0) which analyzes conditions that fall within those listed in Table 14.3.2-1. Analysis experience indicates that this break location most likely causes conditions that result in flow stagnation to occur in the core. Scoping studies with WCOBRA/TRAC have confirmed that the cold leg remains the limiting break location (WCAP-12945-P-A).

For convenience, the large break LOCA transient can be divided into time periods in which specific phenomena occur, such as various hot assembly heatup and cooldown transients. For a typical large break, the blowdown period can be divided into the Critical Heat Flux (CHF) phase, the upward core flow phase, and the downward core flow phase. These are followed by the refill, reflood, and long-term cooling periods. Specific important transient phenomena and heat transfer regimes are discussed below, with the transient results shown in Figures 14.3.2-1A through 14.3.2-1L. (The limiting case was chosen to show a conservative representation of the response to a large break LOCA.)

1) Critical Heat Flux (CHF) Phase (0 - 2 seconds):

Immediately following the cold leg rupture, the break discharge rate is subcooled and high (Figure [14.3.2-1B](#)). The regions of the RCS with the highest initial temperatures (core, upper plenum, upper head, and hot legs) begin to flash to steam, the core flow reverses and the fuel rods begin to undergo departure from nucleate boiling (DNB). The fuel cladding rapidly heats up (Figure [14.3.2-1A](#))

while the core power shuts down due to voiding in the core. This phase is terminated when the water in the lower plenum and downcomer begins to flash (Figures 14.3.2-1F and 14.3.2-1K, respectively). The mixture swells and intact loop pumps, still rotating in single-phase liquid (Figure 14.3.2-1C), push this two-phase mixture into the core.

2) Upward Core Flow Phase (2 - 8 seconds):

Heat transfer is improved as the two-phase mixture is pushed into the core. This phase may be enhanced if the pumps are not degraded, or if the break discharge rate is low due to saturated fluid conditions at the break. If pump degradation is high or the break flow is large, the cooling effect due to upward flow may not be significant. Figure 14.3.2-1C shows the void fraction for one intact loop pump and the broken loop pump. The figure shows that the intact loop pumps are undergoing a head degradation as they transition from single-phase liquid to single-phase vapor. This phase ends as the lower plenum mass is depleted, the loop flow becomes two-phase, and the pump head degrades.

3) Downward Core Flow Phase (8 - 30 seconds):

The loop flow is pushed into the vessel by the intact loop pumps and decreases as the pump flow becomes two-phase. The break flow begins to dominate and pulls flow down through the core, up the downcomer to the broken loop cold leg, and out the break. While liquid and entrained liquid flow provide core cooling, the top of core vapor flow (Figure 14.3.2-1D) best illustrates this phase of core cooling. Once the system has depressurized to the accumulator pressure (Figure 14.3.2-1E), the accumulators begin to inject relatively cold borated water into the intact cold legs (Figure 14.3.2-1H). During this period, due to steam upflow in the downcomer, a portion of the injected ECCS water is calculated to be bypassed around the downcomer and out the break. As the system pressure continues to fall, the break flow, and consequently the downward core flow (i.e. reverse flow in the fuel bundle region), is reduced. The core begins to heat up as the system pressure approaches the containment pressure and the vessel begins to fill with ECCS water (Figure 14.3.2-1J).

4) Refill Period (30 - 40 seconds):

As the refill period begins, the core begins a period of heatup and the vessel begins to fill with ECCS water (Figures 14.3.2-1H and 14.3.2-1I). This period is characterized by a rapid increase in cladding temperatures at all elevations due to the lack of liquid and steam flow in the core region. This period continues until the lower plenum is filled and the bottom of the core begins to reflood and entrainment begins.

5) Reflood Period (40 - 350 seconds):

During the early reflood phase, the accumulators begin to empty and nitrogen enters the system. This forces water into the core, which then boils, causing system re-pressurization and the lower core region begins to quench (Figure 14.3.2-1J). During this time, core cooling may increase due to vapor generation



and liquid entrainment. During the reflood period, the core flow and temperatures are oscillatory as relatively cold water periodically rewets and quenches the hot fuel cladding, which generates steam and causes system re-pressurization. The steam and entrained water must pass through the vessel upper plenum, the hot legs, the steam generators, and the reactor coolant pumps before it is vented out of the break. This flow path resistance is overcome by the downcomer water elevation head, which provides the gravity driven reflood force. From the later stage of blowdown to the beginning of reflood, the accumulators rapidly discharge borated cooling water into the RCS, filling the lower plenum and contributing to the filling of the downcomer. The pumped ECCS water aids in the filling of the downcomer and subsequently supplies water to maintain a full downcomer and complete the reflood period. As the quench front progresses up the core, the PCT location moves higher into the top core region (Figure 14.3.2-1L). Note that PCT location plot is based on the core noding (approximately one node for every 1.8 inch of core elevation). As the vessel continues to fill (Figure 14.3.2-1G), the PCT location is cooled and the early reflood period is terminated.

A brief and less severe second cladding heatup occurs (170 - 200 seconds) due to excessive boiling in the downcomer. The mixing of ECCS water with hot water and steam from the core, in addition to the continued heat transfer from the vessel and its components, reduces the subcooling of ECCS water in the lower plenum and downcomer. The saturation temperature is dictated by the containment pressure. If the liquid temperature in the downcomer reaches saturation, subsequent heat transfer from the vessel and other structures will cause boiling and level swell in the downcomer (Figure 14.3.2-1K). The downcomer liquid will spill out of the broken cold leg and reduce the driving head, which can reduce the reflood rate, causing a late reflood heatup at the upper core elevations.

#### 6) Long-Term Core Cooling

At the end of the WCOBRA/TRAC calculation, the core and downcomer levels are increasing as the pumped safety injection flow exceeds the break flow. The core and downcomer levels would be expected to continue to rise, until the downcomer mixture level approaches the loop elevation. At that point, the break flow would increase, until it roughly matches the injection flowrate. The core would continue to be cooled until the entire core is eventually quenched.

#### 14.3.2.5 Post Analysis of Record Evaluations

In addition to the analyses presented in this section, evaluations and assessments may be performed as needed to address computer code errors and emergent issues, or to support plant changes. The issues or changes are evaluated, and the impact on the Peak Cladding Temperature (PCT) is determined. The resultant increase or decrease in PCT is applied to the analysis of record PCT. The PCTs, including all penalties and benefits, are presented in Table 14.3.2-6. The resultant PCT is demonstrated to be less than the 10 CFR 50.46(b) requirement of 2200 °F.

In addition, 10 CFR 50.46 requires that licensees assess and report the effect of changes to or errors in the evaluation model used in the LOCA analysis. These reports constitute addenda to the analysis of record provided in the UFSAR until the overall changes become significant as

defined by 10 CFR 50.46. If the assessed changes or errors in the evaluation model result in significant changes in calculated PCT, a schedule for formal reanalysis or other action as needed to show compliance will be addressed in the report to the NRC.

Finally, the criteria of 10 CFR 50.46 require that holders and users of the evaluation models establish a number of definitions and processes for assessing changes in the models or their use. Westinghouse, in consultation with the Westinghouse Owner's Group (WOG), developed an approach for compliance with the reporting requirements. This approach is documented in WCAP-13451, *Westinghouse Methodology for Implementation of 10 CFR 50.46 Reporting*. The company provides the NRC with annual and 30-day reports, as applicable, for the Beaver Valley Power Station Unit 1. The company intends to provide future reports required by 10 CFR 50.46 consistent with the approach described in WCAP-13451.

#### 14.3.2.6 Conclusions

It must be demonstrated that there is a high level of probability that the limits set forth in 10 CFR 50.46 are met. The demonstration that these limits are met is as follows:

- (b)(1) The limiting PCT corresponds to a bounding estimate of the 95<sup>th</sup> percentile PCT at the 95-percent confidence level. Since the resulting PCT for the limiting case is 2161 °F, the analysis confirms that 10 CFR 50.46 acceptance criterion (b)(1), i.e., "Peak Cladding Temperature less than 2200 °F," is demonstrated. The results are shown in Table [14.3.2-5](#).
- (b)(2) The maximum cladding oxidation corresponds to a bounding estimate of the 95<sup>th</sup> percentile LMO at the 95-percent confidence level. Since the resulting LMO for the limiting case is 9.22 percent, the analysis confirms that 10 CFR 50.46 acceptance criterion (b)(2), i.e., "Local Maximum Oxidation of the cladding less than 17 percent of the total cladding thickness before oxidation," is demonstrated. The results are shown in Table [14.3.2-5](#).
- (b)(3) The limiting core-wide oxidation corresponds to a bounding estimate of the 95<sup>th</sup> percentile CWO at the 95-percent confidence level. The limiting Hot Assembly Rod (HAR) total maximum oxidation is 0.94 percent. A detailed CWO calculation takes advantage of the core power census that includes many lower power assemblies. Because there is significant margin to the regulatory limit, the CWO value can be conservatively chosen as that calculated for the limiting HAR. A detailed CWO calculation is therefore not needed because the outcome will always be less than 0.94 percent. Since the resulting CWO is 0.94 percent, the analysis confirms that 10 CFR 50.46 acceptance criterion (b)(3), i.e., "Core-Wide Oxidation less than 1 percent of the metal in the cladding cylinders surrounding the fuel, excluding the cladding surrounding the plenum volume," is demonstrated. The results are shown in Table [14.3.2-5](#).

- (b)(4) 10 CFR 50.46 acceptance criterion (b)(4) requires that the calculated changes in core geometry are such that the core remains amenable to cooling. This criterion has historically been satisfied by adherence to criteria (b)(1) and (b)(2), and by assuring that fuel deformation due to combined LOCA and seismic loads is specifically addressed. It has been demonstrated that the PCT and maximum cladding oxidation limits remain in effect for Best-Estimate LOCA applications. The approved methodology (WCAP-12945-P-A) specifies that effects of LOCA and seismic loads on core geometry do not need to be considered unless grid crushing extends beyond the 44 assemblies in the low-power channel. This situation has not been calculated to occur for Beaver Valley Unit 1. Therefore, acceptance criterion (b)(4) is satisfied.
- (b)(5) 10 CFR 50.46 acceptance criterion (b)(5) requires that long-term core cooling be provided following the successful initial operation of the ECCS. Long-term cooling is dependent on the demonstration of continued delivery of cooling water to the core. The manual actions that are currently in place to maintain long-term cooling remain unchanged with the application of the ASTRUM methodology (WCAP-16009-P-A).

Based on the ASTRUM Analysis results (Table 14.3.2-5), it is concluded that Beaver Valley Unit 1 continues to maintain a margin of safety to the limits prescribed by 10 CFR 50.46. A time sequence of events for the limiting case is given in Table 14.3.2-8.

### 14.3.3 Core and Internals Integrity Analysis

#### 14.3.3.1 Internals Evaluation

The forces exerted on the reactor internals and the core following a LOCA are computed by employing the MULTIFLEX 3.0 computer code.

#### 14.3.3.2 Design Criteria

Following a LOCA, the basic requirement is that the station shall be shut down in an orderly manner and cooled down so that fuel cladding temperature is kept within specified limits. This implies that the deformation of the reactor internals must be kept sufficiently small so that the core geometry remains substantially intact to allow core cooling and insertion of a sufficient number of control rods.

After the break, the reduction in water density greatly reduces the reactivity of the core, thus making the core subcritical, causing reactor shutdown independent of the control rods. In other words, the core is subcritical whether or not the rods are tripped. (The subsequent refilling of the core by the ECCS uses borated water to maintain the core in a subcritical state.) Therefore, insertion of most of the control rods further ensures the ability to shut the reactor down and keep it in a safe shutdown condition.

Maximum allowable deflection limitations are established for those regions of the internals that are critical for reactor shutdown. Allowable stress limits are adopted to ensure physical integrity of the components.

In the event of a sudden double-ended reactor coolant system pipe break (complete severance in a few milliseconds), pressure waves are produced in the reactor causing vertical and horizontal excitation of the components. A study has been made to analyze the response of the reactor vessel internal structures under these conditions.

#### 14.3.3.3 Dynamic System Analysis of Reactor Internals under Loss of Coolant Accident (LOCA)

The response of reactor internals components due to an excitation produced by complete severance of a branch line pipe is analyzed. Assuming a pipe break occurs in a very short period of time of 1 millisecond, the rapid drop of pressure at the break produces a disturbance that propagates along the primary loop and excites the internal structures.

The LOCA breaks considered for the Beaver Valley Unit 1 (DLW) consist of breaks located at the Accumulator line and the Residual Heat Removal line (RHR). The LOCA hydraulic forcing functions (horizontal and vertical forces) that were used in the analyses were generated using the MULTIFLEX 3.0 computer code described by Takeuchi et. al., (WCAP-9735 Rev. 1, "Multiflex 3.0-A Fortran IV Computer Program for Analyzing Thermal-Hydraulic-Structural System Dynamics (III) Advanced Beam Model).

#### Mathematical Model of the Reactor Pressure Vessel (RPV) System

The mathematical model of the RPV system is a three-dimensional nonlinear finite element model that represents dynamic characteristics of the reactor vessel/internals/fuel in the six geometric degrees of freedom. The RPV system model was developed using the WECAN computer code (Westinghouse Electric Computer Analysis). The WECAN finite element model consists of three concentric structural sub-models connected by nonlinear impact elements and stiffness matrices. The first sub-model represents the reactor vessel shell and associated components. The reactor vessel is restrained by reactor vessel supports and by the attached primary coolant piping. The reactor vessel support system is represented by stiffness matrices.

The second sub-model represents the reactor core barrel assembly (core barrel and thermal shield), lower support plate, tie plates, and secondary core support components. This sub-model is physically located inside the first, and is connected to it by a stiffness matrix at the internals support ledge. Core barrel to vessel shell impact is represented by nonlinear elements at the core barrel flange, core barrel nozzle, and lower radial support locations.

The third and innermost sub-model represents the upper support plate, guide tubes, support columns, upper and lower core plates, and the fuel. This sub-model includes the specific properties of the Westinghouse 17x17 Robust Fuel Assembly with Intermediate Flow Mixing devices (IFMS). The third sub-model is connected to the first and second by stiffness matrices and nonlinear elements.

The WECAN computer code, which is used to determine the response of the reactor vessel and its internals, is a general purpose finite element code. In the finite element approach, the structure is divided into a finite number of members or elements. The inertia and stiffness matrices, as well as the force array, are first calculated for each element in the local coordinates. Employing appropriate transformation, the element global matrices and arrays are then computed. Finally, the global element matrices and arrays are assembled into the global structural matrices and arrays, and used for dynamic solution of the differential equation of motion for the structure:

$$[M]\{\ddot{U}\} + [D]\{\dot{U}\} + [K]\{U\} = \{F\} \quad (\text{Equation 1})$$

where,

[M]	= Global inertia matrix
[D]	= Global damping matrix
[K]	= Global stiffness matrix
{ $\ddot{U}$ }	= Acceleration array
{ $\dot{U}$ }	= Velocity array
{U}	= Displacement array
{F}	= Force array, including impact, thrust forces, hydraulic forces, constraints, and weight.

WECAN solves equation (1) using the nonlinear modal superposition theory. An initial computer run is made to calculate the eigenvalues (frequencies) and eigenvectors (mode shapes) for the mathematical model. This information is stored, and is used in a subsequent computer run that solves equation (1). The first time step performs a static solution of equation (1) to determine the initial displacements of the structure due to deadweight and normal operating hydraulic forces. After the initial time step, WECAN calculates the dynamic solution of equation (1). Time history nodal displacements and impact forces are stored for post-processing.

The following typical discrete elements from the WECAN finite element library are used to represent the reactor vessel and internals components:

- Three-dimensional elastic pipe
- Three-dimensional mass with rotary inertia
- Three-dimensional beam
- Three-dimensional linear spring
- Concentric impact element
- Linear impact element
- 6 x 6 stiffness matrix
- 18 Card stiffness matrix
- 18 Card mass matrix
- Three-dimensional friction element

### Analytical Methods

The RPV system finite element model as described above was used to perform the LOCA analysis. Following a postulated LOCA pipe rupture, forces are imposed on the reactor vessel and its internals. These forces result from the release of the pressurized primary system coolant. The release of pressurized coolant results in traveling depressurization waves in the primary system. These depressurization waves are characterized by a wavefront with low pressure on one side and high pressure on the other. The wavefront translates and reflects throughout the primary system until the system is completely depressurized. The rapid depressurization results in transient hydraulic loads on the mechanical equipment of the system.

The LOCA loads applied to the reactor pressure vessel system consist of (a) reactor internal hydraulic loads (vertical and horizontal), and (b) reactor coolant loop mechanical loads. All the loads are calculated individually and combined in a time-history manner.

### RPV Internal Hydraulic Loads

Depressurization waves propagate from the postulated break location into the reactor vessel through either a hot leg or a cold leg nozzle.

After a postulated break in the cold leg, the depressurization path for waves entering the reactor vessel is through the nozzle into the region between the core barrel and reactor vessel. This region is called the down-corner annulus. The initial waves propagate up, around, and down the down-corner annulus, then up through the region circumferentially enclosed by the core barrel; that is, the fuel region.

The region of the down-corner annulus close to the break depressurizes rapidly but, because of restricted flow areas and finite wave speed (approximately 3,000 feet per second), the opposite side of the core barrel remains at a high pressure. This results in a net horizontal force on the core barrel and reactor pressure vessel. As the depressurization wave propagates around the down-corner annulus and up through the core, the barrel differential pressure reduces, and similarly, the resulting hydraulic forces drop.

In the case of a postulated break in the hot leg, the waves follow a dissimilar depressurization path, passing through the outlet nozzle and directly into the upper internals region, depressurizing the core and entering the down-corner annulus from the bottom exit of the core barrel. Thus, after a break in the hot leg, the down-corner annulus would be depressurized with very little difference in pressure across the outside diameter of the core barrel.

A hot leg break produces less horizontal force because the depressurization wave travels directly to the inside of the core barrel (so that the down-corner annulus is not directly involved) and internal differential pressures are not as large as for a cold leg break. Since the differential pressure is less for a hot leg break, the horizontal force applied to the core barrel is less for a hot leg break than for a cold leg break. For breaks in both the hot leg and cold leg, the depressurization waves would continue to propagate by reflection and translation through the reactor vessel and loops.

The MULTIFLEX computer code described by Takeuchi calculates the hydraulic transients within the entire primary coolant system. It considers subcooled, transition, and two-phase (saturated) blowdown regimes. The MULTIFLEX program employs the method of characteristics to solve the conservation laws, and assumes one-dimensionality of flow and homogeneity of the liquid-vapor mixture.

The MULTIFLEX code considers a coupled fluid-structure interaction by accounting for the deflection of constraining boundaries, which are represented by separate spring-mass oscillator systems. A beam model of the core support barrel has been developed from the structural properties of the core barrel. In this model, the cylindrical barrel is vertically divided into various segments, and the pressure, as well as the wall motions, are projected onto the plane parallel to the broken inlet nozzle. The spatial pressure variation at each time step is transformed into 10 horizontal forces, which act on the 10 mass points of the beam model. Each flexible wall is bounded on either side by a hydraulic flow path. The motion of the flexible walls is determined by solving the global equations of motion for the masses representing the forced vibration of an undamped beam.

#### Reactor Coolant Loop Mechanical Loads

The reactor coolant loop mechanical loads are applied to the RPV nozzles by the primary coolant loop piping. The loop mechanical loads result from the release of normal operating forces present in the pipe prior to the separation as well as transient hydraulic forces in the reactor coolant system. The magnitudes of the loop release forces are determined by performing a reactor coolant loop analysis for normal operating loads (pressure, thermal, and deadweight). The loads existing in the pipe at the postulated break location are calculated and are “released” at the initiation of the LOCA transient by application of the loads to the broken piping ends. These forces are applied with a ramp time of 1 millisecond because of the assumed instantaneous break opening time. For breaks in the branch lines the force applied at the reactor vessel would be insignificant. The restraints on the main coolant piping would eliminate any force to the reactor vessel caused by a break in the branch line.

#### Results of the Analysis

The severity of a postulated break in a reactor vessel is related to three factors: the distance from the reactor vessel to the break location, the break opening area, and the break opening time. The nature of the decompression following a LOCA, as controlled by the internals structural configuration previously discussed, results in larger reactor internal hydraulic forces for pipe breaks in the cold leg than in the hot leg (for breaks of similar area and distance from the RPV). Pipe breaks farther away from the reactor vessel are less severe because the pressure wave attenuates as it propagates toward the reactor vessel. The LOCA hydraulic and mechanical loads described in the previous sections were applied to the WECAN model of the reactor pressure vessel system.

The results of LOCA analysis include time history displacements and nonlinear impact forces for all major components. The time history displacements of upper core plate, lower core plate and core barrel at the upper core plate elevation are provided as input for the reactor core evaluations. The impact forces calculated at the vessel-internals interfaces are used to evaluate the structural integrity of the reactor vessel and its internals. Using appropriate post-processors, component linear forces are also calculated.

### Components Subjected to Transverse Excitations

The loading from the hydraulic pressure transient on the upper core barrel is represented by a dynamic pressure wave.

The dynamic stability and the maximum distortion of the upper core barrel is analyzed. The response to the initial peak of the pressure wave is obtained neglecting the effect of the water and solid-water interaction in limiting the response of the core barrel.

The analysis shows that the upper barrel does not collapse during a hot leg break and that it has an allowable stress distribution during a cold leg break.

The guide tubes are studied applying the blowdown forces to the structures and calculating the resulting deflections. The guide tubes are considered as being elastically supported at the upper plate and simply supported at the lower end with variable cross-section. Consideration is given to the frequencies and amplitudes of the forcing function and the response is computed to ensure that the deflections do not prevent rod insertion.

Results of the analysis show that the deformation of the guide tubes is within the limits established experimentally to ensure control rod insertion.

#### Allowable Deflection

##### 1. Upper Barrel

The upper barrel deformation has the following limits:

- a. To ensure reactor trip and to avoid disturbing the RCC guide structure, the barrel should not interfere with any guide tubes. This condition requires a stability check to ensure that the barrel will not buckle under the accident loads. The minimum distance between guide tube and barrel is 8.77 inches. This value is adopted as the limit above which "no loss of function" can no longer be guaranteed. An allowable deflection of 4.38 inches has been selected.
- b. To ensure core cooling, the outward movement of the upper barrel must be such that the inlet flow from the unbroken cold legs should not be impaired. From this condition an outward barrel deflection of 1.50 inches in front of the inlet nozzle has been established as the "no loss of function" value. An allowable deflection of 1.00 inches has been selected.

##### 2. RCC Guide Tubes

The guide tubes in the upper core support package housing control rods required for reactor shutdown have the following deflection limit:

The maximum horizontal deflection as a beam should not exceed 1.6 inches over the length of the guide tube. An allowable distortion of 1.0 inches has been selected.



The limitations for this case are related to the stability of the thimbles in the upper end. The upper end of the thimbles shall not experience stresses above the buckling compressive stresses because any buckling of the upper end of the thimbles will distort the guide line and could affect the free fall of the control rod.

### 3. Upper Package

The local deformation of the upper core plate where a guide tube is located shall be below 0.100 inch. This deformation will cause the plate to contact the guide tube since the clearance between plate and guide tube is 0.1 inch. This limit will prevent the guide tubes from being put in compression.

For a plate local deformation of 0.150 inch, the guide tube will be compressed and deformed transversely to the established upper limit and consequently the value of 0.150 inch is adopted as the maximum core plate local deformation, with an allowable deformation of 0.100 inch.

#### 14.3.4 Containment Evaluation

##### 14.3.4.1 Design Bases

The design of the atmospheric containment structure is based on the following criteria:

1. The peak calculated containment atmosphere pressure shall not exceed the design pressure of 45 psig.
2. The containment pressure shall be reduced to less than 50% of the peak calculated pressure for the design basis loss-of-coolant accident within 24 hours after the postulated accident.

The peak containment pressure due to a postulated loss-of-coolant accident (LOCA) occurs after a double-ended rupture (DER) of a reactor coolant hot leg and is a function of the initial total pressure and average temperature of the containment atmosphere, the containment free volume, the passive heat sink inventory in the containment, and the rates of mass and energy released to the containment. The passive heat sinks in the containment are considered to be at the same initial temperature as the initial average containment atmosphere temperature. Maximizing the initial containment total pressure and average atmospheric temperature maximizes the calculated peak pressure.

The ability to reduce the containment pressure to less than 50% of the peak calculated pressure within 24 hours for a postulated Loss-of-Coolant accident depends on the mass of air in the containment, on the design of the containment depressurization system (both quench spray and recirculation spray subsystems, see Section 6.4), and on the river water temperatures.

In summary, the containment structure is sized for criterion 1 and the containment depressurization system is sized in accordance with criterion 2.

The reactor is assumed to be operating at the maximum core thermal power of 2917.4 MWt (which includes uncertainty allowance) and to have been operating at this power long enough to have reached its equilibrium concentration of fission products. Coincident with the LOCA, a complete loss of all offsite electric power is assumed. For the minimum engineered safety features case, one emergency diesel generator starts and operates to supply emergency power.

The minimum engineered safety features that are assumed to be activated to limit the consequences of the LOCA are as follows:

1. Emergency core cooling by
  - a. All of three nitrogen-pressurized accumulators
  - b. One out of three charging pumps
  - c. One out of two low-head safety injection (LHSI) pumps
2. Containment depressurization by
  - a. One out of two trains of the quench spray subsystem and
  - b. One out of two trains of the recirculation spray subsystem (i.e., one inside recirculation spray pump and one outside recirculation spray pump).

The emergency diesel generator provides the power to operate the pumps. The accumulators are passive and discharge into the Reactor Coolant System (RCS) when the RCS pressure drops below the accumulator pressure.

#### 14.3.4.2 LOCA Mass and Energy Release

##### 14.3.4.2.1 LOCA Mass and Energy Release Safety Analysis

The uncontrolled release of pressurized high temperature reactor coolant, or loss-of-coolant accident (LOCA), results in release of steam and water into the containment. This, in turn, results in increases in the local subcompartment pressures, and an increase in the global containment pressure and temperature.

The long-term LOCA mass and energy (M&E) releases are utilized as input to the containment analysis. The containment analysis demonstrates that the containment safeguards systems successfully mitigate the consequences of all current licensing basis LOCAs without exceeding the current containment design basis pressure or temperature.

The short-term LOCA mass and energy releases, addressed in Section 14.3.4.5, are used as input to the subcompartment analysis. The subcompartment analysis addresses the short pressure pulse (generally less than 3 seconds) accompanying a high-energy line pipe break within that subcompartment. The subcompartment analysis demonstrates the resultant pressures and temperatures are within the current design basis values for all current licensing basis breaks.

## Introduction

The LOCA mass and energy release analysis was performed at a core power (including uncertainty allowance) of 2917.4 MWt.

The LOCA mass and energy releases were generated using the March 1979 LOCA mass and energy release model described in Reference 15. These releases were used in the containment response calculation.

The Westinghouse generated LOCA mass and energy releases for the first hour were used in the MAAP-DBA containment response analysis. After this time, the break enthalpy is calculated, along with the containment response by using MAAP-DBA.

This section describes the LOCA mass and energy release calculation methodology for the hypothetical double-ended pump suction (DEPS) and double-ended hot-leg (DEHL) break cases. It also explains that the analysis of the DEPS and DEHL LOCAs bounds all current licensing basis LOCAs, including the double-ended cold leg (DECL) break.

## Input Parameters and Assumptions

All input parameters are chosen consistent with accepted analysis methodology. Some of the most critical items are the RCS initial conditions, core decay heat, safety injection flow, and primary and secondary metal mass and steam generator heat release modeling. Specific assumptions concerning each of these items are discussed next. Tables [14.3.4-1](#), [14.3.4-2](#) and [14.3.4-3](#) present key data assumed in the analysis.

The core rated power adjusted for uncertainty allowance was used in the analysis. As previously noted, the use of RCS operating temperatures to bound the highest average coolant temperature range were used as bounding analysis conditions. The use of higher temperatures is conservative because the initial fluid energy is based on coolant temperatures that are at the maximum levels attained in steady state operation. Additionally, an allowance to account for instrument error and deadband is reflected in the initial RCS temperatures. The selection of the limiting pressure is considered to affect the blowdown phase results only, since this represents the initial pressure of the RCS. The RCS rapidly depressurizes from this value until the point at which it equilibrates with containment pressure.

The rate at which the RCS blows down is initially more severe at the higher RCS pressure. Additionally the RCS has a higher fluid density at the higher pressure (assuming a constant temperature) and subsequently has a higher RCS mass available for releases. Thus, 2250 psia plus uncertainty was selected for the initial pressure as the limiting case for the long-term mass and energy release calculations.

The selection of the fuel design features for the long-term mass and energy release calculation is based on the need to conservatively maximize the energy stored in the fuel at the beginning of the postulated accident (i.e., to maximize the core stored energy). Thus, the analysis conservatively accounts for the stored energy in the core.

The nominal RCS volume is increased to maximize the initial RCS mass and energy.

A uniform steam generator tube plugging (SGTP) level is modeled. This assumption maximizes the reactor coolant volume and fluid release by considering the RCS fluid in all SG tubes. During the post-blowdown period the steam generators are active heat sources, as significant energy remains in the secondary metal and secondary mass that has the potential to be transferred to the primary side. The SGTP assumption maximizes heat transfer area and therefore, the transfer of secondary heat across the SG tubes. Additionally, this assumption reduces the reactor coolant loop resistance, which reduces the pressure drop upstream of the break for the pump suction breaks and increases break flow. Thus, the analysis very conservatively accounts for the level of SGTP.

The initial steam generator fluid mass is calculated at full power, and then increased by 10% to cover uncertainties. Conservative steam generator water and metal masses were used.

Portions of the SG secondary metal, such as the upper elliptical head, upper shell, and miscellaneous upper internals, have poor heat transfer due to their location in the steam region. The mass of this metal was conservatively chosen. The stored energy in this metal will be transferred to the RCS and released to the containment at a much slower rate and is not considered during the first hour of the LOCA mass and energy release calculation for the double-ended pump suction breaks. The stored energy in the rest of the SG secondary metal and fluid is released to the containment within the first hour.

After one hour, the Westinghouse LOCA mass and energy calculation has extracted all of the stored energy from the RCS, except for the stored metal energy in the steam generator upper internals and upper elliptical heads. This energy is assumed to be removed at a constant rate over the next six hours and is added to the core decay heat as an energy source for the long-term steaming rate calculation.

Regarding safety injection flow, the mass and energy release calculation considered configurations/failures to conservatively bound respective alignments. These cases include (1) a Minimum Safeguards case with one Charging/High Head Injection pump (HHSI) and one Low Head Safety Injection (LHSI) pump and (2) a Maximum Safeguards case with two HHSI and two LHSI pumps.

In summary, the following assumptions were employed so that the LOCA mass and energy releases are conservatively calculated, thereby maximizing the energy release to containment:

1. The nominal RCS volume is increased by 3 percent (1.6-percent allowance for thermal expansion and 1.4 percent for uncertainty)
2. The reactor is assumed to be operating at full core rated power (2900 MWT) and an allowance for uncertainty allowance is included.
3. The full power core-stored energy (above T-avg) is increased by 15 percent to account for fuel manufacturing tolerances and an additional allowance is included to account for fuel densification.
4. The RCS is assumed to be at the maximum expected full power operating temperature and an allowance for temperature measurement uncertainty allowance of +4.0°F is added. These uncertainties conservatively include both deadband and bias.

5. The RCS is assumed to be at the nominal RCS pressure and an allowance for pressure measurement uncertainty (+40 psi) is added.
6. Conservatively high heat transfer coefficients (i.e., steam generator primary/secondary heat transfer and reactor coolant system metal heat transfer) are modeled. The SG secondary stored energy is released in one hour. All of the additional stored energy in the upper elliptical head, upper shell, and miscellaneous upper internals, is released at a constant rate over the next 6 hours.
7. The LOCA back-pressure is assumed to remain at the containment design pressure (45 psig). This assumption determines the end of the blowdown phase and minimizes the safety injection flow rate during the reflood phase.
8. A uniform SGTP level of 0% is assumed. This assumption:
  - Maximizes reactor coolant volume and fluid release,
  - Maximizes heat transfer area across the SG tubes,
  - Reduces coolant loop resistance, which reduces the  $\Delta P$  upstream of the break for the pump suction breaks and increases break flow.
9. The full power SG level is used to calculate the initial secondary mass and 10% is added to cover uncertainty.

#### Description of Analyses

The Westinghouse LOCA Mass and Energy Release Model for Containment Design (Reference 15) is used for the long-term LOCA mass and energy release calculations. This evaluation model has been reviewed and approved generically by the Nuclear Regulatory Commission (NRC). The approval letter is included with Reference 15.

#### LOCA Mass and Energy Release Phases

The containment system receives mass and energy releases following a postulated break in the RCS. These releases continue over a time period, which, for the LOCA mass and energy release analysis, is typically divided into four phases.

1. Blowdown – the period of time from accident initiation (when the reactor is at steady state operation) to the time that the RCS and containment reach an equilibrium state.
2. Refill – the period of time when the lower plenum is being filled by accumulator and Emergency Core Cooling System (ECCS) water. At the end of blowdown, a large amount of water remains in the cold legs, downcomer, and lower plenum. To conservatively consider the refill period for the purpose of containment mass and energy releases, it is assumed that this water is instantaneously transferred to the lower plenum along with sufficient accumulator water to completely fill the lower plenum. This allows an uninterrupted release of mass and energy releases to containment. Thus, the refill period is conservatively neglected in the mass and energy release calculation.

3. Reflood – begins when the water from the lower plenum enters the core and ends when the core is completely quenched.
4. Post-reflood (Froth) – describes the period following the reflood phase. For the pump suction break, a two-phase mixture exits the core, passes through the hot legs, and is superheated in the steam generators prior to exiting the break as steam. After the broken loop steam generator cools, the break flow becomes two-phase.

#### Computer Codes

The Reference 15 mass and energy release evaluation model is comprised of mass and energy release versions of the following codes: SATAN VI, WREFLOOD, FROTH, and EPITOME. These codes were used to calculate the LOCA mass and energy releases for the containment peak pressure and temperature calculation.

SATAN VI calculates blowdown, the first portion of the thermal-hydraulic transient following break initiation, including pressure, enthalpy, density, mass and energy flow rates, and energy transfer between primary and secondary systems as a function of time.

The WREFLOOD code addresses the portion of the LOCA transient where the core reflooding phase occurs after the primary coolant system has depressurized (blowdown) due to the loss of water through the break and when water supplied by the ECCS refills the reactor vessel and provides cooling to the core. The most important feature of WREFLOOD is the steam/water mixing model, discussed later in this section.

FROTH models the post-reflood portion of the transient. The FROTH code calculates the heat release from the energy stored in the secondary fluid and metal masses, excluding the upper internals and upper elliptical head. This part of the steam generator metal mass is not actively cooled by the two-phase fluid circulating through steam generator tubes and takes longer to cooldown.

EPITOME continues the FROTH post-reflood portion of the transient from the time at which the secondary equilibrates to containment design pressure to the end of the transient (1 hour). It also compiles a summary of data on the entire transient, including formal instantaneous mass and energy release tables and mass and energy releases balance tables with data at critical times.

After one hour, the Westinghouse LOCA mass and energy release calculation has extracted all of the stored energy from the RCS, except for the stored metal energy in the steam generator upper internals and upper elliptical heads. This energy is assumed to be removed at a constant rate over the next six hours and is added to the core decay heat as an energy source for the long-term steaming rate calculation.

#### Break Size and Location

Generic studies (Reference 15, Section 3) have been performed to determine the effect of postulated break size on the LOCA mass and energy releases. The double-ended guillotine break has been found to be limiting due to larger mass flow rates during the blowdown phase of the transient. During the reflood and post-reflood phases, the break size has little effect on the releases.

Three distinct locations in the reactor coolant system loop can be postulated for pipe rupture for any release purposes:

- Hot leg (between vessel and steam generator)
- Cold leg (between pump and vessel)
- Pump suction (between steam generator and pump)

The DEHL break location yields the highest blowdown mass and energy release rates (Reference 15, Section 3.3). Although the core flooding rate would be the highest for this break location, the amount of energy released from the steam generator secondary side is minimal because the majority of fluid that exits the core vents directly to containment, bypassing the steam generators. As a result, the reflood mass and energy releases are reduced significantly as compared to either the pump suction, or cold-leg break locations where the core exit mixture must pass through the steam generators before venting through the break. Studies have confirmed that there is no reflood peak (i.e., from the end of the blowdown period the containment pressure would continually decrease) for the hot leg break. Therefore, the mass and energy releases for the blowdown phase of the hot-leg break are calculated and used in the containment peak pressure and temperature response calculation.

Studies have determined that the blowdown transient for the DEHL break is, in general, less limiting than that for the pump suction break (Reference 15, Section 3.3). The cold leg blowdown is faster than that of the pump suction break, and more mass is released into the containment. However, the core heat transfer is greatly reduced, and this results in a considerably lower energy release into containment. The flooding rate during the reflood phase is greatly reduced, and the energy release rate into the containment is reduced. Therefore, the cold-leg break is bounded by other breaks and no further evaluation is necessary.

The pump suction break combines the effects of the relatively high core-flooding rate, as in the hot-leg break, and the additional stored energy in the steam generators. As a result, the pump suction break yields the highest energy flow rates during the post-blowdown period by including all of the available energy of the RCS in calculating the releases to containment.

Therefore, the break locations that were analyzed for this program were the DEPS rupture (10.46 ft<sup>2</sup>) and the DEHL rupture (9.15 ft<sup>2</sup>). LOCA mass and energy releases have been calculated for the blowdown, reflood, and post-reflood phases for the DEPS cases. For the DEHL case, the releases were calculated only for the blowdown phase with this methodology.

#### Application of Single-Failure Criterion

The mass and energy release calculation assumes a complete loss of all offsite power coincident with the LOCA. The emergency diesel generators are actuated to provide power for the safety injection system. The combination of signal delay plus diesel delay and additional delays in starting the ECCS pumps results in the delivery of SI after the end of blowdown.

Two cases were analyzed to assess the effects of a single failure in the mass and energy release calculation. The first case assumes a single failure of one of the emergency diesel generators, resulting in the loss of one train of safeguards equipment. This, in combination with other conservative assumptions (maximum resistances, minimum pump head-flow curves), minimizes the safety injection flow rate. The second case assumes a failure in the containment spray system. The safety injection flow rate for this case is maximized by assuming both trains of safeguards equipment are operating and by including other conservative assumptions (minimum resistances, maximum pump head-flow curves).

### Regulatory Guidance

A large LOCA is classified as an ANS Condition IV event, a limiting fault. The guidance presented in the Standard Review Plan Section 6.2.1.3 involved following:

- 10 CFR 50, Appendix A
- 10 CFR 50, Appendix K, paragraph I.A

To meet this guidance, the following must be addressed:

- Sources of energy
- Break size and location

Calculation of each phase of the accident

### Results

Blowdown Mass and Energy Release Data (Tables [14.3.4-4](#), [14.3.4-5](#), [14.3.4-6](#), [14.3.4-7](#), [14.3.4-8](#), [14.3.4-9](#), [14.3.4-10](#), and [14.3.4-11](#))

The SATAN-VI code is used for computing the blowdown transient. The code utilizes the control volume (element) approach with the capability for modeling a large variety of thermal fluid system configurations. The fluid properties are considered uniform, and thermodynamic equilibrium is assumed in each element. A point kinetics model is used with weighted feedback effects. The major feedback effects include moderator density, moderator temperature, and Doppler broadening. A critical flow calculation for subcooled (modified Zaloudek), two-phase (Moody), or superheated break flow is incorporated into the analysis. The methodology for the use of this model is described in Reference 15.

Table [14.3.4-4](#) presents the calculated mass and energy release for the blowdown phase of the DEHL break. For the hot-leg break mass and energy release tables, break path 1 refers to the mass and energy releases exiting from the reactor vessel side of the break; and break path 2 refers to the mass and energy releases exiting from the steam generator side of the break.

Table [14.3.4-5](#) presents the calculated mass and energy releases for the blowdown phase of the DEPS break with either minimum or maximum ECCS flows. For the pump suction breaks, break path 1 in the mass and energy release tables refers to the mass and energy releases exiting from the steam generator side of the break; break path 2 refers to the mass and energy releases exiting from the pump side of the break.



### Reflood Mass and Energy Release Data

The WREFLOOD code is used for computing the reflood transient. The WREFLOOD code consists of two basic hydraulic models—one for the contents of the reactor vessel and one for the coolant loops. The two models are coupled through the interchange of the boundary conditions applied at the vessel outlet nozzles and at the top of the downcomer. Additional transient phenomena, such as pumped safety injection and accumulators, reactor coolant pump performance, and steam generator releases are included as auxiliary equations that interact with the basic models as required. The WREFLOOD code permits the capability to calculate variations during the core reflooding transient of basic parameters such as core flooding rate, core and downcomer water levels, fluid thermodynamic conditions (pressure, enthalpy, density) throughout the primary system, and mass flow rates through the primary system. The code permits hydraulic modeling of the two flow paths available for discharging steam and entrained water from the core to the break, the path through the broken loop and the path through the unbroken loops.

A complete thermal equilibrium mixing condition for the steam and ECCS injection water during the reflood phase has been assumed for each loop receiving ECCS water. This is consistent with the usage and application of the (Reference 15) mass and energy release evaluation model in recent analyses, for example, D.C. Cook (Reference 22). Even though the Reference 15 model credits steam/water mixing only in the intact loop and not in the broken loop, the justification, applicability, and NRC approval for using the mixing model in the broken loop has been documented (Reference 23). Moreover, this assumption is supported by test data and is further discussed below.

The model assumes a complete mixing condition (i.e., thermal equilibrium) for the steam/water interaction. The complete mixing process, however, is made up of two distinct physical processes. The first is a two-phase interaction with condensation of steam by cold ECCS water. The second is a single-phase mixing of condensate and ECCS water. Since the steam release is the most important influence to the containment pressure transient, the steam condensation part of the mixing process is the only part that needs to be considered. (Any spillage directly heats only the sump.)

The most applicable steam/water mixing test data has been reviewed for validation of the REFLOOD steam/water mixing model. This data, generated in 1/3-scale tests (Reference 23), are the largest scale data available and thus, most clearly simulate the flow regimes and gravitational effects that would occur in a Pressurized Water Reactor (PWR). These tests were designed specifically to study the steam/water interaction for PWR reflood conditions.

A group of 1/3-scale tests corresponds directly to the reflood conditions. The injection flow rates for this group cover all phases and mixing conditions calculated during the reflood transient. The data from these tests were reviewed and discussed in detail in Reference 15. For all of these tests, the data clearly indicate the occurrence of very effective mixing with rapid steam condensation. The mixing model used in the REFLOOD calculation is therefore wholly supported by the 1/3-scale steam/water mixing data. Descriptions of the test and test results are contained in References 22 and 23.

The calculated DEPS reflood phase LOCA mass and energy releases are given in Table 14.3.4-6 for the minimum safeguards case and in Table 14.3.4-9 for the maximum safeguards case. The transient responses of the principal parameters during reflood are given in Table 14.3.4-7 for the DEPS minimum safeguards case and in Table 14.3.4-10 for the DEPS maximum safeguards case.

#### Post-Reflood Mass and Energy Release Data

The FROTH code (Reference 20) is used for computing the post-reflood transient. The FROTH code calculates the heat release rates resulting from a two-phase mixture present in the steam generator tubes. The mass and energy releases that occur during this phase are typically superheated due to the depressurization and equilibration of the broken-loop and intact-loop steam generators. During this phase of the transient, the RCS has equilibrated with the containment pressure, but the steam generators contain a secondary inventory at an enthalpy that is much higher than the primary side. Therefore, there is a significant amount of reverse heat transfer that occurs. Steam is produced in the core due to core decay heat. For a pump suction break, a two-phase fluid exits the core, flows through the hot legs, and becomes superheated as it passes through the steam generator. Once the broken loop cools, the break flow becomes two-phase. During the FROTH calculation, ECCS injection is addressed for both the injection phase and the recirculation phase. The FROTH code calculation stops when the secondary side equilibrates to the saturation temperature ( $T_{sat}$ ) at the containment design pressure. After this point, the EPITOME code completes the SG depressurization. The methodology for the use of this model is described in Reference 15. (See subsection 14.3.4.2.1.7.5 and subsection 14.3.4.2.1.7.6 for additional information.)

Table 14.3.4-8 presents the two-phase post-reflood mass and energy release data for the double-ended pump suction case minimum safeguards case. Table 14.3.4-11 present the two-phase post-reflood mass and energy release data for the double-ended pump suction maximum safeguards case.

#### Decay Heat Model

The American Nuclear Society Standard ANSI/ANS-5.1-1979 (Reference 75) has been used for the determination of decay heat in the mass and energy release analysis. Table 14.3.4-12 lists the generic decay heat curve used in the BVPS-1 mass and energy release calculations applying the Reference 15 LOCA mass and energy release methodology.

Significant assumptions in the generation of the decay heat curve for use in the LOCA mass and energy release analysis include the following:

- Decay heat sources considered are fission product decay and heavy element decay of U-239 and Np-239.
- Decay heat power from the following fissioning isotopes are included: U-238, U-235, and Pu-239.

- Fission rate is constant over the operating history of maximum power level.
- The factor accounting for neutron capture in fission products has been taken from Equation 11 of Reference 6, up to 10,000 seconds and from Table 10 of Reference 6, beyond 10,000 seconds.
- The fuel has been assumed to be at full power for  $10^8$  seconds.
- The number of atoms of U-239 produced per second has been assumed to be equal to 70 percent of the fission rate.
- The total recoverable energy associated with one fission has been assumed to be 200 MeV/fission.
- Two-sigma uncertainty (two times the standard deviation) has been applied to the fission product decay.

Based upon NRC staff review, Safety Evaluation Report (SER) of the March 1979 evaluation model (Reference 15), use of the ANS Standard ANSI/ANS-5.1-1979 decay heat model was approved for the calculation of mass and energy releases to the containment following a LOCA.

#### Steam Generator Equilibration and Depressurization

Steam generator equilibration and depressurization is the process by which secondary side energy is removed from the steam generators in stages. The FROTH computer code calculates the heat removal from the secondary mass until the secondary temperature is the saturation temperature ( $T_{sat}$ ) at the containment design pressure. After the FROTH calculations, the EPITOME code continues the FROTH calculation for SG cooldown removing steam generator secondary energy at different rates (i.e., first and second stage rates). The first stage rate is applied until the steam generator reaches  $T_{sat}$  at the user specified intermediate equilibration pressure, when the secondary pressure is assumed to reach the containment pressure. Then the second stage rate is used until the final depressurization, when the secondary reaches the reference temperature of  $T_{sat}$  at 14.7 psia, or 212°F. The heat removal of the broken-loop and intact-loop steam generators are calculated separately.

During the FROTH calculations, steam generator heat removal rates are calculated using the secondary side temperature, primary side temperature, and a secondary side heat transfer coefficient determined using a modified McAdam's correlation. Steam generator energy is removed during the FROTH transient until the secondary side temperature reaches saturation temperature at the containment design pressure. The constant heat removal rate used during the first heat removal stage is based on the final heat removal rate calculated by FROTH. The SG energy available to be released during the first stage interval is determined by calculating the difference in secondary energy available at the containment design pressure and that at the (lower) user specified intermediate equilibration pressure, assuming saturated conditions. The intermediate equilibrium pressures are chosen as discussed in Reference 15, Sections 2.3 and 3.3. This energy is then divided by the first stage energy removal rate, resulting in an intermediate equilibration time. At this time, the rate of energy release drops substantially to the

second stage rate. The second stage rate is determined as the fraction of the difference in secondary energy available between the intermediate equilibration and final depressurization at 212°F, and the time difference from the time of the intermediate equilibration to the user-specified time of the final depressurization at 212°F. With current methodology (Reference 15), all of the secondary energy remaining after the intermediate equilibration is conservatively assumed to be released by imposing a mandatory cooldown and subsequent depressurization down to atmospheric pressure at 3600 seconds, i.e., 14.7 psia and 212°F.

### Long Term Mass & Energy Releases

The long-term (greater than 3600 seconds) mass and energy release calculations are performed through user defined input functions which is an option in the MAAP-DBA code (Reference 21). This method of determining the long-term mass and energy releases is consistent with past applications of the Reference 15 methodology. These user defined functions are characterized for the long term discharge from the break for both a mixed discharge and for an unmixed discharge of steam and water. In both cases, the flow rates that are used are those calculated by the EPITOME code and only the specific enthalpies of the discharge flows are calculated to represent the influence of the time dependent RCS injection temperature as the containment cools.

### Sources of Mass and Energy

The sources of mass considered in the LOCA mass and energy release analysis are given in Tables 14.3.4-13, 14.3.4-14, and 14.3.4-15. These sources are the reactor coolant system, accumulators, and pumped safety injection.

The energy inventories considered in the LOCA mass and energy release analysis are given in Tables 14.3.4-16, 14.3.4-17 and 14.3.4-18. The energy sources are listed below.

- RCS water
- Accumulator water (all three inject)
- Pumped SI water
- Decay heat
- Core stored energy
- RCS metal (includes the reactor vessel and internals, hot and cold leg piping, SG inlet and outlet plenums, and SG tubes)
- SG metal (includes transition cone, shell, wrapper, and other internals)

Note: The DEHL cases also conservatively include the upper internals and upper elliptical head.

- SG secondary energy (includes fluid mass and steam mass)

- Secondary transfer of energy (feedwater into, and steam out of, the SG secondary)

The energy reference points are as follows.

- Available energy: 212°F; 14.7 psia
- Total energy content: 32°F; 14.7 psia

The mass and energy inventories are presented at the following times, as appropriate:

- Time zero (initial conditions)
- End of blowdown time
- End of refill time
- End of reflood time
- Time of broken loop steam generator equilibration to pressure setpoint
- Time of intact loop steam generator equilibration to pressure setpoint
- Time of full depressurization (3600 seconds)

The Zirc-water reaction energy was not considered in the mass and energy release data presented because the clad temperature was not assumed to increase high enough for the rate of the Zirc-water reaction to be of any significance.

The analyses described in the previous sections were based on a maximum RWST temperature of 65°F.

### Conclusions

Plant specific LOCA mass and energy release analyses were developed using approved design basis methodology. The results of this analysis were provided for use in the containment analysis.

The consideration of the various energy sources in the long-term mass and energy release analysis provides assurance that all available sources of energy have been included in this analysis. Thus, the review guidelines presented in Standard Review Plan Section 6.2.1.3 have been satisfied.

#### 14.3.4.2.2 MAAP-DBA Code

##### Method of Analysis

The MAAP-DBA code generalized containment model (21) was used to determine the containment response. The containment assessment for a design basis application was performed consistent with the NRC guidance provided in the Standard Review Plan. This includes the use of Tagami and Uchida heat transfer correlations for the quantification of the passive heat sink responses. The temperatures and pressures acting on the containment building and its supporting mechanical and electrical systems were analyzed to ensure that the containment parameters do not exceed the plant's design bases events acceptance criteria.

Those design bases events include the rupture of a pipe in the Reactor Coolant System (LOCA) and the Main Steam Line Break (MSLB) between the top of the steam generator and the penetration through the containment wall (See Section 5.2.2 for the MSLB results). LOCA breaks were evaluated at hot leg, cold leg, and pump suction locations. All these design bases events assumed a 2917.4 MWt core power. Evaluations for the limiting containment design basis events were evaluated to assess the peak containment pressure, peak containment gas temperature, long term temperatures within the containment, and the peak liner temperatures attributes. To ensure that the most conservative value of each of the attributes was identified and evaluated, the most conservative value (max or min) of each input parameter for each attribute was selected.

The mass and energy released to the containment can also vary depending upon a combination of variables such as break size, break location, single active failure, power level, and containment air pressure at the time of the break. The consequences of the breaks can further vary dependent on a variety of possible single active failures that may occur concurrent with the breaks and affect the availability of engineered safety features (ESFs). Single active failures that were considered for LOCA response to identify the “worst single failure” that maximizes the challenge to the containment integrity include:

- the failure of a single train of engineered safety features such as might occur with the failure of a Diesel Generator (DG) coincident with a loss of off-site power,
- the failure of a single train of low head safety injection (LHSI),
- the single failure of the containment isolation phase B signal (CIB), which would result in the failure of one complete train of quench and recirculation sprays to start, which means that the remaining train of sprays would be available to cool the containment atmosphere,
- The failure of a river water pump to supply cooling water to one train of the recirculation spray heat exchangers (two heat exchangers) which are part of the containment heat removal system.
- The failure of a timer start relay which would result in the failure of one train of recirculation spray.

Operational conditions in the reactor coolant system including the reactor and steam generators were also examined for the worst possible conditions that could influence the mass and energy releases from the break. Section 14.3.4.2.1 discusses the spectrum of LOCA mass and energy releases used as input to the containment analysis.

Thus, the containment analyses were performed in a manner that ensured that the evaluations identified and examined the most severe challenges to successful operation of the containment and its supporting mechanical and electrical safety systems.

### Application of MAAP DBA to Containment Analysis

The MAAP DBA Generalized Containment Model (GCM) was used for DBA evaluations (Reference 21).

#### Parameter File/Nodalization

##### Nodalization

The application of the MAAP-DBA containment model to a commercial nuclear power plant begins with the characterization of the containment building geometry, emergency safeguard systems, etc., in a plant specific parameter file. While this parameter file includes specifications for the entire plant (including the reactor coolant system), the application of the MAAP-DBA containment model to the large LOCA and MSLB design basis evaluations, with the external specification of the mass and energy releases into the containment, only requires that the containment information be qualified for the specific plant. The remaining information has been developed for the BVPS RCS designs such that it can also be used for medium and small break LOCA evaluations.

When formulating a containment parameter file, the most important decision lies in the specification of the number of nodes used to represent the building. To be consistent with the previous BVPS DBA analyses, the evaluations for peak pressure and temperature are performed using single node models. However, those evaluations which are sensitive to potential water accumulation (holdup) in various locations within the building are performed with multi-node models, i.e., 18 nodes for BVPS-1.

There are a few guidelines to be followed for multi-node models.

1. Each building region which is a separate room or compartment with limited connections (flow paths) to the remainder of the building should be treated as a separate node.
2. Typically the design basis accident conditions include analyses for a large break RCS LOCA as well as evaluations for a main steam line break. For those accident analyses requiring a multi-node model such as maximum recirculation sump temperature following a large break LOCA, the containment nodalization should include the region surrounding the reactor coolant system, the loop compartment(s), and the region above the operating deck as individual nodes. In this regard, the LOCA conditions considered include any sensitivities related to whether the LOCA is postulated to occur in any of the reactor coolant loops. Consequently, if the reactor coolant loops are in one large compartment, a single node is sufficient. Conversely, if the loop compartments and other RCS components, such as the pressurizer, are in individual rooms, then the nodalization scheme should be expanded to include each of these compartments as a separate node.
3. An important parameter of the DBA evaluations is the sump temperature under accident conditions. Thus, that region in the bottom of the containment which includes the recirculation sump and the floor of the containment outside the reactor cavity needs to be considered as a separate node.

4. The nodalization scheme needs to be sufficient to represent the potential for light gas stratification in the top of the containment building. Consequently, there should be at least two nodes (one above the other) in the region above the operating deck where light gases, such as steam and/or hydrogen could accumulate. This is the only region of the Beaver Valley Containment model that uses multiple nodes to represent the given region.

#### Flow Paths/Junctions

Multi-node models also require specification of the junctions (flow paths) connecting the various nodes. These are defined in the TOPOLOGY section of the parameter file. These junctions include doorways, hatchways, open areas, grating, etc. These junctions enable the major flow transport paths to be clearly specified and quantified with respect to their available area, their potential to be flooded by water accumulation, the potential for water accumulation within containment nodes, etc. Hence, this topology description is important in providing a realistic multi-node characterization, including the potential for global and countercurrent natural circulation, of the containment response to DBA conditions.

#### Structural Heat Sinks

Structural heat sink information including the surface areas, thicknesses, materials, whether they are steel lined, whether the outer surface is painted, etc., is also described in the parameter file. During DBA conditions the heat sink response is typically sufficiently slow that only a few heat sinks have the thermal conduction developed through the entire width of the heat sink. Nonetheless the MAAP-DBA parameter file has the capability for all of these heat sinks to be identified as two-sided structures, thereby enabling the parameter file to be used for DBA evaluations as well as for accident analyses evaluations over an extended time period, i.e., hours or days. To accomplish this, the node facing each heat sink surface is identified in the parameter file, i.e., a heat sink face is pointed to the specific node with which it interacts, and its opposite face is pointed to another node.

#### Engineered Safeguards

Engineered safeguards that are specific to the containment are also defined in the parameter file, including the containment spray pumps, and the heat exchangers that are used to remove decay heat from the containment during recirculation. The configuration of the ECCS and containment spray injection pumps must be specified in terms of:

- those pumps which take suction only from the Refueling Water Storage Tank (RWST),
- those pumps which take suction from the RWST and are switched over to take suction from the containment sump at containment recirculation,
- those pumps which only take suction from the containment sump under recirculation conditions.

Heat removal capabilities (if any) must be identified with the type of pumping system. Loss of function related to the single failure criterion are addressed in the input decks assembled for each sequence. The parameter file is meant to represent the nominal operating condition for specific systems. As part of this, the configuration also defines whether any pumps are “piggybacked” to the discharge of a lower pressure pump to increase their discharge pressure.



### Treatment of the Mass and Energy Releases

As discussed in Section 14.3.4.2.1, there are a number of LOCA accident conditions that are analyzed for the containment response. The discharge from the break location is the mass and energy source that is input into the containment analysis.

There are two means of treating the mass and energy releases input to MAAP-DBA. For instance, the evaluations for the maximum temperatures within containment following an accident focus on those set of conditions which result in the hottest steam being released to the containment atmosphere, i.e., a double-ended break where the mass and energy streams from the two sides of the break (the hot water flow rate from the cold leg side and the steam flow from the steam generator side) are discharged into the containment atmosphere as separate streams. Conversely, the evaluations for the minimum available NPSH focus on those conditions which could result in the maximum sump temperature and the largest recirculation flow rate to maximize the frictional losses. In this case, the mass and energy releases from the two sides of the guillotine break are mixed together before entering the containment such that there is minimal steam released to the containment environment and the temperature of the water added to the containment sump is maximized. Therefore, from this description, the mass and energy releases for a similar type of break are manipulated to cover the potential uncertainties related to the break configuration and how this influences the specific attributes that must be evaluated to ensure that the containment is capable of remaining within its design basis envelope for all of the accident conditions considered.

For those accident sequences, which result in the long term response of the containment, after containment recirculation, the mass and energy releases from the RCS are dependent upon the temperature of the containment sump due to the recirculated and injected water. (The sump water may pass through a heat exchanger prior to this injection). Since the sump temperature changes with time, long term evaluations require feedback from the containment evaluation. Specifically, the mass and energy releases need the sump water temperature history such that long term analyses properly incorporate the decreasing temperature of the containment sump. Because of this, the long-term (greater than 3600 seconds) mass and energy release calculations are performed with the MAAP-DBA code. These input functions are used to incorporate the sump water temperature history, and are consistent with the methodology discussed in Section 14.3.4.2.1. These user defined functions are characterized for the long term discharge from the break for both a mixed discharge and for an unmixed discharge of steam and water. In both cases, the flow rates that are used are those calculated with the methodology discussed in Section 14.3.4.2.1 and only the specific enthalpies of the discharge flows are calculated to represent the influence of the time dependent RCS injection temperature as the containment cools.

### Influence of Varying Containment Operating Conditions

Another aspect of the evaluation is the spectrum of operating conditions that could be experienced by the containment at the time that the accident is initiated. For example, the containment pressure may vary between 12.8 and 14.2 psia. Furthermore, the containment atmosphere temperature could be at its maximum value or its minimum value. These types of operating parameters have an influence on the specific attribute being evaluated, and the different boundaries of these operating conditions were investigated to determine the set of conditions which maximizes the challenge to the attributes being evaluated.

### Uncertainty on the MAAP-DBA Modeling Parameters

The previous discussion focuses on those uncertainties related to the containment operating envelope. These must also be combined with those uncertainties associated with the physical model parameters identified in the containment evaluation. As an example, the condensation model has an uncertainty related to the data that were used to formulate the empirical representation and its comparison with the spectrum of condensation experiments reported in the literature. These uncertainty boundaries were investigated with respect to the specific containment analysis being performed. For example, the condensation rate should be minimized for those evaluations which are focused on the possible peak containment pressure but would be maximized for those which are focused on the maximum liner temperature under design basis accident conditions.

### MAAP-DBA Modeling Approach

As noted previously, the MAAP-DBA model utilizes both single node and multi-node models to address the spectrum of DBA analyses. Unit specific single node models are used for the peak pressure and peak temperature analyses and the unit specific multi-node models are used for those analyses which are influenced by water holdup in subcompartments. These two approaches are outlined below.

### Single Node Containment Model

The design basis containment response calculations are implemented consistent with the intent of the Standard Review Plan. The containment peak pressure and temperature responses for large LOCA and main steamline breaks use the Tagami and Uchida heat transfer correlations to conservatively quantify the participation of the passive heat sinks. Implementation of these heat transfer correlations leads to the use of a single node containment model. Thus, the total containment volume and passive containment heat sinks are incorporated in a single node containment model that is applied for quantifying the peak pressure, peak gas temperature, and maximum containment liner temperature for the spectrum of main steamline break and large LOCA breaks. Furthermore, the containment liner temperature response is biased toward maximizing the energy transfer by using a multiplier of four (consistent with NUREG-0588) on the Tagami and Uchida heat transfer coefficients per the BVPS-1 current licensing basis.

### Multiple Node Containment Model

The assessment of some of the long-term containment response attributes is conducted with a multiple node containment model. Specifically, the large break LOCA NPSH, the small break LOCA NPSH, and the large and small break LOCA sump water temperature attributes implement a multiple node model. The sump water level and temperature histories are a key results to quantifying these specific attributes. Thus, the relative delivery rate and removal of water inventory from the containment sump and lower compartment influence the NPSH and sump temperature histories. Water hold-up from the break or spray injection sources in containment subcompartments directly influences the sump water level and temperature histories. Additionally, the distribution of containment sprays as they are collected on the operating deck floor can also influence these attributes. Thus, a multiple node containment configuration that identifies the elevations and sizes of junctions connecting the various containment regions is implemented for these evaluations.

The multiple node model uses natural convection heat transfer models for calculating the energy transfer rate to the containment heat sinks distributed through these multiple nodes. The natural convection heat transfer models are biased to minimize the calculated available NPSH.

#### Input Parameters, Assumptions and Model

Table 14.3-5a lists the key input data utilized in the containment analysis.

Based on detailed drawing reviews and site visits and considering the plant-specific features, it was determined that the containment would most appropriately be represented with an 18 node model of the containment (see Figures 14.3-45, 14.3-46 and 14.3-47). This scheme enables the model to represent the individual compartments for each of the three Reactor Coolant System (RCS) loops, the recirculation sump region, the reactor cavity region, the annular region outside of the cooling loops, and three nodes above the operating deck. Using multiple nodes above the operating deck enables the stratification of light gases to be calculated when this is part of the evaluation. The physical flow paths between the containment compartments are also included, as junctions, in the containment model. The junction areas and loss coefficients are based on the plant dimensions and are summarized in Table 14.3-6. MAAP-DBA calculates the quasi steady state nodal pressure distribution at each time step such that inertial effects due to flow acceleration are not required nor calculated due to the relatively slow containment pressurization (containment pressure benchmarks have demonstrated this behavior). Thus, inertial coefficients for each junction are not included in the parameter file.

One principal input element for the MAAP-DBA code is the parameter file which defines the containment geometry, nominal operating conditions, pump curves, etc.

Major parts of the parameter file include the individual nodal volumes that make up the total containment volume, the volume vs. height function of these nodes such that water accumulation can be properly evaluated, the structural and containment heat sinks within these individual nodes, the surface characterization of the heat sink in terms of whether the surface is painted, how it is painted (number of layers, their thicknesses and the thermal conductivity of each layer), whether the heat sink is concrete, steel or steel lined concrete, etc. Furthermore, the setpoints for system actuation, pump curves, heat exchanger capacities, etc., are also contained in the unit-specific parameter file. The containment node volumes, metal heat sink areas and masses, and concrete heat sink areas and thicknesses included in the containment model, are tabulated in Tables 14.3-7 and 14.3-8. The heat sinks include structural steel, concrete liners, ventilation ducts and supports, pipes, pipe supports and restraints, and heavy equipment.

The characteristics of the containment spray systems (header elevations and flow rates) are also included in the parameter file. A quench spray (QS) system is actuated on a containment high-high pressure signal and, after a start delay, directs cold water from the RWST to the quench spray ring header in containment.

After a RWST low level, coincident with a containment pressure high-high signal, a recirculation spray (RS) system is actuated, which directs water from the containment recirculation sump, through a heat exchanger, and then to the recirculation spray ring header in containment. Containment heat removal is accomplished by the RS heat exchanger.

### Acceptance Criteria

An acceptance criterion was developed for each of the types of analyses being performed. These are as follows:

- peak containment pressure less than 45 psig and the pressure is less than half the peak pressure within 24 hours,
- peak liner temperature less than 280°F.

#### 14.3.4.3 Pressure Transient Results

Containment analysis were conducted for large break LOCAs including a double-ended hot leg break (DEHL) and a double-ended pump suction break (DEPS). See Section 14.3.4.2.1 for discussion of the mass and energy releases.

Table 14.3-16 summarizes the peak containment pressures for the large break LOCA cases. The pressures are reported as psig and referenced to an atmospheric pressure of 14.3 psi. As illustrated by this table, all of these sequences result in a pressurization which is less than the design basis value of 45 psig.

Figure 14.3-56 illustrates the containment pressure and temperature time history for the DEHL Break case. Figure 14.3-56a and Figure 14.3-56b illustrate the containment pressure and temperature time histories in the break node for the DEPS Break cases.

The sequence of events are summarized in Tables 14.3-17a, 14.3-17b, and 14.3-17c.

As mentioned previously, the acceptability of the results for the containment pressure is that the design basis break conditions analyzed using design basis methodology for the mass and energy releases to the containment must be less than the design basis structural capability of 45 psig. As demonstrated by analyses for various types of break conditions and mass and energy releases, these results meet the acceptance criteria of less than 45 psig. Also, the calculated pressure transients demonstrate that the containment pressure is reduced to below one-half of the peak pressure within 24 hours.

### Quench and Recirculation Spray

The containment depressurization system discharges water into the containment via the quench spray and recirculation spray headers. Heat transfer between both the quench and recirculation sprays and the containment atmosphere is computed in each time interval.

The recirculation spray subsystems reject heat through coolers to river water. The recirculation spray headers are located approximately 80 ft above the main operating floor.

The quench spray subsystems spray chilled water from the refueling water storage tank into the containment via the quench spray headers located approximately 96 ft above the main operating floor.

The quench spray subsystem flow rate is determined as a function of the difference between containment total pressure and the RWST water level. This is based upon the pump head versus capacity curve and pressure losses in lines, headers and nozzles.

The initial height of water in the RWST, referenced against the suction point, is an input parameter to the MAAP-DBA computer program. The height of the column of water is computed throughout the run based on the summation of flows out of the tank.

#### Quench and Recirculation Spray Effectiveness

Heat and mass transfer to the spray droplets from the quench and recirculation sprays are both calculated. The important spray system input quantities for these calculations are the spray flow rate, the spray water temperature, the initial droplet diameter, and the spray nozzle height. The important gas phase input quantities are the pressure, gas temperature, and the partial pressure of water vapor. The mass and energy flow rates transferred to the gas phase by evaporation, condensation, and convective heat transfer are calculated. Spray droplets are assumed to enter the containment at the spray nozzle height at their terminal velocity and drift downward until they either strike the water surface that collects on the floor of the compartment or they evaporate. Typically, the droplets enter at a cold temperature below the dewpoint of water vapor in the gas. Moisture in the gas condenses on the droplets, which are heated by convective heat transfer as well as by latent heat. The droplets rise in temperature past the dewpoint and begin to evaporate. They asymptotically reach the wetbulb temperature where the convective heat transfer to the droplet is just balanced by evaporative cooling. The evaporating droplet continues to drift downward until it is entirely evaporated or it has reached the floor of the compartment.

#### 14.3.4.4 Post-DBA Hydrogen Generation

The NRC eliminated from 10 CFR 50.44, "Combustible gas control for nuclear power reactors," the postulated design-basis LOCA hydrogen release, and requirements for hydrogen control systems to mitigate such a release. These provisions were eliminated since it was determined that such a hydrogen release is not risk significant.

10 CFR 50.44(b)(1) requires that all containments have a capability for ensuring a mixed atmosphere.

Convective mixing associated with containment spray system operation ensures a uniform mixture of hydrogen within the containment.

The BVPS-1 containment is similar to the Surry Power Station - Units 1 and 2 for which it has been established that adequate mixing of the containment atmosphere by containment spray systems is achieved.<sup>(66)</sup> As BVPS-1 has the capability for ensuring a mixed atmosphere, it complies with 10 CFR 50.44(b)(1).

#### 14.3.4.5 Analysis of Containment Subcompartments

The containment subcompartments comprise the reactor cavity, steam generator cubicles, and pressurizer cubicle. Since application of Leak-Before-Break (LBB) to the design of the permanent reactor cavity water seal and to the design of the reactor cavity drain excludes consideration of large bore pipe breaks inside the lower reactor cavity (below the reactor cavity water seal), the reactor cavity analysis is excluded. Furthermore, the application of LBB criteria eliminates the reactor coolant system primary pipe breaks and the pressurizer surge line break inside the steam generator cubicles and pressurizer cubicle, respectively.

Since the original subcompartment analyses for the steam generator cubicles and the pressurizer cubicle did not take the LBB credit, the existing conservative analyses, which bound the smaller pipe breaks within the cubicles, are retained as historical calculations for the steam generator and pressurizer cubicle wall design.

The subcompartment pressure analyses make use of the following initial conditions:

1. Initial pressure = 9.5 psia. (12 psia for the pressurizer superstructure).
2. Initial Relative Humidity = 46 % (50% for the pressurizer superstructure)
3. Initial Temperature = 105°F (70°F for the pressurizer superstructure)

The operating range of the subcompartments at atmospheric operation are 12.8 – 14.2 psia (pressure), 15-100% (relative humidity), and 70 – 105°F (temperature).

In general, the use of minimum initial pressure, relative humidity, and temperature is conservative for cubicle pressurization. However, the impact of initial conditions on the cubicle pressurization is considered to be minimal due to sufficient cubicle wall design margins.

Double-ended ruptures of a hot leg and the surge line were assumed for the steam generator and pressurizer cubicles, respectively. A double-ended rupture of the spray line is assumed for the Pressurizer Superstructure (above El. 767 ft-10 inches).

Mass and energy release rates shown in Tables 14.3-20 and 14.3-21 were computed by assuming frictionless Moody flow from the reactor vessel side of the break, while the flow from the steam generator side incorporates the effect of friction.

The release rates for the slot break or single-ended rupture (which is equivalent to one pipe flow area) shown in Table 14.3-21 were computed assuming frictionless Moody flow.

The mass and energy rates for the surge line and spray line DER, shown in Tables 14.3-22 and 14.3-23 were supplied by Westinghouse (Note that the 10 percent margin Westinghouse has applied for the surge line DER was removed prior to use of the rates).

Outflow from the cubicles is computed in CUPAT using the LOCTVS vent flow model.

### Free Volume and Vent Areas

The Table 14.3-32 provides a tabulation of the free volume and vent areas for each interior compartment analyzed: (See Figure 14.3-82 for a schematic presentation of volumes and vent areas for the steam generator and pressurizer cubicles).

### Mass and Enthalpy Release Rates

Tables of mass and enthalpy release rates are shown in Tables 14.3-20 through 14.3-23. The blowdown calculations make use of Moody flow with friction for saturated effluent and an adaption of the Zaloudek correlation for subcooled effluent.

### Jet Force Impingement

The following is a description of the analyses and results for the evaluation performed for jet forces impinging on the walls of interior compartments.

Calculation of the total jet force from a postulated rupture is based on Moody's theoretical model<sup>(43)(44)(45)</sup> and Fauske's experimental data<sup>(46)</sup>. It is assumed that the retarding action of the total jet force is constant at all axial locations. The jet impingement pressure on a distant object will be computed by assuming that the jet stream expands conically at a solid angle of twenty degrees.

For normal impingement, the jet impingement force on a distant object is equal to the product of the jet impingement pressure and the intercepted jet area. If the object intercepts the jet stream with a curved or inclined surface area, then the drag force between the jet and the object will be taken as the jet impingement force.

Within the steam generator cubicles, various mechanisms for pipe breaks allowing for jet impingement on the walls were considered. The most critical break from the point of view of structural integrity is that which occurs as a longitudinal split on the axis of the cold or hot leg (see Figure 14.3-98). Longitudinal splits are considered to be elliptical in shape with major and minor axes of 2D inches and 1/2D inches, respectively. The split location is picked at a point along the pipe run such that its full length can be propagated without affecting valve-pipe, or equipment-nozzle welds. Where pipe assemblies shorter than 2D in length are encountered, the pipe split is limited to 1/2D times pipe length, but never exceeding the cross sectional area of the pipe. For this specific orientation of break, an elasto-plastic analysis of the cubicle wall is performed to ensure the wall has sufficient ductility to absorb the energy of the jet force. The jet force resulting from the pipe break is shown by Figure 14.3-97. This force is computed by the summation of momentum expulsion rate and the exit plate pressure force. The Punching shear capacity of the loaded section of wall is designed to accommodate the jet impingement. The cubicle pressure buildup for a longitudinal split of a hot leg is assumed to act concurrently with jet impingement.

It should be noted that any orientation of the longitudinal split, other than the 3 o'clock  $\pm$  1 radian in the cold leg or 9 o'clock  $\pm$  1 radian in the hot leg looking radially inward (see Figure 14.3-98), would not overstress the cubicle walls beyond their elastic capacity. Further, every other conceivable break such as a double-ended rupture or longitudinal split of the pressurizer surge line was analyzed. Magnitudes of loading were derived as previously stated, and the stresses

within the cubicle walls and floors were found to be within elastic ranges. A double-ended rupture of either the hot or cold leg causing jet impingement on the shield wall was not considered possible because for circumferential breaks along a straight run of pipe restrained at the ends, the reaction of the jet on the pipe tends to center the pipe about the original pipe run axis. The reactor coolant loops represent short stiff sections of piping and as such, vibration and plastic hinge formation due to instability need not be considered. For the hot and cold leg circumferential breaks considered, no pipe whip is possible, thus the jets from each end of the break work in opposition to one another, resulting in an undefined steam and water release. Therefore, only the pressure and temperature effects on the cubicles were considered for these specific breaks.

### Steam Generator Cubicles

The three steam generator cubicles were each modeled by a single node, with the assumption of instantaneous and complete mixing of steam and air. Figure 14.3-99 indicates the arrangement within the cubicles and vent locations for a typical steam generator cubicle. These cubicles are open volumes with no restrictions to flow, as can be seen from Figures 5.1-1, 5.1-2, 5.1-3, 5.1-4, 5.1-5, 5.1-6, and 5.1-7.

For the steam generator cubicles, the line break which produces the highest cubicle pressure is a double-ended rupture of a hot leg. Since the peak pressure for the steam generator cubicles occurs approximately 1 second after the accident, the line break that discharges the most mass and energy to the cubicle during this time produces the highest peak pressure in the cubicle.

Back pressure for the steam generator cubicles was determined by first computing the vent flow directly to the containment from cubicle 1A (which has the least vent area) from a base run in which a constant back pressure was assumed, then making a containment transient pressure run with the mass and energy release rates computed from the vent flows. The resulting pressure transient was then input as back pressure for the subcompartment pressure analysis. The vent flow to the containment as a function of time was then compared to the original vent flow value (with constant back pressure) and found to be almost identical.

### Pressurizer Cubicle

A multi-node (4-node) model was developed for the pressurizer superstructure (above El. 767 ft-10 inches) in order to predict the pressure response following a spray line DER. The computer program THREED<sup>(107)</sup> was used to calculate the pressure transient using Westinghouse mass and energy release data (see Figure 14.3-89).

The pressurizer cubicle (for the surge line DER) was analyzed with two nodes using a multinode version of the CUPAT computer program. The two nodes (upper and lower pressurizer cubicles) are separated by a floor at the 738 ft 10 inch elevation. Two different break locations in the surge line were analyzed. One postulated location of a surge line DER is in the lower pressurizer cubicle (between El. 718 ft 6 inch and 738 ft 10 inch) which vents to the upper pressurizer cubicle (above El. 738 ft 10 inch) and to the containment. The other postulated location is in the upper pressurizer cubicle which can vent to the lower pressurizer cubicle and the containment (see Figure 14.3-91).



The air duct that surrounds the lower part of the neutron shield wall beneath the steam generator compartments was to eliminate any potential blockage of flow from the cubicle vent areas. In the analysis it was assumed that the duct would fail, thus eliminating any resistance to vent flow from the steam generator cubicles.

The back pressure for the pressurizer cubicles was determined in a manner similar to that used for the steam generator cubicles.

#### Compartment Design Capability

The peak differential pressures associated with the interior steam generator cubicles, loops A, B and C, and the pressurizer cubicle, upper and lower compartments, plotted as differential pressure vs. time are shown on Figures 14.3-86, 14.3-87, 14.3-88, 14.3-89, 14.3-90, 14.3-91, and 14.3-92.

In order to compare the design capability of the compartment to the loadings described above, the failure capacity of the structures has been determined utilizing yield line techniques.

The limiting pressure for the steam generator cubicles has been calculated to be 28 psi; for the pressurizer cubicle, both upper and lower compartments, 24 psi; and for pressurizer superstructure, 5 psi. Under the above differential pressures the cubicles will perform so that no loss of function of safety related equipment will result.

#### Results

Figures 14.3-86, 14.3-87, 14.3-88, 14.3-90, and 14.3-92 graphically show the pressure response (differential pressure) of the components as a function of time.

The maximum differential pressure across the wall of the pressurizer superstructure at a power level of 2910 MWt is approximately 2.3 psi, which is below the design pressure of 5 psi.

It should be noted that all of the above plots represent differential pressures between the cubicle and the containment free volume.

The effect of the extended power uprate on the subcompartment analyses is due to the reduction in the RCS temperature. This results in a higher mass flow rate into the subcompartment and consequently a higher rate of pressurization of the subcompartment. Since the peak pressure is reached within the subcompartment in less than 3 seconds, the effect of the power uprate and steam generator design are not significant.

#### 14.3.5 Radiological Consequences

This section addresses the radiological consequences of the postulated design basis accident. Although the preceding thermal and hydraulic analyses concluded that there would be little if any core damage, the analyses described in this section are based on assumptions that assume major core damage resulting in release of significant radionuclides to the containment.

#### 14.3.5.1 Fission Product Cleanup

The containment depressurization system (section 6.4) is designed to reduce post accident containment pressure by condensing released steam and is designed to absorb iodine present in the containment atmosphere in inorganic vapor form and in particulate form with chemical spray.

In the effectively sprayed region, fission product cleanup is actively accomplished by the quench and recirculation spray systems and passively by transport of particulates to the spray droplets and heat sink surfaces as a result of steam condensation on these surfaces (diffusiophoresis). In the unsprayed region, only passive gravitational settling promotes particulate removal.

The bounding fission product cleanup calculation for Units 1 and 2 is performed with the containment at atmospheric conditions and with power uprating conditions. The estimated dose consequences following a LOCA reflect the changes in the recirculation spray system operation incorporated as part of the resolution to GSI-191, associated sump strainer modification and change in buffering agent from sodium hydroxide to sodium tetraborate.

##### Removal of Particulates by Sprays

The particulates are effectively removed from the containment atmosphere by the quench and recirculation spray systems. The particulate removal rate is calculated with Stone & Webster's proprietary SWNAUA Computer Program<sup>(96)</sup>. The SWNAUA Program is a derivative of the NAUA/MOD4 Computer Program<sup>(97)</sup> which has been modified for DBA calculations to include a conservative model for aerosol removal by sprays.

The model correlations that were implemented into SWNAUA tend to underestimate the spray removal coefficient. The spray model was originally described in Reference 98. For the effectively sprayed region of the containment, SWNAUA employs only the conservatively developed spray removal model and conservative condensation rates for the diffusiophoresis calculation when performing DBA calculations. While agglomeration is considered, its impact on the resulting particulate removal rates is negligible. In summary, the aerosol removal rates calculated by SWNAUA are conservative lower bound estimates.

There are several aerosol mechanics phenomena that promote the depletion of aerosols from the containment atmosphere. These include the natural phenomena of agglomeration, gravitational settling, diffusional plate-out, and diffusiophoresis; and removal by fluid mechanical interaction with the falling droplets that enter the containment atmosphere through the spray system nozzles. The particulate removal calculation for the effectively sprayed region takes credit for the removal effectiveness of only diffusiophoresis and sprays. Agglomeration of the aerosol is considered. If gravitational settling and diffusional plate-out were considered, the spray removal coefficients would be slightly reduced but the total removal effectiveness by all removal mechanisms would increase. In the unsprayed region, only gravitational settling of aerosols is credited.

The spray model in SWNAUA evaluates the particulate removal efficiency for each particle size in the aerosol by the following mechanisms: inertial impaction, interception, and Brownian diffusion. The aerosol removal constant due to spray is presented in NUREG-0772<sup>(99)</sup> as:

$$\lambda_{\text{spray}} = \frac{3 F_m h \varepsilon}{4 R_{\text{sp}} \rho_w V} \times \frac{V_{\text{spray}} - V_{\text{sed}}}{V_{\text{spray}}}$$

where

$\lambda_{\text{spray}}$	=	Particulate removal constant for spray
$F_m$	=	Spray mass flow rate
$h$	=	Spray fall height
$\varepsilon$	=	Collision efficiency
$R_{\text{sp}}$	=	Spray droplet radius
$\rho_w$	=	Density of the spray droplet
$V$	=	Effectively sprayed volume of containment
$V_{\text{spray}}$	=	Velocity of the spray droplets
$V_{\text{sed}}$	=	Aerosol sedimentation velocity

The collision efficiency is divided into three contributing mechanisms as described in BMI-2104<sup>(100)</sup>:

$$\varepsilon = \varepsilon_i + \varepsilon_r + \varepsilon_d$$

where

$\varepsilon_i$	=	Efficiency due to inertial impaction
$\varepsilon_r$	=	Efficiency due to interception
$\varepsilon_d$	=	Efficiency due to Brownian diffusion

For viscous flow around the spray droplet, the inertial impaction efficiency is given in NUREG-0772<sup>(99)</sup>:

$$\varepsilon_i = \frac{1}{\left[ 1 + \frac{0.75 \ln(2 \text{ Stk})}{\text{Stk} - 1.214} \right]^2}$$

The critical Stokes number,  $Stk$ , for viscous flow is 1.214; for  $Stk$  below this value, the model assumes the efficiency of inertial impaction is 0. The  $Stk$  is calculated from BMI-2104<sup>(100)</sup>:

$$Stk = \frac{2 \rho_p r^2 C_c (v_{\text{spray}} - v_{\text{sed}})}{9 \mu R_{\text{sp}}}$$

where

- $r$  = Aerosol particle radius
- $\rho_p$  = Aerosol density
- $C_c$  = Cunningham slip correction factor
- $\mu$  = Gas viscosity

For droplet sizes typical of nuclear plant spray systems, the data of Walton and Woolcock<sup>(101)</sup> show that the inertial impaction efficiency will be closer to that predicted for potential flow around the droplet. Calvert<sup>(102)</sup> fitted this data to the expression:

$$\varepsilon_i = \left( \frac{Stk}{Stk + 0.7} \right)^2$$

The inertial impaction efficiency predicted by this equation is always higher than that predicted by the viscous flow expression given above. Calvert's fit is employed in this calculation.

For the remaining constituents of the collision efficiency, the spray model employs an interception efficiency of the form:

$$\varepsilon_r \cong \frac{3}{2} \left( \frac{r}{R_{\text{sp}}} \right)^2 \times \left( 1 - \frac{1}{3} \frac{r}{R_{\text{sp}}} \right)$$

which is a conservative approximation of the expression given by BMI-2104<sup>(100)</sup>. The efficiency due to Brownian motion is also taken from this report:

$$\varepsilon_d = 3.5 Pe^{-2/3}$$

where

- $Pe$  = Peclet number
- =  $2v_{\text{spray}}R_{\text{sp}}/D_B$
- $D_B$  = Aerosol diffusion coefficient
- =  $k_{\text{Boltz}}TB$  (Fuchs, Reference 103, p. 181)

- $k_{\text{Boltz}}$  = Boltzmann constant
- =  $1.3804 \times 10^{-16}$  erg/K
- $T$  = Temperature, K

Fuchs (Reference 103, p. 27) gives the aerosol mobility, B:

$$B = \frac{C_c}{6 \pi \mu r}$$

In most cases, the collision efficiency is dominated by inertial impaction, but for small aerosols, Brownian diffusion may become dominant. The inertial impaction efficiency increases as aerosol size is increased, whereas the Brownian diffusion increases as aerosol size decreases.

The model can handle a distribution of up to 20 droplet radii with the spray removal efficiency being determined for each aerosol size bin. However, the droplet diameter distribution can be accurately represented by a single diameter equal to the mass mean diameter<sup>(98)</sup>.

The bounding plant parameters for Units 1 and 2 are listed below.

Bounding Plant Parameters for Fission Product Cleanup Calculations

Parameter	Value
Sprayed Containment Volume	$3.1973 \times 10^{10}$ cm <sup>3</sup>
Fall Height	2,403 cm
Spray Flow Rate	1,821 gpm (120-2,080 sec)
	2,956 gpm (2,080-3,870 sec)
	6,108 gpm (3,870-10,938 sec)
	3,267 gpm (10,938-346,000 sec)
Spray droplet radius	
Mass mean radius	500 μm (120-346,000 sec)

The containment pressure, temperature, relative humidity, and steam condensing rate transients following the NUREG-1465 style DBA are presented in Table 14.3-12.

### Description of Aerosol

The chemical composition of the aerosol is important only as it relates to the density of aerosol utilized in the development of spray lambdas. The chemical composition during the gap release phase is assumed to be predominantly CsOH. The chemical composition during the in-vessel release phase is assumed to be 20 percent CsOH, 20 percent indium, and 60 percent silver. These compositions are based on a review of the SASCHA experimental results. The aerosol input data for SWNAUA are provided below.

#### **Description of Aerosol**

Minimum Aerosol Radius	1.0E-07 cm
Maximum Aerosol Radius	1.0E-02 cm
Maximum Number of Aerosol Size Bins	100
From 30 sec to 1830.0 sec	
Aerosol Injection Rate	6.13 (gm/sec)
Mean Geometric Radius	7.5E-06 cm
Geometric Standard Deviation	1.56
Aerosol Density	3.7 gm/cc
From 1830 sec to 6510.0 sec	
Aerosol Injection Rate	58.53 (gm/sec)
Mean Geometric Radius	4.0E-05 cm
Geometric Standard Deviation	1.46
Aerosol Density	4.6 gm/cc

### Removal of Particulates by Diffusiophoresis

Diffusiophoresis entrains particulate matter in steam as it flows toward condensation surfaces. In this calculation, steam is assumed to condense on the spray droplets, on particulate matter, and on heat sinks. The diffusiophoresis model in the SWNAUA computer code is the same as that in the NAUA/MOD4 computer code.

The steam condensation rates used by SWNAUA are calculated by the LOCTIC computer code<sup>(104)</sup>. The LOCTIC code calculates conservative DBA containment pressure and temperature responses. Because LOCTIC predicts a conservatively high containment pressure transient, the rate of steam condensation from the containment atmosphere is minimized. The steam condensation rates that are input to the diffusiophoresis calculation of SWNAUA are taken as the steam removal rates from the containment atmosphere determined by LOCTIC.

The coefficient for removal of particulates from the effectively sprayed and unsprayed regions of the containment are plotted versus time in Figures 14.3-100 and 14.3-101, respectively. For the effectively sprayed region, the aerosol removal is due to sprays and diffusiophoresis. The particulate removal coefficient in the unsprayed region is due to gravitational settling only.

### Removal of Elemental Iodine

The calculated removal rate for elemental iodine in the vapor phase by sprays always exceeds  $20 \text{ hr}^{-1}$ , the maximum value permitted by NUREG-0800, Standard Review Plan Section 6.5.2<sup>(105)</sup>. Therefore, elemental iodine is conservatively assumed to be removed by sprays at either the same rate as the aerosol particles when the aerosol removal rate is lower than  $20 \text{ hr}^{-1}$  or at  $20 \text{ hr}^{-1}$  when the aerosol removal rate is calculated to be higher than the NRC limit.

A plateout removal coefficient for elemental iodine is calculated with the model provided in NUREG-0800, Standard Review Plan Section 6.5.2<sup>(105)</sup>. In the effectively sprayed region, a minimum plateout coefficient of  $2 \text{ hr}^{-1}$  is calculated.

No credit is taken for elemental iodine removal in the unsprayed region.

### Effectively Sprayed Containment Volume Fraction

The sprayed volume fraction of the containment is determined by superimposing spray patterns for various spray nozzle orientations onto containment arrangement drawings. The sprayed volume is the volume of unblocked spray patterns. The spray patterns are based on the nozzle manufacturer's laboratory tests at atmospheric conditions. The patterns have been compressed to account for the higher density atmosphere that exists during a DBA. The effectively sprayed volume is calculated by combining highly mixed unsprayed regions with directly sprayed regions.

The effective spray coverage fraction is determined to be 63.0 percent of the containment free volume. The concentration of fission products is expected to be uniform in the containment volume above the operating floor since this volume is open with very few obstructions to mixing. The sprayed volume is taken as the free volume above the operating floor plus the volume below the operating floor that is covered by recirculation spray. Actually, the whole containment is expected to be uniform in fission product concentration based on the discussion below, but the sprayed volume fraction has been limited to 63.0 percent.

### Containment Mixing

The mixing rate between the effectively sprayed volume and the unsprayed volume of the containment is assumed to be  $2 \text{ hr}^{-1}$ , the rate permitted by NUREG-0800, the Standard Review Plan Section 6.5.2<sup>(105)</sup>.

#### 14.3.5.2 Release Pathways for DBA Case

The DBA LOCA dose analysis supporting BVPS-1 utilizes input parameter values that are bounding for an event at either Unit 1 or Unit 2, Alternative Source Terms (AST) methodology as outlined in 10 CFR 50.67 and Regulatory Guide 1.183, and a core power level of 2918 MWt.

A LOCA would increase the pressure in the containment, initiating containment isolation auxiliary feedwater, emergency core cooling, and containment spray. Normal ventilation in the auxiliary and contiguous buildings is realigned and the engineered safety features (ESF) areas are aligned and exhausted by the supplementary leak collection and release system (SLCRS). However, no credit is taken for filtration of the containment and ESF leakage prior to release to the environment.

Due to the rapid pressure transient expected following a LOCA, the Containment Isolation Phase B (CIB) signal, which initiates the control room isolation and emergency ventilation system, is assumed to occur at T=0 hours.

The analysis assumes a Loss of Offsite Power (LOOP) at T=0 hours. The impact of a LOOP at a more unfavorable time following the accident, such as during the fuel release phase, is not addressed per NRC Information Notice 93-17. The need to evaluate a design basis event assuming a simultaneous or subsequent LOOP is based on the cause/effect relationship between the two events (an example illustrated in IN 93-17 is that a LOCA results in a turbine trip and a loss of generation to the grid, thus causing grid instability and a LOOP a few seconds later; i.e., a reactor trip could result in a LOOP). IN 93-17 concludes that plant design should reflect all credible sequences of the LOCA/LOOP, but states that a sequence of a LOCA and an unrelated LOOP (which would be the case if a LOOP was assumed to occur 1 to 2 hours after the event) is of very low probability and is not a concern.

The doses to personnel in the control room following a LOCA are discussed later on in this section, in Section 11.3.5 and provided in Table 14.1-1A. Input parameters used for the LOCA dose assessment including estimated doses to the population at the exclusion area boundary (EAB) and at the low population zone (LPZ) outer boundary are provided in Table 14.3-14a. The dose consequences following a LOCA are due to releases from the containment vacuum release system prior to containment isolation, containment leakage, ESF leakage, and back-leakage to the RWST. Figure 14B-1 of Appendix 14.B illustrates the release pathway of containment leakage.

#### Containment Vacuum System Release Source

It is assumed that the containment Vacuum System is operating at the initiation of the LOCA and that the release is terminated as part of containment isolation. In accordance with Regulatory Guide 1.183 the entire RCS inventory, assumed to be at levels in Table 14B-15 is released to the containment at T=0 hours. It is conservatively assumed that 100% of the volatiles are instantaneously and homogeneously mixed in containment atmosphere. Containment pressurization (due to the RCS mass and energy release), combined with the relief line cross-sectional area, results in a release of containment atmosphere to the environment.



Since the release is isolated before the onset of the gap phase release assumed to be at 30 seconds, no fuel damage releases are postulated.

Per Regulatory Guide 1.183, the chemical form of the iodine released from the RCS is assumed to be 97% elemental and 3% organic. The containment Vacuum System line is routed to the Process Vent which is located on top of the BVPS-1 Cooling Tower. However, since the associated piping is non-seismic, it is conservatively assumed that the release occurs at the containment wall.

No credit is taken for processing this release via the safety related ventilation exhaust and filtration system that services the areas contiguous to containment; i.e., the Supplementary Leak Collection System (SLCRS) filters. To ensure bounding values, the atmospheric dispersion factors utilized for this release reflects the worst value between the containment wall release point and the SLCRS release point for 0-2 hr time period.

Table 14.3-14a tabulates the significant input parameters and assumptions used in determining the radiological consequence due to the containment vacuum release pathway. An assessment of the activity release via this pathway demonstrates that its contribution to the site boundary and control room dose is negligible.

#### Containment Leakage Source

The inventory of fission products in the reactor core available for release via containment leakage following a LOCA is based on Table 14B-1A which represents a conservative equilibrium reactor core inventory of dose significant isotopes, assuming maximum full power operation at a core power level of 2918 MWt, and taking into consideration fuel enrichment and burnup.

The fission products released from the fuel are assumed to mix instantaneously and homogeneously throughout the free air volume of the primary containment as it is released from the core. Containment sprays are utilized as one of the primary means of fission product cleanup following a LOCA. BVPS design includes a containment quench spray and a containment recirculation spray system at each of the units. Following post LOCA containment pressurization, the quench spray system is automatically initiated by the CIB signal, and injects cooling water from the refueling water storage tank (RWST), into the containment, via the quench spray system spray headers. Based on an assumption of a LOOP coincident with the LOCA, the quench spray is assumed to be initiated, at either unit, by approximately T=120 secs, and is available until depletion of the RWST inventory based on maximum ESF. The recirculation spray system takes suction from the containment sump and provides recirculation spray inside containment via the recirculation spray headers. Credit for recirculation spray is taken up to 4 days post-LOCA.

In accordance with Regulatory Guide 1.183, two fuel release phases are considered for DBA analyses: (a) the gap release and (b) the early In-Vessel release.

Since the BVPS long term sump pH is controlled to values of 7 and greater, the chemical form of the radioiodine released from the fuel is assumed as provided on Table 14.3-14a. With the exception of noble gases; elemental and organic iodine, all fission products released are assumed to be in particulate form.

The activity released from the core during each release phase is modeled as increasing in a linear fashion over the duration of the phase. The release into the containment is assumed to terminate at the end of the early in-vessel phase.

In the "effectively" sprayed region the activity transport model takes credit for aerosol removal due to steam condensation and via containment recirculation and quench sprays based on spray flowrates associated with minimum ESF. It considers mixing between the sprayed and unsprayed regions of the containment, reduction in airborne radioactivity in the containment by concentration dependent aerosol removal lambdas, and isotopic in-growth due to decay.

Since, using the SRP 6.5.2 methodology, the calculated elemental iodine spray removal lambdas are greater than  $20 \text{ hr}^{-1}$ , it is conservatively assumed that the sprays remove the elemental iodine at the same rate as the aerosols when the aerosol removal rates are less than  $20 \text{ hr}^{-1}$ , and at  $20 \text{ hr}^{-1}$  when the aerosol removal rate is greater than  $20 \text{ hr}^{-1}$ . In the effectively sprayed region, a minimum plateout coefficient of  $2 \text{ hr}^{-1}$  is calculated for BVPS. This allows a maximum elemental iodine removal rate in the effectively sprayed region, during the spray period, of  $22 \text{ hr}^{-1}$ .

In the unsprayed region, the aerosol removal lambdas reflect gravitational setting. No credit is taken for elemental iodine removal in the unsprayed region.

Since the spray removal coefficients are based on calculated time dependent airborne aerosol mass, there is no restriction on the DF for particulate iodine. The maximum DF for elemental iodine is based on SRP 6.5.2.

Mixing between the "effectively" sprayed and unsprayed regions of the containment is assumed for the duration of the accident. Though higher mixing rates are expected, the dose analysis conservatively assumes a mixing rate of 2 unsprayed volumes per hour in accordance with the default value noted in SRP 6.5.2.

Current BVPS design includes providing sufficient amount of sodium tetraborate (NaTB) to the containment sump water which ensures a long term sump pH of 7 or greater. Consequently, iodine re-evolution is not addressed. The definition of long term as it relates to sump pH and iodine re-evolution post LOCA is based on NUREG/CR 5732.

Radioactivity is assumed to leak from both the sprayed and unsprayed region to the environment at the containment technical specification leak rate for the first day, and half that leakage rate for the remaining duration of the accident (i.e., 29 days). No credit is taken for processing the containment leakage via the safety related ventilation exhaust and filtration system that services the areas contiguous to containment; i.e., the Supplementary Leak Collection System (SLCRS) filters. To ensure bounding values, the atmospheric dispersion factors utilized for the containment release path reflects the worst value between the containment wall release point and the SLCRS release point for each time period.

Table 14.3-14a tabulates all significant input parameters and assumptions used in determining the radiological consequence due to containment leakage.

### ESF and RWST Back-leakage

With the exception of noble gases, all the fission products released from the core in the gap and early in-vessel release phases are assumed to be instantaneously and homogeneously mixed in the primary containment sump water at the time of release from the fuel. The minimum sump volume increases to a steady state minimum value of 326,000 gallons two hours after the LOCA. Three sump volume values are utilized in the transport model. Up to the first half hour after the LOCA, the sump volume is about 44% of the final value. For the next one and half-hours the sump volume is about 58% of the final value. For the remainder of the accident the steady state minimum sump volume is utilized. In accordance with Regulatory Guide 1.183, with the exception of iodine, all radioactive materials in the recirculating liquid are assumed to be retained in the liquid phase. The subsequent environmental radioactivity release is discussed below:

- ESF leakage: Equipment carrying sump fluids and located outside containment are postulated to leak at twice the expected value of 5700 cc/hr (BVPS-1 value) into the auxiliary building. ESF leakage is expected starting at initiation of the recirculation spray. Note that due to the long-term nature of this release, minor variations in the start time of this release will not significantly impact the resultant doses. As noted in Regulatory Guide 1.183, the fraction of total iodine in the liquid that becomes airborne should be assumed to be equal to the fraction of the leakage that flashes to vapor. The flash fraction (using Regulatory Guide 1.183 methodology) associated with this temperature is calculated to be less than 10%. Consequently, in accordance with Regulatory Guide 1.183, 10% of the halogens associated with this leakage is assumed to become airborne and are exhausted (without mixing and without holdup) to the environment via the SLCRS vent located on top of Containment. In accordance with Regulatory Guide 1.183, the chemical form of the iodine released from the sump water is 97% elemental and 3% organic. No credit is taken for the SLCRS filters.
- RWST Back-leakage: Sump water back-leakage into the RWST (located in the Yard) is postulated to occur at twice the expected leakrate of 1 gpm, to be released directly to the environment via the RWST vent. Sump water begins to leak into the RWST after the LOCA. The iodine begins to flow out of the RWST and disperses to the environment. A significant portion of the iodine associated with the RWST back-leakage is retained within the tank due to equilibrium iodine distribution balance between the RWST gas and liquid phases (i.e., a time dependent iodine partition coefficient). The analysis includes sodium tetraborate (NaTB) as the buffering agent for sump water pH control. Environmental airborne iodine activity resulting from RWST leakage is assumed to be 97% elemental and 3% organic. In the dose model, this phenomenon is modeled using a series of effective environmental release rate lambdas from the RWST vent. The analysis of RWST back-leakage envelopes the RWST design modifications for ECCS switchover level setpoint and maximum temperature.

Table [14.3-14a](#) tabulates all significant input parameters and assumptions used in determining the radiological consequence due to ESF and RWST back-leakage.

### Direct Dose

The direct dose is due to activity in the atmosphere and sump of the containment building and from contained sources in systems carrying radioactive LOCA fluid outside containment. The shielding provided by the containment structure and other buildings, plus the distance factor are considered in the evaluation of the direct doses to the control room and offsite locations. Contained sources that contribute to the direct shine dose in the control room are described later on in this section. Note that contained sources are an insignificant contributor to the dose at the EAB and LPZ.

### Control Room Habitability

Beaver Valley Power Station is served by a single control room that supports both units. The joint control room is serviced by two ventilation intakes, one assigned to BVPS-1 and the other to BVPS-2. These air intakes are utilized for both the normal as well as the accident mode.

During normal plant operation, both ventilation intakes are operable providing a total supply of 500 cfm of unfiltered outside air makeup which includes all potential inleakage and uncertainties.

Upon receipt of a containment isolation Phase B signal, or a high radiation signal from the control room area monitors, the normal outside air supply dampers automatically close, thus isolating the control room envelope (CRE). This signal also initiates the Unit 2 control room emergency ventilation system (CREVS). On detection of failure of one train, the second train is automatically initiated after a short time delay.

In the unlikely event that neither of the BVPS-2 CREVS trains can be put in service, operator action may be utilized to initiate the BVPS-1 CREVS train. This unlikely scenario is utilized in the DBA dose consequence analyses to allow flexibility in taking out a BVPS-2 CREVS train for maintenance.

CREVS is capable of providing the CRE with a sufficient supply of air to meet the pressurization requirements. The system is capable of maintaining the ambient pressure slightly above atmospheric pressure for an indefinite period of time after the accident. Each CREVS can draw outside air through a filter assembly which consists of a HEPA filter and carbon adsorber with removal efficiency of 99% for the particulate aerosols and 98% for the radioiodines. These emergency supply filtration units and associated air handling equipment are designed to Seismic Category I and Safety Class 3 requirements.

The control room ventilation recirculation flow is not filtered, but remains in service during emergency conditions to maintain the control room within design temperature limits.

The BVPS control rooms (CR) are contained in a single CRE, which is therefore modeled as a single region. Isotopic concentrations in areas outside the CRE are assumed to be comparable to the isotopic concentrations at the CRE intake locations.

The atmospheric dispersion factors for the various combinations of release point/receptor applicable for all accidents, are provided in Tables [2.2-12A](#) and [2.2-12B](#).

The atmospheric dispersion factors associated with CRE inleakage are assumed to be the same as those utilized for the CRE intake. Control room tracer gas tests have indicated that potential sources of unfiltered inleakage into the CRE during the post accident pressurization mode are the normal operation dampers associated with the CRE ventilation system to which it is reasonable to assign the same X/Q as that of the CRE air intake.

The other source of inleakage is potentially that associated with door seals. This inleakage, plus an allowance of 10 cfm for ingress and egress, is assigned to the door leading into the control room that is considered the point of primary access. This door is located at grade level and in-between the BVPS-1 and BVPS-2 control room air intakes. It is located close enough to the referenced air intakes to allow the assumption that the X/Q associated with this source of inleakage would be reasonably similar to that associated with the air intakes.

Use of conservative estimates in the accident dose consequence analyses for CRE unfiltered inleakage that envelope the results of tracer gas testing provides margin for surveillance tests.

Taking into account Loss of Offsite Power (LOOP), the maximum estimated delay following a LOCA in attaining control room isolation after receipt of a CIB signal to switch from CRE normal operation to emergency ventilation mode, which accounts for delays due to Emergency Diesel Generator start, sequencing and damper movement/re-alignment.

Since the LOCA is intended to be bounding for an event at either unit, no credit is taken for automatic initiation of CREVS. Rather it is assumed that operator action will be necessary to initiate the CREVS, and that a pressurized control room will be available. As discussed above, in the event one of the BVPS-2 trains is out of service, and the second train fails to start, operator action will be utilized to initiate the BVPS-1 CREVS. Operator action to initiate the BVPS CREVS and availability of a pressurized CRE at 30 minutes is assumed for all of the DBAs that credit CREVS.

To support development of bounding CRE doses the most limiting X/Q associated with the release point/receptor for an event in either unit is utilized for the LOCA. The CRE post-accident ventilation model utilized in the LOCA dose analysis correspond to an assumed "single intake" which utilizes the worst case atmospheric dispersion factor (X/Q) from release points associated with accidents at either unit, to the limiting CRE intake. This approach has also been used for all of the DBA dose consequence analyses that are intended to be bounding.

For the LOCA, a CRE unfiltered inleakage is conservatively assumed during the time it is isolated. This value is based on the results of tracer gas testing in the isolated mode, and includes a 10 cfm unfiltered inleakage due to ingress/egress as well as a margin to address potential future deterioration. The analysis takes into account measured inleakage using mean values of the tracer gas test measurements.

The CREVS intake flow includes allowance for measurement uncertainties. For the LOCA and all of the other DBAs, the CRE unfiltered inleakage during the emergency pressurization mode is conservatively assumed (includes 10 cfm unfiltered inleakage due to ingress/egress) to reflect the results of tracer gas testing in the pressurized mode, and margin. The analysis takes into account measured inleakage using mean values of the tracer gas test measurements.

For reasons outlined below, the dose model uses the minimum intake flow rate in the pressurized mode as it is considered to be more limiting. Although the intake of radioisotopes is higher at the larger intake rate, it is small compared to the radioactivity entering the control room, in both cases, due to unfiltered inleakage. Consequently, the depletion of airborne activity in the CRE via the higher exhaust rate make the lower intake rate more limiting from a dose consequence perspective. This argument holds true because the Committed Effective Dose Equivalent (CEDE) from inhalation is far more limiting than the Deep Dose Equivalent (DDE) from immersion which is principally from noble gases.

The control room operator doses following a LOCA include contributions due to cloud immersion, external plume shine, airborne activity shine through penetrations in adjoining areas, direct shine from sources in the RWST and from the buildup of activity on the control room intake filters. The direct dose from sources inside the containment and RWST were found to be an insignificant dose contributor.

Table 14.3-14a lists key assumptions/parameters associated with BVPS control room design utilized for the LOCA dose analyses. The results of these calculations are provided in Table 14.1-1A.

### Dose Model

The radiological consequences from a postulated LOCA are analyzed in accordance with the guidance provided in Regulatory Guide 1.183. S&W computer code PERC2 is utilized in the analysis. PERC2 is a multiple compartment activity transport code which calculates the Committed Effective Dose Equivalent (CEDE) from inhalation and the Deep Dose Equivalent (DDE) from submersion due to halogens, noble gases and other nuclides at the offsite locations and in the control room. The Total Effective Dose Equivalent (TEDE) is the sum of CEDE and DDE. The dose calculation model is described in Appendix 14B and is consistent with the regulatory guidance. Table 14.3-14a tabulates all significant input parameters and assumptions used in determining the radiological consequences of a LOCA.

The environmental releases resulting from the LOCA are used in conjunction with the atmospheric dispersion values given in Table 2.2-12A or Table 2.2-12B, whichever is more limiting.

The estimated worst 2-hour EAB dose (occurs between 0.5-2.5 hrs) and LPZ doses for the duration of the accident are provided in Table 14.1-1B and are within the regulatory limit of 25 rem TEDE specified in 10 CFR 50.67<sup>(36)</sup>. The estimated control room operator dose due to a LOCA at either unit is presented in Table 14.1-1A and is within the regulatory limit of 5 rem TEDE specified in 10 CFR 50.67<sup>(36)</sup>.

#### 14.3.6 Summary of Loss-of-Coolant Accident Effects on the Reactor Coolant System, the Containment and on Offsite Doses

For breaks up to and including the double-ended severance of a reactor primary coolant pipe, the Emergency Core Cooling System (ECCS) with minimum engineered safety features prevents clad melting and ensures that the core remains in place and substantially intact with its essential heat transfer geometry preserved. The ECCS design meets the core cooling criteria with substantial margin for all cases.

The basic requirement of the ECCS following any LOCA, including the double-ended severance of a reactor primary coolant pipe, is that sufficient integrity be maintained to permit the safe and orderly shutdown of the reactor. This implies that the core must remain essentially intact and deformation of internals must be sufficiently small that reactor coolant loop flow and, particularly, adequate safety injection flow will not be impeded. The ability to insert control rods to the extent necessary to provide shutdown following the accident must be maintained. The analysis indicates that these criteria are met. The analysis of the effects of injecting safety injection water into the RCS following a postulated LOCA shows that the integrity of the reactor vessel is never violated and core cooling is not jeopardized.

The containment structure is capable of containing, without loss of integrity and undue hazard to the public, breaks up to and including the double-ended severance of a reactor coolant pipe. The containment depressurization system removes heat and airborne fission products from the containment atmosphere and returns the containment to conditions that are close to atmospheric pressure. The recirculation spray subsystems transfer the heat from the containment to the river water system, thereby removing fission decay heat, reducing the pressure to near atmospheric and maintaining the containment pressure near atmospheric.

Using conservative values of the containment leak rate, containment spray iodine removal coefficients and meteorological dispersion coefficients for the BVPS-1 site, the offsite radiation doses as a result of the LOCA are found to be below the guidelines set forth in 10 CFR 50.67.

References to Section 14.3

1. Lee, H., Rupprecht, S.D., Tauche, W.D., Schwarz, W.R., "Westinghouse Small Break ECCS Evaluation Model Using the NOTRUMP Code," WCAP-10054-P-A, August 1985.
2. Meyer, P.E., "NOTRUMP, A Nodal Transient Small Break and General Network Code," WCAP-10079-P-A, August 1985.
3. J. M. Hellman, "Fuel Densification Experimental Results and Model for Reactor Application," WCAP-8219, Westinghouse Electric Corporation (October 1973).
4. F. M. Bordelon, et al., "LOCTA-IV Program: Loss-of-Coolant Transient Analysis," WCAP-8301-P, WCAP-8305-NP, Westinghouse Electric Corporation (June 1974).
5. Deleted by Revision 23.
6. Deleted by Revision 23.
7. Deleted by Revision 23.
8. Deleted by Revision 23.
9. Deleted by Revision 23.
10. F. M. Bordelon, and E. T. Murphy, "Containment Pressure Analysis Code (COCO)," WCAP-8327 (Proprietary Version), WCAP-8326 (Non-Proprietary Version), Westinghouse Electric Corporation (June 1974).
11. Johnson, W. J. (Westinghouse) letter to Murley, T. E. (USNRC), NS-NRC-89-3463, October 5, 1989
12. Deleted by Revision 0.
13. Deleted by Revision 23.
14. S. Fabric, Computer Program WHAM for Calculation of Pressure, Velocity and Force Transient in a Liquid-Filled Piping Network," Report No. 67-49-R, Kaiser Engineers (November 1967).
15. WCAP-10325-P-A, (Proprietary), WCAP-10326-A (Nonproprietary), "Westinghouse LOCA Mass & Energy Release Model for Containment Design – March 1979 Version," May 1983.
20. WCAP-8264-P-A, Rev. 1 (Proprietary), WCAP-8312-A (Nonproprietary), "Westinghouse Mass and Energy Release Data for Containment Design," August 1975
21. Beaver Valley Power Station Pre-Application Report dated November 2003 submitted to the NRC by FENOC letter L-03-188 on November 24, 2003.



References to Section 14.3 (CONT'D)

22. Docket No. 50-315, "Amendment No. 126, Facility Operating License No. DPR-58 (TAC No. 7106), for D. C. Cook Nuclear Plant BVPS-1," June 9, 1989.
23. EPRI 294-2, Mixing of Emergency Core Cooling Water with Steam; 1/3 Scale Test and Summary," (WCAP-8423), Final Report, June 1975.
24. Deleted by Revision 2.
25. NU-092, Version 15, Level 01, "THREED-A Sub-compartment Transient Response Code", by J.C. Boyle, Reissue: August, 1988 (Stone & Webster Proprietary).
26. Final Draft, Safety Evaluation Report, Beaver Valley Power Station, Unit 2, Docket No. 50-412, June, 1985, Section 6.2.1.2.
27. Deleted by Revision 2.
28. Deleted by Revision 2.
29. Deleted by Revision 2.
30. Deleted by Revision 0.
31. Deleted by Revision 23.
32. Deleted by Revision 0.
33. Deleted by Revision 0.
34. Deleted by Revision 0.
35. Deleted by Revision 0.
36. Deleted by Revision 0.
37. Deleted by Revision 23.
38. Stone & Webster letter from W. J. L. Kennedy to Dr. Peter A. Morris, Director of Reactor Licensing, Atomic Energy Commission, Subject: 70 percent of the available core sensible heat by the reactor vessel blowdown ends (December 6, 1971).
39. T. Tagami, "Interim Report on Safety Assessments and Facilities Establishment Project in Japan for Period Ending June, 1965 (No. 1)," Section IV (February 28, 1966).
40. Deleted by Revision 23.
41. Deleted by Revision 23.
42. Letter from J. H. Noble, Stone & Webster Engineering Corporation, to Mr. Samuel Jensch, USAEC, Subject: "Heat Transfer to Containment Spray Particles" (October 2, 1970).
43. F. J. Moody, "Maximum Two-Phase Vessel Blowdown for Pipes," Transactions of the American Society of Mechanical Engineers, Journal of Heat Transfer (August 1967).

References to Section 14.3 (CONT'D)

44. F. J. Moody, "Prediction of Blowdown Thrust and Jet Forces," Paper No. 69-HT-31 American Society of Mechanical Engineers.
45. F. J. Moody, "Time Dependent Pipe Forces Caused by Blowdown and Flow Stoppage," Paper No. 73-FE-23 American Society of Mechanical Engineers.
46. H. K. Fauske, "The Discharge of Saturated Water Through Tubes," Chemical Engineering Progress Symposium Series, No. 59, Vol. 61., pp 210-216.
47. Deleted by Revision 0.
48. Deleted by Revision 0.
49. Deleted by Revision 2
50. Deleted by Revision 0.
51. Deleted by Revision 0.
52. Deleted by Revision 0.
53. Deleted by Revision 23.
54. Deleted by Revision 23.
55. Deleted by Revision 0.
56. Deleted by Revision 0.
57. F. Kreith, Principles of Heat Transfer, International Textbook Company (1966).
58. Deleted by Revision 7.
59. Deleted by Revision 23.
60. Deleted by Revision 7.
61. Deleted by Revision 7.
62. Deleted by Revision 7.
63. Deleted by Revision 7.
64. Deleted by Revision 7.
65. Deleted by Revision 7.
66. Safety Evaluation in the Matter of Virginia Electric Power Company, Surry Power Stations Units 1 and 2, Docket Numbers 50-280 and 50-281, pp. 57-58, Atomic Energy Commission (February 23, 1972).

67. NUREG-0772, "Technical Bases for Estimating Fission Product Behavior During LWR Accidents," Appendix E, June 1981.
68. Deleted by Revision 20
69. Deleted by Revision 20
70. Deleted by Revision 20
71. Deleted by Revision 20
72. Deleted by Revision 12
73. Deleted by Revision 22.
74. Deleted by Revision 23.
75. "American National Standard for Decay Heat Power in Light Water Reactors," ANSI/ANS - 5.1 - 1979, American Nuclear Society, August 1979.
76. D.C. Slaughterback, "A Review of Heat Transfer Coefficients for Condensing Steam in a Containment Building Following a Loss of Coolant Accident," Interim Task Report, Subtask 4.2.2.1, Idaho Nuclear Corporation, January 1970.
77. "PWR FLECHT Final Report," WCAP - 7665, Westinghouse Electric Corporation, April 1971.
78. Deleted by Revision 23.
79. Deleted by Revision 23.
80. Letter from K. E. Halliday (Duquesne Light Company) to G. D. Simmers (Westinghouse), Subject: BV Unit 1 Increased SGTP and Reduced TDF Program, ND1MNE:6312, October 12, 1992. (LOCA Parameters.)
81. Deleted by Revision 23.
82. Deleted by Revision 23.
83. Letter from J. M. Hall (Westinghouse) to N. R. Tonet (Duquesne Light Company), Subject: BV Units 1&2 10 CFR 50.46 Notification and Reporting Information, DLW-93-202, January 29, 1993.
84. Deleted by Revision 23.
85. Deleted by Revision 23.
86. Deleted by Revision 23.
87. 10 CFR 50.67, "Accident Source Term."

References to Section 14.3 (CONT'D)

88. Regulatory Guide 1.183, Revision 0, "Alternative Radiological Source Terms for Evaluating Design Basis Accidents at Nuclear Power Reactors," July 2000.
89. NRC Information Notice 93-17, Revision 1, "Safety Systems Response to Loss of Coolant and Loss of Offsite Power," March 25, 1994 (original issue March 8, 1993).
90. NUREG/CR-5732, "Iodine Chemical Forms in LWR Severe Accidents - Final Report," April 1992.
91. S&W Proprietary Computer Code, PERC2, "Passive Evolutionary Regulatory Consequence Code," NU-226, V00, L01.
92. Industry Computer Code SCALE 4.3, "Modular Code System for Performing Standardized Computer Analyses for Licensing Evaluation for Workstations And Personal Computers," Control Module SAS2H, Version 3.1, developed by ORNL (S&W Program NU-230, V05, L03).
93. Industry Computer Code ARCON96, "Atmospheric Relative Concentrations in Building Wakes" developed by PNL (S&W Program EN-292, V00, L00).
94. S&W Proprietary Computer Code, SWNAUA, "Aerosol Behavior in Condensing Atmosphere," NU-185, V02, L00.
95. S&W Computer Code, SW-QADCGGP, "A Combinatorial Geometry Version of QAD-5A," NU-222, V00, L02.
96. Lischer, D.J., User's Manual, Aerosol Behavior in a Condensing Atmosphere (SWNAUA), June 1993, (Stone & Webster Proprietary).
97. Bunz, H., Kayro, M., Schöck, W., 1982, NAUA/Mod4 - A Code for Calculating Aerosol Behaviour in LWR Core Melt Accidents, Code Description and User Manual, KfK.
98. Elia, Frank A. Jr. and Lischer, D. Jeffrey, Advanced Method for Calculating the Removal of Airborne Particles with Sprays, 1993, ASME paper no. 93-WA/SERA-5.
99. NUREG-0772, 1981, "Technical Bases for Estimating Fission Product Behavior During LWR Accidents."
100. Battelle Columbus Laboratories, BMI-2104, Vol. III, draft report, 1984, "Radionuclide Release Under Specific LWR Accident Conditions."
101. Walton, W. H., and Woolcock, A., 1960, "The Suppression of Airborne Dust by Water Spray," Interm. J. Air Pollution 3, 129-153.
102. Calvert, S., 1970, "Venturi and Other Atomizing Scrubbers Efficiency and Pressure Drop," AIChE Journal 16, 392-396.

References to Section 14.3 (CONT'D)

103. Fuchs, N.A., 1964, "The Mechanics of Aerosols," revised and enlarged edition, Dover Publications, Inc.
104. Cho, J. H., User's Manual, Loss of Coolant Transient Inside Containment (LOCTIC), January 1993, (Stone & Webster Proprietary).
105. NUREG-0800, 1988, Standard Review Plan, "Containment Spray as a Fission Product Cleanup System," Section 6.5.2, Revision 2.
106. "Acceptance Criteria for Emergency Core Cooling Systems for Light Water Cooled Nuclear Power Reactors: 10 CFR 50.46 and Appendix K of 10 CFR 50.46," Federal Register, Volume 39, Number 3, January 4, 1974.
107. Foster, J.P., et al., Westinghouse Improved Performance Analysis and Design Model (PAD 4.0), WCAP-15063-P-A, Revision 1, with Errata, 2000.
108. Federal Register, "Emergency Core Cooling Systems: Revisions to Acceptance Criteria," V53, N180, pp. 35996-36005, September 16, 1988.
109. USNRC Regulatory Guide 1.157, "Best-Estimate Calculations of Emergency Core Cooling System Performances," May 1989.
110. Boyack, B., et al., 1989, "Qualifying Reactor Safety Margins: Application of Code Scaling Applicability and Uncertainty (CSAU) Evaluation Methodology to a Large Break Loss-of-Coolant-Accident," NUREG/CR-5249.
111. Letter, R. C. Jones (USNRC) to N. J. Liparulo (W), "Acceptance for Referencing of the Topical Report WCAP-12945 (P), Westinghouse Code Qualification Document for Best Estimate Loss-of-Coolant Analysis," June 28, 1996.
112. Bajorek, S. M., et al., 1998, "Westinghouse Code Qualification Document for Best Estimate Loss of Coolant Accident Analysis," WCAP 12945-P-A (Proprietary), Volume I, Revision 2, and Volumes II-V, Revision 1, and WCAP-14747 (Non-Proprietary).
113. SECY-83-472, Information Report from W. J. Dircks to the Commissioners, "Emergency Core Cooling System Analysis Methods," November 17, 1983.
114. Branch Technical Position CSB 6-1, "Minimum Containment Pressure Model for PWR ECCS Performance Evaluation," July 1981.
115. Thompson, C. D. et. al., "Addendum to the Westinghouse ECCS Evaluation Model Using the NOTRUMP Code: Safety Injection into the Broken Loop and COSI Condensation Model," WCAP-10054-P-A, Addendum 2, Rev. 1, July 1997.
116. Amendment 271: BVPS-1 Containment Conversion From SubAtmospheric to Atmospheric Operating Conditions, February 6, 2006.

References to Section 14.3 (CONT'D)

117. Amendment 272: BVPS-1 Applicability of Westinghouse Topical Report WCAP-12945-0-A, " Volume 1 (Revision 2) 1996 and Volume 2-5 (Revision 1), 'Code Qualification Document for Best Estimate LOCA (BELOCA) Analysis' March 1998, February 6, 2006.
118. Amendment 273: BVPS-1 Steam Generator (SG) Replacement, February 9, 2006.
119. Amendment 281: Control Room Envelope Habitability in accordance with Technical Specification Task Force Traveler 448, February 15, 2008.
120. Amendment 286: Beaver Valley Power Station, Unit 1 - Issuance of Amendment Regarding Automated Statistical Treatment of Uncertainty Method Implementation for Large-Break-Loss-Of-Coolant Accident Analysis, July 1, 2010.
121. WCAP-16009-P-A, "Realistic Large Break LOCA Evaluation Methodology Using the Automated Statistical Treatment of Uncertainty Method (ASTRUM)," (Westinghouse Proprietary), 2005.
122. WCAP-13451, "Westinghouse Methodology for Implementation of 10 CFR 50.46 Reporting," October 1992.
123. WCAP-17052-P, "Best Estimate Analysis of the Large-Break Loss-of-Coolant Accident for Beaver Valley Unit 1 Nuclear Plant Using the ASTRUM Methodology," March 2009.
124. WCAP-12610-P-A & CENPD-404-P-A Addendum 1-A, "Optimized ZIRLO™," July 2006.

BVPS UFSAR UNIT 1

TABLES FOR SECTION 14

Table 14.0-1

## LIST OF CONDITIONS

A typical list of Condition I events is listed below:

1. Steady state and shutdown operations
  - a. Power operation (15 to 100 percent of full power)
  - b. Startup (or standby) (critical, 0 to 15 percent of full power)
  - c. Hot shutdown (subcritical, residual heat removal system isolated)
  - d. Cold shutdown (subcritical, residual heat removal system in operation)
  - e. Refueling
2. Operation with permissible deviations

Various deviations which may occur during continued operation as permitted by the plant Technical Specifications must be considered in conjunction with other operational modes. These include:

  - a. Operation with components or systems out of service (such as power operation with a reactor coolant pump out of service)
  - b. Leakage from fuel with cladding defects
  - c. Activity in the reactor coolant
    1. Fission products
    2. Corrosion products
    3. Tritium
  - d. Operation with steam generator leaks up to the maximum allowed by Technical Specifications
3. Operational transients
  - a. Plant heatup and cooldown (up to 100 F per hr for the Reactor Coolant System (RCS); 200 F per hr for the pressurizer)
  - b. Step load changes (up to  $\pm 10$  percent)
  - c. Ramp load changes (up to 5 percent per minute)



Table 14.1-1A

POSTULATED CONTROL ROOM ACCIDENT DOSE, REM  
(Design Basis Accidents at Unit 1)

Accident	Control Room Operator	
	TEDE (rem)	Notes
Loss of Coolant Accident (LOCA)	2.5 (0.61)	1
Control Rod Ejection Accident (CREA)	1.3	2, 3
Main Steam Line Break (MSLB)		3, 5
PIS	0.5	
CIS	0.66	
Steam Generator Tube Rupture (SGTR)		5, 6
PIS	1.96	
CIS	0.68	
Fuel Handling Accident	2.36	5
Locked Rotor Accident (LRA)	2.2	6
Loss of AC Power (LACP)	< 2.2	4, 6
Small Line Break Outside Containment (SLB)	0.7	6

Notes:

- (1) Control room isolation actuated by CIB signal. CR in emergency pressurization mode by T=30 mins due to manual operator action. Dose shown in parenthesis for the LOCA represents that portion of the total dose that is the contribution of direct shine from contained sources/external cloud.
- (2) Dose values are based on the containment release scenario. The dose consequences based on the secondary side release scenario is 0.06 Rem.
- (3) Control room isolation and in emergency pressurization mode by T=30 mins due to manual operator action
- (4) Dose from a postulated Loss of AC Power is bounded by the Locked Rotor Accident.
- (5) The CR is purged for 30 minutes at 16,200 cfm following termination of the environmental releases. The purge initiation times used in the accident analyses are listed below:
  - MSLB: 24 hrs
  - SGTR: 8 hrs
  - FHA: 2 hrs
- (6) The following accidents do not take credit for CREVS operations: SGTR, LRA, LACP, SLB outside Containment

Table 14.1-1B

BEAVER VALLEY POWER STATION BVPS-1  
EXCLUSION AREA BOUNDARY AND LOW POPULATION DOSES (TEDE)

Accident	EAB Dose (rem) <sup>(1,3)</sup>	LPZ Dose (rem) <sup>(2)</sup>	Regulatory Limit (rem)
Loss of Coolant Accident	16.5	3.0	25
Control Rod Ejection Accident <sup>(4)</sup>	3.1	1.5	6.3
Main Steam Line Break (U1) <sup>(5)</sup>	0.08	0.01	25(PIS)
	0.11	0.04	2.5(CIS)
Steam Generator Tube Rupture (U1) <sup>(5)</sup>	2.27	0.14	25(PIS)
	0.93	0.06	2.5(CIS)
Locked Rotor Accident	2	0.33	2.5
Loss of AC Power	(Note 6)	(Note 6)	2.5
Fuel Handling Accident	2.02	0.12	6.3
Small Line Break Outside Containment	0.23	0.012	2.5

Notes:

- (1) EAB Doses are based on the worst 2-hour period following the onset of the event.
- (2) LPZ Doses are based on the duration of the release.
- (3) Except as noted, the maximum 2 hr dose for the EAB is based on the 0-2 hr period:
  - LOCA: 0.5 to 2.5 hr
  - LR: 6 to 8 hr
- (4) Dose values are based on the containment release scenario. The dose consequences based on the secondary side release scenario are 1 Rem (EAB) and 0.1 Rem (LPZ).
- (5) PIS: Pre-accident iodine spike; CIS: Concurrent iodine spike.
- (6) Dose from a postulated Loss of AC Power is bounded by the Locked Rotor Accident.

Table 14.1-2

TIME SEQUENCE OF EVENTS FOR CONDITION II EVENTS

<u>Accident</u>	<u>Event</u>	<u>Time (sec)</u>
Uncontrolled RCCA Withdrawal from a Subcritical Condition	Initiation of uncontrolled rod withdrawal from $10^{-9}$ of nominal power	0
	Power range high neutron flux low setpoint reached	10.4
	Peak nuclear power occurs	10.6
	Rods begin to fall into core	10.9
	Minimum DNBR occurs	12.6
	Peak heat flux occurs	12.6
	Peak average clad temperature occurs at the hot spot	13.1
	Peak average fuel temperature occurs at the hot spot	13.3
Uncontrolled RCCA Withdrawal at Power 1. Case A	Initiation of uncontrolled RCCA withdrawal at maximum reactivity insertion rate ( $8.0 \times 10^{-4} \Delta k/\text{second}$ )	0
	Power range high neutron flux high trip point reached	1.4
	Rods begin to fall into core	1.9
	Minimum DNBR occurs	2.9

Table 14.1-2 (CONT'D)

TIME SEQUENCE OF EVENTS FOR CONDITION II EVENTS

<u>Accident</u>	<u>Event</u>	<u>Time (sec)</u>	
2. Case B	Initiation of uncontrolled RCCA withdrawal at a small reactivity insertion rate ( $0.8 \times 10^{-5} \Delta k/\text{second}$ )	0	
	Overtemperature $\Delta T$ reactor trip signal initiated	104.1	
	Rods begin to fall into core	106.1	
	Minimum DNBR occurs	107.1	
Uncontrolled Boron Dilution			
1. Dilution During Full Power Operation	a. Automatic Reactor Control	Dilution begins; low-low rod insertion limit alarm	0
		Loss of shutdown margin	> 900
	b. Manual Reactor Control	Dilution begins	0
		Reactor trip setpoint reached for overtemperature $\Delta T$	72
	Loss of shutdown margin	> 972	
2. Dilution During Start-up	Dilution begins	0	
	Source range reactor trip	0	
	Loss of shutdown margin	> 900	
Partial Loss of Forced Coolant Flow (3 Loops Operating, 1 RCP Coasting Down)	Coastdown begins	0	
	Low flow reactor trip	1.6	
	Rods begin to drop	2.6	
	Minimum DNBR occurs	3.7	

Table 14.1-2 (CONT'D)

TIME SEQUENCE OF EVENTS FOR CONDITION II EVENTS

<u>Accident</u>	<u>Event</u>	<u>Time (sec)</u>
Loss of External Electrical Load		
1. With pressurizer pressure control	Loss of electrical load/turbine trip	0.0
	Initiation of steam release from steam generator safety valves	9.0
	Overtemperature $\Delta T$ reactor trip setpoint reached	12.3
	Rods begin to drop	14.3
	Minimum DNBR (1.72) occurs	15.6
2. Without pressurizer pressure control	Loss of electrical load/turbine trip	0.0
	High pressurizer pressure setpoint reached	5.5
	Rods begin to drop	7.5
	Peak pressurizer pressure occurs	8.3
	Initiation of steam release from steam generator safety valves	8.6

(1) DNBR does not decrease below its initial value.

Table 14.1-2 (CONT'D)

TIME SEQUENCE OF EVENTS FOR CONDITION II EVENTS

<u>Accident</u>	<u>Event</u>	<u>Time (sec)</u>
Loss of Normal Feedwater	Main feedwater flow stops	10.0
	Low-low steam generator level setpoint reached	63.3
	Rods begin to drop	65.3
	Auxiliary feedwater flow is started	123.3
	Feedwater lines are purged and cold auxiliary feedwater is delivered to three steam generators	586.0
	Core decay heat plus pump heat decreases to auxiliary feedwater heat removal capability	~1100.0
	Peak water level in pressurizer occurs	1274.0
Loss of Non-Emergency AC Power	Main feedwater flow stops	10.0
	Low-low steam generator level setpoint reached	63.6
	Rods begin to drop	65.6
	Reactor coolant pumps begin to coast down	67.6
	Peak water level in pressurizer occurs	844.0
	Auxiliary feedwater flow is started	123.6
	Feedwater lines are purged and cold auxiliary feedwater is delivered to three steam generators	587.0
	Core decay heat decreases to auxiliary feedwater heat removal capability	~750

Table 14.1-2 (CONT'D)

TIME SEQUENCE OF EVENTS FOR CONDITION II EVENTS

<u>Accident</u>	<u>Event</u>	<u>Time (sec)</u>
Excessive feedwater at full load	One main feedwater control valve fails fully open	0
	Minimum DNBR occurs	111.0
	Feedwater flow isolated due to high-high steam generator water level	118.9

Table 14.1-2 (CONT'D)

TIME SEQUENCE OF EVENTS FOR CONDITION II EVENTS

<u>Accident</u>	<u>Event</u>	<u>Time (sec)</u>
Accidental depressurization of the Reactor Coolant System	Inadvertent opening of one RCS safety valve	0
	Low pressurizer pressure trip setpoint reached	16.9
	Rods begin to drop	18.9
	Minimum DNBR occurs	19.8
Inadvertent Operation of ECCS during Power Operation	Charging pumps begin injecting borated water	0
	Low pressure trip point reached	116
	Rods begin to drop	118



Table 14.1-3

PARAMETERS USED IN CONTROL ROOM HABITABILITY ANALYSIS  
OF THE LOSS OF AC POWERED AUXILIARIES ACCIDENT<sup>(1)(2)</sup>

Core Power Level	2918 MWt
Minimum Reactor Coolant Mass	340,711 lbm
Primary to Secondary SG tube leakage	450 gpd @ STP
Melted Fuel Percentage	0%
Failed Fuel Percentage	0%
<b>Secondary Side Parameters</b>	
Minimum Post-Accident SG Liquid Mass	101,799 lbm per SG
Iodine Species released to Environment	97% elemental; 3% organic
Iodine Partition Coefficient in SGs	100 (all tubes submerged)
Particulate Carry-Over Fraction in SGs	0.0025
Steam Releases from SGs	0-2 hr (348,000 lbm) 2-8 hr (778,000 lbm)
Termination of releases from SGs	8 hours
Fraction of Noble Gas Released	1.0 (Released to Environment without holdup)
Environmental Release Point	MSSVs/ADVs
Control Room $\chi/Q$ values	Limiting Values of Table 2.2-12a and Unit 2 UFSAR Table 15.0-14a (i.e., BVPS-1 MSSVs/ADVs to BVPS-1 CR Intake)

**CR Emergency Ventilation: Initiation  
Signal/Timing**

CR is maintained under Normal Operation  
ventilation

**Note:**

- (1) This analysis was originally performed in 1987 in support of plant modifications converting the Unit 1 Control Room to a common Unit 1 - Unit 2 facility. The radiological consequences of this event were not required to be evaluated as part of the licensing basis for Unit 1.
- (2) Bounding parameter values are used to encompass an event at either unit.

Table 14.2-2

TIME SEQUENCE OF EVENTS FOR  
CONDITION IV EVENTS

<u>Accident</u>	<u>Event</u>	<u>Time (Sec.)</u> <u>3-Loop</u>
Major Secondary System Pipe Rupture at Hot Zero Power Conditions	Steam Line Ruptures	0
	Low Steam Pressure SI setpoint is reached	0.7
	SI pumps start	27.7
	Feedwater isolation occurs	30.7
	Criticality attained	29.6
	Borated water reaches loops Minimum DNBR reached	~74.2 277.8
Major Secondary System Pipe Rupture at Hot Full Power Conditions	Steam Line Ruptures	0
	Overpower $\Delta T$ Reactor Trip Setpoint Reached	31.5
	Rods Begin to Drop	33.5
	Minimum DNBR Occurs	34.0
	Peak Core Heat Flux Occurs	34.1

Table 14.2-2 (CONT'D)

TIME SEQUENCE OF EVENTS FOR  
CONDITION IV EVENTS

<u>Accident</u>	<u>Event</u>	<u>Time (Sec.)</u>
Rupture of Main Feed Pipe  1. With Offsite Power	Feedline rupture occurs	10.0
	Low steam pressure setpoint reached in faulted loop	19.0
	Low-low steam generator water level reached in faulted loop	22.0
	Rods begin to drop	24.0
	All main steamline isolation valves closed	27.0
	First steam generator safety valve setpoint reached in an intact steam generator	35.6
	Auxiliary feedwater initiation	79.0
	Feedwater lines are purged and cold auxiliary feedwater is delivered to intact steam generators	804
	Hot and Cold Leg temperatures begin to decrease	~2900.0

Table 14.2-2 (CONT'D)

TIME SEQUENCE OF EVENTS FOR  
CONDITION IV EVENTS

<u>Accident</u>	<u>Event</u>	<u>Time (Sec.)</u>
Rupture of Main Feed Pipe		
2. Without Offsite Power	Feedline rupture occurs	10.0
	Low steam pressure setpoint reached in faulted loop	19.0
	Low-low steam generator level reached in faulted loop	22.0
	Rods begin to drop	24.0
	Reactor coolant pumps begin to coast down	26.0
	All main steamline isolation valves closed	27.0
	First steam generator safety valve setpoint reached in an intact steam generator	36.0
	Auxiliary feedwater initiation	79.0
	Feedwater lines are purged and cold auxiliary feedwater is delivered to intact steam generators	804.0
	Hot & Cold Leg temperatures being to decrease.	~1500

Table 14.2-2 (CONT'D)

TIME SEQUENCE OF EVENTS FOR  
CONDITION IV EVENTS

<u>Accident</u>	<u>Event</u>	<u>Time (sec)</u>
Rod Cluster Control Assembly Ejection		
1. Beginning-of-Life, Full Power	Initiation of rod ejection	0.0
	Power range high neutron flux setpoint reached	0.06
	Peak nuclear power occurs	0.13
	Rods begin to fall	0.56
	Peak fuel average temperature occurs	2.39
	Peak clad average temperature occurs	2.46
	Peak heat flux occurs	2.47
2. End-of-Life, Zero Power	Initiation of rod ejection	0.0
	Power range high neutron flux low setpoint reached	0.17
	Peak nuclear power occurs	0.20
	Rods begin to fall	0.67
	Peak clad average temperature occurs	1.39
	Peak heat flux occurs	1.39
	Peak fuel average temperature occurs	1.82

Table 14.2-3

PARAMETERS USED IN THE ANALYSIS OF THE ROD CLUSTER CONTROL  
ASSEMBLY EJECTION ACCIDENT

<u>Time in Life</u>	<u>Beginning</u>	<u>Beginning</u>	<u>End</u>	<u>End</u>
Power Level, %	100.6	0	100.6	0
Ejected rod worth, %Δk	0.20	0.70	0.21	0.98
Delayed Neutron Fraction, %	0.55	0.55	0.47	0.47
Feedback Reactivity Weighting	1.5	1.866	1.567	3.620
Trip Reactivity, %Δk	4.0	2.0	4.0	2.0
Fq Before Rod Ejection	2.52	---	2.52	---
Fq After Rod Ejection	7.11	10.0	7.6	25.00
Number of Operating RC Pumps	3	2	3	2
Max Fuel Pellet Average Temperature, °F	4136	2568	4008	3914
Max Fuel Center Temperature, °F	4969	3037	4869	4441
Max Fuel Stored Energy, cal/gm	181.6	103.4	174.7	169.8
Fuel Melt (%)	<10	0	<10	0

Table 14.2-4a

SUMMARY OF RESULTS FOR LOCKED ROTOR TRANSIENTS

	<u>3 Loops Operating</u>	
Maximum Reactor Coolant Pressure (psia)	2826	
Maximum Cladding Temperature at Core Hot Spot, (°F)	1884	
Zirc-Water Reaction at Core Hot Spot (weight %)	0.41	

TIME SEQUENCE OF EVENTS

<u>Accident</u>	<u>Event</u>	<u>Time (sec)</u>	
Locked Rotor 3 Loops Operating	1 reactor coolant pump rotor locks	0.0	
	Low flow trip point reached	0.04	
	Rods begin to drop	1.04	
	Maximum reactor coolant system pressure occurs	3.4	
	Peak clad temperature occurs	3.8	

Table 14.2-4b

PARAMETERS USED IN RADIOLOGICAL ANALYSIS  
OF THE LOCKED ROTOR ACCIDENT<sup>(1)</sup>

Core Power Level	2,918 MWt
Minimum Reactor Coolant Mass	340,711 lbm
Primary to Secondary SG tube leakage	450 gpd @ STP
Melted Fuel Percentage	0%
Failed Fuel Percentage	20%
Core Activity of Isotopes	Table 14B-1A
Radial Peaking Factor	1.75
Fraction of Core Inventory in Fuel gap	I-131 (8%) Kr-85 (10%) Other Noble Gases (5%) Alkali Metals (12%)
Iodine Chemical Form in Gap	4.85% elemental 95% CsI 0.15% Organic
<b>Secondary Side Parameters</b>	
Minimum Post-Accident SG Liquid Mass	101,799 lbm per SG
Iodine Species released to Environment	97% elemental; 3% organic
Iodine Partition Coefficient in SGs	100 (all tubes submerged)
Particulate Carry-Over Fraction in SGs	0.0025
Steam Releases from SGs	0-2 hr (348,000 lbm) 2-8 hr (778,000 lbm)
Termination of releases from SGs	8 hours
Fraction of Noble Gas Released	1.0 (Released to Environment without holdup)
Environmental Release Point	MSSVs/ADVs
Control Room $\chi/Q$ Values	Limiting values of Table 2.2-12a and Unit 2 UFSAR Table 15.0-14a (i.e., BVPS-1 MSSVs/ ADVs to BVPS-1 CR Intake)

**CR emergency Ventilation: Initiation Signal/Timing**

CR is maintained under Normal Operation ventilation

Note:

(1) Bounding parameter values are used to encompass an event at either unit.



Table 14.2-5

## TIME SEQUENCE OF EVENTS FOR CONDITION III EVENTS

<u>Accident</u>	<u>Event</u>	<u>Time (sec)</u>
Complete Loss of Forced Reactor Coolant Flow (Frequency Decay)	Coastdown begins	0.0
	Low reactor coolant flow trip point reached	1.7
	Rods begin to drop	2.7
	Minimum DNBR occurs	4.6

Table 14.2-6

PARAMETERS USED IN RADIOLOGICAL ANALYSIS OF THE FUEL HANDLING ACCIDENT

Core Power Level	2918 MWt
Number of Rods in Fuel Assemblies	264
Total Number of Fuel Assemblies	157
Number of Damaged Rods	137
Decay Time Prior to Fuel Movement	100 hours
Radial Peaking Factor	1.75
Fraction of Core Inventory in gap	I-131 (8%) Kr-85 (10%) Other Noble Gases (5%) Other Halides (5%) Alkali Metals (12%)
Core Activity of Noble Gases and Halogens of T=100 hrs Iodine Form of gap release before scrubbing	Table 14.2-6a 99.85% elemental 0.15% Organic
Min depth of water in Fuel Pool or Reactor Cavity	23 ft.
Scrubbing Decontamination Factors	Iodine (200) Noble Gas (1) Particulates ( $\infty$ )
Rate of Release from Fuel Environmental Release Rate (unfiltered) within a 2-hour period	PUFF All airborne activity
Environmental Release Points Accident in Fuel Pool Area	More Restrictive of Ventilation Vent or SLCRS
Accident in Containment	More Restrictive of Equipment Hatch, containment wall or SLCRS
CR Emergency Ventilation: Initiation Signal/Timing Control room is maintained in normal ventilation mode Control room purge initiation (Manual) Time and Rate	2 hours after DBA @ 16,200 for 30 min.

Table 14.2-6a

CORE ACTIVITY OF NOBLE GASES AND HALOGENS  
100-HOURS AFTER SHUTDOWN

<u>Nuclide</u>	<u>Composite Core Activity (Ci)</u>
KR-85	8.27E+05
KR-85M	3.77E+00
XE-127	9.50E+00
XE-129M	4.49E+03
XE-131M	1.00E+06
XE-133	1.11E+08
XE-133M	2.07E+06
XE-135	2.13E+05
XE-135M	6.51E+02
BR-82	4.25E+04
I-129	2.86E+00
I-130	7.64E+03
I-131	5.62E+07
I-132	4.74E+07
I-133	5.86E+06
I-135	3.98E+03

TABLE 14.2-9

PARAMETERS USED IN RADIOLOGICAL ANALYSIS  
OF THE STEAM GENERATOR TUBE RUPTURE ACCIDENT

Core Power Level	2918 MWt
Reactor Coolant Mass	373,100 lbm
Break Flow to Faulted Steam Generator	0-225 sec (21,900 lbm) 225-1800 sec (128,000 lbm)
Time of Reactor Trip	225 sec
Termination of Release from Faulted SG	1800 seconds
Fraction of Break Flow that Flashes	0-225 sec (0.2227) 225-1800 sec (0.1645)
Leakage Rate to Intact Steam Generators	150 gpd @ STP for each SG
Failed/Melted Fuel Percentage	0%
RCS Tech Spec Iodine & NG Concentration	Table 14B-15 (0.35 µCi/gm DE-I131)
RCS Equilibrium Iodine Appearance Rates	Table 14B-16 (0.35 µCi/gm DE-I131)
Pre-Accident Iodine Spike Activity	Table 14B-16 (21 µCi/gm DE-I131)
Accident Initiated Spike Appearance Rate	335 times equilibrium
Duration of Accident Initiated Spike	4 hours
<b>Secondary System Release Parameters</b>	
Intact SG Liquid Mass (min)	91,000 lbm
Faulted SG Liquid Mass (min)	91,000 lbm
Initial SG Liquid Mass per Steam Generators	96,000 lbm
Tech Spec Activity in SG liquid	Table 14B-15 (0.1 µCi/gm DE-I131)
Form of All Iodine Released to the Environment via Steam Generators	97% elemental; 3% organic
Iodine Partition Coefficient (unflashed portion)	100 (all tubes submerged)
Fraction of Iodine Released (flashed portion)	1.0 (Released without holdup)
Fraction of Noble Gas Released from any SG	1.0 (Released without holdup)
Partition Factor in Condenser	100 elemental iodine 1 organic iodine / Noble Gases
Steam Flowrate to Condenser	0-225 sec (1207.407 lbm/sec per SG)
Faulted SG Steam Releases via MSSV/ADVs	225 sec - 1800 sec (68,900 lbm)
Intact SG Steam Releases via MSSV/ADVs	225 sec - 7200 sec (417,100 lbm) 2 hr - 8 hr (979,500 lbm) 8 hr - 16 hr (658,400 lbm) 16 hr - 24 hr (546,700 lbm)
Termination of Release from SGs	24 hours
Environmental Release Points	0-225 sec (Condenser Air Ejector) 225 sec - 24 hours (MSSVs/ADVs)
Control Room x/Q values	MSSVs/ADVs to BVPS-1 CR Intake & Air Ejector to BVPS-1 CR Intake (From Table 2.2-12a)
<b>CR Emergency Ventilation: Initiation Signal/Timing</b>	
Control room is maintained in normal ventilation mode	
CR Purge Initiation (Manual)Time and Rate	8 hours after DBA @16,200 cfm (min) for 30 minutes

TABLE 14.2-10

PARAMETERS USED IN MAIN STEAM LINE BREAK ANALYSIS

Core Power Level	2918 MWt
Reactor Coolant Mass (min)	340,711 lbm
Leakrate into Faulted Steam Generator	150 gpd @ STP
Amount of Accident Induced Leakage (AIL) into Faulted SG.	N/A
Maximum time to cool RCS to 212F	19 hrs
Leakrate into Intact Steam Generators	300 gpd total from 2 SGs @ STP
Failed/Melted Fuel Percentage	0%
RCS Tech Spec Iodine and NG Concentration	Table 14B-15 (0.35 $\mu$ Ci/gm DE-I131)
RCS Equilibrium Iodine Appearance Rates	Table 14B-16 (0.35 $\mu$ Ci/gm DE-I131)
Pre-Accident Iodine Spike Activity	Table 14B-16 (21 $\mu$ Ci/gm DE-I131)
Accident Initiated Spike Appearance Rate	500 times equilibrium appearance rates
Duration of Accident Initiated Spike	4 hours
<b>Secondary System Release Parameters</b>	97% elemental; 3% organic
Iodine Species released to Environment	Table 14B-15 (0.1 $\mu$ Ci/gm DE-I131)
Tech Spec Activity in SG liquid	100 (all tubes submerged)
Iodine Partition Coefficient in Intact SG	1.0 (Released without holdup)
Fraction of Noble Gas Released from Intact SG	1.0 (Released without holdup)
Fraction of Iodine Released form Faulted SG	1.0 (Released without holdup)
Fraction of Noble Gas Released from faulted SG	101,799 lbm per SG
Minimum Post-Accident Intact SG Liquid Mass	101,799 lbm
Maximum Initial Liquid in each SG	0-2 hr (345,000 lbm)
Steam Releases from Intact SG	2-8 hr (734,000 lbm)
	Instantaneous
Dryout of Faulted SG	19 hours
Termination of release from Faulted SG	8 hours
Termination of release from Intact SG	Break Point
Release Point: Faulted SG	MSSV/ADVs
Release Point: Intact SG	
Control Room $\chi$ /Q values	MSSVs/ADVs to BVPS-1 CR Intake & Break location to BVPS-1 CR Intake (From Table 2.2-12a)
<b>CR emergency Ventilation: Initiation Signal/Timing Manual</b>	T=30 minutes
CR pressurized and in Emergency Mode	24 hours after DBA
Control Room Purge (Time/Rate)	@16,200 cfm (min) for 30 minutes

TABLE 14.2-12

PARAMETERS USED IN RADIOLOGICAL ANALYSIS  
OF THE RCCA EJECTION ACCIDENT

**Containment Pathway Parameters**

Power Level	2918 MWth
Minimum Free Volume	1.75E+6 ft <sup>3</sup>
Containment Leakrate (0-24 hr)	0.1% vol fractions per day
Containment Leakrate (1-30 day)	0.05% vol fractions per day
Failed Fuel Percentage	10%
Percentage of Core Inventory in Fuel Gap	10% (noble gases & halogens)
Melted Fuel Percentage	0.25%
Percentage of Core Inventory in melted fuel released to Containment Atmosphere	100% Noble Gas; 25% Halogens
Chemical Form of Iodine in Failed/Melted fuel	4.85% elemental; 95% CsI 0.15% organic
Radial Peaking Factor	1.75
Core Activity Release Timing	PUFF
Form of Failed/Melted Iodine in the Containment Atmosphere	97% elemental; 3% organic
Equilibrium Core Activity	Table <a href="#">14B-1a</a>
Termination of Containment Release	30 days
Environmental Release Point	Containment wall/SLCRS Vent (Containment Top)
Control Room $\chi/Q$ Values	Limiting values of Table 2.2-12a and Unit 2 UFSAR Table 15.0-14a

**Secondary Side Pathway Parameters**

Minimum Reactor Coolant Mass	340,711 lbm
Primary-to-Secondary Leakrate	150 gpd per SG @ STP, 450 gpd total
Termination of Primary-to-Secondary Leakage	2500 secs
Fraction of Failed/Melted Fuel	Same as Containment Pathway
Percentage of Core Inventory in melted fuel released to Reactor Coolant	100% Noble Gas; 50% Halogens
Iodine Species released to Environment	97% elemental; 3% organic
Iodine Partition Coefficient	100 (all tubes submerged)
Fraction of Noble Gas Released	1.0 (Released to Environ without holdup)

TABLE 14.2-12 (CONT'D)

PARAMETERS USED IN RADIOLOGICAL ANALYSIS  
OF THE RCCA EJECTION ACCIDENT

Minimum Post-Accident SG Liquid Mass	99,217 lbm per SG
Steam Releases per SG	0-150 secs: 900 lbs/sec
	150-300 secs 300 lbs/sec
	300-2500 secs 150 lbs/sec
	2500 secs-8 hrs 776,000 lbs
Termination of Release from SGs	8 hours
Environmental Release Point	MSSVs/ADVs
Control Room $\chi/Q$ Values	Limiting values of Table 2.2-12a and Unit 2 UFSAR Table 15.0-14a
<b>CR Emergency Ventilation: Initiation Signal/Timing</b>	
Initiation time	30 minutes by manual operation

Table 14.3-1e

SMALL BREAK LOCA  
 TIME SEQUENCE OF EVENT  
 (2900 MWt Core Power / Westinghouse Model 54F Steam Generator)

Break Size	1.5-inch	2-inch	2.25-inch	2.5-inch	2.75-inch	3-inch	3.25-inch	4-inch	6-inch
Break Initiation	0	0	0	0	0	0	0	0	0
Reactor Trip Signal	54.1	29.0	22.5	17.9	14.6	12.3	10.6	7.3	4.4
S-Signal	75.9	42.4	33.9	27.9	23.8	20.8	18.6	14.4	10.2
Accumulator Injection	N/A	4017	2378	1821	1438	1138	996	637	290
PCT Time <sup>(3)</sup>	(1)	3160.3	2417.0	2209.8	1723.7	1386.4	1215.8	780.2	2209.2
Transient Termination	N/A	(2)	(2)	(2)	(2)	(2)	(2)	(2)	(2)

Notes:

- (1) It has been judged that no core uncover of any consequence will take place and the 1.5-inch case is non-limiting. Therefore no PCT calculations were performed.
- (2) For the cases where core recovery is greater than the transient time, basis for transient termination can be concluded based on some or all of the following: (1) The RCS system pressure is decreasing which will increase SI flow, (2) Total RCS system mass is increasing due to SI flow exceeding break flow, and (3) Core mixture level has begun to increase and is expected to continue for the remainder of the accident.
- (3) The limiting time-in-life for the 2.75-inch break case for PCT was determined to be at 8,000 MWD/MTU. All other PCT times are for beginning-of-life (BOL).



Table 14.3-1f

SMALL BREAK LOCA<sup>(1)</sup>  
 FUEL CLADDING DATA  
 (2900 MWt Core Power / Westinghouse Model 54F Steam Generators)

Break Size (in)	2	2.25	2.5 <sup>(2)</sup>	2.75 <sup>(3)</sup>	3	3.25	4	6
PCT (°F)	1723.1	1804.8	1796.0	1895.0	1777.6	1617.0	1334.2	1267.9
PCT Elevation (ft)	12	12	12	12	11.75	11.5	11.25	11.5
Hot Rod Burst Time (sec)	N/A	N/A	1770.2	1721.7	N/A	N/A	N/A	N/A
Hot Rod Burst Elevation (ft)	N/A	N/A	11.75	12	N/A	N/A	N/A	N/A
Max. Local ZrO <sub>2</sub> Reaction (%)	3.15	3.6	11.07	8.82	2.87	1.19	0.14	0.12
Max. Local ZrO <sub>2</sub> Elev. (ft)	12	12	11.75	12	11.75	11.5	11.25	11.5
Core-Wide Avg. ZrO <sub>2</sub> (%)	<1.0	<1.0	<1.0	<1.0	<1.0	<1.0	<1.0	<1.0

Notes:

1. A 1.5-inch break size NOTRUMP case was also analyzed, but because it resulted in minimal core uncover, a PCT for that break was not calculated.
2. The limiting time-in-life for the 2.5-inch break case for transient oxidation was determined to be at 20,000 MWD/MTU
3. The limiting time-in-life for the 2.75-inch break case for PCT was determined to be at 8,000 MWD/MTU.

Table 14.3-1g

PEAK CLAD TEMPERATURE INCLUDING ALL PENALTIES AND BENEFITS  
SMALL BREAK LOCA

PCT for Analysis of Record	1895 °F
PCT Assessments Allocated to AOR	
a. None	N/A °F
SBLOCA PCT for Comparison to 10 CFR 50.46 Requirements	1895 °F

The maximum fuel element cladding temperature shall not exceed 2200 °F per 10 CFR 50.46(b)(1).

Table 14.3-2b

PLANT PARAMETERS USED IN SMALL BREAK LOCA

Core Power	100.6 of 2900 MWt
Total Core Peaking Factor (FQ)	2.40
Hot Channel Factor (FDH)	1.62
LOCA Hot Assembly Peaking Factor (P-bar-HA)	1.42
Peak Linear Power	13.17 kw/ft
Baffle-Barrel Configuration	Converted Upflow
Steam Generator Tube Plugging	10% (Up to 10% in any or all) (Note 3)
Minimum Auxiliary Feedwater Flow Rate	98 gpm/SG
Reactor Coolant System Initial Conditions	
Vessel Flowrate	248,520 gpm (82,840 gpm/loop)
Vessel Inlet Temperature	540.95°F
Vessel Outlet Temperature	619.05°F
Maximum System Pressure, including uncertainties	2300 psia
Cold Leg Accumulator	
Minimum Cover Pressure	625 psia
Accumulator Water Volume	957 ft <sup>3</sup> (Note 1)
Maximum Water Temperature	105°F
Fuel Analyzed	Westinghouse 17x17 Robust Fuel Assembly (RFA) with IFMs

(1) The accumulator is modeled as 957 ft<sup>3</sup> nominal water volume (measured to tank outlet neglecting unusable water volume) without crediting the average 57 ft<sup>3</sup>/loop volume between the tank outlet and the first Reactor Coolant System check valve.

Table 14.3-5a

KEY INPUT DATA TO MAAP-DBA (PEAK PRESSURE CALCULATIONS)

Containment volume	1,751,734 ft <sup>3</sup>
Initial containment pressure	14.2 psia
Initial containment temperature	108°F
Initial containment relative humidity	15%
Steel liner to concrete gap effective heat transfer coefficient	100 BTU/hr/ft <sup>2</sup> /°F
Paint thickness on carbon steel heat sinks	0.0065 inches
Effective heat transfer coefficient for the paint on the carbon steel	462 BTU/hr/ft <sup>2</sup> /°F
Paint thickness on concrete heat sinks	0.005 inches
Effective heat transfer coefficient for the paint on the concrete heat sinks	200 BTU/hr/ft <sup>2</sup> /°F
Zinc thickness on carbon steel	0.0251 in
RWST temperature	65°F
Containment high-high quench spray setpoint	BVPS-1 used 26.8 psia
Containment high (SI actuation, FW isolation and CIA) safety analysis limit setpoint range	22 psia
Containment intermediate high-high (steam line isolation) safety analysis limit setpoint	24 psia
Start delay for quench spray	≤ 43.9 seconds
Quench spray flow rate	variable, determined by pump curve
Start delay for recirculation spray	variable, determined by RWST drawdown

Table 14.3-5b

PHYSICAL CONSTANTS FOR CONTAINMENT AND COOLANT SYSTEM MATERIALS

<u>Material Designation</u>	<u>Material</u>	<u>Conductivity Btu/Hr-Sq Ft-(F/Ft)</u>	<u>Specific Heat, Btu/Lb-F</u>	<u>Density Lb/Cu Ft</u>
1	Carbon Steel	31	0.11	490
2	Stainless Steel	11	0.11	490
3	Concrete <sup>(1)</sup>	0.8	0.21	145
4	Popcorn Concrete	0.8	0.21	120

Paint on Carbon Steel

Min unit thermal conductance = 462 Btu/hr-ft<sup>2</sup> - °F

Max unit thermal conductance = 2526 Btu/ hr-ft<sup>2</sup> - °F

Paint on Concrete

Min unit thermal conductance = 200 Btu/hr-ft<sup>2</sup> - °F

Max unit thermal conductance = 933 Btu/hr-ft<sup>2</sup> - °F

Table 14.3-6

BEAVER VALLEY MAAP-DBA PARAMETER FILE SUMMARY OF  
JUNCTION FLOW AREAS

Junction Number	Upstream Node Number	Downstream Node Number	Junction Flow Area (ft <sup>2</sup> )	Junction Loss Coefficient
1	1	4	3.14	.618
2	1	5	6.0	.583
3	1	7	6.0	.583
4	1	9	6.0	.583
5	2	4	417.0	.510
6	2	5	160.0	.540
7	2	6	33.5	.526
8	2	7	155.0	.518
9	2	8	976.0	1.0
10	2	9	140.6	.545
11	2	10	1166.0	.894
12	2	11	1166.0	.894
13	3	5	28.0	.546
14	13	12	903.2	1.0
15	4	5	28.0	.546
16	4	10	517.8	.511
17	5	6	56.0	.535
18	5	15	384.8	.590
19	6	7	56.0	.535
20	6	11	56.0	.535
21	6	15	64.2	.617
22	7	15	389.4	.584
23	8	11	800.0	.516
24	8	15	673.4	.894
25	9	10	56.0	.535
26	9	15	389.4	.584
27	11	10	493.3	1.0
28	10	12	1257.3	.894
29	11	13	1257.3	.894
30	12	15	792.3	.535
31	13	15	130.0	.522
32	17	16	7980.0	1.0

**TABLE 14.3-6 (CONT'D)****BEAVER VALLEY MAAP-DBA PARAMETER FILE SUMMARY OF  
JUNCTION FLOW AREAS**

Junction Number	Upstream Node Number	Downstream Node Number	Junction Flow Area (ft <sup>2</sup> )	Junction Loss Coefficient
33	16	15	8120.0	1.0
34	16	13	1822.0	1.0
35	16	12	1822.0	1.0
36	15	14	926	1.0
37	18	2	0.0	.756
38	14	1	23.38	.538
41	14	18	.0491	.572
42	1	2	0.785	.474
43	14	18	324	1.0
44	15	18	210	1.0

Note: Junction 39 represents design basis leakage and 40 is the containment failure junction set to add when containment pressure exceeds a pre-set value.

Table 14.3-7

## BEAVER VALLEY MAAP-DBA PARAMETER FILE SUMMARY OF CONTAINMENT NOMINAL VOLUMES AND METAL HEAT SINKS

	BVPS-1 Net Free Volume (ft <sup>3</sup> )	Metal Heat Sinks	
		Mass (lbm)	Surface Area (ft <sup>2</sup> )
1 Reactor cavity	11826	425,023	2,975
2 Lower compartment	198039	655,459	60,526
3 Instrument room	30872	1,094	216
4 RHR platform	31264	17,446	431
5 Loop C compartment	52311	264,057	8,744
6 PZR compartment	48637	50,933	2,431
7 Loop B compartment	49141	267,633	11,410
8 RV head laydown area	45542	17,075	2,898
9 Loop A compartment	51429	284,087	11,462
10 Lower annulus south (BVPS-1) or north (BVPS-2) half	85457	299,948	41,642
11 Lower annulus north (BVPS-1) or south (BVPS-2) half	85663	280,947	37,869
12 Upper annulus south (BVPS-1) or north (BVPS-2) half	80082	148,581	24,295
13 Upper annulus north (BVPS-1) or south (BVPS-2) half	80294	224,330	23,716
14 Refueling cavity	26668	131,960	5,522
15 Upper compartment cylindrical section	347071	481,486	15,339
16 Upper compartment lower dome region	413,523	583,731	34,062
17 Upper compartment upper dome region	108,635	0	0
18 Refueling cavity <sup>(3)</sup>	7572	0	0
TOTAL	1,754,025	4,133,789	283,537

## Notes:

1. Metal heat sinks do not include major equipment, such as steam generators or RCS loop piping. Realistic heat sink values without any uncertainty included.
2. The containment steel liner mass is included with concrete heat sinks, therefore the liner mass is not reflected in the metal heat sink summary.
3. Unit 1 uses two nodes for refueling cavity because of HS configuration.



Table 14.3-8

BEAVER VALLEY MAAP-DBA PARAMETER FILE SUMMARY OF CONTAINMENT CONCRETE  
HEAT SINKS

Heat Sink #	Description	Total Thickness ft	One-Sided Area ft <sup>2</sup>	No. Sides Inside Ctmt	Total Area ft <sup>2</sup>
1	Shield wall to lower	4.50	1,524	2	3,049
2	Refuel cavity wall to loop B	4.00	958	2	1,915
3	Shield wall to loop C	4.50	195	2	389
4	Refuel cavity wall to PZR	4.00	924	2	1,848
5	Shield wall to loop B	4.50	211	2	421
6	Shield wall to RV laydown	4.50	62	2	124
7	Shield wall to loop A	4.50	155	2	309
8	Instrument tunnel to lower	3.00	954	2	1,908
9	Refuel cavity wall to loop C	4.00	826	2	1,653
10	Reactor cavity floor <sup>(1)</sup>	10.00	621	1	621
11	14 crane wall support columns	2.00	1,646	2	3,293
12	Lower compartment floor	10.00	10,094	1	10,094
13	Lower compartment outer wall <sup>(1)</sup>	4.50	8,445	1	8,445
14	Instrument room floor	4.00	1,017	2	2,034
15	Instrument room wall to loop C	3.25	929	2	1,858
16	Instrument room wall to loop A	3.25	704	2	1,408
17	Instrument room crane wall	2.00	1,545	2	3,091
18	Instrument room ceiling	2.00	923	2	1,846
19	Loop C floor	4.50	912	2	1,824
20	Loop C wall to PZR	3.00	1,043	2	2,085
21	Loop C crane wall	2.75	2,290	2	4,579
22	SG cubicle support columns	3.50	633	2	1,265
23	Loop C ceiling	2.00	923	2	1,846
24	PZR floor	2.00	880	2	1,761
25	PZR wall to loop B	3.00	1,253	2	2,506
26	PZR crane wall	2.00	2,568	2	5,136
27	PZR intermediate deck	4.00	984	2	1,969
28	PZR ceiling	2.00	923	2	1,846
29	Loop B floor	4.50	914	2	1,828
30	Loop B wall to RV head laydown	3.00	717	2	1,435

Table 14.3-8 (CONT'D)

BEAVER VALLEY MAAP-DBA PARAMETER FILE SUMMARY OF CONTAINMENT CONCRETE  
HEAT SINKS

Heat Sink #	Description	Total Thickness ft	One-Sided Area ft <sup>2</sup>	No. Sides Inside Ctmt	Total Area ft <sup>2</sup>
31	Loop B crane wall	2.75	1,768	2	3,536
32	Loop B intermediate roof	6.00	131	2	261
33	Loop B ceiling	2.00	923	2	1,846
34	RV head laydown wall to fuel transfer canal	4.00	885	2	1,771
35	RV head laydown crane wall	2.75	915	2	1,829
36	RV head laydown ceiling	2.00	923	2	1,846
37	Loop A floor	4.50	1,082	2	2,165
38	Loop A crane wall	2.75	2,114	2	4,228
39	Loop A wall to fuel transfer canal	4.00	1,623	2	3,247
40	Loop A interior walls	2.00	271	2	543
41	Loop A ceiling	2.00	923	2	1,846
42	Lower annulus south half outer wall <sup>(1)</sup>	4.50	8,432	1	8,432
43	Lower annulus north half outer wall <sup>(1)</sup>	4.50	8,432	1	8,432
44	Upper annulus south half crane wall	2.75	8,226	2	16,452
45	Upper annulus south half outer wall <sup>(1)</sup>	4.50	7,569	1	7,569
46	Upper annulus north half crane wall	2.75	9,038	2	18,076
47	Upper annulus north half outer wall <sup>(1)</sup>	4.50	7,569	1	7,569
48	Fuel transfer canal floor	4.00	471	2	942
49	Lower dome outer wall	2.50	9,929	1	9,929
50	Upper dome outer wall	2.50	8,774	1	8,774
51	Pressurizer interior walls	2.00	527	2	1,054
52	Instrument room interior wall	1.25	147	2	295
53	RV laydown to Loop A misc wall	3.00	164	2	328

Table 14.3-8 (CONT'D)

BEAVER VALLEY MAAP-DBA PARAMETER FILE SUMMARY OF CONTAINMENT CONCRETE  
HEAT SINKS

Heat Sink #	Description	Total Thickness ft	One-Sided Area ft <sup>2</sup>	No. Sides Inside Cmt	Total Area ft <sup>2</sup>
54	Support beam at 718'-6"	4.50	274	2	548
55	Cubicle walls above op. deck	1.50	3,262	2	6,523
56	RHR room wall to Loop C	3.25	539	2	1,078
57	RHR room wall to Loop A	3.25	568	2	1,135
58	RHR room crane wall	2.75	1,342	2	2,684
59	Refuel cavity wall to upper annulus south half	4.00	1,033	2	2,066
60	Refuel cavity wall to upper annulus north half	4.00	1,181	2	2,361
61	Containment shell sections with embedment plates in lower compartment <sup>(1)</sup>	4.50	338	1	338
62	Containment shell sections with embedment plates in lower south annulus <sup>(1)</sup>	4.50	492	1	492
63	Containment shell sections with embedment plates in lower north annulus <sup>(1)</sup>	4.50	492	1	492
64	Containment shell sections with embedment plates in upper south annulus <sup>(1)</sup>	4.50	525	1	525
65	Containment shell sections with embedment plates in upper north annulus <sup>(1)</sup>	4.50	525	1	525
66	Lower dome sections with embedment plates	2.50	3,313	1	3,313
67	Upper dome sections with embedment plates	2.50	2,922	1	2,922
68	Wall Adjacent to Reactor Enclosure	3.00	705	2	1,410
69	Cubicle	1.50	1,590	2	3,179
70	Elevator Pit	1.00	94	2	188

Table 14.3-8 (CONT'D)

BEAVER VALLEY MAAP-DBA PARAMETER FILE SUMMARY OF CONTAINMENT CONCRETE  
HEAT SINKS

Heat Sink #	Description	Total Thickness ft	One-Sided Area ft <sup>2</sup>	No. Sides Inside Ctmt	Total Area ft <sup>2</sup>
71	Unlined portion of lower compartment outer wall	4.50	640	1	640
72	Unlined portion of lower annulus south half outer wall	4.50	836	1	836
73	Unlined portion of lower annulus north half outer wall	4.50	836	1	836
74	Unlined portion of upper annulus south half outer wall	4.50	856	1	856
75	Unlined portion of upper annulus north half outer wall	4.50	856	1	856
TOTAL					217,155

## Notes:

(1) Includes painted carbon steel liner and gap resistance between liner and concrete.

TABLE 14.3-10

PARAMETERS USED IN CONTROL ROOM HABITABILITY ANALYSIS  
OF THE SMALL LINE BREAK ACCIDENT<sup>1,2,3</sup>

Core Power Level	2,918 MWt
Minimum Reactor Coolant Mass	340,711 lbm
CVCS letdown line break - mass flow rate	16.79 lbm/s
Break Flow Flash Fraction	37%
Time to isolate break-	15 minutes
Melted Fuel Percentage	0%
Failed Fuel Percentage	0%
RCS Tech Spec NG & Iodine Concentration	Table 14B-15 (0.35 $\mu$ Ci/gm DE-I131)
RCS Equilibrium Iodine Appearance Rates	Table 14B-16 (0.35 $\mu$ Ci/gm DE-I131)
Accident Initiated Spike Appearance Rate	500 times equilibrium
Duration of Accident Initiated Spike	4 hours
Iodine Species released to Environment	97% elemental; 3% organic
SLCRS Filter Efficiency	0%
Environmental Release Point	Ventilation Vent
Control Room $\chi$ /Q values	Limiting Values of Table 2.2-12a and Unit 2 UFSAR Table 15.0-14a (i.e., BVPS-1 Ventilation Vent to BVPS-1 CR Intake)

**CR Emergency Ventilation: Initiation  
Signal/Timing**

CR is maintained under Normal Operation ventilation

**Notes**

- (1) Bounding parameter values are used to encompass an event at either unit
- (2) This analysis was originally performed in 1987 in support of plant modifications converting the Unit 1 Control Room to a common Unit 1 - Unit 2 facility. The radiological consequences of this event were not required to be evaluated as part of the licensing basis for Unit 1.
- (3) The dose acceptance criteria utilized for off-site locations was the most limiting set forth in RG 1.183 of 2.5 rem TEDE. The estimated worst 2-hour EAB dose is 0.23 rem TEDE. The estimated LPZ doses for the duration of the accident is 0.012 rem TEDE. The estimated control room operator dose due to a small line break outside containment at either unit is presented in Table 14.1-1A and is within the regulatory limit of 5 rem TEDE specified in 10 CFR 50.67

Table 14.3-12

CONTAINMENT THERMODYNAMIC DATA - LOSS OF COOLANT ACCIDENT

Time (sec)	Pressure (psia)	Time (sec)	Temp (°F)	Time (sec)	Steam Condensing Rates (gm/sec)	Time (sec)	Relative Humidity Fraction
0.0	14.2	0.0	108.0	0.0	0.0	0.0	0.500
17.3	56.5	17.3	266.7	40.0	277315.0	5.0	0.579
40.1	52.3	40.1	258.9	80.1	120655.9	10.0	1.000
80.2	51.5	80.2	256.0	120.2	101211.8	345600.0	1.000
120.6	50.0	120.6	253.2	160.2	84363.2		
160.2	49.0	160.2	251.3	200.2	74004.4		
200.2	48.3	200.2	250.0	240.2	66345.6		
240.2	47.8	240.2	249.4	280.7	61909.1		
280.7	47.6	280.7	248.9	321.0	58435.7		
321.0	47.4	321.0	248.5	361.0	55660.3		
361.0	47.4	361.0	248.4	401.0	53361.2		
401.0	47.3	401.0	248.3	441.0	51477.6		
441.0	47.3	441.0	248.3	481.0	49833.9		
481.0	47.4	481.0	248.3	522.1	48459.7		
522.1	47.5	522.1	248.4	562.1	47186.3		
562.1	47.6	562.1	248.6	602.1	47106.8		
602.1	47.7	602.1	248.9	642.1	46142.9		
642.1	47.9	642.1	249.2	682.1	45339.0		
682.1	48.1	682.1	249.5	722.1	44671.6		
722.1	48.2	722.1	249.8	762.1	44046.5		
762.1	48.4	762.1	250.1	802.1	43450.6		
802.1	48.6	802.1	250.5	842.1	40987.5		
842.1	48.9	842.1	250.9	882.1	39002.2		
882.1	48.6	882.1	250.4	922.1	36625.6		
922.1	48.3	922.1	249.8	962.1	35511.8		
962.1	48.0	962.1	249.2	1002.1	34577.7		
1002.1	47.7	1002.1	248.6	1042.1	33760.2		
1042.1	47.4	1042.1	248.1	1082.1	33031.9		
1082.1	47.2	1082.1	247.7	1122.1	32376.9		
1122.1	47.0	1122.1	247.3	1162.1	31885.7		

Table 14.3-12 (Continued)

CONTAINMENT THERMODYNAMIC DATA - LOSS OF COOLANT ACCIDENT

Time (sec)	Pressure (psia)	Time (sec)	Temp (°F)	Time (sec)	Steam Condensing Rates (gm/sec)	Time (sec)	Relative Humidity Fraction
1162.1	46.8	1162.1	246.9	1202.1	31344.1		
1202.1	46.6	1202.1	246.6	1242.1	32338.9		
1242.1	46.5	1242.1	246.3	1282.1	31822.6		
1282.1	46.3	1282.1	246.0	1322.1	31350.0		
1322.1	46.2	1322.1	245.7	1362.1	30936.6		
1362.1	46.1	1362.1	245.4	1402.1	30555.2		
1402.1	45.9	1402.1	245.2	1442.1	30201.4		
1442.1	45.8	1442.1	244.9	1482.1	29871.6		
1482.1	45.7	1482.1	244.7	1522.1	29563.9		
1522.1	45.6	1522.1	244.5	1562.1	29183.4		
1562.1	45.4	1562.1	244.1	1602.1	28593.4		
1602.1	45.2	1602.1	243.6	1642.1	28094.8		
1642.1	45.0	1642.1	243.2	1682.1	27661.6		
1682.1	44.8	1682.1	242.8	1722.1	27262.5		
1722.1	44.6	1722.1	242.4	1800.1	26465.3		
1762.1	44.4	1762.1	242.0	2004.0	25498.4		
1804.0	44.2	1804.0	241.6	2766.0	22197.8		
1844.0	44.0	1844.0	241.2	3006.0	18874.7		
1884.0	43.8	1884.0	240.8	3221.1	18440.8		
1924.0	43.6	1924.0	240.5	3248.4	19906.7		
1964.0	43.5	1964.0	240.1	3548.4	10768.3		
2004.0	43.3	2004.0	239.8	4049.5	13086.0		
2044.0	43.1	2044.0	239.4	4359.5	13219.0		
2078.0	43.0	2078.0	239.1	4759.5	8477.6		
2093.0	43.0	2080.0	239.1	4959.5	10098.2		
2140.0	42.8	2081.0	239.3	5059.5	10485.0		
2170.0	42.1	2100.0	239.1	5159.5	10929.1		
2212.0	41.0	2152.4	238.2	5259.5	11132.0		
2252.0	40.1	2200.0	234.3	5363.8	5848.9		
2350.0	37.9	2252.0	231.3	5463.8	8500.4		
2450.0	35.9	2966.0	204.2	5563.8	9584.6		

Table 14.3-12 (Continued)

CONTAINMENT THERMODYNAMIC DATA - LOSS OF COOLANT ACCIDENT

Time (sec)	Pressure (psia)	Time (sec)	Temp (°F)	Time (sec)	Steam Condensing Rates (gm/sec)	Time (sec)	Relative Humidity Fraction
2550.0	34.2	3609.5	197.5	5663.8	10343.7		
2650.0	32.6	3877.5	192.8	5763.8	10871.0		
2750.0	31.3	3955.5	190.0	5863.8	11164.7		
3446.5	29.0	4749.5	180.1	6563.8	11990.7		
3849.5	27.4	4849.5	183.7	6663.8	12075.3		
3955.5	27.0	5749.5	191.2	7163.8	12071.2		
4749.5	24.9	6749.5	191.4	7324.9	10980.8		
4849.5	25.3	7263.9	192.6	10025.8	10025.0		
5949.5	27.2	18074.7	188.9	10338.5	10042.1		
6749.5	27.2	35998.0	180.5	10938.5	10167.3		
7263.9	27.4	72198.0	170.9	11054.8	5388.5		
18074.7	26.8	144020.0	162.6	11154.8	6717.8		
35998.0	24.9	259020.0	155.3	11254.8	7739.4		
72198.0	23.1	346020.0	150.4	11354.8	8311.9		
144020.0	21.7			11454.8	8594.5		
259020.0	20.8			11554.8	8780.4		
346020.0	20.2			11569.0	5020.2		
				11682.9	6267.3		
				11782.9	7467.5		
				11882.9	8111.2		
				13882.9	9063.9		
				15082.9	8838.6		
				27200.0	7407.0		
				36000.0	6962.0		
				72000.0	5866.0		
				86400.0	5609.0		
				142920.0	5077.0		
				335920.0	4044.0		
				345920.0	3942.0		



TABLE 14.3-14a

PARAMETERS USED IN EVALUATING THE  
RADIOLOGICAL CONSEQUENCES OF A LOSS-OF-COOLANT ACCIDENT

A. Core Parameters

- |    |                          |      |
|----|--------------------------|------|
| 1. | Core Power (MWt)         | 2918 |
| 2. | Fuel Cycle Length (days) | 548  |

B. Radiation Source Terms

1. Puff release of 100% of the Reactor Coolant Inventory to the containment atmosphere. RCS activity concentrations are listed in Table 14B-15 and in BVPS-2 UFSAR Table 15.0-8c.
2. Core inventory release timing
 

gap phase	Onset: 30 sec. Duration: 30 min.
early-in-vessel phase	Onset: 30.5 min. Duration: 1.3 hours
3. Elements in each group and Release Fractions Released from the Core to Containment Atm Following LOCA (BVPS Unit 1 core activity is listed in Table 14B-1A and is the same as BVPS-2).

<u>Group</u>	<u>Gap Release phase</u>	<u>Early In-Vessel Release phase</u>	<u>Nuclides</u>
Noble Gas	0.05	0.95	Xe, Kr, Rn, H
Halogens	0.05	0.35	I, Br
Alkali Metals	0.05	0.25	Cs, Rb
Tellurium Group		0.05	Te, Sb, Se, Sn, In, Ge, Ga, Cd, As, Ag
Barium, Strontium		0.02	Ba, Sr, Ra
Noble Metals		0.0025	Ru, Rh, Pd, Mo, Tc, Co
Cerium Group		0.0005	Ce, Pu, Np, Th, U, Pa, Cf, Ac
Lanthanides		0.0002	La, Zr, Nd, Eu, Nb, Pm, Pr, Sm, Y, Cm, Am, Gd, Ho, Tb, Dy

4. Elements in each group and Release Fractions Released from the Core to Sump Following LOCA (BVPS Unit 1 core activity is listed in Table 14B-1A and is the same as BVPS-2).

<u>Group</u>	<u>Gap Release phase</u>	<u>Early In-Vessel Release phase</u>	<u>Nuclides</u>
Noble Gas	0	0	Xe, Kr, Rn, H
Halogens	0.05	0.35	I, Br
Alkali Metals	0.05	0.25	Cs, Rb
Tellurium Group		0.05	Te, Sb, Se, Sn, In, Ge, Ga, Cd, As, Ag
Barium, Strontium		0.02	Ba, Sr, Ra
Noble Metals		0.0025	Ru, Rh, Pd, Mo, Tc, Co
Cerium Group		0.0005	Ce, Pu, Np, Th, U, Pa, Cf, Ac
Lanthanides		0.0002	La, Zr, Nd, Eu, Nb, Pm, Pr, Sm, Y, Cm, Am, Gd, Ho, Tb, Dy

TABLE 14.3-14a (Continued)

PARAMETERS USED IN EVALUATING THE  
RADIOLOGICAL CONSEQUENCES OF A LOSS-OF-COOLANT ACCIDENT

5. Iodine form of core activity released

From the Containment atmosphere due to melted and failed fuel	95% cesium iodide 4.85% elemental 0.15% organic
From the Sump water due to melted and failed fuel	97% elemental 3% organic

C. Data and Assumptions Used to Estimate Containment Airborne Activity Released

1. Containment Vacuum Relief Line release	2200 scfm for 5 seconds	
2. Containment leakage rate (%/day)		
a. From t=0 to 24 hours	0.1	
b. From t=1 to 30 days	0.05	
3. Containment leakage duration (day)	30	
4. Containment minimum free volume (ft <sup>3</sup> )	1,750,000	
5. Containment spray coverage (%)	63	
6. Spray deposition effectiveness and timing aerosols		
a. beginning of spray effectiveness	120 seconds	
b. ending of spray effectiveness	96 hours	
elemental iodine		
c. beginning of spray effectiveness	120 seconds	
d. ending of spray effectiveness	6.4 hours	
7. Natural deposition mechanisms and timing		
<u>Sprayed region</u>		
aerosols		
a. beginning of effectiveness	30 seconds	
b. ending of effectiveness	96 hours	
elemental iodine		
c. beginning of effectiveness	30 seconds	
d. ending of effectiveness	6.4 hours	
<u>Unsprayed region</u>		
aerosols		
e. beginning of effectiveness	30 seconds	
f. ending of effectiveness	10 hours	
elemental iodine	Not credited	

TABLE 14.3-14a (Continued)

PARAMETERS USED IN EVALUATING THE  
RADIOLOGICAL CONSEQUENCES OF A LOSS-OF-COOLANT ACCIDENT

8. Aerosol and Elemental Iodine Removal Coefficients used in LOCA Dose Analysis

Period		Sprayed Region		Unsprayed Region	
From (hour)	To (hour)	Aerosol (hr <sup>-1</sup> )	Elem I (hr <sup>-1</sup> )	Aerosol (hr <sup>-1</sup> )	Elem I (hr <sup>-1</sup> )
0	0.00833	-----	-----	-----	-----
0.00833	0.02139	5.96	2	0.003	0
0.02139	0.02372	5.96	2	0.003	0
0.02372	0.073	3.872	3.872	0.003	0
0.073	0.14096	2.954	2.954	0.003	0
0.14096	0.20056	2.687	2.687	0.003	0
0.20056	0.2686	2.213	2.213	0.004	0
0.2686	0.39841	2.058	2.058	0.004	0
0.39841	0.5	1.971	1.971	0.005	0
0.5	0.50833	1.969	1.969	0.006	0
0.50833	0.51416	1.971	1.971	0.006	0
0.51416	0.54541	7.455	7.455	0.006	0
0.54541	0.62038	8.194	8.194	0.021	0
0.62038	0.71383	13.128	13.128	0.050	0
0.71383	0.82628	14.802	14.802	0.056	0
0.82628	0.98233	15.168	15.168	0.061	0
0.98233	1.0823	15.593	15.593	0.065	0
1.0823	1.33802	25.587	22	0.067	0
1.33802	1.45671	28.641	22	0.073	0
1.45671	1.55529	28.899	22	0.075	0
1.55529	1.79435	29.137	22	0.077	0
1.79435	1.80833	29.34	22	0.079	0
1.80833	1.81353	29.359	22	0.080	0
1.81353	1.83451	16.589	16.589	0.080	0
1.83451	1.88966	9.873	9.873	0.080	0
1.88966	1.99366	6.654	6.654	0.084	0
1.99366	2	6.402	6.402	0.084	0
2	2.07982	5.452	5.452	0.084	0
2.07982	2.18606	4.507	4.507	0.089	0
2.18606	2.34274	3.818	3.818	0.089	0
2.34274	2.49782	3.3	3.3	0.089	0
2.49782	2.66091	2.933	2.933	0.095	0
2.66091	3.00886	2.478	2.478	0.095	0
3.00886	3.47714	1.375	1.375	0.096	0
3.47714	5	1.2	1.2	0.091	0
5	6.4	1.085	1.085	0.086	0
6.4	8	1	0	0.082	0
8	10	0.924	0	0.077	0
10	24	0.7173	0	0	0
24	62.4	0.5766	0	0	0
62.4	96	0.4	0	0	0
96	720	0	0	0	0

TABLE 14.3-14a (Continued)

PARAMETERS USED IN EVALUATING THE  
RADIOLOGICAL CONSEQUENCES OF A LOSS-OF-COOLANT ACCIDENT

9.	Containment mixing rate (unsprayed volumes per hour)	2
10.	Long term pH	>7
11.	Max DF for aerosols	No Restriction
12.	Max DF for elemental iodine	200
13.	SLCRS filter efficiency (%)	Not Credited

D. Data and Assumptions Used to Estimate Sump Activity Releases

1.	ECCS Leakage Assumptions	
a.	Leak Initiation Time (sec)	1200
b.	Leak Rate (cc/hr - doubled in analysis)	5700
c.	Sump Water Volume	
	1200 sec to 30 min (ft <sup>3</sup> )	19,111
	30 min to 2 hours (ft <sup>3</sup> )	25,333
	2 hours to 30 days (ft <sup>3</sup> )	43,577
d.	Iodine Release Fraction	0.1
e.	Sump Temp after 1200 seconds (°F)	250
2.	RWST Back-leakage Assumptions	
a.	Beginning of back-leakage post accident (sec)	1782
b.	Sump water iodine leakage	elemental
c.	Beginning of RWST Release post accident (sec)	3055
d.	End of RWST release post accident (day)	30
e.	Rate of back-leakage to RWST (gpm - doubled in analysis)	1
f.	Iodine release fraction from RWST used in LOCA analysis (values tabulated below)	

Period		RWST Vent Iodine	RWST Vent Gaseous
From (hour)	To (hour)	Release Rate (fraction per day)	Release Rate (fraction per day)
0.84861	1.66667	1.0E-02	0.78
1.66667	1.75	8.0E-03	0.78
1.75	2	6.0E-03	0.78
2	3	4.0E-03	0.78
3	5	2.0E-03	0.48
5	9	1.1E-03	0.48
9	11	1.1E-03	0.098
11	48	2.4E-04	0.098
48	72	1.1E-04	0.05
72	96	3.0E-05	0.05
96	120	1.0E-05	0.05
120	144	6.0E-06	0.042
144	168	2.0E-06	0.042
168	192	1.0E-06	0.042
192	216	8.0E-07	0.042
216	264	7.0E-07	0.042
264	312	6.0E-07	0.042
312	384	5.0E-07	0.042
384	480	4.0E-07	0.042
480	576	3.0E-07	0.042
576	672	2.4E-07	0.042
672	720	2.0E-07	0.042

TABLE 14.3-14a (Continued)

PARAMETERS USED IN EVALUATING THE  
RADIOLOGICAL CONSEQUENCES OF A LOSS-OF-COOLANT ACCIDENT

E. Control Room Parameters

1.	Control Room Volume (ft <sup>3</sup> )	1.73E+5
2.	Control Room Normal Intake including inleakage (cfm)	500
3.	Time when CR is isolated (sec)	77
4.	Infiltration during isolation mode (cfm)	300
5.	Time when CR Emergency Vent is manually initiated (min)	30
6.	Emergency vent flowrate (cfm)	600 to 1030
7.	Control Room intake filter removal efficiency	
	a. aerosols (%)	99
	b. elemental/organic iodine (%)	98
8.	In-leakage during Emergency Vent mode (scfm)	30

|

Table 14.3-16

MAAP-DBA CONTAINMENT PEAK PRESSURE RESULTS FOR A DESIGN BASIS LARGE  
BREAK LOCA BEAVER VALLEY – BVPS-1

Description	Power Level, %	Single Failure	Peak Pressure (psig) <sup>(1)</sup>
6L-DEPS MIN SI	100.6	DG	41.9
7L-DEPS MAX SI	100.6	CIB	41.9
8L-DEHL	100.6	None	43.1

**Single Failures – Failed Equipment**

CIB One train each, QSS, RSS

DG One train each, SI, QSS, RSS

(1) Gauge pressure is referenced to 14.3 psi atmospheric pressure.

Table 14.3-17A

## BVPS-1 DOUBLE-ENDED HOT-LEG BREAK SEQUENCE OF EVENTS

Time (sec)	Event Description
0.0	Break Occurs, Reactor Trip and Loss of Offsite Power are assumed
3.0	Low Pressurizer Pressure SI Setpoint is reached (1745 psia)
1.8	Containment High-High Setpoint is reached
11.9	Broken Loop Accumulator Begins Injecting Water
12.1	Intact Loop Accumulator Begins Injecting Water
15.7	Peak Containment Pressure During Blowdown
22.2	End of Blowdown Phase

Table 14.3-17B

BVPS-1 DOUBLE-ENDED PUMP SUCTION BREAK MINIMUM SAFEGUARDS SEQUENCE  
OF EVENTS

Time (sec)	Event Description
0.0	Break Occurs, Reactor Trip and Loss of Offsite Power are assumed
1.8	Containment High-High Setpoint is reached
3.0	Low Pressurizer Pressure SI Setpoint is reached (1745 psia)
12.9	Broken Loop Accumulator Begins Injecting Water
13.3	Intact Loop Accumulator Begins Injection Water
17.1	Peak Containment Pressure During Blowdown
21	End of Blowdown Phase
30.3	Safety Injection Begins
56.5	Accumulator Water Injection Ends
83.2	Quench Spray is initiated
225.8	End of Reflood Phase
229.9	Recirculation Spray in initiated
2900.0	ECCS Recirculation Begins
3600 <sup>(1)</sup>	Transient Modeling Terminated

<sup>(1)</sup> Except for long term attributes such as EQ profiles, sump water temperature, and hydrogen recombine assessments which may require 1 day or 30 day transients.



Table 14.3-17C

BVPS-1 DOUBLE-ENDED PUMP SUCTION BREAK MAXIMUM SAFEGUARDS SEQUENCE  
OF EVENTS

Time (sec)	Event Description
0.0	Break Occurs, Reactor Trip and Loss of Offsite Power are assumed
3.0	Low Pressurizer Pressure SI Setpoint is reached (1745 psia)
1.8	Containment High-High Setpoint is reached
12.9	Broken Loop Accumulator Begins Injecting Water
13.3	Intact Loop Accumulator Begins Injection Water
17.1	Peak Containment Pressure During Blowdown
21.0	End of Blowdown Phase
30.3	Safety Injection Begins
56.9	Accumulator Water Injection Ends
83.2	Quench Spray is initiated
221.3	End of Reflood Begins
229.9	Recirculation Spray in initiated
2500.0	ECCS Recirculation Begins
3600 <sup>(1)</sup>	Transient Modeling Terminated

<sup>(1)</sup> Except for long term attributes such as EQ profiles, sump water temperature, and hydrogen recombine assessments which may require 1 day or 30 day transients.

Table 14.3-20

STEAM GENERATOR  
CUBIC MASS AND ENERGY INFLOW  
RATES FOR DER OF HOT LEG

<u>Time (seconds)</u>	<u>Mass Flow (lbm/second)</u>	<u>Energy Release (Btu/second)</u>
0.01	132,340	75,556,188
0.02	111,930	63,753,519
0.03	92,700	52,704,513
0.04	77,560	44,034,869
0.05	65,180	36,965,463
0.06	56,470	32,001,769
0.07	56,570	32,063,944
0.08	56,560	32,061,225
0.09	56,530	32,048,744
0.1	56,500	32,033,331
0.2	56,300	31,957,113
0.3	56,070	31,860,119
0.4	55,820	31,753,381
0.5	55,610	31,669,863
0.6	55,360	31,560,488
0.7	55,130	31,467,463
0.8	54,970	31,409,881
0.9	54,790	31,317,606
1.0	54,650	31,290,644
2.0	53,050	30,615,238
3.0	51,240	29,720,069
4.0	49,140	28,553,688
5.0	46,860	27,185,913

Table 14.3-21

STEAM GENERATOR CUBICLE 1A  
 MASS AND ENERGY INFLOW RATES  
 FOR SER OF HOT LEG

<u>Time (seconds)</u>	<u>Mass Flow (lbm/second)</u>	<u>Energy Release (Btu/second)</u>
0.01	93,396	53,400,000
0.02	78,497	44,700,000
0.03	64,859	36,900,000
0.04	54,041	30,700,000
0.05	45,537	25,800,000
0.06	40,040	22,700,000
0.07	40,109	22,800,000
0.08	40,093	22,700,000
0.09	40,078	22,700,000
0.1	40,061	22,700,000
0.2	39,425	22,700,000
0.3	39,785	22,600,000
0.4	39,642	22,600,000
0.5	39,496	22,500,000
0.6	39,340	22,500,000
0.7	39,175	22,400,000
0.8	30,003	22,300,000
0.9	38,887	22,200,000

Table 14.3-22

MASS AND ENERGY RELEASE RATES FOR DER OF  
SURGE LINE IN PRESSURIZER SUBCOMPARTMENT

<u>Time</u> <u>(seconds)</u>	<u>Mass Flow</u> <u>(lbm/second)</u>	<u>Energy Release</u> <u>(Btu/second)</u>
0.0	9,324	5,877,000
0.025	21,170	13,910,000
0.05005	21,131	14,010,000
0.0751	20,810	13,700,000
0.1002	19,440	12,840,000
0.125	18,580	12,320,000
0.150	18,200	12,130,000
0.175	16,470	11,060,000
0.2001	14,570	9,889,000
0.225	14,250	9,768,000
0.250	13,740	9,527,000
0.275	13,550	9,449,000
0.300	13,170	9,229,000
0.325	13,390	9,360,000
0.3501	13,670	9,522,000
0.375	13,460	9,402,000
0.400	13,380	9,347,000
0.4251	13,450	9,358,000
0.450	13,430	9,353,000
0.475	13,530	9,398,000
0.50	13,630	9,447,000
0.6501	13,220	9,163,000
0.80	13,390	9,207,000
1.0	13,460	9,166,000
1.20	13,390	9,049,000
1.375	13,430	8,954,000
1.50	13,570	9,056,000
1.70	14,520	9,576,000
1.80	14,800	9,712,000
1.90	15,000	9,798,000
1.975	15,090	9,829,000
2.10	14,860	9,671,000
2.20	14,560	9,477,000
2.30	14,190	9,242,000
2.40	13,830	9,011,000
2.50	13,510	8,807,000
2.60	13,250	8,635,000
2.70	12,970	8,454,000
3.0	12,780	8,331,000
5.0	9,844	6,425,000

Table 14.3-23

MASS AND ENERGY RELEASE RATES FOR DER OF SPRAY LINE IN PRESSURIZER  
SUBCOMPARTMENT SUPERSTRUCTURE  
(ABOVE EL. 767 FT-10 INCHES)

<u>Time</u> <u>(seconds)</u>	<u>Mass Flow</u> <u>(lbm/second)</u>	<u>Energy Release</u> <u>(Btu/second)</u>
0.0	0.0	0.0
0.02501	2,572.7	1,545,186.3
0.05005	2,561.0	1,537,966.6
0.07509	2,561.0	1,537,893.6
0.1001	2,526.0	1,518,577.2
0.125	2,540.0	1,526,742.5
0.150	2,527.2	1,518,747.0
0.1749	2,519.0	1,515,031.5
0.2001	2,513.2	1,511,293.5
0.2249	2,491.0	1,500,485.2
0.250	2,501.5	1,505,269.8
0.275	2,486.3	1,497,847.7
0.300	2,475.8	1,492,722.5
0.3249	2,463.0	1,486,386.3
0.3501	2,460.6	1,486,027.7
0.375	2,447.8	1,481,012.6
0.400	2,442.0	1,478,417.8
0.4250	2,435.0	1,473,536.5
0.4499	2,421.0	1,469,923.2
0.4749	2,421.0	1,469,661.3
0.500	2,403.5	1,463,068.8
0.650	2,367.3	1,448,110.0
0.800	2,344.0	1,437,356.8
1.00	2,318.3	1,423,449.1
1.20	2,292.6	1,409,429.0
1.375	2,272.8	1,397,984.3
1.50	2,260.0	1,390,809.6
1.70	2,242.5	1,380,435.3
1.7999	2,234.3	1,375,635.0
1.8999	2,226.1	1,371,054.8
1.975	2,221.5	1,367,968.8
2.0999	2,213.3	1,362,906.5
2.20	2,208.6	1,358,970.6
2.2999	2,200.5	1,355,275.3
2.40	2,195.8	1,351,673.3
2.50	2,190.0	1,348,053.3
2.5999	2,185.3	1,344,444.6
2.70	2,179.5	1,340,898.7
3.00	2,163.1	1,329,747.6

Table 14.3-32

CONTAINMENT SUBCOMPARTMENT  
FREE VOLUME AND VENT AREAS

<u>Compartment</u>	<u>Free Volume, ft<sup>3</sup></u>	<u>Vent Area, ft<sup>2</sup></u>	
		<u>To Containment</u>	<u>To Other Cubicles</u>
Steam Generator Cubicles			
1A	42,719	562.0	0.0
1B	33,699	582	(2)
1C	39,421	579.0	(2)
Pressurizer Cubicle			
Upper	20,916	175 <sup>(3)</sup>	114
Lower	18,887	118.5 <sup>(3)</sup>	114
Superstructure (above El. 767 ft. 10 in.)	11,755	75.3	20

---

(1) Deleted

(2) Vent paths to other cubicles neglected, see Figure 14.3-82.

(3) Vent paths to steam generator cubicles are included in vents to containment since steam generator cubicles are larger than either upper or lower pressurizer cubicle and have much greater vent area to containment than vent area credit taken.

Table 14.3.2-1

PLANT OPERATING RANGE ANALYZED BY THE BEST-ESTIMATE  
LARGE-BREAK LOCA ANALYSIS FOR BEAVER VALLEY UNIT 1

	<u>Parameter</u>	<u>Analyzed Value or Range</u>
<b>1.0</b>	<b>Plant Physical Description</b>	
	a) Dimensions	Nominal
	b) Pressurizer location	On an intact loop <sup>(4)</sup>
	c) Hot assembly location	Anywhere in core <sup>(1)</sup>
	d) Hot assembly type <sup>(2)</sup>	17x17 RFA-2 Fuel with ZIRLO <sup>®</sup> (5) cladding, non-IFBA or IFBA
	e) Steam generator tube plugging level	≤ 22%
	f) Fuel assembly type <sup>(2)</sup>	17x17 RFA-2 Fuel with ZIRLO <sup>®</sup> (5) cladding, non-IFBA or IFBA
<b>2.0</b>	<b>Plant Initial Operating Conditions</b>	
	<b>2.1 Reactor Power</b>	
	a) Maximum Core power	2900 MWt
	b) Peak heat flux hot channel factor ( $F_Q$ ) <sup>(2)</sup>	≤ 2.52
	c) Peak hot rod enthalpy rise hot channel factor ( $F_{\Delta H}$ ) <sup>(2)</sup>	≤ 1.75
	d) Hot assembly radial peaking factor ( $\bar{P}_{HA}$ ) <sup>(2)</sup>	≤ 1.75/1.04
	e) Hot assembly heat flux hot channel factor ( $F_{QHA}$ )	≤ 2.52/1.04
	f) Axial power distribution ( $P_{BOT}$ , $P_{MID}$ ) <sup>(2)</sup>	Figure 14.3.1-2
	g) Low power region relative power ( $P_{LOW}$ ) <sup>(2)</sup>	$0.20 \leq P_{LOW} \leq 0.60$
	h) Hot assembly burnup	≤ 75,000 MWD/MTU, lead rod <sup>(1)(3)</sup>
	i) Moderator Temperature Coefficient (MTC)	≤ 0 at hot full power (HFP)
	j) Typical cycle length	18 months
	k) Minimum core average burnup <sup>(2)</sup>	≥ 10,000 MWD/MTU
	l) Maximum steady state depletion, $F_Q$ <sup>(2)</sup>	2.2
	<b>2.2 Fluid Conditions</b>	
	a) $T_{AVG}$	$566.2 - 4.0^\circ\text{F} \leq T_{AVG} \leq 580.0 + 4.0^\circ\text{F}$
	b) Pressurizer pressure	$2250 - 50 \text{ psia} \leq P_{RCS} \leq 2250 + 50 \text{ psia}$
	c) Minimum thermal design flow	87,200 gpm/loop
	d) Upper head design	$T_{HOT}$
	e) Pressurizer level (at hot full power)	826 ft <sup>3</sup> (High $T_{AVG}$ ) 611 ft <sup>3</sup> (Low $T_{AVG}$ )

TABLE 14.3.2-1 (Continued)

PLANT OPERATING RANGE ANALYZED BY THE BEST-ESTIMATE  
LARGE-BREAK LOCA ANALYSIS FOR BEAVER VALLEY UNIT 1

<u>Parameter</u>	<u>Analyzed Value or Range</u>
f) Accumulator temperature	$70^{\circ}\text{F} \leq T_{\text{ACC}} \leq 108^{\circ}\text{F}$
g) Accumulator pressure	$575.0 \text{ psia} \leq P_{\text{ACC}} \leq 716.0 \text{ psia}$
h) Accumulator liquid volume	$893 \text{ ft}^3 \leq V_{\text{ACC}} \leq 1022 \text{ ft}^3$
i) Minimum accumulator boron	2300 ppm
<b>3.0 Accident Boundary Conditions</b>	
a) Minimum safety injection flow	Table 14.3.1-4a and 14.3.1-4b
b) Safety injection temperature	$45^{\circ}\text{F} \leq \text{SI Temp} \leq 65^{\circ}\text{F}$
c) Safety injection delay	17 seconds (with offsite power) 27 seconds (with LOOP)
d) Containment modeling	Bounded, See Figures 14.3.2-3 and raw data in Tables 14.3.2-2, 14.3.2-3, and 14.3.2-7
e) Initial containment pressure	12.8 psia (minimum) 14.2 psia (maximum)
f) Containment spray initiation delay (post- accident)	23 sec (with offsite power) 38 sec (with LOOP)
g) Containment Fan Coolers	N/A
h) Single failure	Loss of one ECCS train

**Notes:**

- Peripheral locations will not physically be lead power assembly.
- In the Westinghouse Reload Safety Analysis Checklist (RSAC) process, this parameter is identified as a key safety analysis parameter that could be impacted by a fuel reload.
- The fuel temperature and rod internal pressure data is only provided up to 62,000 MWD/MTU. In addition, the hot assembly/hot rod will not have a burnup this high in ASTRUM analyses.
- Analyzing the pressurizer as being located on an intact loop is limiting per Westinghouse methodology.
- Optimized ZIRLO™ fuel cladding has been evaluated as an acceptable fuel cladding material.



Table 14.3.2-2

## LARGE BREAK LOCA CONTAINMENT DATA

<b>Net Free Volume</b>	1.80 x 10 <sup>6</sup> ft <sup>3</sup>
<b>Initial Conditions</b>	
Pressure	12.8 psia (minimum) 14.2 psia (maximum)
Temperature	70°F
RWST Temperature	45°F
Temperature outside containment (air/ground)	-20°F/32°F
<b>Spray System</b>	
Post Accident spray system initiation delay	38 sec with LOOP 23 sec without LOOP
Maximum spray system delivered flow (both pumps operating)	See Table 14.3.2-2a
<b>Containment Fan Coolers</b>	N/A

Table 14.3.2-2a

MAXIMUM CONTAINMENT SPRAY FLOW RATE

RWST Level (feet)	Containment Pressure (psig)	Maximum Two Pump Spray Flow Rate (Delivered to Spray Headers) Gallons per minute
51.5	0	4982
0	0	4538
51.5	45	4040
0	45	3489

Table 14.3.2-3

LARGE BREAK CONTAINMENT - HEAT SINK DATA  
STRUCTURAL HEAT SINKS

Wall	TAir (°F)	Area (ft <sup>2</sup> )	Height (ft)	Tinit (°F)	Thickness (in)
1 Painted Concrete	70	133,215	10	70	0.00375 Paint 12.0 Concrete
2 Stainless Steel Piping and Containment Sump Strainer Structural Commodities	70	14,244	10	70	0.221 Stainless Steel
3 Galvanized Structural Steel	70	22,041	10	70	0.0625 Galvanized Steel
4 Galvanized Ventilation Ducts	70	15,856	10	70	0.125 Galvanized Steel
5 Carbon Structural Steel	70	7,034	10	70	0.00475 Paint 0.0647 Carbon Steel
6 Carbon Structural Steel	70	67,479	10	70	0.00475 Paint 0.125 Carbon Steel
7 Carbon Steel Liner/Concrete Shell	-20	42,469	10	70	0.00475 Paint 0.375 Carbon Steel 54.0 Concrete
7A Carbon Steel Liner/Concrete Shell	-20	4,258	10	70	0.00475 Paint 0.1875 Carbon Steel 54.0 Concrete
8 Carbon Steel Liner/Concrete Dome	-20	19,638	10	70	0.00475 Paint 0.5 Carbon Steel 30.0 Concrete
9 Carbon Steel Liner/ Concrete Dome Liner Plates	-20	9,036	10	70	0.00475 Paint 1.0 Carbon Steel 30.0 Concrete
10 Concrete/Carbon Steel	32	11,251	10	70	0.00375 Paint 24.0 Concrete 0.25 Carbon Steel 120.0 Concrete
11 Carbon Structural Steel, Ducts, and Equipment	70	28,514	10	70	0.00475 Paint 0.1883 Carbon Steel
12 Carbon Structural Steel, Pipe Supports, and Piping	70	45,738	10	70	0.00475 Paint 0.2565 Carbon Steel
13 Carbon Structural Steel	70	21,484	10	70	0.00475 Paint 0.3233 Carbon Steel
14 Stainless Steel Refueling Cavity Liner/Concrete	70	6,697	10	70	0.25 Stainless Steel 24.0 Concrete

Table 14.3.2-3 (CONT'D)

LARGE BREAK CONTAINMENT - HEAT SINK DATA  
STRUCTURAL HEAT SINKS

Wall	TAir (°F)	Area (ft <sup>2</sup> )	Height (ft)	Tinit (°F)	Thickness (in)
15 Stainless Steel Refueling Cavity Liner/Concrete	70	1,674	10	70	1.0 Stainless Steel 48.0 Concrete
16 Carbon Steel Equipment	70	32,214	10	70	0.00475 Paint 0.438 Carbon Steel
17 Carbon Steel Pipe Rupture Restraints and Structural Steel	70	11,269	10	70	0.00475 Paint 0.6064 Carbon Steel
18 Carbon Steel Pipe Rupture Restraints	70	2,615	10	70	0.00475 Paint 1.0312 Carbon Steel
19 Carbon Steel Equipment and Structural Steel	70	3,843	10	70	0.00475 Paint 1.4683 Carbon Steel
20 Carbon Steel Equipment	70	7,648	10	70	0.00475 Paint 4.593 Carbon Steel
21 Galvanized Steel (Conduits, Cable Trays, etc)	70	33,465	10	70	0.121 Galvanized Steel

Table 14.3.2-4

BEAVER VALLEY UNIT 1 BEST ESTIMATE LARGE BREAK LOCA TOTAL MINIMUM  
INJECTED SI FLOW HIGH HEAD SAFETY INJECTION (HHSI) AND LOW HEAD SAFETY  
INJECTION (LHSI) FROM TWO INTACT LOOPS

<b>RCS Pressure (psig)</b>	<b>Total Injected Flow Rate (gpm)</b>
0	2433.0
10	2272.1
20	2106.1
50	1569.1
100	338.1
105	278.4
150	270.4
200	261.4
400	219.2
600	173.4

Table 14.3.2-5

## BEAVER VALLEY UNIT 1 BEST-ESTIMATE LARGE BREAK LOCA RESULTS

<b>ASTRUM Result</b>	<b>Value</b>	<b>Criteria</b>
95/95 PCT (°F)	2161	< 2,200
95/95 LMO (%)	9.22	< 17
95/95 CWO (%)	0.94	< 1

Table 14.3.2-6

PEAK CLAD TEMPERATURE INCLUDING ALL PENALTIES AND BENEFITS  
BEST ESTIMATE LARGE BREAK LOCA (ASTRUM)

PCT for Analysis of Record (AOR)	2161 °F	
a. PAD Data Evaluation	+2 °F	
b. Design Input Changes with Respect to Plant Operation	-485 °F	
c. Evaluation of Pellet Thermal Conductivity Degradation and Peaking Factor Burndown	+156 °F	
d. Revised Heat Transfer Multiplier Distributions	-1 °F	
e. Error in Burst Strain Application	+7 °F	
ASTRUM LBLOCA PCT for Comparison to 10 CFR 50.46 Requirements	1840 °F	

The maximum fuel element cladding temperature shall not exceed 2200 °F per 10 CFR 50.46(b)(1).

Evaluation Basis

$F_Q = 2.4$        $F_{\Delta H}^N = 1.62$       Steam Generator Tube Plugging = 5%

Table 14.3.2-7a

LARGE BREAK LOCA MASS & ENERGY RELEASES FROM BCL VESSEL SIDE  
USED FOR COCO CALCULATIONS

Time [s]	Mass Flow Rate [lb <sub>m</sub> /s]	Energy Flow [BTU/s]
0.0	0	0
0.5	53642	28698260
1	47647	25607680
2	30975	17160713
3	25850	14370028
4	22972	12805631
5	20949	11667155
10	7263	5435647
15	5949	2157622
20	3540	661196
25	-117	0
30	-50	0
35	-12.4	0
40	9308	1115922
45	921	366997
50	208	155440
55	86	73872
60	45	44678
65	18	16384
70	71	67778
75	85	74976
80	53	38741
85	82	72927
90	50	51563
95	116	72159
100	666	196928
110	164	77883
120	763	209627
130	325	104583
140	287	84661
150	68	40819
160	34	30022
170	44	26330
180	275	89335



Table 14.3.2-7a (CONT'D)

LARGE BREAK LOCA MASS & ENERGY RELEASES FROM BCL VESSEL SIDE  
USED FOR COCO CALCULATIONS

Time [s]	Mass Flow Rate [lb <sub>m</sub> /s]	Energy Flow [BTU/s]
190	121	56695
200	615	158714
210	111	53756
220	343	98774
230	217	72813
240	117	51712
250	233	82918
260	320	99995
270	405	109619
280	68	31947
290	82	40590
300	301	93188
310	292	95293
320	54	38990
330	245	77002
340	242	82097
350	71	48700
360	119	51457
370	152	70050
380	78	49692
390	165	71491
400	209	74937
410	168	74527
420	182	74298
430	132	68420
440	133	65198
450	328	104977
475	370	126403
500	215	75003

[s] = Seconds

[lb<sub>m</sub>/s] = Pounds mass per Second

[BTU/s] = British Thermal Unit per Second

Table 14.3.2-7b

LARGE BREAK LOCA MASS & ENERGY RELEASES FROM RCP SIDE  
USED FOR COCO CALCULATIONS

Time [s]	Mass Flow Rate [lb <sub>m</sub> /s]	Energy Flow [BTU/s]
0.0	9245.7	4978829
0.5	24773	13234390
1	24190	13096108
2	19204	10852074
3	14333	8382252
4	10428	6510084
5	7923	5397657
10	3279	276484
15	735	794186
20	166	201146
25	-16	0
30	-14	0
35	76.5	84287
40	161	197731
45	97	120327
50	45	57357
55	28	35007
60	49	61835
65	34	42778
70	42	52726
75	56	71891
80	31	39539
85	47	59432
90	35	44764
95	45	57414
100	48	60457
110	45	56995
120	39	49310
130	39	49411
140	30.6	38984
150	29	36275
160	28	35374
170	29	37074
180	36	45305

Table 14.3.2-7b (CONT'D)

LARGE BREAK LOCA MASS & ENERGY RELEASES FROM RCP SIDE  
USED FOR COCO CALCULATIONS

Time [s]	Mass Flow Rate [lb <sub>m</sub> /s]	Energy Flow [BTU/s]
190	34	43547
200	33	42327
210	32	40429
220	31	39519
230	32	40459
240	31	38816
250	36	45967
260	33	41319
270	36	46192
280	33	41407
290	33	41482
300	33	41994
310	36	45272
320	31	39461
330	34	43274
340	33	42050
350	35	43716
360	37	47309
370	38	48039
380	39	49649
390	44	55380
400	41	51575
410	43	53958
420	42	53093
430	44	55267
440	43	53955
450	49	60070
475	55	66150
500	39	49018

[s] = Seconds

[lb<sub>m</sub>/s] = Pounds mass per Second

[BTU/s] = British Thermal Unit per Second

Table 14.3.2-8

## SEQUENCE OF EVENTS FOR THE LIMITING CASE

<b>Event</b>	<b>Time (sec)</b>
Start of Transient	0.0
Safety Injection Signal	4.5
Accumulator Injection Begins	9.5
Safety Injection Begins	21.5
End of Blowdown	25
Bottom of Core Recovery	32
Accumulator Empty	36.5
PCT Occurs	79
Quench Time	350
End of Transient	500

Table 14.3.4-1

System Parameters Initial Conditions For Thermal Uprate

Parameters	Value
Core Thermal Power (MWT)*	2917.4
Reactor Coolant System Total Flowrate (lbm/sec)	27583.3
Vessel Outlet Temperature (°F)*	621.0
Core Inlet Temperature (°F)*	547.1
Vessel Average Temperature (°F)*	584.0
Initial Steam Generator Steam Pressure (psia)	831.0
Steam Generator Design	54F
Steam Generator Tube Plugging (percent)	0
Initial Steam Generator Secondary Side Mass (lbm)*	131011
Assumed Maximum Containment Backpressure (psia)	59.7
Accumulator	
Water Volume (ft <sup>3</sup> ) per accumulator	1077.6
N <sub>2</sub> Cover Gas Pressure (psia)	575
Temperature (°F)	105**

Notes:

\* The Core Power, RCS Temperature, and Secondary Side Mass values listed above include uncertainty allowance.

\*\* This value is lower than the containment maximum average temperature limit of 108°F, however, it is a conservative value for the accumulators which are located in the lowest part of the containment structure.

Table 14.3.4-2  
 Safety Injection Flow Minimum Safeguards

RCS Pressure (psig)	Total Flow (GPM)
Injection Mode (Reflood Phase)	
0	3825.5
20	3564.3
50	3131.0
100	2226.5
150	716.2
200	430.0
400	407.4
600	383.7
Cold Leg Recirculation Mode	
0	3072

Note:

A maximum Safety Injection Temperature of 65°F was used during the Injection Phase and 190°F was used during the Recirculation Phase.

Table 14.3.4-3

## Safety Injection Flow Maximum Safeguards

RCS Pressure (psig)	Total Flow (GPM)
Injection Mode (Reflood Phase)	
0	5842
50	5092
100	4208
120	3792
200	840
400	807
600	771
Cold Leg Recirculation Mode	
0	5050

## Note:

A maximum Safety Injection Temperature of 65°F was used during the Injection Phase and 210°F was conservatively used during the Recirculation Phase.

Table 14.3.4-4

## Double-Ended Hot-Leg Break Blowdown Mass and Energy Releases

Time (sec)	Break Path No. 1 Flow*		Break Path No. 2 Flow**	
	(lbm/sec)	(Thousand Btu/sec)	(lbm/sec)	(Thousand Btu/sec)
.00000	.0	.0	.0	.0
.00109	46610.3	29915.0	46609.0	29913.2
.00217	46171.1	29631.7	45920.8	29466.0
.102	40888.4	26595.7	26652.5	17066.7
.202	34830.1	22703.4	24188.7	15421.5
.301	34365.7	22340.8	21479.3	13551.9
.401	33362.0	21670.6	20111.0	12505.6
.502	32543.3	21137.8	19219.3	11768.5
.602	32400.5	21041.1	18623.3	11240.1
.701	32436.3	21072.0	18078.9	10773.7
.801	32107.7	20896.9	17712.0	10435.1
.902	31571.8	20609.5	17373.3	10132.5
1.00	31218.0	20462.9	17100.0	9886.2
1.10	30928.9	20388.1	16879.7	9682.7
1.20	30649.9	20327.7	16690.5	9508.9
1.30	30289.1	20209.0	16570.8	9382.3
1.40	29888.2	20061.2	16500.6	9291.2
1.50	29438.5	19883.7	16479.3	9232.7
1.60	28922.9	19662.4	16497.3	9200.5
1.70	28364.9	19411.2	16545.5	9188.7
1.80	27764.4	19131.6	16616.8	9192.0
1.90	27156.7	18842.2	16699.0	9204.7



Table 14.3.4-4 (CONT'D)

## Double-Ended Hot-Leg Break Blowdown Mass and Energy Releases

Time (sec)	Break Path No. 1 Flow*		Break Path No. 2 Flow**	
	(lbm/sec)	(Thousand Btu/sec)	(lbm/sec)	(Thousand Btu/sec)
2.00	26532.2	18533.8	16782.8	9221.6
2.10	25871.9	18192.5	16866.1	9241.1
2.20	25212.8	17842.4	16946.6	9262.2
2.30	24578.1	17498.1	17018.4	9281.9
2.40	23935.1	17136.6	17083.1	9300.5
2.50	23325.2	16784.4	17135.3	9315.0
2.60	22739.8	16439.3	17176.0	9325.6
2.70	22130.0	16060.4	17202.5	9330.7
2.80	21577.5	15708.7	17214.9	9330.2
2.90	21072.8	15379.1	17213.8	9323.9
3.00	20603.5	15058.0	17199.0	9311.7
3.10	20202.3	14772.6	17172.1	9294.2
3.20	19843.0	14503.8	17133.9	9271.6
3.30	19524.4	14252.5	17085.3	9244.3
3.40	19261.1	14031.5	17027.9	9213.0
3.50	19028.5	13822.9	16961.2	9177.4
3.60	18836.3	13637.0	16887.5	9138.5
3.70	18677.3	13468.2	16805.9	9095.8
3.80	18544.7	13313.6	16718.2	9050.2
3.90	18442.3	13177.6	16624.5	9001.7
4.00	18359.6	13052.5	16524.6	8950.1
4.20	18273.5	12852.5	16306.8	8837.9
4.40	18340.4	12746.9	16060.9	8711.3
4.60	18506.2	12704.7	15771.4	8561.9
4.80	18750.4	12712.0	15445.0	8393.7
5.00	19128.9	12776.4	15156.7	8247.6
5.20	11682.8	8813.9	14816.1	8073.4

Table 14.3.4-4 (CONT'D)

## Double-Ended Hot-Leg Break Blowdown Mass and Energy Releases

Time (sec)	Break Path No. 1 Flow*		Break Path No. 2 Flow**	
	(lbm/sec)	(Thousand Btu/sec)	(lbm/sec)	(Thousand Btu/sec)
5.40	14643.7	10645.5	14397.9	7857.2
5.60	14898.3	10688.8	13971.4	7637.6
5.80	15008.0	10665.4	13539.2	7416.2
6.00	15156.1	10667.5	13119.7	7202.8
6.20	15174.3	10585.0	12700.5	6990.0
6.40	15336.2	10598.2	12263.7	6767.8
6.60	15527.5	10585.2	11801.5	6531.1
6.80	15482.1	10491.5	11349.4	6300.0
7.00	15702.1	10504.6	10916.8	6079.2
7.20	15893.2	10518.8	10485.2	5858.2
7.40	16024.3	10513.6	10064.4	5642.8
7.60	16107.2	10492.1	9668.2	5440.3
7.80	16148.5	10454.6	9293.9	5248.9
8.00	16119.3	10385.1	8944.0	5069.9
8.20	15958.6	10252.6	8609.1	4898.7
8.40	15625.0	10031.1	8294.6	4737.9
8.60	15170.5	9749.6	7995.3	4585.0
8.80	14748.8	9491.8	7712.3	4440.6
9.00	14393.7	9273.6	7436.6	4300.4
9.20	14068.3	9075.3	7179.3	4170.2
9.40	13724.8	8869.0	6930.8	4045.0
9.60	13352.6	8648.4	6691.7	3925.2
9.80	12969.0	8423.4	6464.9	3812.4
10.0	12584.8	8200.0	6245.8	3704.0
10.2	12206.3	7981.6	6032.6	3599.2
10.2	12201.1	7978.7	6029.4	3597.6
10.4	11835.1	7769.2	5827.1	3499.1
10.6	11478.2	7567.2	5632.8	3405.2

Table 14.3.4-4 (CONT'D)

## Double-Ended Hot-Leg Break Blowdown Mass and Energy Releases

Time (sec)	Break Path No. 1 Flow*		Break Path No. 2 Flow**	
	(lbm/sec)	(Thousand Btu/sec)	(lbm/sec)	(Thousand Btu/sec)
10.8	11119.0	7366.3	5441.3	3313.5
11.0	10764.3	7170.4	5257.3	3226.0
11.2	10418.7	6982.3	5081.4	3143.0
11.4	10069.4	6795.1	4908.0	3061.9
11.6	9730.1	6615.6	4742.4	2985.0
11.8	9392.9	6441.0	4581.3	2910.7
12.0	9060.8	6272.5	4427.1	2840.3
12.2	8730.1	6108.2	4276.9	2771.8
12.4	8377.0	5935.4	4130.8	2705.6
12.6	7976.2	5743.3	3986.3	2640.2
12.8	7525.1	5534.6	3843.8	2575.6
13.0	7008.5	5303.3	3697.5	2509.5
13.2	6434.8	5054.9	3545.5	2441.6
13.4	5813.9	4786.1	3383.2	2370.9
13.6	5180.9	4506.3	3209.9	2297.4
13.8	4555.9	4214.7	3025.3	2221.8
14.0	3937.2	3883.0	2826.6	2142.8
14.2	3302.4	3490.6	2616.7	2061.2
14.4	2792.1	3101.8	2386.7	1972.0
14.6	2428.7	2787.1	2127.2	1870.8
14.8	2143.0	2511.8	1837.1	1775.6
15.0	1902.1	2263.5	1519.1	1678.0
15.2	1702.5	2051.7	1218.4	1482.7
15.4	1507.3	1833.7	996.7	1233.5
15.6	1342.1	1646.4	868.8	1081.0
15.8	1184.2	1464.9	782.2	976.3
16.0	1065.4	1332.2	700.9	876.5
16.2	948.1	1191.8	613.8	768.3

Table 14.3.4-4 (CONT'D)

## Double-Ended Hot-Leg Break Blowdown Mass and Energy Releases

Time (sec)	Break Path No. 1 Flow*		Break Path No. 2 Flow**	
	(lbm/sec)	(Thousand Btu/sec)	(lbm/sec)	(Thousand Btu/sec)
16.4	869.2	1097.1	526.9	660.8
16.6	780.6	987.2	455.6	573.0
16.8	684.1	866.3	395.9	498.7
17.0	596.1	755.8	346.2	436.7
17.2	518.0	657.5	288.9	365.0
17.4	444.3	564.5	238.3	301.8
17.6	371.4	472.2	200.4	254.4
17.8	297.7	379.0	157.2	200.0
18.0	212.1	270.0	111.5	142.4
18.2	61.3	77.6	55.9	71.8
18.4	278.9	357.9	103.7	133.5
18.6	124.1	159.4	82.5	105.8
18.8	125.0	161.2	103.0	132.4
19.0	177.5	229.6	95.8	123.3
19.2	195.9	253.8	99.0	127.4
19.4	197.0	255.3	102.7	131.9
19.6	178.7	231.8	77.2	99.4
19.8	219.4	283.8	65.5	84.6
20.0	253.2	327.8	73.9	95.8
20.2	321.2	414.7	85.8	111.0
20.4	403.6	517.7	91.4	117.9
20.6	422.6	540.8	110.9	142.8
20.8	450.8	556.9	103.0	132.4
21.0	378.2	473.0	140.9	180.9
21.2	372.1	466.7	95.8	122.9
21.4	470.3	576.9	97.0	124.7
21.6	445.8	554.6	83.6	107.8
21.8	323.4	408.0	78.3	101.0

Table 14.3.4-4 (CONT'D)

Double-Ended Hot-Leg Break Blowdown Mass and Energy Releases

Time (sec)	Break Path No. 1 Flow*		Break Path No. 2 Flow**	
	(lbm/sec)	(Thousand Btu/sec)	(lbm/sec)	(Thousand Btu/sec)
22.0	91.9	119.4	57.3	74.1
22.2	.0	.0	.0	.0

\* Mass and Energy exiting from the RV side of the break

\*\* Mass and Energy exiting from the SG side of the break

Table 14.3.4-5

Double-Ended Pump Suction Break Blowdown Mass and Energy Releases  
(Same for all DEPS Runs)

Time (sec)	Break Path No. 1 Flow*		Break Path No. 2 Flow**	
	(lbm/sec)	(Thousand Btu/sec)	(lbm/sec)	(Thousand Btu/sec)
.00000	.0	.0	.0	.0
.00111	86328.0	46576.4	40275.9	21682.3
.101	40307.9	21771.0	20311.6	10927.4
.202	47126.9	25635.7	22479.2	12101.8
.301	46925.4	25755.9	23012.6	12401.0
.401	47194.3	26187.2	22696.1	12244.5
.501	46805.7	26295.2	21992.2	11874.6
.602	44647.8	25398.6	21311.8	11513.8
.701	44824.0	25789.8	20823.0	11253.7
.801	44733.7	25996.8	20440.3	11050.7
.902	44015.3	25812.1	20143.1	10894.0
1.00	42956.2	25407.3	19924.0	10778.4
1.10	41899.1	24991.3	19757.3	10690.3
1.20	40878.9	24586.9	19662.8	10640.7
1.30	39938.6	24215.4	19641.5	10630.2
1.40	39096.9	23890.2	19657.0	10639.1
1.50	38373.8	23621.3	19640.1	10629.4
1.60	37726.9	23387.2	19589.6	10600.9
1.70	37058.7	23137.4	19540.4	10573.0
1.80	36340.3	22862.4	19516.2	10558.9
1.90	35600.6	22590.9	19471.2	10533.6
2.00	34792.4	22295.7	19360.1	10472.2
2.10	33760.9	21876.9	19182.1	10374.5
2.20	32417.3	21261.7	18960.4	10253.2
2.30	31045.2	20629.4	18605.5	10060.2
2.40	29602.3	19943.2	18277.5	9882.0

Table 14.3.4-5 (CONT'D)

Double-Ended Pump Suction Break Blowdown Mass and Energy Releases  
(Same for all DEPS Runs)

Time (sec)	Break Path No. 1 Flow*		Break Path No. 2 Flow**	
	(lbm/sec)	(Thousand Btu/sec)	(lbm/sec)	(Thousand Btu/sec)
2.50	27463.0	18739.7	17936.0	9696.5
2.60	23679.2	16340.9	17641.3	9537.0
2.70	21310.6	14895.4	17357.6	9383.7
2.80	19830.4	13995.2	17045.5	9215.4
2.90	18412.1	13061.0	16763.1	9063.7
3.00	17352.9	12355.2	16520.0	8933.8
3.10	16489.3	11779.6	16289.7	8811.0
3.20	15741.3	11280.8	16069.6	8693.8
3.30	15119.1	10871.2	15874.8	8590.9
3.40	14582.9	10522.2	15718.9	8508.6
3.50	14068.0	10184.6	15521.4	8403.6
3.60	13598.1	9878.9	15358.9	8317.9
3.70	13195.3	9620.9	15200.7	8234.4
3.80	12848.5	9398.2	15046.2	8152.9
3.90	12534.6	9192.1	14892.8	8072.0
4.00	12254.3	9004.7	14758.6	8001.5
4.20	11804.1	8699.6	14501.7	7866.7
4.40	11428.7	8440.7	14271.1	7746.3
4.60	11111.7	8222.9	14050.8	7631.4
4.80	10854.3	8047.0	13803.2	7501.7
5.00	10625.4	7891.7	13298.2	7232.2
5.20	10387.8	7734.9	13076.4	7116.6
5.40	10158.5	7588.8	14660.0	7987.7
5.60	9979.2	7472.2	14500.8	7904.9
5.80	9867.5	7399.2	14305.8	7805.4
6.00	10258.8	7702.6	14222.2	7765.8
6.20	10209.2	8045.0	13904.0	7597.7

Table 14.3.4-5 (CONT'D)

Double-Ended Pump Suction Break Blowdown Mass and Energy Releases  
(Same for all DEPS Runs)

Time (sec)	Break Path No. 1 Flow*		Break Path No. 2 Flow**	
	(lbm/sec)	(Thousand Btu/sec)	(lbm/sec)	(Thousand Btu/sec)
6.40	8820.8	7744.0	13698.0	7491.8
6.60	7980.5	7358.6	13464.7	7369.7
6.80	7742.2	7116.4	13146.0	7199.8
7.00	7759.1	6953.3	12832.5	7031.6
7.20	7902.8	6845.9	12642.0	6929.6
7.40	8045.0	6745.7	12550.2	6878.6
7.60	8144.0	6676.1	12413.3	6798.7
7.80	8169.6	6591.9	12200.0	6675.0
8.00	8181.2	6511.3	11982.0	6550.3
8.20	8174.8	6427.7	11826.8	6461.8
8.40	8133.7	6335.0	11671.9	6374.0
8.60	8062.2	6238.2	11478.2	6264.8
8.80	7963.5	6139.8	11293.7	6161.1
9.00	7842.4	6042.5	11137.9	6073.7
9.20	7699.6	5944.5	10969.5	5979.6
9.40	7543.8	5848.6	10792.4	5881.0
9.60	7379.2	5754.7	10630.2	5791.1
9.80	7214.3	5667.4	10466.2	5700.6
10.0	7041.0	5573.6	10287.9	5602.5
10.2	6874.7	5480.9	10118.8	5510.1
10.4	6713.8	5388.1	9952.1	5419.4
10.6	6555.8	5294.2	9781.7	5326.9
10.8	6405.4	5202.4	9617.2	5237.6
11.0	6259.3	5111.1	9455.8	5150.1
11.2	6113.6	5017.1	9295.6	5063.1
11.4	5958.1	4915.0	9106.9	4960.6
11.6	5798.1	4806.1	8935.7	4868.4
11.8	5641.3	4689.2	8769.4	4779.2



Table 14.3.4-5 (CONT'D)

Double-Ended Pump Suction Break Blowdown Mass and Energy Releases  
(Same for all DEPS Runs)

Time (sec)	Break Path No. 1 Flow*		Break Path No. 2 Flow**	
	(lbm/sec)	(Thousand Btu/sec)	(lbm/sec)	(Thousand Btu/sec)
12.0	5496.8	4571.0	8592.3	4683.6
12.2	5362.4	4454.7	8422.7	4592.4
12.4	5230.1	4338.5	8249.6	4499.4
12.6	5097.1	4222.0	8076.6	4406.5
12.8	4969.7	4110.6	7823.7	4269.0
13.0	4854.9	4009.5	7562.6	4128.6
13.2	4755.8	3921.2	7443.0	4062.0
13.4	4660.4	3841.7	7191.8	3898.8
13.6	4568.5	3773.9	7174.9	3839.4
13.8	4475.3	3714.9	7115.1	3741.6
14.0	4377.6	3662.4	7093.4	3655.2
14.2	4269.4	3614.1	6979.8	3522.7
14.4	4151.4	3570.4	6652.7	3288.2
14.6	4023.0	3533.2	6385.1	3088.0
14.8	3885.7	3499.2	6162.4	2922.3
15.0	3738.5	3469.7	5919.0	2759.5
15.2	3584.2	3445.7	5730.1	2630.4
15.4	3418.0	3424.9	5546.7	2511.2
15.6	3214.1	3381.6	5340.3	2387.9
15.8	2890.7	3246.9	4903.2	2164.0
16.0	2564.9	3058.2	4538.9	1969.6
16.2	2319.6	2840.7	4324.6	1839.9
16.4	2102.1	2594.6	4027.6	1683.4
16.6	1918.7	2377.3	3595.4	1476.0
16.8	1760.6	2187.8	3166.8	1272.4
17.0	1627.6	2027.0	2789.1	1091.8
17.2	1499.8	1871.3	2516.2	958.2
17.4	1379.0	1723.6	2346.9	869.9

Table 14.3.4-5 (CONT'D)

Double-Ended Pump Suction Break Blowdown Mass and Energy Releases  
(Same for all DEPS Runs)

Time (sec)	Break Path No. 1 Flow*		Break Path No. 2 Flow**	
	(lbm/sec)	(Thousand Btu/sec)	(lbm/sec)	(Thousand Btu/sec)
17.6	1248.8	1563.3	2291.2	828.2
17.8	1136.7	1425.4	2258.2	797.2
18.0	1032.7	1296.6	2304.1	793.3
18.2	825.2	1036.9	2301.4	771.9
18.4	586.6	738.3	1958.1	645.6
18.6	419.1	528.6	1583.8	517.9
18.8	292.7	369.6	1217.3	396.9
19.0	191.8	242.5	972.4	317.2
19.2	117.5	148.8	784.0	256.2
19.4	14.8	18.8	848.2	277.8
19.6	.0	.0	939.8	306.5
19.8	.0	.0	987.4	319.3
20.0	.0	.0	976.1	313.9
20.2	.0	.0	908.2	291.5
20.4	.0	.0	789.9	253.7
20.6	.0	.0	604.1	194.7
20.8	.0	.0	295.9	96.0
21.0	.0	.0	.0	.0

\* Mass and Energy exiting the SG side of the break

\*\* Mass and Energy exiting the pump side of the break

Table 14.3.4-6  
 Double-Ended Pump Suction Break Minimum Safeguards Reflood Mass and Energy Releases

Time (sec)	Break Path No. 1 Flow*		Break Path No. 2 Flow**	
	(lbm/sec)	(Thousand Btu/sec)	(lbm/sec)	(Thousand Btu/sec)
21.5	.0	.0	.0	.0
21.7	.0	.0	.0	.0
21.8	.0	.0	.0	.0
21.9	.0	.0	.0	.0
21.9	.0	.0	.0	.0
22.0	70.1	82.6	.0	.0
22.1	30.4	35.8	.0	.0
22.2	32.1	37.8	.0	.0
22.3	37.1	43.7	.0	.0
22.4	46.9	55.2	.0	.0
22.5	54.3	63.9	.0	.0
22.6	61.3	72.2	.0	.0
22.7	67.9	80.0	.0	.0
22.8	72.8	85.8	.0	.0
22.9	77.6	91.4	.0	.0
23.0	81.1	95.5	.0	.0
23.0	82.2	96.8	.0	.0
23.1	86.6	102.0	.0	.0
23.2	90.9	107.0	.0	.0
23.3	94.9	111.8	.0	.0
23.4	98.9	116.5	.0	.0
23.5	102.7	121.0	.0	.0
23.6	106.4	125.3	.0	.0
23.7	110.0	129.5	.0	.0
23.8	113.5	133.7	.0	.0
23.9	116.9	137.7	.0	.0
24.0	120.2	141.6	.0	.0

Table 14.3.4-6 (CONT'D)

## Double-Ended Pump Suction Break Minimum Safeguards Reflood Mass and Energy Releases

Time (sec)	Break Path No. 1 Flow*		Break Path No. 2 Flow**	
	(lbm/sec)	(Thousand Btu/sec)	(lbm/sec)	(Thousand Btu/sec)
25.0	149.6	176.3	.0	.0
26.1	444.3	526.3	4349.7	497.9
26.7	445.8	528.2	4348.1	504.3
27.1	442.6	524.3	4317.1	502.1
28.1	433.1	512.9	4224.7	494.5
29.1	423.0	500.8	4126.1	485.9
30.1	413.0	488.9	4027.4	477.1
31.2	428.2	507.0	4198.7	476.7
31.3	427.2	505.9	4189.5	475.9
32.2	419.1	496.2	4109.6	468.5
33.2	410.4	485.9	4023.7	460.5
34.2	402.2	476.0	3941.1	452.8
35.2	394.3	466.6	3861.6	445.4
36.2	386.8	457.7	3785.2	438.2
37.2	379.6	449.1	3711.7	431.3
38.2	372.8	441.0	3641.0	424.7
39.2	366.2	433.2	3573.0	418.3
40.2	360.0	425.7	3507.3	412.2
41.2	354.0	418.6	3444.0	406.2
42.2	348.2	411.8	3382.8	400.5
43.2	342.7	405.2	3323.7	394.9
44.1	337.9	399.5	3272.1	390.1
44.2	337.4	398.9	3266.5	389.6
45.2	332.3	392.8	3211.1	384.4
46.2	327.4	387.0	3157.4	379.3
47.2	322.6	381.3	3105.3	374.4
48.2	318.1	375.9	3054.7	369.6

Table 14.3.4-6 (CONT'D)

## Double-Ended Pump Suction Break Minimum Safeguards Reflood Mass and Energy Releases

Time (sec)	Break Path No. 1 Flow*		Break Path No. 2 Flow**	
	(lbm/sec)	(Thousand Btu/sec)	(lbm/sec)	(Thousand Btu/sec)
49.2	313.6	370.6	3005.5	364.9
50.2	309.3	365.5	2957.7	360.4
51.2	305.2	360.6	2911.2	356.0
51.8	302.8	357.7	2883.8	353.4
52.2	301.2	355.8	2865.8	351.7
53.2	297.3	351.2	2821.7	347.5
54.2	293.5	346.7	2778.6	343.4
55.2	289.8	342.3	2736.5	339.4
56.2	231.3	272.9	1995.3	273.5
57.2	260.8	307.8	237.8	116.6
58.2	261.3	308.5	237.9	116.9
59.2	256.3	302.6	236.1	114.4
60.2	251.4	296.7	234.3	112.0
61.2	246.5	291.0	232.6	109.7
62.2	241.7	285.3	230.9	107.4
63.2	236.8	279.5	229.2	105.1
64.2	232.4	274.2	227.6	103.0
65.2	228.1	269.2	226.1	101.0
66.2	224.0	264.3	224.7	99.1
67.2	220.0	259.6	223.3	97.2
68.2	216.1	255.0	222.0	95.4
69.2	212.4	250.5	220.7	93.7
70.2	208.7	246.2	219.4	92.1
70.4	208.0	245.3	219.1	91.7
71.2	205.1	242.0	218.2	90.4
72.2	201.7	237.9	217.0	88.9
73.2	198.3	233.9	215.8	87.4

Table 14.3.4-6 (CONT'D)

## Double-Ended Pump Suction Break Minimum Safeguards Reflood Mass and Energy Releases

Time (sec)	Break Path No. 1 Flow*		Break Path No. 2 Flow**	
	(lbm/sec)	(Thousand Btu/sec)	(lbm/sec)	(Thousand Btu/sec)
74.2	195.0	230.0	214.7	85.9
75.2	191.9	226.3	213.6	84.5
76.2	188.8	222.6	212.6	83.2
77.2	185.8	219.1	211.5	81.9
78.2	182.9	215.6	210.6	80.6
79.2	180.0	212.3	209.6	79.4
80.2	177.3	209.0	208.7	78.2
81.2	174.6	205.9	207.8	77.1
82.2	172.1	202.9	207.0	76.0
84.2	167.2	197.1	205.4	73.9
86.2	162.6	191.7	203.9	72.0
88.2	158.4	186.7	202.5	70.3
90.2	154.4	182.0	201.3	68.7
92.2	150.7	177.7	200.1	67.2
94.2	147.4	173.7	199.1	65.8
94.3	147.2	173.5	199.0	65.8
96.2	144.3	170.0	198.1	64.6
98.2	141.4	166.7	197.2	63.5
100.2	138.8	163.6	196.4	62.4
102.2	136.4	160.7	195.7	61.5
104.2	134.2	158.2	195.0	60.6
106.2	132.2	155.8	194.4	59.9
108.2	130.5	153.7	193.9	59.2
110.2	128.9	151.8	193.4	58.5
112.2	127.4	150.1	192.9	58.0
114.2	126.1	148.6	192.5	57.5
116.2	125.0	147.2	192.2	57.0

Table 14.3.4-6 (CONT'D)

## Double-Ended Pump Suction Break Minimum Safeguards Reflood Mass and Energy Releases

Time (sec)	Break Path No. 1 Flow*		Break Path No. 2 Flow**	
	(lbm/sec)	(Thousand Btu/sec)	(lbm/sec)	(Thousand Btu/sec)
118.2	124.0	146.0	191.9	56.6
120.2	123.1	145.0	191.6	56.3
122.2	122.3	144.1	191.4	55.9
123.3	121.9	143.6	191.2	55.8
124.2	121.6	143.3	191.1	55.7
126.2	121.0	142.6	190.9	55.4
128.2	120.5	142.0	190.8	55.2
130.2	120.1	141.5	190.6	55.0
132.2	119.7	141.1	190.5	54.9
134.2	119.5	140.8	190.4	54.7
136.2	119.2	140.5	190.3	54.6
138.2	119.1	140.3	190.2	54.5
140.2	119.0	140.2	190.2	54.5
142.2	118.9	140.1	190.1	54.4
144.2	118.9	140.0	190.1	54.3
146.2	118.9	140.0	190.1	54.3
148.2	118.9	140.1	190.0	54.3
150.2	119.0	140.2	190.0	54.3
152.2	119.0	140.3	190.0	54.3
154.2	119.1	140.4	190.0	54.3
155.3	119.2	140.5	190.0	54.3
156.2	119.3	140.5	190.0	54.3
158.2	119.4	140.7	190.1	54.3

Table 14.3.4-6 (CONT'D)

## Double-Ended Pump Suction Break Minimum Safeguards Reflood Mass and Energy Releases

Time (sec)	Break Path No. 1 Flow*		Break Path No. 2 Flow**	
	(lbm/sec)	(Thousand Btu/sec)	(lbm/sec)	(Thousand Btu/sec)
160.2	119.6	140.9	190.1	54.3
162.2	119.8	141.1	190.1	54.4
164.2	119.9	141.3	190.1	54.4
166.2	120.1	141.6	190.2	54.4
168.2	120.4	141.8	190.2	54.5
170.2	120.6	142.1	190.2	54.5
172.2	121.3	142.9	190.5	54.8
174.2	121.8	143.6	191.1	55.0
176.2	122.3	144.1	192.1	55.4
178.2	122.7	144.6	193.4	55.8
180.2	123.1	145.0	195.0	56.2
182.2	123.3	145.3	196.8	56.7
184.2	123.5	145.6	198.9	57.2
186.2	123.7	145.7	201.1	57.7
188.2	123.7	145.7	203.5	58.2
189.0	123.7	145.7	204.5	58.4
190.2	123.6	145.7	206.0	58.7
192.2	123.5	145.5	208.7	59.3
194.2	123.2	145.2	211.4	59.8
196.2	122.8	144.7	214.3	60.4
198.2	122.3	144.1	217.4	60.9
200.2	121.7	143.4	220.5	61.5
202.2	121.0	142.5	223.8	62.1
204.2	120.1	141.5	227.2	62.6
206.2	119.1	140.3	230.6	63.2
208.2	118.0	139.0	234.2	63.8
210.2	116.7	137.5	237.9	64.3



Table 14.3.4-6 (CONT'D)

Double-Ended Pump Suction Break Minimum Safeguards Reflood Mass and Energy Releases

Time (sec)	Break Path No. 1 Flow*		Break Path No. 2 Flow**	
	(lbm/sec)	(Thousand Btu/sec)	(lbm/sec)	(Thousand Btu/sec)
212.2	115.3	135.8	241.7	64.9
214.2	113.7	134.0	245.6	65.5
216.2	112.0	132.0	249.6	66.1
218.2	110.2	129.8	253.6	66.6
220.2	109.0	128.4	256.8	67.0
222.2	108.6	128.0	258.7	67.0
224.2	108.3	127.5	260.5	67.0
225.8	107.9	127.2	261.8	67.0

\* Mass and Energy exiting the SG side of the break

\*\* Mass and Energy exiting the pump side of the break

Table 14.3.4-7  
 Double-Ended Pump Suction Break - Minimum Safeguards  
 Principle Parameters During Reflood

Time (sec)	Flooding		Carryover Fraction	Core Height (ft)	Downcomer Height (ft)	Flow Frac	Total	Injection Accum (lbm/sec)	Spill	Enthalpy (Btu/lbm)
	Temp (°F)	Rate (in/sec)								
21.0	221.0	.000	.000	.00	.00	.333	.0	.0	.0	.00
21.7	217.0	22.982	.000	.54	1.98	.000	7125.9	7125.9	.0	74.49
21.9	213.6	28.149	.000	1.07	1.93	.000	7029.8	7029.8	.0	74.49
23.0	211.4	2.916	.313	1.50	6.03	.426	6674.2	6674.2	.0	74.49
23.9	210.9	2.797	.442	1.64	9.78	.455	6432.7	6432.7	.0	74.49
26.1	209.4	5.028	.617	1.92	15.62	.687	5432.3	5432.3	.0	74.49
26.7	208.8	4.811	.647	2.01	15.63	.684	5301.0	5301.0	.0	74.49
27.1	208.5	4.679	.662	2.06	15.63	.684	5230.7	5230.7	.0	74.49
30.1	206.6	4.099	.715	2.39	15.63	.677	4788.1	4788.1	.0	74.49
31.2	206.1	4.154	.724	2.50	15.63	.683	4969.0	4581.7	.0	71.27
31.3	206.0	4.143	.725	2.51	15.63	.683	4957.1	4569.6	.0	71.26
37.2	204.5	3.658	.746	3.01	15.63	.668	4367.9	3967.3	.0	70.71
44.1	204.3	3.309	.754	3.50	15.63	.652	3852.4	3441.3	.0	70.09
51.8	205.2	3.033	.756	4.00	15.63	.635	3405.9	2986.4	.0	69.41
56.2	206.1	2.545	.752	4.26	15.63	.582	2409.9	1975.5	.0	67.05
57.2	206.3	2.756	.755	4.32	15.54	.606	428.9	.0	.0	33.22
61.2	207.6	2.613	.754	4.54	14.89	.602	430.7	.0	.0	33.22

Table 14.3.4-7 (CONT'D)

Double-Ended Pump Suction Break - Minimum Safeguards  
Principle Parameters During Reflood

Time (sec)	Flooding			Core Height (ft)	Downcomer Height (ft)	Flow Frac	Total	Injection Accum (lbm/sec)	Spill	Enthalpy (Btu/lbm)
	Temp (°F)	Rate (in/sec)	Carryover Fraction							
70.4	212.2	2.282	.750	5.00	13.79	.584	436.2	.0	.0	33.22
82.2	220.1	1.975	.747	5.53	12.99	.561	439.9	.0	.0	33.22
94.3	228.8	1.763	.745	6.00	12.69	.539	442.1	.0	.0	33.22
110.2	238.3	1.604	.746	6.57	12.77	.518	443.6	.0	.0	33.22
123.3	244.8	1.540	.748	7.00	13.06	.509	444.1	.0	.0	33.22
140.2	252.0	1.505	.752	7.54	13.57	.506	444.4	.0	.0	33.22
155.3	257.6	1.497	.757	8.00	14.09	.507	444.4	.0	.0	33.22
162.2	259.9	1.496	.759	8.21	14.33	.508	444.4	.0	.0	33.22
172.2	263.0	1.501	.763	8.51	14.68	.510	444.4	.0	.0	33.22
182.2	265.9	1.508	.766	8.80	15.00	.514	444.2	.0	.0	33.22
189.0	267.8	1.504	.769	9.00	15.18	.515	444.2	.0	.0	33.22
208.2	272.5	1.442	.773	9.54	15.50	.509	444.6	.0	.0	33.22
225.8	276.1	1.348	.776	10.00	15.60	.497	445.2	.0	.0	33.22

Table 14.3.4-8

Double-Ended Pump Suction Break Minimum  
Safeguards Post-Reflood Mass and Energy Releases

Time (sec)	Break Path No. 1 Flow*		Break Path No. 2 Flow**	
	(lbm/sec)	(Thousand Btu/sec)	(lbm/sec)	(Thousand Btu/sec)
225.9	126.9	159.6	318.6	82.5
230.9	126.6	159.2	319.0	82.5
235.9	127.2	160.0	318.3	82.1
240.9	126.9	159.6	318.7	82.0
245.9	126.5	159.1	319.0	82.0
250.9	127.2	159.9	318.4	81.6
255.9	126.8	159.5	318.7	81.6
260.9	126.4	159.0	319.1	81.5
265.9	126.1	158.5	319.5	81.4
270.9	126.7	159.4	318.8	81.1
275.9	126.3	158.9	319.2	81.0
280.9	126.0	158.4	319.6	81.0
285.9	125.6	157.9	319.9	80.9
290.9	126.2	158.7	319.3	80.5
295.9	125.9	158.3	319.7	80.5
300.9	125.5	157.8	320.1	80.4
305.9	126.1	158.6	319.4	80.1
310.9	125.7	158.1	319.8	80.0
315.9	125.3	157.6	320.2	79.9
320.9	124.9	157.1	320.6	79.9
325.9	125.5	157.9	320.0	79.5
330.9	125.2	157.4	320.4	79.5
335.9	124.8	156.9	320.8	79.4
340.9	125.4	157.6	320.2	79.1
345.9	125.0	157.1	320.6	79.0
350.9	124.6	156.6	321.0	78.9
355.9	125.1	157.4	320.4	78.6

Table 14.3.4-8 (CONT'D)

Double-Ended Pump Suction Break Minimum  
Safeguards Post-Reflood Mass and Energy Releases

Time (sec)	Break Path No. 1 Flow*		Break Path No. 2 Flow**	
	(lbm/sec)	(Thousand Btu/sec)	(lbm/sec)	(Thousand Btu/sec)
360.9	124.7	156.9	320.8	78.5
365.9	124.3	156.3	321.2	78.5
370.9	124.9	157.1	320.6	78.2
375.9	124.5	156.5	321.1	78.1
380.9	124.1	156.0	321.5	78.0
385.9	124.6	156.7	320.9	77.7
390.9	124.2	156.2	321.3	77.6
395.9	123.8	155.7	321.8	77.6
400.9	124.3	156.4	321.2	77.3
405.9	124.0	156.0	321.5	77.2
410.9	123.7	155.6	321.8	77.1
415.9	123.4	155.2	322.1	77.0
420.9	124.1	156.0	321.5	76.6
425.9	123.8	155.6	321.8	76.5
430.9	123.4	155.2	322.1	76.5
435.9	123.1	154.8	322.4	76.4
440.9	123.7	155.6	321.8	76.0
445.9	123.4	155.2	322.1	75.9
450.9	123.1	154.8	322.4	75.8
455.9	123.7	155.6	321.8	78.4
460.9	123.4	155.1	322.2	78.3
465.9	123.0	154.7	322.5	78.2
470.9	122.7	154.3	322.8	78.1
475.9	123.3	155.0	322.2	77.8
480.9	123.0	154.6	322.6	77.7
485.9	122.6	154.2	322.9	77.5
490.9	123.2	154.9	322.4	77.2

Table 14.3.4-8 (CONT'D)

Double-Ended Pump Suction Break Minimum  
Safeguards Post-Reflood Mass and Energy Releases

Time (sec)	Break Path No. 1 Flow*		Break Path No. 2 Flow**	
	(lbm/sec)	(Thousand Btu/sec)	(lbm/sec)	(Thousand Btu/sec)
495.9	122.8	154.5	322.7	77.1
500.9	122.5	154.0	323.1	77.0
505.9	123.0	154.7	322.5	76.7
510.9	122.6	154.2	322.9	76.6
515.9	122.3	153.8	323.2	76.5
520.9	122.8	154.4	322.7	76.2
525.9	122.4	154.0	323.1	76.1
530.9	122.1	153.5	323.5	76.0
535.9	122.6	154.1	323.0	75.6
540.9	122.2	153.7	323.4	75.6
545.9	122.7	154.2	322.9	75.2
550.9	122.3	153.8	323.3	75.1
555.9	121.9	153.3	323.7	75.0
560.9	122.3	153.8	323.2	74.7
565.9	121.9	153.3	323.6	74.6
570.9	122.4	153.9	323.2	74.3
575.9	121.9	153.4	323.6	74.2
580.9	121.5	152.8	324.0	74.1
585.9	121.9	153.3	323.6	73.8
590.9	121.5	152.8	324.0	73.8
595.9	121.9	153.3	323.6	76.2
600.9	121.5	152.8	324.1	76.1
605.9	121.9	153.3	323.7	75.7
610.9	121.5	152.8	324.1	75.6
615.9	121.8	153.2	323.7	75.3
620.9	121.4	152.7	324.1	75.2
625.9	121.8	153.2	323.7	74.9

Table 14.3.4-8 (CONT'D)

Double-Ended Pump Suction Break Minimum  
Safeguards Post-Reflood Mass and Energy Releases

Time (sec)	Break Path No. 1 Flow*		Break Path No. 2 Flow**	
	(lbm/sec)	(Thousand Btu/sec)	(lbm/sec)	(Thousand Btu/sec)
630.9	121.4	152.6	324.2	74.8
635.9	121.7	153.0	323.8	74.5
640.9	121.2	152.5	324.3	74.4
645.9	121.6	152.9	324.0	74.1
650.9	121.1	152.3	324.4	74.0
655.9	121.4	152.6	324.2	73.7
660.9	120.9	152.0	324.6	73.6
665.9	121.2	152.4	324.4	73.3
670.9	121.4	152.7	324.1	73.1
675.9	120.9	152.0	324.7	73.0
680.9	121.1	152.3	324.5	72.7
685.9	121.3	152.5	324.3	72.4
690.9	120.7	151.8	324.8	74.9
695.9	120.9	152.0	324.7	74.7
700.9	121.0	152.2	324.5	74.4
705.9	121.1	152.3	324.4	74.1
710.9	120.5	151.6	325.0	74.0
715.9	120.6	151.7	324.9	73.8
720.9	120.6	151.7	324.9	73.5
725.9	120.7	151.7	324.9	73.3
730.9	120.7	151.7	324.9	73.0
735.9	120.6	151.7	324.9	72.8
740.9	120.6	151.6	325.0	72.6
745.9	120.5	151.5	325.1	72.4
750.9	120.3	151.3	325.2	72.1
755.9	120.2	151.1	325.4	71.9
760.9	120.0	150.9	325.5	71.7

Table 14.3.4-8 (CONT'D)

Double-Ended Pump Suction Break Minimum  
Safeguards Post-Reflood Mass and Energy Releases

Time (sec)	Break Path No. 1 Flow*		Break Path No. 2 Flow**	
	(lbm/sec)	(Thousand Btu/sec)	(lbm/sec)	(Thousand Btu/sec)
765.9	120.4	151.4	325.2	73.9
770.9	120.1	151.0	325.4	73.7
775.9	120.4	151.4	325.2	73.3
780.9	120.0	150.9	325.6	73.2
785.9	120.1	151.1	325.4	72.9
790.9	120.2	151.1	325.4	72.6
795.9	120.2	151.1	325.4	72.3
800.9	120.1	151.0	325.5	72.1
805.9	119.9	150.8	325.6	71.9
810.9	119.6	150.5	325.9	71.7
815.9	119.8	150.6	325.8	71.3
820.9	119.8	150.6	325.8	71.1
825.9	119.6	150.4	326.0	73.3
830.9	119.7	150.5	325.9	72.9
835.9	119.5	150.3	326.0	72.7
840.9	119.5	150.3	326.0	72.4
845.9	119.5	150.3	326.0	72.1
850.9	119.4	150.2	326.1	71.8
855.9	66.2	83.2	379.3	85.5
1273.6	66.2	83.2	379.3	85.5
1273.7	64.6	80.7	381.0	81.5
1275.9	64.5	80.7	381.0	81.2
1547.9	64.5	80.7	381.0	81.2
1548.0	57.9	66.7	387.6	12.9
2900.0	50.4	58.0	395.1	13.1
2900.1	52.1	60.0	355.8	60.9
3600.0	48.6	55.9	359.3	61.5

\* Mass and Energy exiting the SG side of the break

\*\* Mass and Energy exiting the pump side of the break



Table 14.3.4-9

Double-Ended Pump Suction Break Maximum Safeguards Reflood Mass and Energy Releases

Time (sec)	Break Path No. 1 Flow*		Break Path No. 2 Flow**	
	(lbm/sec)	(Thousand Btu/sec)	(lbm/sec)	(Thousand Btu/sec)
21.5	.0	.0	.0	.0
21.7	.0	.0	.0	.0
21.8	.0	.0	.0	.0
21.9	.0	.0	.0	.0
21.9	.0	.0	.0	.0
22.0	70.1	82.6	.0	.0
22.1	30.4	35.8	.0	.0
22.2	32.1	37.8	.0	.0
22.3	37.1	43.7	.0	.0
22.4	46.9	55.2	.0	.0
22.5	54.3	63.9	.0	.0
22.6	61.3	72.2	.0	.0
22.7	67.9	80.0	.0	.0
22.8	72.8	85.8	.0	.0
22.9	77.6	91.4	.0	.0
23.0	81.1	95.5	.0	.0
23.0	82.2	96.8	.0	.0
23.1	86.6	102.0	.0	.0
23.2	90.9	107.0	.0	.0
23.3	94.9	111.8	.0	.0
23.4	98.9	116.5	.0	.0
23.5	102.7	121.0	.0	.0
23.6	106.4	125.3	.0	.0
23.7	110.0	129.5	.0	.0
23.8	113.5	133.7	.0	.0
23.9	116.9	137.7	.0	.0
24.0	120.2	141.6	.0	.0

Table 14.3.4-9 (CONT'D)

## Double-Ended Pump Suction Break Maximum Safeguards Reflood Mass and Energy Releases

Time (sec)	Break Path No. 1 Flow*		Break Path No. 2 Flow**	
	(lbm/sec)	(Thousand Btu/sec)	(lbm/sec)	(Thousand Btu/sec)
25.0	149.6	176.3	.0	.0
26.1	444.3	526.3	4349.7	497.9
26.7	445.8	528.2	4348.1	504.3
27.1	442.6	524.3	4317.1	502.1
28.1	433.1	512.9	4224.7	494.5
29.1	423.0	500.8	4126.1	485.9
30.1	413.0	488.9	4027.4	477.1
31.2	445.9	528.2	4384.6	482.6
31.3	444.9	527.1	4375.5	481.8
32.2	436.8	517.4	4297.0	474.5
33.2	428.1	507.0	4212.4	466.6
34.2	419.9	497.1	4130.9	459.0
35.2	412.0	487.7	4052.4	451.6
36.2	404.4	478.7	3977.0	444.5
37.0	398.6	471.8	3918.7	439.1
37.2	397.2	470.1	3904.4	437.7
38.2	390.4	461.9	3834.6	431.2
39.2	383.8	454.1	3767.3	424.8
40.2	377.5	446.6	3702.4	418.7
41.2	371.5	439.4	3639.8	412.8
42.2	365.7	432.5	3579.3	407.1
43.2	360.1	425.9	3520.8	401.6
43.7	357.4	422.7	3492.2	399.0
44.2	354.8	419.6	3464.2	396.3
45.2	349.6	413.4	3409.4	391.1
46.2	344.7	407.5	3356.3	386.1
47.2	339.9	401.8	3304.8	381.2
48.2	335.3	396.3	3254.7	376.5
49.2	330.8	391.0	3206.1	371.9

Table 14.3.4-9 (CONT'D)

## Double-Ended Pump Suction Break Maximum Safeguards Reflood Mass and Energy Releases

Time (sec)	Break Path No. 1 Flow*		Break Path No. 2 Flow**	
	(lbm/sec)	(Thousand Btu/sec)	(lbm/sec)	(Thousand Btu/sec)
50.2	326.4	385.8	3158.8	367.4
51.1	322.6	381.3	3117.2	363.5
51.2	322.2	380.8	3112.8	363.0
52.2	318.2	376.0	3067.9	358.7
53.2	314.2	371.3	3024.2	354.6
54.2	310.4	366.8	2981.6	350.5
55.2	306.7	362.3	2940.0	346.5
56.2	247.7	292.4	2222.8	283.2
57.2	170.1	200.6	402.3	101.8
58.2	158.8	187.1	428.7	96.9
59.2	158.4	186.7	429.4	96.7
60.2	158.1	186.4	430.0	96.5
61.2	157.8	186.0	430.7	96.3
62.2	157.4	185.6	431.4	96.2
63.2	157.1	185.2	432.1	96.0
64.2	156.8	184.8	432.8	95.9
65.2	156.5	184.4	433.5	95.7
66.2	156.2	184.1	434.2	95.5
67.2	155.8	183.7	434.9	95.4
68.2	155.5	183.3	435.6	95.2
69.2	155.2	183.0	436.3	95.1
70.2	154.9	182.6	437.0	94.9
71.2	154.6	182.2	437.7	94.8
71.5	154.5	182.1	437.9	94.7
72.2	154.3	181.8	438.4	94.6
73.2	154.0	181.5	439.1	94.5
74.2	153.7	181.1	439.8	94.3
75.2	153.4	180.8	440.5	94.2
76.2	153.0	180.4	441.2	94.0

Table 14.3.4-9 (CONT'D)

Double-Ended Pump Suction Break Maximum Safeguards Reflood Mass and Energy Releases

Time (sec)	Break Path No. 1 Flow*		Break Path No. 2 Flow**	
	(lbm/sec)	(Thousand Btu/sec)	(lbm/sec)	(Thousand Btu/sec)
77.2	152.7	180.0	441.9	93.9
78.2	152.4	179.7	442.6	93.8
79.2	152.1	179.3	443.3	93.6
80.2	151.8	178.9	444.0	93.5
81.2	151.5	178.6	444.7	93.3
82.2	151.2	178.2	445.4	93.2
84.2	150.6	177.5	446.9	92.9
86.2	150.0	176.8	448.3	92.6
88.2	149.4	176.1	449.7	92.4
90.2	148.8	175.3	451.2	92.1
92.2	148.2	174.6	452.7	91.8
94.2	147.5	173.9	454.1	91.6
95.8	147.1	173.3	455.3	91.4
96.2	146.9	173.2	455.6	91.3
98.2	146.3	172.4	457.0	91.1
100.2	145.7	171.7	458.5	90.8
102.2	145.1	171.0	459.9	90.5
104.2	144.5	170.2	461.4	90.3
106.2	143.8	169.5	462.8	90.0
108.2	143.2	168.8	464.2	89.7
110.2	142.6	168.0	465.7	89.5
112.2	141.9	167.3	467.1	89.2
114.2	141.3	166.5	468.5	88.9
116.2	140.7	165.8	469.9	88.7
118.2	140.0	165.0	471.3	88.4
120.2	139.4	164.3	472.7	88.1
122.2	138.7	163.5	474.2	87.9
122.3	138.7	163.5	474.2	87.8
124.2	138.1	162.7	475.6	87.6

Table 14.3.4-9 (CONT'D)

Double-Ended Pump Suction Break Maximum Safeguards Reflood Mass and Energy Releases

Time (sec)	Break Path No. 1 Flow*		Break Path No. 2 Flow**	
	(lbm/sec)	(Thousand Btu/sec)	(lbm/sec)	(Thousand Btu/sec)
77.2	152.7	180.0	441.9	93.9
78.2	152.4	179.7	442.6	93.8
79.2	152.1	179.3	443.3	93.6
80.2	151.8	178.9	444.0	93.5
81.2	151.5	178.6	444.7	93.3
82.2	151.2	178.2	445.4	93.2
84.2	150.6	177.5	446.9	92.9
86.2	150.0	176.8	448.3	92.6
88.2	149.4	176.1	449.7	92.4
90.2	148.8	175.3	451.2	92.1
92.2	148.2	174.6	452.7	91.8
94.2	147.5	173.9	454.1	91.6
95.8	147.1	173.3	455.3	91.4
96.2	146.9	173.2	455.6	91.3
98.2	146.3	172.4	457.0	91.1
100.2	145.7	171.7	458.5	90.8
102.2	145.1	171.0	459.9	90.5
104.2	144.5	170.2	461.4	90.3
106.2	143.8	169.5	462.8	90.0
108.2	143.2	168.8	464.2	89.7
110.2	142.6	168.0	465.7	89.5
112.2	141.9	167.3	467.1	89.2
114.2	141.3	166.5	468.5	88.9
116.2	140.7	165.8	469.9	88.7
118.2	140.0	165.0	471.3	88.4
120.2	139.4	164.3	472.7	88.1
122.2	138.7	163.5	474.2	87.9
122.3	138.7	163.5	474.2	87.8
124.2	138.1	162.7	475.6	87.6

Table 14.3.4-9 (CONT'D)

## Double-Ended Pump Suction Break Maximum Safeguards Reflood Mass and Energy Releases

Time (sec)	Break Path No. 1 Flow*		Break Path No. 2 Flow**	
	(lbm/sec)	(Thousand Btu/sec)	(lbm/sec)	(Thousand Btu/sec)
126.2	137.4	162.0	477.0	87.3
128.2	136.8	161.2	478.4	87.0
130.2	136.1	160.4	479.7	86.8
132.2	135.5	159.7	481.1	86.5
134.2	134.8	158.9	482.5	86.2
136.2	134.2	158.1	483.9	86.0
138.2	133.5	157.4	485.3	85.7
140.2	132.9	156.6	486.7	85.4
142.2	132.2	155.8	488.1	85.2
144.2	131.6	155.0	489.4	84.9
146.2	130.9	154.2	490.8	84.6
148.2	130.2	153.5	492.2	84.4
150.2	129.6	152.7	493.5	84.1
151.6	129.1	152.1	494.5	83.9
152.2	128.9	151.9	494.9	83.8
154.2	128.2	151.1	496.3	83.6
156.2	127.6	150.3	497.6	83.3
158.2	126.9	149.5	499.0	83.1
160.2	126.2	148.7	500.4	82.8
162.2	125.5	147.9	501.7	82.5
164.2	124.8	147.1	503.1	82.3
166.2	124.2	146.3	504.5	82.0
168.2	123.5	145.5	505.8	81.7
170.2	122.8	144.7	507.2	81.5
172.2	122.1	143.9	508.5	81.2
174.2	121.4	143.1	509.9	81.0
176.2	120.7	142.3	511.2	80.7
178.2	120.1	141.5	512.6	80.5

Table 14.3.4-9 (CONT'D)

Double-Ended Pump Suction Break Maximum Safeguards Reflood Mass and Energy Releases

Time (sec)	Break Path No. 1 Flow*		Break Path No. 2 Flow**	
	(lbm/sec)	(Thousand Btu/sec)	(lbm/sec)	(Thousand Btu/sec)
180.2	119.4	140.6	513.9	80.2
182.2	118.8	140.0	515.0	80.1
184.2	118.3	139.4	515.9	80.1
184.3	118.3	139.4	515.9	80.1
186.2	117.8	138.8	516.8	80.1
188.2	117.4	138.3	517.7	80.1
190.2	116.9	137.7	518.6	80.0
192.2	116.4	137.2	519.5	80.0
194.2	116.0	136.6	520.3	80.0
196.2	115.5	136.1	521.2	80.0
198.2	115.0	135.5	522.1	79.9
200.2	114.6	135.0	523.0	79.9
202.2	114.1	134.4	523.9	79.9
204.2	113.6	133.9	524.7	79.8
206.2	113.2	133.3	525.6	79.8
208.2	112.7	132.8	526.5	79.8
210.2	112.2	132.2	527.3	79.7
212.2	111.8	131.7	528.2	79.7
214.2	111.3	131.2	529.1	79.6
216.2	110.9	130.6	529.9	79.6
218.2	110.4	130.1	530.8	79.6
220.2	110.0	129.6	531.6	79.5
221.3	109.7	129.3	532.1	79.5

\* Mass and Energy exiting the SG side of the break

\*\* Mass and Energy exiting the pump side of the break

Table 14.3.4-10

## Double-Ended Pump Suction Break - Maximum Safeguards Principle Parameters During Reflood

## Flooding

Time (sec)	Temp (°F)	Rate (in/sec)	Carryover Fraction	Core Height (ft)	Downcomer Height (ft)	Flow Frac	Total	Injection Accum (lbm/sec)	Spill	Enthalpy (Btu/lbm)
21.0	221.0	.000	.000	.00	.00	.333	.0	.0	.0	.00
21.7	217.0	22.982	.000	.54	1.98	.000	7125.9	7125.9	.0	74.49
21.9	213.6	28.149	.000	1.07	1.93	.000	7029.8	7029.8	.0	74.49
23.0	211.4	2.916	.313	1.50	6.03	.426	6674.2	6674.2	.0	74.49
23.9	210.9	2.797	.442	1.64	9.78	.455	6432.7	6432.7	.0	74.49
26.1	209.4	5.028	.617	1.92	15.62	.687	5432.3	5432.3	.0	74.49
26.7	208.8	4.811	.647	2.01	15.63	.684	5301.0	5301.0	.0	74.49
27.1	208.5	4.679	.662	2.06	15.63	.684	5230.7	5230.7	.0	74.49
30.1	206.6	4.099	.715	2.39	15.63	.677	4788.1	4788.1	.0	74.49
31.2	206.0	4.283	.724	2.50	15.63	.690	5183.3	4527.6	.0	69.27
31.3	206.0	4.271	.725	2.51	15.63	.690	5171.4	4515.5	.0	69.26
37.0	204.3	3.792	.747	3.01	15.63	.676	4604.2	3935.6	.0	68.50
43.7	203.9	3.443	.754	3.51	15.63	.661	4102.0	3422.8	.0	67.66
51.1	204.6	3.169	.757	4.00	15.63	.647	3669.1	2981.7	.0	69.41
57.2	205.7	2.126	.744	4.38	15.63	.494	714.3	.0	.0	33.22
60.2	206.5	2.069	.744	4.51	15.63	.494	717.3	.0	.0	33.22
71.6	211.6	2.015	.745	5.00	15.63	.495	717.2	.0	.0	33.22



Table 14.3.4-10 (CONT'D)

Double-Ended Pump Suction Break - Maximum Safeguards Principle Parameters During Reflood

Flooding										
Time (sec)	Temp (°F)	Rate (in/sec)	Carryover Fraction	Core Height (ft)	Downcomer Height (ft)	Flow Frac	Total	Injection Accum (lbm/sec)	Spill	Enthalpy (Btu/lbm)
84.2	219.6	1.954	.748	5.53	15.63	.496	717.2	.0	.0	33.22
95.8	227.9	1.897	.750	6.00	15.63	.497	717.2	.0	.0	33.22
110.2	237.3	1.828	.754	6.56	15.63	.498	717.2	.0	.0	33.22
122.3	243.9	1.770	.756	7.00	15.63	.499	717.2	.0	.0	33.22
138.2	251.4	1.695	.759	7.56	15.63	.499	717.3	.0	.0	33.22
151.6	256.8	1.633	.762	8.00	15.63	.499	717.3	.0	.0	33.22
168.2	262.5	1.556	.765	8.52	15.63	.499	717.3	.0	.0	33.22
184.3	267.2	1.485	.767	9.00	15.63	.500	717.4	.0	.0	33.22
202.2	271.6	1.420	.771	9.50	15.63	.502	717.3	.0	.0	33.22
221.3	275.6	1.352	.775	10.00	15.63	.504	717.3	.0	.0	33.22

Table 14.3.4-11

## Double-Ended Pump Suction Break Maximum Safeguards Post-Reflow Mass and Energy Releases

Time (sec)	Break Path No. 1 Flow*		Break Path No. 2 Flow**	
	(lbm/sec)	(Thousand Btu/sec)	(lbm/sec)	(Thousand Btu/sec)
221.4	129.6	163.0	588.5	92.6
226.4	130.3	163.9	587.8	92.2
231.4	129.9	163.4	588.2	92.2
236.4	129.5	162.9	588.6	92.1
241.4	130.2	163.8	587.9	91.8
246.4	129.8	163.3	588.3	91.7
251.4	129.4	162.8	588.7	91.6
256.4	129.0	162.3	589.1	91.5
261.4	129.7	163.2	588.4	91.2
266.4	129.3	162.7	588.8	91.1
271.4	128.9	162.2	589.2	91.0
276.4	129.6	163.0	588.5	90.7
281.4	129.2	162.5	588.9	90.6
286.4	128.8	162.0	589.3	90.6
291.4	128.4	161.5	589.7	90.5
296.4	129.0	162.3	589.1	90.1
301.4	128.6	161.8	589.5	90.1
306.4	128.2	161.3	589.9	90.0
311.4	128.8	162.1	589.3	89.7
316.4	128.4	161.6	589.7	89.6
321.4	128.0	161.1	590.1	89.5
326.4	128.6	161.8	589.5	89.2
331.4	128.2	161.3	589.9	89.1
336.4	127.8	160.8	590.3	89.0
341.4	128.4	161.5	589.7	88.7
346.4	128.0	161.0	590.1	88.6
351.4	127.5	160.5	590.6	88.6

Table 14.3.4-11 (CONT'D)

Double-Ended Pump Suction Break Maximum Safeguards Post-Reflow Mass and Energy Releases

Time (sec)	Break Path No. 1 Flow*		Break Path No. 2 Flow**	
	(lbm/sec)	(Thousand Btu/sec)	(lbm/sec)	(Thousand Btu/sec)
356.4	128.1	161.2	590.0	88.2
361.4	127.7	160.6	590.4	88.2
366.4	127.3	160.1	590.8	88.1
371.4	127.8	160.8	590.3	87.8
376.4	127.4	160.2	590.7	87.7
381.4	126.9	159.7	591.2	87.6
386.4	127.5	160.4	590.6	87.3
391.4	127.0	159.8	591.1	87.2
396.4	126.6	159.3	591.5	87.2
401.4	127.1	159.9	591.0	86.8
406.4	126.8	159.5	591.3	86.7
411.4	126.5	159.1	591.6	86.6
416.4	127.1	159.9	591.0	86.3
421.4	126.8	159.5	591.3	86.2
426.4	126.4	159.1	591.7	86.1
431.4	126.1	158.7	592.0	86.0
436.4	126.7	159.4	591.4	85.7
441.4	126.4	159.0	591.7	85.6
446.4	126.0	158.5	592.1	85.5
451.4	126.6	159.3	591.5	85.2
456.4	126.2	158.8	591.9	85.1
461.4	125.9	158.4	592.2	85.0
466.4	126.4	159.1	591.7	84.6
471.4	126.1	158.6	592.0	84.6
476.4	125.7	158.2	592.4	84.5
481.4	126.3	158.8	591.8	84.1
486.4	125.9	158.4	592.2	86.8
491.4	125.5	157.9	592.6	86.7
496.4	126.0	158.5	592.1	86.4

Table 14.3.4-11 (CONT'D)

Double-Ended Pump Suction Break Maximum Safeguards Post-Reflood Mass and Energy Releases

Time (sec)	Break Path No. 1 Flow*		Break Path No. 2 Flow**	
	(lbm/sec)	(Thousand Btu/sec)	(lbm/sec)	(Thousand Btu/sec)
501.4	125.6	158.1	592.5	86.3
506.4	125.3	157.6	592.8	86.2
511.4	125.7	158.2	592.4	85.9
516.4	125.4	157.7	592.7	85.8
521.4	125.8	158.3	592.3	85.4
526.4	125.4	157.8	592.7	85.4
531.4	125.0	157.3	593.1	85.3
536.4	125.5	157.8	592.6	84.9
541.4	125.0	157.3	593.1	84.8
546.4	125.5	157.8	592.6	84.5
551.4	125.0	157.3	593.1	84.4
556.4	125.4	157.8	592.7	84.1
561.4	125.0	157.2	593.1	84.0
566.4	125.4	157.7	592.7	83.7
571.4	124.9	157.2	593.2	83.6
576.4	125.3	157.6	592.8	83.3
581.4	124.8	157.0	593.3	83.2
586.4	125.1	157.4	593.0	82.9
591.4	124.7	156.8	593.4	82.9
596.4	125.0	157.2	593.1	82.6
601.4	124.5	156.6	593.6	82.5
606.4	124.8	157.0	593.3	84.8
611.4	124.4	156.4	593.7	84.7
616.4	124.7	156.8	593.4	84.4
621.4	124.2	156.2	593.9	84.3
626.4	124.5	156.6	593.6	84.0
631.4	124.7	156.9	593.4	83.7
636.4	124.2	156.3	593.9	83.6

Table 14.3.4-11 (CONT'D)

Double-Ended Pump Suction Break Maximum Safeguards Post-Reflood Mass and Energy Releases

Time (sec)	Break Path No. 1 Flow*		Break Path No. 2 Flow**	
	(lbm/sec)	(Thousand Btu/sec)	(lbm/sec)	(Thousand Btu/sec)
641.4	124.4	156.5	593.7	83.4
646.4	123.9	155.9	594.2	83.3
651.4	124.1	156.1	594.0	83.0
656.4	124.3	156.3	593.8	82.7
661.4	124.4	156.5	593.7	82.4
666.4	123.8	155.8	594.3	82.4
671.4	124.0	155.9	594.1	82.1
676.4	124.1	156.1	594.0	81.8
681.4	124.1	156.2	594.0	81.6
686.4	124.2	156.2	593.9	81.3
691.4	123.5	155.4	594.6	83.8
696.4	123.5	155.4	594.6	83.6
701.4	123.5	155.4	594.6	83.3
706.4	123.4	155.3	594.7	83.1
711.4	123.4	155.2	594.7	82.8
716.4	123.9	155.9	594.2	82.5
721.4	123.7	155.7	594.4	82.2
726.4	123.5	155.4	594.6	82.0
731.4	123.3	155.1	594.8	81.8
736.4	123.6	155.5	594.5	81.5
741.4	123.3	155.1	594.8	81.3
746.4	123.5	155.4	594.6	81.0
751.4	123.1	154.9	595.0	80.9
756.4	123.2	155.0	594.9	83.0
761.4	123.2	155.0	594.9	82.7
766.4	123.2	155.0	594.9	82.5
771.4	123.0	154.8	595.1	82.2
776.4	123.3	155.1	594.8	81.9

Table 14.3.4-11 (CONT'D)

Double-Ended Pump Suction Break Maximum Safeguards Post-Reflood Mass and Energy Releases

Time (sec)	Break Path No. 1 Flow*		Break Path No. 2 Flow**	
	(lbm/sec)	(Thousand Btu/sec)	(lbm/sec)	(Thousand Btu/sec)
781.4	122.9	154.6	595.2	81.7
786.4	122.9	154.7	595.2	81.4
791.4	122.8	154.5	595.3	81.2
796.4	122.9	154.7	595.2	80.8
801.4	122.9	154.6	595.2	80.6
806.4	122.5	154.2	595.6	80.4
811.4	122.8	154.4	595.3	80.0
816.4	122.5	154.1	595.6	82.2
821.4	122.5	154.1	595.6	81.9
826.4	66.7	83.9	651.4	96.2
1242.0	66.7	83.9	651.4	96.2
1242.1	64.3	80.5	653.8	92.1
1246.4	64.2	80.4	653.9	91.4
1543.3	64.2	80.4	653.9	91.4
1543.4	56.5	65.0	661.6	22.0
2500.0	50.7	58.3	667.4	22.2
2500.1	53.5	61.5	612.6	113.9
3600.0	47.9	55.1	618.2	114.9

\* Mass and Energy exiting the SG side of the break

\*\* Mass and Energy exiting the pump side of the break

Table 14.3.4-12

LOCA Mass and Energy Release Analysis ANS 1979 Core Decay Heat  
Power Fraction

Time (sec)	ANS 1979 Decay Heat Fraction
10	0.053876
15	0.050401
20	0.048018
40	0.042401
60	0.039244
80	0.037065
100	0.035466
150	0.032724
200	0.030936
400	0.027078
600	0.024931
800	0.023389
1000	0.022156
1500	0.019921
2000	0.018315
4000	0.014781
6000	0.013040
8000	0.012000
10000	0.011262
15000	0.010097
20000	0.009350
40000	0.007778
60000	0.006958
80000	0.006424

Table 14.3.4-12 (CONT'D)

LOCA Mass and Energy Release Analysis ANS 1979 Core Decay Heat  
Power Fraction

Time (sec)	ANS 1979 Decay Heat Fraction
100000	0.006021
150000	0.005323
400000	0.003770
600000	0.003201
800000	0.002834
1000000	0.002580
2592000	0.001745



Table 14.3.4-13

Double-Ended Hot-Leg Break Mass Balance

		Time (Sec)		
		.00	22.20	22.20*
		Mass (Thousand lbm)		
Initial	In RCS and ACC	621.13	621.13	621.13
Added Mass	Pumped Injection	.00	.00	.00
	Total Added	.00	.00	.00
Total Available		621.13	621.13	621.13
Distribution	Reactor Coolant	420.62	80.27	80.27
	Accumulator	200.51	138.05	138.05
	Total Contents	621.13	218.32	218.32
Effluent	Break Flow	.00	402.79	402.79
	ECCS Spill	.00	.00	.00
	Total Effluent	.00	402.79	402.79
Total Accountable		621.13	621.12	621.12

\* This time is the bottom of core recovery time, which is identical to the end of blowdown time due to the assumption of instantaneous refill.

Table 14.3.4-14

Double-Ended Pump Suction Break Mass Balance Minimum Safeguards

		Time (Sec)						
		.00	21.00 <sup>(1)</sup>	21.00 <sup>(2)</sup>	225.80 <sup>(3)</sup>	1273.73 <sup>(4)</sup>	1547.89 <sup>(5)</sup>	3600.00 <sup>(6)</sup>
		Mass (Thousand lbm)						
Initial	In RCS & Accumulator	621.20	621.20	621.20	621.20	621.20	621.20	621.20
Added Mass	Pumped Injection	.00	.00	.00	85.65	552.50	674.64	1562.59
	Total Added	.00	.00	.00	85.65	552.50	674.64	1562.59
Total Available		621.20	621.20	621.20	706.84	1173.69	1295.84	2183.78
Distribution	Reactor Coolant	420.68	42.50	56.19	101.84	101.84	101.84	101.84
	Accumulator	200.51	159.91	146.22	.00	.00	.00	.00
	Total Contents	621.20	202.42	202.42	101.84	101.84	101.84	101.84
Effluent	Break Flow	.00	418.77	418.77	596.32	1063.17	1185.31	2073.26
	ECCS Spill	.00	.00	.00	.00	.00	.00	.00
	Total Effluent	.00	418.77	418.77	596.32	1063.17	1185.31	2073.26
Total Accountable		621.20	621.18	621.18	698.16	1165.01	1287.15	2175.10

Notes:

- (1) End of Blowdown
- (2) Bottom of core recovery time, which is identical to the end of blowdown time due to the assumption of instantaneous refill.
- (3) End of Reflood
- (4) Time at which the Broken Loop SG equilibrates at the first intermediate pressure
- (5) Time at which the Intact Loop SG equilibrates at the second intermediate pressure
- (6) Time at which both SGs equilibrate to 14.7 psia

Table 14.3.4-15

Double-Ended Pump Suction Break Mass Balance Maximum Safeguards

		Time (Sec)						
		.00	21.00 <sup>(1)</sup>	21.00 <sup>(2)</sup>	221.30 <sup>(3)</sup>	1242.08 <sup>(4)</sup>	1543.28 <sup>(5)</sup>	3600.00 <sup>(6)</sup>
		Mass (Thousand lbm)						
Initial	In RCS & Accumulator	621.20	621.20	621.20	621.20	621.20	621.20	621.20
Added Mass	Pumped Injection	.00	.00	.00	135.94	868.89	1085.19	2504.92
	Total Added	.00	.00	.00	135.94	868.89	1085.19	2504.92
Total Available		621.20	621.20	621.20	757.14	1490.09	1706.38	3126.11
Distribution	Reactor Coolant	420.68	42.50	56.19	102.02	102.02	102.02	102.02
	Accumulator	200.51	159.91	146.22	.00	.00	.00	.00
	Total Contents	621.20	202.42	202.42	102.02	102.02	102.02	102.02
Effluent	Break Flow	.00	418.77	418.77	646.44	1379.39	1595.68	3015.41
	ECCS Spill	.00	.00	.00	.00	.00	.00	.00
	Total Effluent	.00	418.77	418.77	646.44	1379.39	1595.68	3015.41
Total Accountable		621.20	621.18	621.18	748.46	1481.40	1697.70	3117.43

Notes:

- (1) End of Blowdown
- (2) Bottom of core recovery time, which is identical to the end of blowdown time due to the assumption of instantaneous refill
- (3) End of Reflood
- (4) Time at which the Broken Loop SG equilibrates at the first intermediate pressure.
- (5) Time at which the Intact Loop SG equilibrates at the second intermediate pressure.
- (6) Time at which both SGs equilibrate to 14.7 psia.

Table 14.3.4-16  
 Double-Ended Hot-Leg Break Energy Balance

		Time (Sec)		
		.00	22.20	22.20*
		Energy (Million Btu)		
Initial Energy	In RCS, Acc, SG	667.41	667.41	667.41
Added Energy	Pumped Injection	.00	.00	.00
	Decay Heat	.00	6.28	6.28
	Heat From Secondary	.00	-.20	-.20
	Total Added	.00	6.08	6.08
Total Available		667.41	673.49	673.49
Distribution	Reactor Coolant	247.64	17.46	17.46
	Accumulator	14.95	10.29	10.29
	Core Stored	22.89	9.64	9.64
	Primary Metal	124.37	116.25	116.25
	Secondary Metal	74.99	74.79	74.79
	Steam Generator	182.56	181.95	181.95
	Total Contents	667.41	410.38	410.38
Effluent	Break Flow	.00	262.62	262.62
	ECCS Spill	.00	.00	.00
	Total Effluent	.00	262.62	262.62
Total Accountable		667.41	673.00	673.00

\* This time is the bottom of core recovery time, which is identical to the end of blowdown time due to the assumption of instantaneous refill.

Table 14.3.4-17  
 Double-Ended Pump Suction Break Energy Balance Minimum Safeguards

		Time (Sec)						
		.00	21.00 <sup>(1)</sup>	21.00 <sup>(2)</sup>	225.80 <sup>(3)</sup>	1273.73 <sup>(4)</sup>	1547.89 <sup>(5)</sup>	3600.00 <sup>(6)</sup>
		Energy (Million Btu)						
Initial Energy	In RCS, Acc, SG	663.25	663.25	663.25	663.25	663.25	663.25	663.25
Added Energy	Pumped Injection	.00	.00	.00	2.85	18.35	22.41	87.58
	Decay Heat	.00	5.72	5.72	25.78	96.42	111.84	209.75
	Heat From Secondary	.00	-.84	-.84	-.84	2.96	2.98	2.98
	Total Added	.00	4.88	4.88	27.79	117.74	137.22	300.31
Total Available		663.25	668.13	668.13	691.04	780.99	800.47	963.56
Distribution	Reactor Coolant	247.55	10.59	11.61	26.78	26.78	26.78	26.78
	Accumulator	14.95	11.92	10.90	.00	.00	.00	.00
	Core Stored	22.82	12.24	12.24	3.91	3.20	3.14	2.71
	Primary Metal	120.95	113.82	113.82	93.30	50.68	45.55	39.50
	Secondary Metal	45.38	45.75	45.75	41.87	23.55	20.23	17.60
	Steam Generator	211.59	213.69	213.69	192.31	105.75	90.93	79.36
	Total Contents	663.25	408.01	408.01	358.18	209.96	186.63	165.95
Effluent	Break Flow	.00	259.63	259.63	324.54	562.71	584.39	769.66
	ECCS Spill	.00	.00	.00	.00	.00	.00	.00
	Total Effluent	.00	259.63	259.63	324.54	562.71	584.39	769.66
Total Accountable		663.25	667.65	667.65	682.72	772.67	771.02	935.61

Notes:

- (1) End of Blowdown
- (2) Bottom of core recovery time. This time is identical to the end of blowdown time due to the assumption of instantaneous refill.
- (3) End of Reflood
- (4) Time at which the Broken Loop SG equilibrates at the first intermediate pressure
- (5) Time at which the Intact Loop SG equilibrates at the second intermediate pressure
- (6) Time at which both SGs equilibrate to 14.7 psia

Table 14.3.4-18

Double-Ended Pump Suction Break Energy Balance - Maximum Safeguards

					Time (sec)			
		.00	21.00 <sup>(1)</sup>	21.00 <sup>(2)</sup>	221.30 <sup>(3)</sup>	1242.08 <sup>(4)</sup>	1543.28 <sup>(5)</sup>	3600.00 <sup>(6)</sup>
		Energy (Million Btu)						
Initial Energy	In RCS, Acc, SG	663.25	663.25	663.25	663.25	663.25	663.25	663.25
Added Energy	Pumped Injection	.00	.00	.00	4.52	28.86	36.05	189.48
	Decay Heat	.00	5.72	5.72	25.40	94.58	111.58	209.73
	Heat From Secondary	.00	-.84	-.84	-.84	2.87	2.90	2.90
	Total Added	.00	4.88	4.88	29.08	126.31	150.52	402.10
Total Available		663.25	668.13	668.13	692.33	789.56	813.77	1065.36
Distribution	Reactor Coolant	247.55	10.59	11.61	26.80	26.80	26.80	26.80
	Accumulator	14.95	11.92	10.90	.00	.00	.00	.00
	Core Stored	22.82	12.24	12.24	3.91	3.13	3.08	2.71
	Primary Metal	120.95	113.82	113.82	92.86	50.18	44.57	39.47
	Secondary Metal	45.38	45.75	45.75	41.76	23.44	19.78	17.58
	Steam Generator	211.59	213.69	213.69	191.70	105.22	88.86	79.18
	Total Contents	663.25	408.01	408.01	357.04	208.78	183.09	165.73
Effluent	Break Flow	.00	259.63	259.63	326.97	572.46	600.87	870.97
	ECCS Spill	.00	.00	.00	.00	.00	.00	.00
	Total Effluent	.00	259.63	259.63	326.97	572.46	600.87	870.97
Total Accountable		663.25	667.65	667.65	684.01	781.25	783.96	1036.70

Notes:

- (1) End of Blowdown
- (2) Bottom of core recovery time. This time is identical to the end of blowdown time due to the assumption of instantaneous refill.
- (3) End of Reflood
- (4) Time at which the Broken Loop SG equilibrates at the first intermediate pressure.
- (5) Time at which the Intact Loop SG equilibrates at the second intermediate pressure.
- (6) Time at which both SGs equilibrate to 14.7 psia.

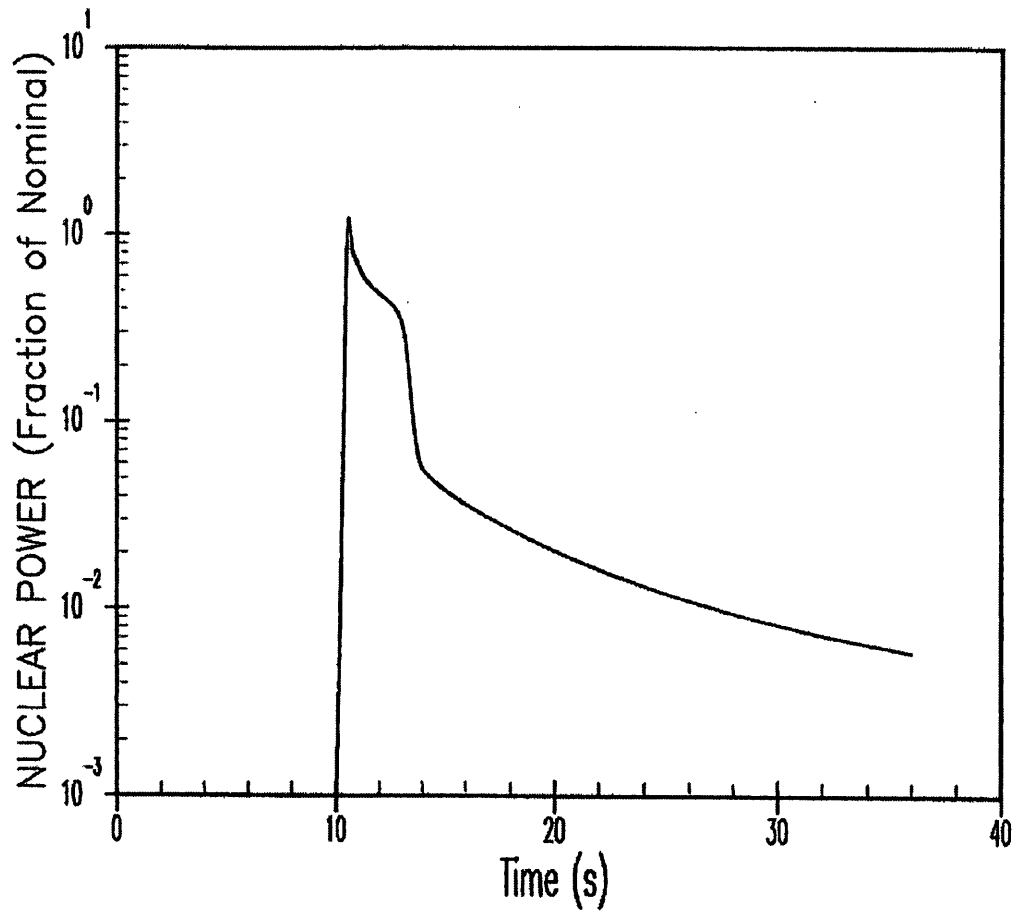


FIGURE 14.1-1

UNCONTROLLED ROD WITHDRAWAL  
FROM A SUBCRITICAL CONDITION

NUCLEAR POWER VERSUS TIME

BEAVER VALLEY POWER STATION UNIT NO. 1  
UPDATED FINAL SAFETY ANALYSIS REPORT

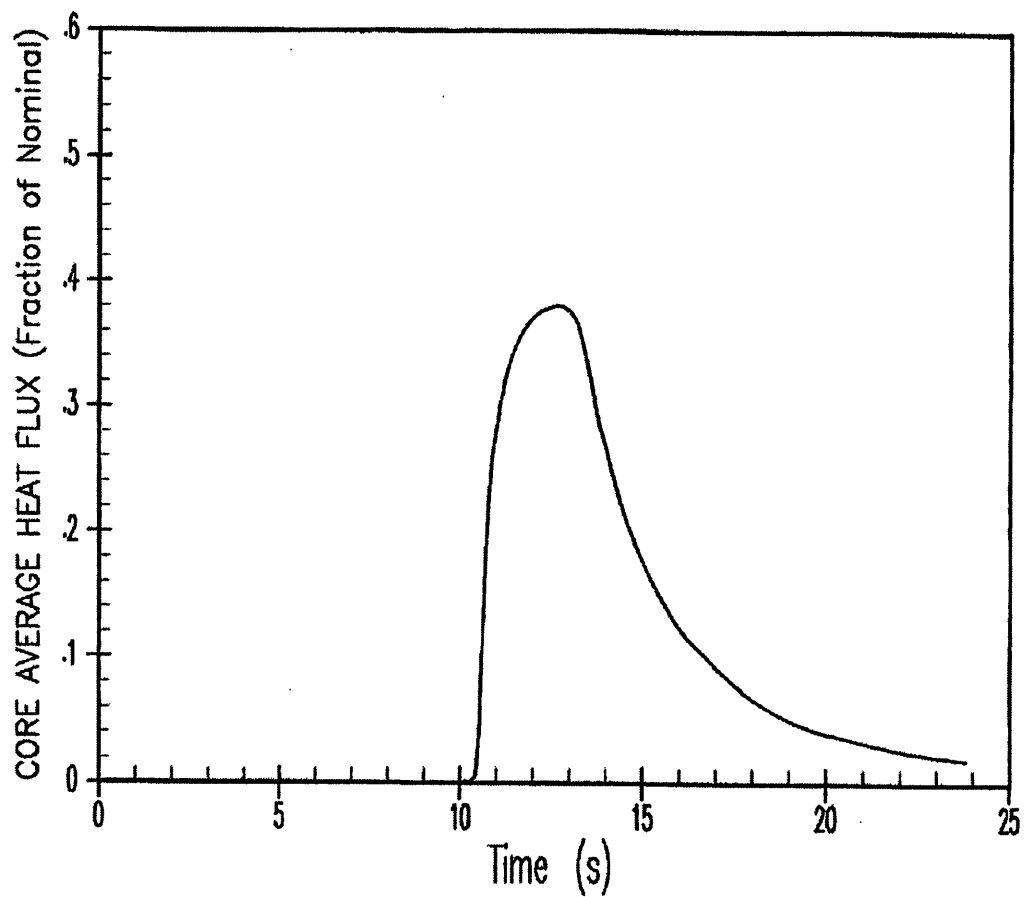


FIGURE 14.1-2

UNCONTROLLED ROD WITHDRAWAL  
FROM A SUBCRITICAL CONDITION

CORE HEAT FLUX VERSUS TIME

BEAVER VALLEY POWER STATION UNIT NO. 1  
UPDATED FINAL SAFETY ANALYSIS REPORT



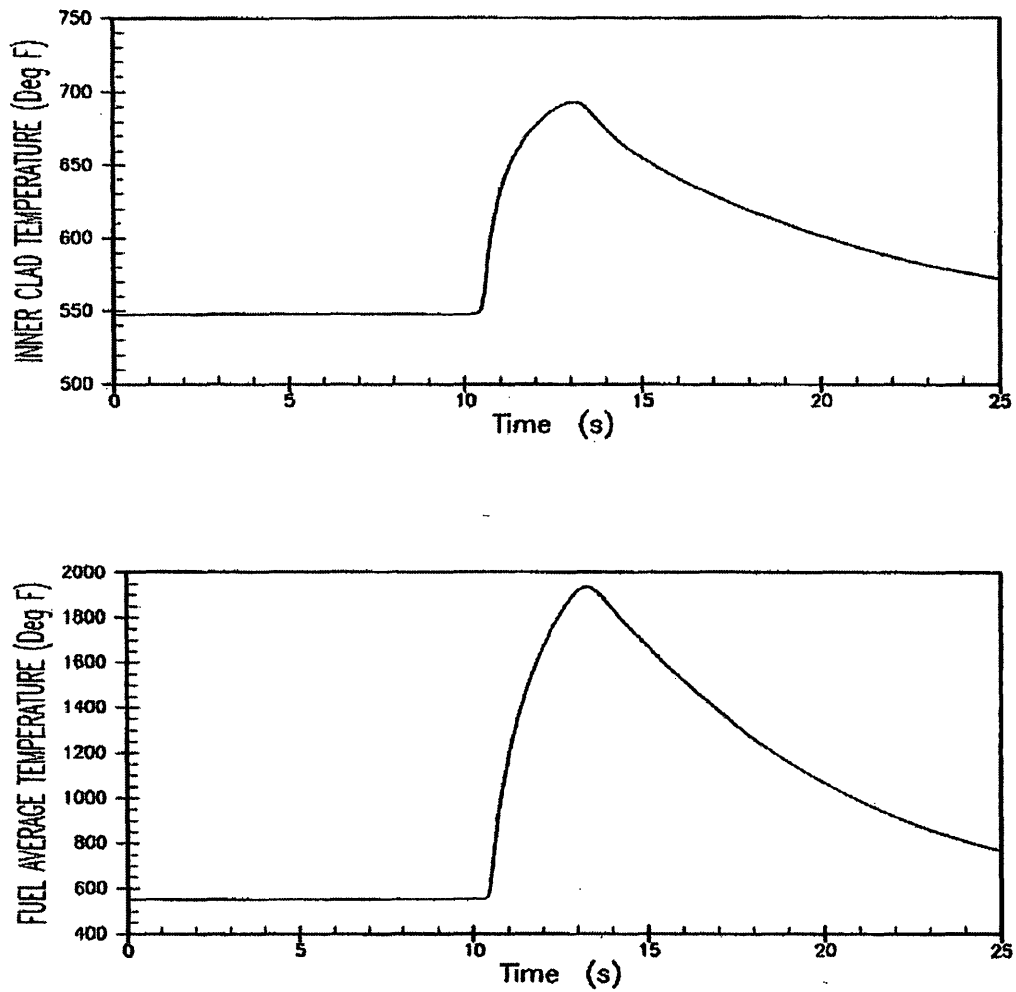


FIGURE 14.1-3

UNCONTROLLED ROD WITHDRAWAL  
FROM A SUBCRITICAL CONDITION

CORE HEAT FLUX VERSUS TIME

BEAVER VALLEY POWER STATION UNIT NO. 1  
UPDATED FINAL SAFETY ANALYSIS REPORT

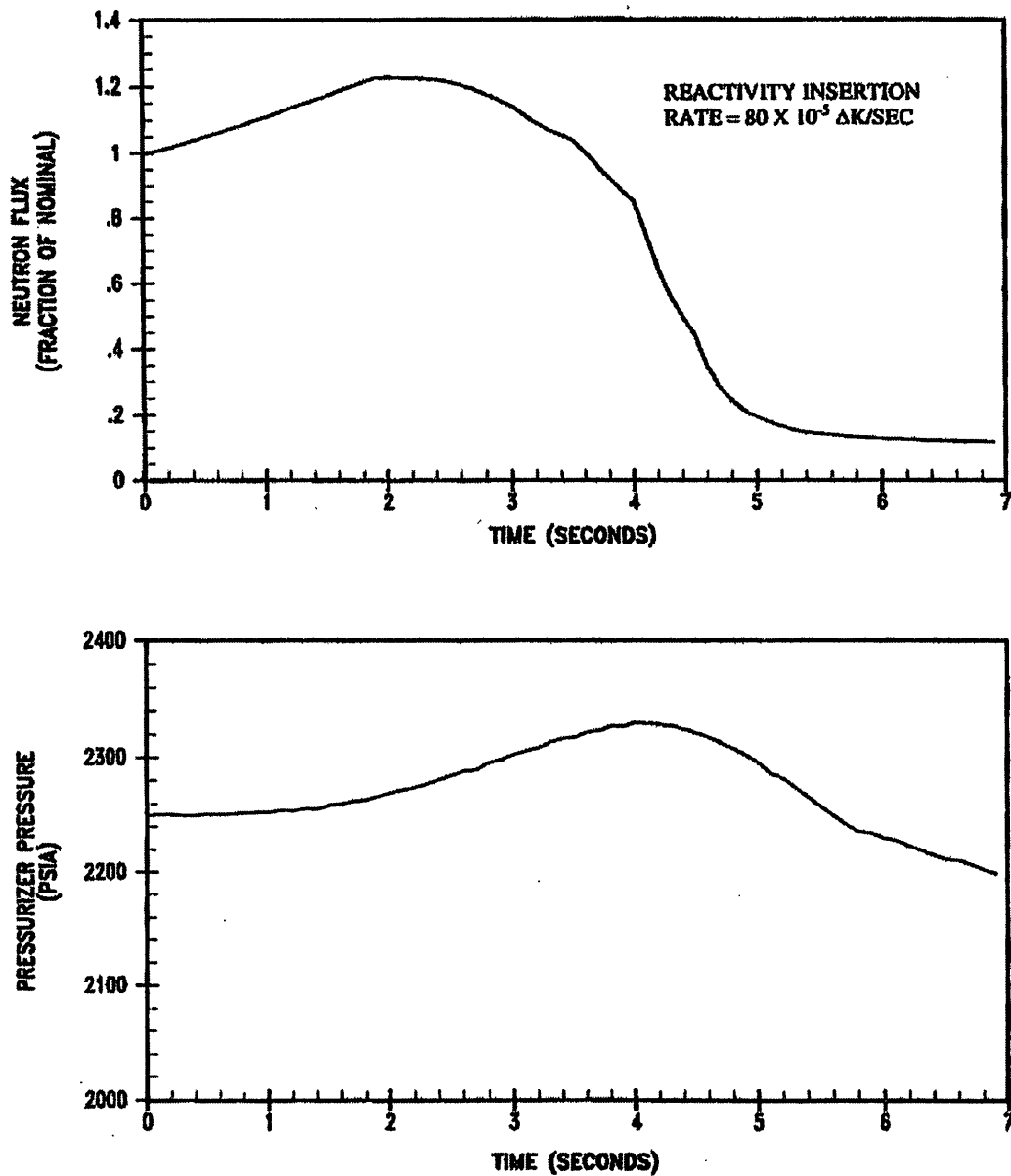


FIGURE 14.1-4

TRANSIENT RESPONSE FOR UNCONTROLLED  
ROD WITHDRAWAL FROM FULL POWER  
TERMINATED BY HIGH NEUTRON FLUX TRIP

BEAVER VALLEY POWER STATION UNIT NO. 1  
UPDATED FINAL SAFETY ANALYSIS REPORT

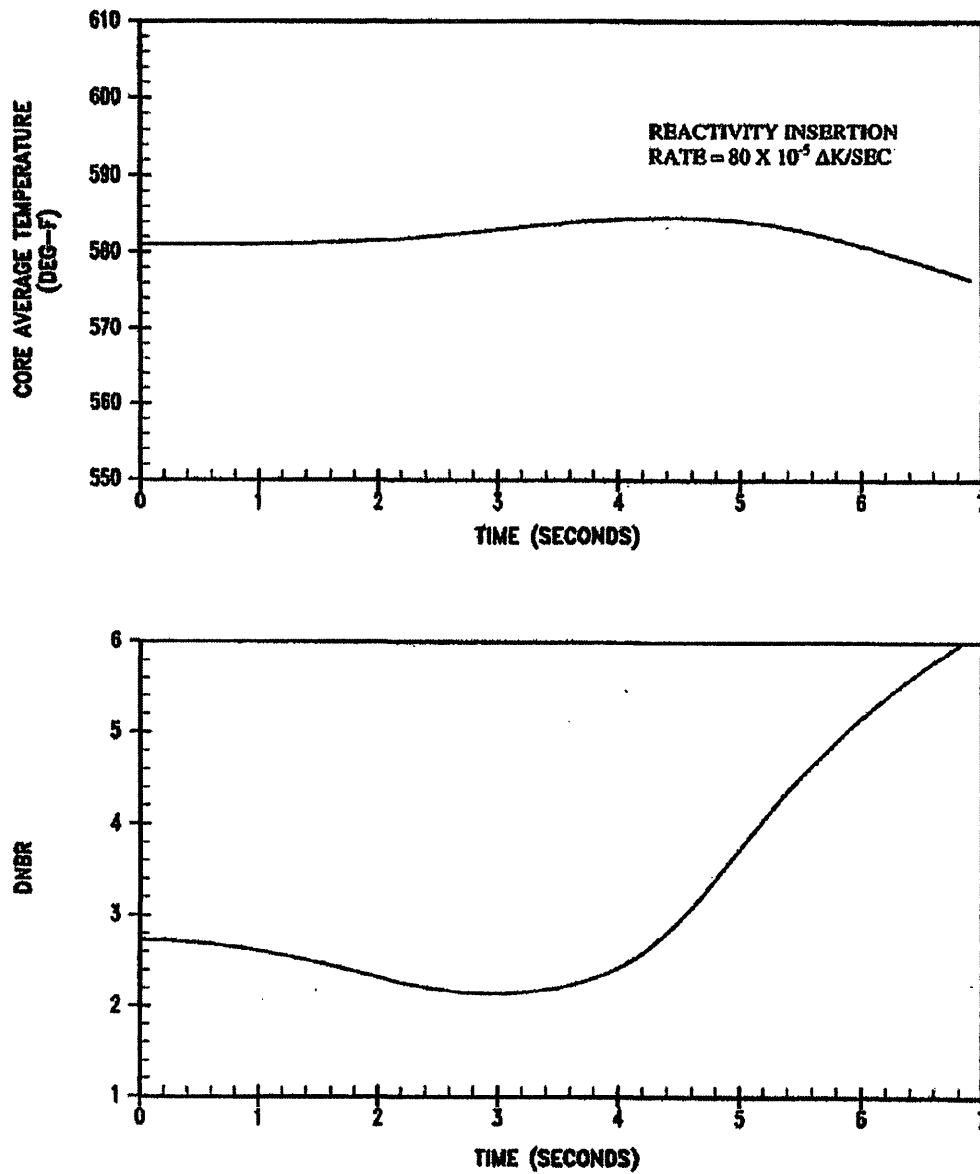


FIGURE 14.1-5

TRANSIENT RESPONSE FOR UNCONTROLLED  
ROD WITHDRAWAL FROM FULL POWER  
TERMINATED BY HIGH NEUTRON FLUX TRIP

BEAVER VALLEY POWER STATION UNIT NO. 1  
UPDATED FINAL SAFETY ANALYSIS REPORT

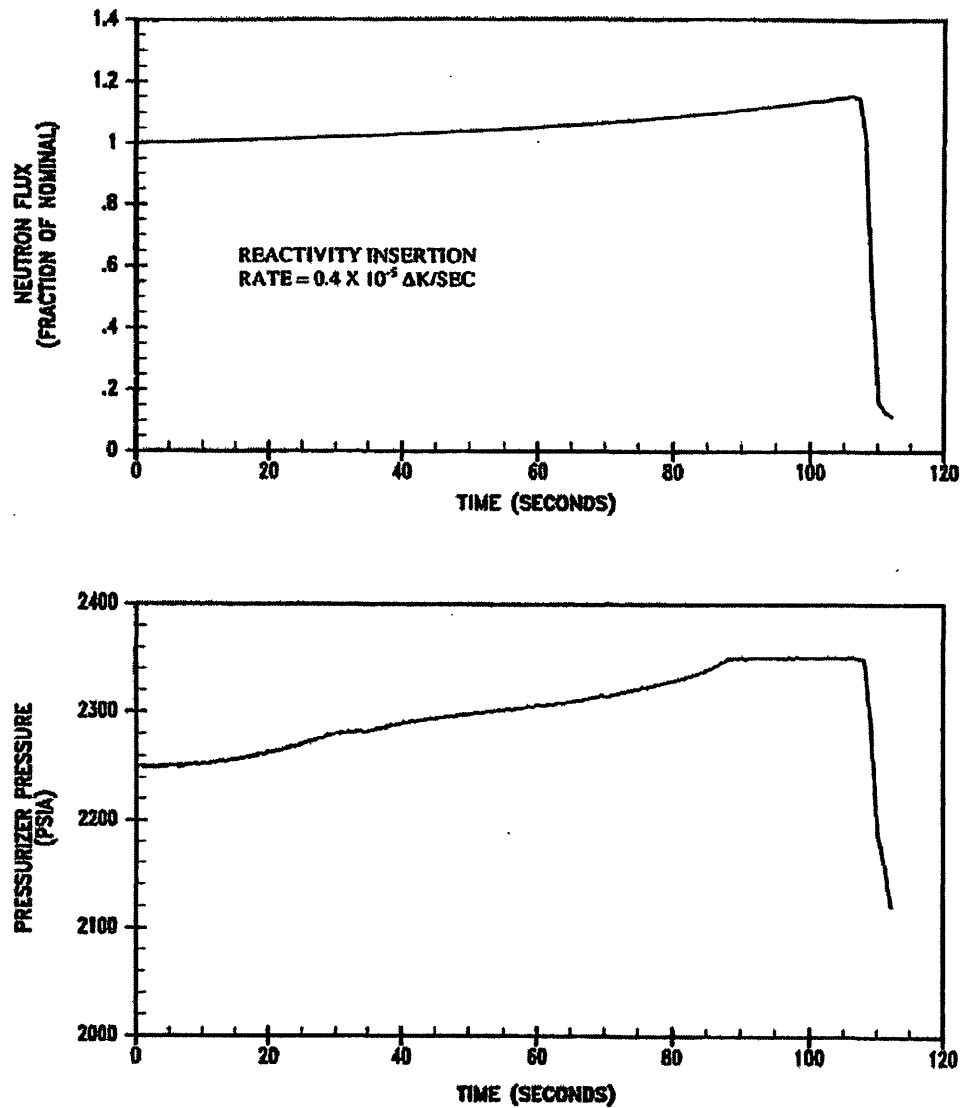


FIGURE 14.1-6

TRANSIENT RESPONSE FOR UNCONTROLLED  
ROD WITHDRAWAL FROM FULL POWER  
TERMINATED BY OVERTEMPERATURE DELTA-T TRIP  
BEAVER VALLEY POWER STATION UNIT NO. 1  
UPDATED FINAL SAFETY ANALYSIS REPORT

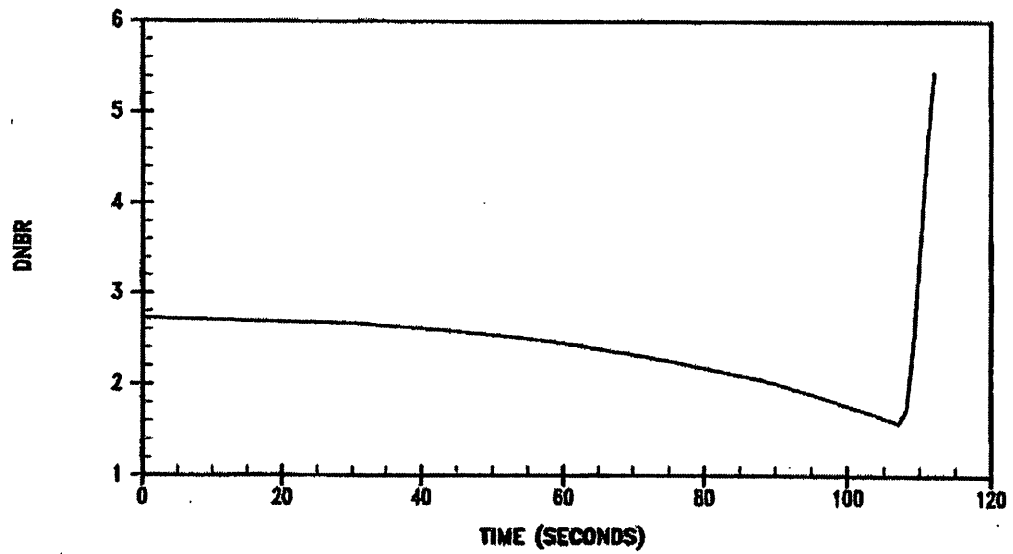
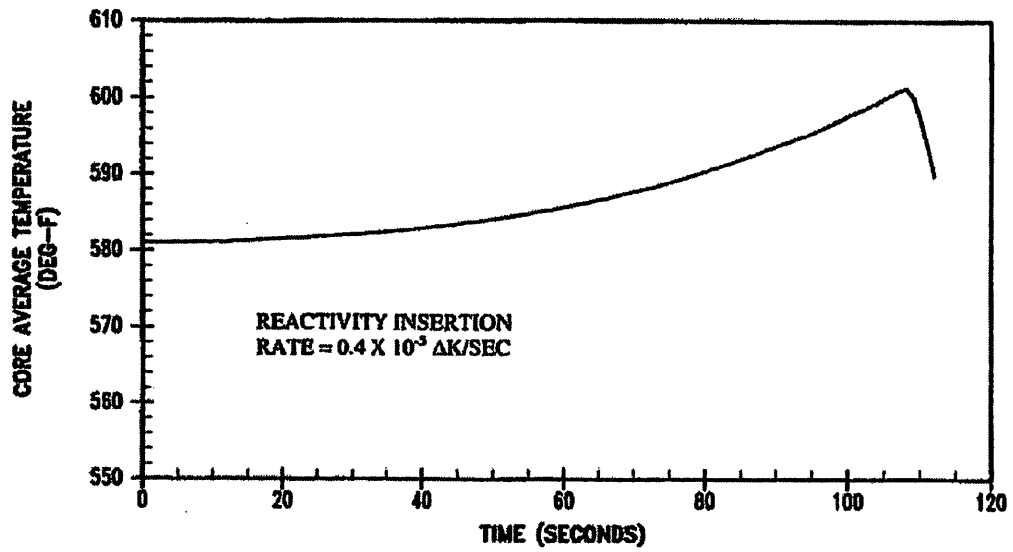


FIGURE 14.1-7

TRANSIENT RESPONSE FOR UNCONTROLLED  
ROD WITHDRAWAL FROM FULL POWER  
TERMINATED BY OVERTEMPERATURE DELTA-T TRIP

BEAVER VALLEY POWER STATION UNIT NO. 1  
UPDATED FINAL SAFETY ANALYSIS REPORT

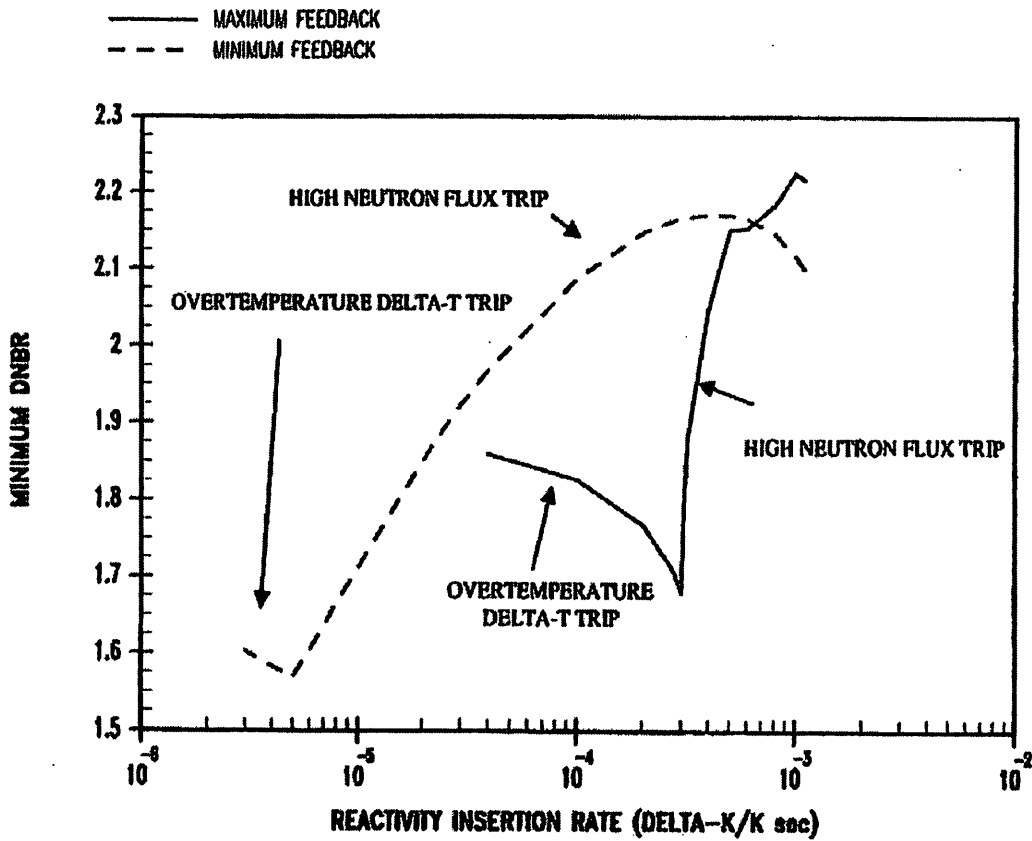


FIGURE 14.1-8

EFFECT OF REACTIVITY INSERTION RATE ON MINIMUM DNBR FOR A ROD WITHDRAWAL ACCIDENT FROM 100% POWER

BEAVER VALLEY POWER STATION UNIT NO. 1  
 UPDATED FINAL SAFETY ANALYSIS REPORT

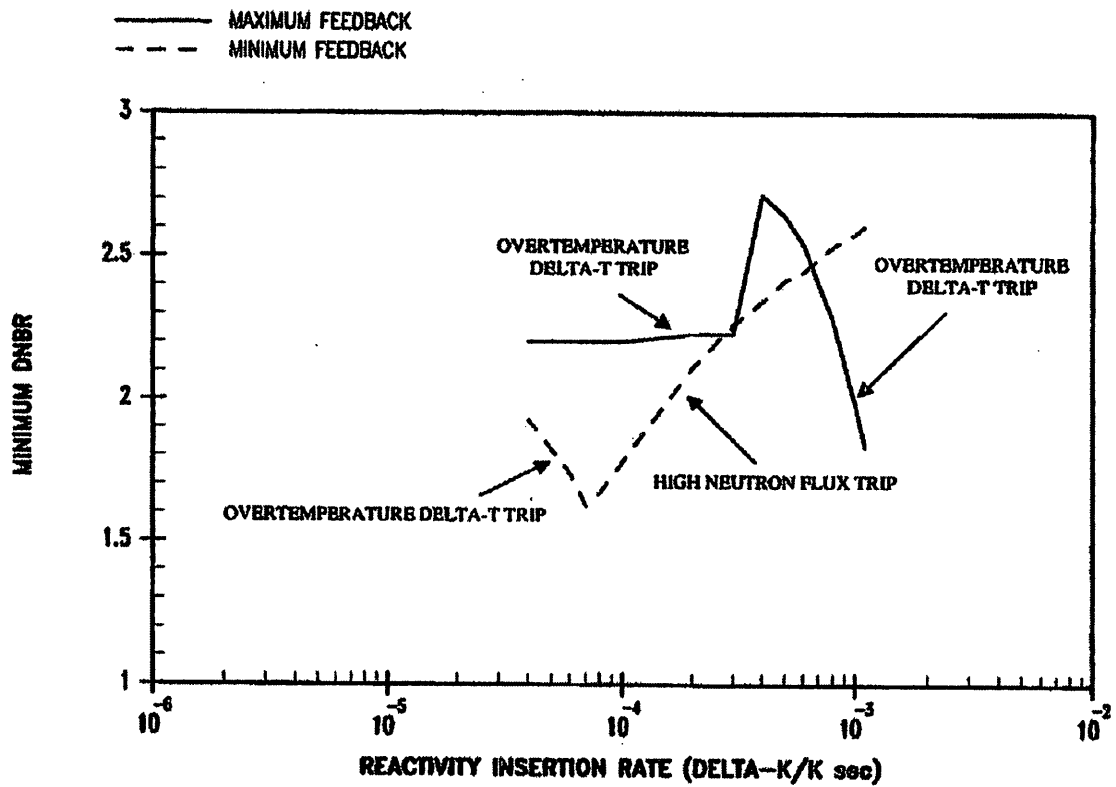


FIGURE 14.1-9

EFFECT OF REACTIVITY INSERTION RATE  
ON MINIMUM DNBR FOR A ROD WITHDRAWAL  
ACCIDENT FROM 60% POWER

BEAVER VALLEY POWER STATION UNIT NO. 1  
UPDATED FINAL SAFETY ANALYSIS REPORT

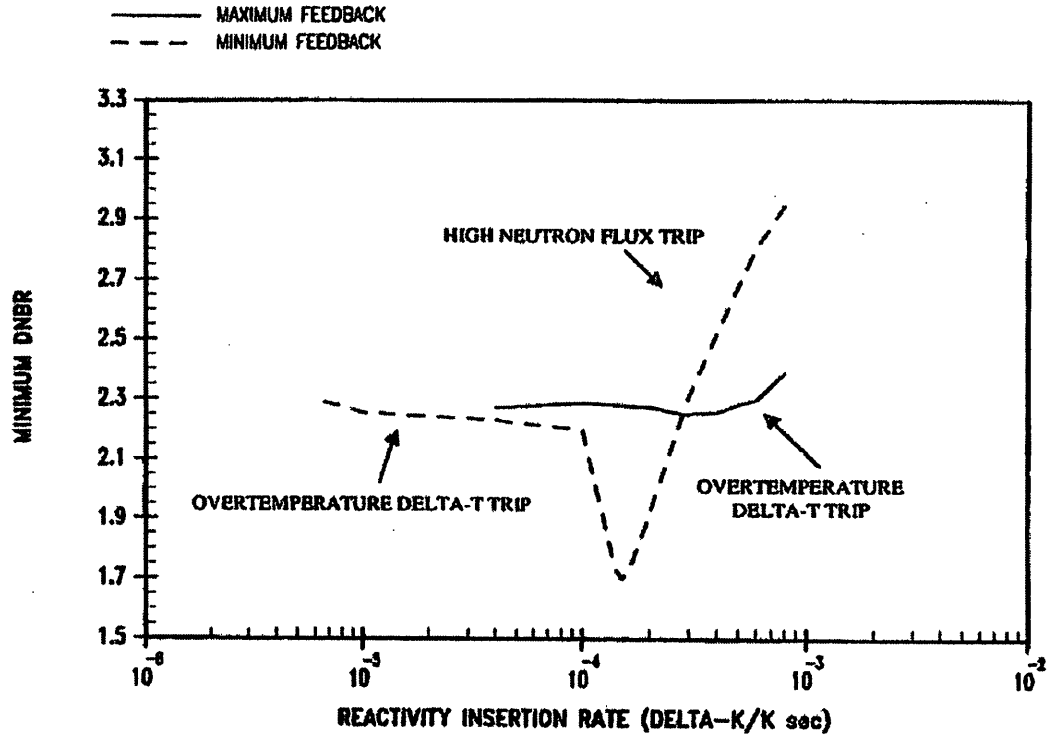


FIGURE 14.1-10

EFFECT OF REACTIVITY INSERTION RATE ON MINIMUM DNBR FOR A ROD WITHDRAWAL ACCIDENT FROM 10% POWER

BEAVER VALLEY POWER STATION UNIT NO. 1  
UPDATED FINAL SAFETY ANALYSIS REPORT



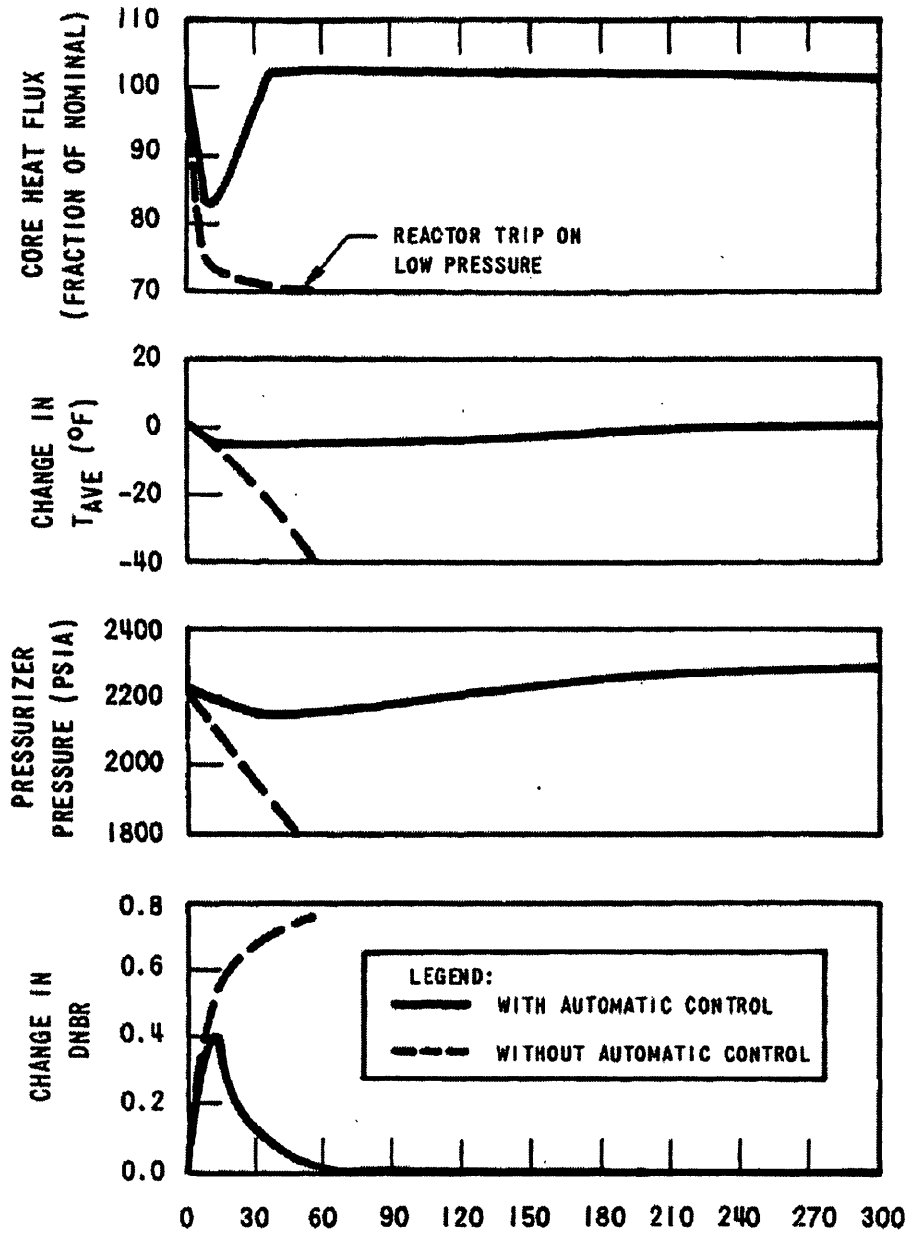


FIGURE 14-1-11  
 TRANSIENT RESPONSE TO DROPPED ROD  
 CLUSTER CONTROL ASSEMBLY  
 BEAVER VALLEY POWER STATION UNIT NO. 1  
 UPDATED FINAL SAFETY ANALYSIS REPORT

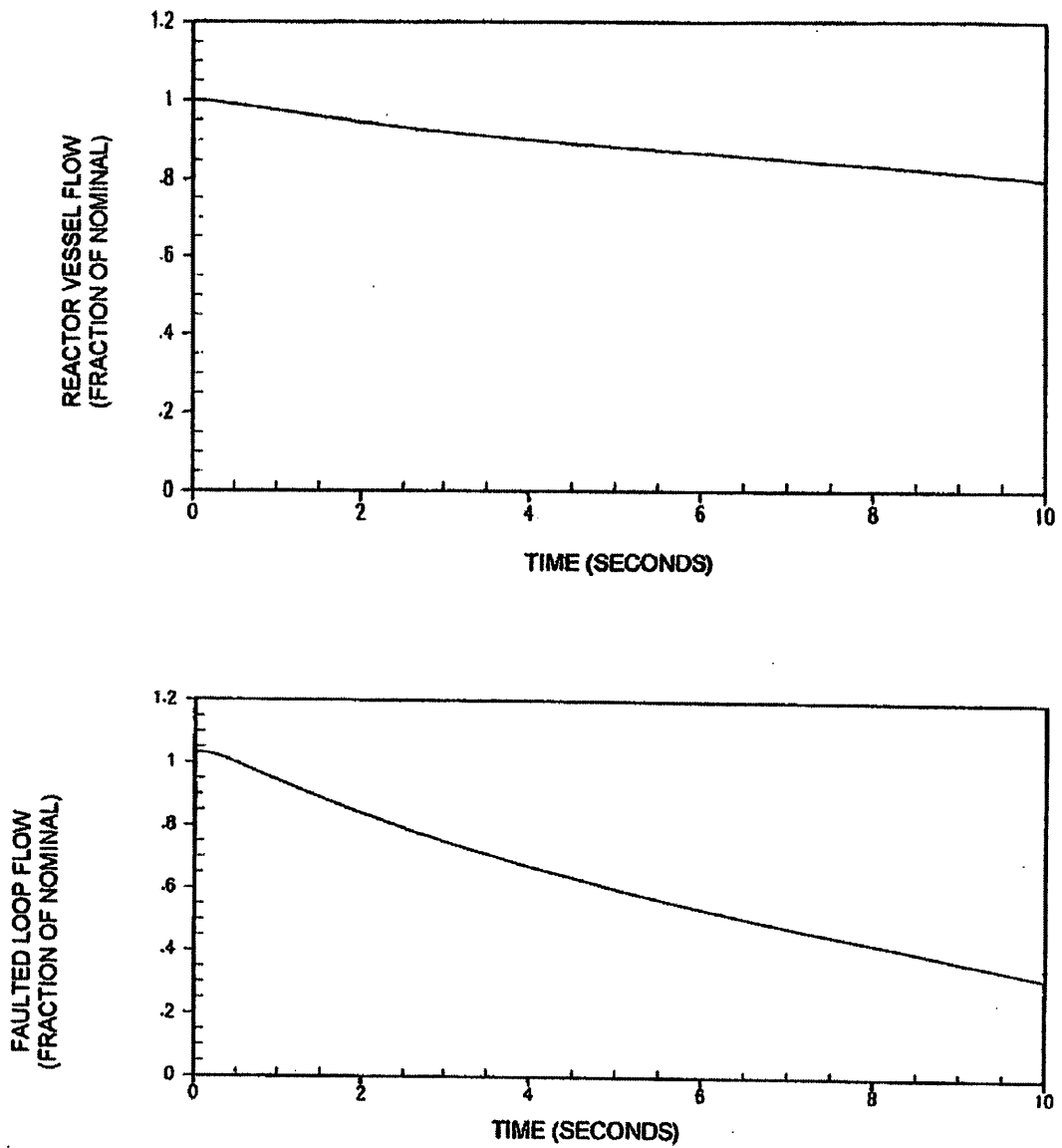


FIGURE 14.1-13

REACTOR VESSEL AND FAULTED LOOP  
FLOW TRANSIENTS FOR PARTIAL LOSS  
OF FLOW-ONE PUMP COASTING DOWN

BEAVER VALLEY POWER STATION UNIT NO.1  
UPDATED FINAL SAFETY ANALYSIS REPORT

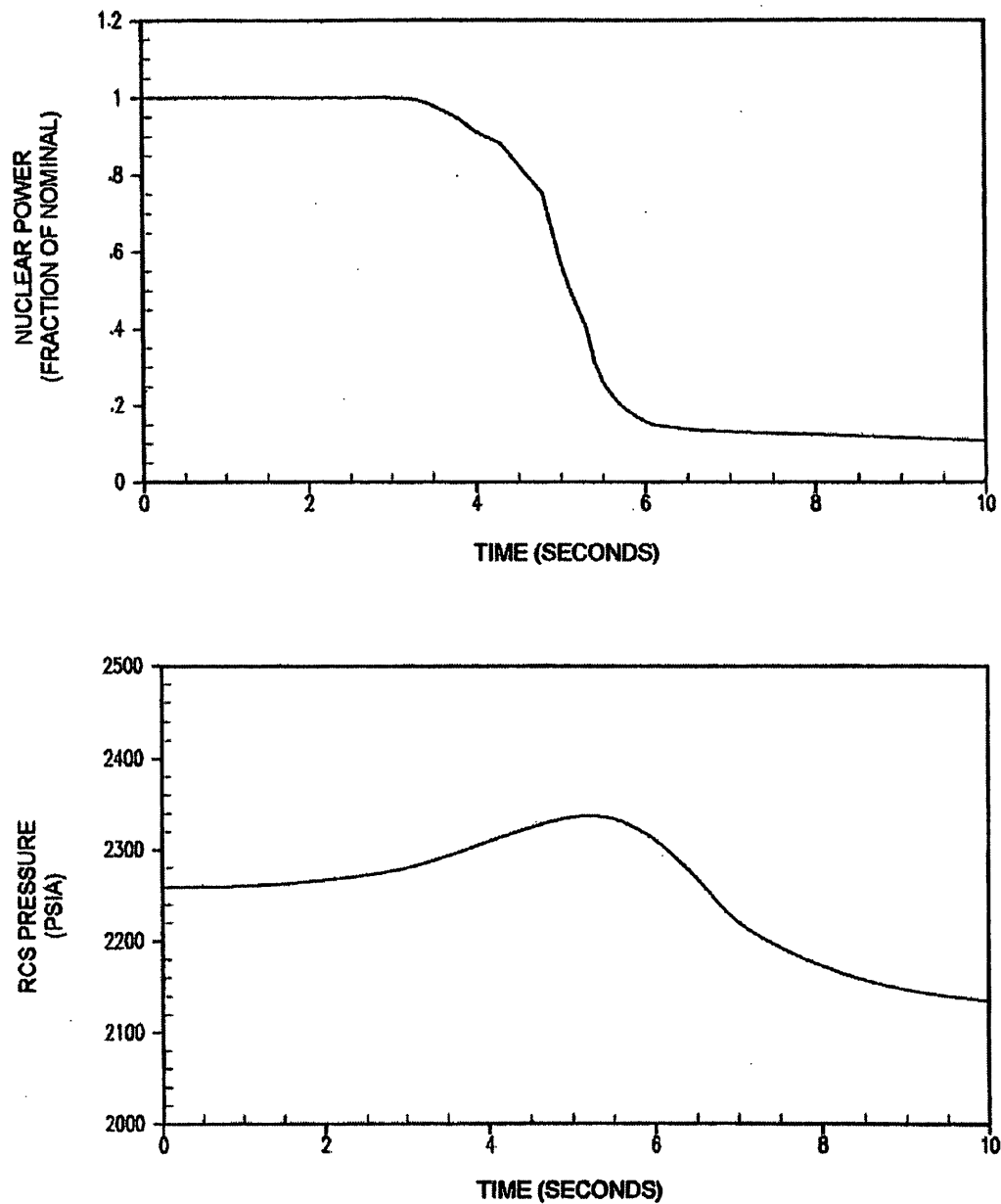


FIGURE 14.1-14

NUCLEAR POWER AND RCS PRESSURE  
TRANSIENTS FOR PARTIAL LOSS OF FLOW-  
ONE PUMP COASTING DOWN

BEAVER VALLEY POWER STATION UNIT NO. 1  
UPDATED FINAL SAFETY ANALYSIS REPORT

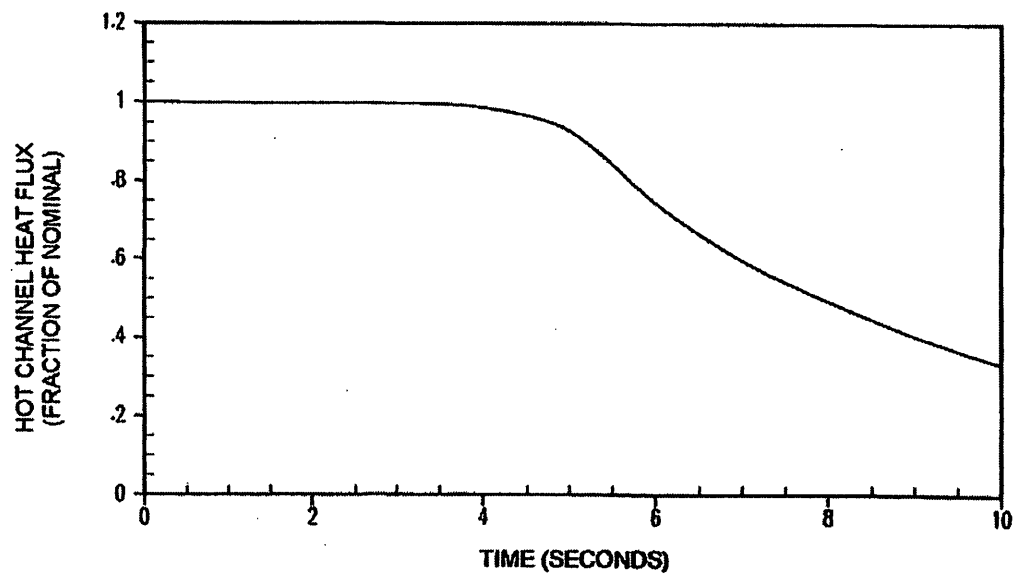
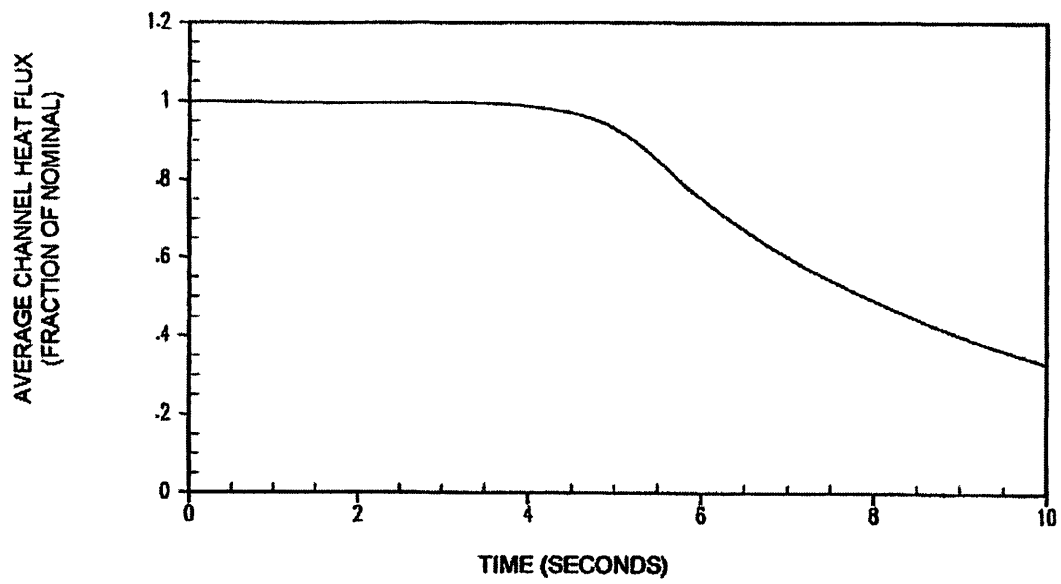


FIGURE 14.1-15

AVERAGE CHANNEL AND HOT CHANNEL  
HEAT FLUX TRANSIENTS FOR PARTIAL  
LOSS OF FLOW-ONE PUMP COASTING DOWN

BEAVER VALLEY POWER STATION UNIT NO.1  
UPDATED FINAL SAFETY ANALYSIS REPORT

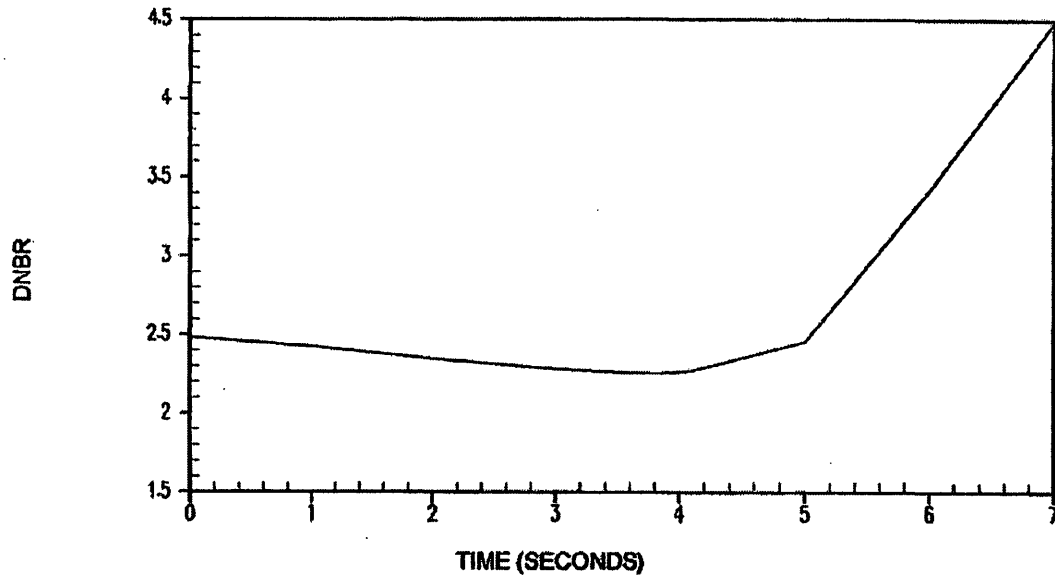


FIGURE 14.1-16

DNBR VERSUS TIME FOR PARTIAL LOSS OF FLOW-ONE PUMP COASTING DOWN

BEAVER VALLEY POWER STATION UNIT NO.1  
UPDATED FINAL SAFETY ANALYSIS REPORT

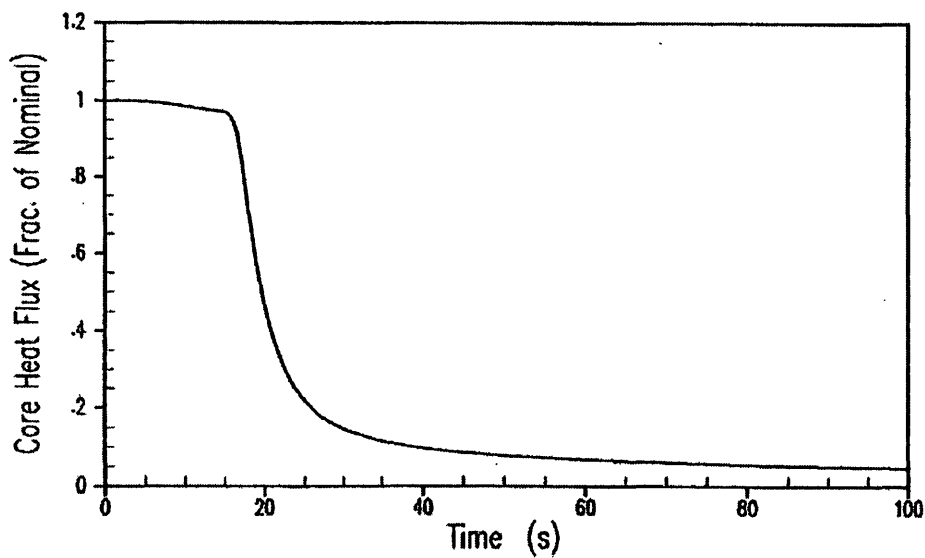
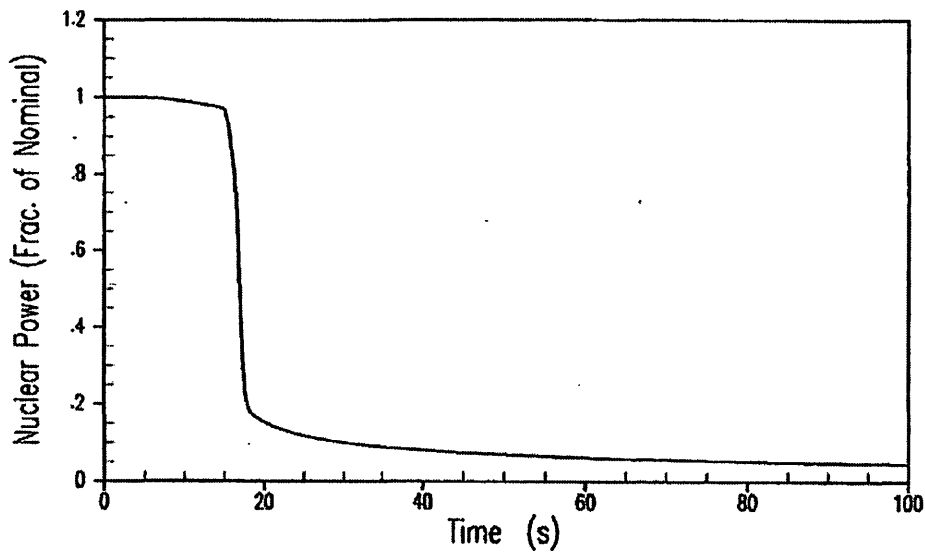


FIGURE 14.1-23

LOSS OF LOAD ACCIDENT WITH  
PRESSURIZER SPRAY AND POWER-  
OPERATED RELIEF VALVES

BEAVER VALLEY POWER STATION UNIT NO. 1  
UPDATED FINAL SAFETY ANALYSIS REPORT

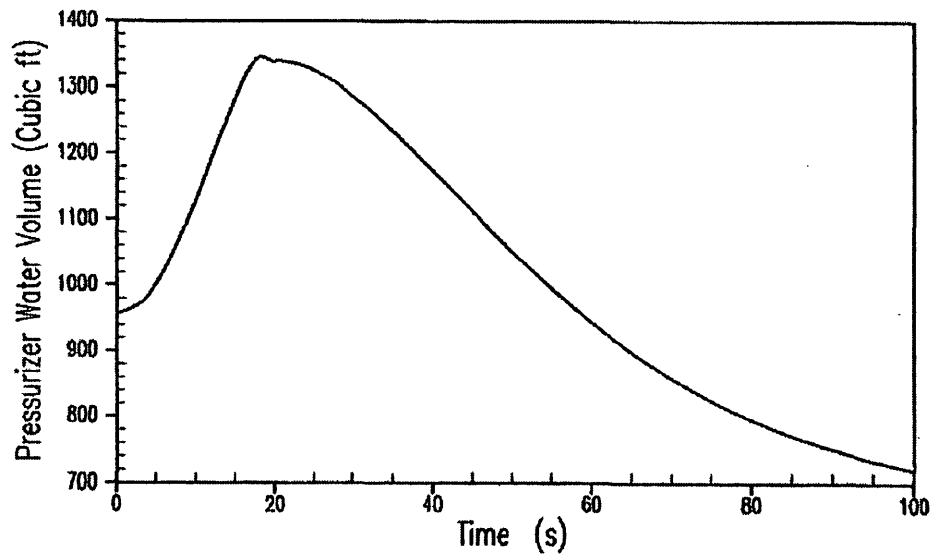
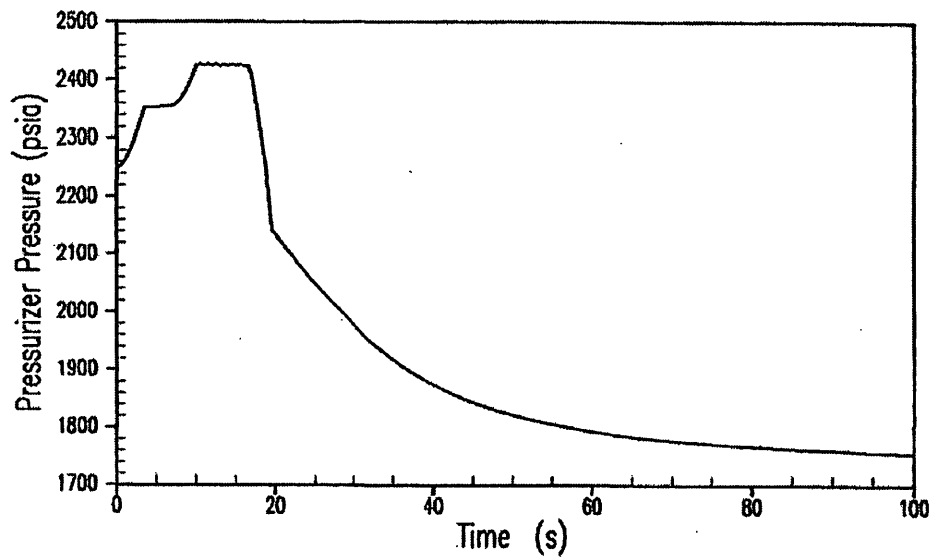


FIGURE 14.1-24  
LOSS OF LOAD ACCIDENT WITH  
PRESSURIZER SPRAY AND POWER  
OPERATED RELIEF VALVES  
BEAVER VALLEY POWER STATION UNIT NO. 1  
UPDATED FINAL SAFETY ANALYSIS REPORT

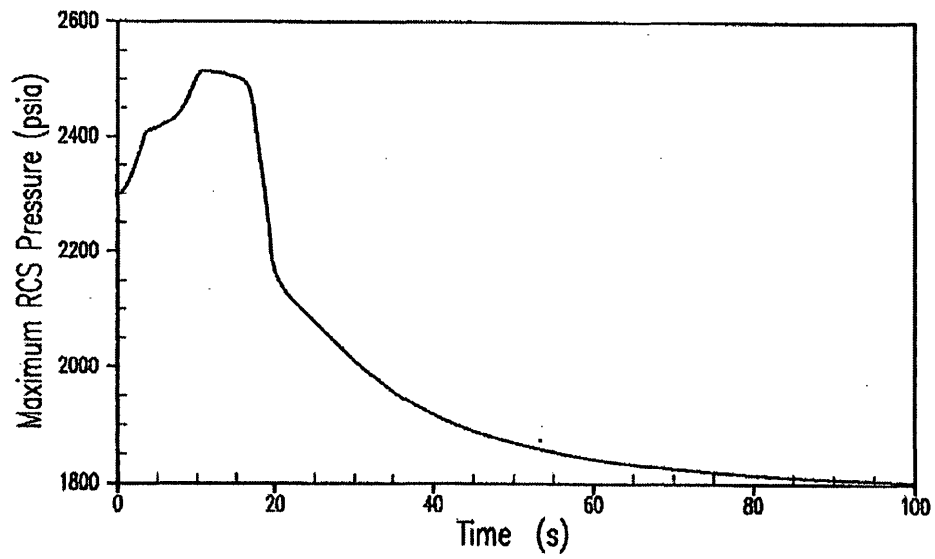
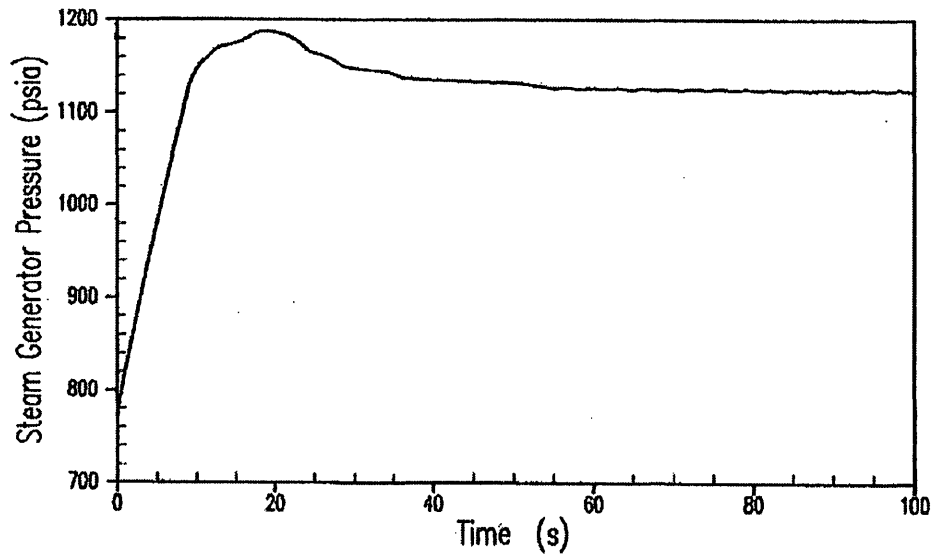


FIGURE 14.1-25

LOSS OF LOAD ACCIDENT WITH  
 PRESSURIZER SPRAY AND POWER  
 OPERATED RELIEF VALVES

BEAVER VALLEY POWER STATION UNIT NO. 1  
 UPDATED FINAL SAFETY ANALYSIS REPORT



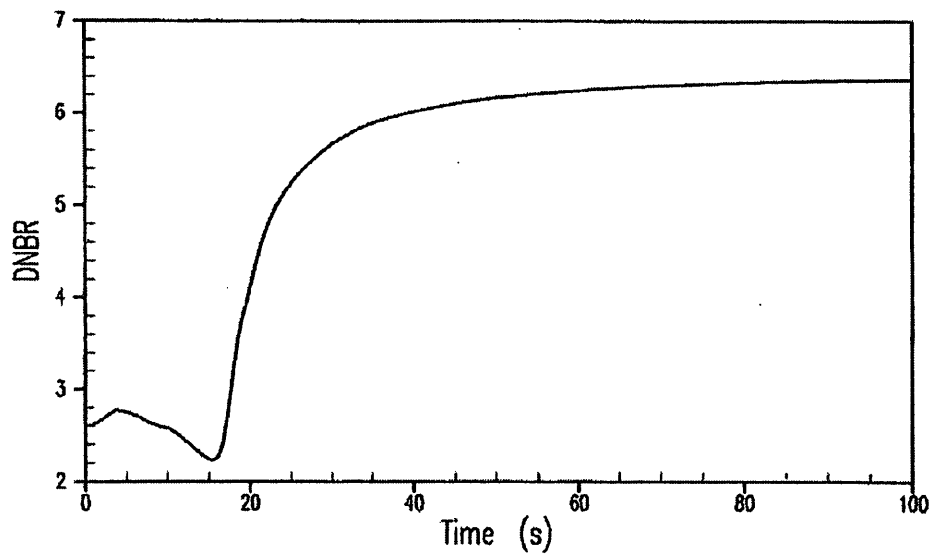
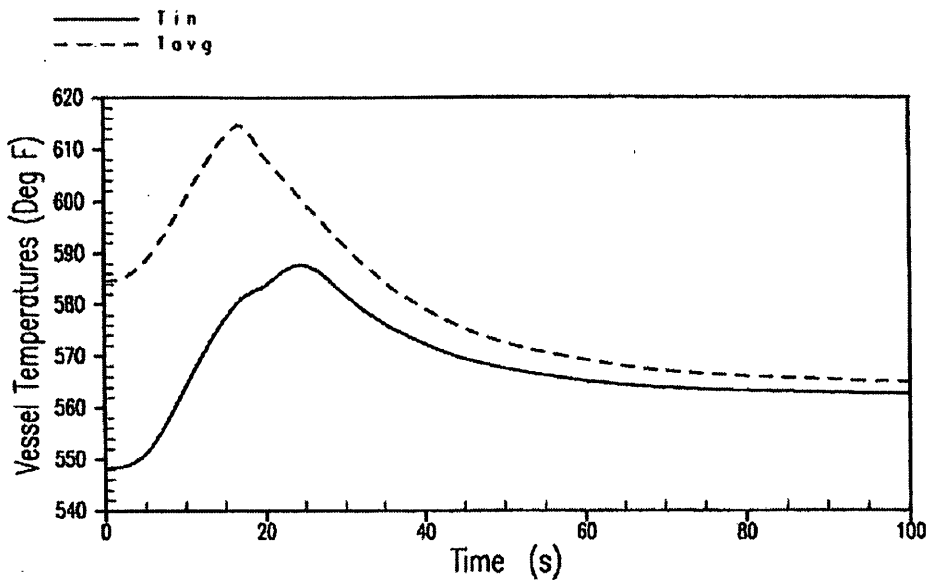


FIGURE 14.1-26

LOSS OF LOAD ACCIDENT WITH  
PRESSURIZED SPRAY AND POWER  
OPERATED RELIEF VALVES

BEAVER VALLEY POWER STATION UNIT NO. 1  
UPDATED FINAL SAFETY ANALYSIS REPORT

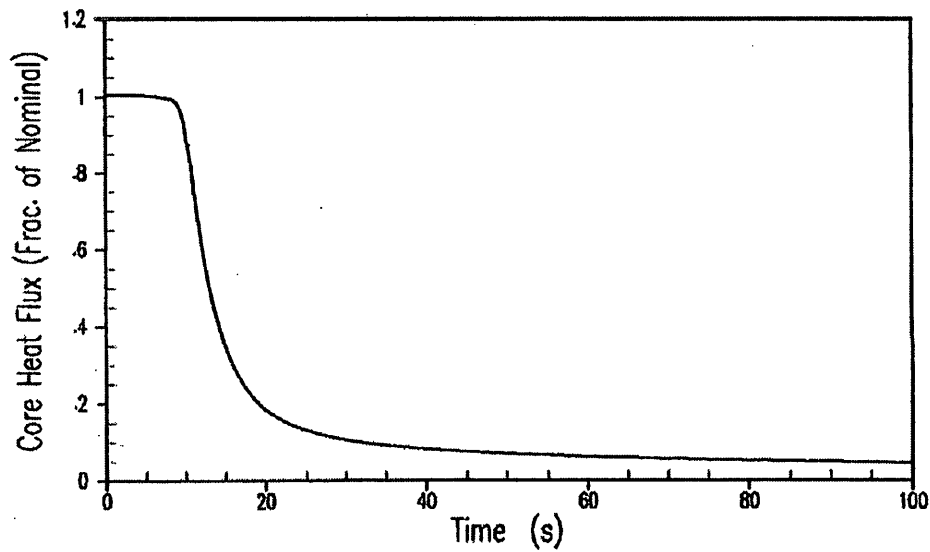
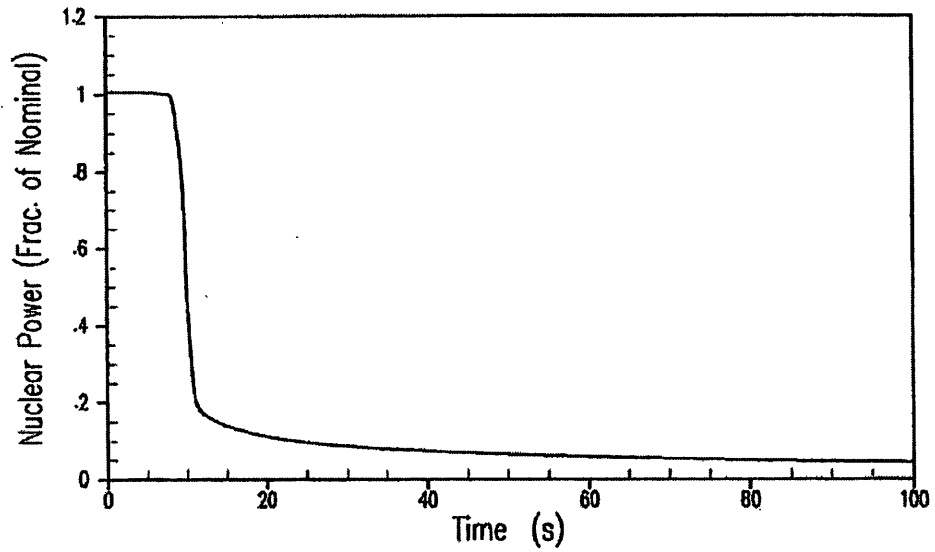


FIGURE 14.1-27

LOSS OF LOAD ACCIDENT WITHOUT  
PRESSURIZER SPRAY AND POWER  
OPERATED RELIEF VALVES

BEAVER VALLEY POWER STATION UNIT NO. 1  
UPDATED FINAL SAFETY ANALYSIS REPORT

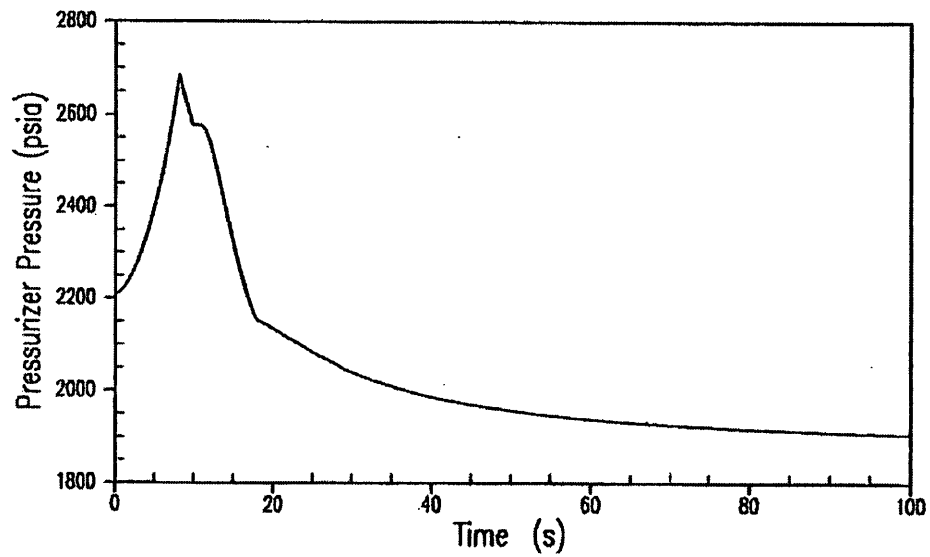
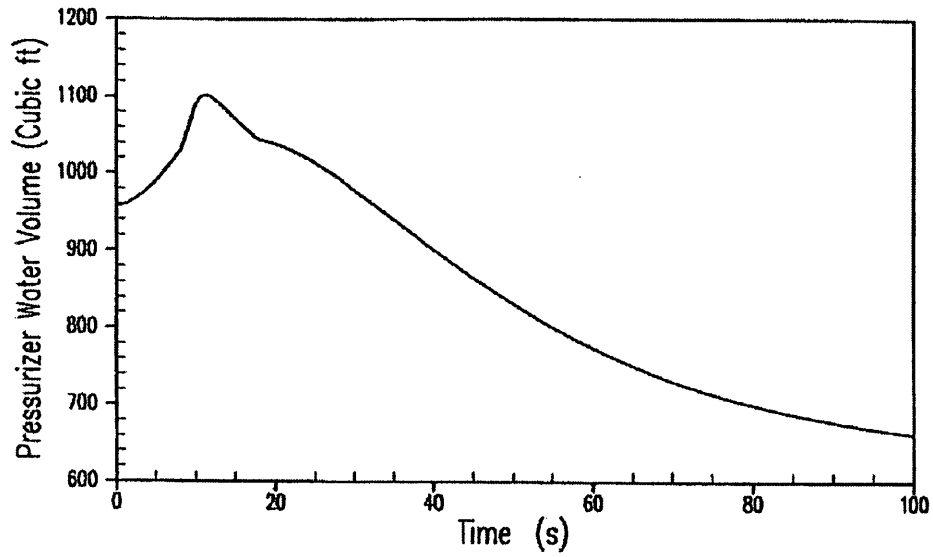


FIGURE 14.1-28

LOSS OF LOAD ACCIDENT WITHOUT  
PRESSURIZER SPRAY AND POWER  
OPERATED RELIEF VALVES

BEAVER VALLEY POWER STATION UNIT NO. 1  
UPDATED FINAL SAFETY ANALYSIS REPORT

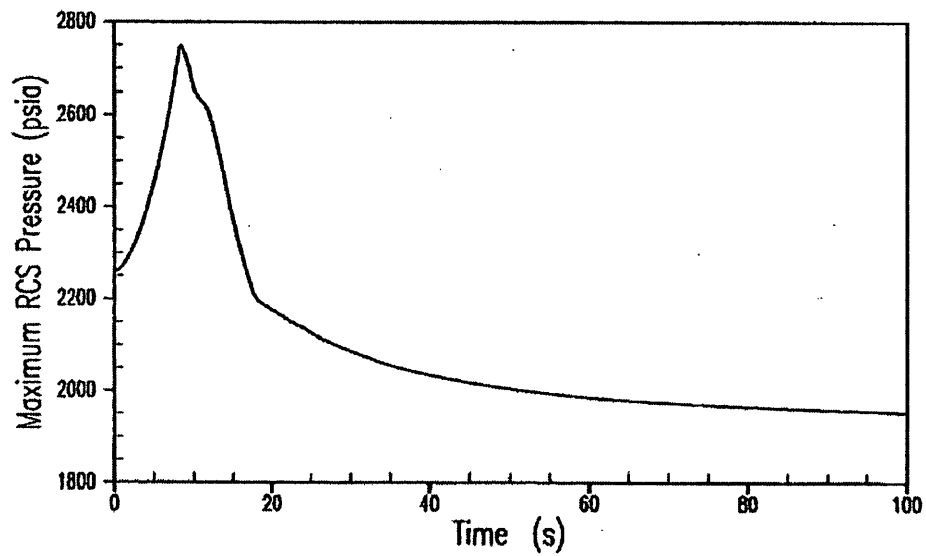
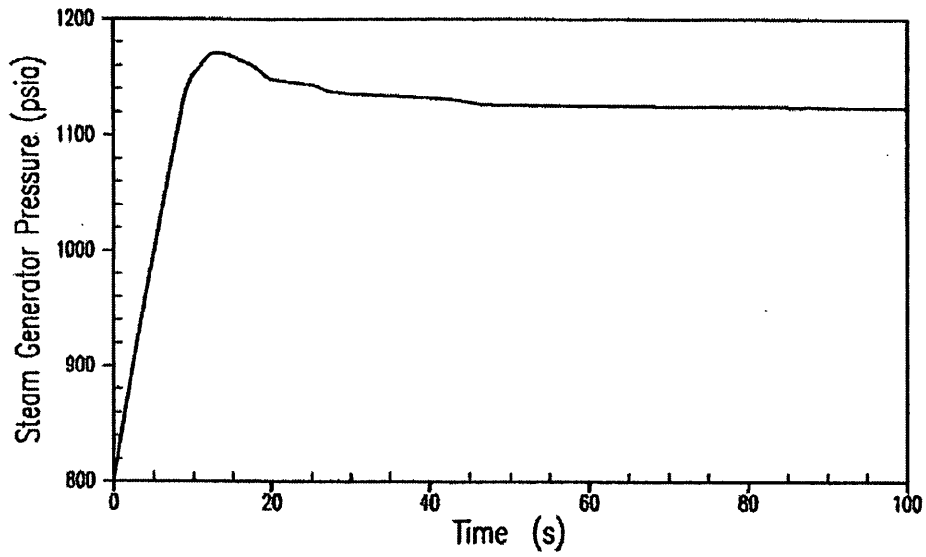


FIGURE 14.1-29

LOSS OF LOAD ACCIDENT WITHOUT  
PRESSURIZER SPRAY AND POWER  
OPERATED RELIEF VALVES

BEAVER VALLEY POWER STATION UNIT NO. 1  
UPDATED FINAL SAFETY ANALYSIS REPORT

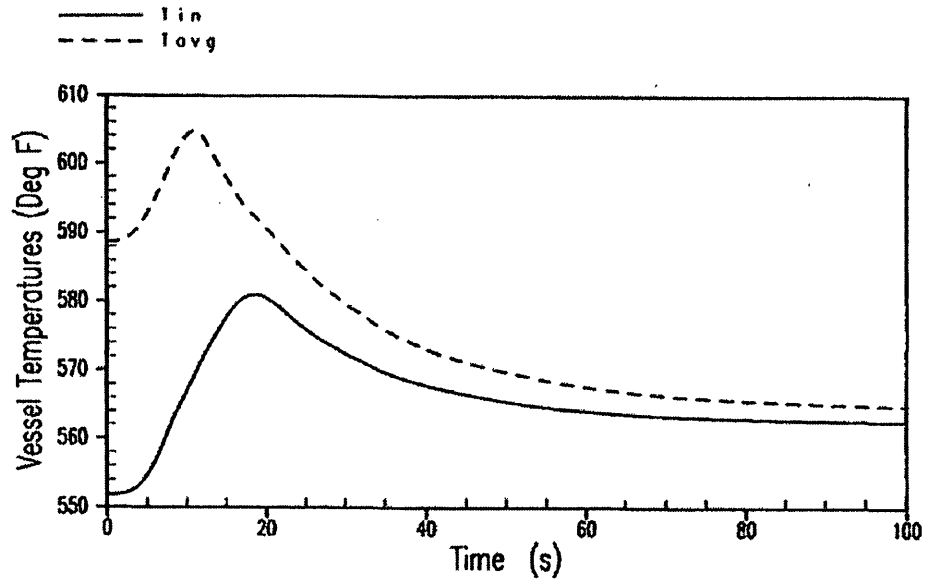


FIGURE 14.1-30

LOSS OF LOAD ACCIDENT WITHOUT  
PRESSURIZER SPRAY AND POWER  
OPERATED RELIEF VALVES

BEAVER VALLEY POWER STATION UNIT NO. 1  
UPDATED FINAL SAFETY ANALYSIS REPORT

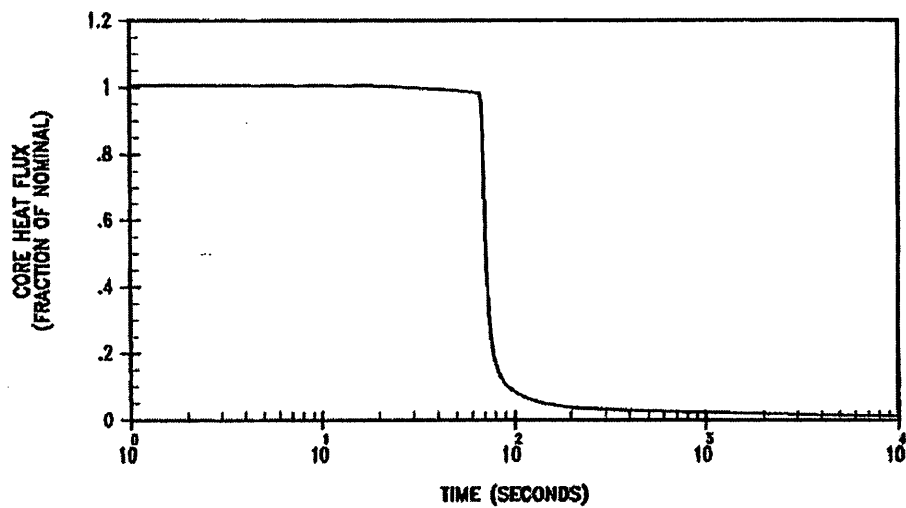
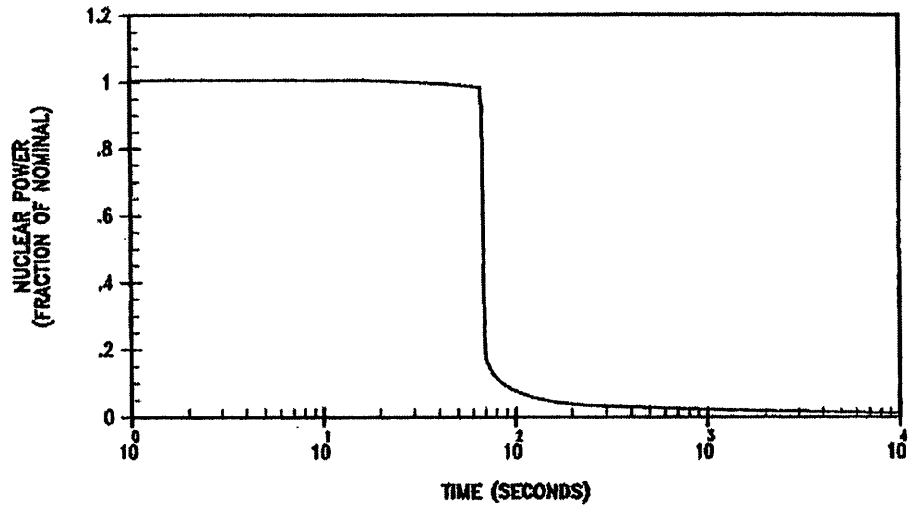


FIGURE 14.1-31

NUCLEAR POWER AND CORE HEAT  
FLUX TRANSIENTS FOR LOSS OF  
NORMAL FEEDWATER

BEAVER VALLEY POWER STATION UNIT NO. 1  
UPDATED FINAL SAFETY ANALYSIS REPORT

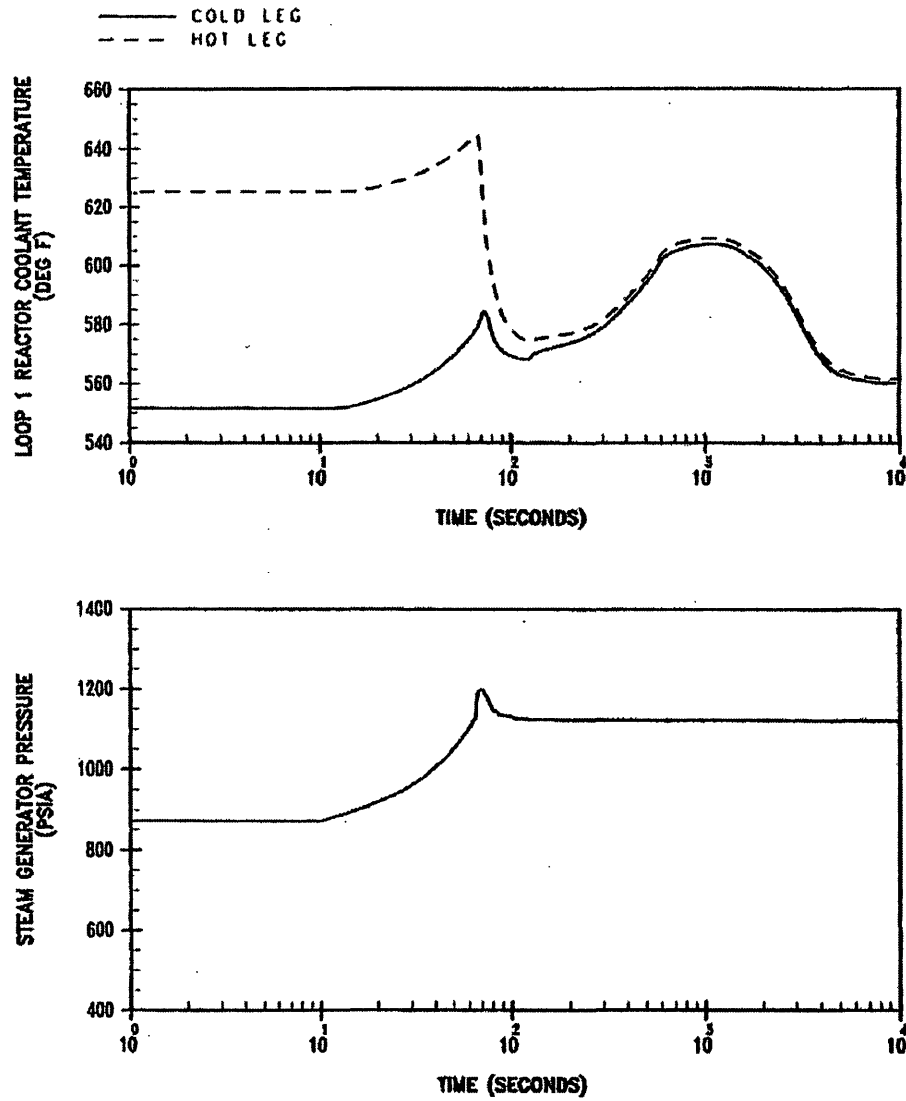


FIGURE 14.1-31A

REACTOR COOLANT TEMPERATURE AND  
STEAM GENERATOR PRESSURE TRANSIENTS  
FOR LOSS OF NORMAL FEEDWATER

BEAVER VALLEY POWER STATION UNIT NO. 1  
UPDATED FINAL SAFETY ANALYSIS REPORT

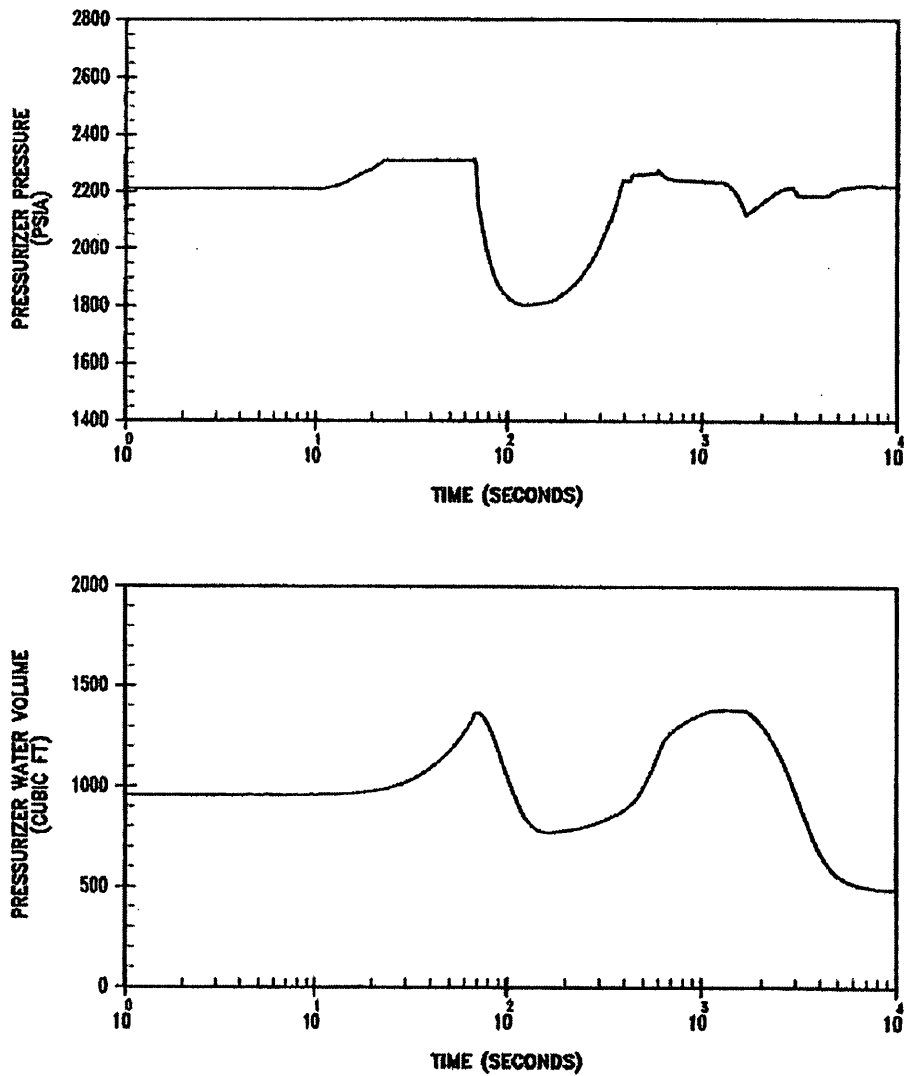


FIGURE 14.1-31B

PRESSURIZER PRESSURE AND WATER  
VOLUME TRANSIENTS FOR LOSS OF  
NORMAL FEEDWATER

BEAVER VALLEY POWER STATION UNIT NO. 1  
UPDATED FINAL SAFETY ANALYSIS REPORT



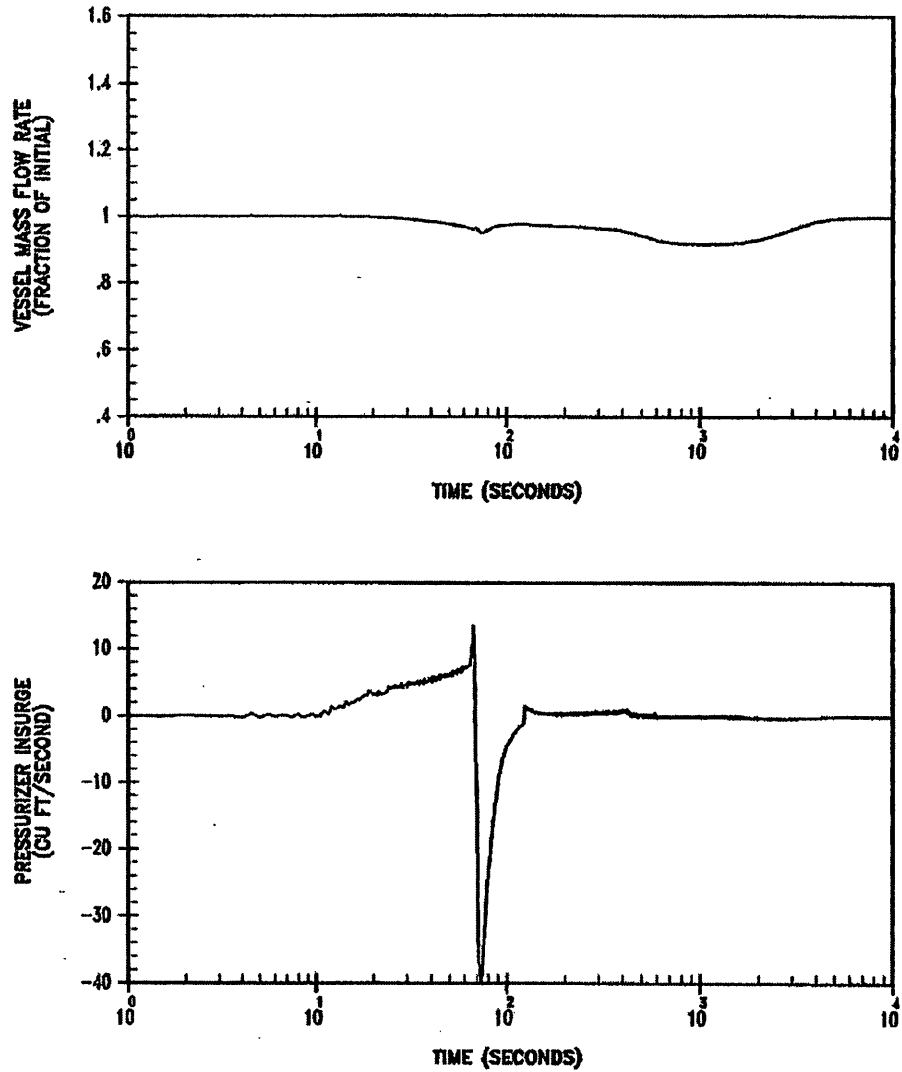


FIGURE 14.1-31C

VESSEL MASS FLOW RATE AND  
PRESSURIZER INSURGE TRANSIENTS FOR  
LOSS OF NORMAL FEEDWATER

BEAVER VALLEY POWER STATION UNIT NO. 1  
UPDATED FINAL SAFETY ANALYSIS REPORT

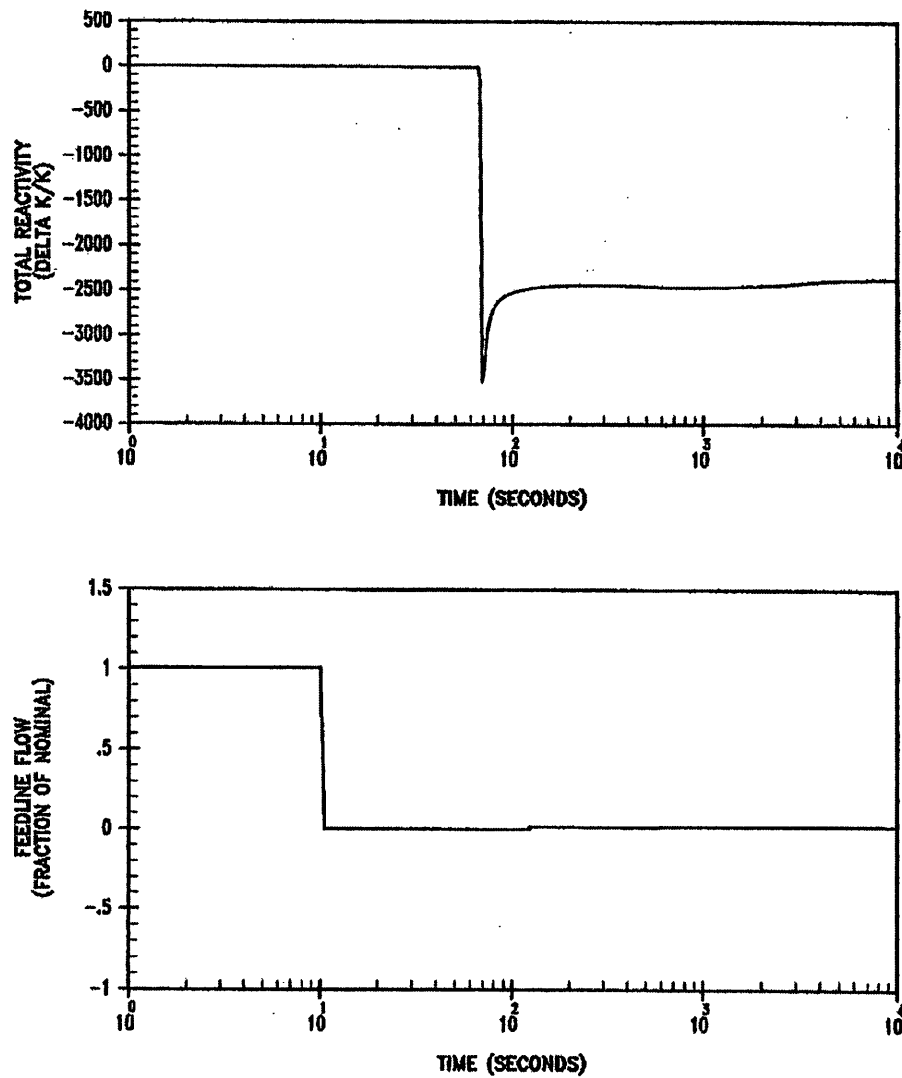


FIGURE 14.1-31D

CORE REACTIVITY TRANSIENT AND  
FEEDLINE FLOW TRANSIENT FOR  
LOSS OF NORMAL FEEDWATER

BEAVER VALLEY POWER STATION UNIT NO. 1  
UPDATED FINAL SAFETY ANALYSIS REPORT

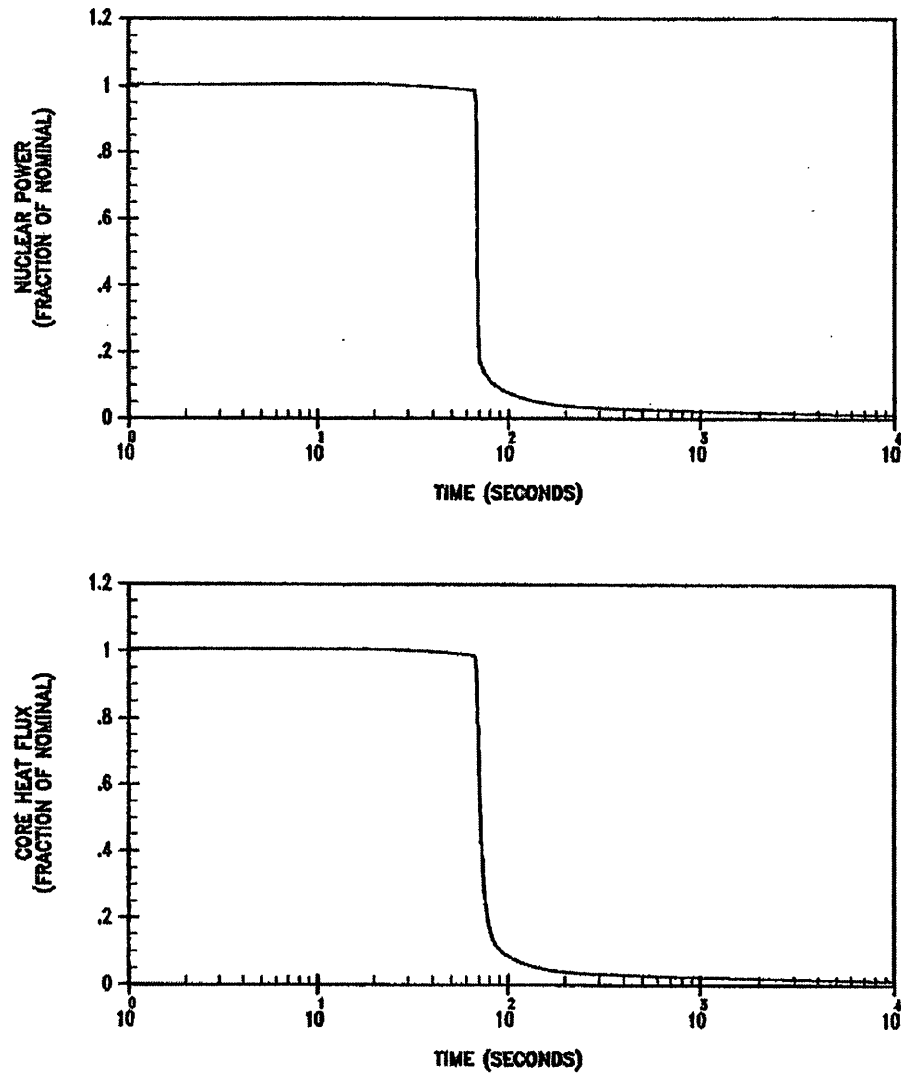


FIGURE 14.1-31E

NUCLEAR POWER AND CORE HEAT FLUX  
TRANSIENTS FOR LOSS OF AC POWER

BEAVER VALLEY POWER STATION UNIT NO. 1  
UPDATED FINAL SAFETY ANALYSIS REPORT

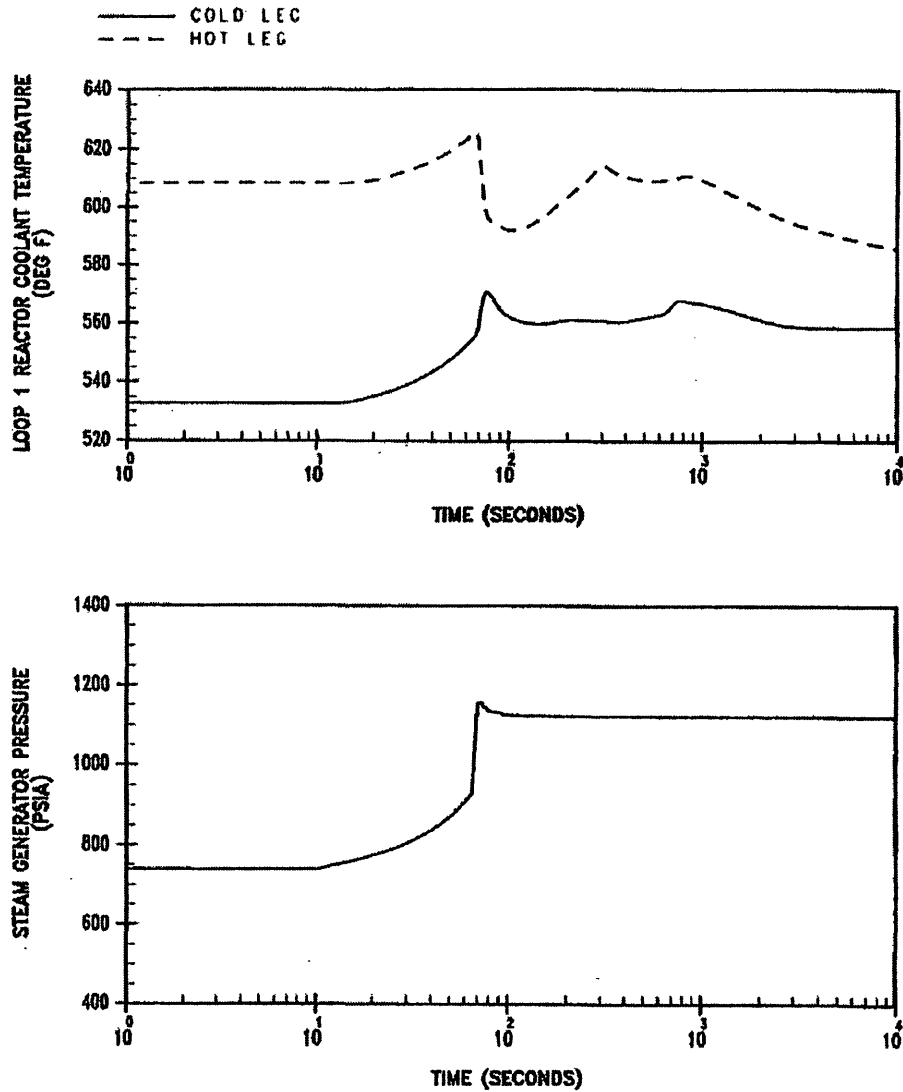


FIGURE 14.1-31F

REACTOR COOLANT TEMPERATURE AND  
 STEAM GENERATOR PRESSURE TRANSIENTS  
 LOSS OF AC POWER

BEAVER VALLEY POWER STATION UNIT NO. 1  
 UPDATED FINAL SAFETY ANALYSIS REPORT

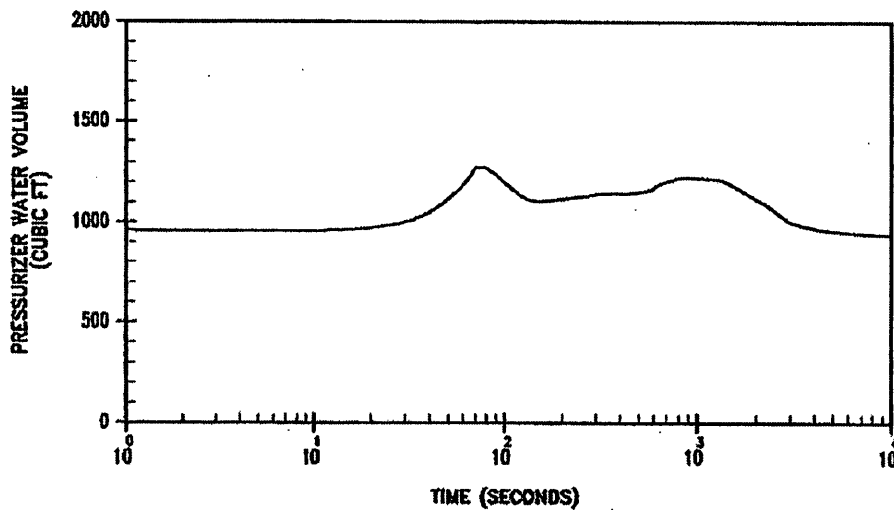
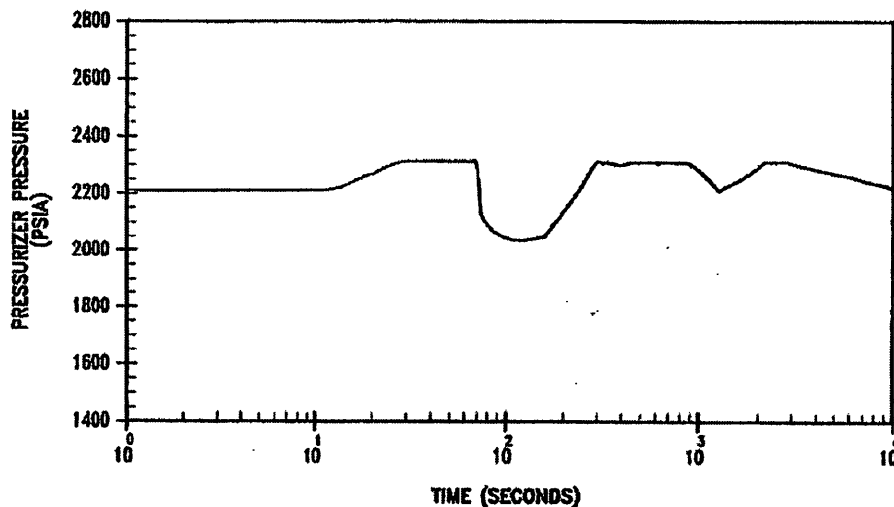


FIGURE 14.1-31G

PRESSURIZER PRESSURE AND WATER VOLUME TRANSIENTS LOSS OF AC POWER

BEAVER VALLEY POWER STATION UNIT NO. 1  
 UPDATED FINAL SAFETY ANALYSIS REPORT

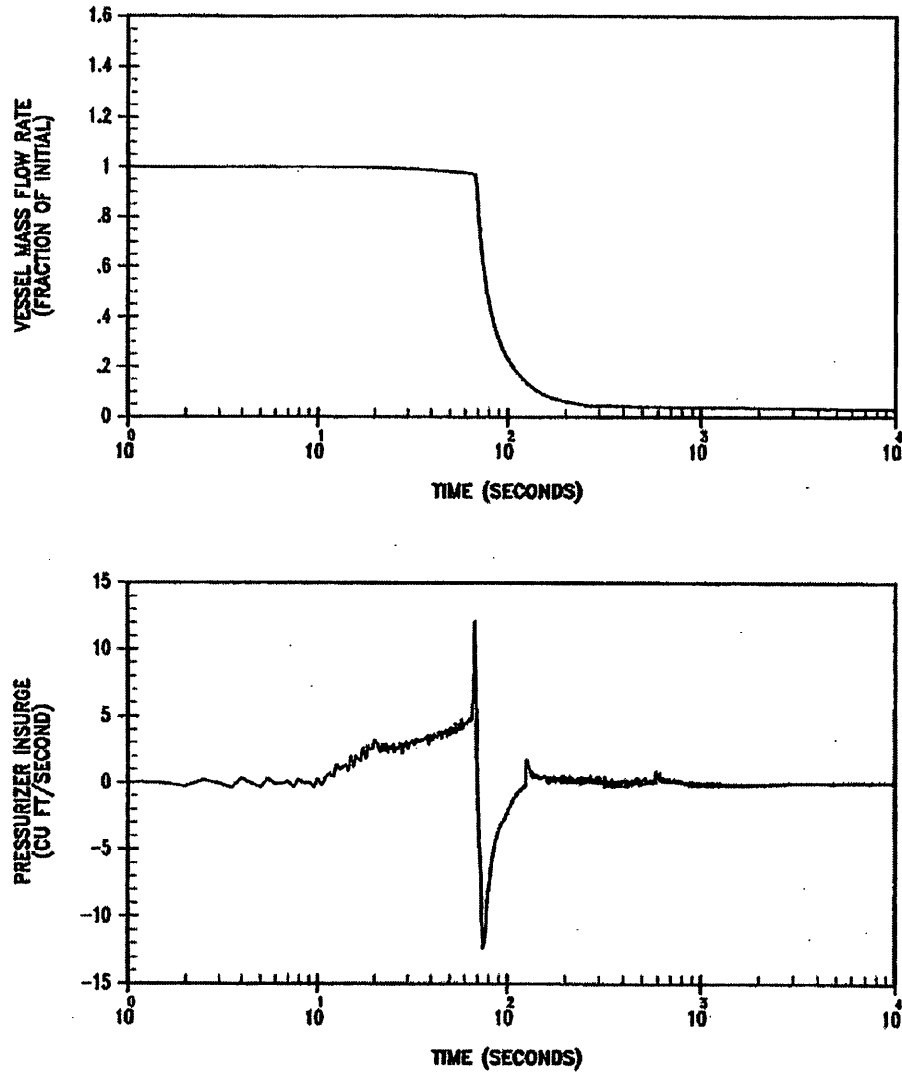


FIGURE 14.1-31H

VESSEL MASS FLOW RATE AND PRESSURIZER  
INSURGE TRANSIENTS LOSS OF AC POWER

BEAVER VALLEY POWER STATION UNIT NO. 1  
UPDATED FINAL SAFETY ANALYSIS REPORT

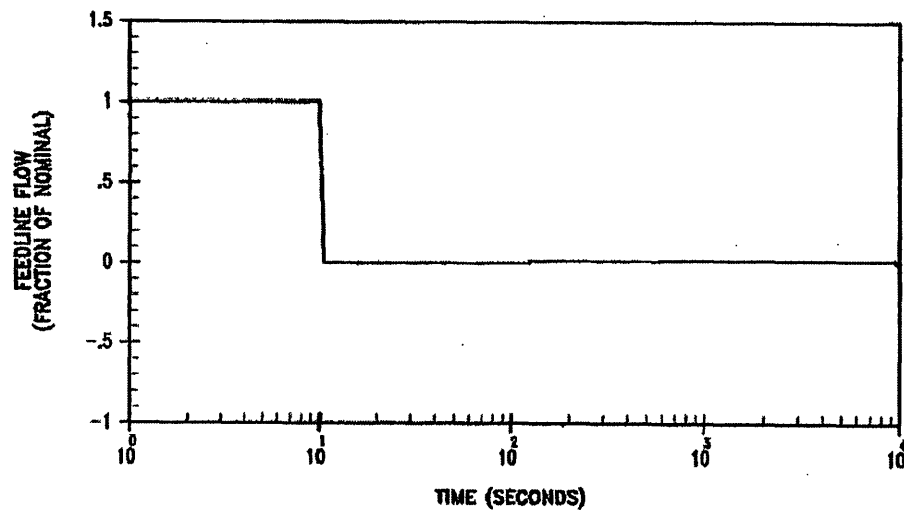
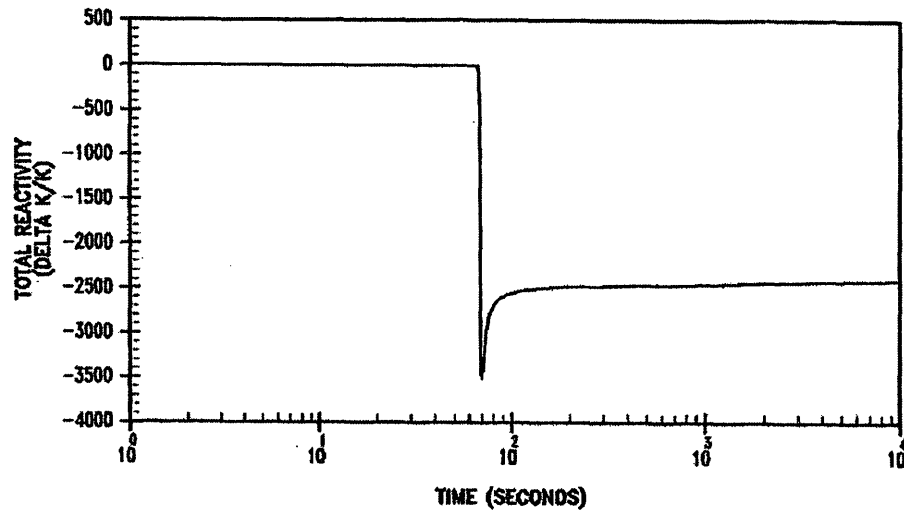


FIGURE 14.1-31I

CORE REACTIVITY TRANSIENT AND FEEDLINE  
FLOW TRANSIENT FOR LOSS OF AC POWER

BEAVER VALLEY POWER STATION UNIT NO. 1  
UPDATED FINAL SAFETY ANALYSIS REPORT

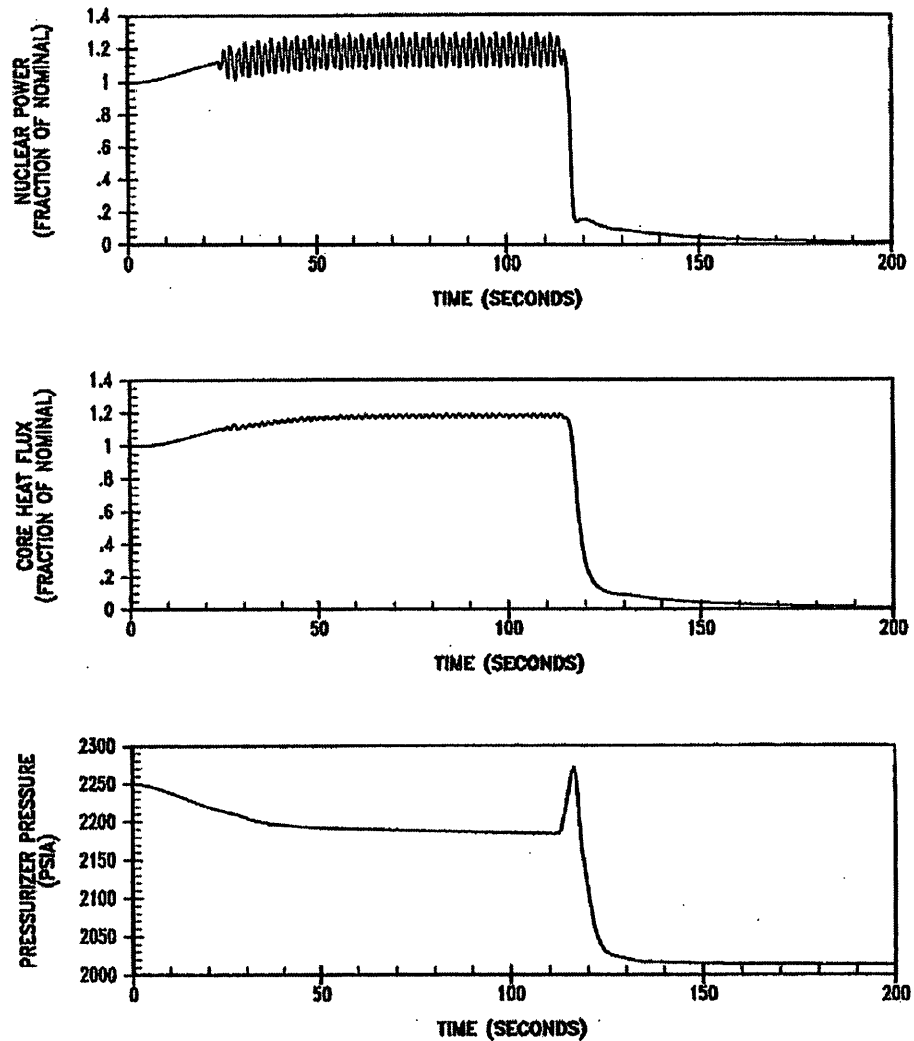


FIGURE 14.1-32A

NUCLEAR POWER, CORE HEAT FLUX AND PRESSURIZER  
PRESSURE TRANSIENTS FOR FEEDWATER CONTROL VALVE  
MALFUNCTION AT FULL POWER, AUTOMATIC ROD CONTROL

BEAVER VALLEY POWER STATION UNIT NO. 1  
UPDATED FINAL SAFETY ANALYSIS REPORT



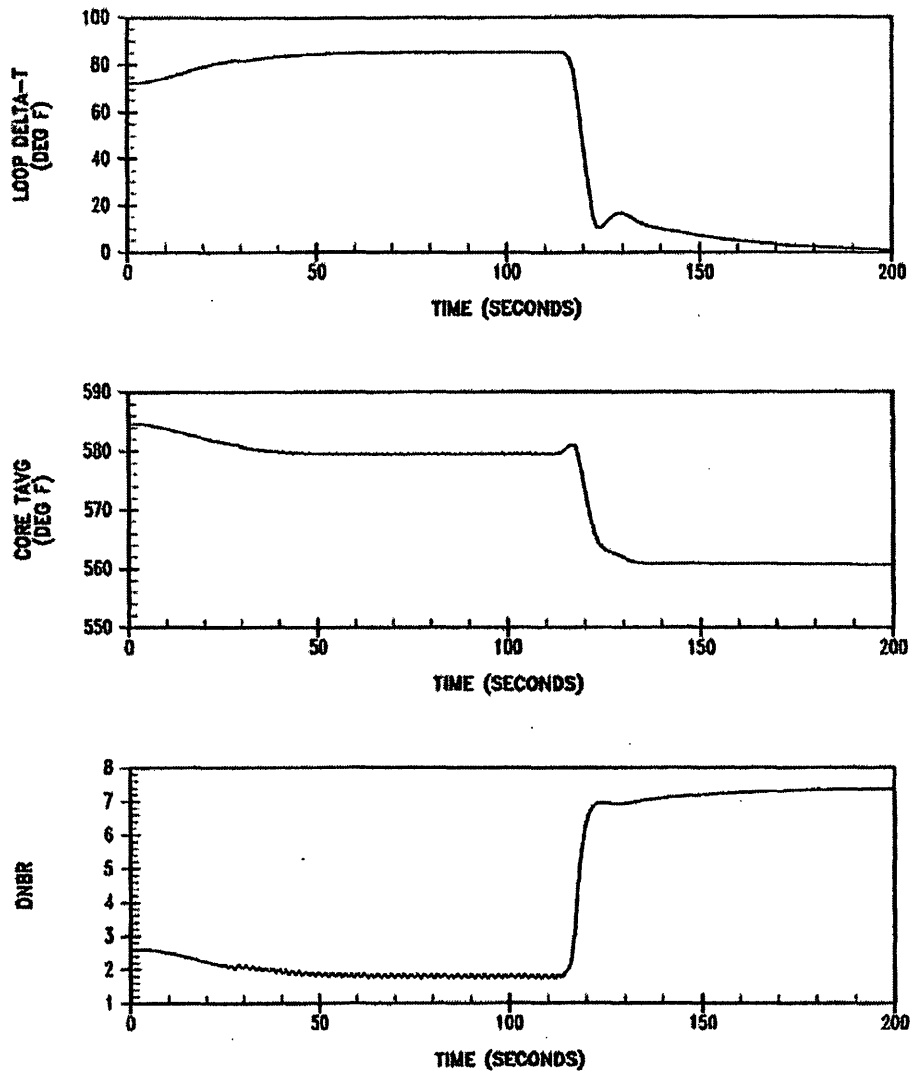


FIGURE 14.1-32B

LOOP DELTA-T, CORE AVERAGE TEMPERATURE  
AND DNBR TRANSIENTS FOR FEEDWATER  
CONTROL VALVE MALFUNCTION AT FULL  
POWER, AUTOMATIC ROD CONTROL

BEAVER VALLEY POWER STATION UNIT NO. 1  
UPDATED FINAL SAFETY ANALYSIS REPORT

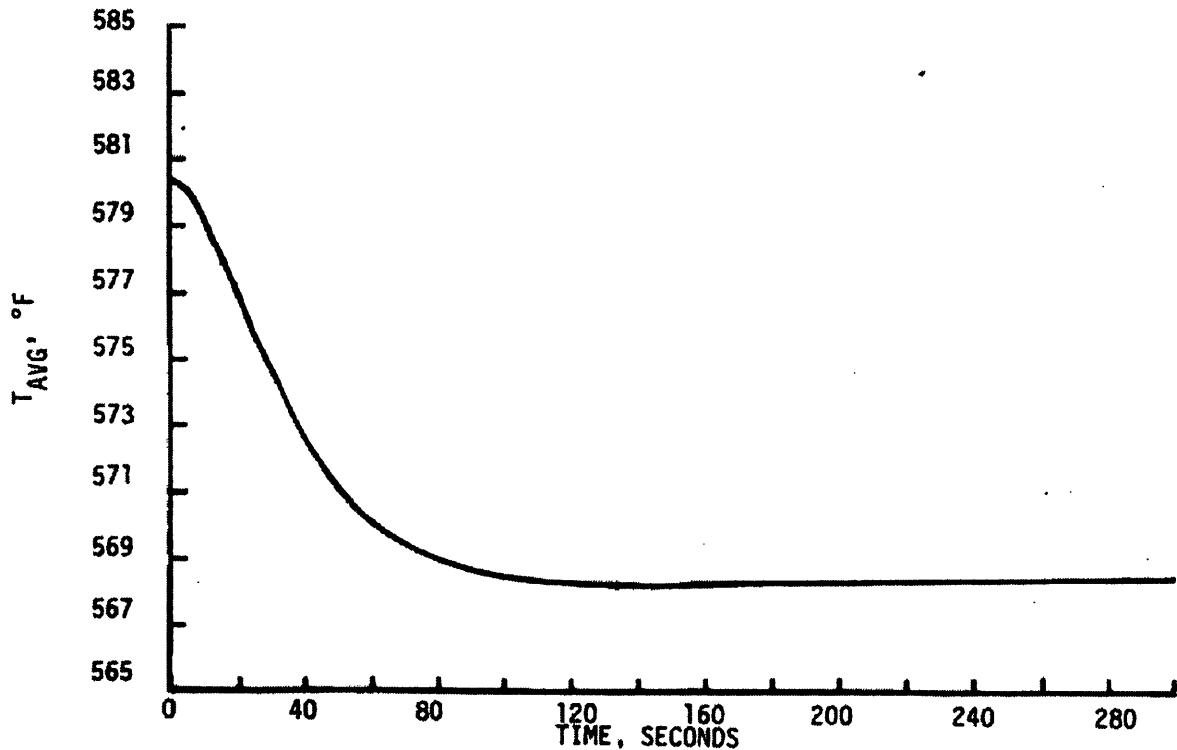
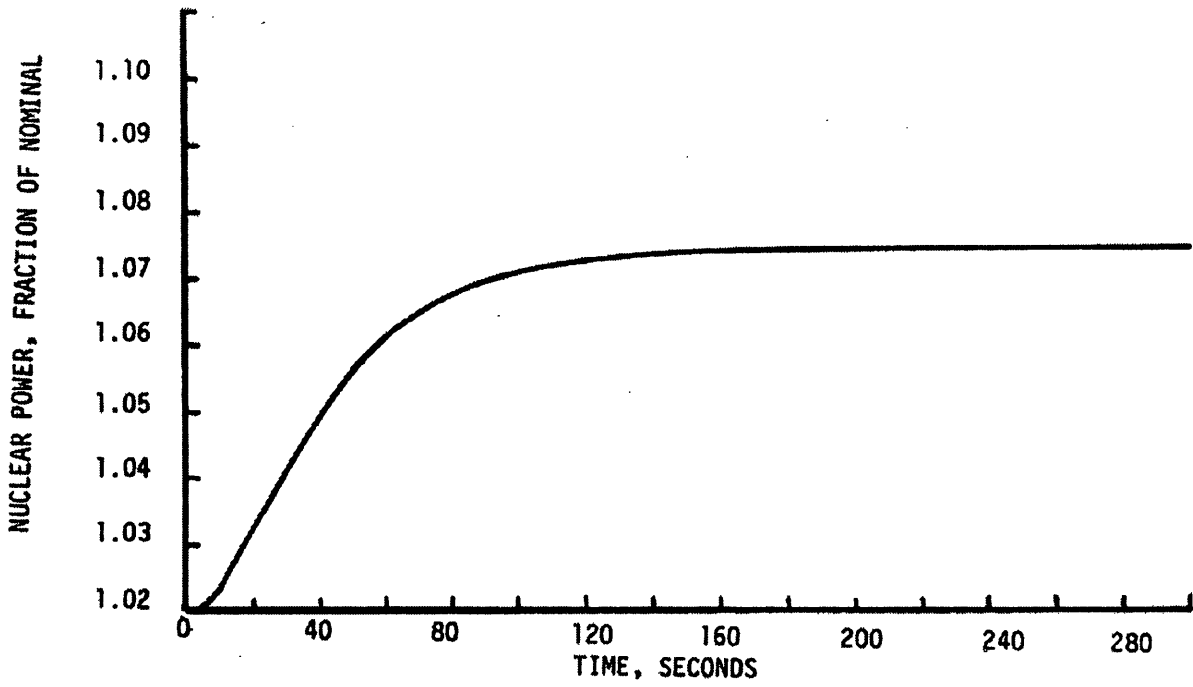


FIGURE 14-1-33  
EXCESSIVE LOAD INCREASE WITHOUT  
ROD CONTROL, BEGINNING OF LIFE  
BEAVER VALLEY POWER STATION UNIT NO. 1  
UPDATED FINAL SAFETY ANALYSIS REPORT

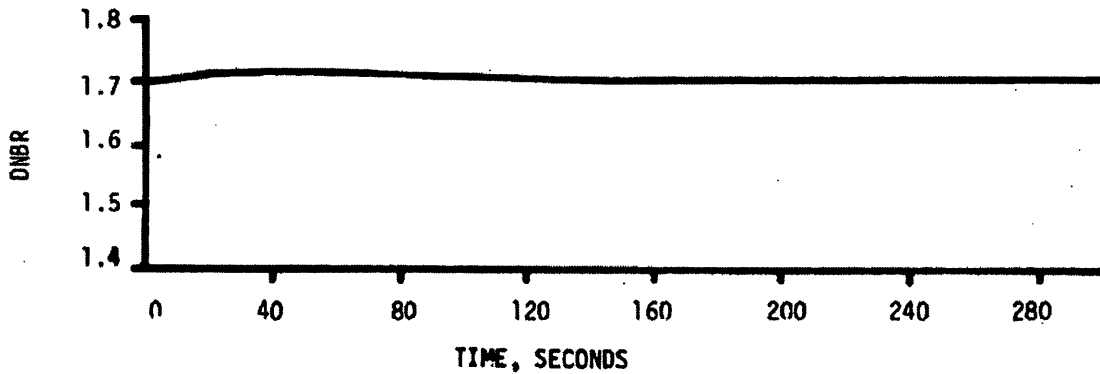
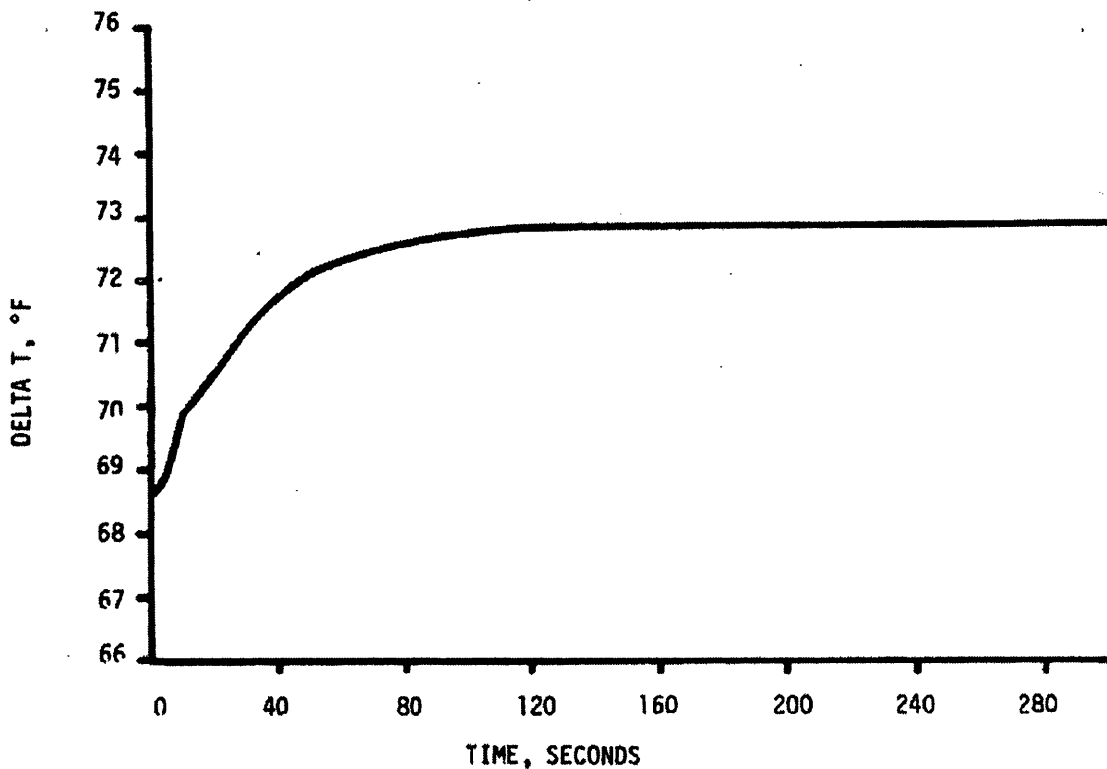
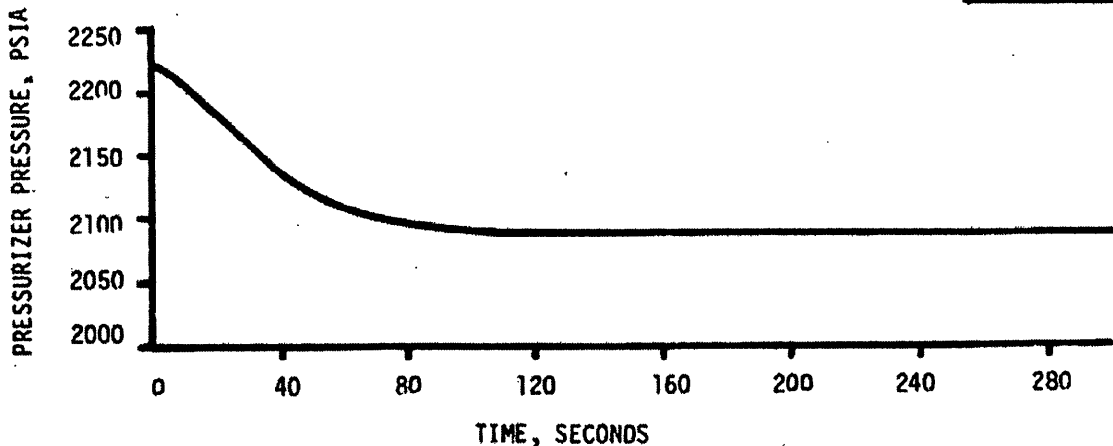


FIGURE 14-1-34  
EXCESSIVE LOAD INCREASE WITHOUT  
ROD CONTROL, BEGINNING OF LIFE  
BEAVER VALLEY POWER STATION UNIT NO. 1  
UPDATED FINAL SAFETY ANALYSIS REPORT

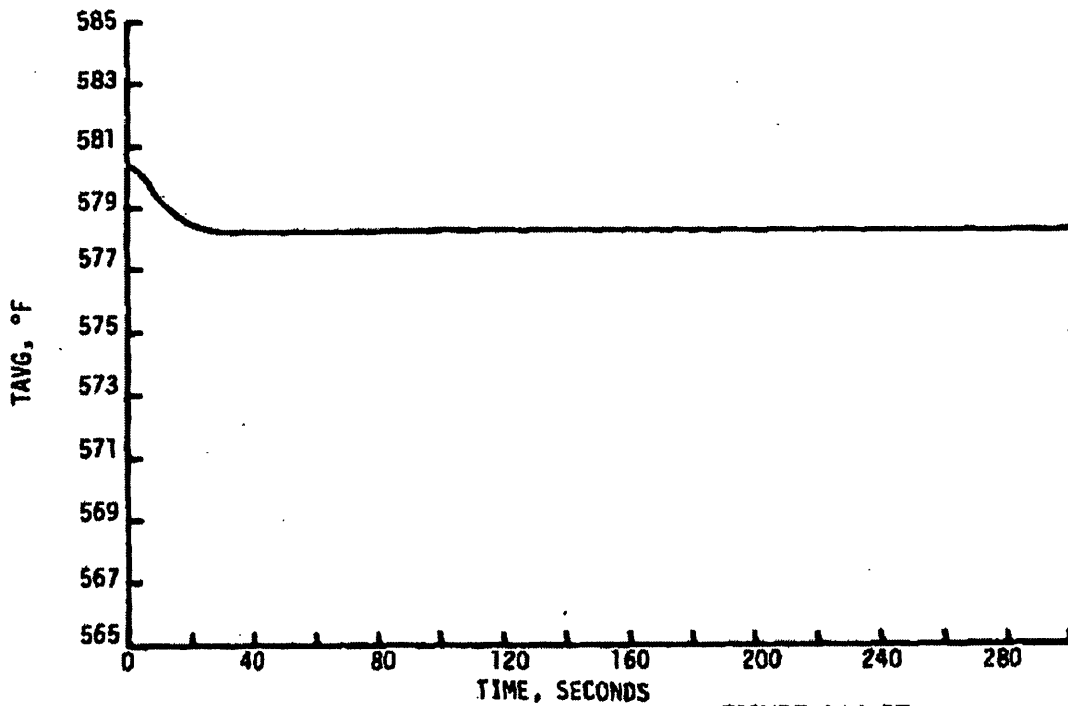
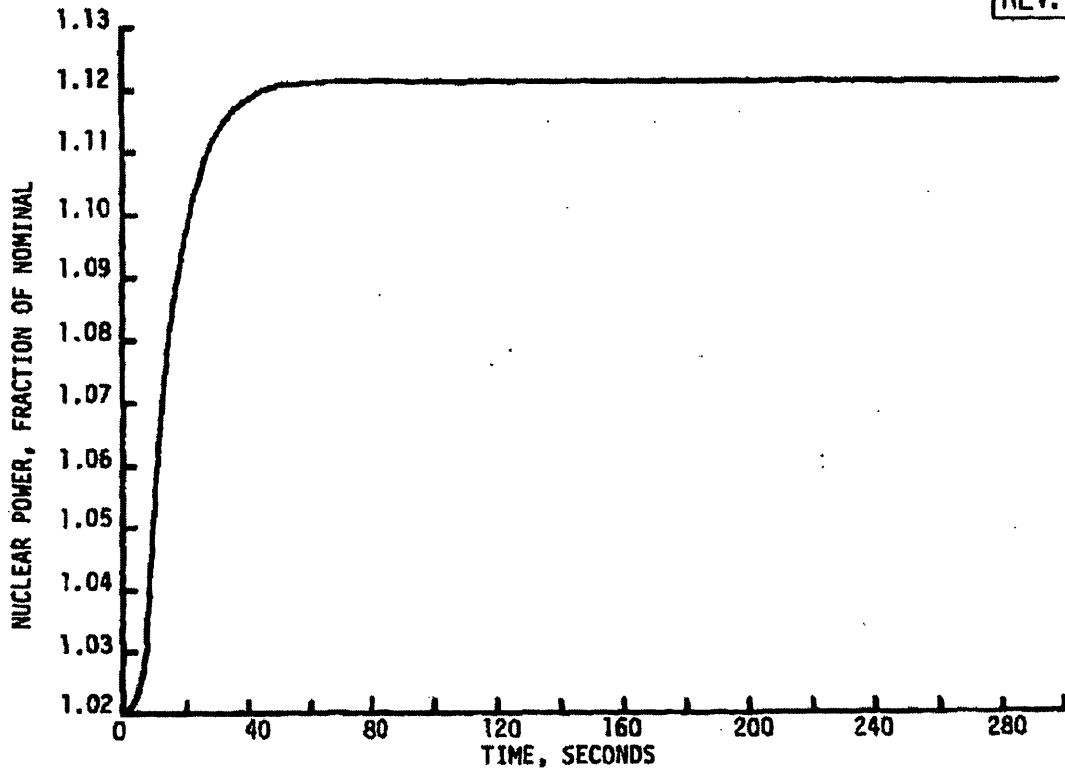


FIGURE 14.1-35  
EXCESSIVE LOAD INCREASE WITHOUT  
ROD CONTROL, END OF LIFE  
BEAVER VALLEY POWER STATION UNIT 1  
UPDATED FINAL SAFETY ANALYSIS REPORT

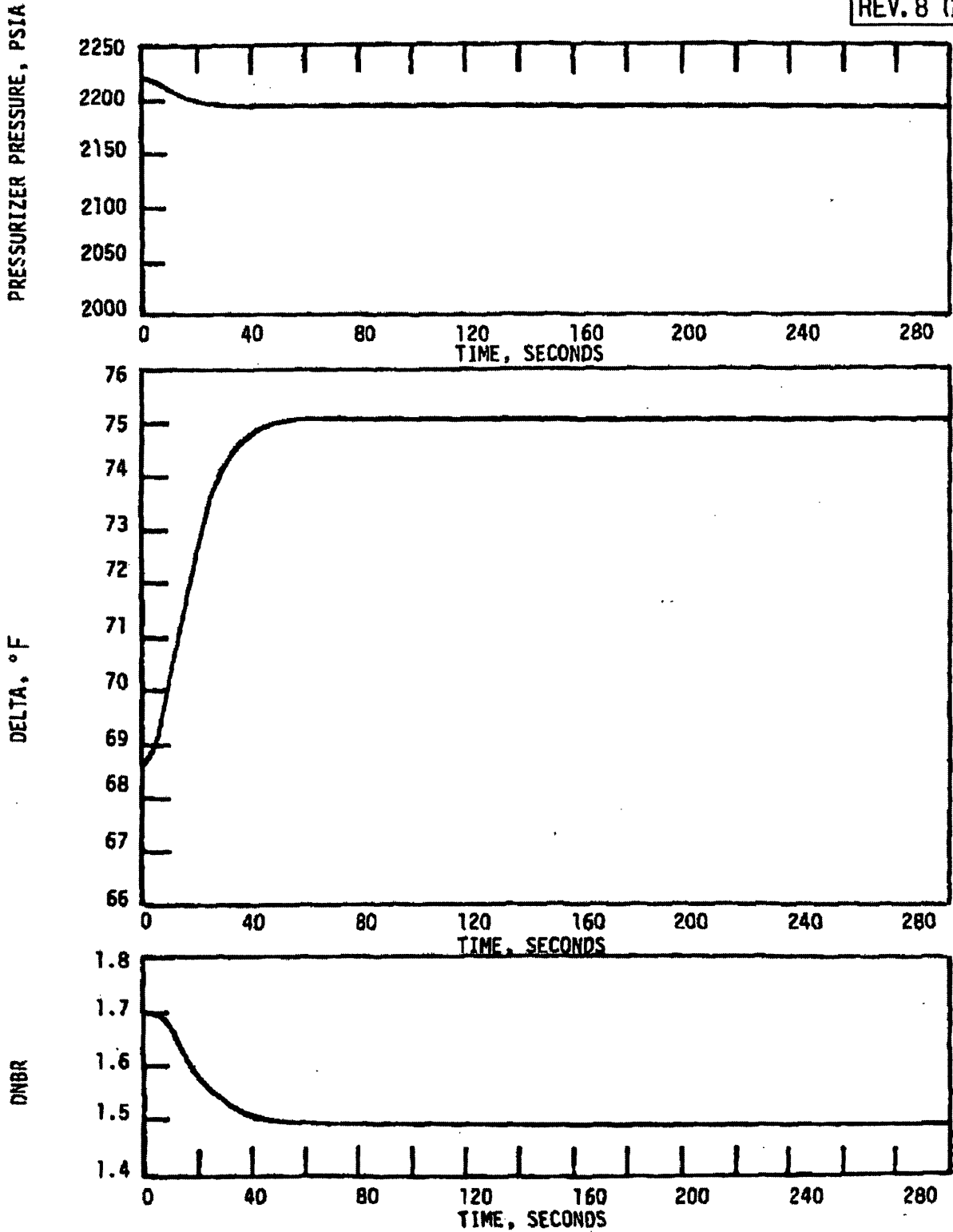


FIGURE 14.1-36  
EXCESSIVE LOAD INCREASE WITHOUT  
ROD CONTROL, END OF LIFE  
BEAVER VALLEY POWER STATION UNIT 1  
UPDATED FINAL SAFETY ANALYSIS REPORT

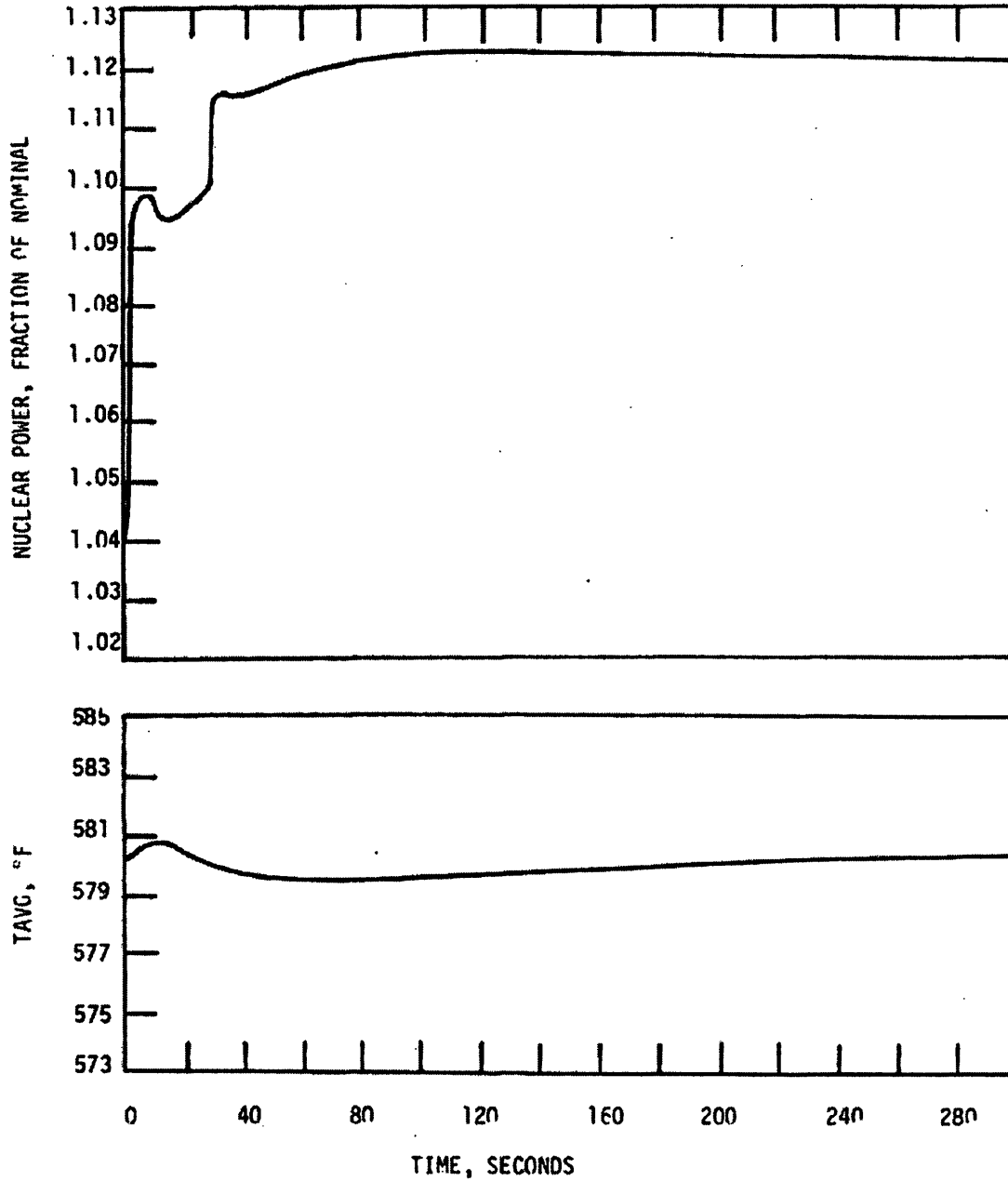
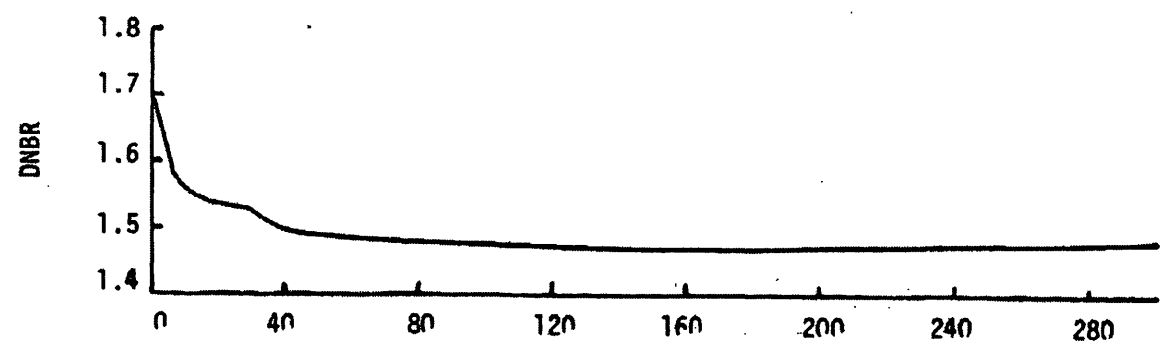
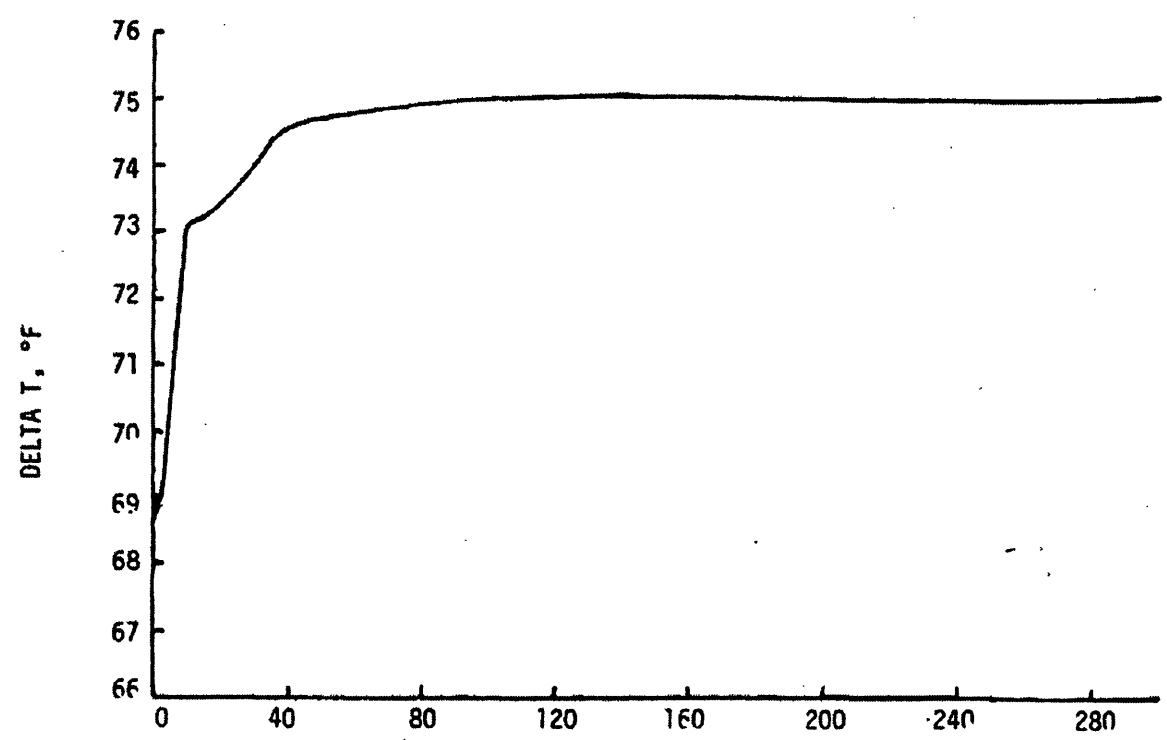
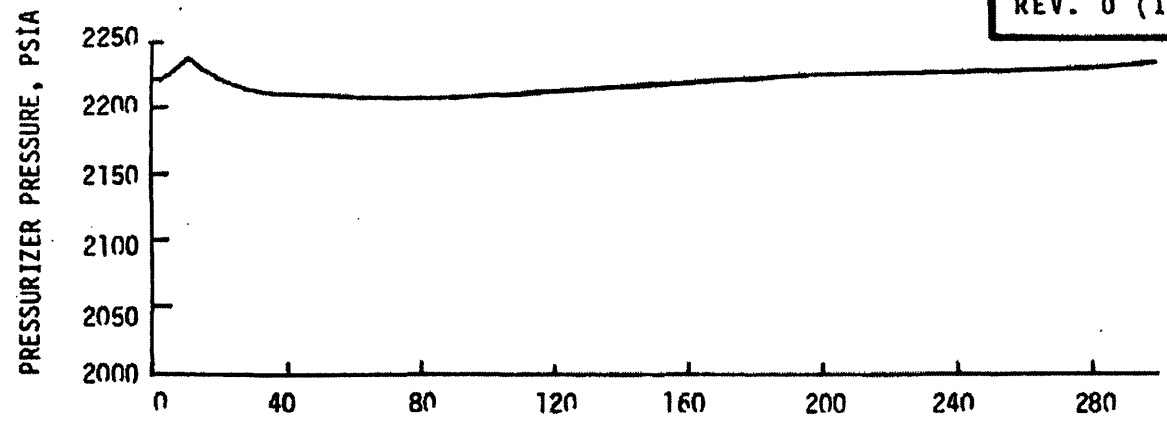


FIGURE 14.1-37  
EXCESSIVE LOAD INCREASE WITH  
ROD CONTROL, BEGINNING OF LIFE  
BEAVER VALLEY POWER STATION UNIT NO. 1  
UPDATED FINAL SAFETY ANALYSIS REPORT



TIME, SECONDS

FIGURE 14-1-38  
EXCESSIVE LOAD INCREASE WITH  
ROD CONTROL, BEGINNING OF LIFE  
BEAVER VALLEY POWER STATION UNIT NO. 1  
UPDATED FINAL SAFETY ANALYSIS REPORT

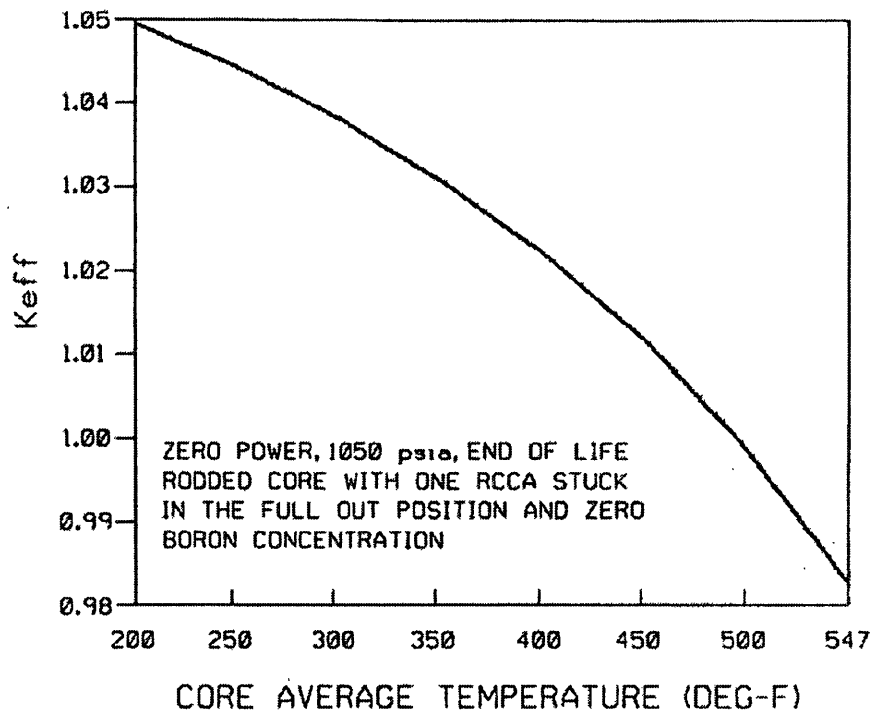


FIGURE 14.1-41

VARIATION OF  $K_{eff}$  WITH  
CORE TEMPERATURESBEAVER VALLEY POWER STATION UNIT NO. 1  
UPDATED FINAL SAFETY ANALYSIS REPORT



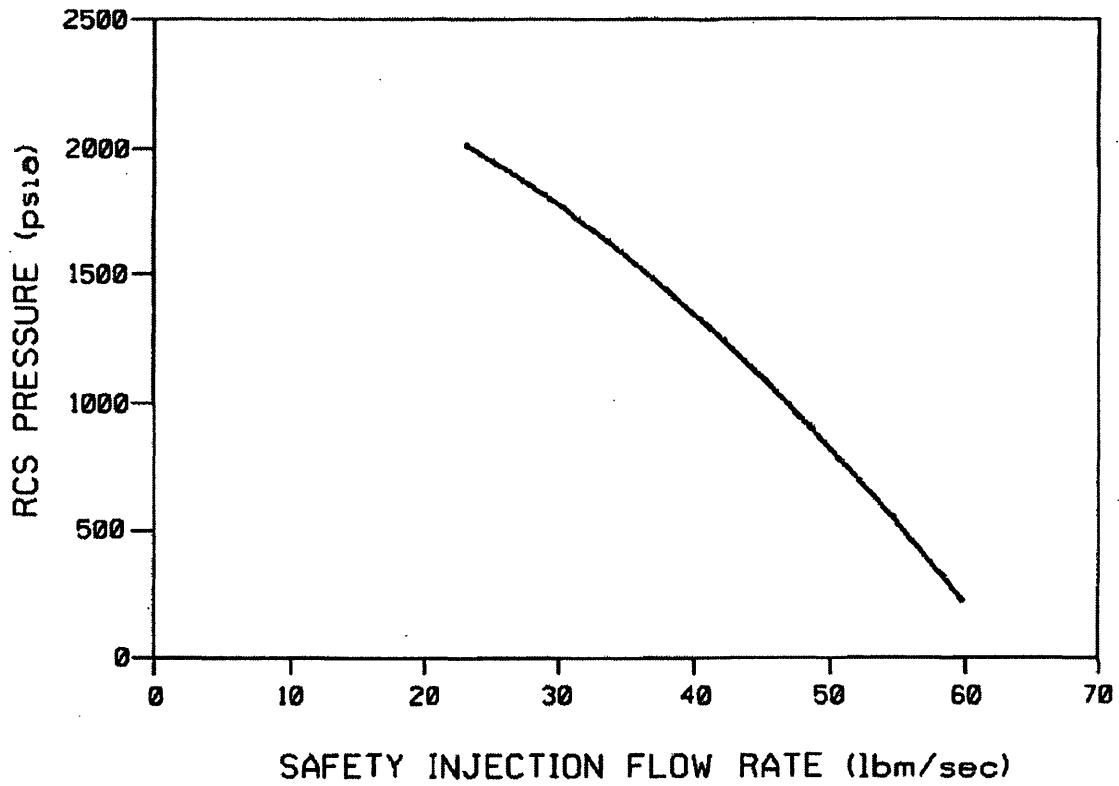


FIGURE 14.1-42

SAFETY INJECTION FLOW  
VERSUS RCS PRESSURE

BEAVER VALLEY POWER STATION UNIT NO. 1  
UPDATED FINAL SAFETY ANALYSIS REPORT

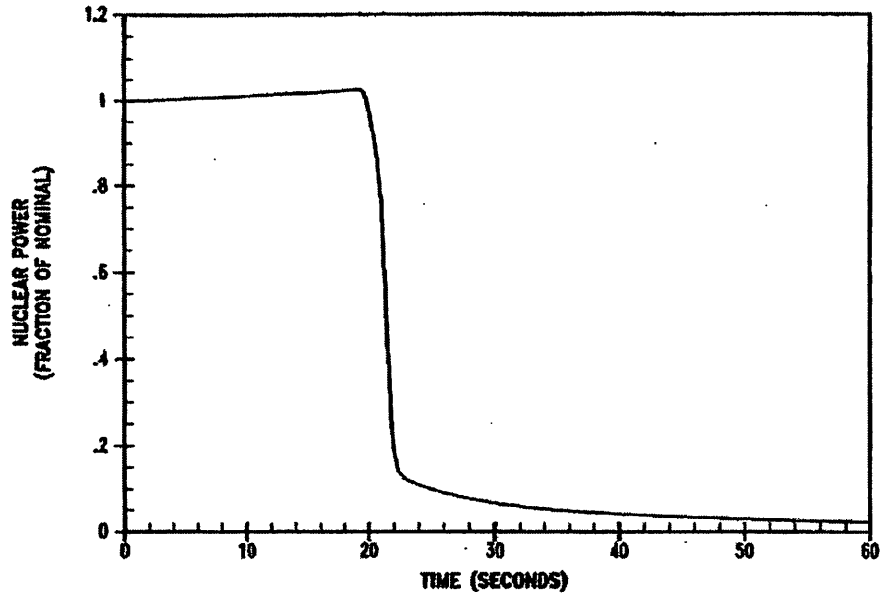


FIGURE 14.1-44

NUCLEAR POWER TRANSIENT FOR  
ACCIDENTAL RCS DEPRESSURIZATION

BEAVER VALLEY POWER STATION UNIT NO. 1  
UPDATED FINAL SAFETY ANALYSIS REPORT

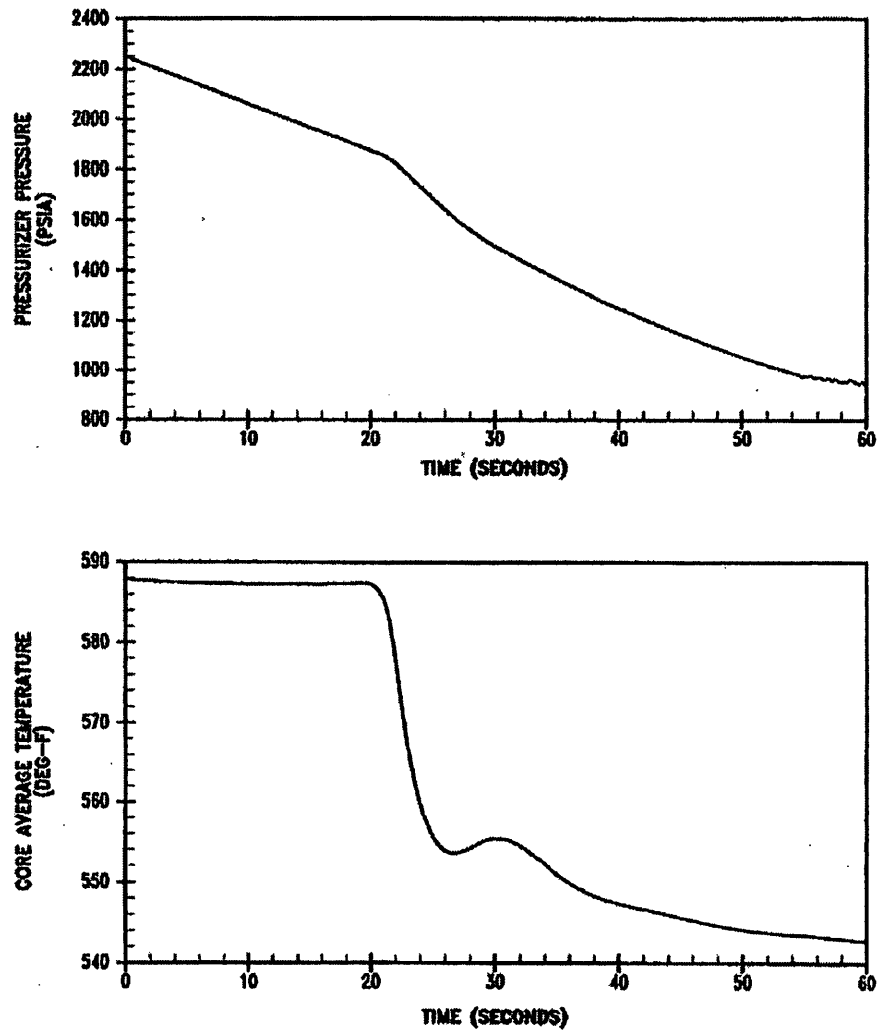


FIGURE 14.1-45

PRESSURIZER PRESSURE AND CORE  
 AVERAGE TEMPERATURE TRANSIENTS  
 FOR ACCIDENTAL RCS DEPRESSURIZATION

BEAVER VALLEY POWER STATION UNIT NO. 1  
 UPDATED FINAL SAFETY ANALYSIS REPORT

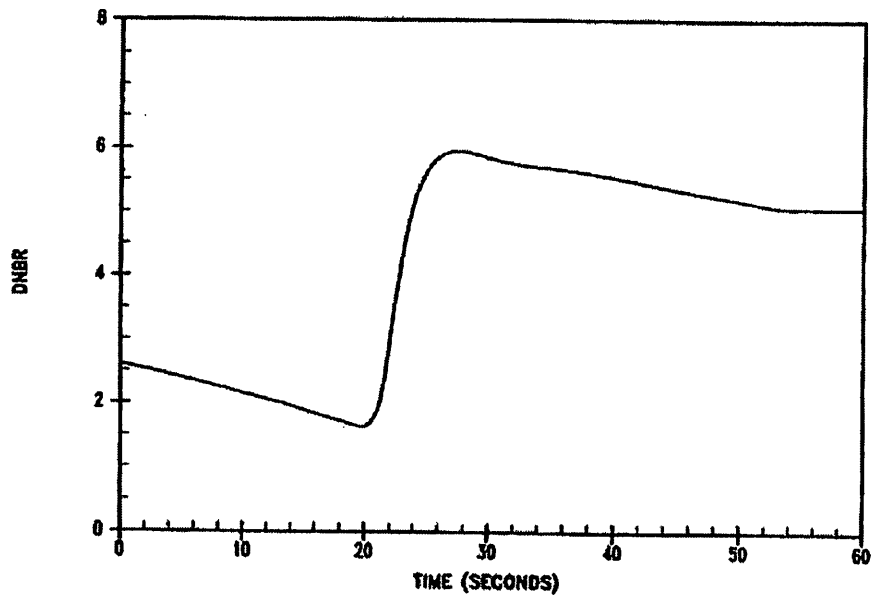
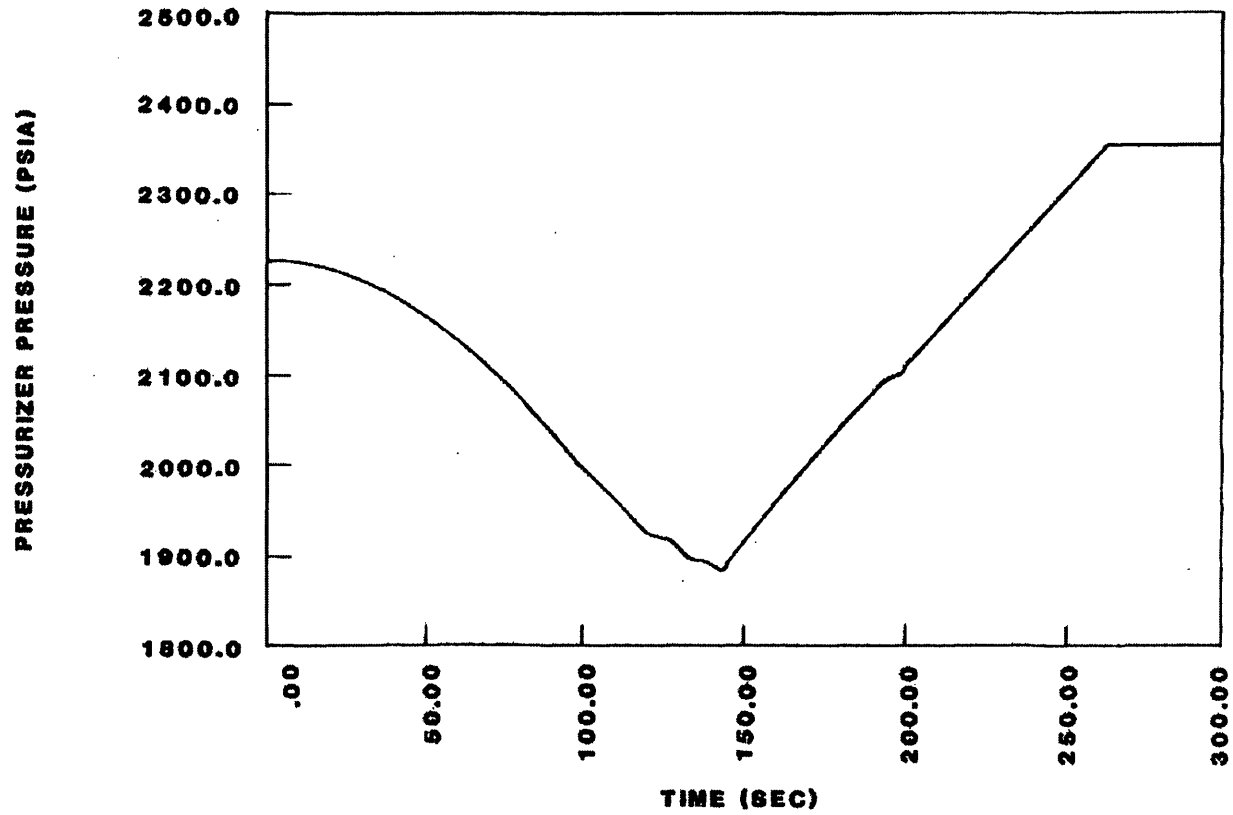
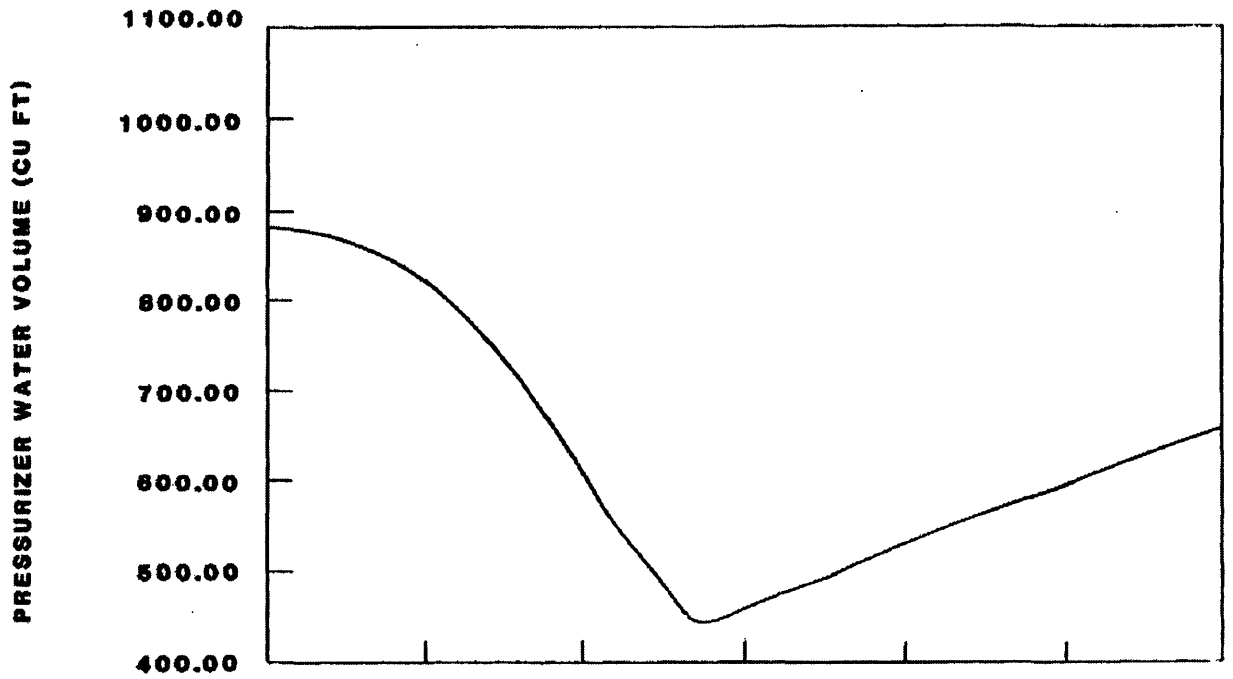
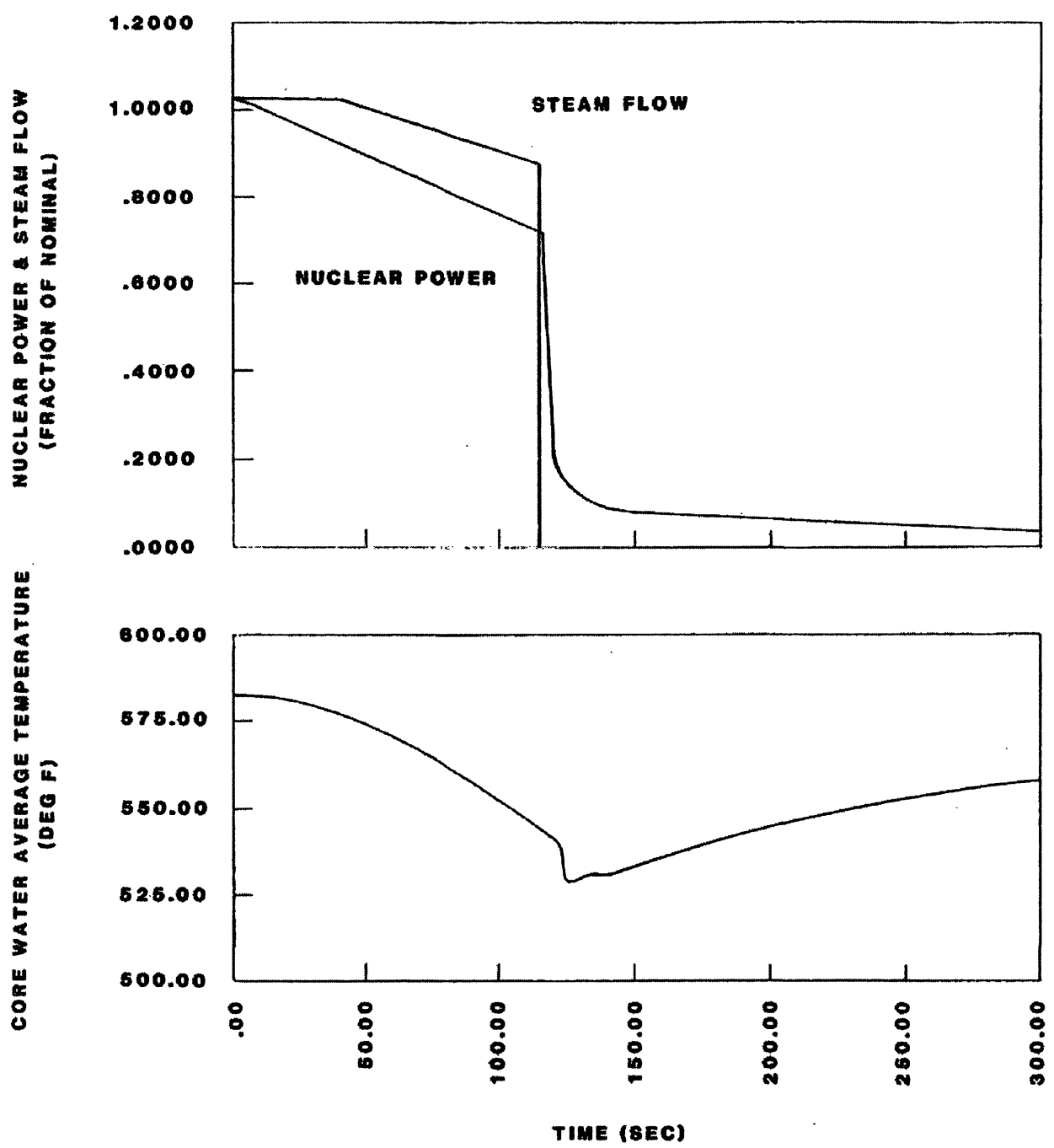


FIGURE 14.1-46

DNBR TRANSIENT  
FOR ACCIDENTAL RCS DEPRESSURIZATION  
BEAVER VALLEY POWER STATION UNIT NO. 1  
UPDATED FINAL SAFETY ANALYSIS REPORT



**FIGURE 14.1-47**  
**SPURIOUS ACTUATION OF SAFETY**  
**INJECTION SYSTEM AT POWER**  
**BEAVER VALLEY POWER STATION UNIT NO. 1**  
**UPDATED FINAL SAFETY ANALYSIS REPORT**



**FIGURE 14.1-48**  
**SPURIOUS ACTUATION OF SAFETY**  
**INJECTION SYSTEM AT POWER**  
**BEAVER VALLEY POWER STATION UNIT NO. 1**  
**UPDATED FINAL SAFETY ANALYSIS REPORT**

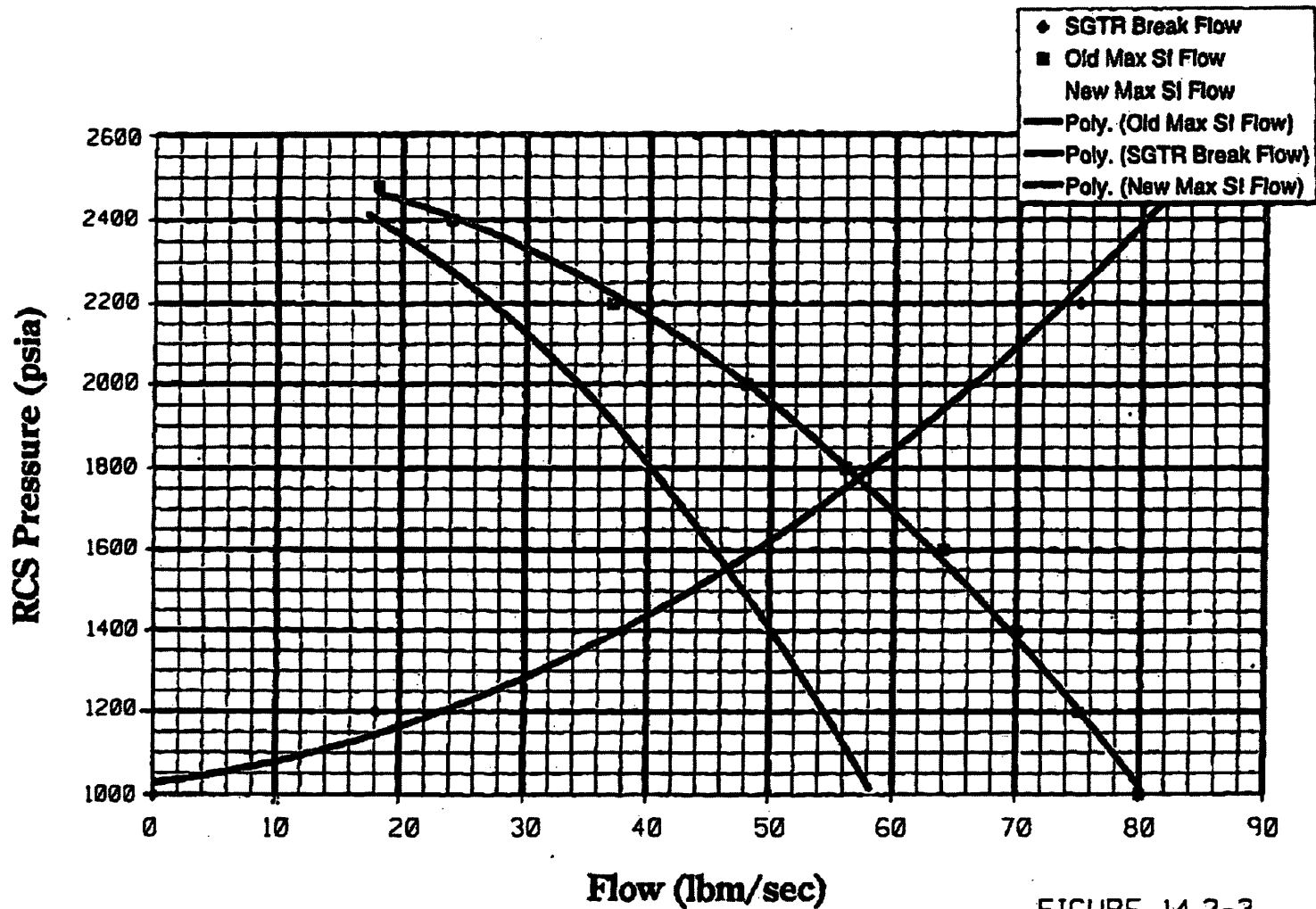


FIGURE 14.2-3

STEAM GENERATOR TUBE RUPTURE  
 OLD/NEW EQUILIBRIUM BREAK FLOW

BEAVER VALLEY POWER STATION UNIT NO. 1  
 UPDATED FINAL SAFETY ANALYSIS REPORT

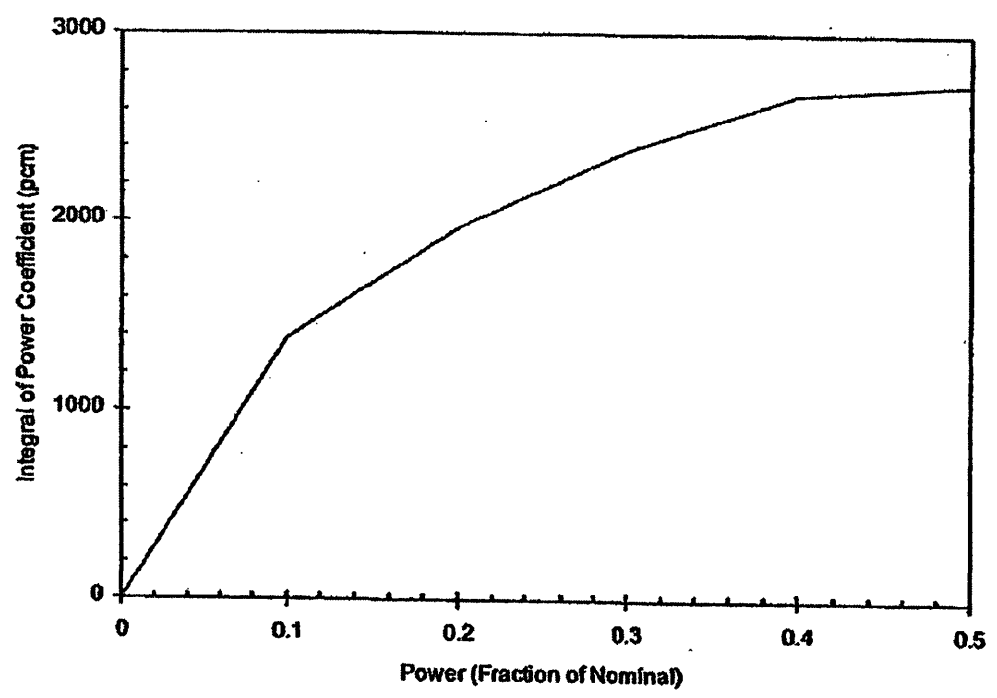


FIGURE 14.2-4

VARIATION OF REACTIVITY WITH POWER AT  
CONSTANT CORE AVERAGE TEMPERATURE

BEAVER VALLEY POWER STATION UNIT NO. 1  
UPDATED FINAL SAFETY ANALYSIS REPORT



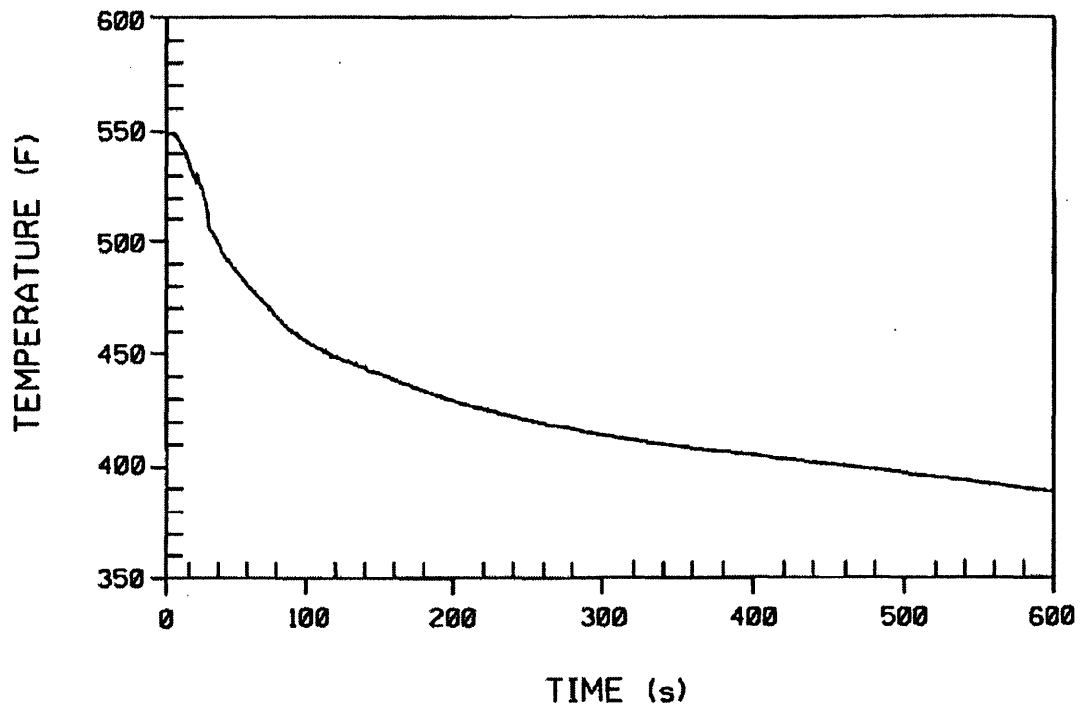


FIGURE 14.2-5

CORE AVERAGE TEMPERATURE TRANSIENT  
FOR STEAM LINE BREAK AT EXIT OF STEAM  
GENERATOR WITH OFFSITE POWER

BEAVER VALLEY POWER STATION UNIT NO. 1  
UPDATED FINAL SAFETY ANALYSIS REPORT

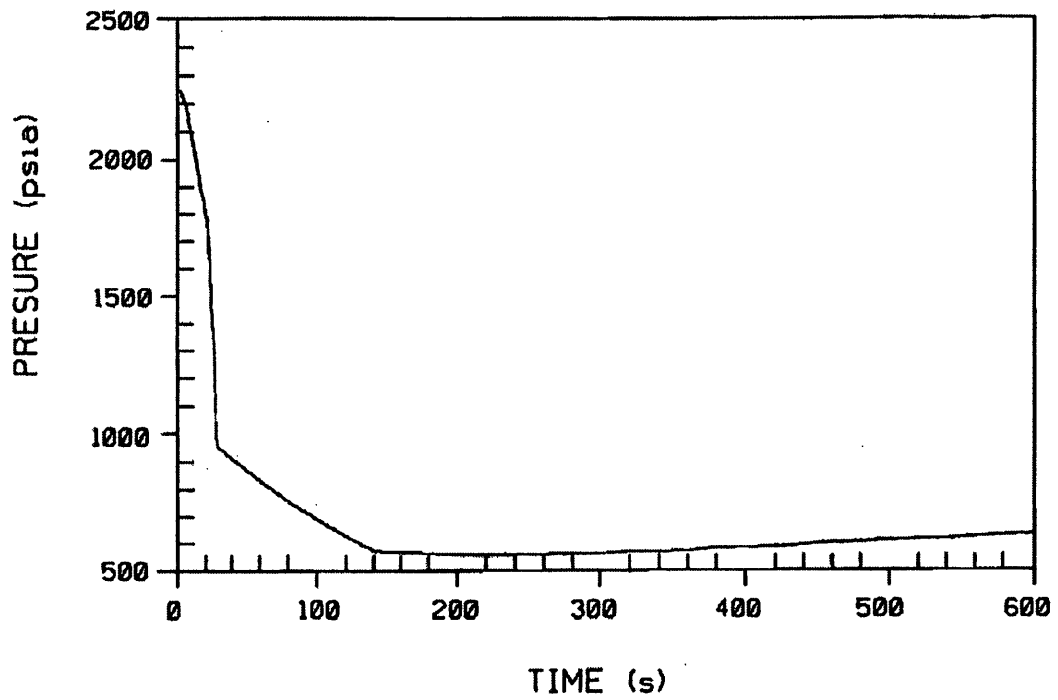


FIGURE 14.2-6

RCS PRESSURE TRANSIENT FOR STEAM  
LINE BREAK AT EXIT OF STEAM GENERATOR  
WITH OFFSITE POWER

BEAVER VALLEY POWER STATION UNIT NO. 1  
UPDATED FINAL SAFETY ANALYSIS REPORT

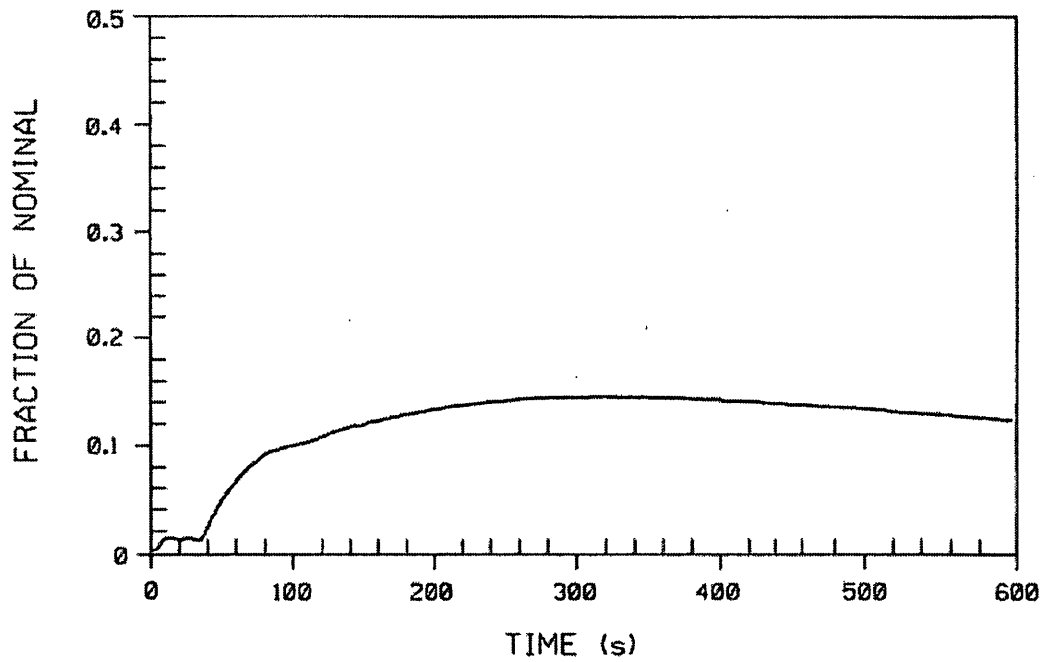


FIGURE 14.2-7

CORE HEAT FLUX TRANSIENT FOR STEAM  
LINE BREAK AT EXIT OF STEAM GENERATOR  
WITH OFFSITE POWER

BEAVER VALLEY POWER STATION UNIT NO. 1  
UPDATED FINAL SAFETY ANALYSIS REPORT

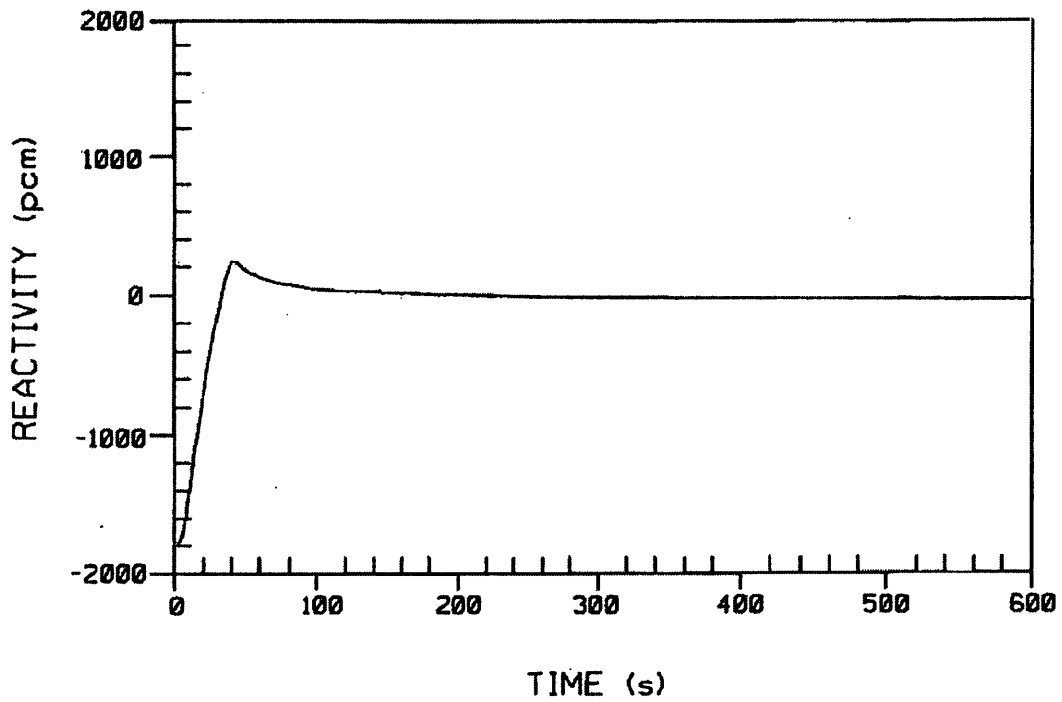


FIGURE 14.2-8

CORE REACTIVITY TRANSIENT FOR STEAM  
LINE BREAK AT EXIT OF STEAM GENERATOR  
WITH OFFSITE POWER

BEAVER VALLEY POWER STATION UNIT NO. 1  
UPDATED FINAL SAFETY ANALYSIS REPORT

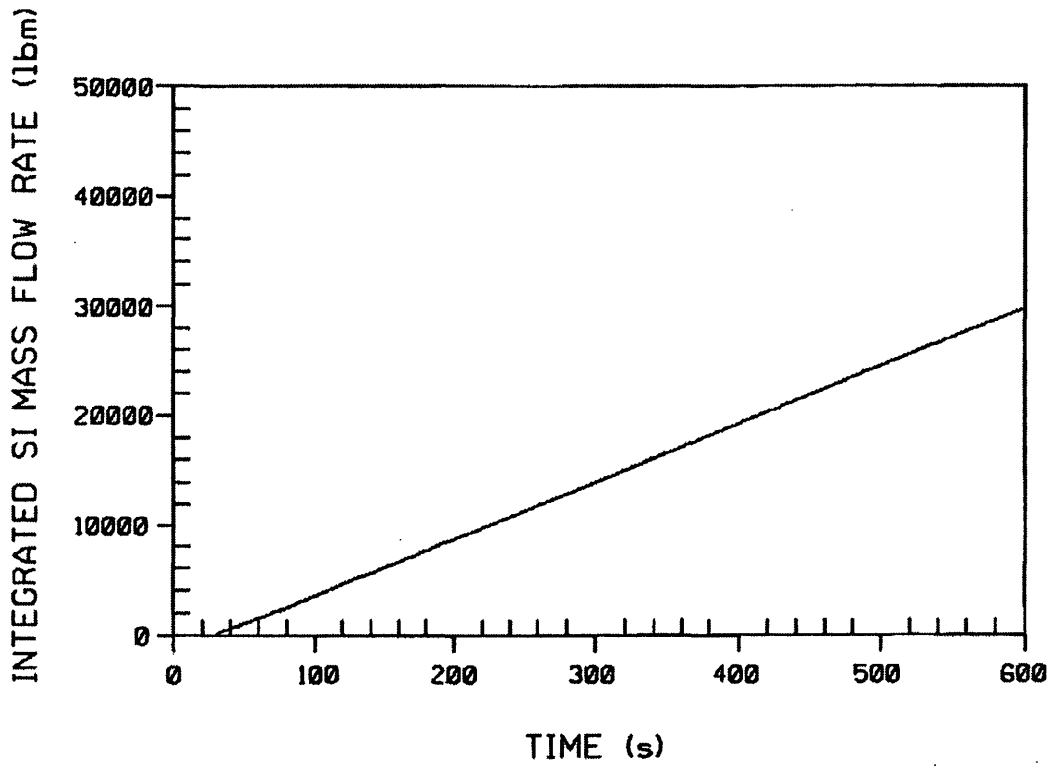


FIGURE 14.2-9

INTEGRATED SAFETY INJECTION FLOW RATE  
OF BORATED WATER FOR STEAM LINE  
BREAK AT EXIT OF STEAM GENERATOR  
WITH OFFSITE POWER

BEAVER VALLEY POWER STATION UNIT NO. 1  
UPDATED FINAL SAFETY ANALYSIS REPORT

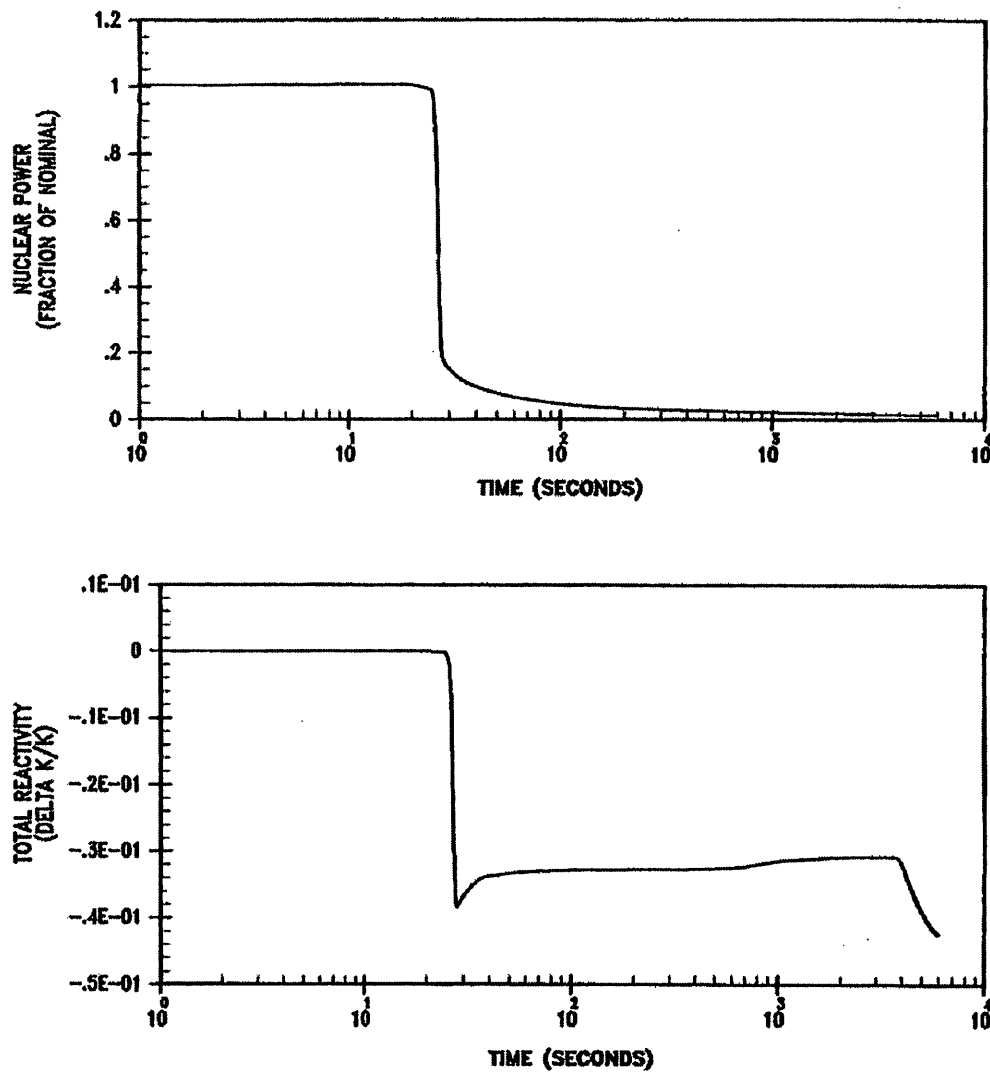


FIGURE 14.2-10A

NUCLEAR POWER AND TOTAL REACTIVITY  
TRANSIENTS FOR MAJOR RUPTURE  
OF A MAIN FEEDWATER PIPE WITH  
OFFSITE POWER AVAILABLE

BEAVER VALLEY POWER STATION UNIT NO. 1  
UPDATED FINAL SAFETY ANALYSIS REPORT

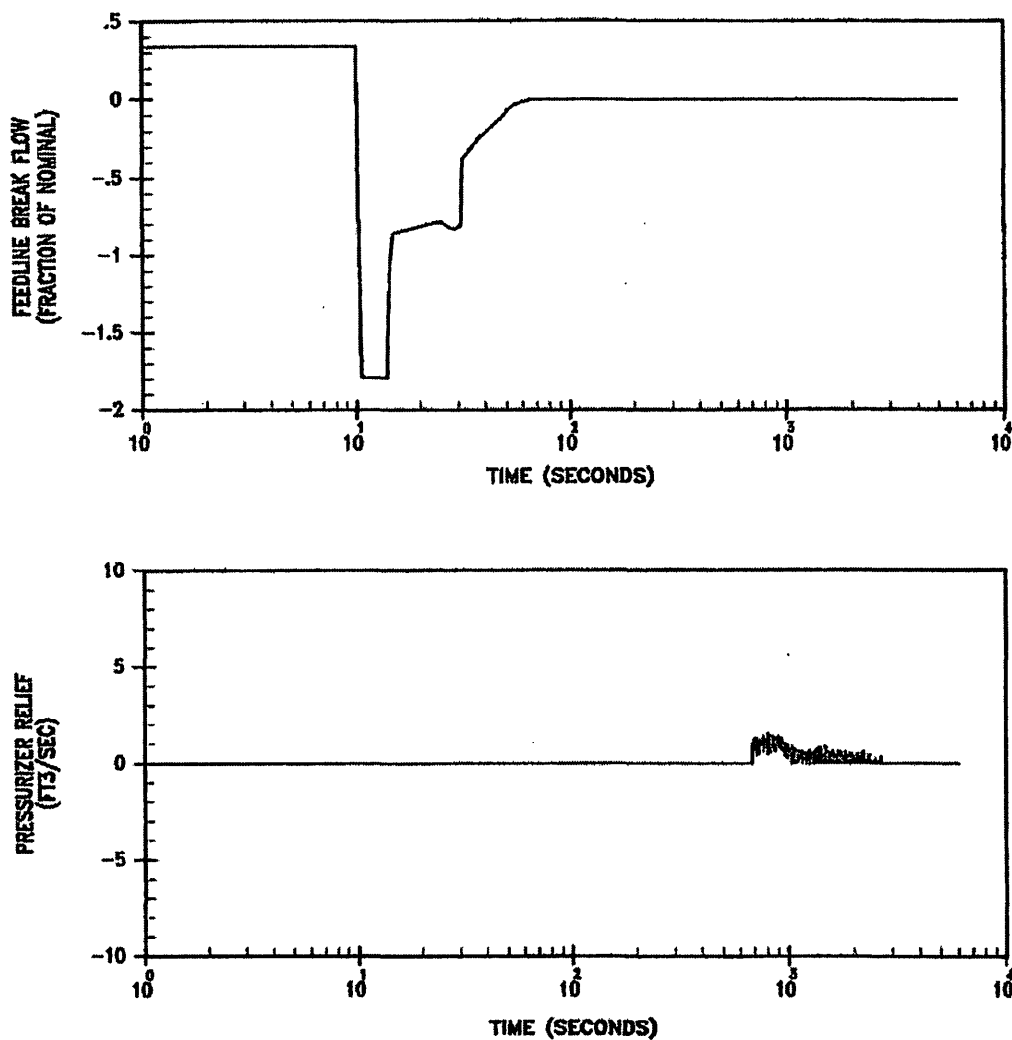


FIGURE 14.2-10B

FEEDLINE BREAK FLOW AND PRESSURIZER  
RELIEF TRANSIENTS FOR MAJOR RUPTURE  
OF A MAIN FEEDWATER PIPE WITH  
OFFSITE POWER AVAILABLE

BEAVER VALLEY POWER STATION UNIT NO. 1  
UPDATED FINAL SAFETY ANALYSIS REPORT

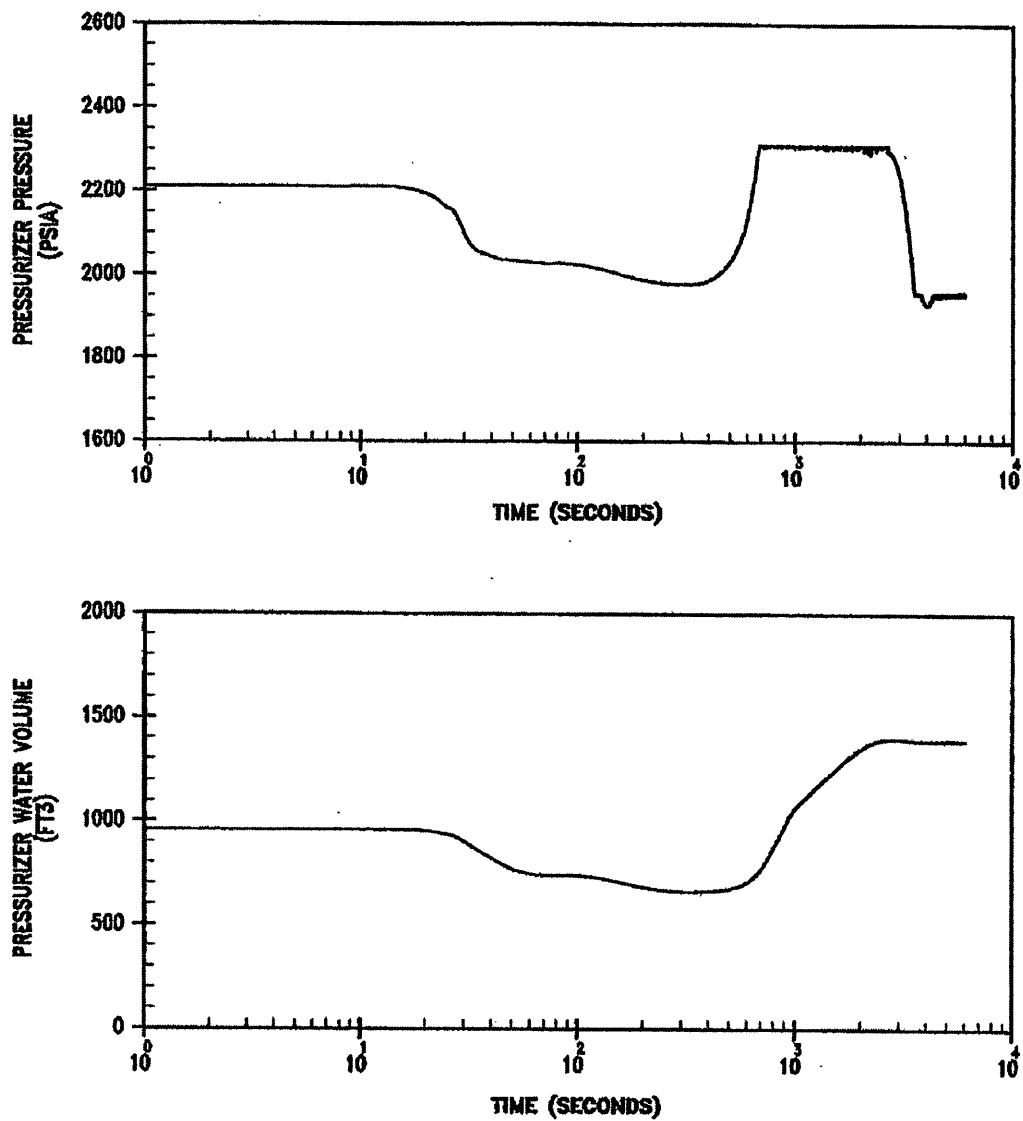


FIGURE 14.2-10C

PRESSURIZER PRESSURE AND PRESSURIZER  
WATER VOLUME TRANSIENTS FOR MAJOR  
RUPTURE OF A MAIN FEEDWATER PIPE  
WITH OFFSITE POWER AVAILABLE

BEAVER VALLEY POWER STATION UNIT NO. 1  
UPDATED FINAL SAFETY ANALYSIS REPORT



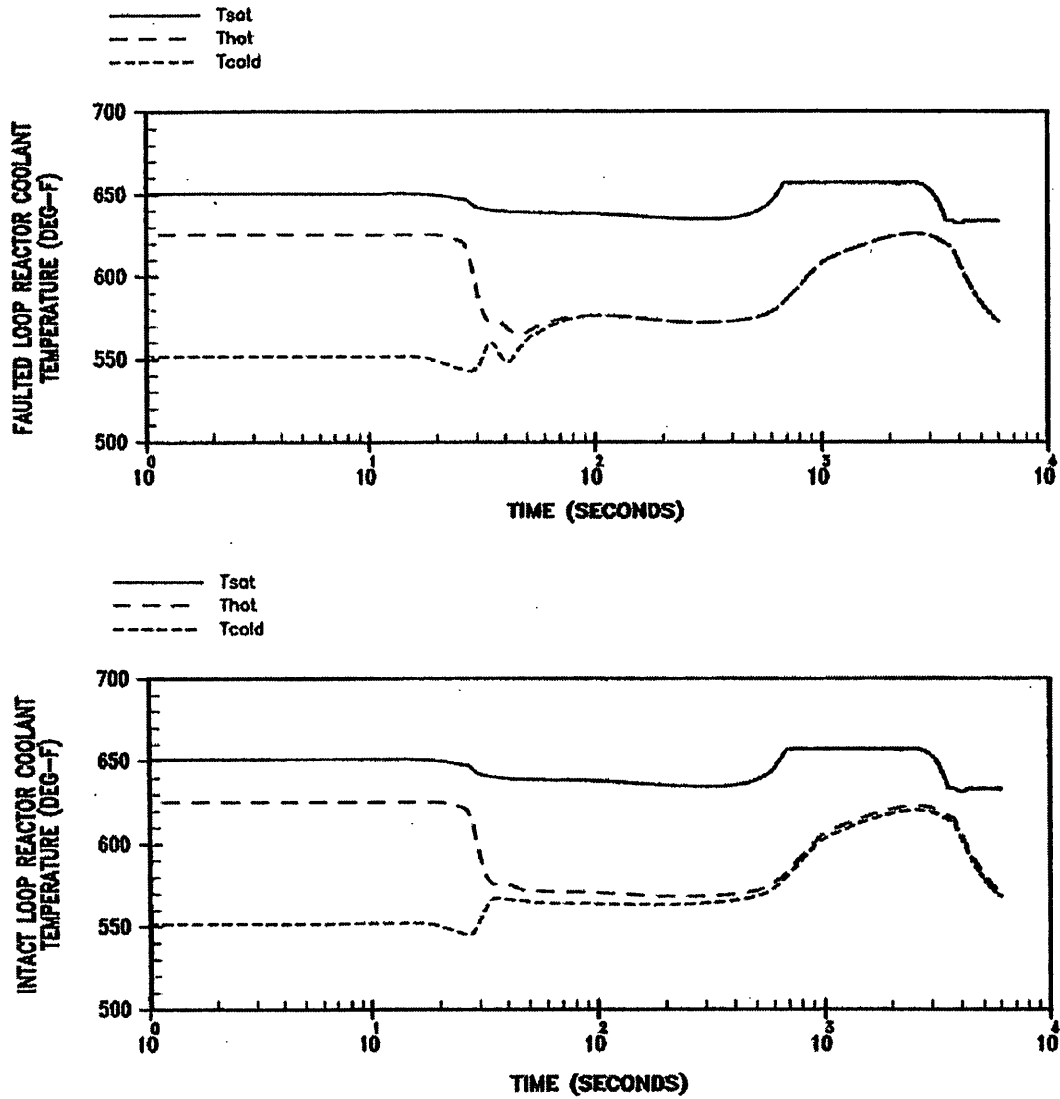


FIGURE 14.2-10D

LOOP TEMPERATURES FOR MAJOR RUPTURE  
OF A MAIN FEEDWATER PIPE WITH  
OFFSITE POWER AVAILABLE

BEAVER VALLEY POWER STATION UNIT NO. 1  
UPDATED FINAL SAFETY ANALYSIS REPORT

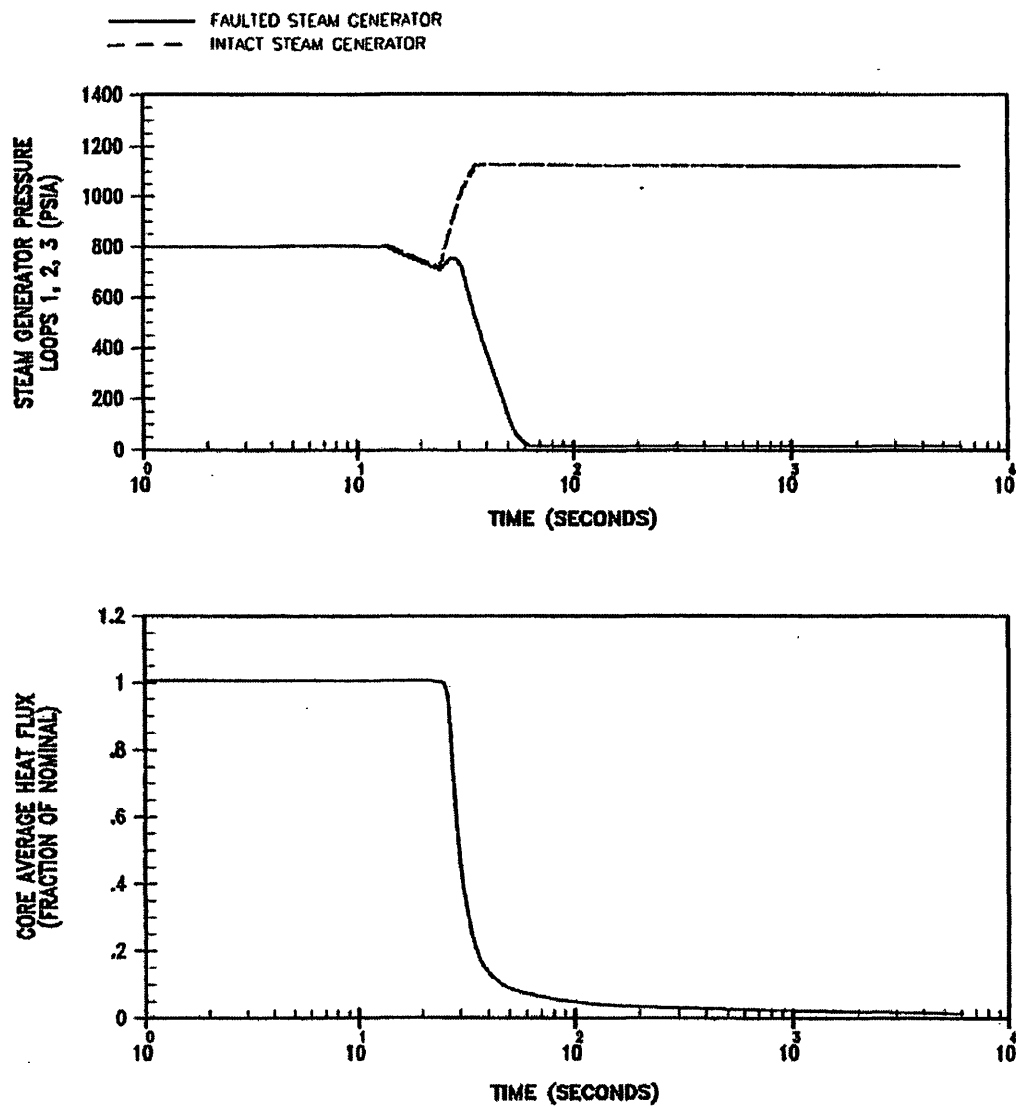


FIGURE 14.2-10E

STEAM GENERATOR PRESSURE AND CORE  
 HEAT FLUX TRANSIENTS FOR MAJOR RUPTURE  
 OF A MAIN FEEDWATER PIPE WITH  
 OFFSITE POWER AVAILABLE

BEAVER VALLEY POWER STATION UNIT NO. 1  
 UPDATED FINAL SAFETY ANALYSIS REPORT

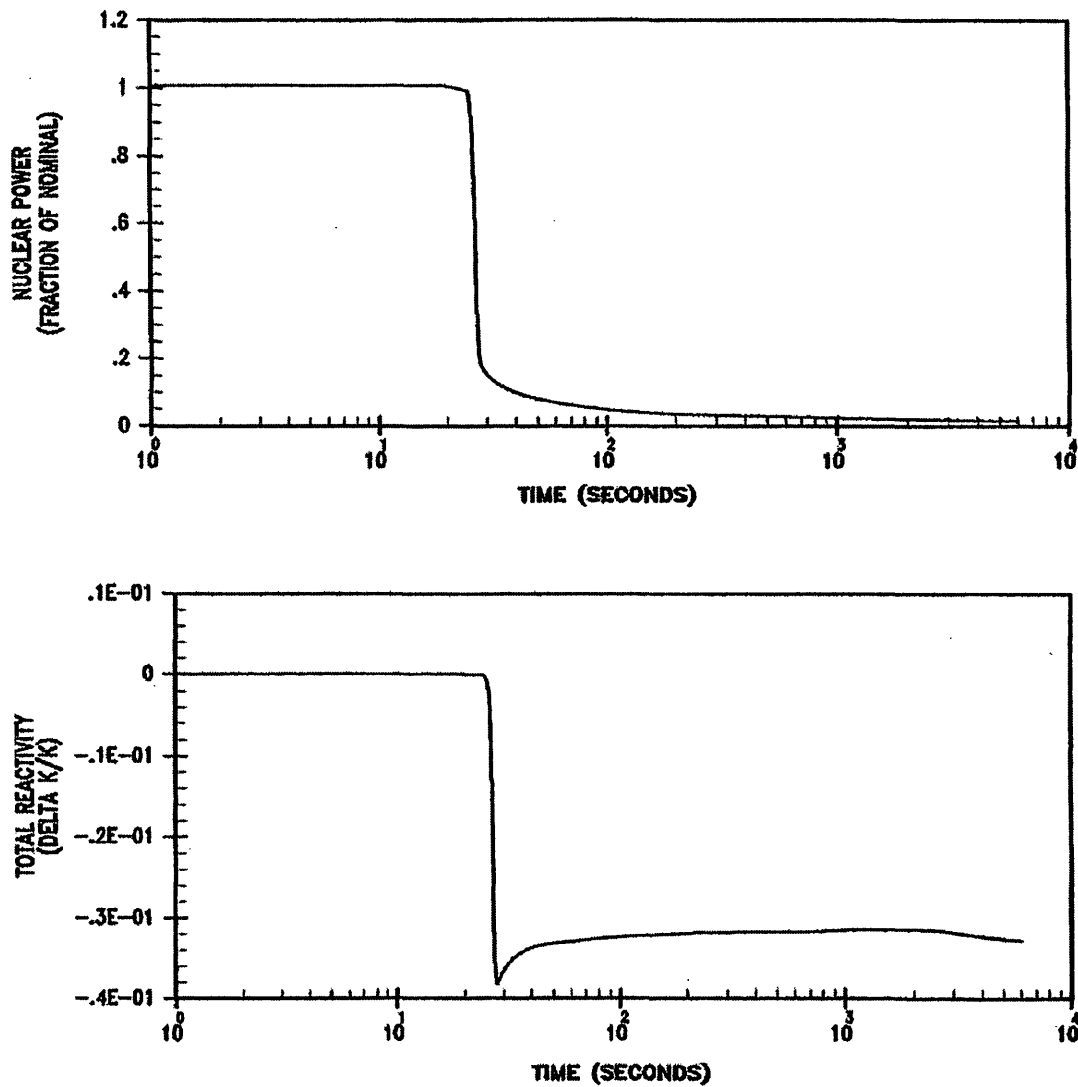


FIGURE 14.2-10F

NUCLEAR POWER AND TOTAL REACTIVITY  
TRANSIENTS FOR A MAJOR RUPTURE  
OF A MAIN FEEDWATER PIPE WITHOUT  
OFFSITE POWER AVAILABLE

BEAVER VALLEY POWER STATION UNIT NO. 1  
UPDATED FINAL SAFETY ANALYSIS REPORT

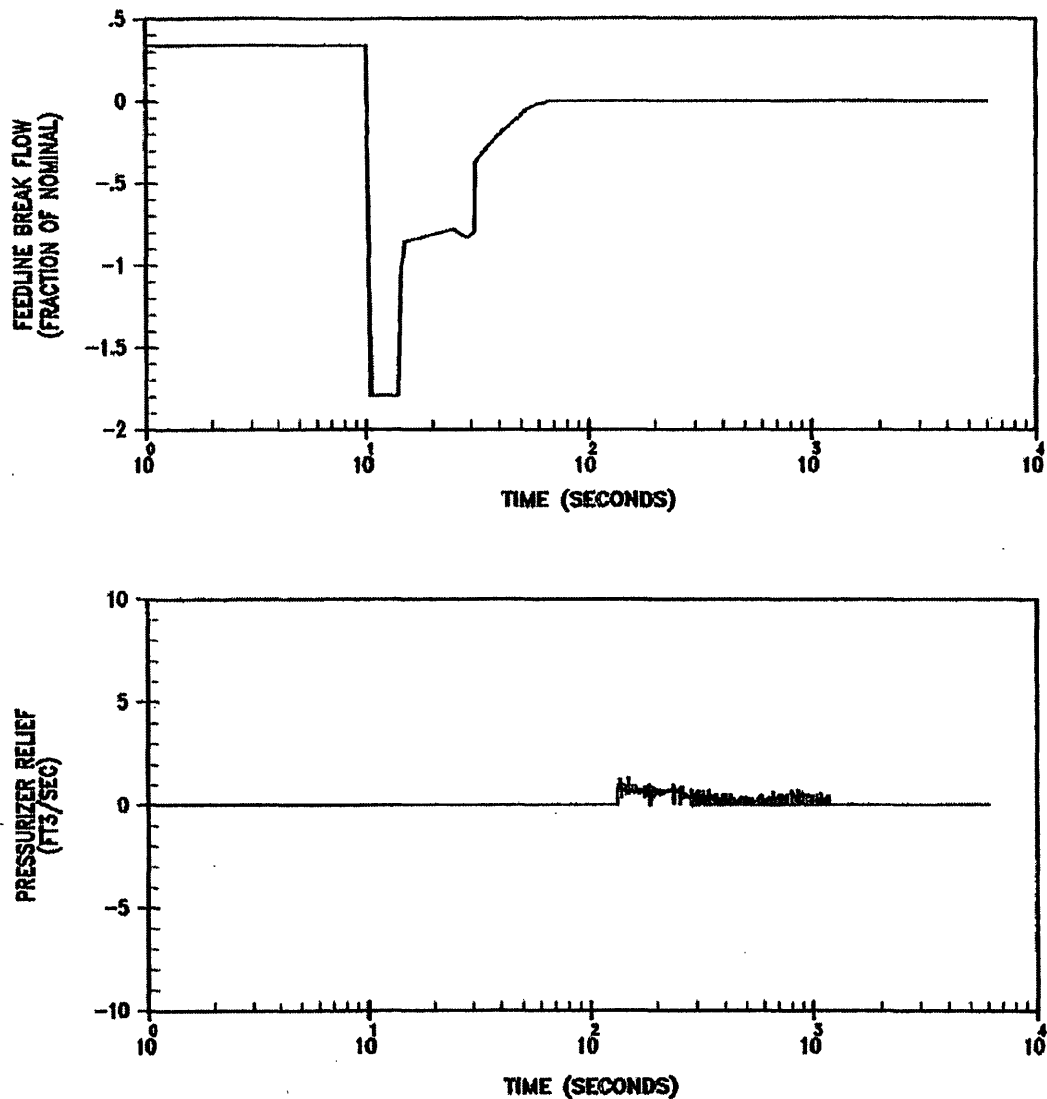


FIGURE 14.2-10G

FEEDLINE BREAK FLOW AND PRESSURIZER RELIEF TRANSIENTS FOR MAJOR RUPTURE OF A MAIN FEEDWATER PIPE WITHOUT OFFSITE POWER AVAILABLE

BEAVER VALLEY POWER STATION UNIT NO. 1  
UPDATED FINAL SAFETY ANALYSIS REPORT

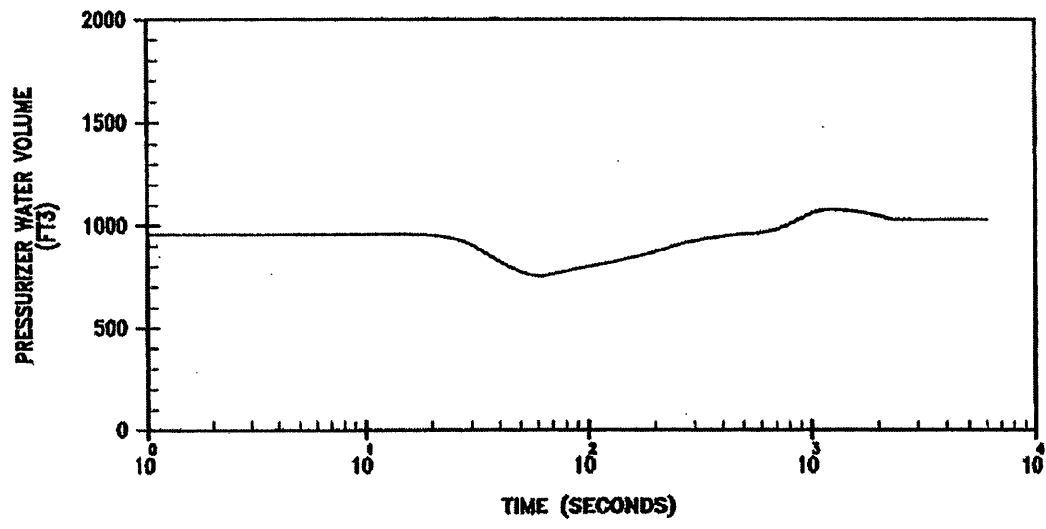
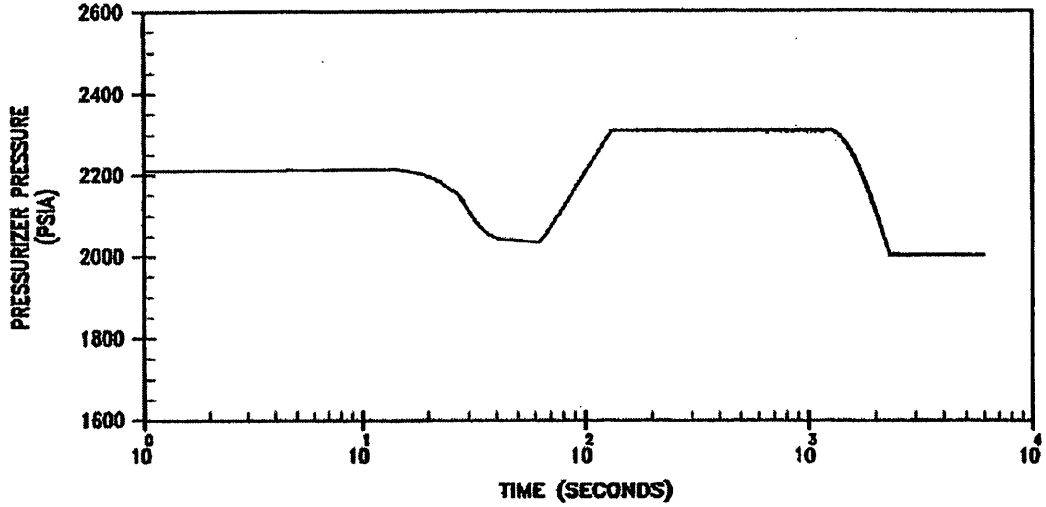


FIGURE 14.2-10H

PRESSURIZER PRESSURE AND PRESSURIZER WATER VOLUME TRANSIENTS FOR MAJOR RUPTURE OF A MAIN FEEDWATER PIPE WITHOUT OFFSITE POWER AVAILABLE

BEAVER VALLEY POWER STATION UNIT NO. 1  
UPDATED FINAL SAFETY ANALYSIS REPORT

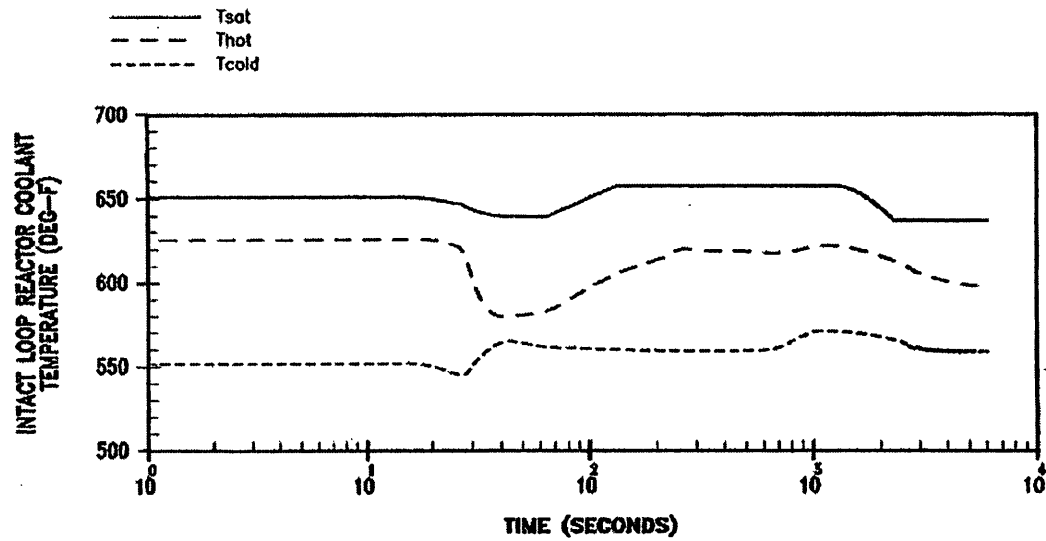
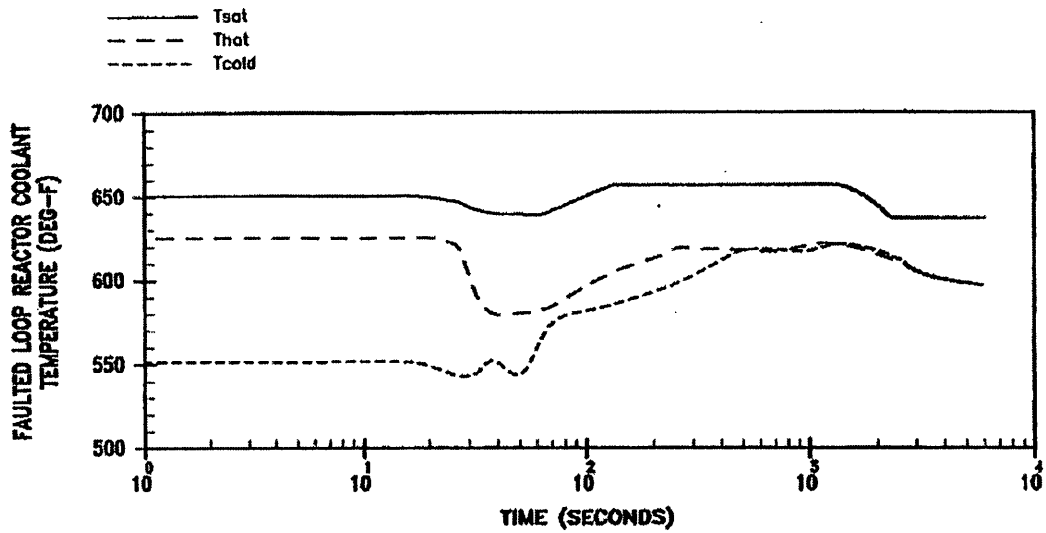


FIGURE 14.2-10I

LOOP TEMPERATURES FOR MAJOR RUPTURE  
OF A MAIN FEEDWATER PIPE  
WITHOUT OFFSITE POWER AVAILABLE

BEAVER VALLEY POWER STATION UNIT NO. 1  
UPDATED FINAL SAFETY ANALYSIS REPORT

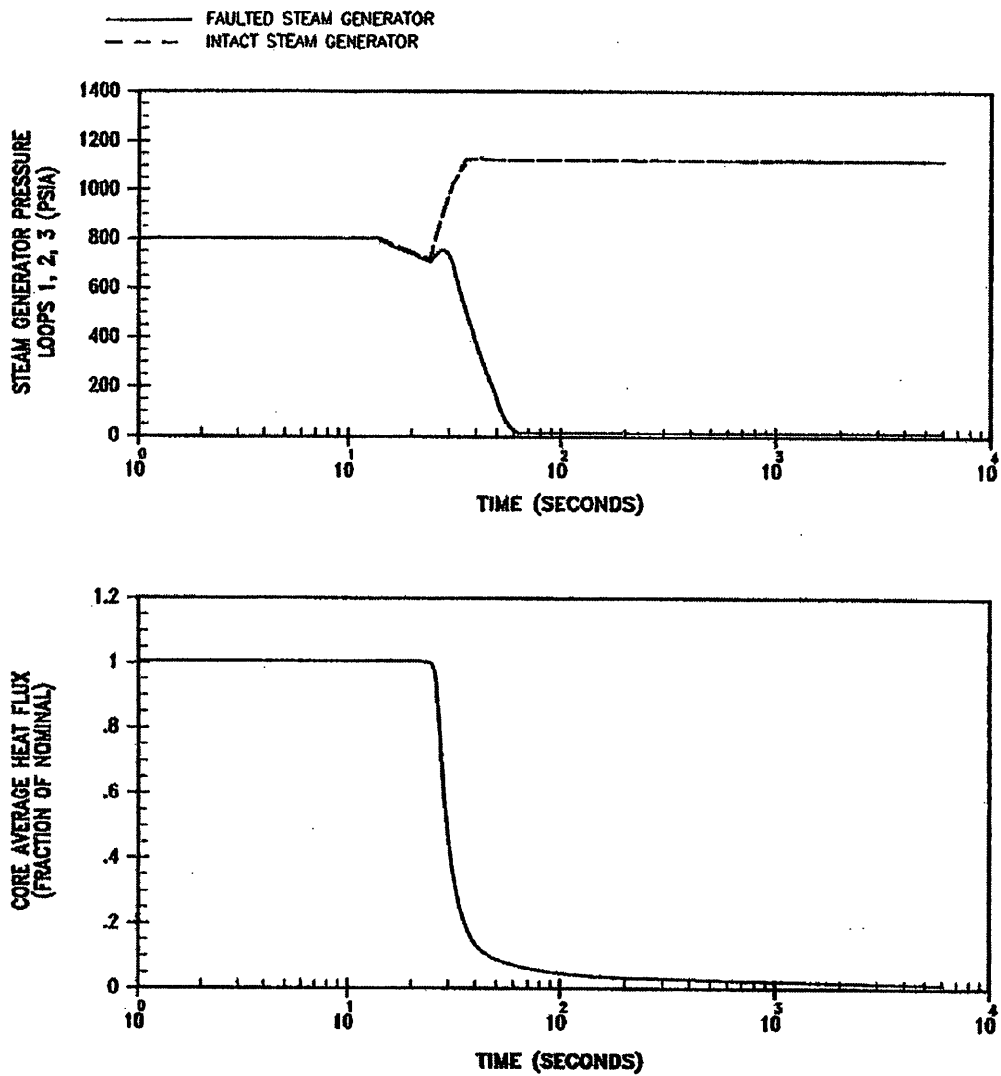


FIGURE 14.2-10J

STEAM GENERATOR PRESSURE AND CORE  
 HEAT FLUX TRANSIENTS FOR MAJOR  
 RUPTURE OF A MAIN FEEDWATER PIPE  
 WITHOUT OFFSITE POWER AVAILABLE

BEAVER VALLEY POWER STATION UNIT NO. 1  
 UPDATED FINAL SAFETY ANALYSIS REPORT

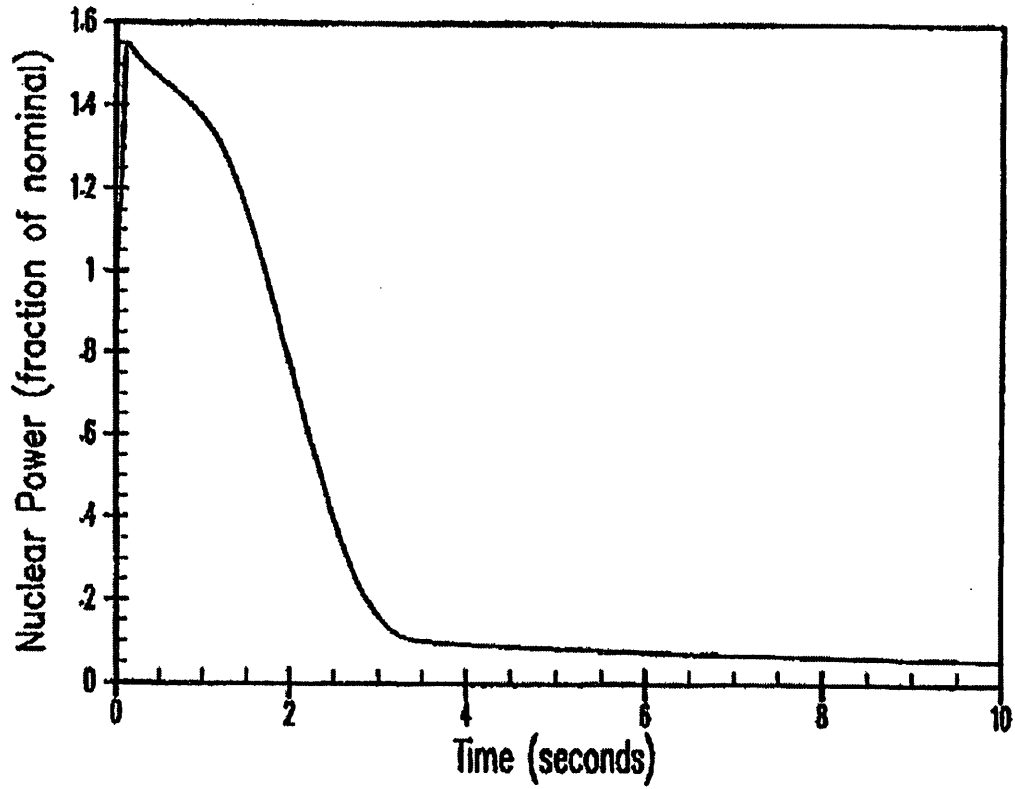


FIGURE 14.2-11

NUCLEAR POWER TRANSIENT  
BOL-HFP EJECTION ACCIDENT

BEAVER VALLEY POWER STATION UNIT NO. 1  
UPDATED FINAL SAFETY ANALYSIS REPORT



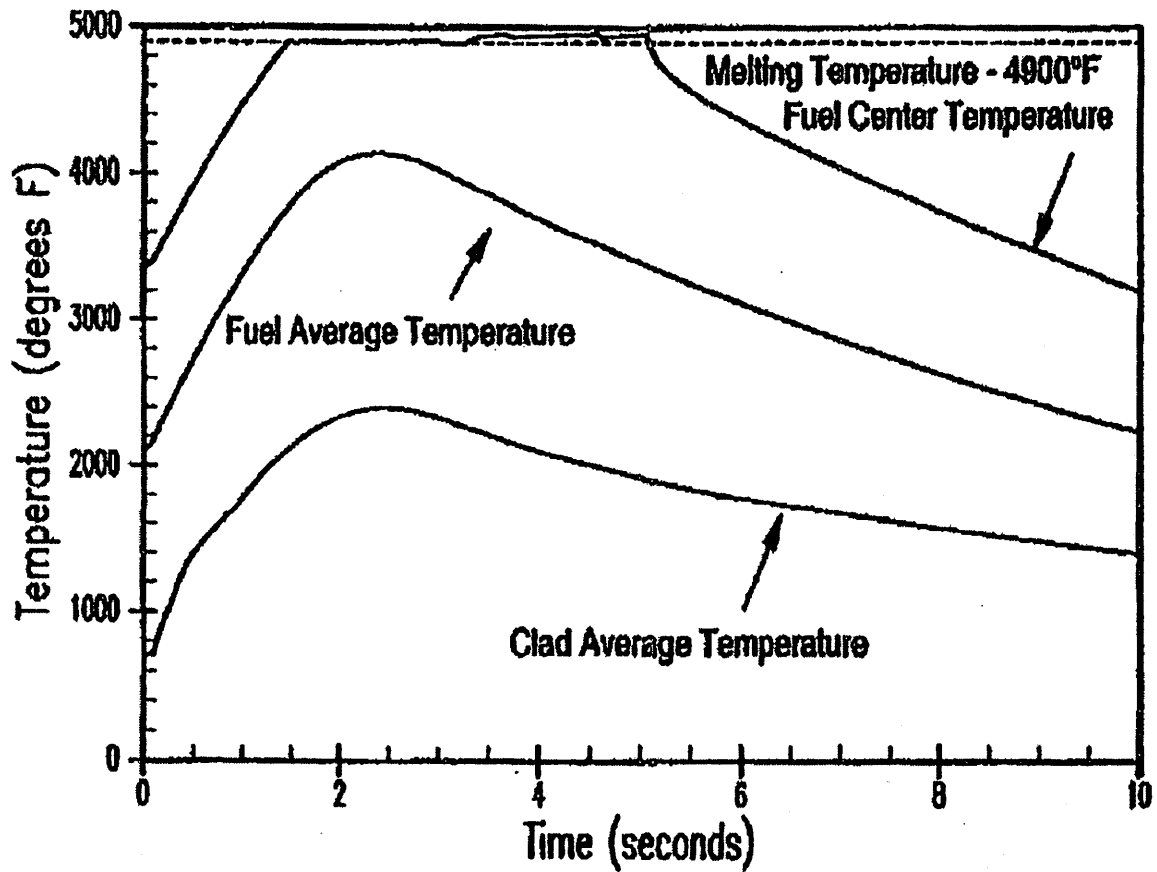


FIGURE 14.2-12

PEAK FUEL AND CLAD AVERAGE  
TEMPERATURE VERSUS TIME  
BOL-HFP EJECTION ACCIDENT

BEAVER VALLEY POWER STATION UNIT NO. 1  
UPDATED FINAL SAFETY ANALYSIS REPORT

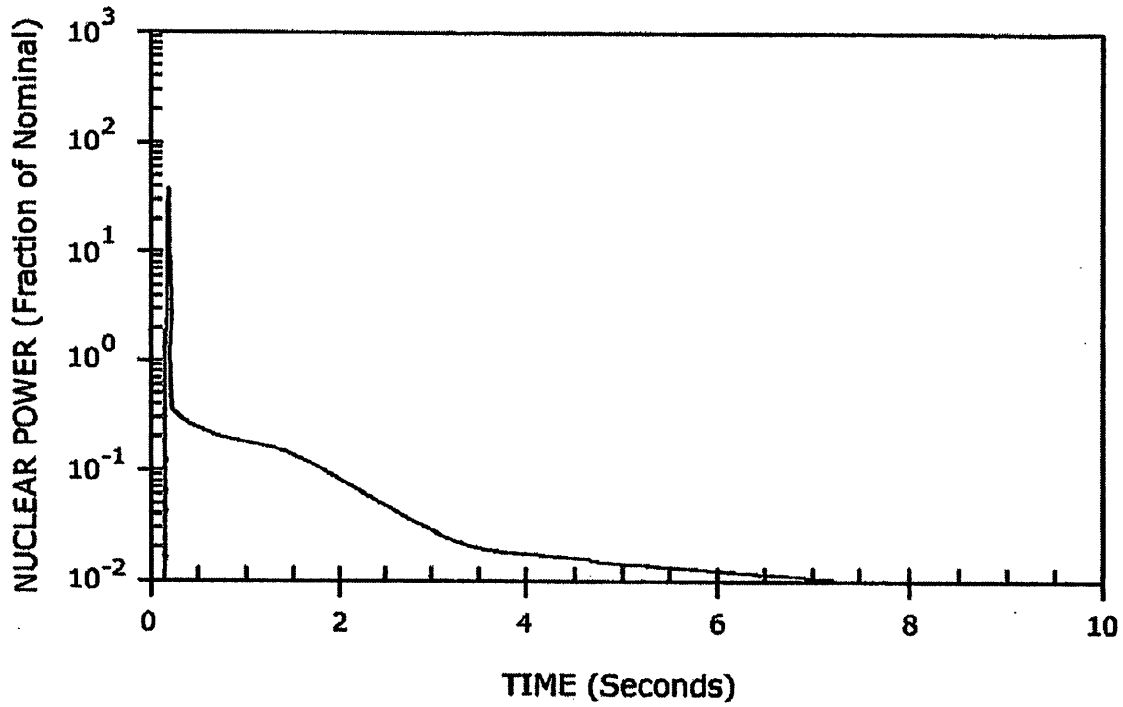


FIGURE 14.2-13

NUCLEAR POWER TRANSIENT  
EOL-HZP EJECTION ACCIDENT

BEAVER VALLEY POWER STATION UNIT NO. 1  
UPDATED FINAL SAFETY ANALYSIS REPORT

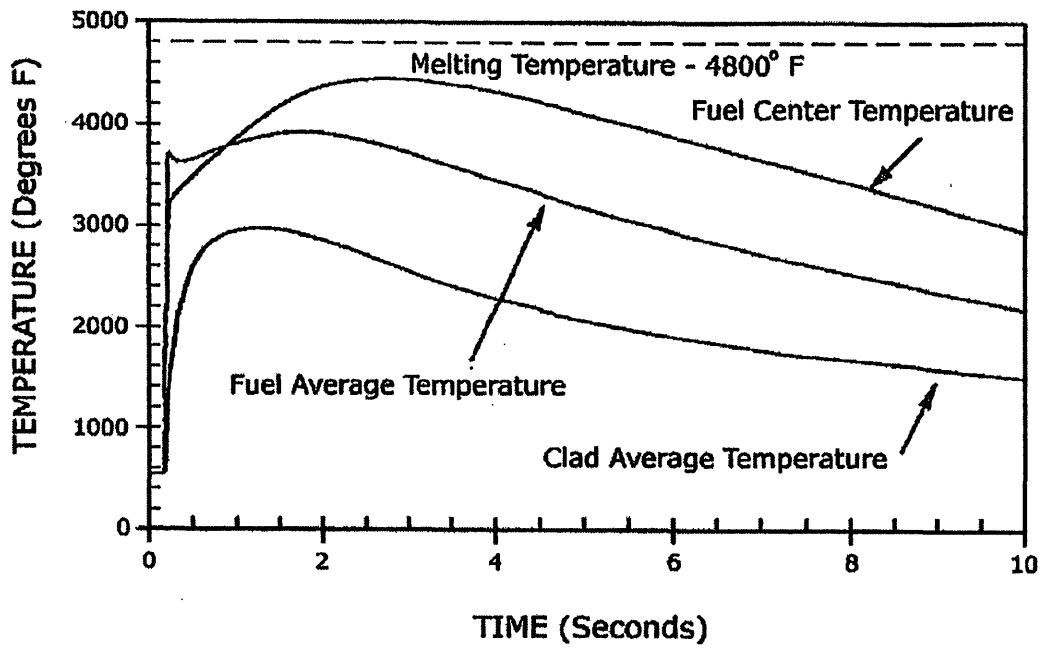


FIGURE 14.2-14

PEAK FUEL AND CLAD AVERAGE  
TEMPERATURE VERSUS TIME  
EOL-HZP EJECTION ACCIDENT

BEAVER VALLEY POWER STATION UNIT NO. 1  
UPDATED FINAL SAFETY ANALYSIS REPORT

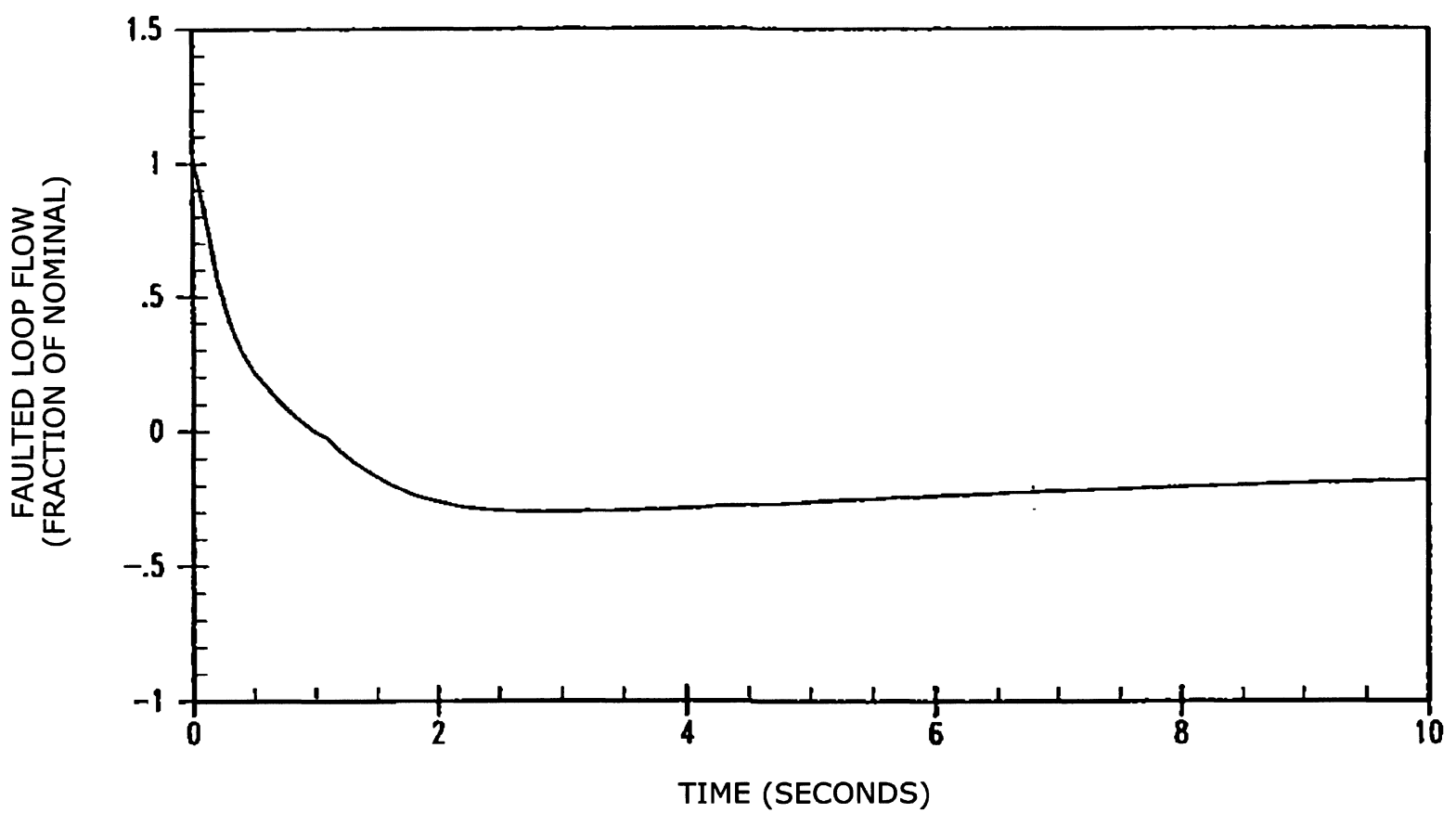
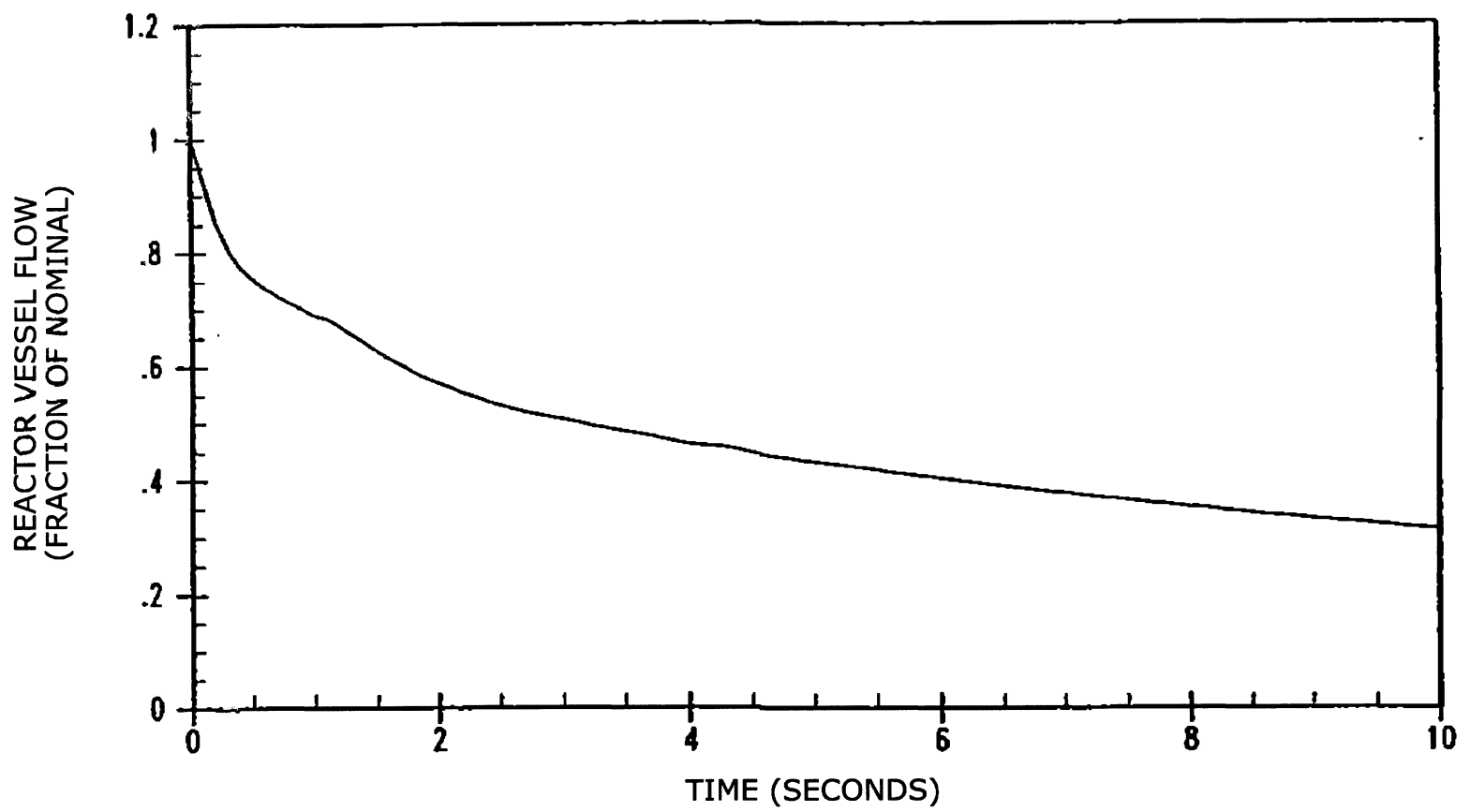


FIGURE 14.2-15

REACTOR VESSEL AND FAULTED LOOP FLOW  
TRANSIENTS FOR THREE LOOP OPERATION,  
ONE LOCKED ROTOR

BEAVER VALLEY POWER STATION UNIT NO. 1  
UPDATED FINAL SAFETY ANALYSIS REPORT

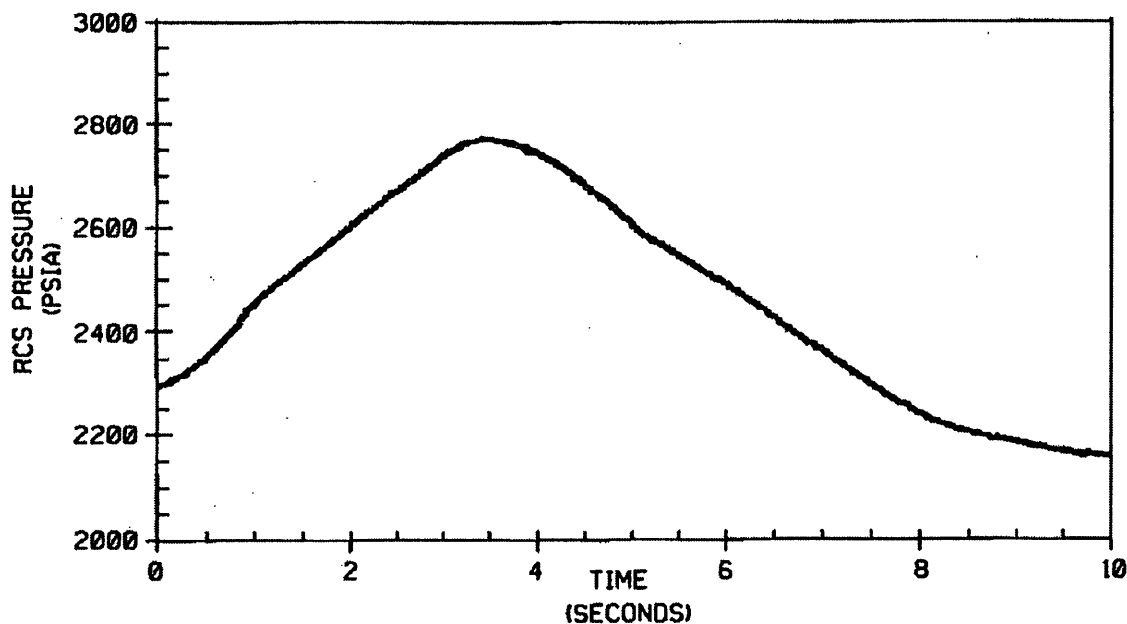
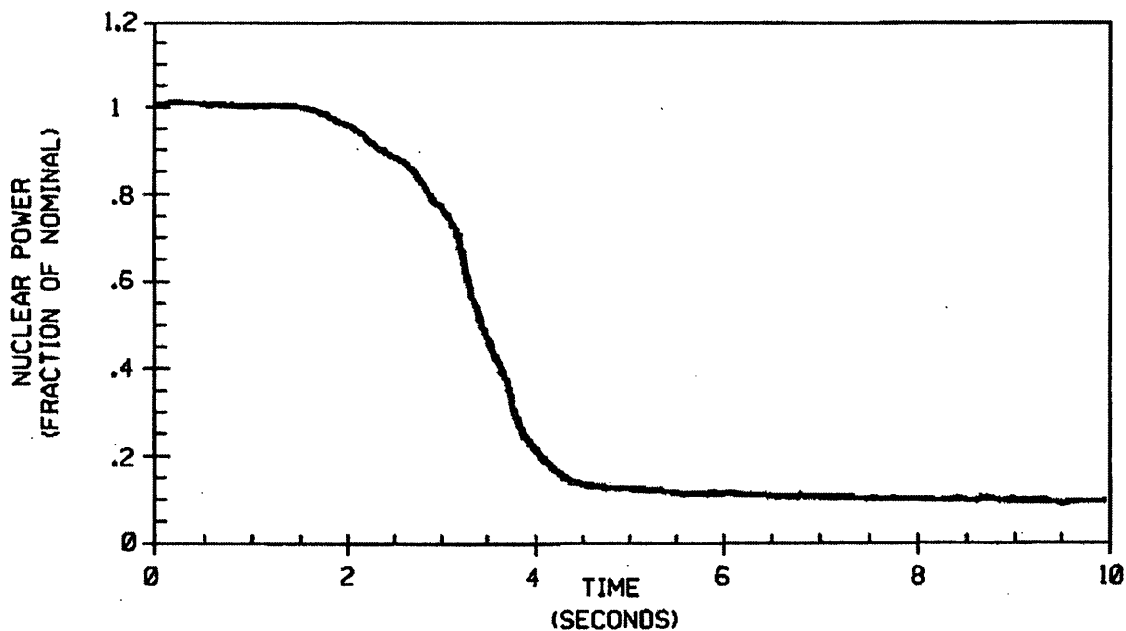


FIGURE 14.2-16

NUCLEAR POWER AND REACTOR COOLANT SYSTEM PRESSURE FOR THREE LOOP OPERATION, ONE LOCKED ROTOR

BEAVER VALLEY POWER STATION UNIT NO. 1  
 UPDATED FINAL SAFETY ANALYSIS REPORT

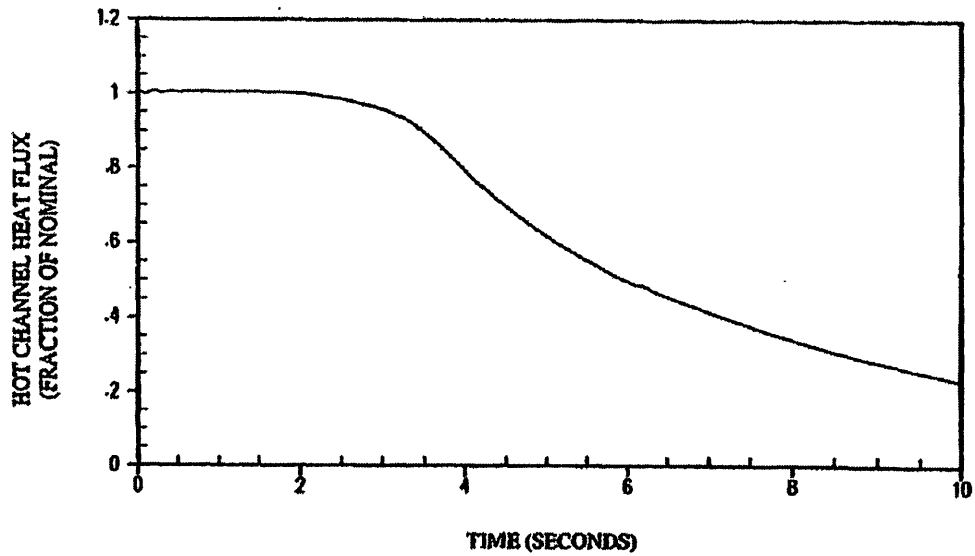
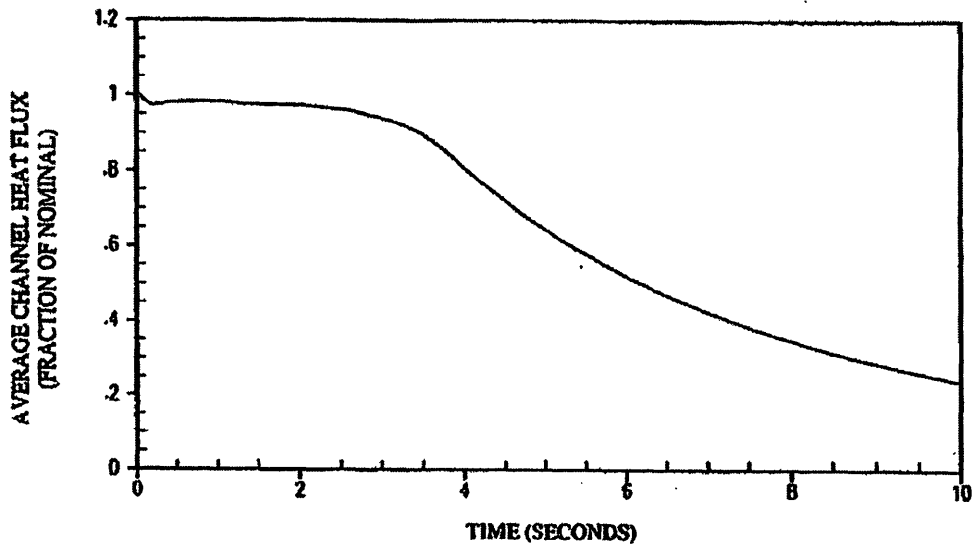


FIGURE 14.2-17

AVERAGE CHANNEL AND HOT CHANNEL  
HEAT FLUX TRANSIENTS FOR THREE LOOP  
OPERATION, ONE LOCKED ROTOR

BEAVER VALLEY POWER STATION UNIT NO. 1  
UPDATED FINAL SAFETY ANALYSIS REPORT

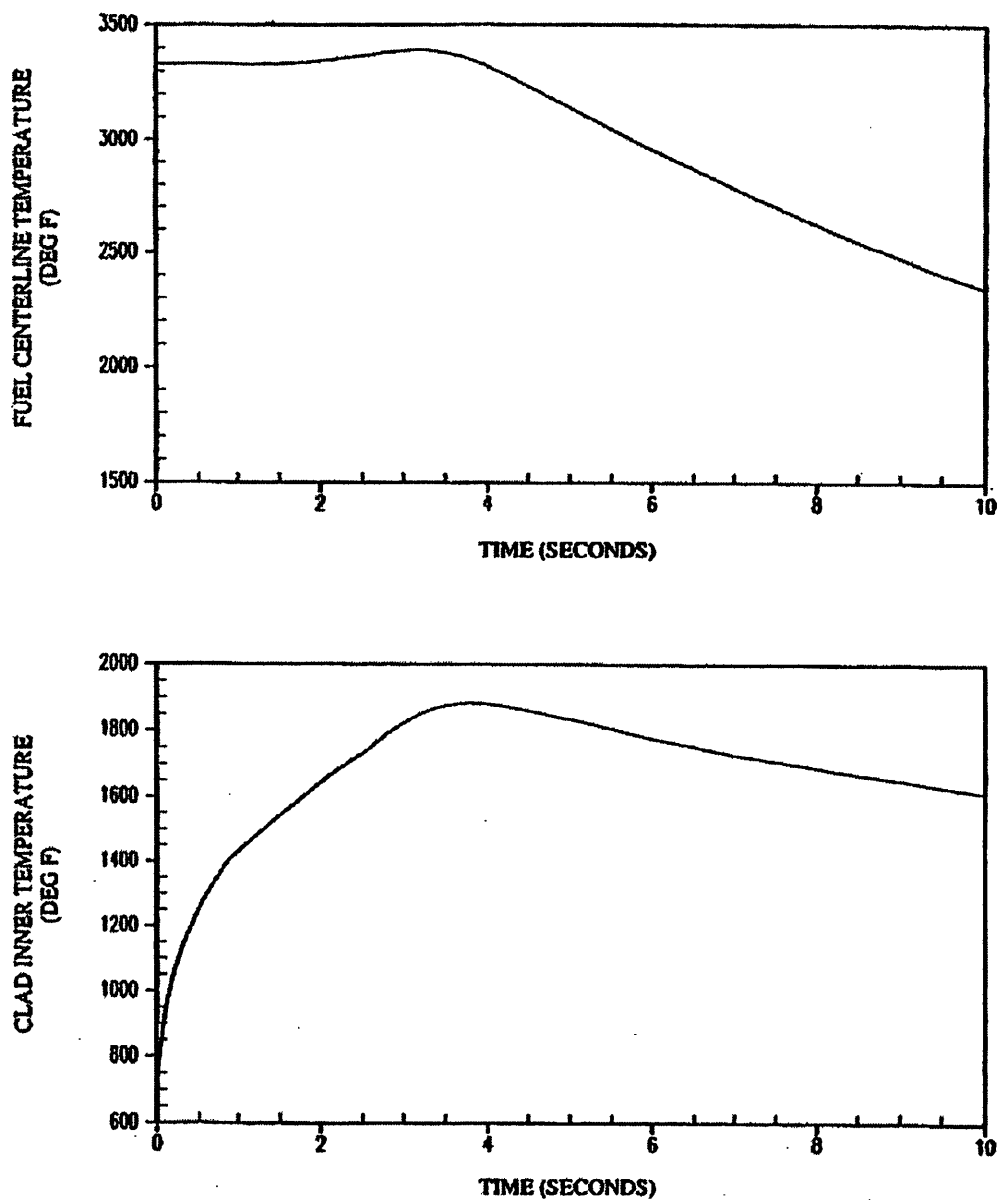
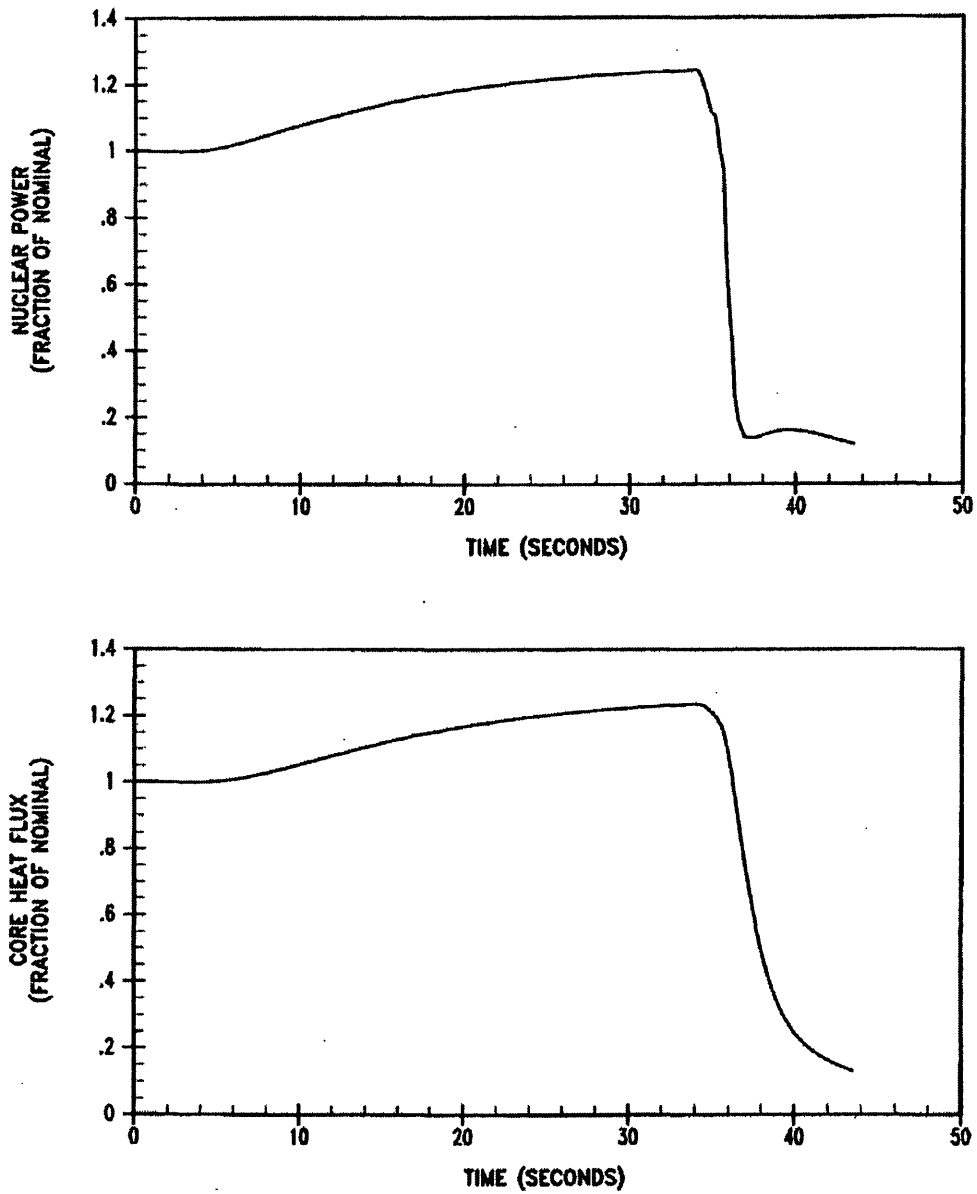


FIGURE 14.2-18

MAXIMUM CLAD AND FUEL CENTERLINE  
TEMPERATURES AT HOT SPOT FOR THREE  
LOOP OPERATION, ONE LOCKED ROTOR

BEAVER VALLEY POWER STATION UNIT NO. 1  
UPDATED FINAL SAFETY ANALYSIS REPORT



**FIGURE 14.2-19**

**STEAM SYSTEM PIPING FAILURE AT POWER –  
0.60 FT<sup>2</sup> BREAK – NUCLEAR POWER AND  
CORE HEAT FLUX TRANSIENTS**

**BEAVER VALLEY POWER STATION UNIT 1  
UPDATED FINAL SAFETY ANALYSIS REPORT**



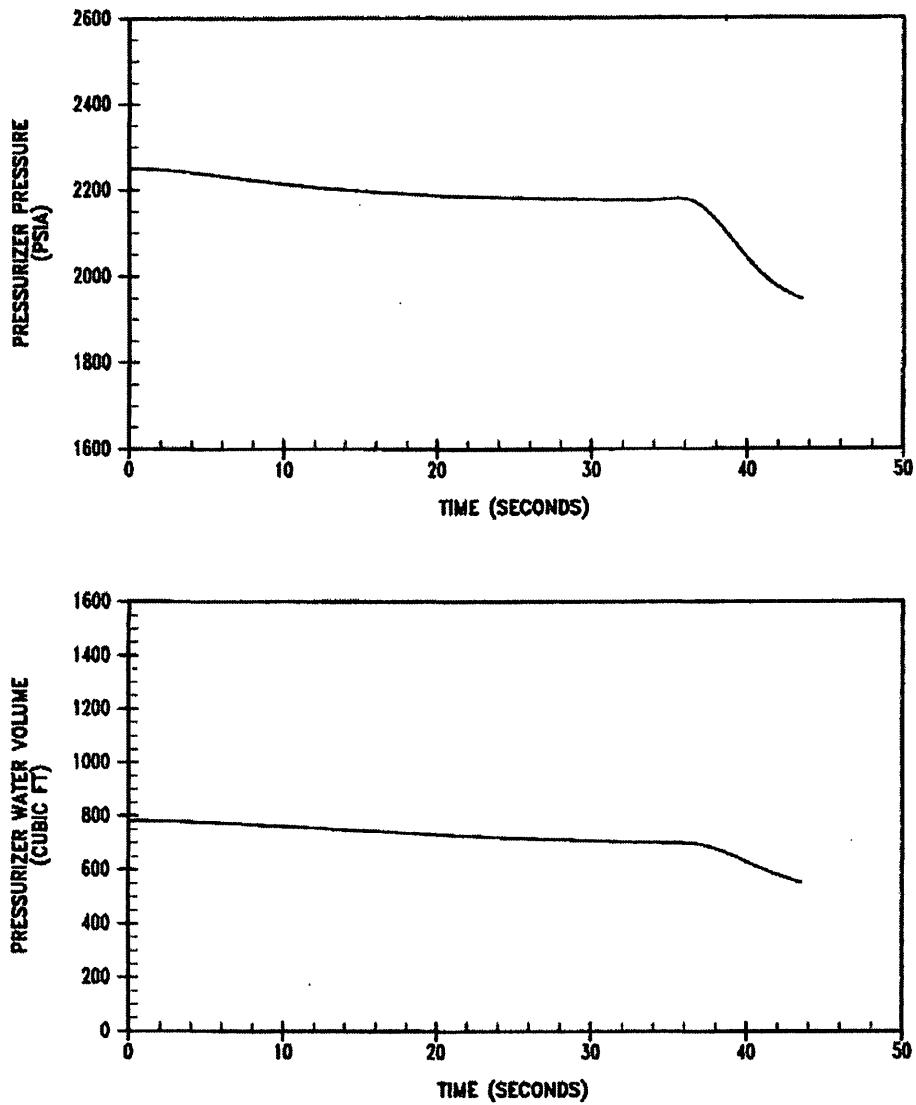


**FIGURE 14.2-20**

**STEAM SYSTEM PIPING FAILURE AT POWER –  
0.60 FT<sup>2</sup> BREAK – PRESSURIZER PRESSURE  
AND WATER VOLUME TRANSIENTS**

**BEAVER VALLEY POWER STATION UNIT 1  
UPDATED FINAL SAFETY ANALYSIS REPORT**

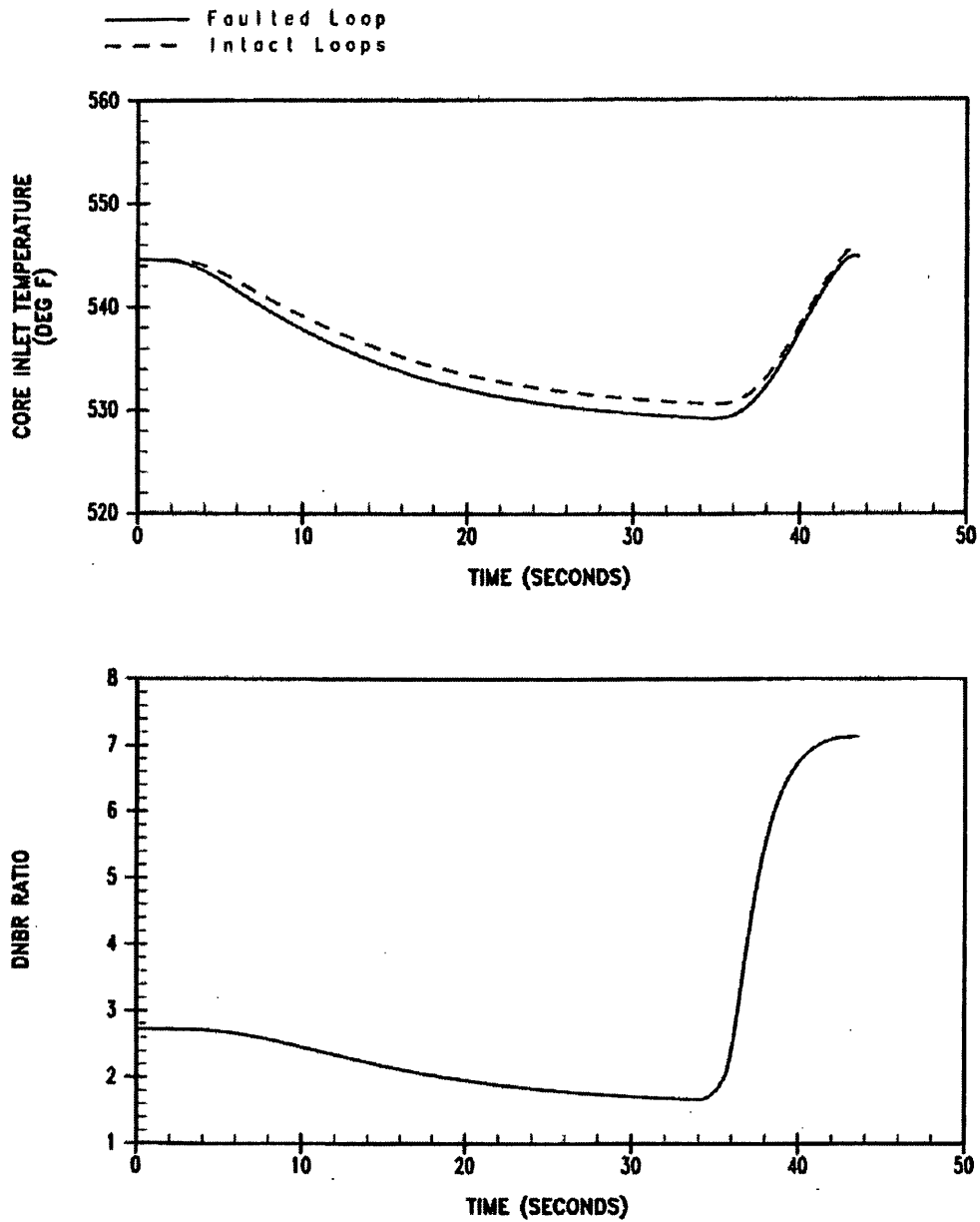


**FIGURE 14.2-21**

**STEAM SYSTEM PIPING FAILURE AT POWER –  
0.60 FT<sup>2</sup> BREAK – CORE INLET TEMPERATURE  
TRANSIENT AND DNR RATIO VERSUS TIME**

**BEAVER VALLEY POWER STATION UNIT 1  
UPDATED FINAL SAFETY ANALYSIS REPORT**

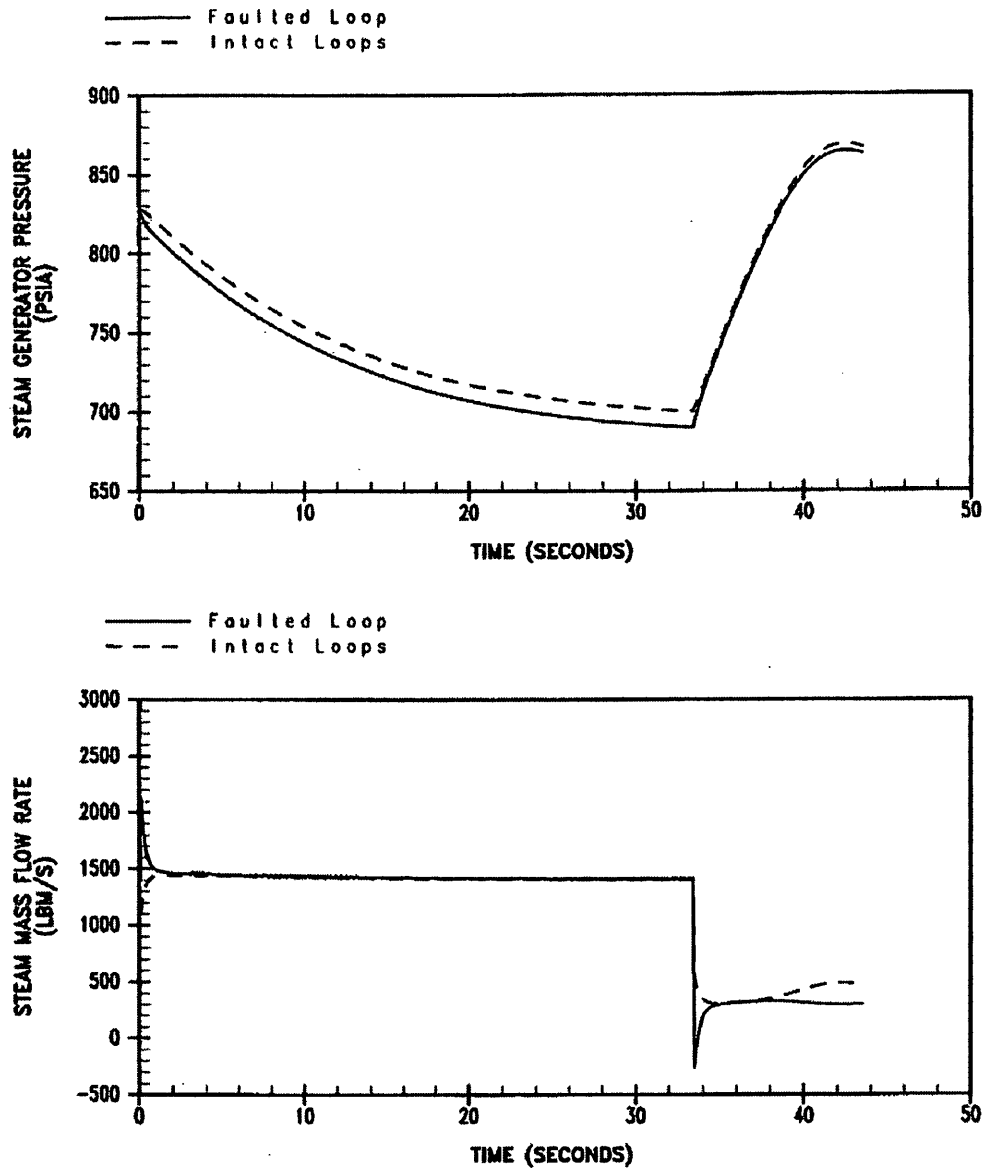
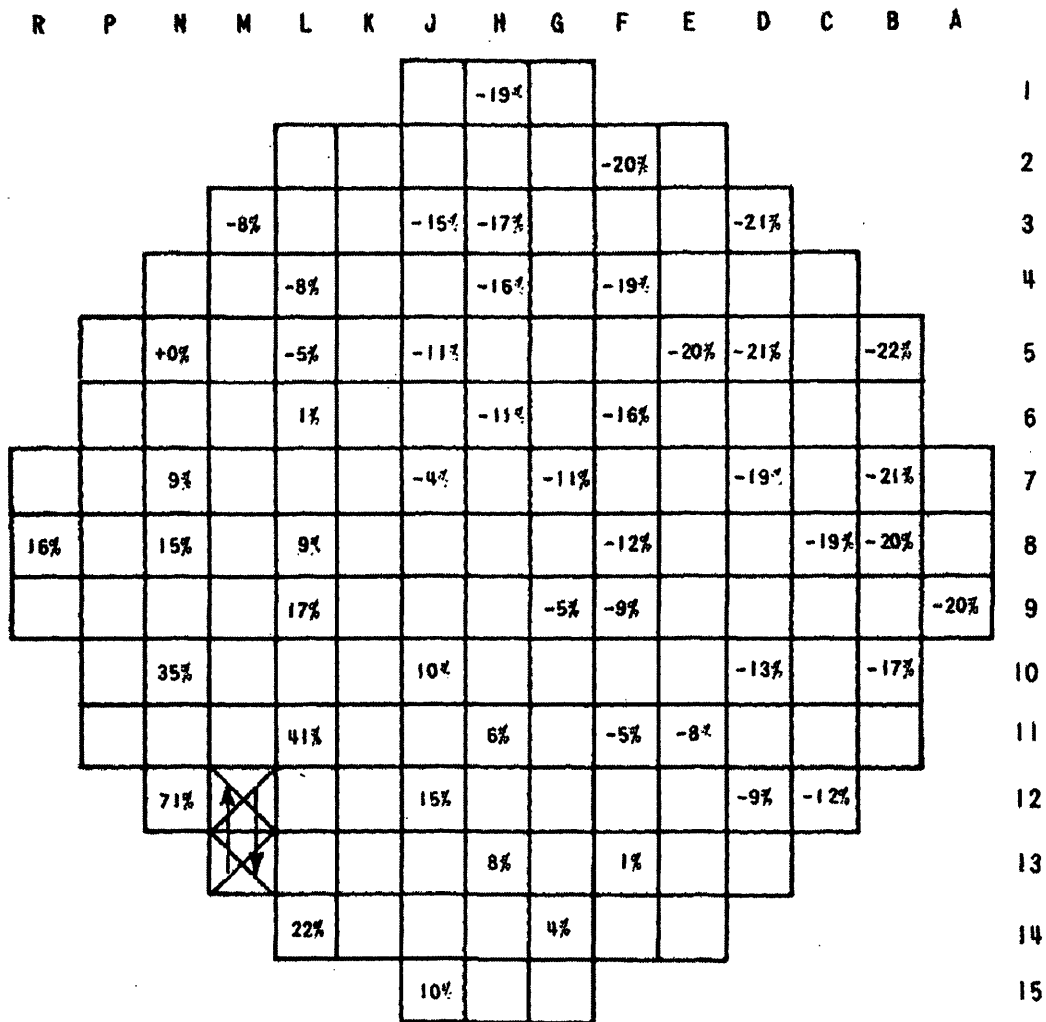


FIGURE 14.2-22

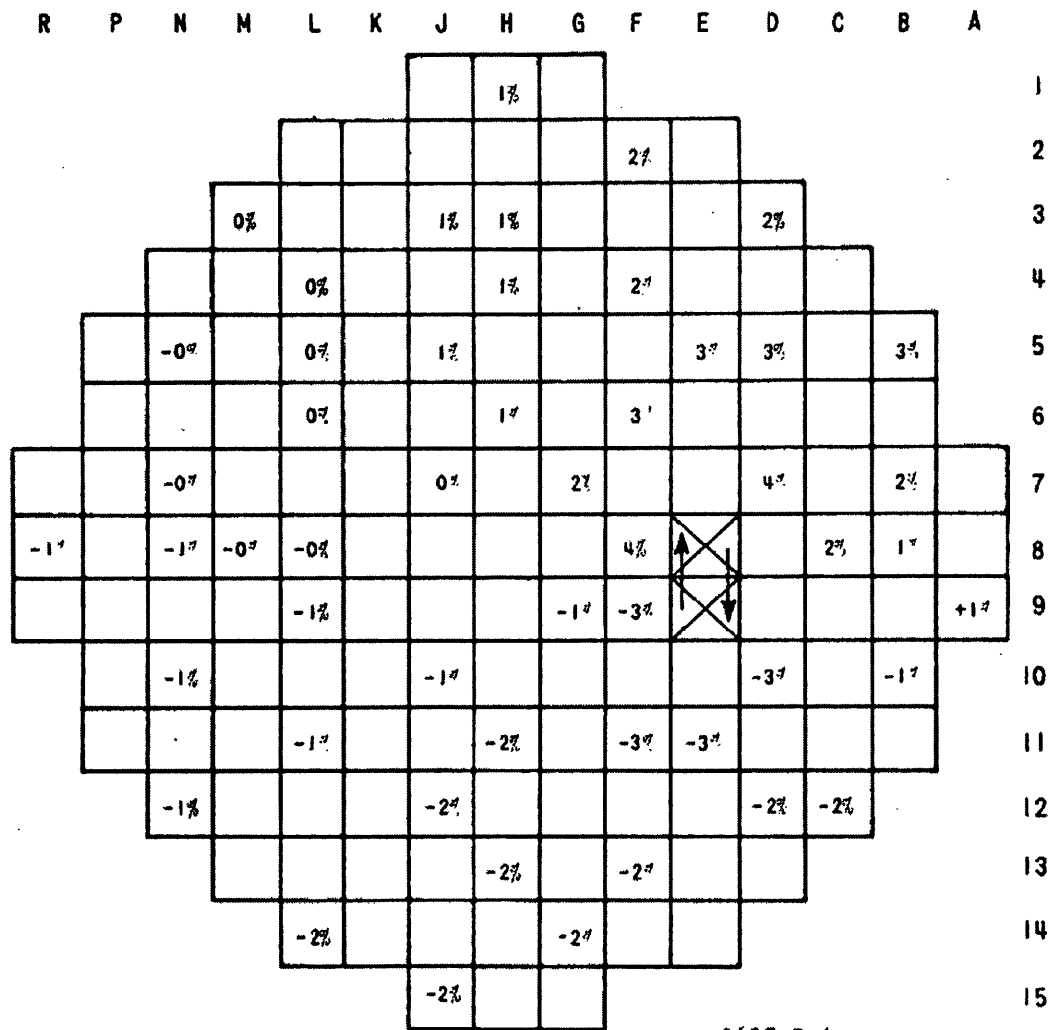
**STEAM SYSTEM PIPING FAILURE AT POWER –  
0.60 FT<sup>2</sup> BREAK – STEAM GENERATOR  
PRESSURE AND STEAM MASS FLOW  
TRANSIENTS**

**BEAVER VALLEY POWER STATION UNIT 1  
UPDATED FINAL SAFETY ANALYSIS REPORT**



CASE A

FIGURE 14.2-25  
 INTERCHANGE BETWEEN REGION 1 AND  
 REGION 3 ASSEMBLY  
 BEAVER VALLEY POWER STATION UNIT NO. 1  
 UPDATED FINAL SAFETY ANALYSIS REPORT



CASE B-1

FIGURE 14.2-26  
 INTERCHANGE BETWEEN REGION 1 AND  
 REGION 2 ASSEMBLY, BURNABLE POISON  
 RODS BEING RETAINED BY THE REGION 2  
 ASSEMBLY  
 BEAVER VALLEY POWER STATION UNIT NO. 1  
 UPDATED FINAL SAFETY ANALYSIS REPORT

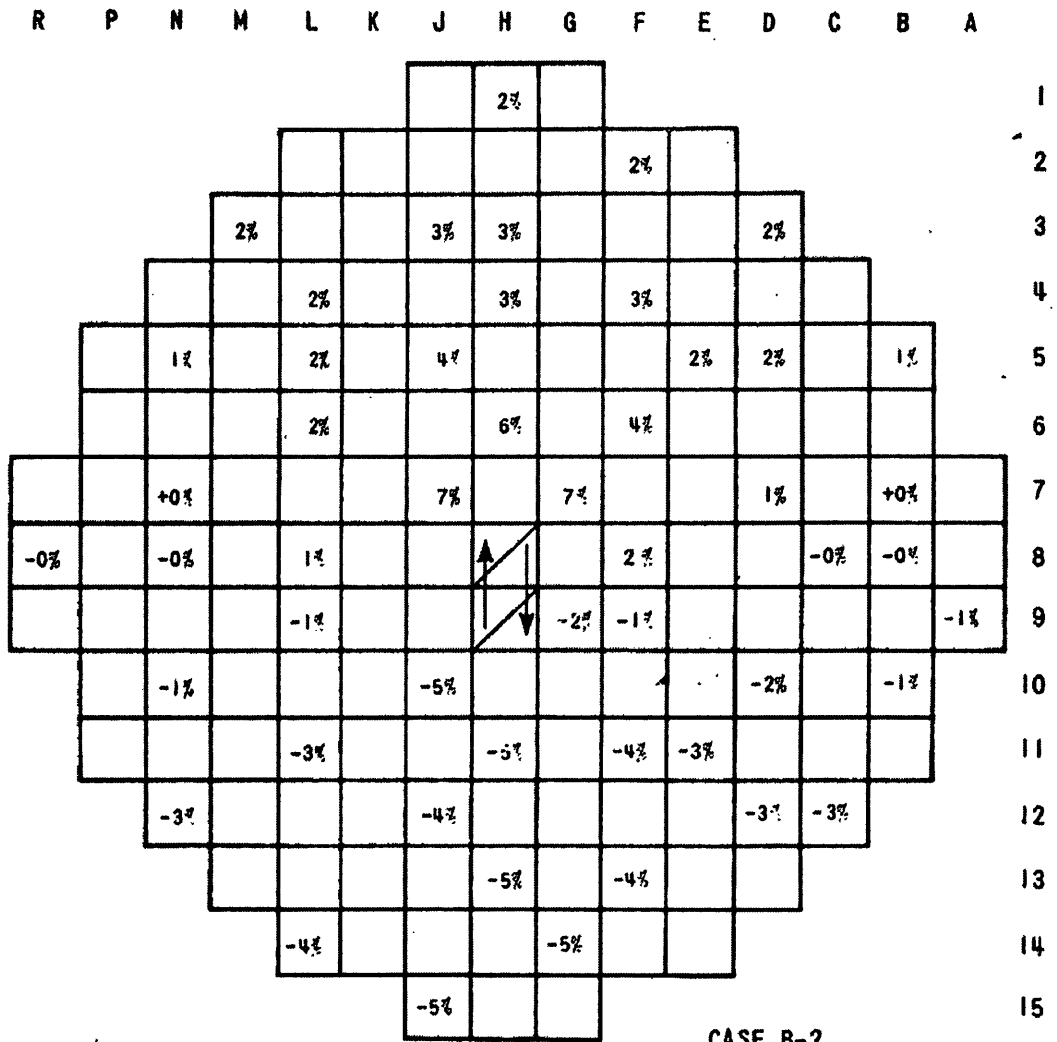
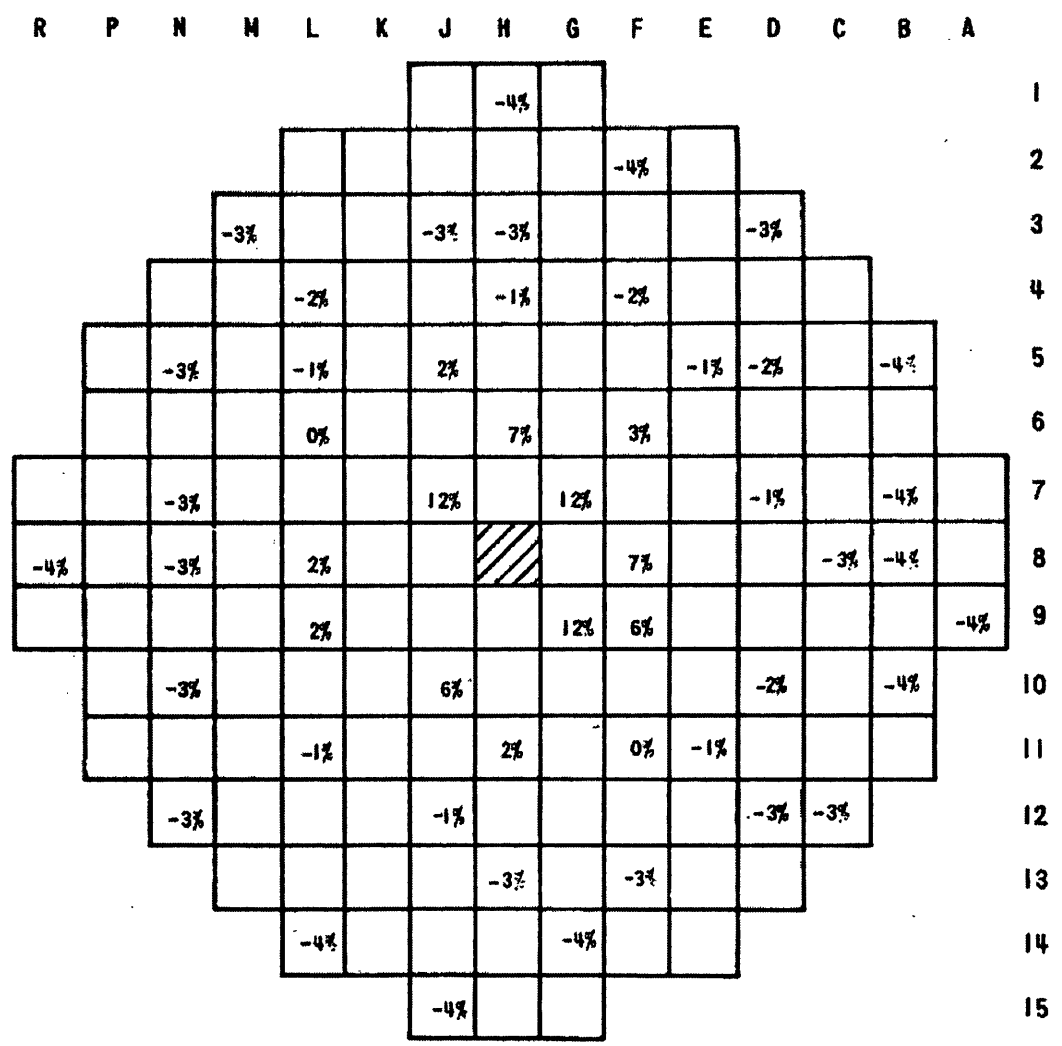


FIGURE 14-2-27  
 INTERCHANGE BETWEEN REGION 1 AND  
 REGION 2 ASSEMBLY, BURNABLE POISON  
 RODS BEING TRANSFERRED TO REGION 1  
 ASSEMBLY  
 BEAVER VALLEY POWER STATION UNIT NO. 1  
 UPDATED FINAL SAFETY ANALYSIS REPORT



CASE C

FIGURE 14-2-28  
 ENRICHMENT ERROR: A REGION 2 ASSEMBLY  
 LOADED INTO THE CORE CENTRAL POSITION  
 BEAVER VALLEY POWER STATION UNIT NO. 1  
 UPDATED FINAL SAFETY ANALYSIS REPORT

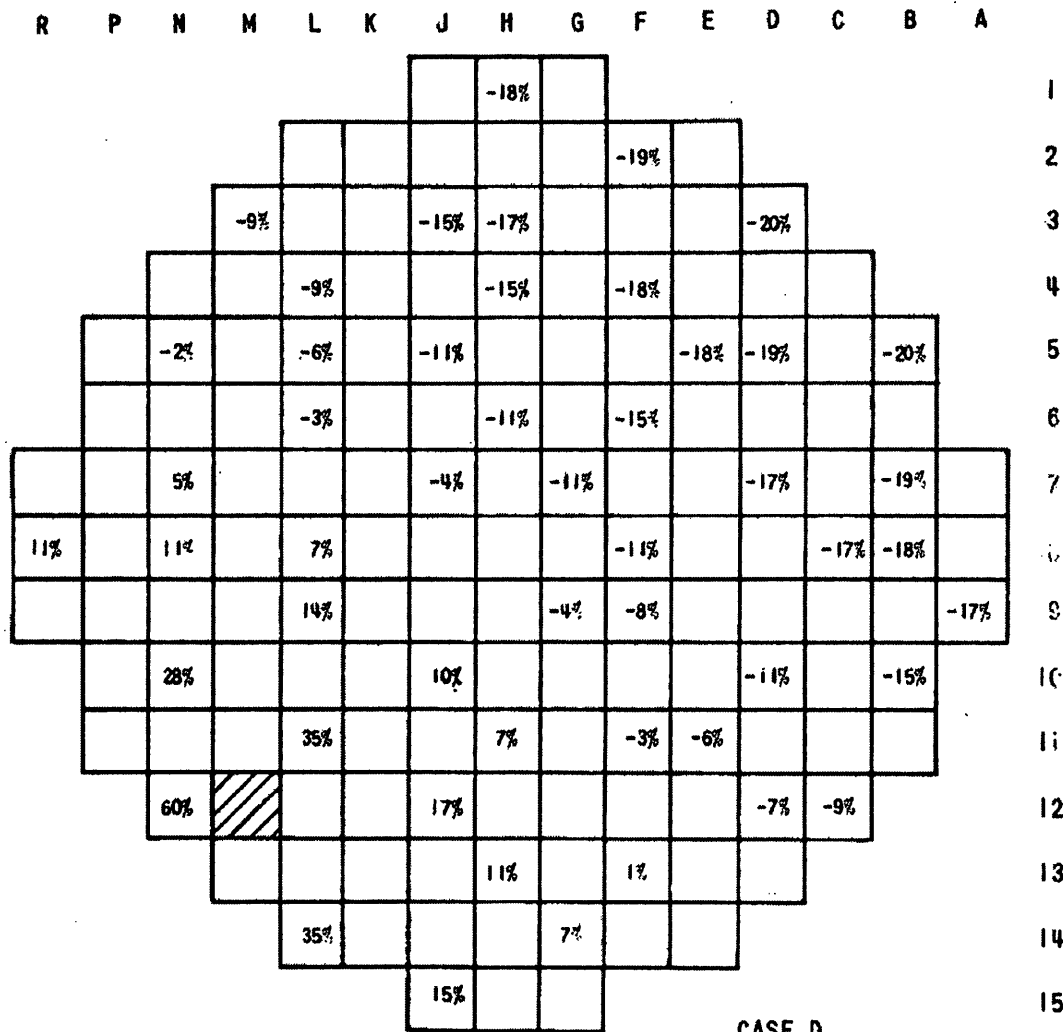


FIGURE 14-2-29  
 LOADING A REGION 2 ASSEMBLY INTO A  
 REGION 1 POSITION NEAR CORE PERIPHERY  
 BEAVER VALLEY POWER STATION UNIT NO. 1  
 UPDATED FINAL SAFETY ANALYSIS REPORT



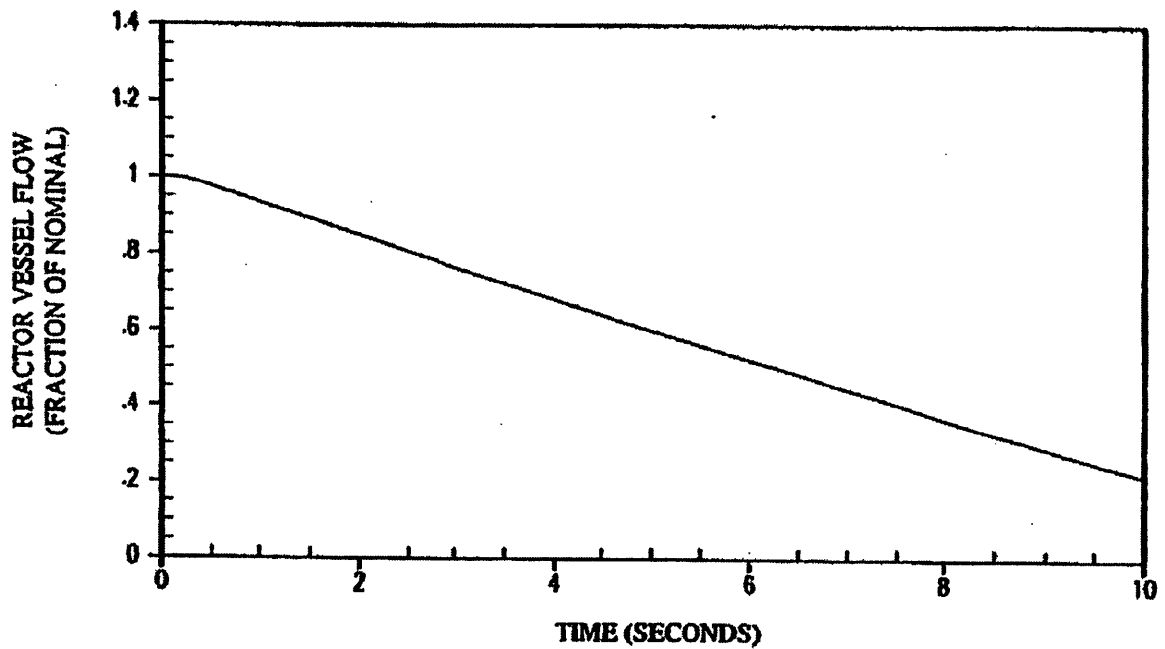


FIGURE 14.2-30

CORE FLOW COASTDOWN VERSUS TIME FOR  
THREE LOOPS IN OPERATION, COMPLETE  
LOSS OF FLOW, FREQUENCY DECAY

BEAVER VALLEY POWER STATION UNIT NO. 1  
UPDATED FINAL SAFETY ANALYSIS REPORT

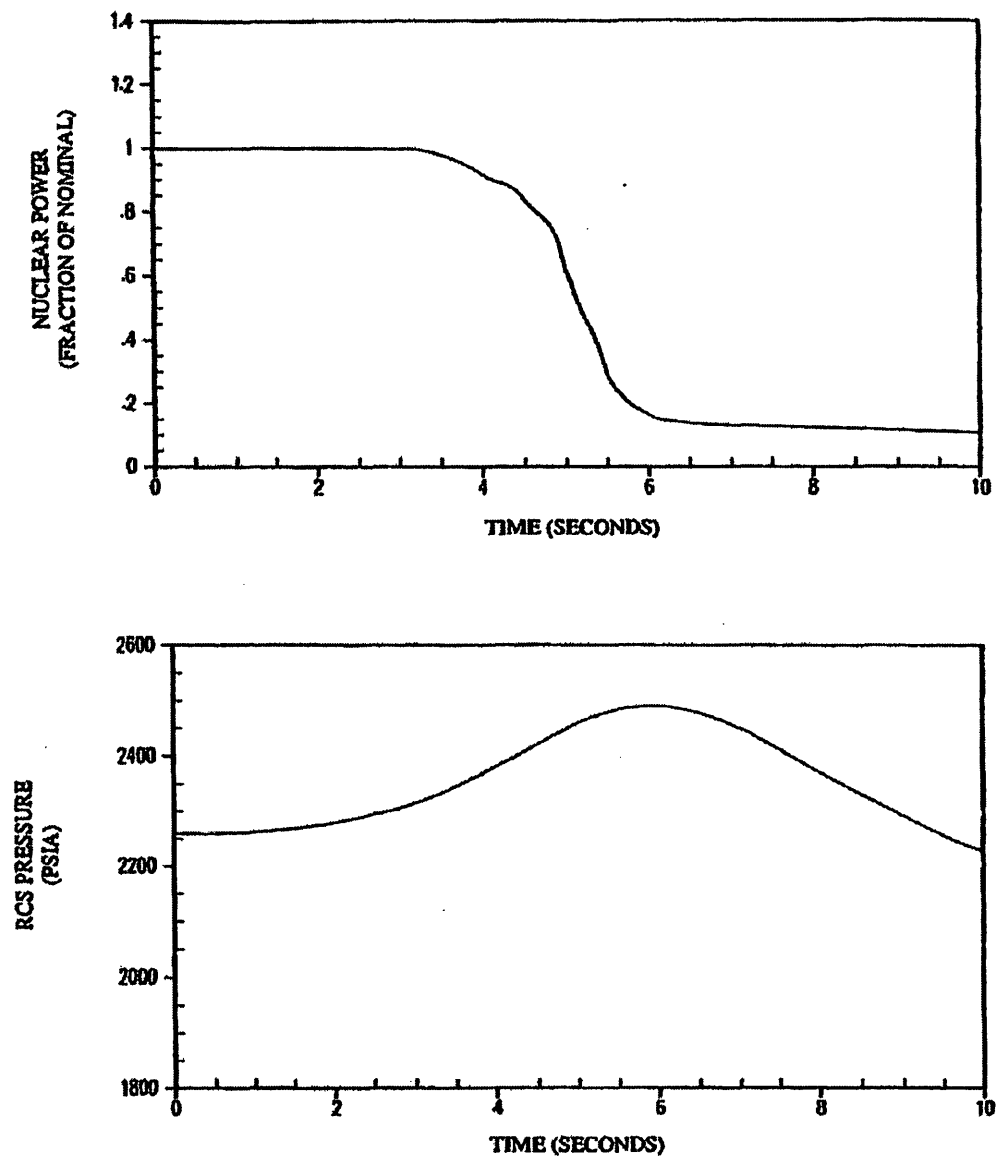


FIGURE 14.2-31

NUCLEAR POWER TRANSIENTS AND  
PRESSURIZER PRESSURE TRANSIENTS FOR  
THREE LOOPS IN OPERATION, THREE LOOPS  
COASTING DOWN, COMPLETE LOSS OF FLOW

BEAVER VALLEY POWER STATION UNIT NO. 1  
UPDATED FINAL SAFETY ANALYSIS REPORT

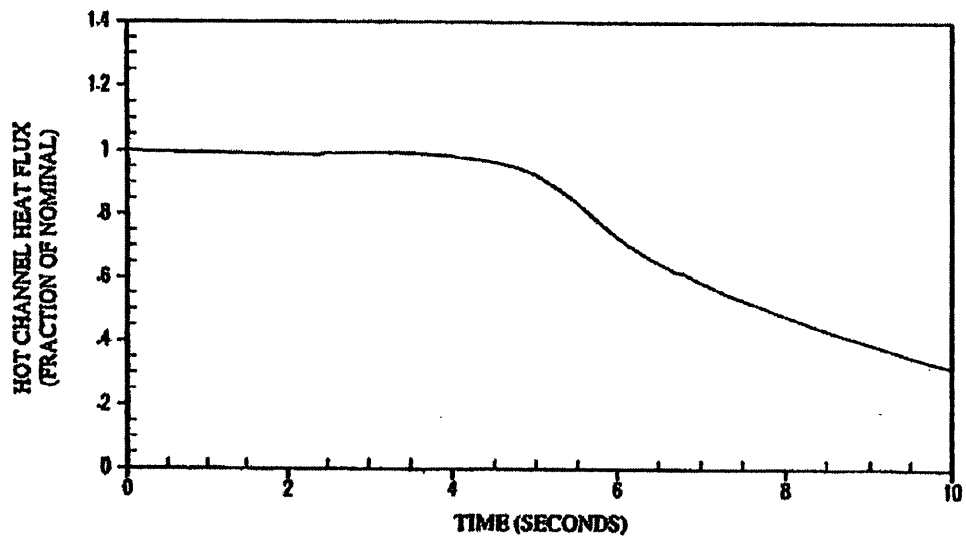
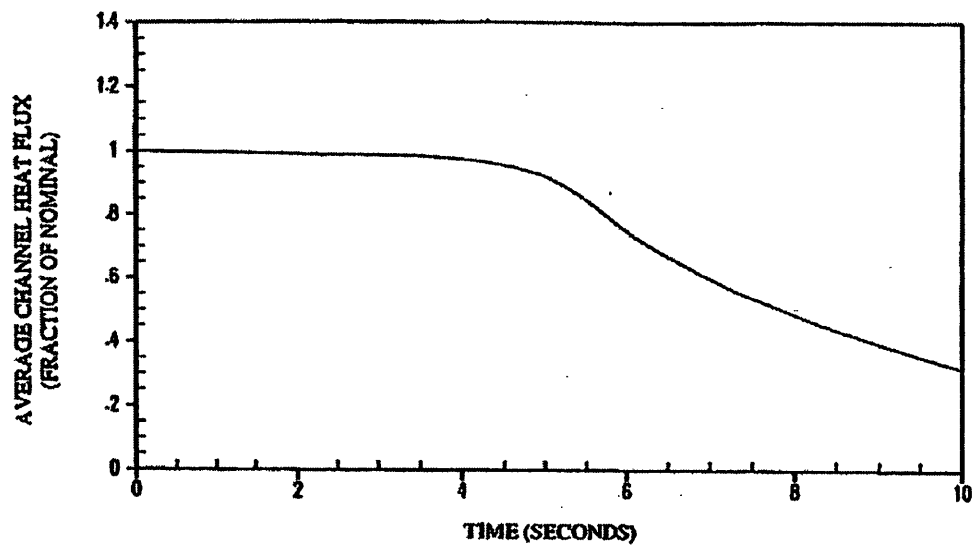


FIGURE 14.2-32

AVERAGE CHANNEL AND HOT CHANNEL  
HEAT FLUX TRANSIENTS FOR THREE LOOPS  
IN OPERATION, COMPLETE LOSS OF FLOW,  
FREQUENCY DECAY

BEAVER VALLEY POWER STATION UNIT NO. 1  
UPDATED FINAL SAFETY ANALYSIS REPORT

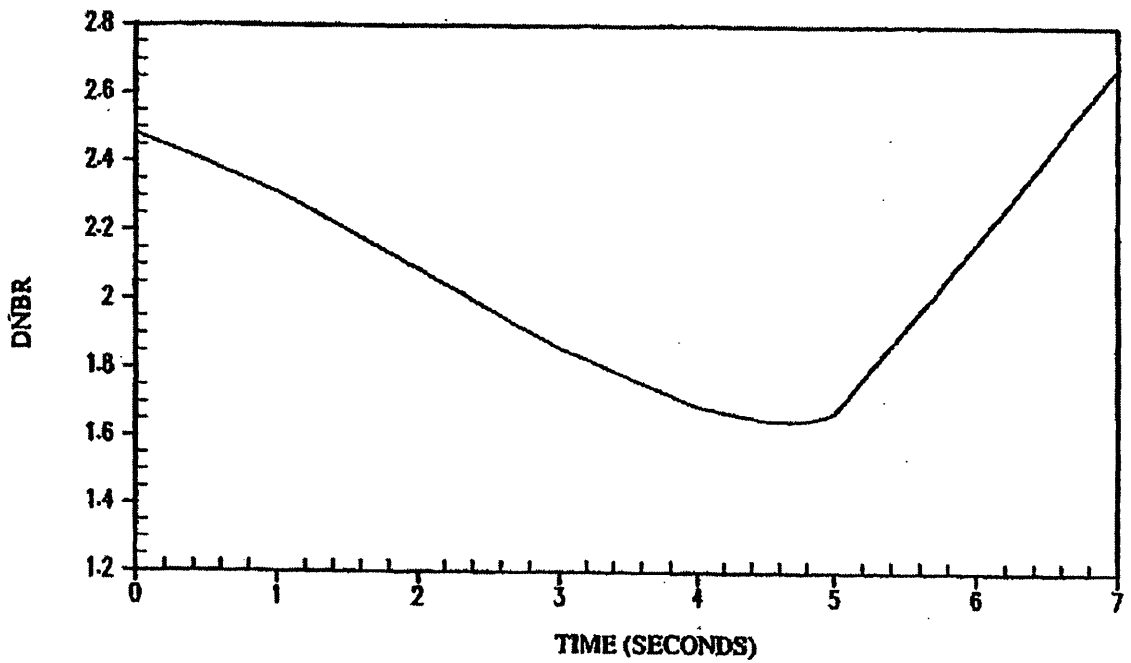


FIGURE 14.2-33

DNBR VERSUS TIME FOR THREE LOOPS  
IN OPERATION, THREE PUMPS COASTING  
DOWN, COMPLETE LOSS OF FLOW

BEAVER VALLEY POWER STATION UNIT NO. 1  
UPDATED FINAL SAFETY ANALYSIS REPORT

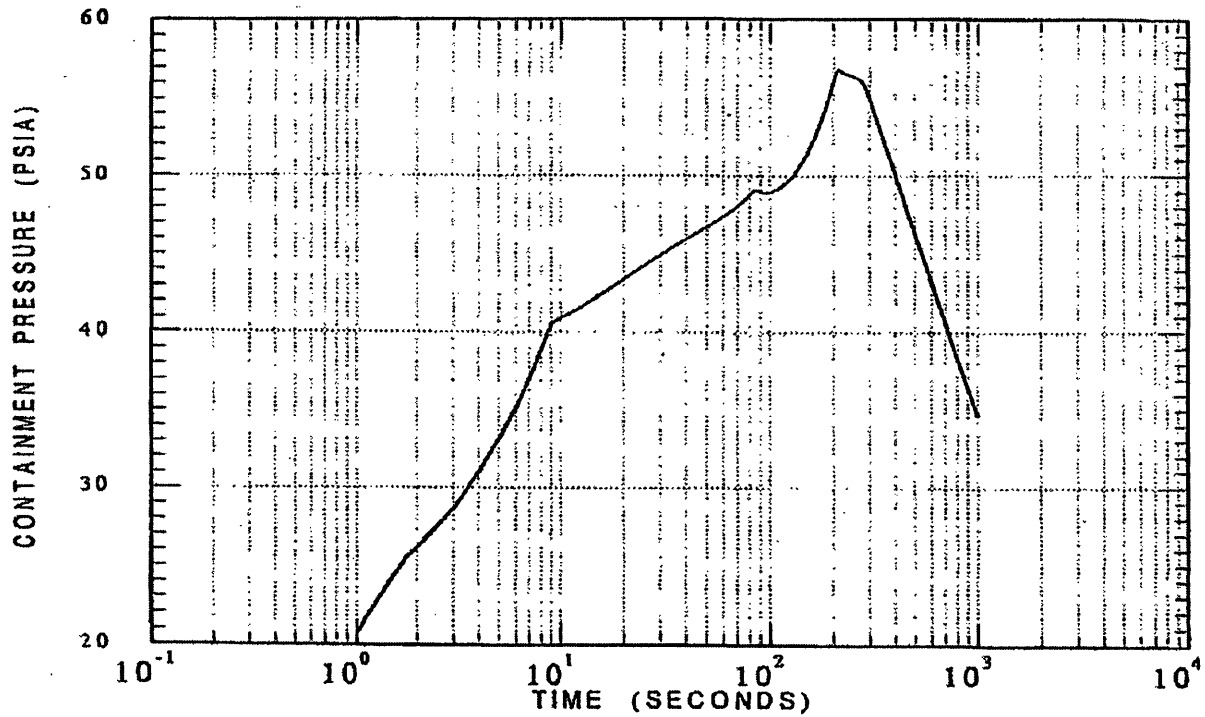


FIGURE 14.2-34

CONTAINMENT PRESSURE PEAK PRESSURE  
ANALYSIS MAIN STEAMLINE BREAK  
(30% POWER) 1.4ft<sup>2</sup> DER, MSCV SAF

BEAVER VALLEY POWER STATION UNIT NO. 1  
UPDATED FINAL SAFETY ANALYSIS REPORT

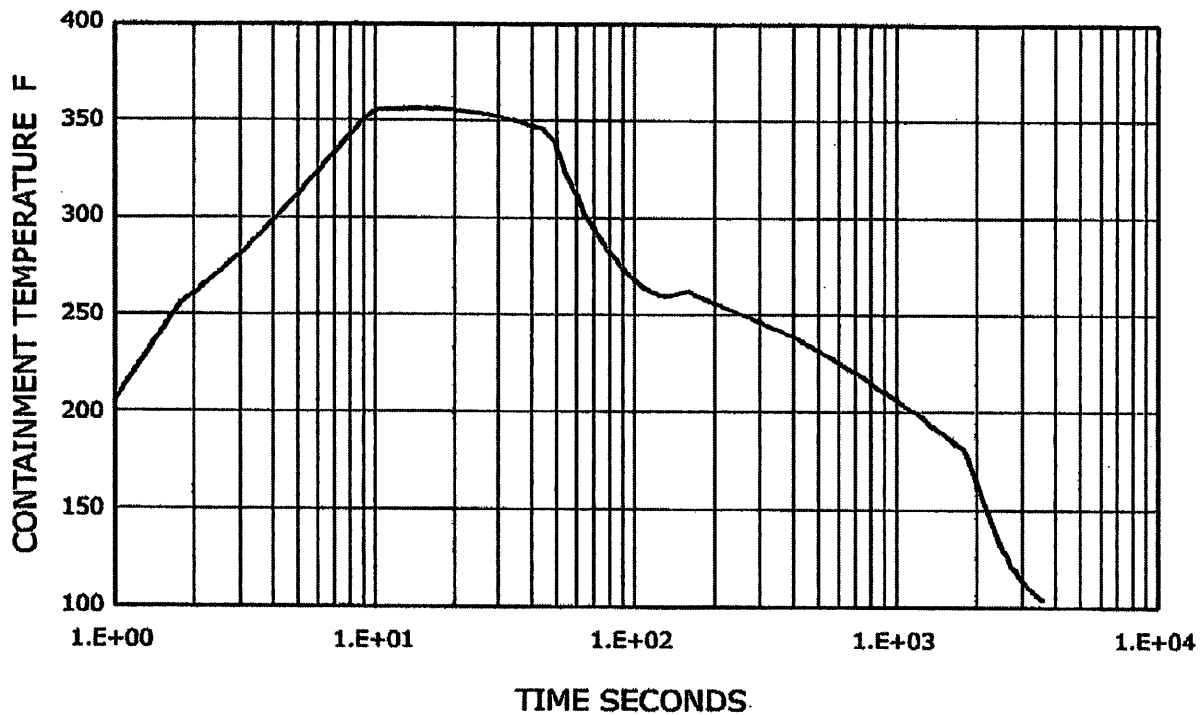


FIGURE 14.2-35

CONTAINMENT ATMOSPHERIC TEMPERATURE PEAK  
TEMPERATURE ANALYSIS MAIN STEAMLINE BREAK  
(100% POWER) 1.4ft<sup>2</sup> DER, MSCV SAF

BEAVER VALLEY POWER STATION UNIT NO. 1  
UPDATED FINAL SAFETY ANALYSIS REPORT

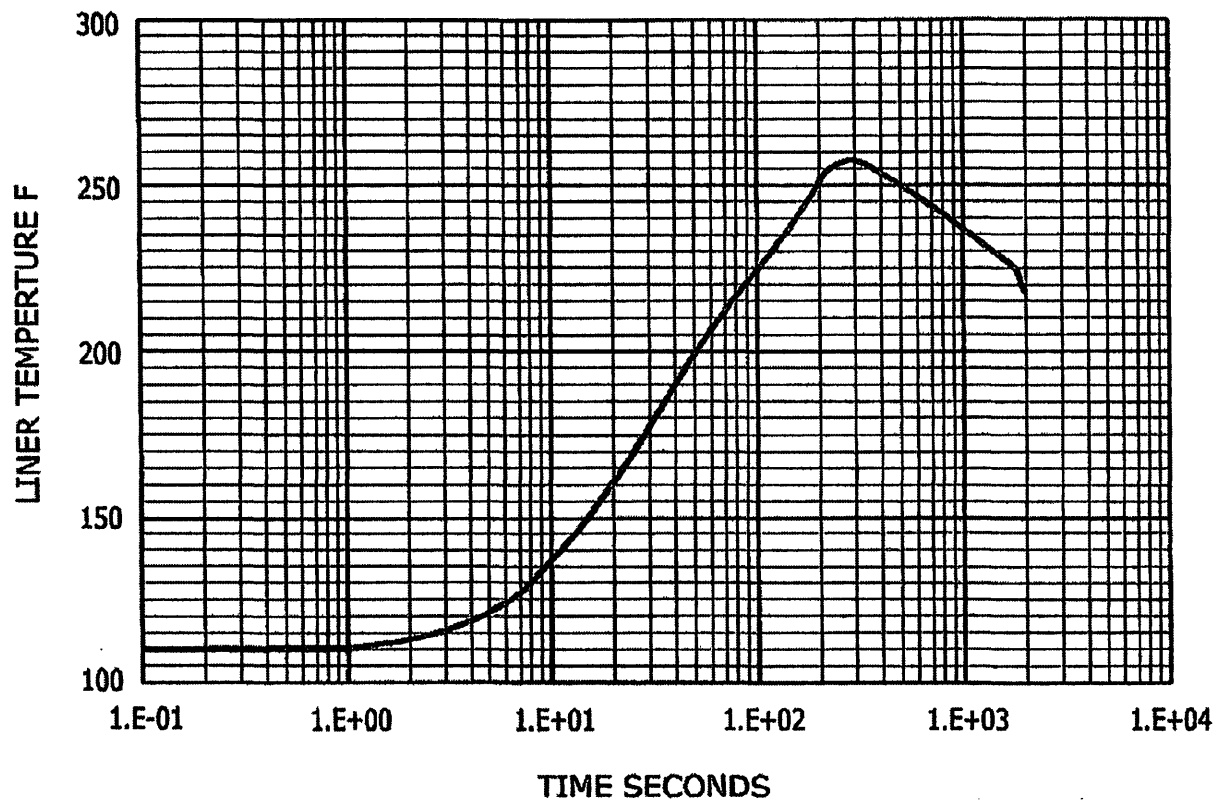
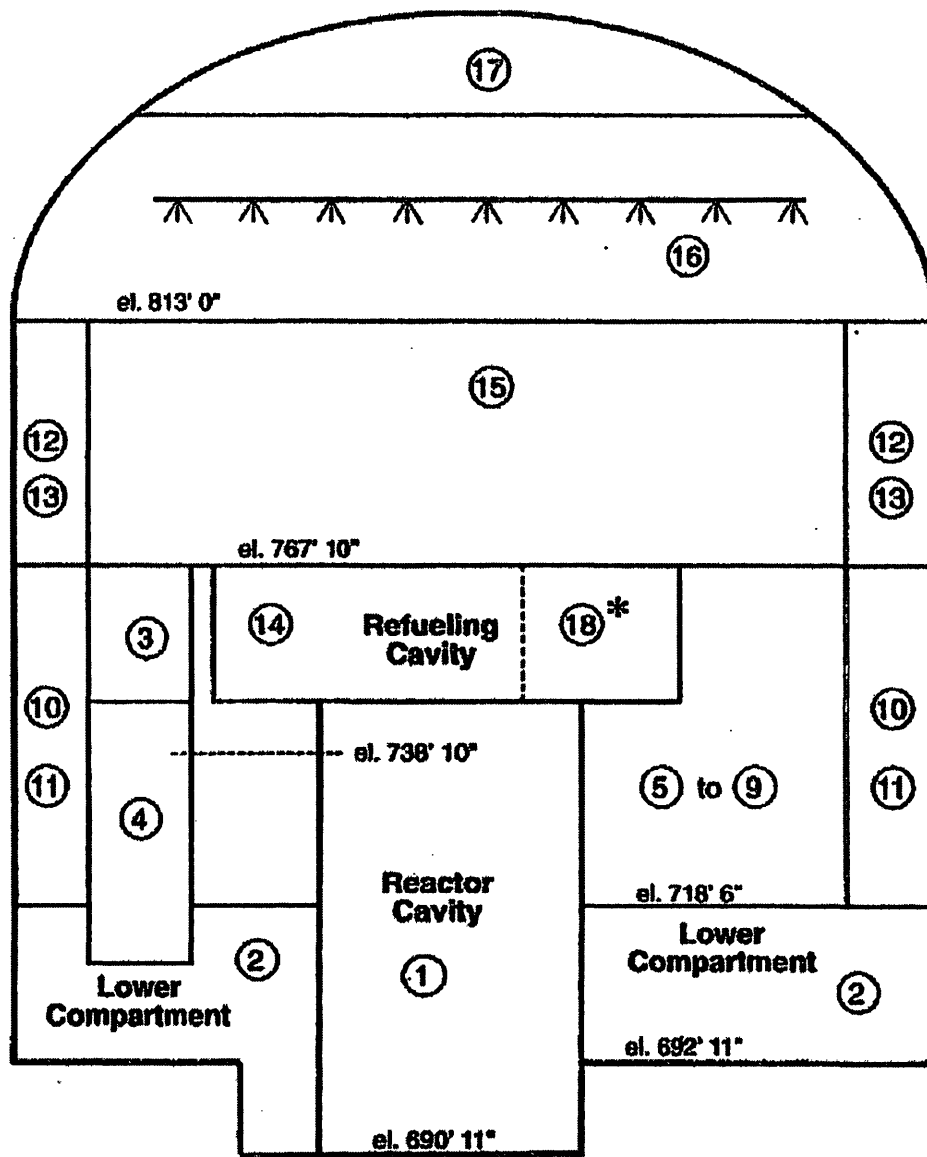


FIGURE 14.2-36

CONTAINMENT LINER TEMPERATURE PEAK  
TEMPERATURE ANALYSIS, MAIN STEAMLINE  
BREAK (30% POWER) 1.4ft<sup>2</sup> DER, MSCV SAF

BEAVER VALLEY POWER STATION UNIT NO. 1  
UPDATED FINAL SAFETY ANALYSIS REPORT



\*Refueling cavity is modeled as two nodes (14 and 18) in Unit 1.

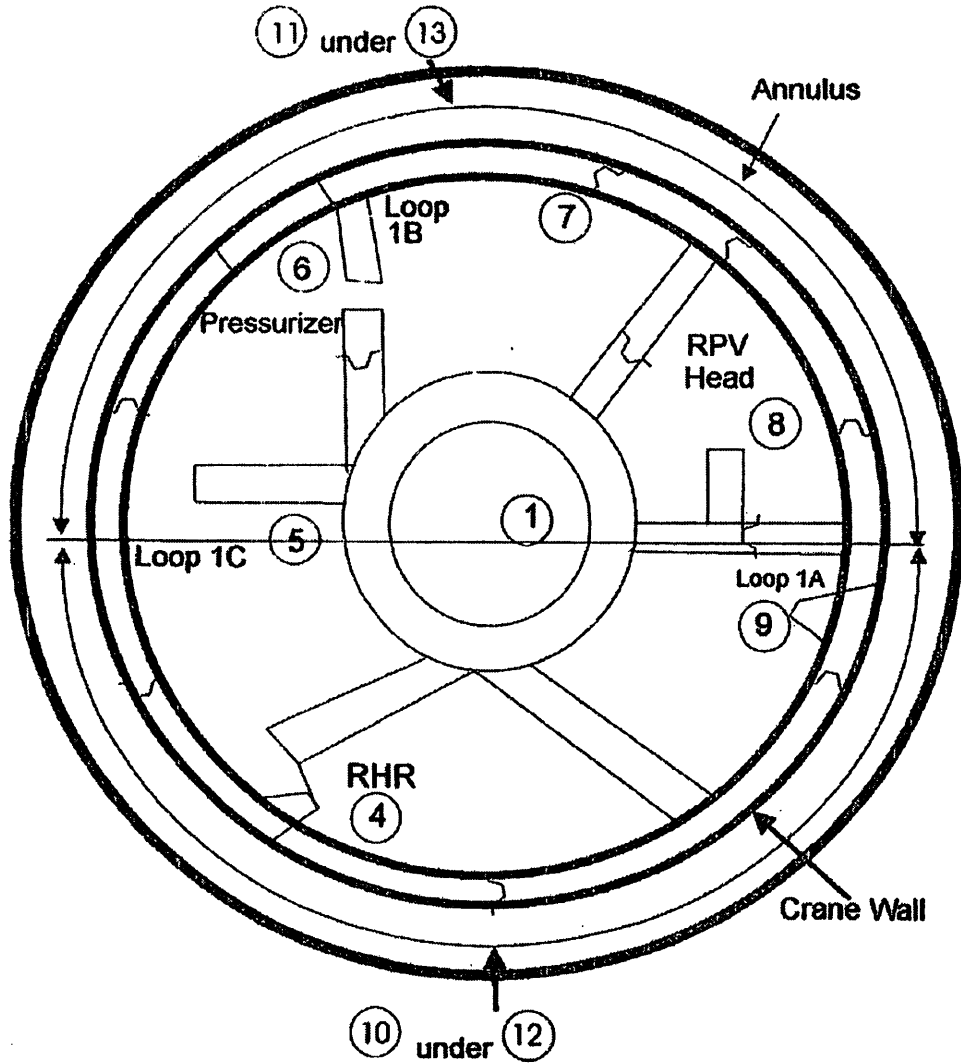
FIGURE 14.3-45

MAAP-DBA CONTAINMENT NODALIZATION  
FOR BVPS-1

BEAVER VALLEY POWER STATION UNIT No. 1  
UPDATED FINAL SAFETY ANALYSIS REPORT



N  
(Unit 1)



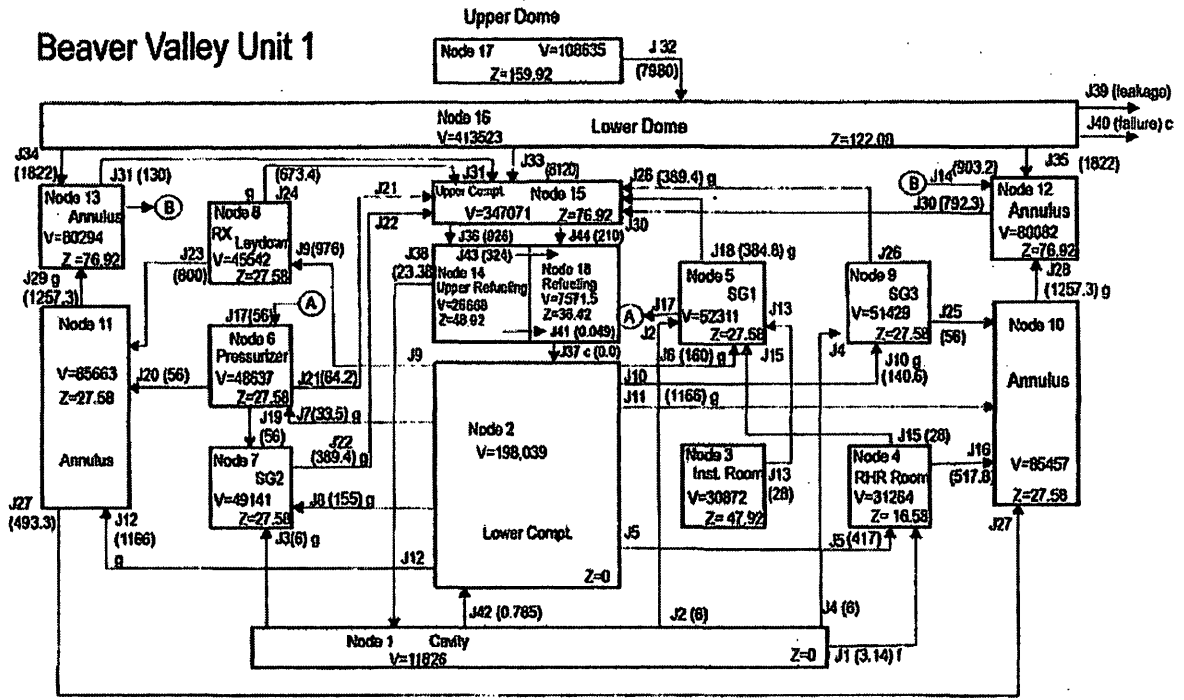
WB022001.CDR 4-26-2002

FIGURE 14.3-46

MAAP-DBA CONTAINMENT NODALIZATION  
(PLAN VIEW)

BEAVER VALLEY POWER STATION UNIT No. 1  
UPDATED FINAL SAFETY ANALYSIS REPORT

Beaver Valley Unit 1



WB02000.CDR 12-10-2002

Notes: (1) Jn (A) g,c  
 Jn: Junction number  
 (A): Junction flow area (ft.<sup>2</sup>)  
 g: Junction with grating and/or stairs  
 c: junction normally closed  
 f: junction opens on set ΔP

(2) Inside the node  
 V is volume (ft.<sup>3</sup>) and  
 Z is elevation (ft.)

FIGURE 14.3-47

MAAP-DBA NODE AND JUNCTION  
 ARRANGEMENT FOR BVPS-1

BEAVER VALLEY POWER STATION UNIT No. 1  
 UPDATED FINAL SAFETY ANALYSIS REPORT

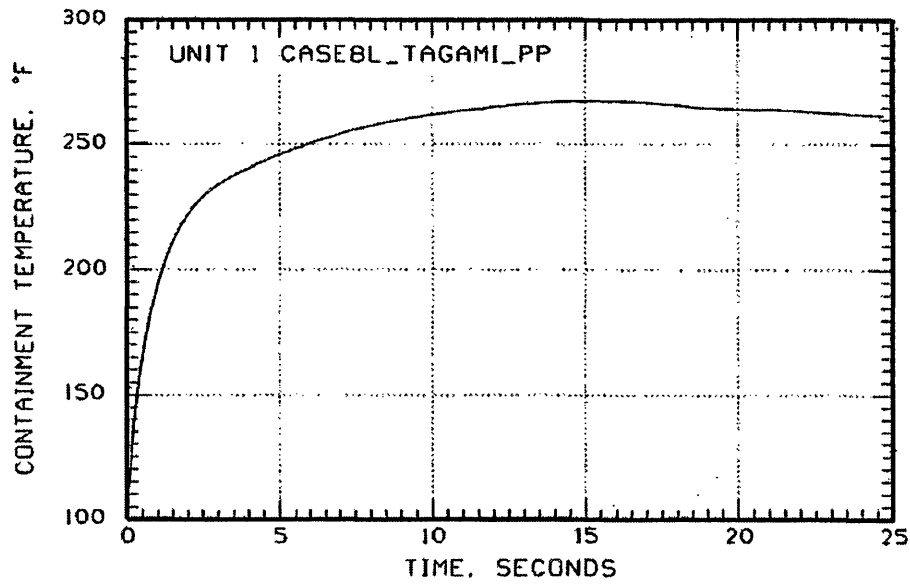
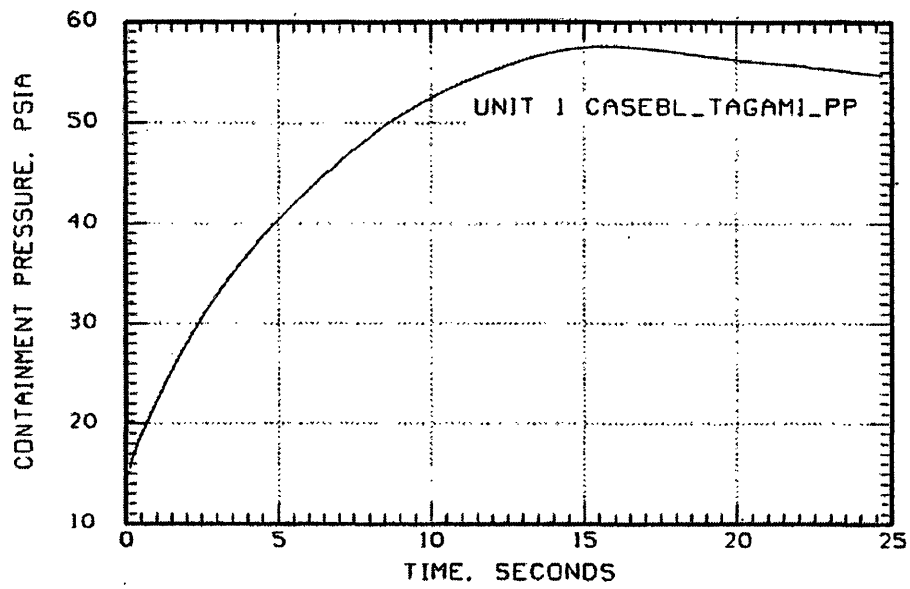


FIGURE 14.3-56

CONTAINMENT PRESSURE & TEMPERATURE  
TIME-HISTORY FOR THE DEHL BREAK CASE

BEAVER VALLEY POWER STATION UNIT No. 1  
UPDATED FINAL SAFETY ANALYSIS REPORT

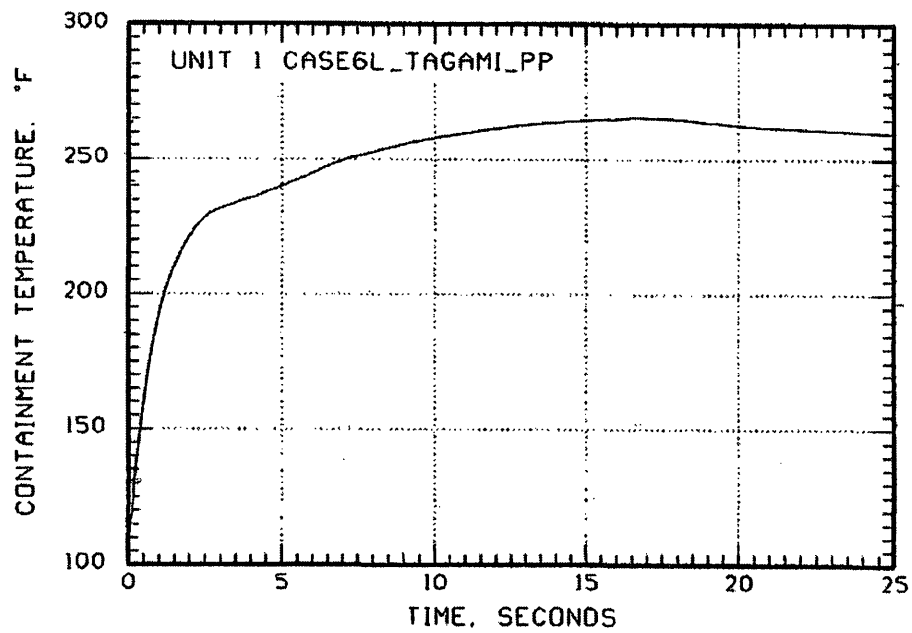
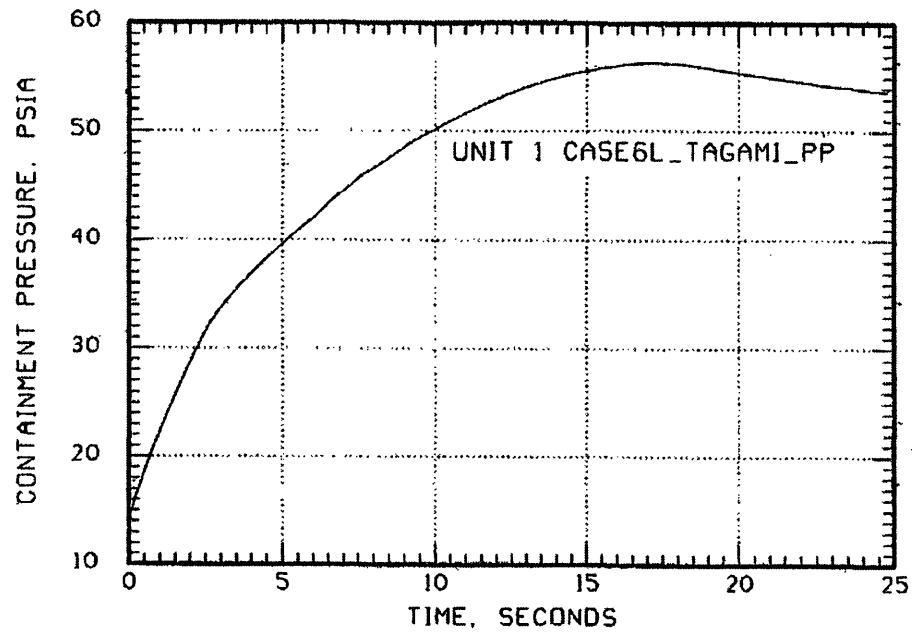


FIGURE 14.3-56A

CONTAINMENT PRESSURE & TEMPERATURE TIME-HISTORY FOR THE DEPS MINIMUM SI BREAK CASE

BEAVER VALLEY POWER STATION UNIT No. 1  
UPDATED FINAL SAFETY ANALYSIS REPORT

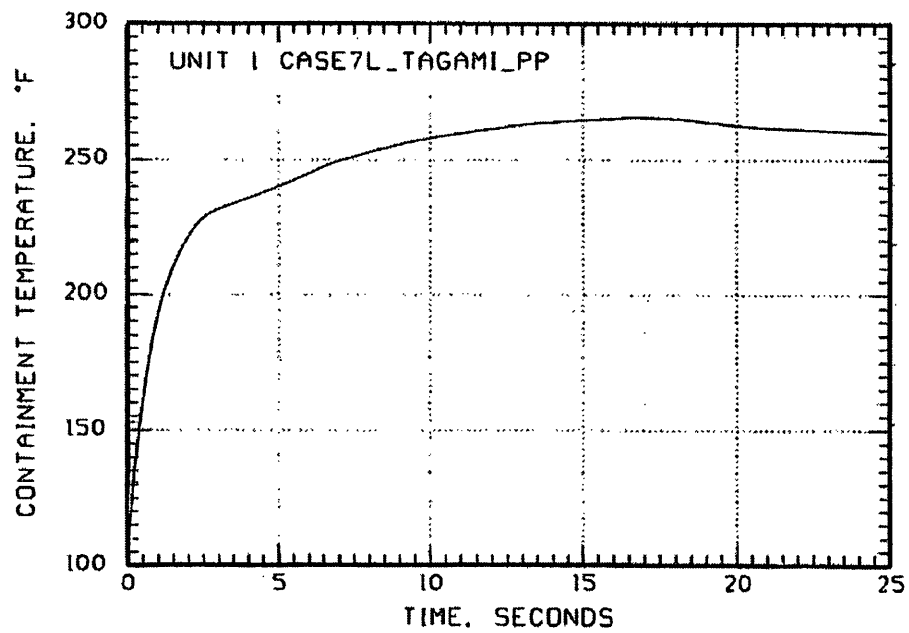
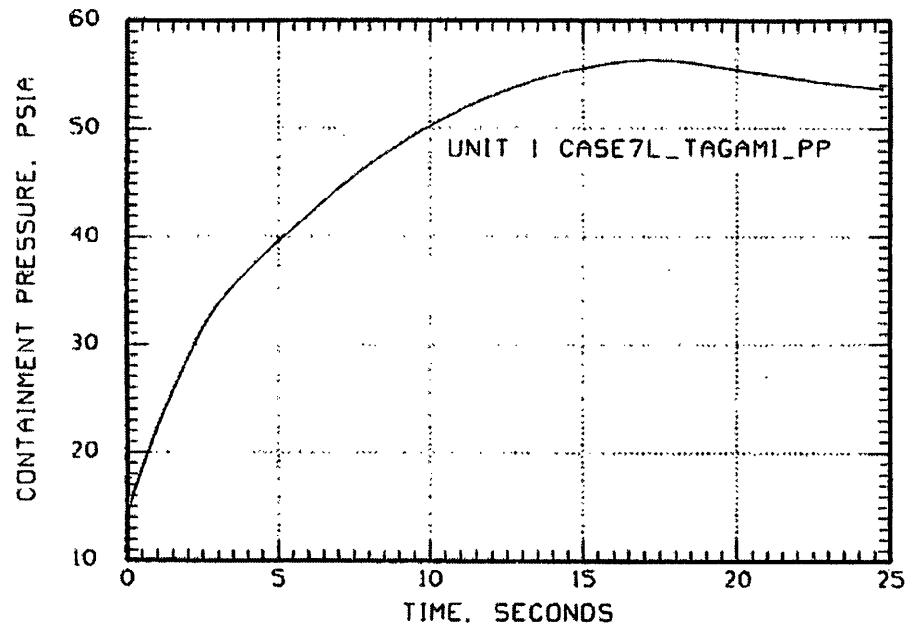
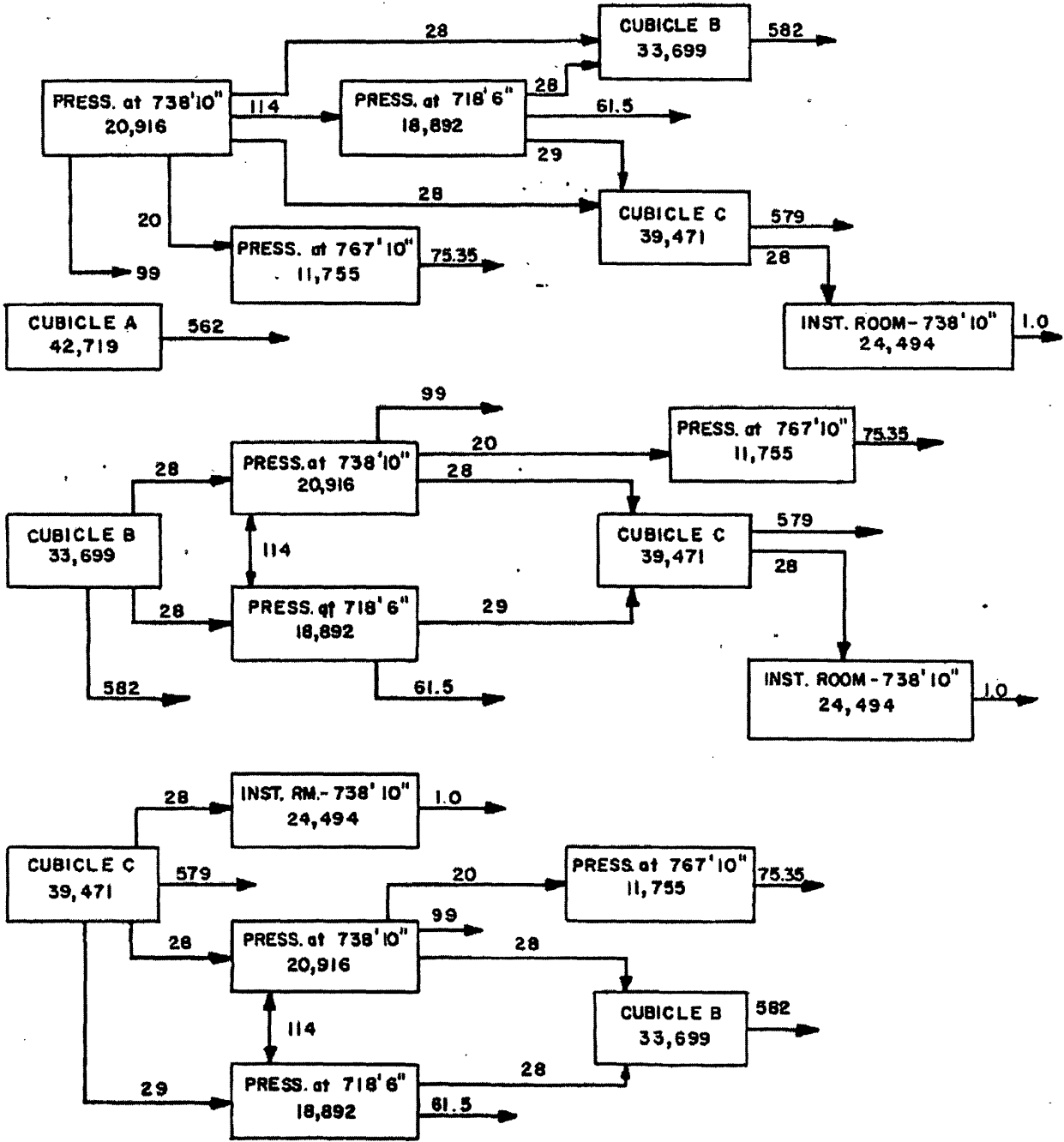


FIGURE 14.3-56B

CONTAINMENT PRESSURE & TEMPERATURE TIME-HISTORY FOR THE DEPS MAXIMUM SI BREAK CASE

BEAVER VALLEY POWER STATION UNIT No. 1  
UPDATED FINAL SAFETY ANALYSIS REPORT



NOTE:  
 VOLUMES IN FT<sup>3</sup>  
 VENT AREAS IN FT<sup>2</sup>

FIGURE 14-5-82  
 FREE VOLUMES AND VENT AREAS FOR  
 STEAM GENERATOR AND PRESSURIZER  
 CUBICLE  
 BEAVER VALLEY POWER STATION UNIT NO. 1  
 UPDATED FINAL SAFETY ANALYSIS REPORT

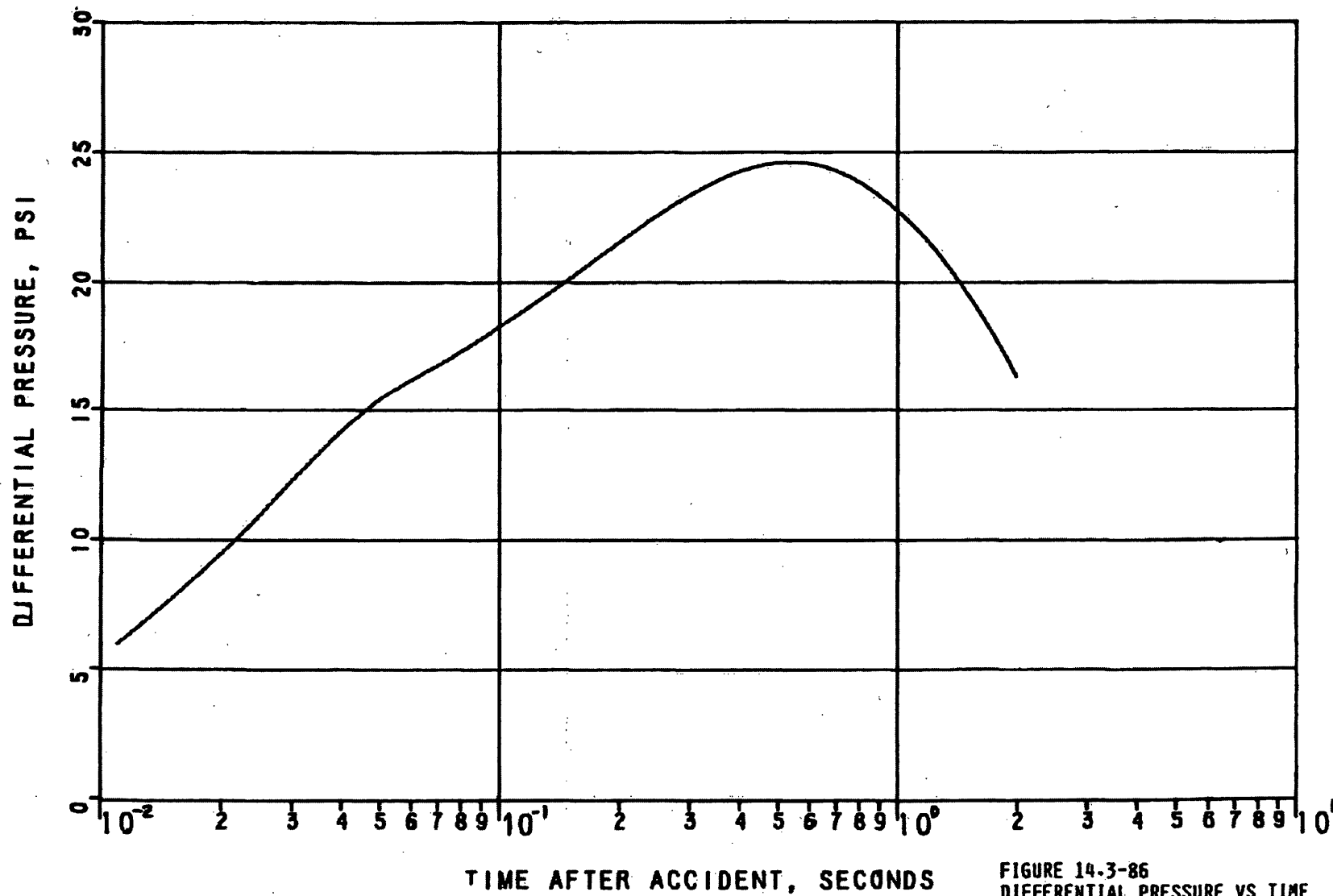


FIGURE 14.3-86  
 DIFFERENTIAL PRESSURE VS TIME  
 STEAM GENERATOR CUBICLE A  
 HOT LEG DER  
 BEAVER VALLEY POWER STATION UNIT NO. 1  
 UPDATED FINAL SAFETY ANALYSIS REPORT

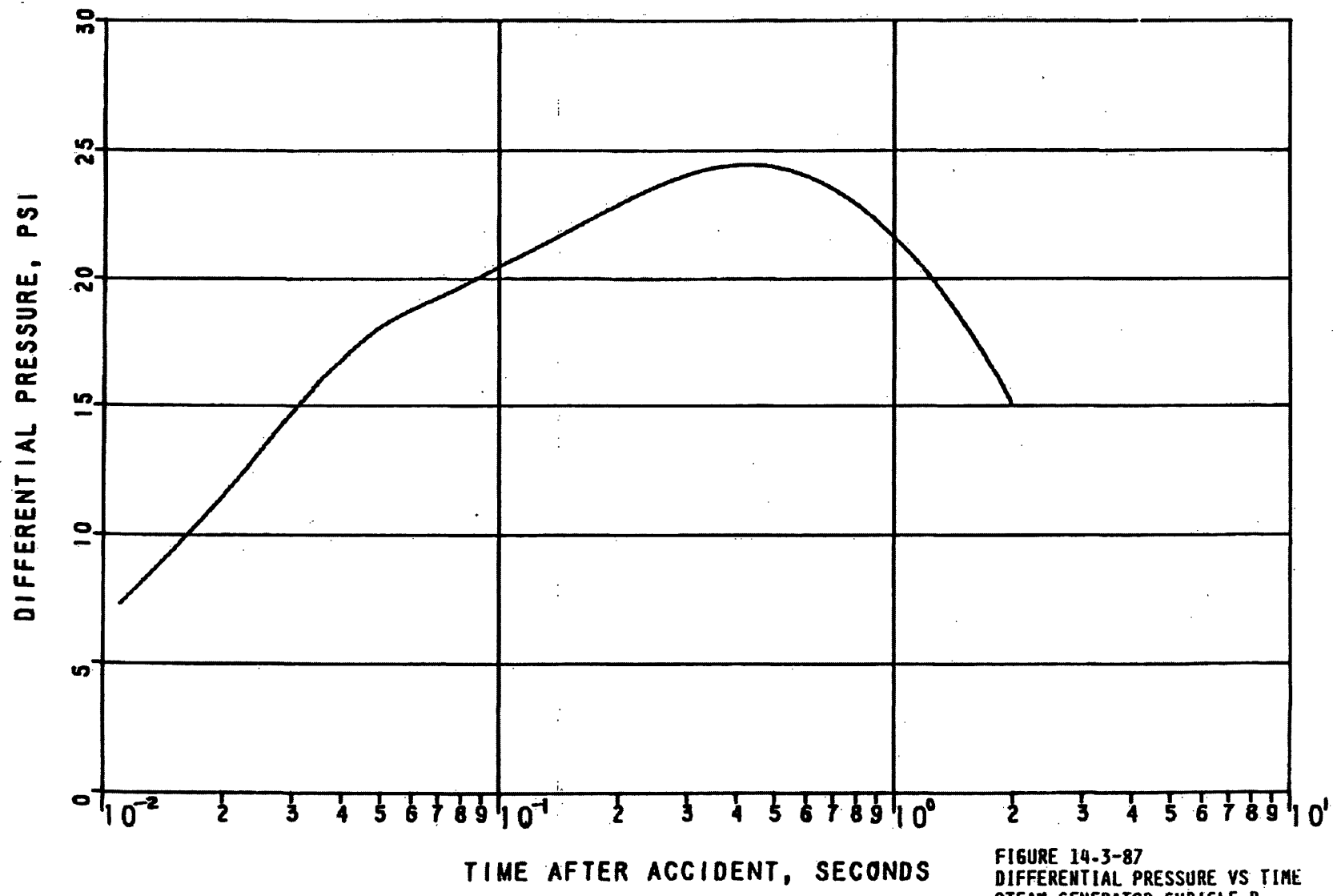


FIGURE 14-3-87  
DIFFERENTIAL PRESSURE VS TIME  
STEAM GENERATOR CUBICLE B  
HOT LEG DER  
BEAVER VALLEY POWER STATION UNIT NO. 1  
UPDATED FINAL SAFETY ANALYSIS REPORT



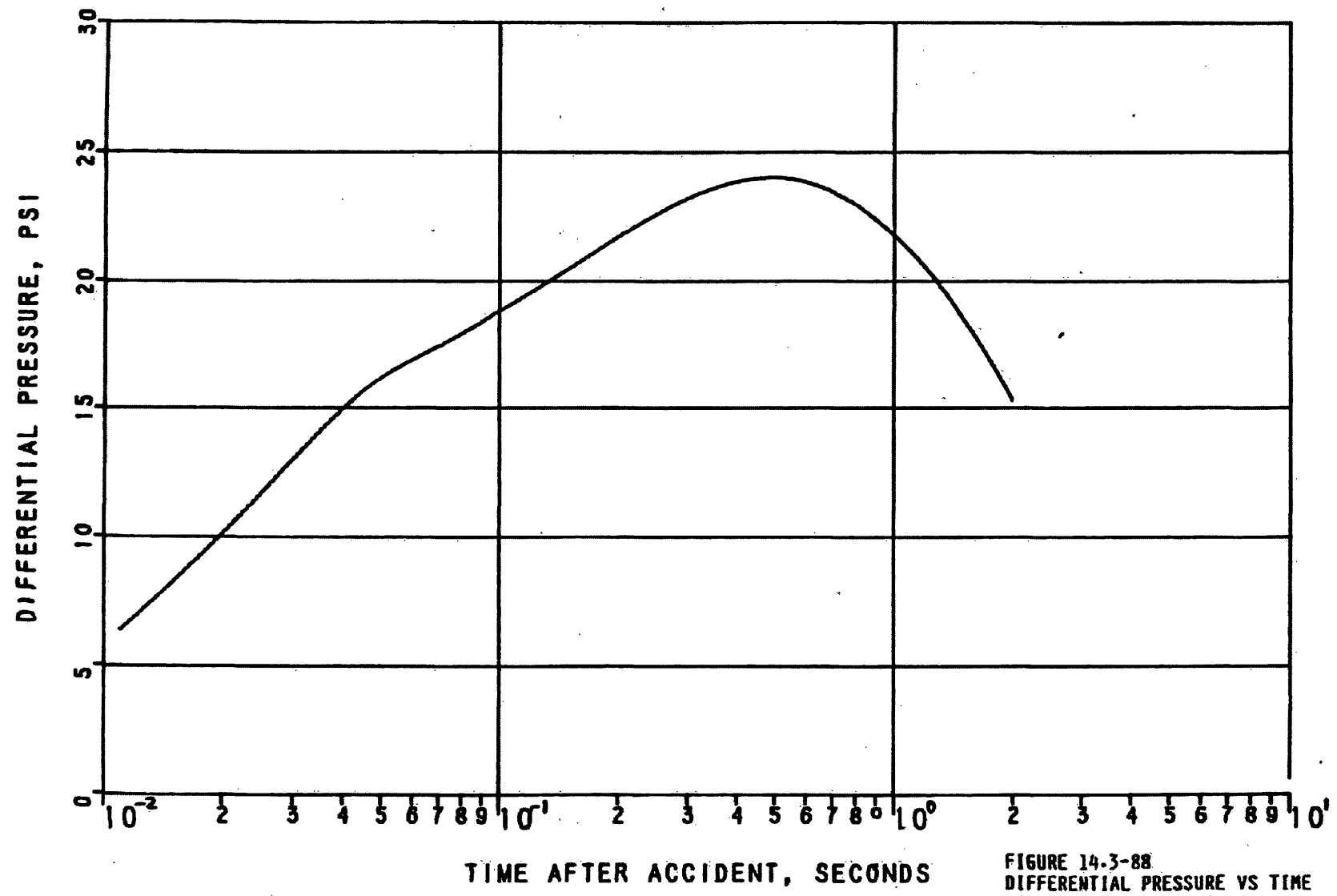


FIGURE 14-3-88  
DIFFERENTIAL PRESSURE VS TIME  
STEAM GENERATOR CUBICLE C  
HOT LEG DER  
BEAVER VALLEY POWER STATION UNIT NO. 1  
UPDATED FINAL SAFETY ANALYSIS REPORT

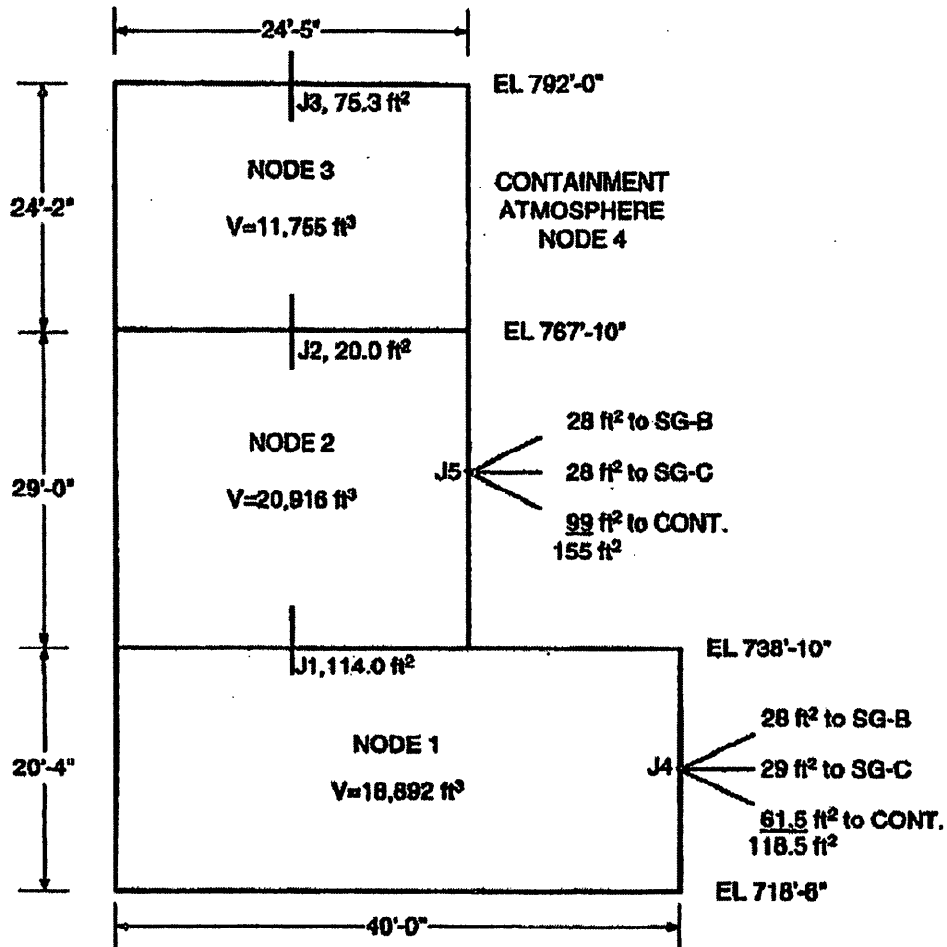


FIGURE 14.3-89

PRESSURIZER NODAL CONFIGURATION  
 4-NODE, 5-JUNCTION MODEL SPRAY  
 LINE BREAK IN NODE 3

BEAVER VALLEY POWER STATION UNIT NO. 1  
 UPDATED FINAL SAFETY ANALYSIS REPORT

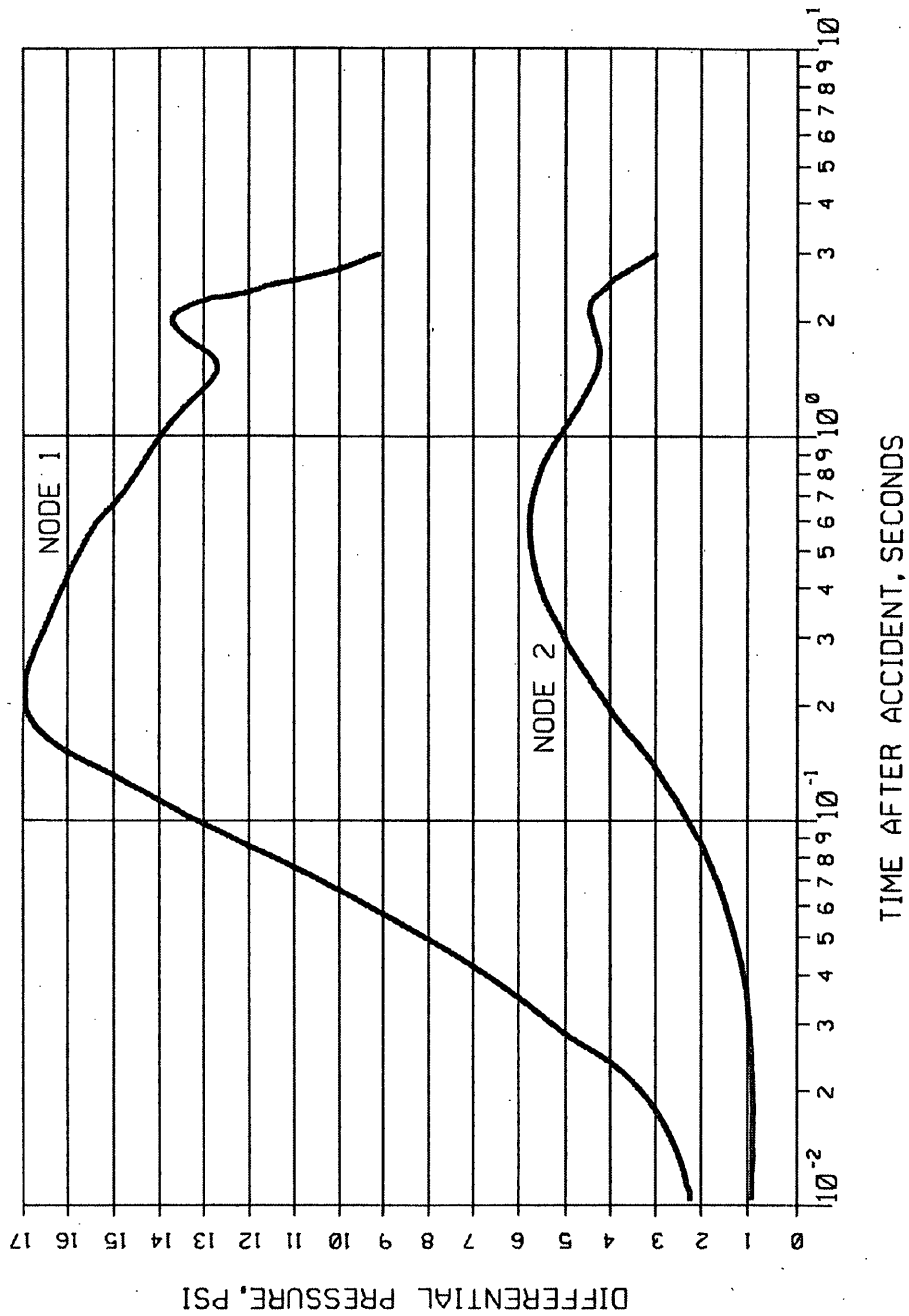
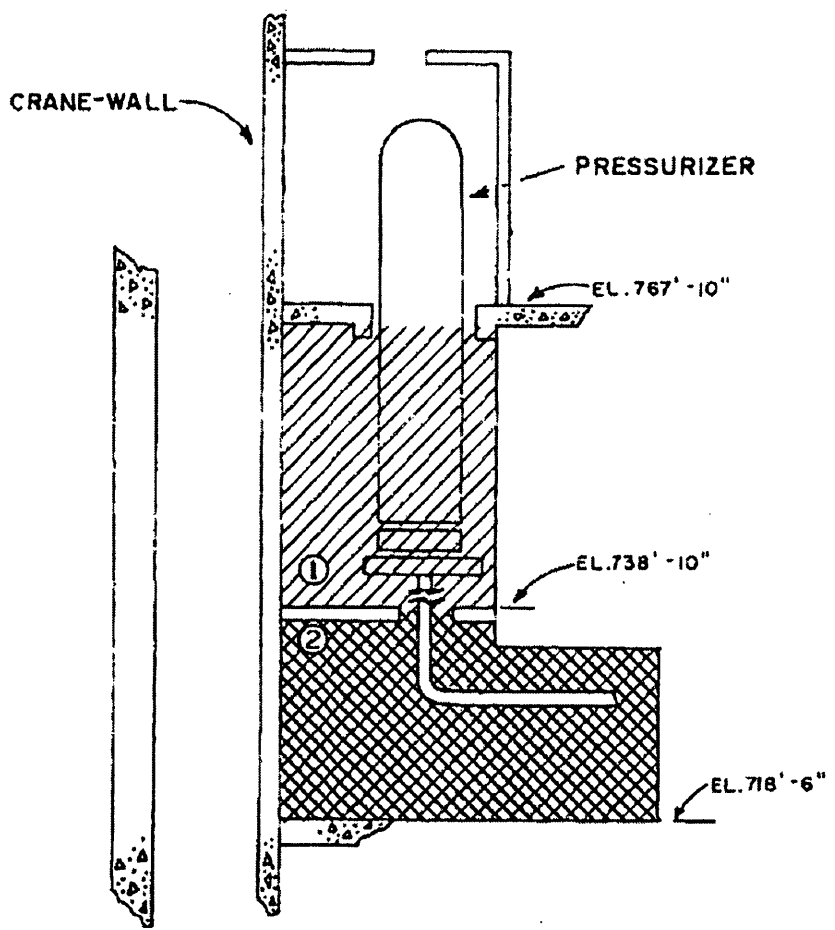


FIGURE 14.3-90

PRESSURE DIFFERENTIAL VS TIME  
PRESSURIZER CUBICLE (2 NODE MODEL)

BEAVER VALLEY POWER STATION UNIT NO. 1  
UPDATED FINAL SAFETY ANALYSIS REPORT





NODE	①		NET VOLUME = 20,916 FT
			VENT AREA = 175 FT
VENT AREA NODE ① TO NODE ② =			114 FT
NODE	②		NET VOLUME = 18,892 FT
			VENT AREA = 118.5 FT

FIGURE 14.3-91  
 NODAL CONFIGURATION FOR PRESSURIZER  
 COMPARTMENTS (MIDDLE NODE 1 & LOWER NODE 2)  
 BEAVER VALLEY POWER STATION UNIT NO. 1  
 UPDATED FINAL SAFETY ANALYSIS REPORT

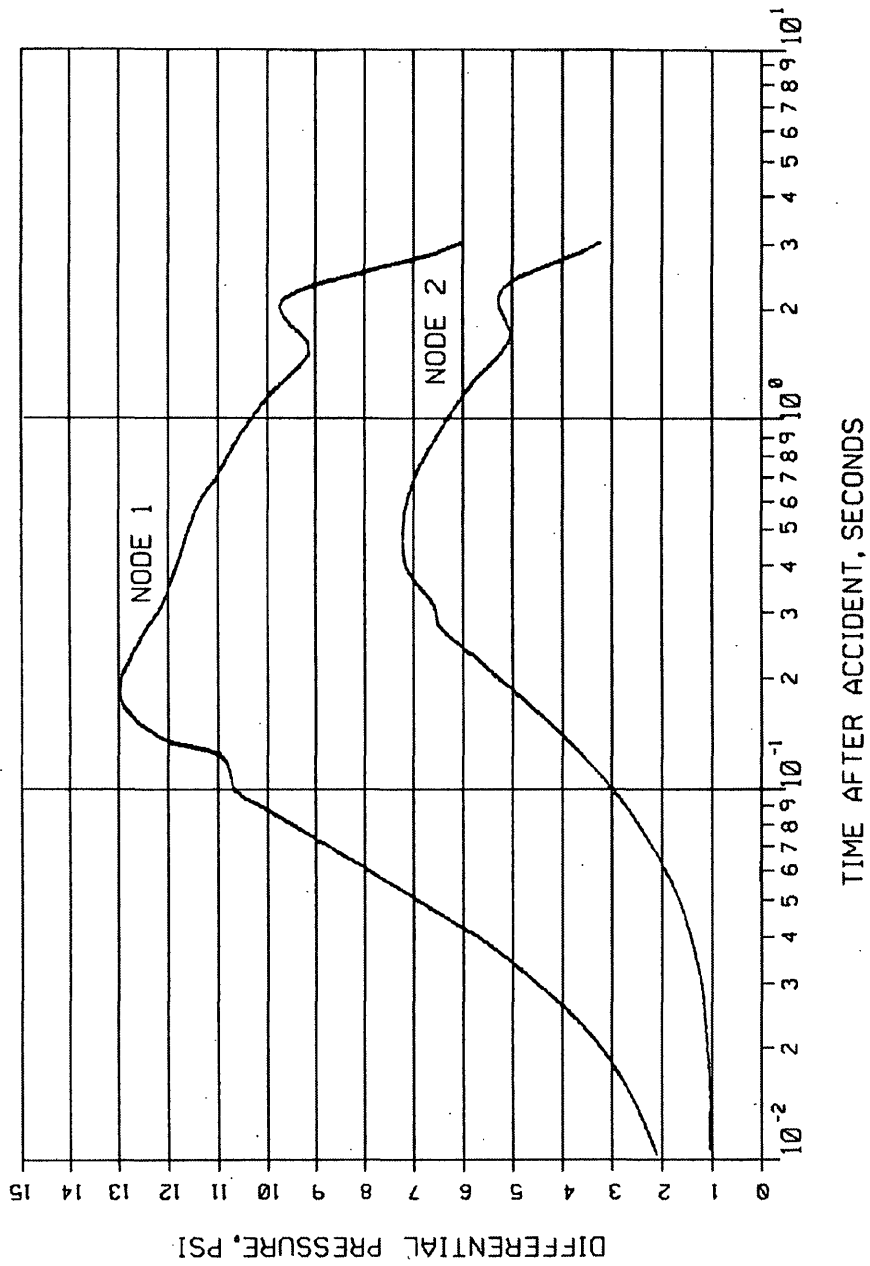


FIGURE 14.3-92

PRESSURE DIFFERENTIAL VS TIME  
PRESSURIZER CUBICLE (2 NODE MODEL)

BEAVER VALLEY POWER STATION UNIT NO. 1  
UPDATED FINAL SAFETY ANALYSIS REPORT

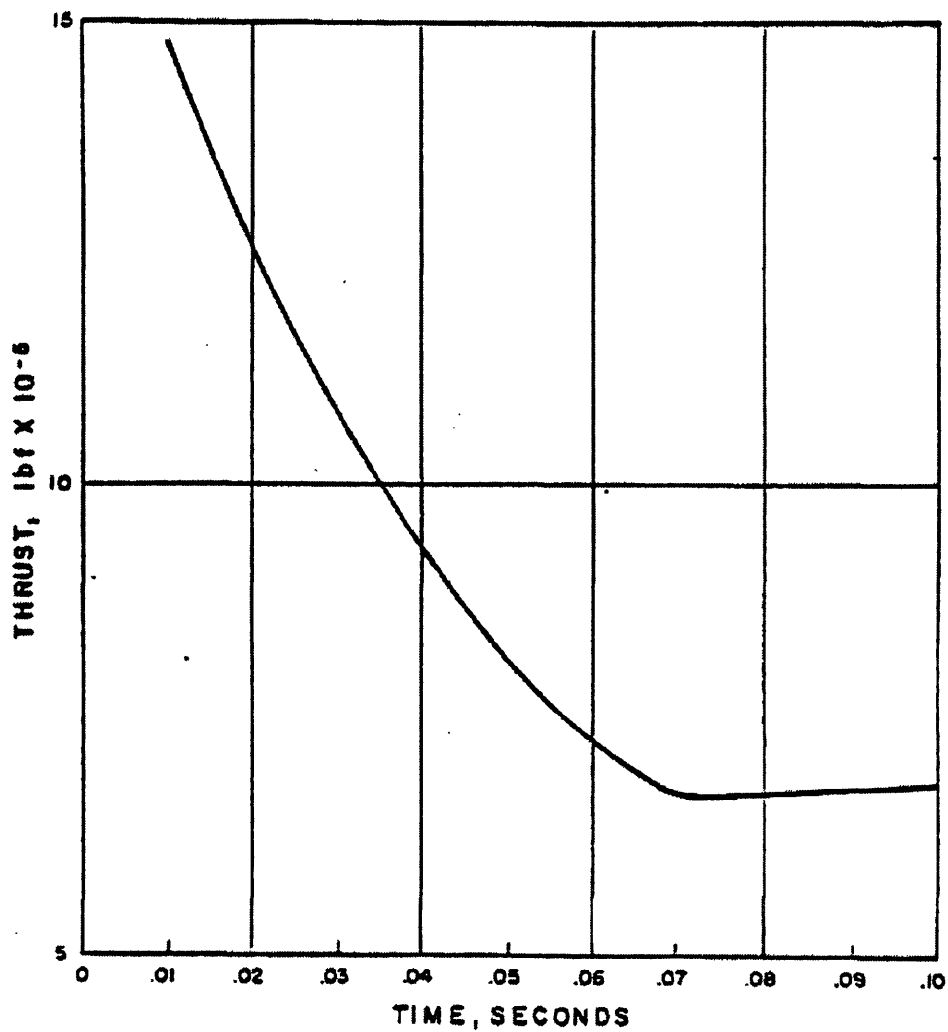
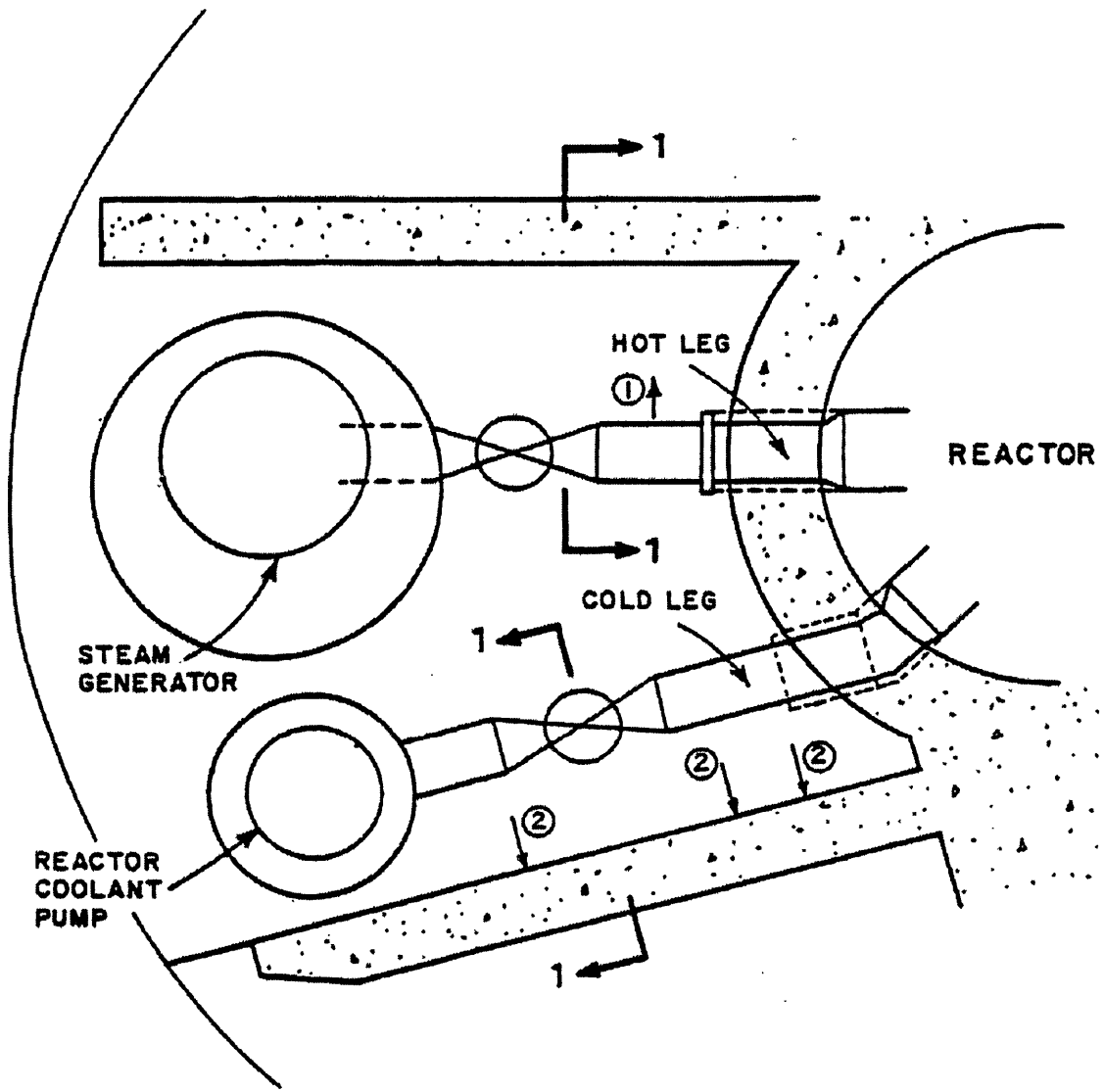


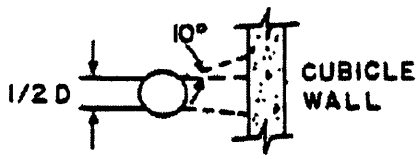
FIGURE 14-3-97  
THRUST FORCE AS A FUNCTION  
OF TIME AFTER A COLD LEG DER  
BEAVER VALLEY POWER STATION UNIT NO. 1  
UPDATED FINAL SAFETY ANALYSIS REPORT



HOT LEG  
REACTOR  
STEAM GENERATOR  
COLD LEG

REACTOR COOLANT PUMP

LEGEND:  
① HOT LEG LONGITUDINAL SPLIT  
② COLD LEG LONGITUDINAL SPLIT



1-1

FIGURE 14-3-98  
JET FORCES ON TYPICAL  
STEAM GENERATOR CUBICLE  
BEAVER VALLEY POWER STATION UNIT NO. 1  
UPDATED FINAL SAFETY ANALYSIS REPORT

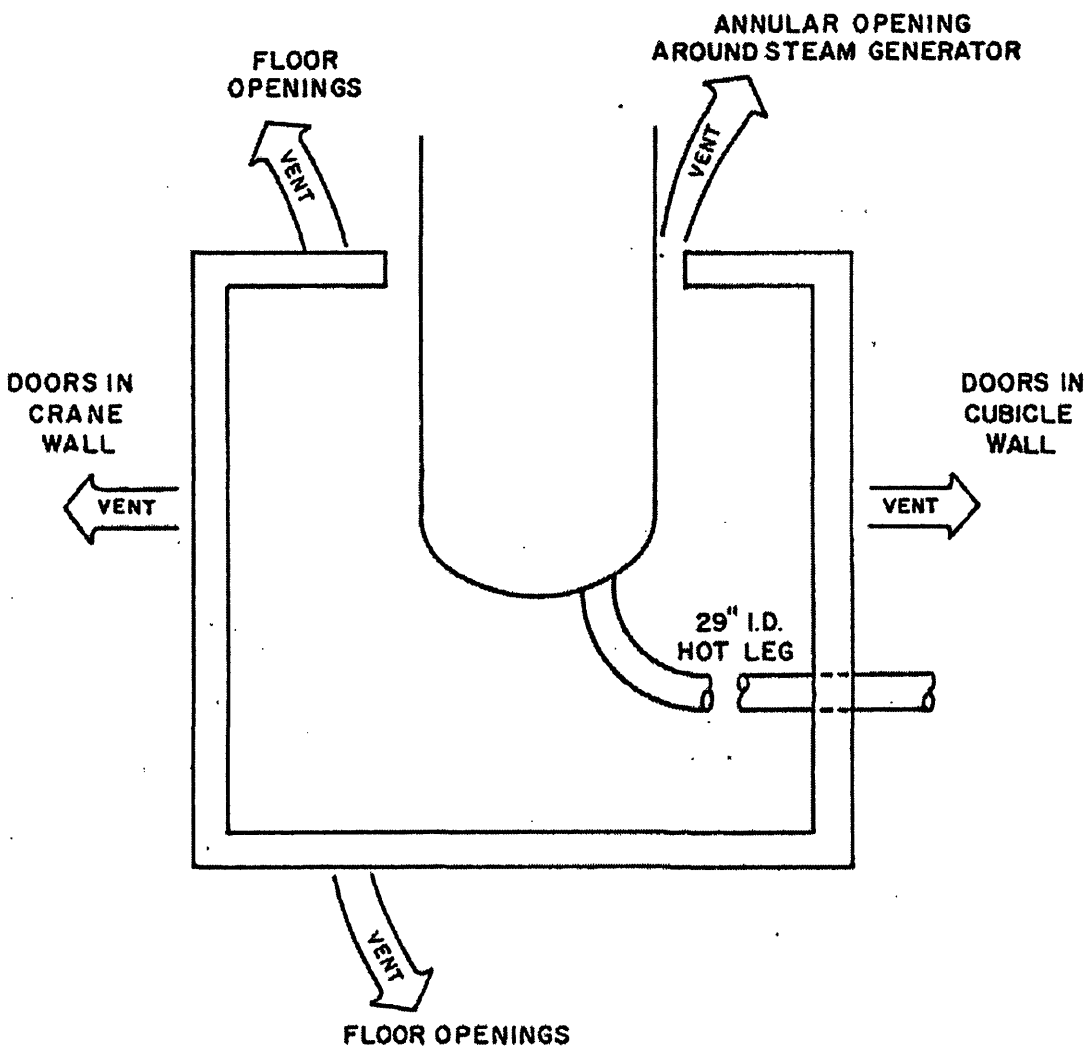


FIGURE 14-3-99  
TYPICAL STEAM GENERATOR  
CUBICLE CONFIGURATION  
BEAVER VALLEY POWER STATION UNIT NO. 1  
UPDATED FINAL SAFETY ANALYSIS REPORT



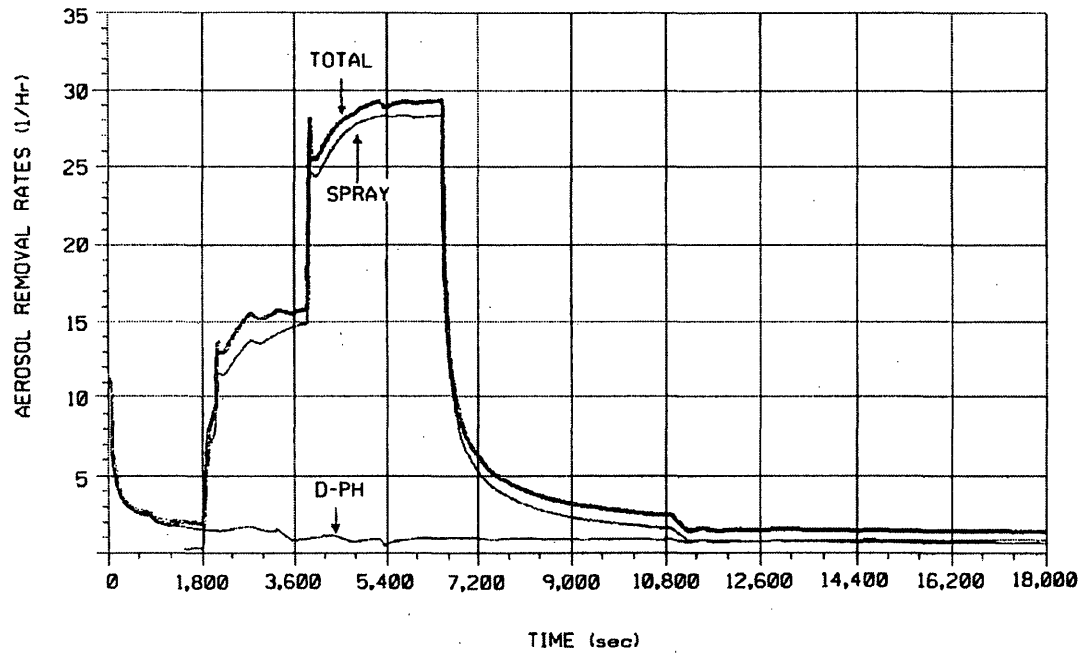


FIGURE 14.3-100

AEROSOL REMOVAL RATES WITHIN SPRAYED  
REGION (NUREG-1465 HLLDR MIN CASE)

BEAVER VALLEY POWER STATION UNIT NO. 1  
UPDATED FINAL SAFETY ANALYSIS REPORT

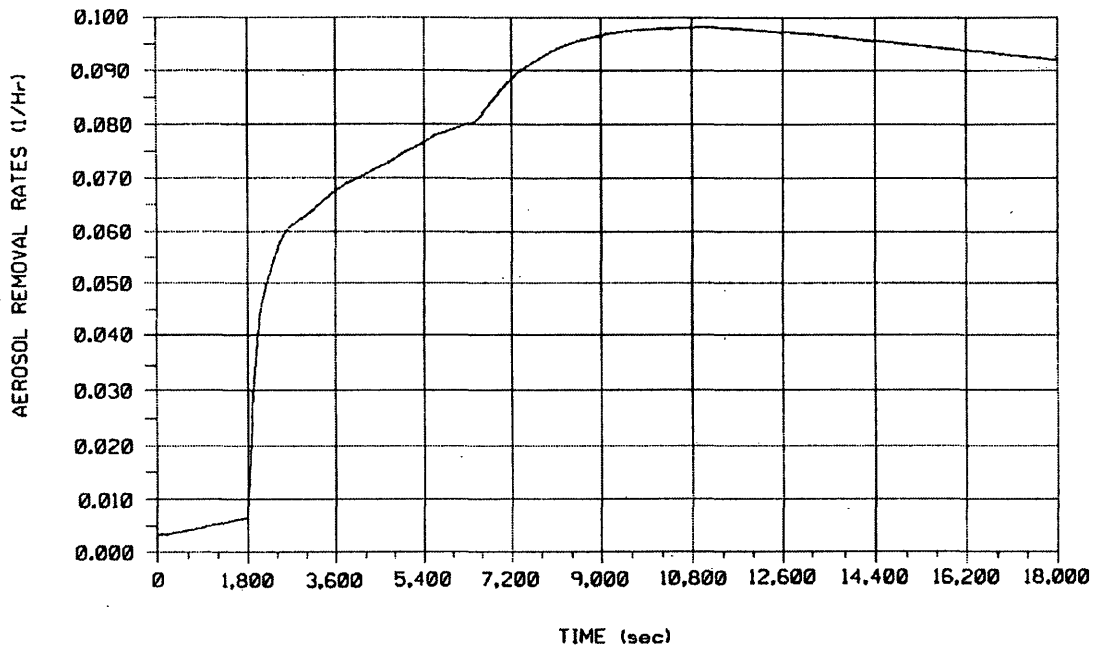


FIGURE 14.3-101

AEROSOL REMOVAL RATES WITHIN UNSPRAYED  
REGION (NUREG-1465 HLDR MIN CASE)

BEAVER VALLEY POWER STATION UNIT NO. 1  
UPDATED FINAL SAFETY ANALYSIS REPORT

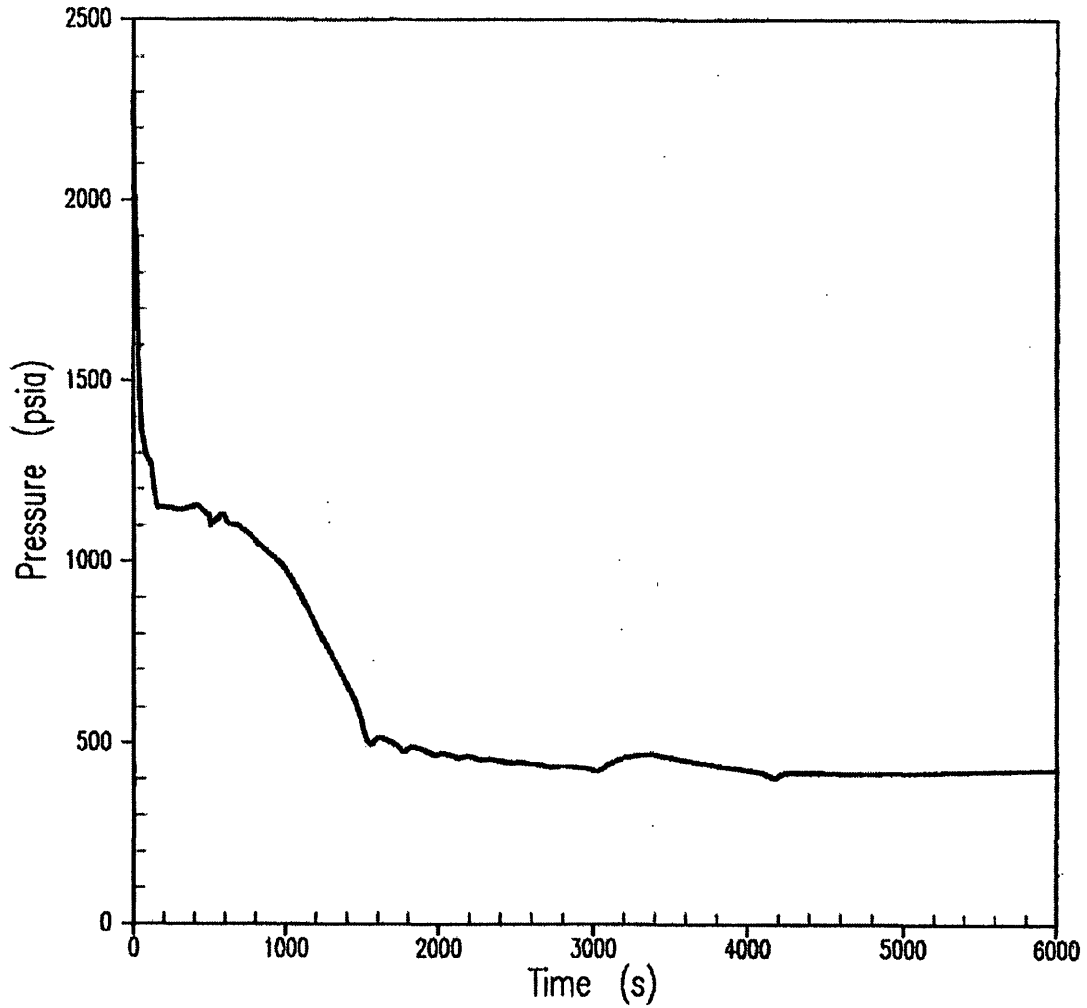


FIGURE 14.3.1-2

2.75-INCH BREAK  
RCS PRESSURE

BEAVER VALLEY POWER STATION UNIT NO. 1  
UPDATED FINAL SAFETY ANALYSIS REPORT

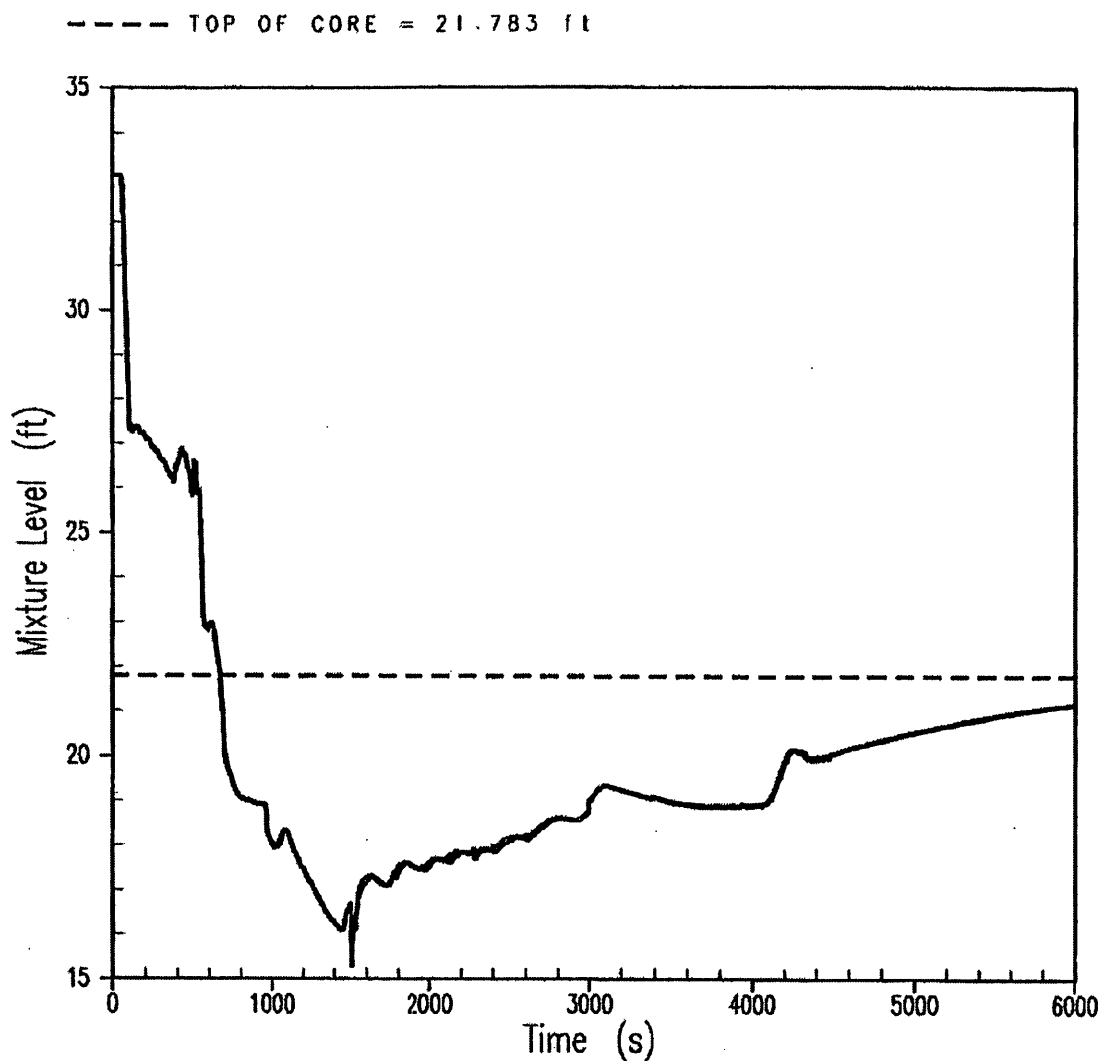


FIGURE 14.3.1-3

2.75-INCH BREAK  
CORE MIXTURE LEVEL

BEAVER VALLEY POWER STATION UNIT NO. 1  
UPDATED FINAL SAFETY ANALYSIS REPORT

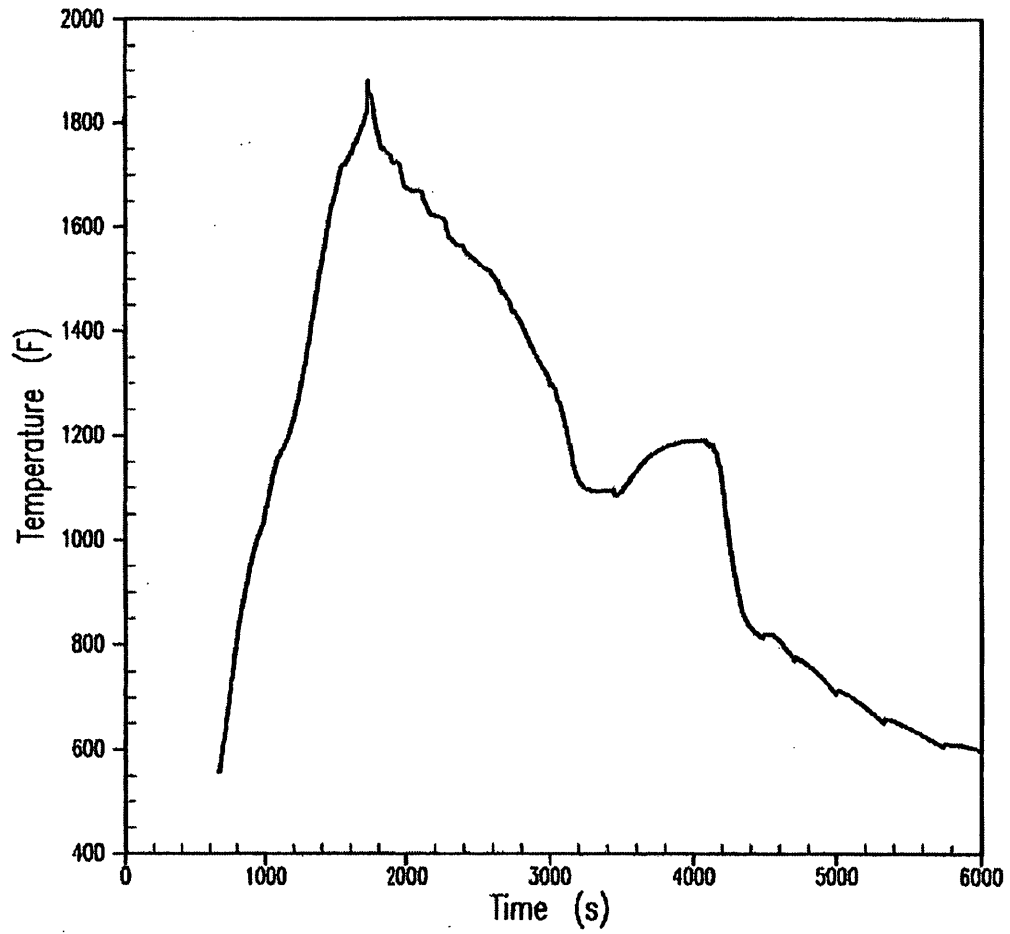


FIGURE 14.3.1-4

2.75-INCH BREAK  
PEAK CLAD TEMPERATURE

BEAVER VALLEY POWER STATION UNIT NO. 1  
UPDATED FINAL SAFETY ANALYSIS REPORT

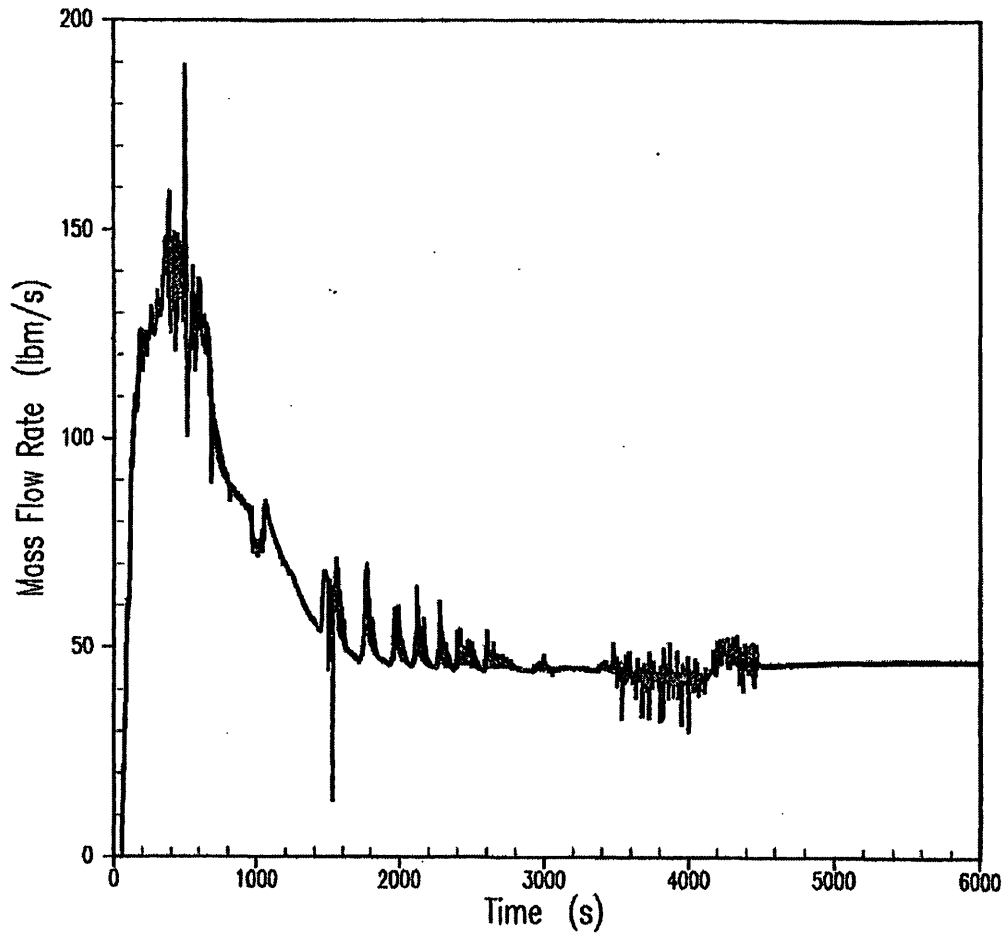


FIGURE 14.3.1-5

STEAM FLOW (2.75-INCH)

BEAVER VALLEY POWER STATION UNIT NO. 1  
UPDATED FINAL SAFETY ANALYSIS REPORT

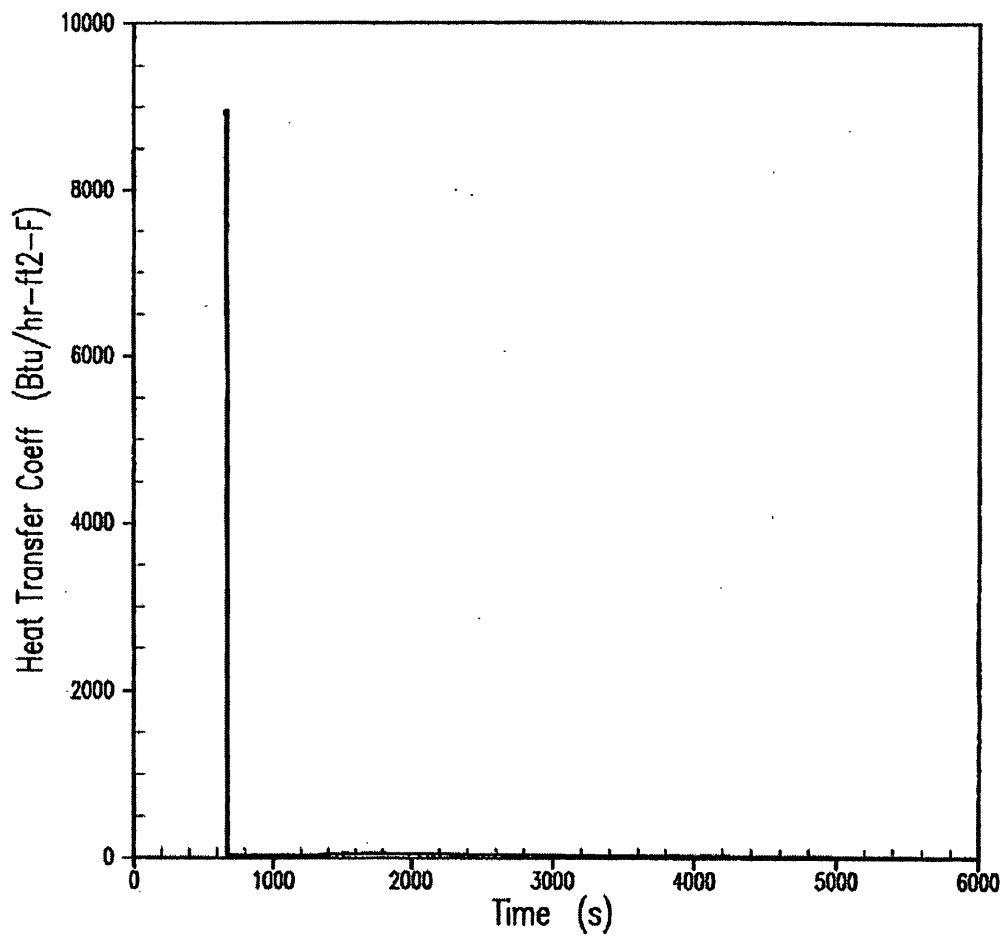


FIGURE 14.3.1-6

2.75-INCH BREAK  
ROD FILM HEAT TRANSFER COEFFICIENT

BEAVER VALLEY POWER STATION UNIT NO. 1  
UPDATED FINAL SAFETY ANALYSIS REPORT

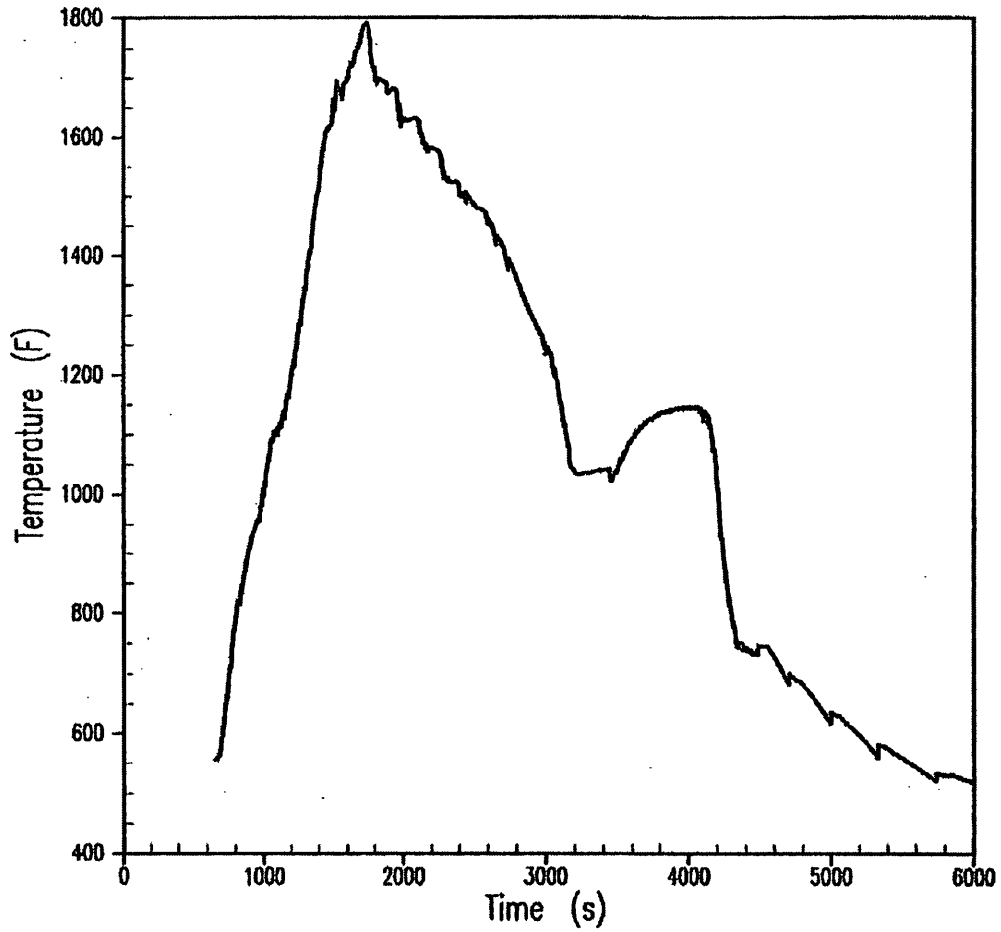


FIGURE 14.3.1-7

2.75-INCH BREAK  
HOT SPOT FLUID TEMPERATURE

BEAVER VALLEY POWER STATION UNIT NO. 1  
UPDATED FINAL SAFETY ANALYSIS REPORT



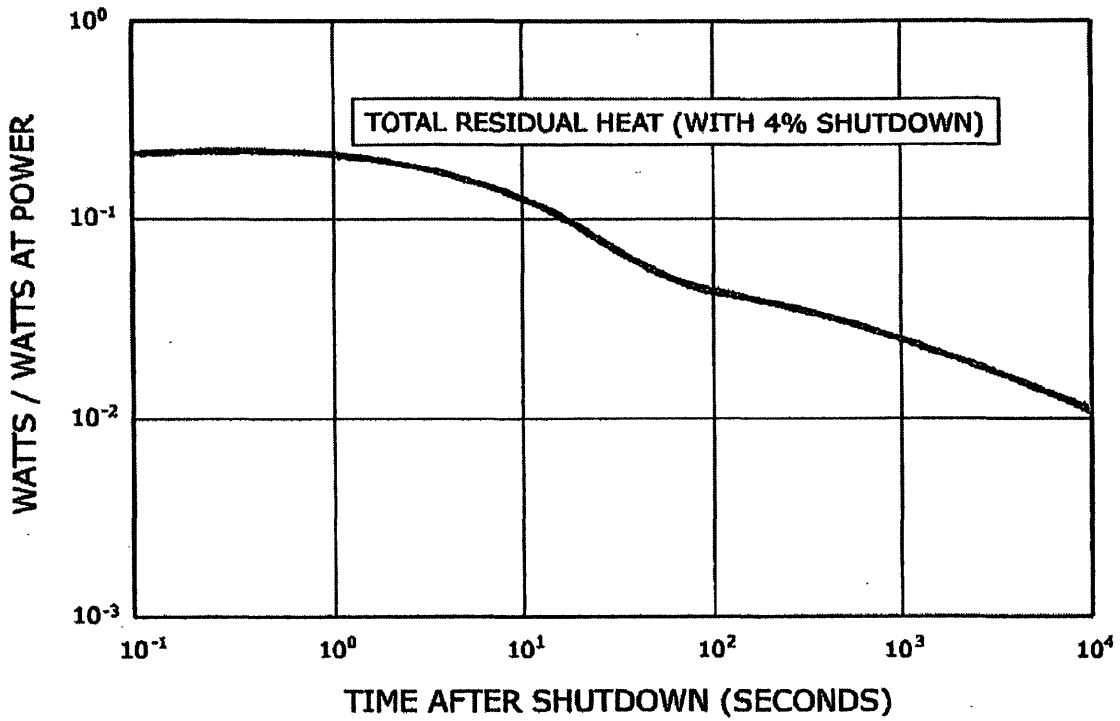


FIGURE 14.3.1-8  
CORE POWER TRANSIENT  
BEAVER VALLEY POWER STATION UNIT NO. 1  
UPDATED FINAL SAFETY ANALYSIS REPORT

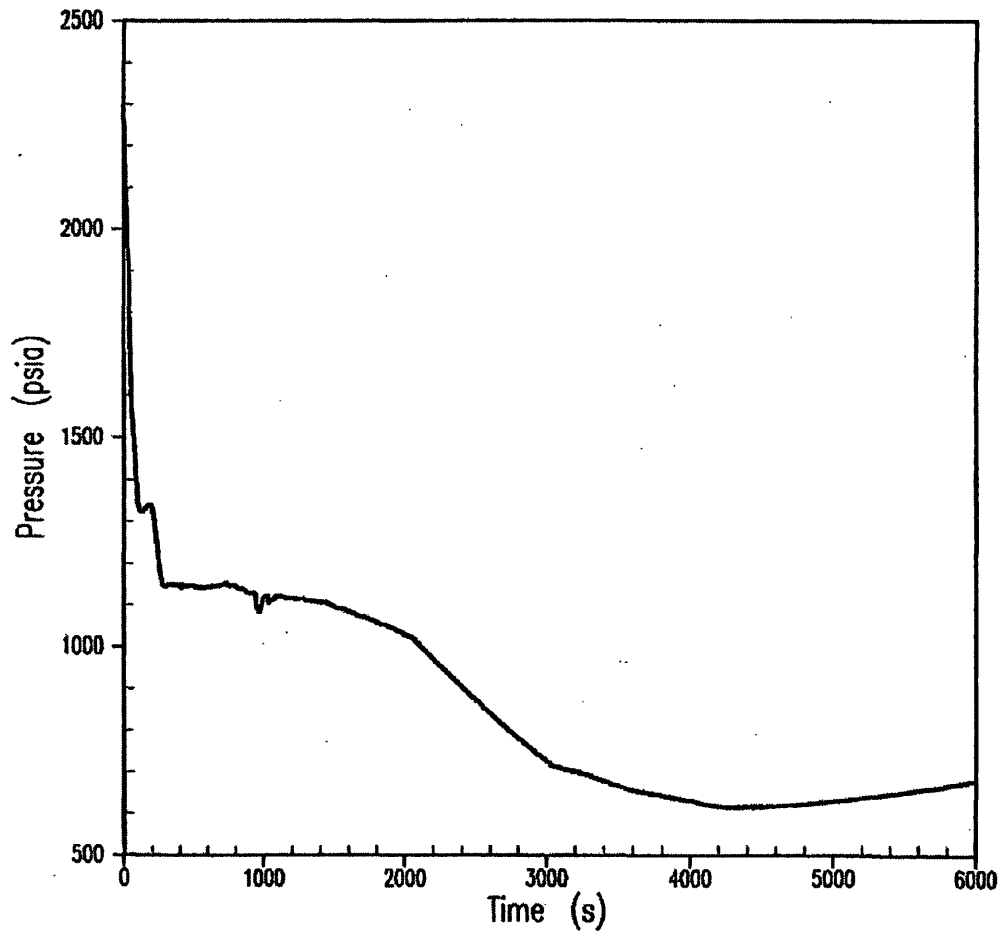


FIGURE 14.3.1-9A

2-INCH BREAK  
RCS PRESSURE

BEAVER VALLEY POWER STATION UNIT NO. 1  
UPDATED FINAL SAFETY ANALYSIS REPORT

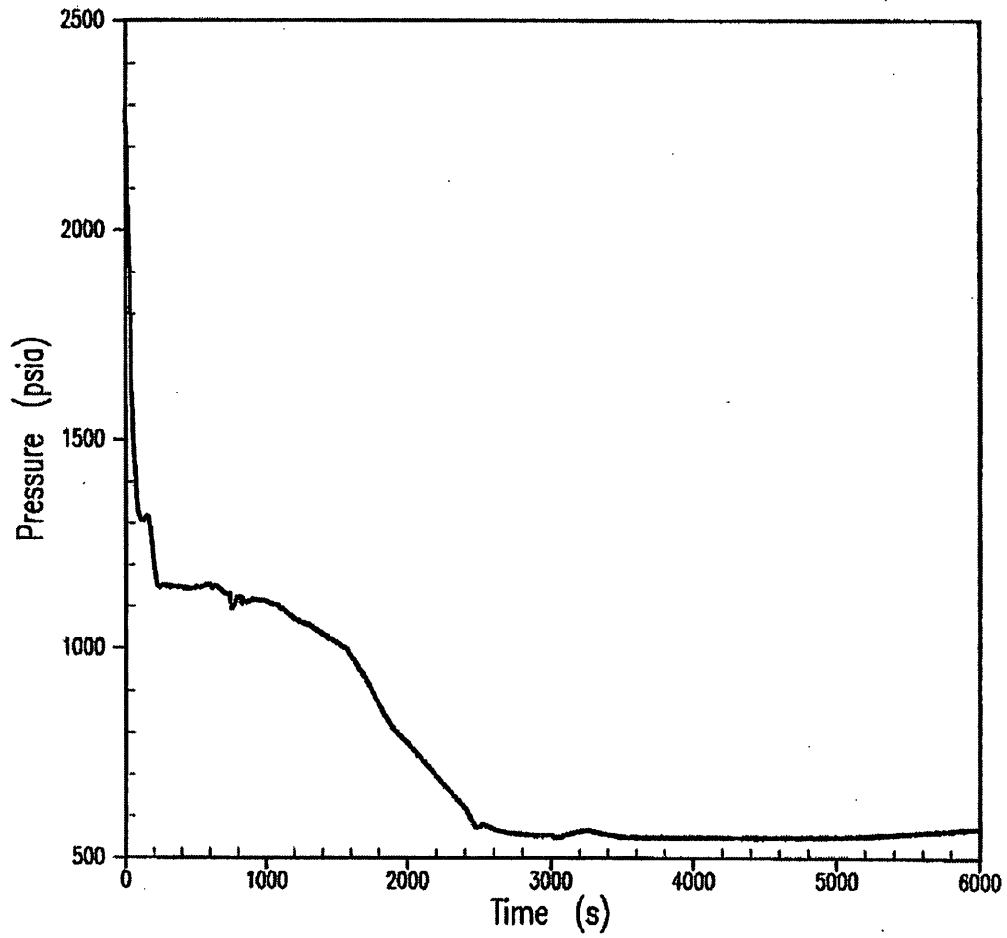


FIGURE 14.3.1-9B

2.25-INCH BREAK  
RCS PRESSURE

BEAVER VALLEY POWER STATION UNIT NO. 1  
UPDATED FINAL SAFETY ANALYSIS REPORT

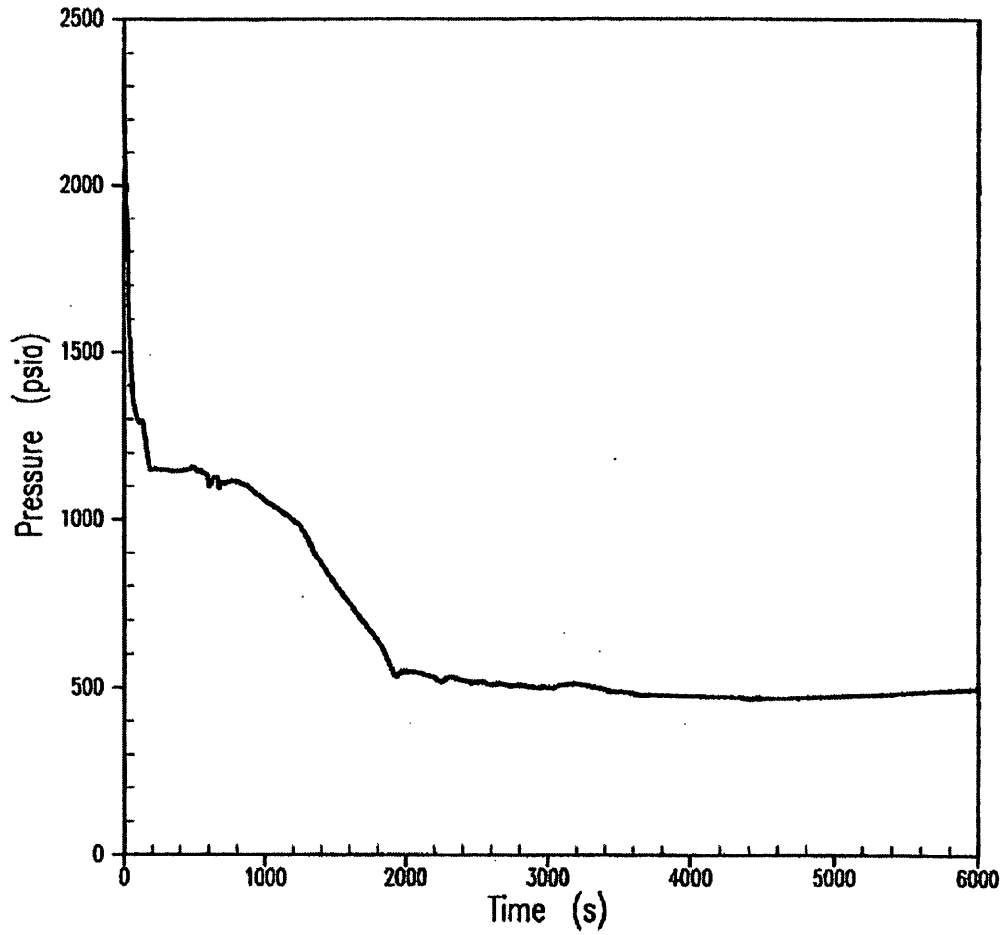


FIGURE 14.3.1-9C

2.5-INCH BREAK  
RCS PRESSURE

BEAVER VALLEY POWER STATION UNIT NO. 1  
UPDATED FINAL SAFETY ANALYSIS REPORT

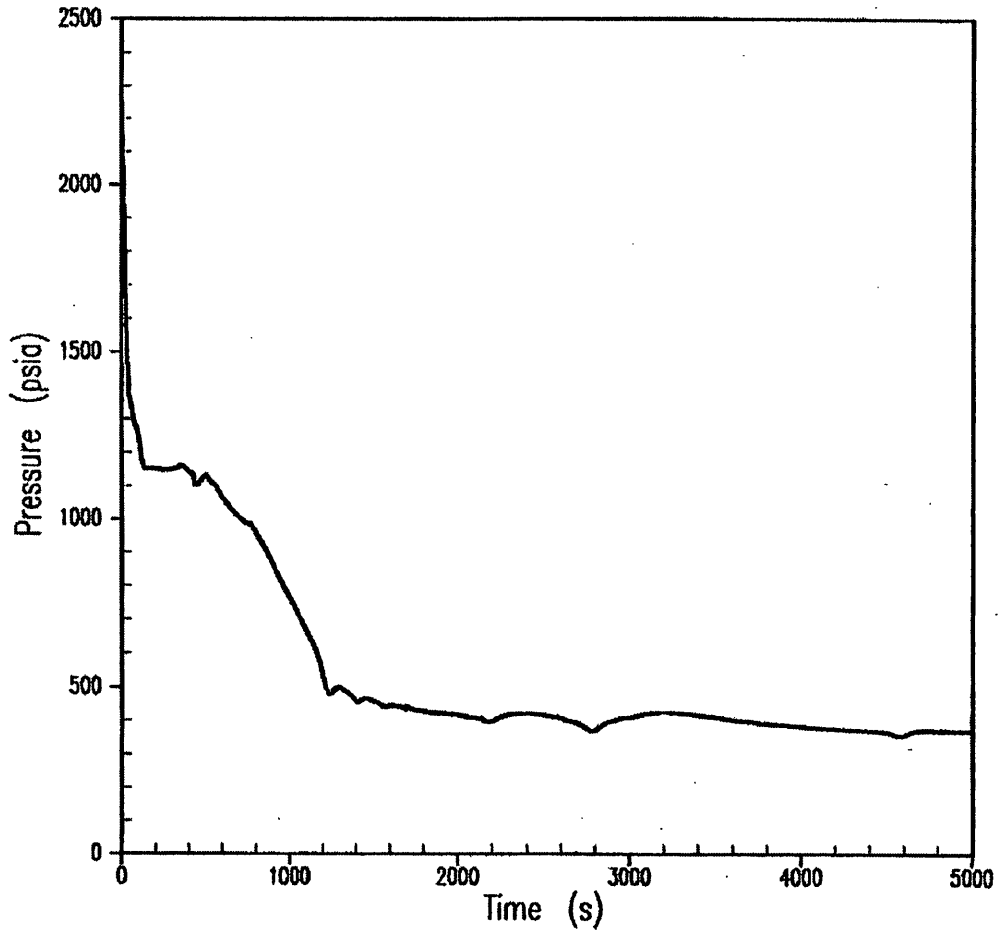


FIGURE 14.3.1-9D

3-INCH BREAK  
RCS PRESSURE

BEAVER VALLEY POWER STATION UNIT NO. 1  
UPDATED FINAL SAFETY ANALYSIS REPORT

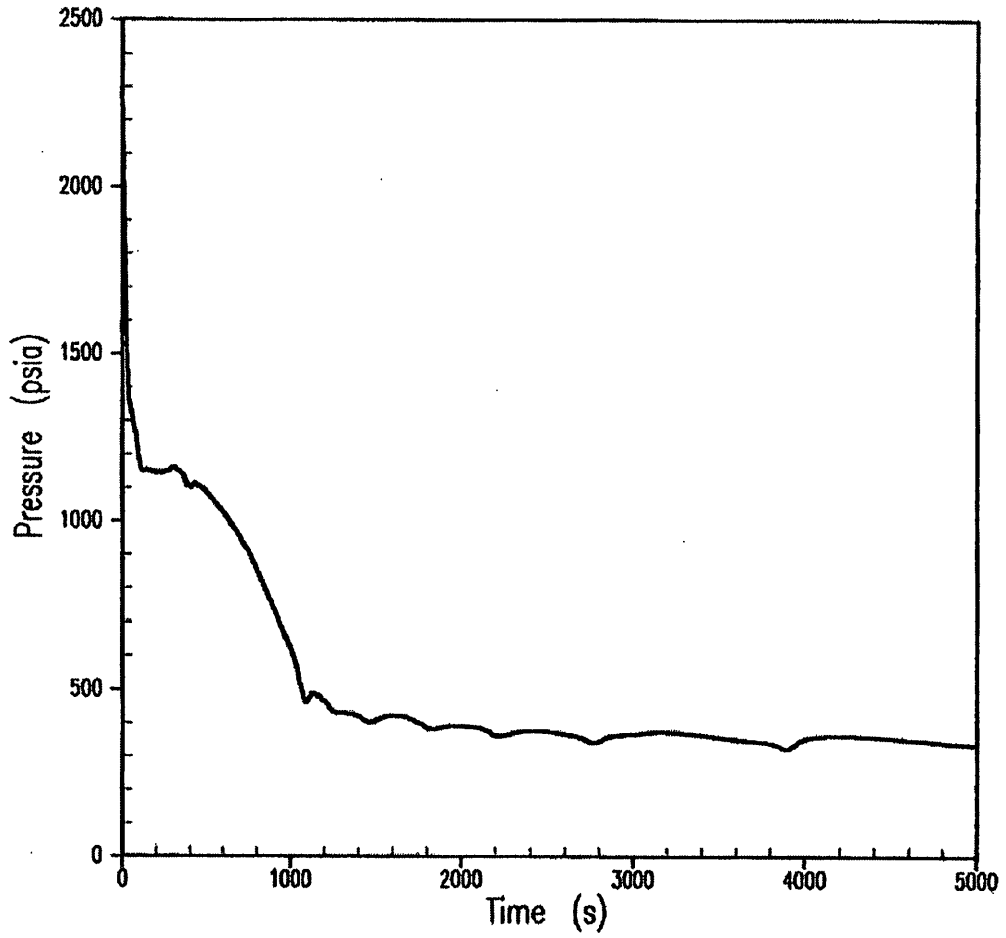


FIGURE 14.3.1-9E

3.25-INCH BREAK  
RCS PRESSURE

BEAVER VALLEY POWER STATION UNIT NO. 1  
UPDATED FINAL SAFETY ANALYSIS REPORT

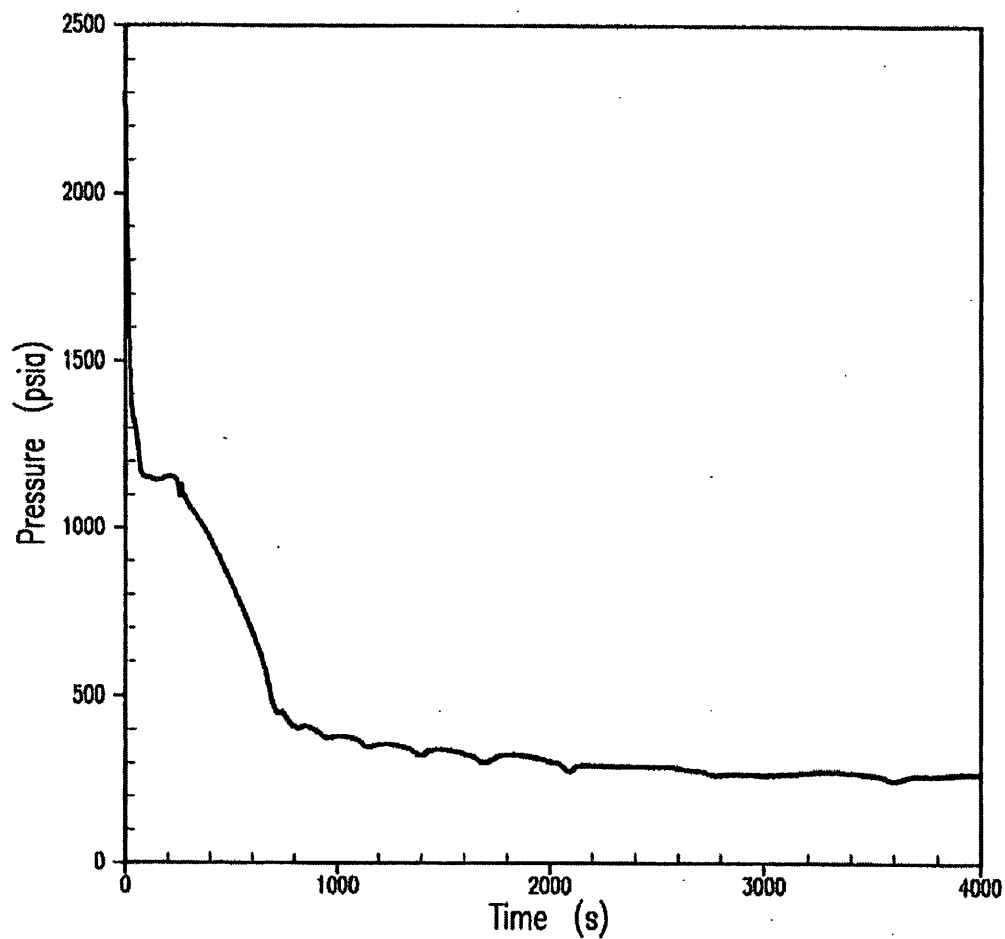


FIGURE 14.3.1-9F

4-INCH BREAK  
RCS PRESSURE

BEAVER VALLEY POWER STATION UNIT NO. 1  
UPDATED FINAL SAFETY ANALYSIS REPORT

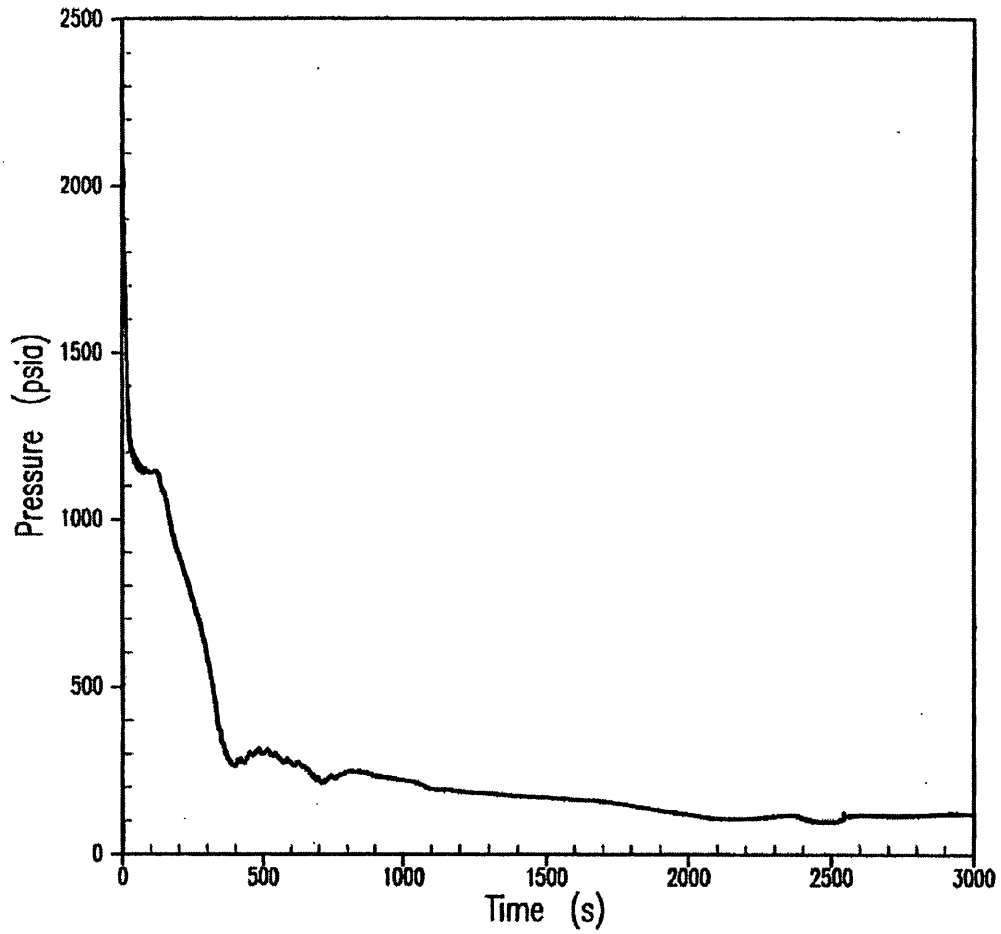


FIGURE 14.3.1-9G

6-INCH BREAK  
RCS PRESSURE

BEAVER VALLEY POWER STATION UNIT NO. 1  
UPDATED FINAL SAFETY ANALYSIS REPORT



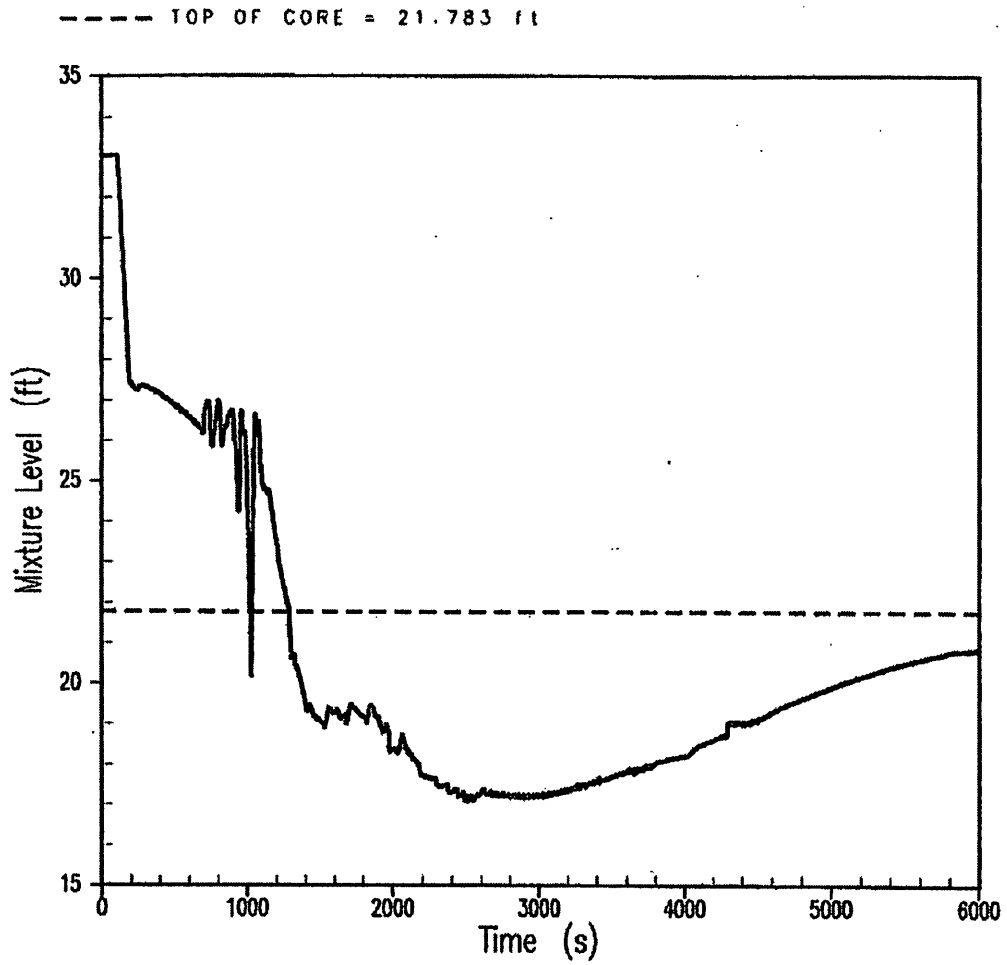


FIGURE 14.3.1-10A

2-INCH BREAK  
CORE MIXTURE LEVEL

BEAVER VALLEY POWER STATION UNIT NO. 1  
UPDATED FINAL SAFETY ANALYSIS REPORT

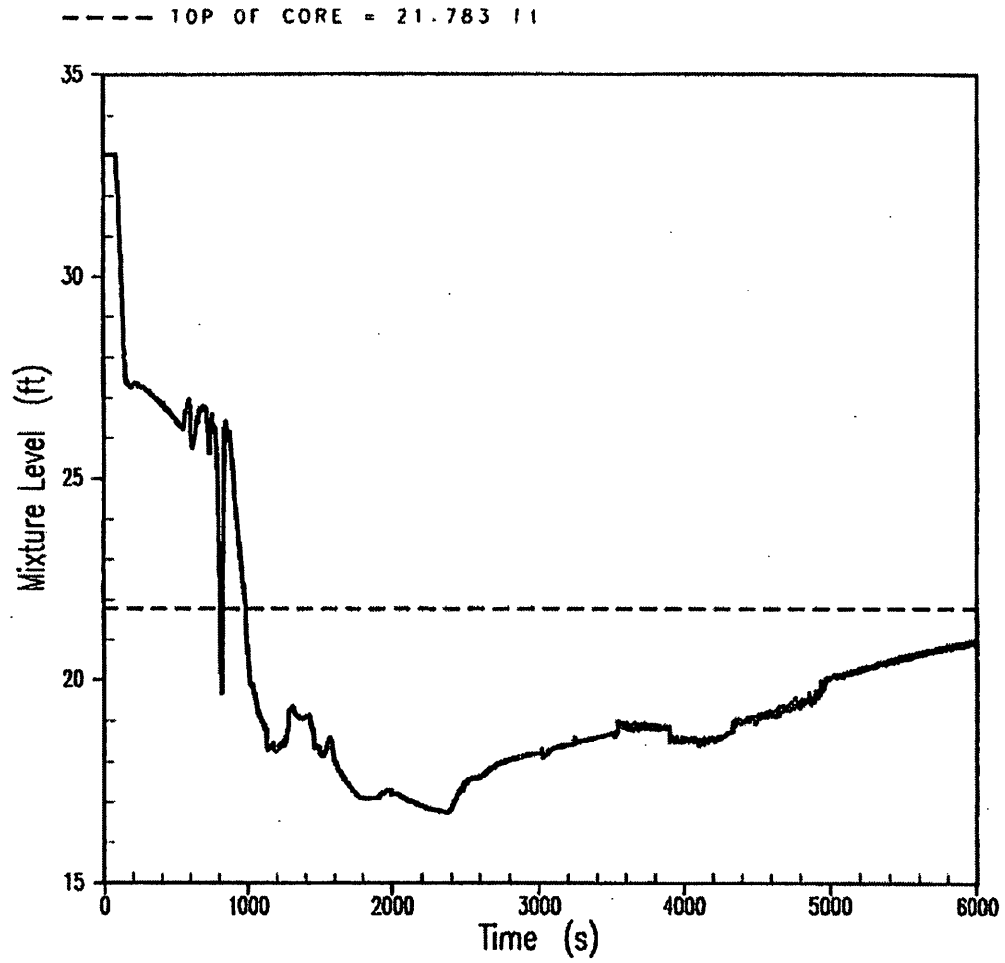


FIGURE 14.3.1-10B

2.25-INCH BREAK  
CORE MIXTURE LEVEL

BEAVER VALLEY POWER STATION UNIT NO. 1  
UPDATED FINAL SAFETY ANALYSIS REPORT

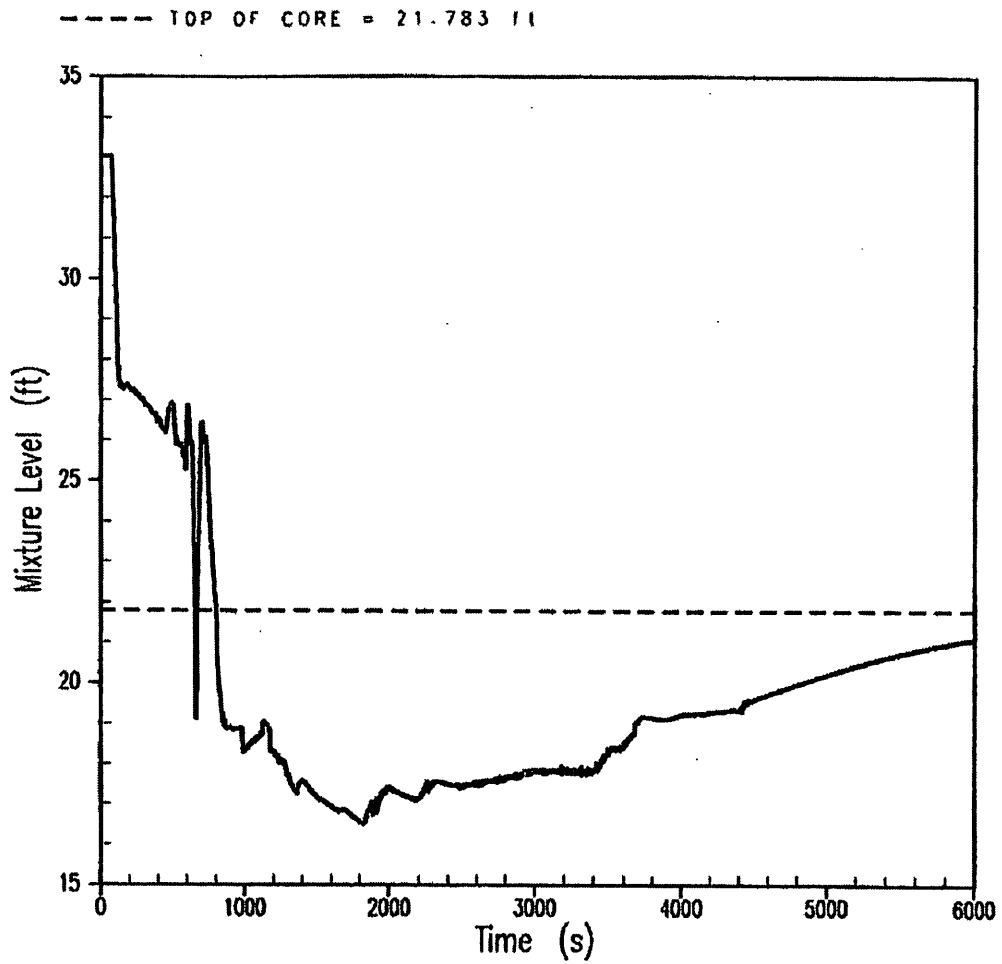


FIGURE 14.3.1-10C

2.5-INCH BREAK  
CORE MIXTURE LEVEL

BEAVER VALLEY POWER STATION UNIT NO. 1  
UPDATED FINAL SAFETY ANALYSIS REPORT

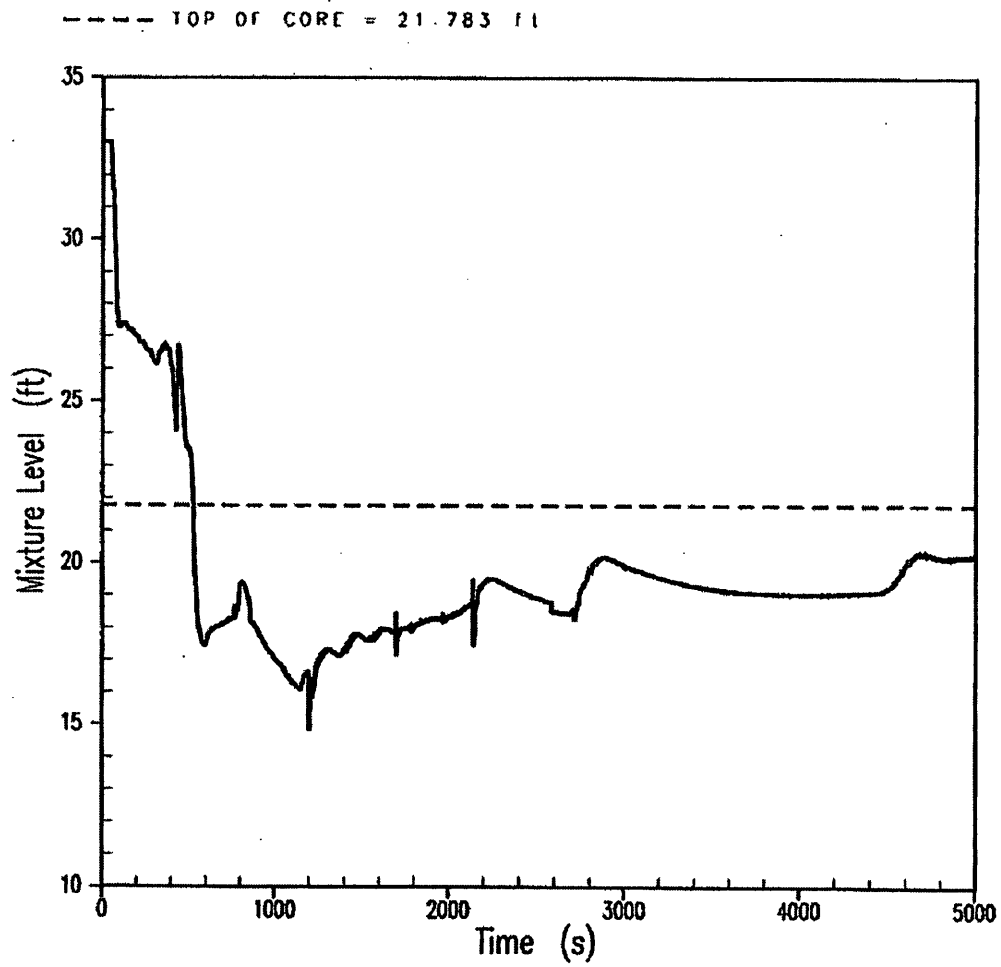


FIGURE 14.3.1-10D

3-INCH BREAK  
CORE MIXTURE LEVEL

BEAVER VALLEY POWER STATION UNIT NO. 1  
UPDATED FINAL SAFETY ANALYSIS REPORT

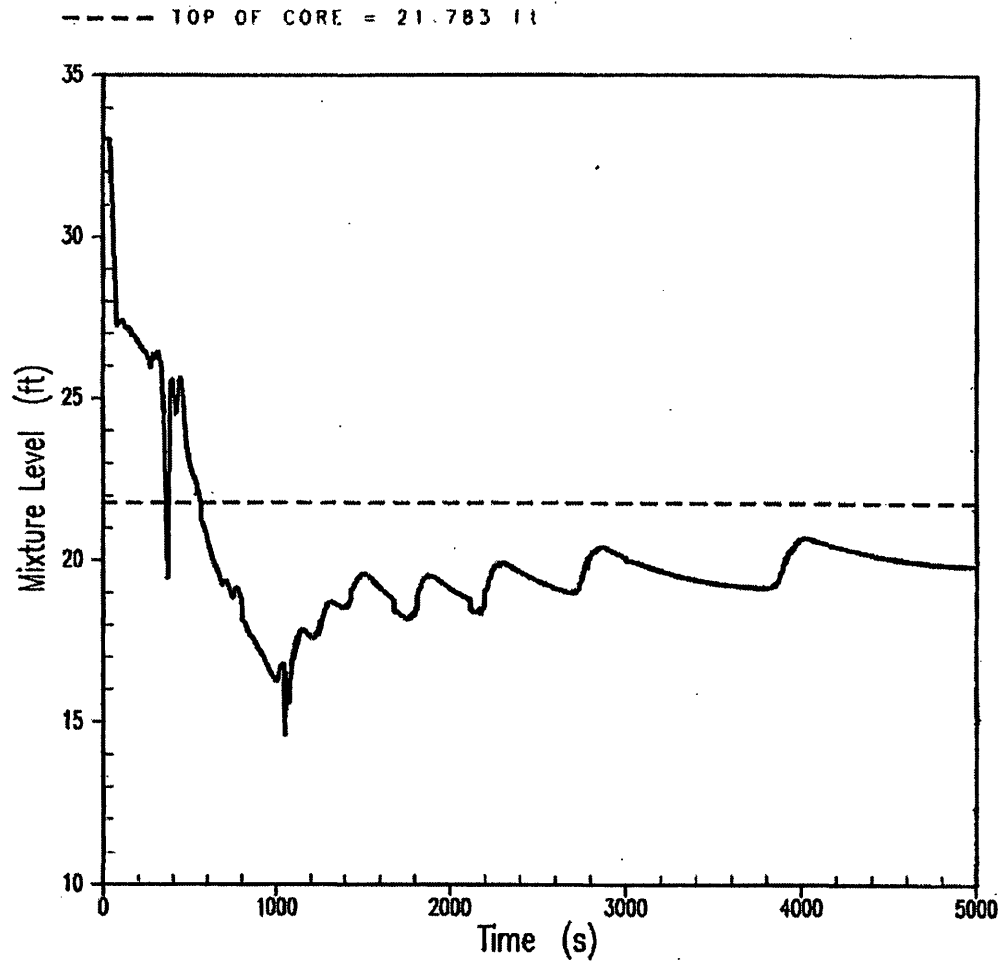


FIGURE 14.3.1-10E

3.25-INCH BREAK  
CORE MIXTURE LEVEL

BEAVER VALLEY POWER STATION UNIT NO. 1  
UPDATED FINAL SAFETY ANALYSIS REPORT

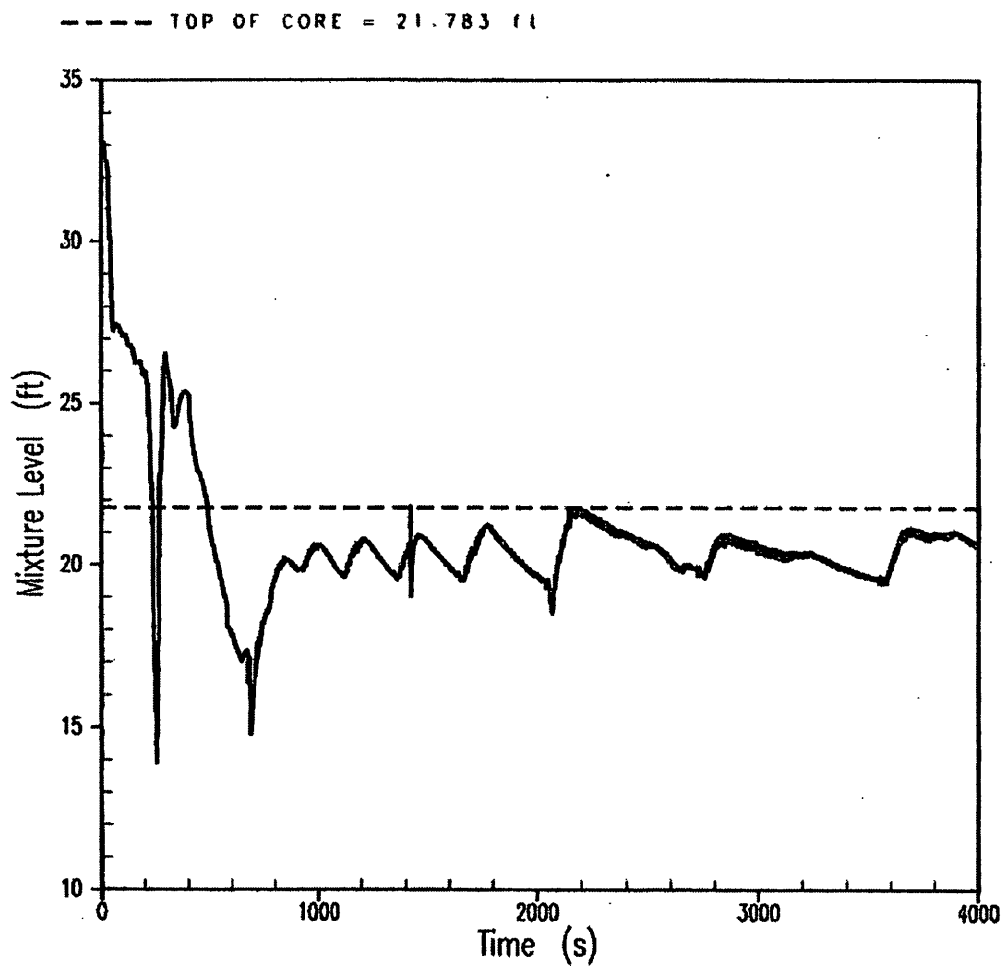


FIGURE 14.3.1-10F

4-INCH BREAK  
CORE MIXTURE LEVEL

BEAVER VALLEY POWER STATION UNIT NO.1  
UPDATED FINAL SAFETY ANALYSIS REPORT

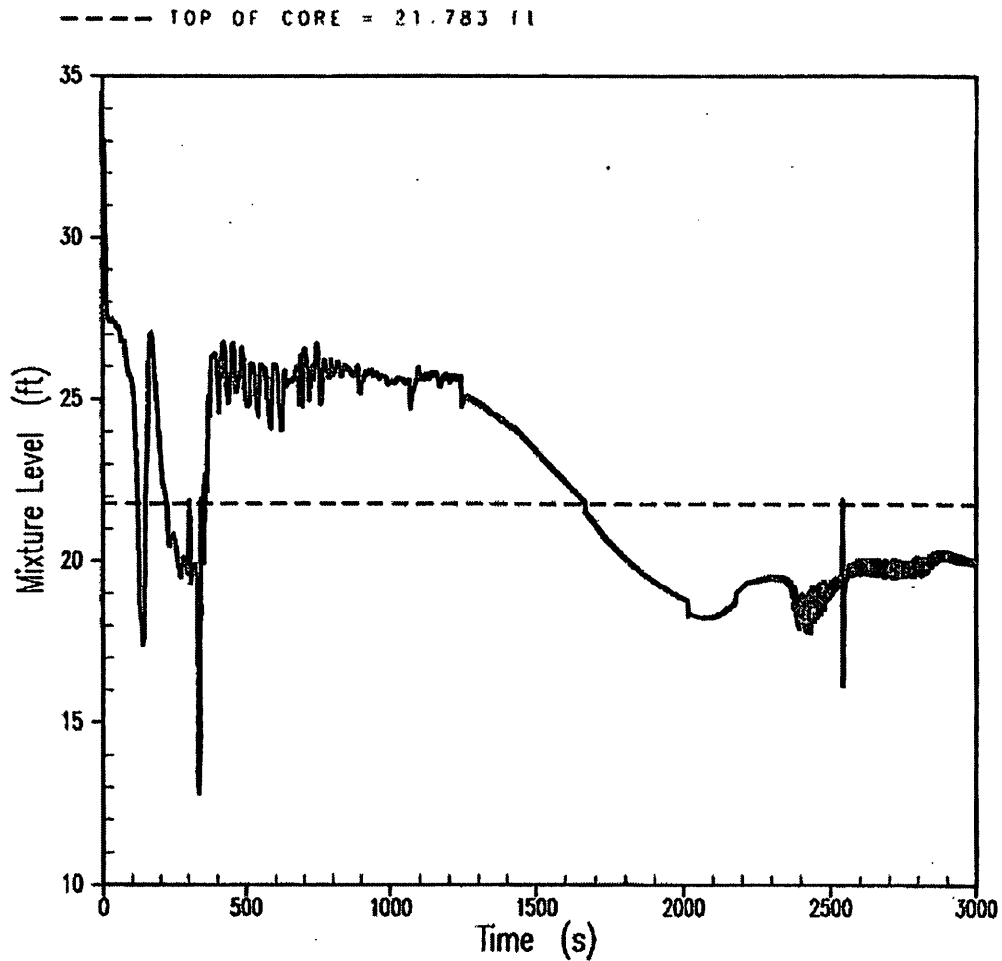


FIGURE 14.3.1-10G

6-INCH BREAK  
CORE MIXTURE LEVEL

BEAVER VALLEY POWER STATION UNIT NO. 1  
UPDATED FINAL SAFETY ANALYSIS REPORT

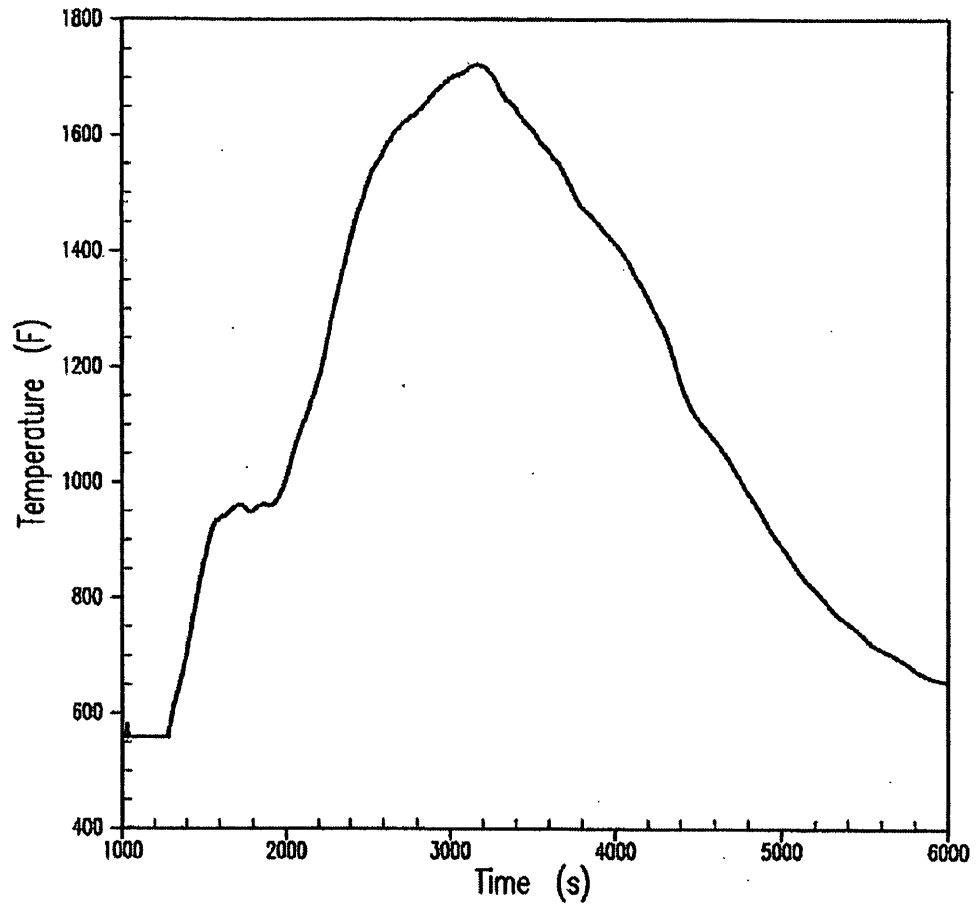


FIGURE 14.3.1-11A

2-INCH BREAK  
PEAK CLAD TEMPERATURE

BEAVER VALLEY POWER STATION UNIT NO. 1  
UPDATED FINAL SAFETY ANALYSIS REPORT



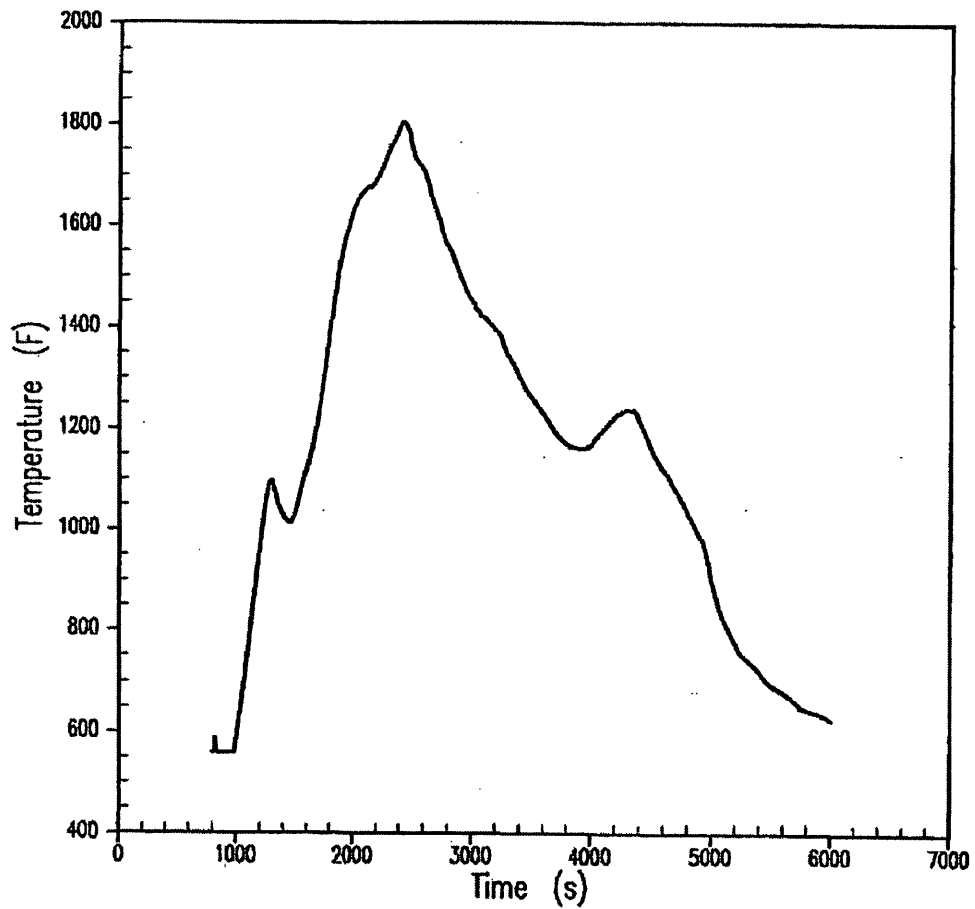


FIGURE 14.3.1-11B

2.25-INCH BREAK  
PEAK CLAD TEMPERATURE

BEAVER VALLEY POWER STATION UNIT NO. 1  
UPDATED FINAL SAFETY ANALYSIS REPORT

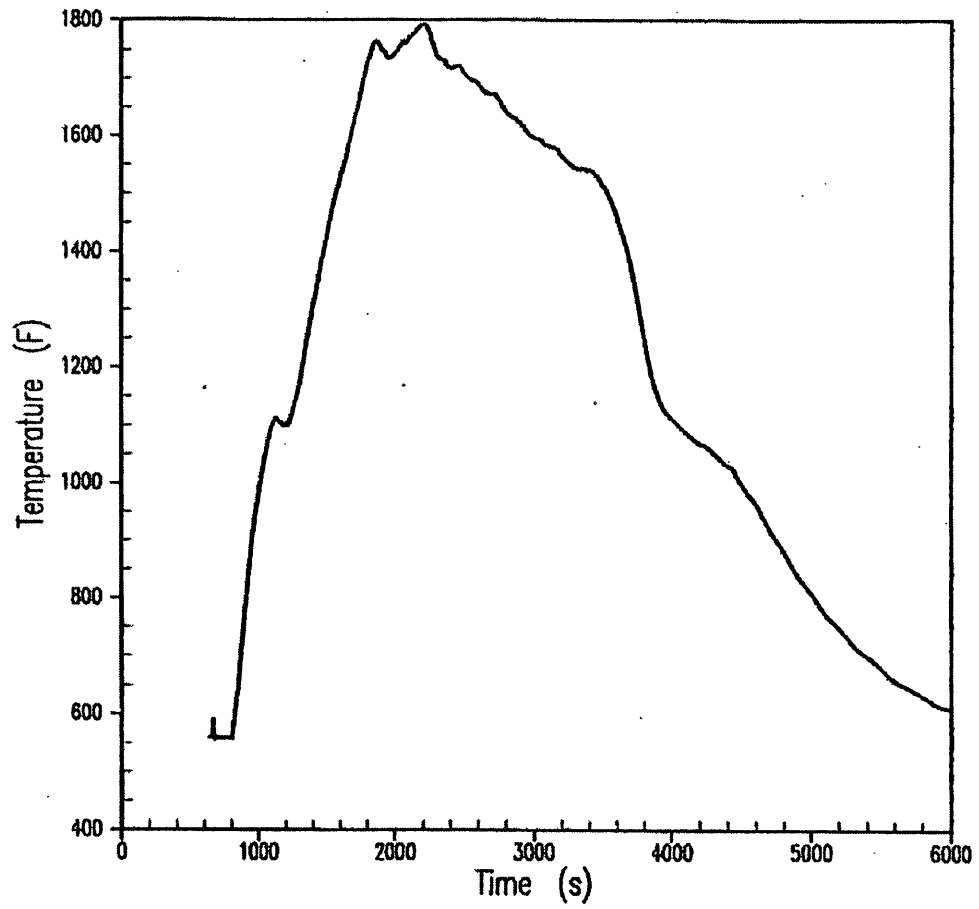


FIGURE 14.3.1-11C

2.5-INCH BREAK  
PEAK CLAD TEMPERATURE

BEAVER VALLEY POWER STATION UNIT NO. 1  
UPDATED FINAL SAFETY ANALYSIS REPORT

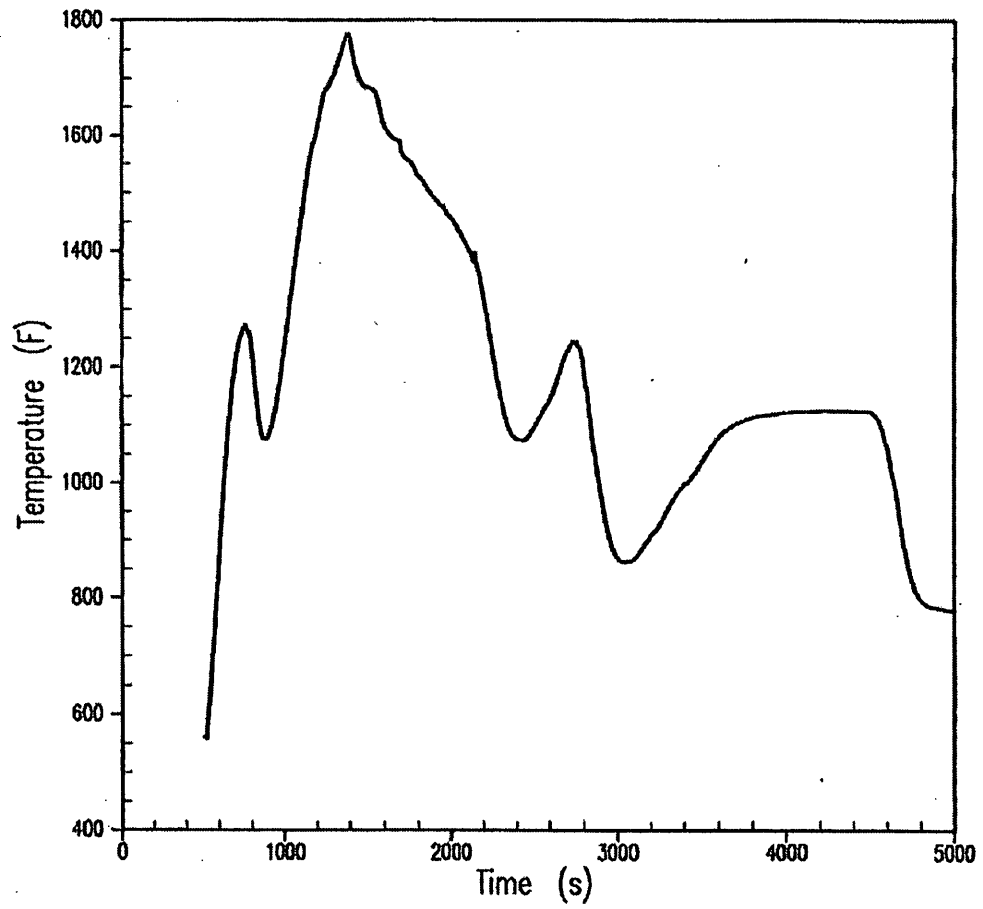


FIGURE 14.3.1-11D

3-INCH BREAK  
PEAK CLAD TEMPERATURE

BEAVER VALLEY POWER STATION UNIT NO. 1  
UPDATED FINAL SAFETY ANALYSIS REPORT

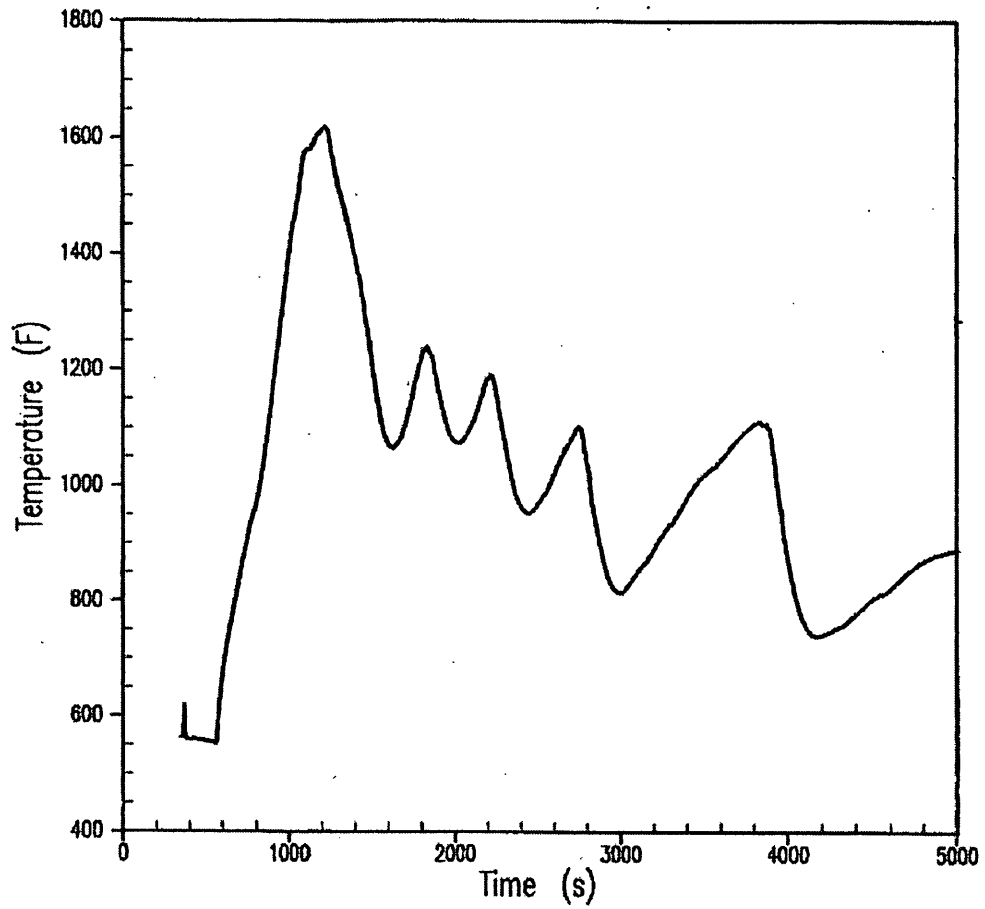


FIGURE 14.3.1-11E

3.25-INCH BREAK  
PEAK CLAD TEMPERATURE

BEAVER VALLEY POWER STATION UNIT NO. 1  
UPDATED FINAL SAFETY ANALYSIS REPORT

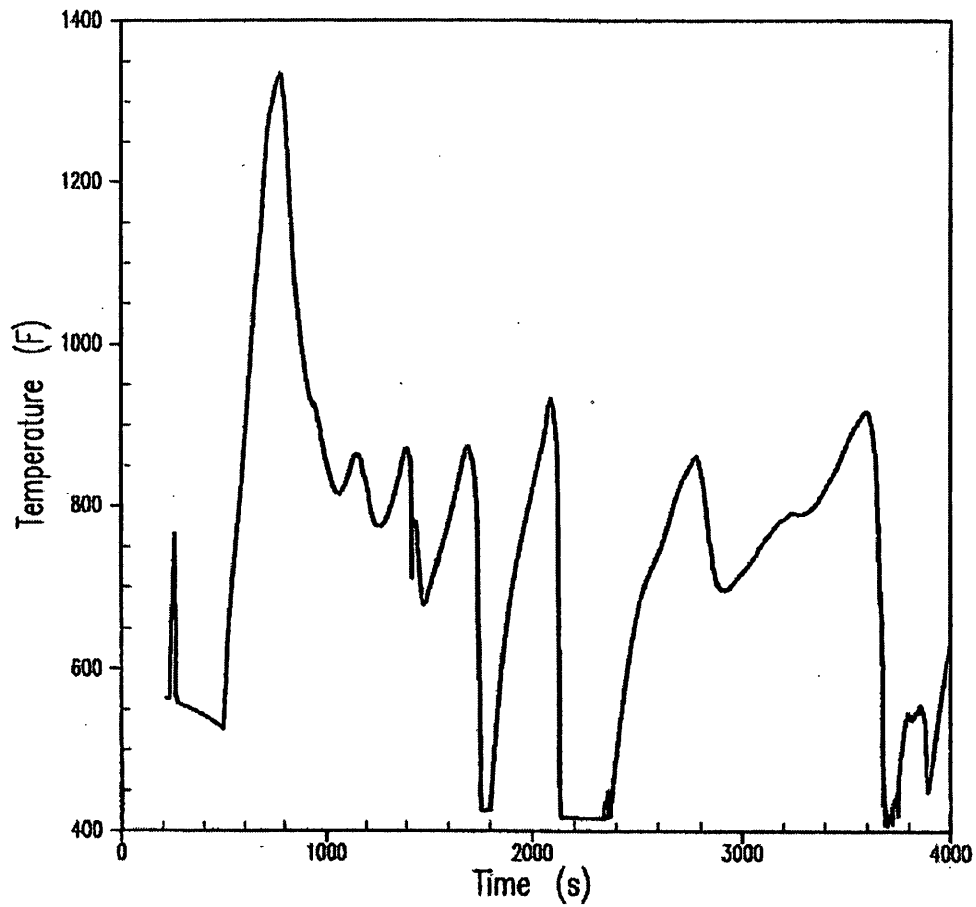


FIGURE 14.3.1-11F

4-INCH BREAK  
PEAK CLAD TEMPERATURE

BEAVER VALLEY POWER STATION UNIT NO. 1  
UPDATED FINAL SAFETY ANALYSIS REPORT

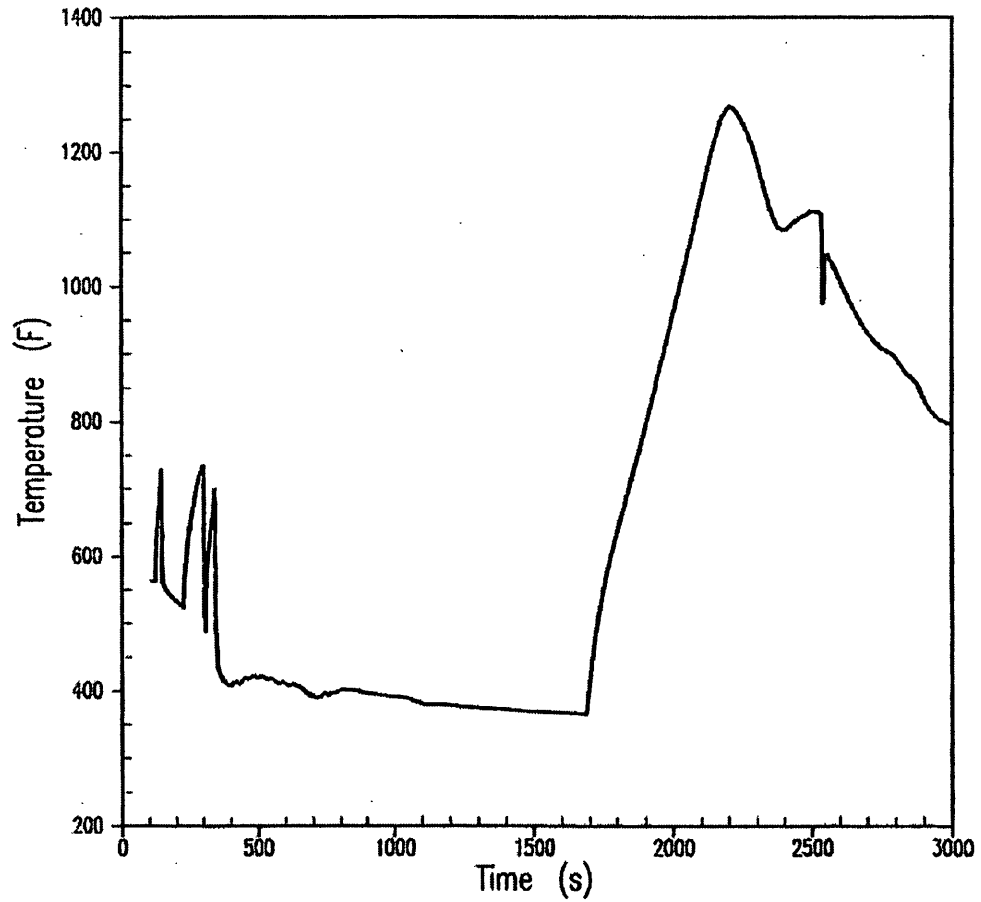


FIGURE 14.3.1-11G

6-INCH BREAK  
PEAK CLAD TEMPERATURE

BEAVER VALLEY POWER STATION UNIT NO. 1  
UPDATED FINAL SAFETY ANALYSIS REPORT

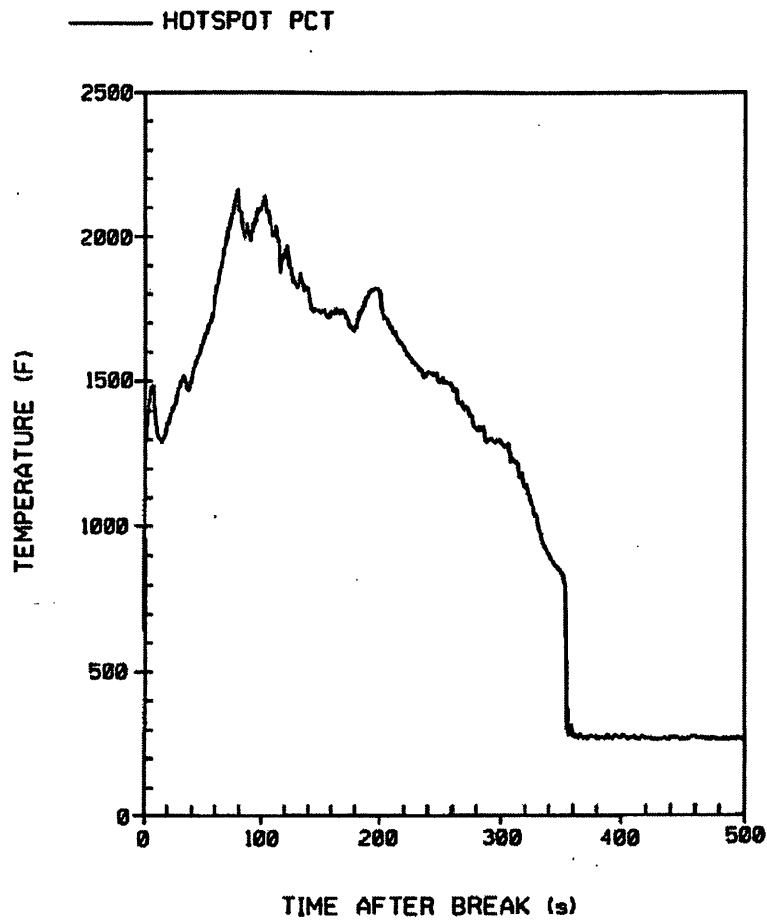


FIGURE 14.3.2-1A

LIMITING CASE  
CLADDING TEMPERATURE  
AT THE PCT ELEVATION

BEAVER VALLEY POWER STATION UNIT NO. 1  
UPDATED FINAL SAFETY ANALYSIS REPORT

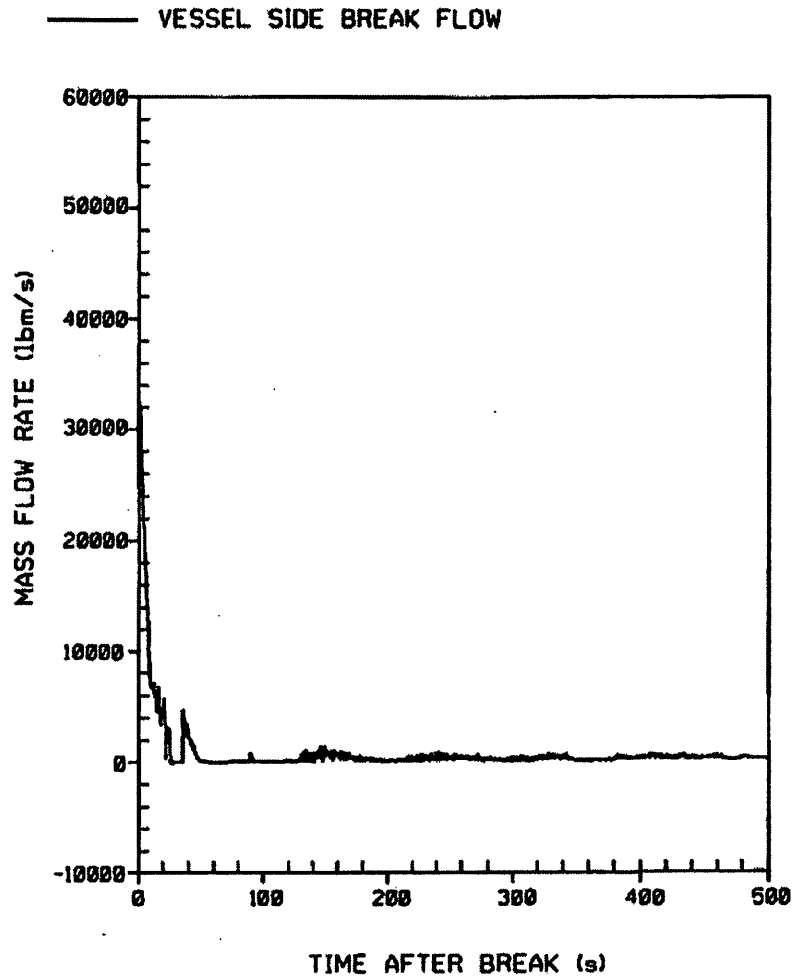


FIGURE 14.3.2-1B

LIMITING CASE  
VESSEL SIDE BREAK FLOW

BEAVER VALLEY POWER STATION UNIT NO. 1  
UPDATED FINAL SAFETY ANALYSIS REPORT



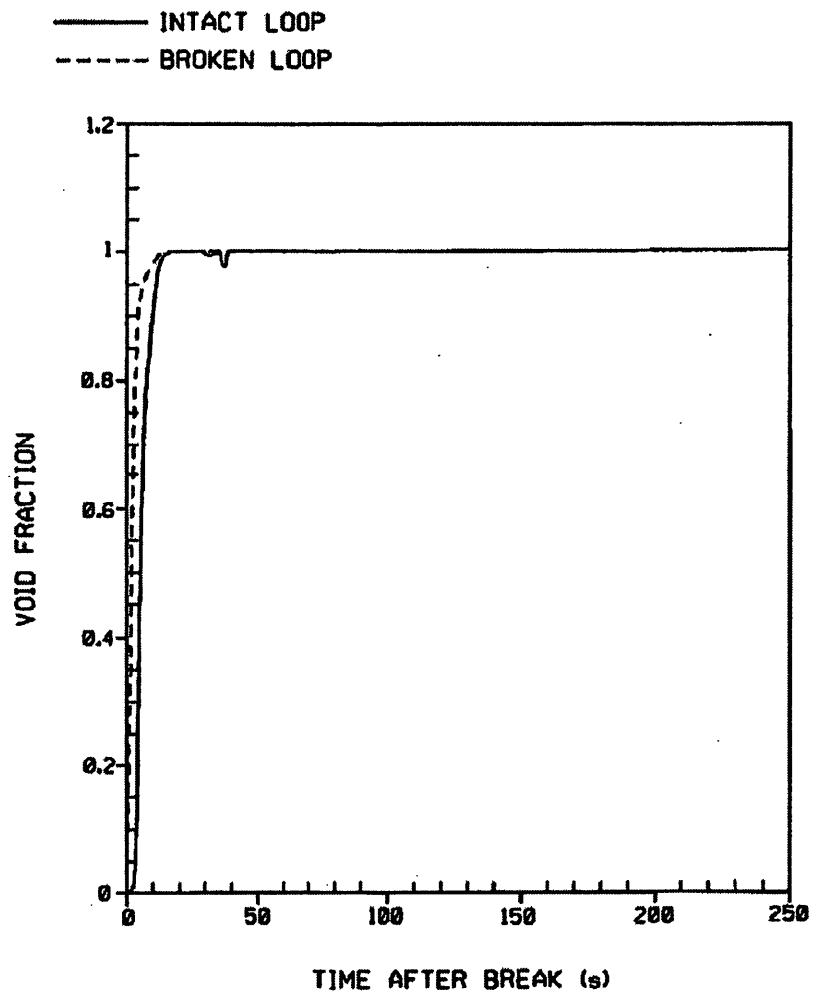


FIGURE 14.3.2-1C

LIMITING CASE  
BROKEN AND INTACT LOOP PUMP  
VOID FRACTION

BEAVER VALLEY POWER STATION UNIT NO. 1  
UPDATED FINAL SAFETY ANALYSIS REPORT

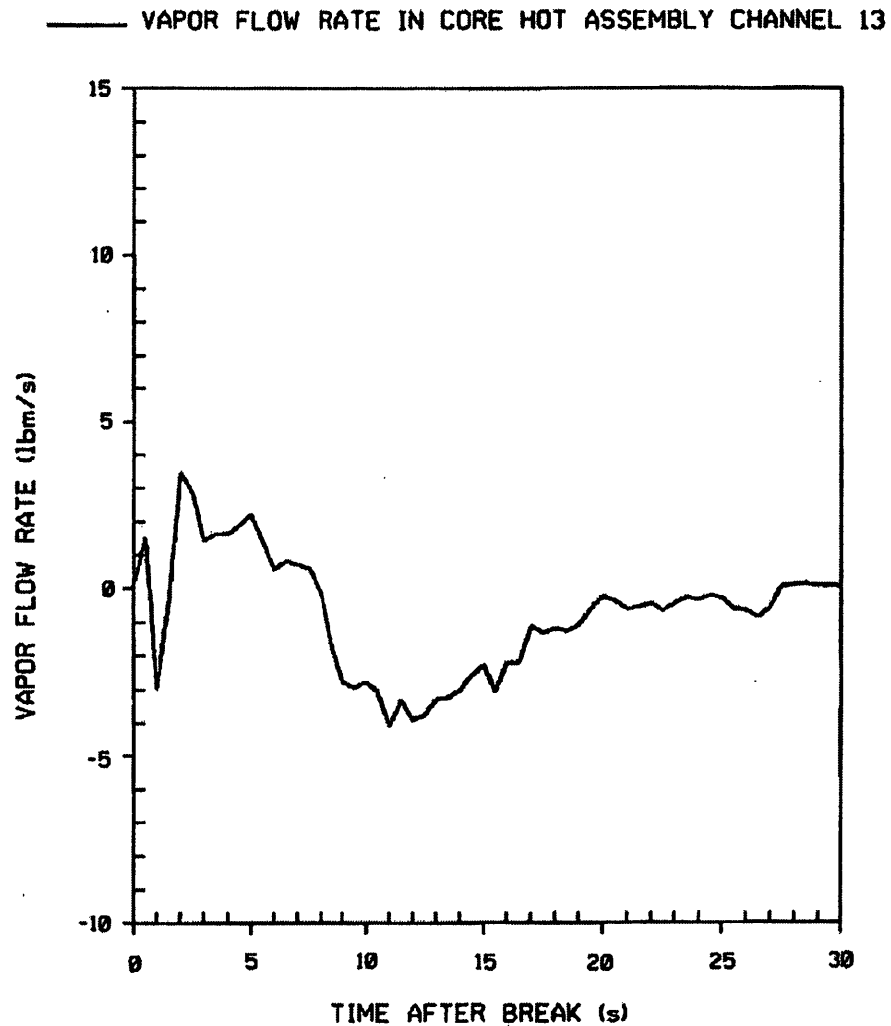


FIGURE 14.3.2-1D

LIMITING CASE  
HOT ASSEMBLY  
TOP OF CORE VAPOR FLOW

BEAVER VALLEY POWER STATION UNIT NO. 1  
UPDATED FINAL SAFETY ANALYSIS REPORT

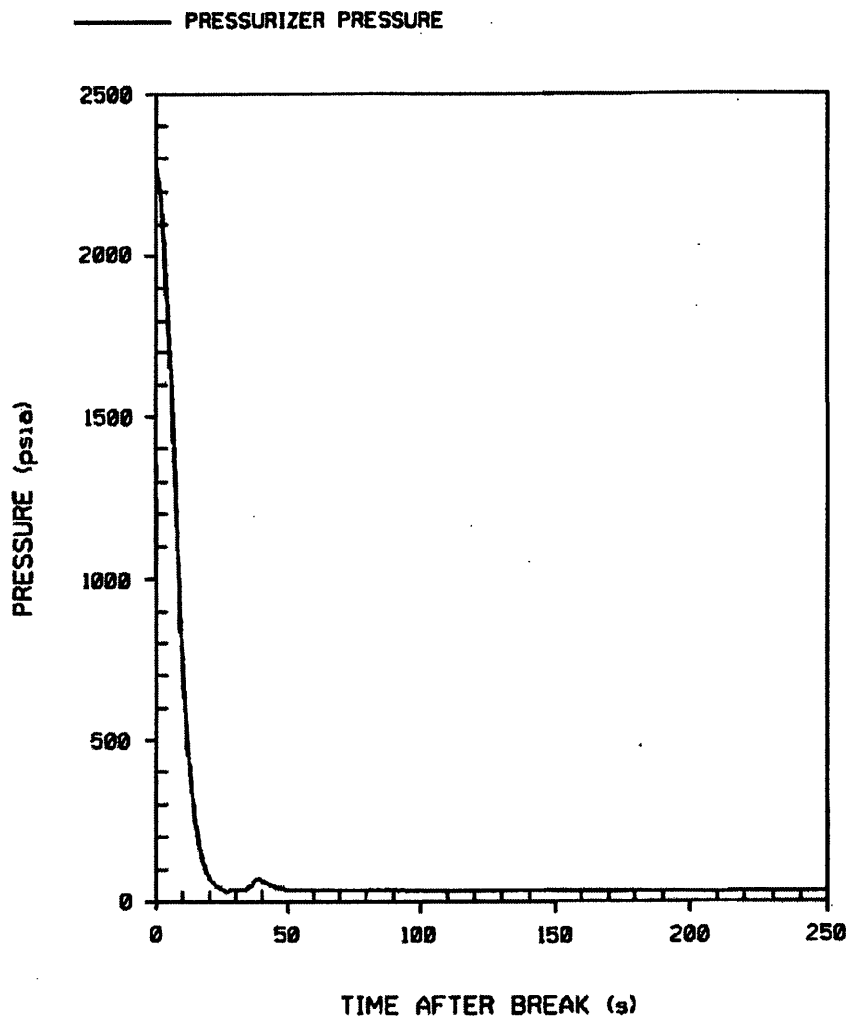
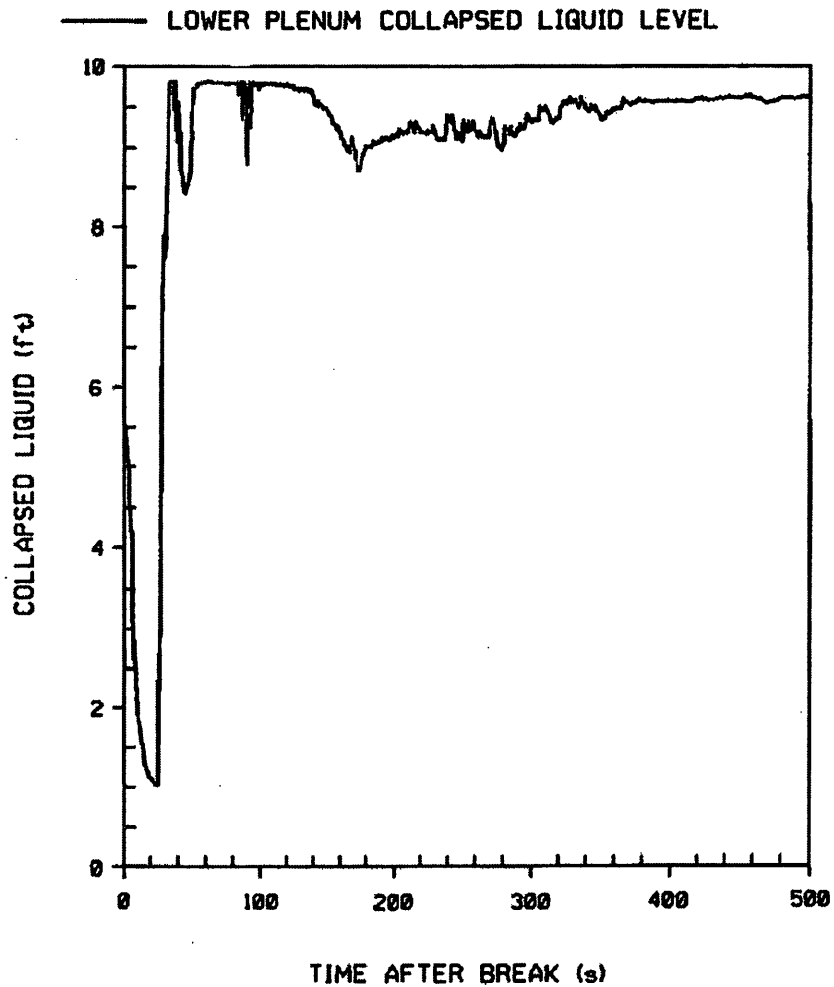


FIGURE 14.3.2-1E

LIMITING CASE  
PRESSURIZER PRESSURE

BEAVER VALLEY POWER STATION UNIT NO. 1  
UPDATED FINAL SAFETY ANALYSIS REPORT



\* THE REFERENCE POINT FOR THE LOWER PLENUM LIQUID LEVEL IS THE BOTTOM OF THE VESSEL

FIGURE 14.3.2-1F

LIMITING PCT  
LOWER PLENUM COLLAPSED LIQUID LEVEL \*

BEAVER VALLEY POWER STATION UNIT NO. 1  
UPDATED FINAL SAFETY ANALYSIS REPORT

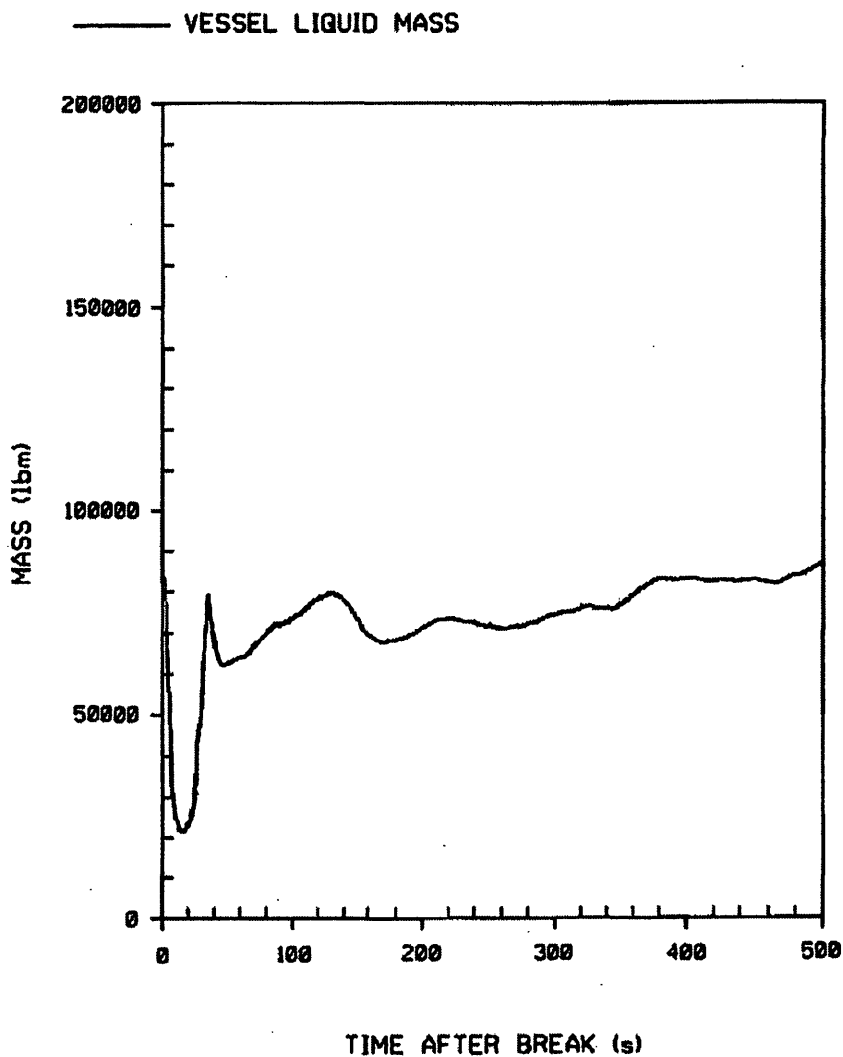


FIGURE 14.3.2-1G

LIMITING CASE  
VESSEL FLUID MASS

BEAVER VALLEY POWER STATION UNIT NO. 1  
UPDATED FINAL SAFETY ANALYSIS REPORT

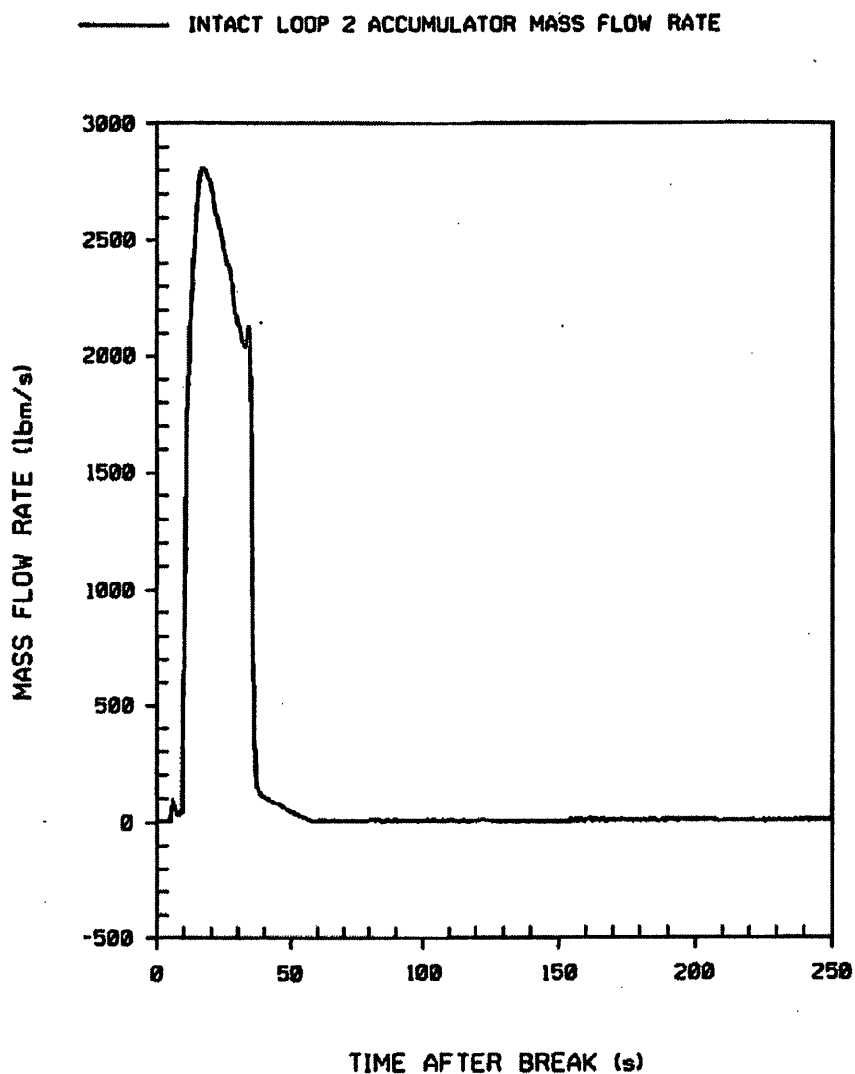


FIGURE 14.3.2-1H

LIMITING CASE  
LOOP 2 ACCUMULATOR FLOW

BEAVER VALLEY POWER STATION UNIT NO. 1  
UPDATED FINAL SAFETY ANALYSIS REPORT

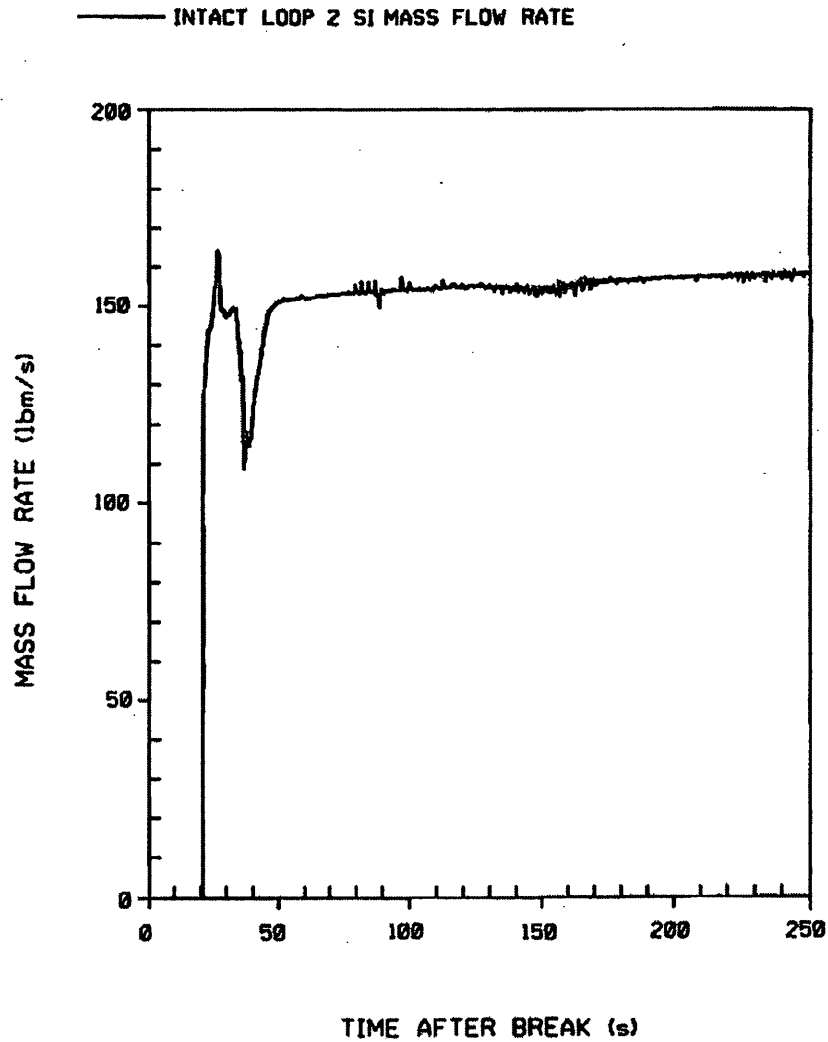
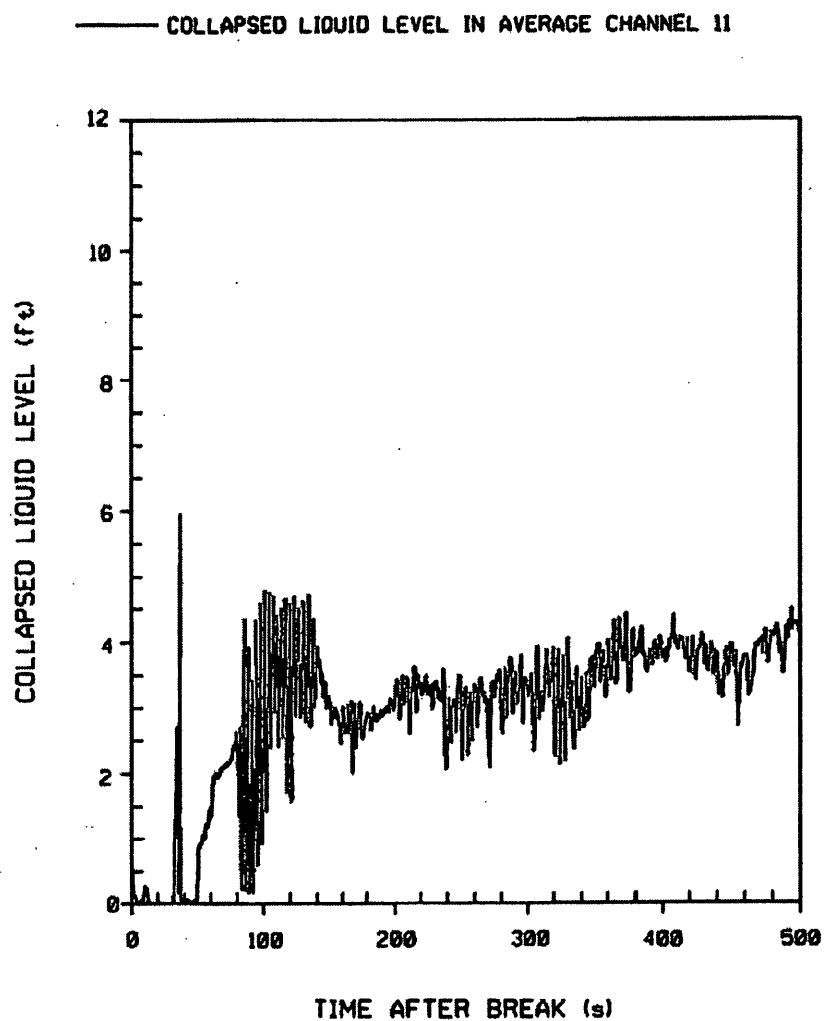


FIGURE 14.3.2-1I

SAFETY INJECTION FLOW  
FOR THE LIMITING PCT CASE

BEAVER VALLEY POWER STATION UNIT NO. 1  
UPDATED FINAL SAFETY ANALYSIS REPORT



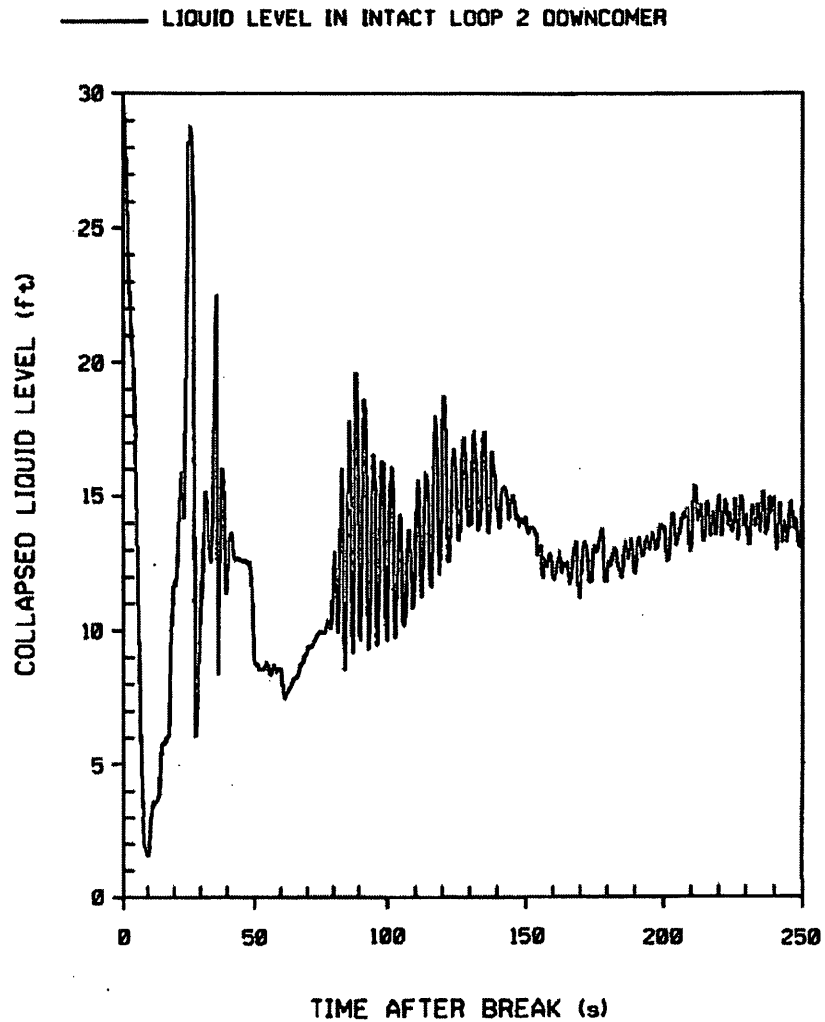
\* THE REFERENCE POINT FOR THE COLLAPSED LIQUID LEVEL IS THE BOTTOM OF THE ACTIVE FUEL

FIGURE 14.3.2-1J

LIMITING CASE  
CORE AVERAGE CHANNEL  
COLLAPSED LIQUID LEVEL\*

BEAVER VALLEY POWER STATION UNIT NO. 1  
UPDATED FINAL SAFETY ANALYSIS REPORT



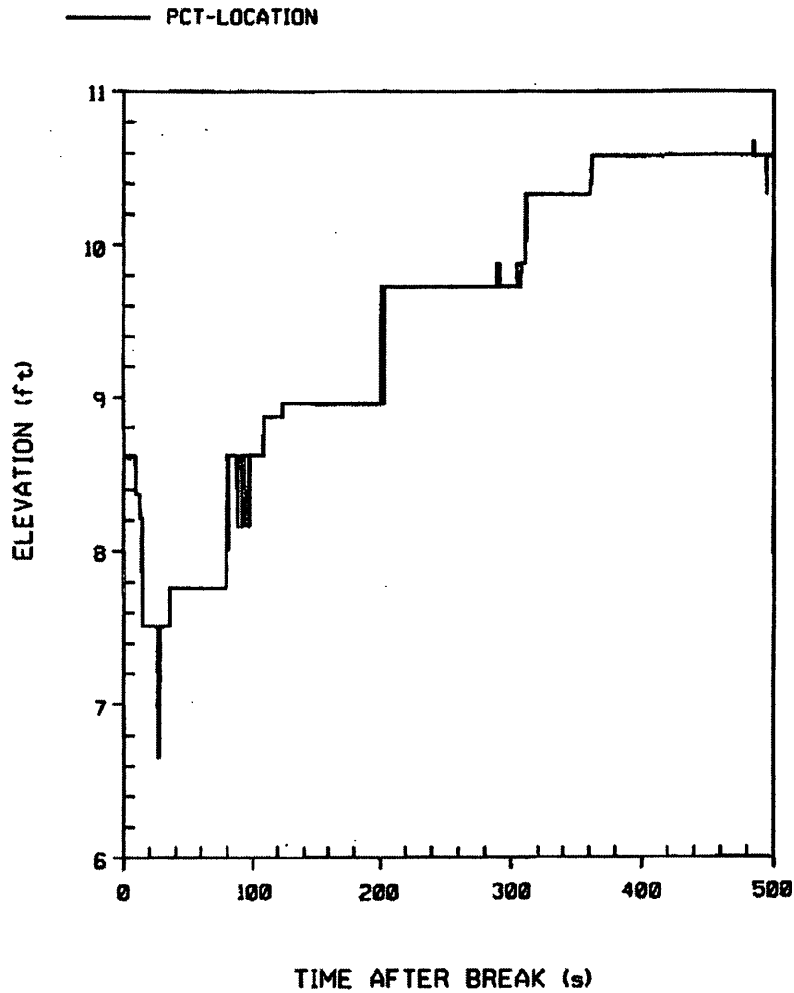


\* THE REFERENCE POINT FOR THE DOWNCOMER LIQUID LEVEL IS THE BOTTOM OF THE VESSEL

FIGURE 14.3.2-1K

LIMITING CASE  
 LOOP 2 DOWNCOMER  
 COLLAPSED LIQUID LEVEL \*

BEAVER VALLEY POWER STATION UNIT NO. 1  
 UPDATED FINAL SAFETY ANALYSIS REPORT



\* THE REFERENCE POINT FOR THE PCT ELEVATION  
IS THE BOTTOM OF THE ACTIVE FUEL

FIGURE 14.3.2-1L

PEAK CLAD TEMPERATURE ELEVATION \*  
FOR THE HOT ROD  
FOR THE LIMITING PCT CASE

BEAVER VALLEY POWER STATION UNIT NO. 1  
UPDATED FINAL SAFETY ANALYSIS REPORT

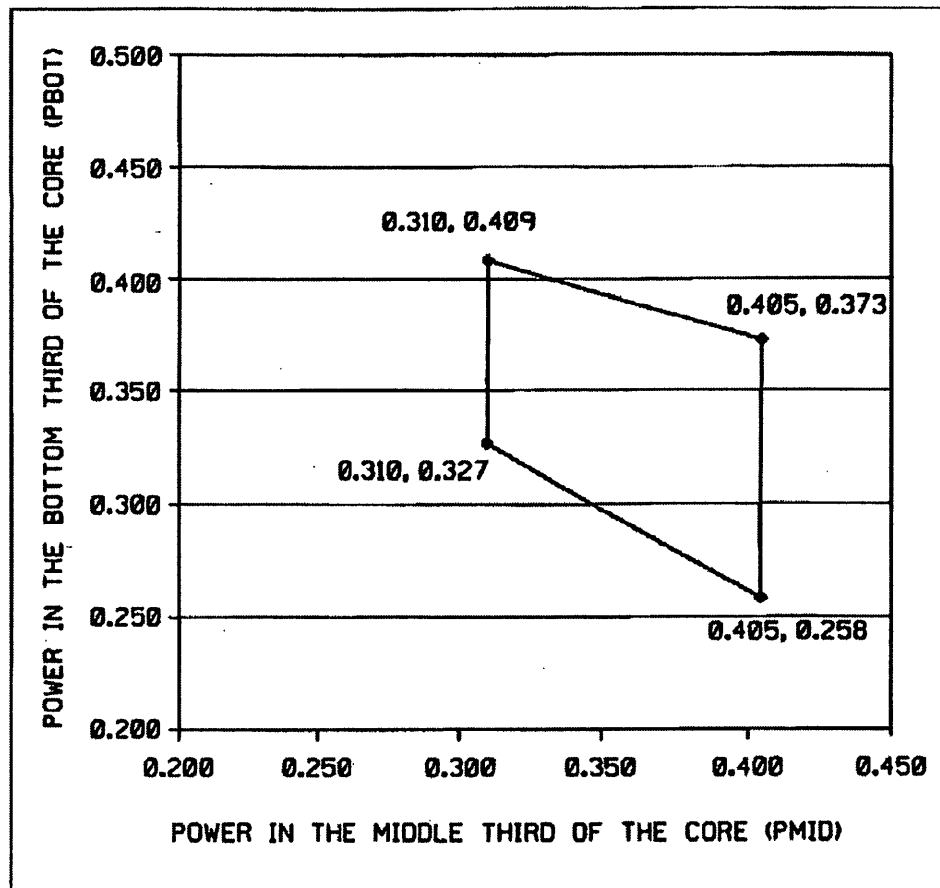


FIGURE 14.3.2-2

BELOCA  
ANALYSIS AXIAL POWER SHAPE  
OPERATING SPACE ENVELOPE

BEAVER VALLEY POWER STATION UNIT NO. 1  
UPDATED FINAL SAFETY ANALYSIS REPORT

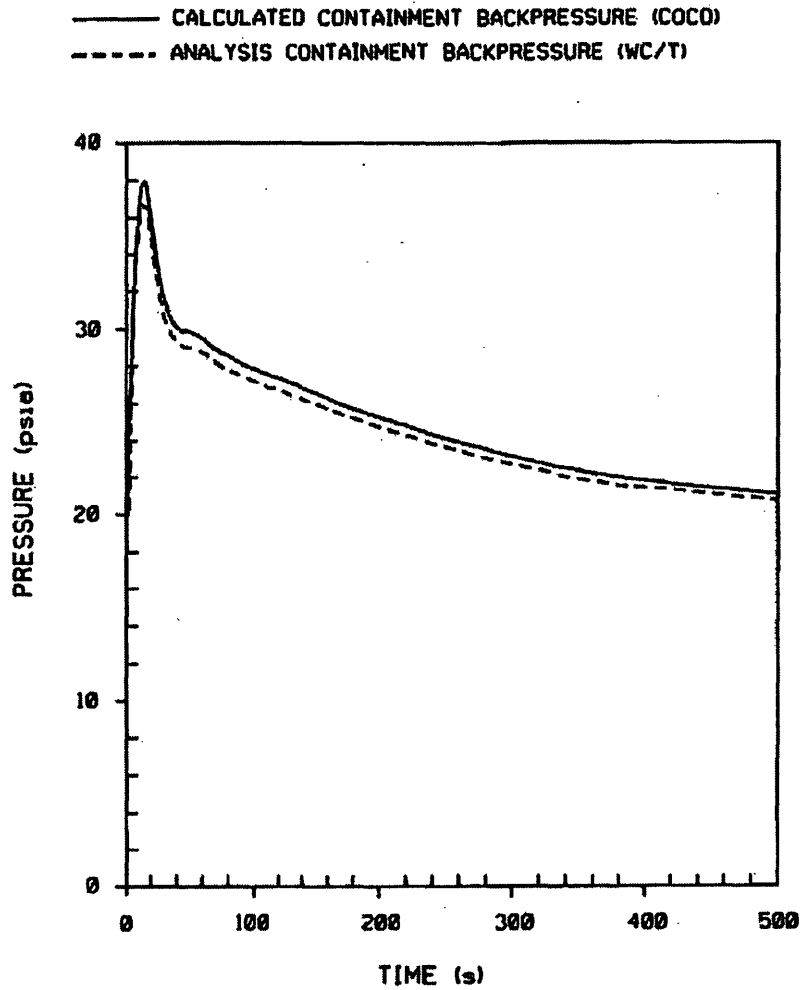


FIGURE 14.3.2-3

WCOBRA/TRAC ASSUMED BACKPRESSURE versus  
CALCULATED CONTAINMENT BACKPRESSURE

BEAVER VALLEY POWER STATION UNIT NO. 1  
UPDATED FINAL SAFETY ANALYSIS REPORT

APPENDIX 14BRADIATION SOURCES AND DOSE CALCULATION METHODOLOGY

This appendix presents the quantities of radioactive isotopes present in the core, fuel rod gap and coolant. A brief discussion of the derivation of these quantities and the dose calculation methodology used in the assessment of the radiological consequences of the postulated accidents is also included.

## 14B.1 ACTIVITIES IN THE CORE

Activities in the core were calculated using the computer code ORIGEN as described in NUREG/CR-0200, and using parameter values specific to the physical and chemical makeup of the fuel and to the reactor operation. Because uranium enrichments may change from cycle to cycle and these changes may cause an increase in certain nuclides, core radionuclide inventory is calculated for a minimum expected enrichment and again for a maximum expected enrichment. The assumed core inventory used in radiological analysis is composed of a selection of the maximum value for each nuclide for the range of expected enrichments. These inventories are given in Table 14B-1A.

The core inventory presented in Table 14B-1A is based on an analyzed core power level of 2918 MWt and is used for the design basis accident dose consequence analyses.

## 14B.2 ACTIVITIES IN THE FUEL ROD GAP FOR NON-LOCA EVENTS

Table 3 in Regulatory Guide 1.183, specifies the fraction of fission product inventory in the fuel rod gap to be used for non-LOCA accidents. The footnote identifies that the applicability of Table 3 is limited to LWR fuel with peak burnups of 62 GWD/MTU "provided that the maximum linear heat generation rate does not exceed 6.3 kW/ft peak rod average power for burnups exceeding 54 GWD/MTU." The gap fractions utilized for the non-LOCA events at BVPS-1 which could result in fuel failure, are consistent with the requirements for RG 1.183 and are listed below.

<b>Nuclide Group</b>	<b>Regulatory Guide 1.183 Gap Fraction for Non-LOCA Events excluding the CREA (Note 1)</b>
I-131	0.08
Kr-85	0.10
Other Noble Gases	0.05
Other Halogens	0.05
Alkali Metals	0.12

<b>Nuclide Group</b>	<b>Regulatory Guide 1.183 Gap Fraction for Non-LOCA Events excluding the CREA (Note 1)</b>
<p><u>Note 1:</u> In accordance with RG 1.183, the gap fraction associated with the Control Rod Ejection Accident is as follows:</p> <p style="padding-left: 40px;">Noble Gases : 10%</p> <p style="padding-left: 40px;">Halogens: 10%</p>	

The core inventory of noble gases, halogens and alkali metals are presented in Table 14B-1A.

### 14B.3 FUEL HANDLING SOURCES

Activities in the core were calculated using the computer code ORIGEN as described in NUREG/CR-0200, and using parameter values specific to the physical and chemical makeup of the fuel and to the reactor operation. Because uranium enrichments may change from cycle to cycle and these changes may cause an increase in certain nuclides, core radionuclide inventory is calculated for a minimum expected enrichment and again for a maximum expected enrichment. The assumed core inventory used in radiological analysis is composed of a selection of the maximum value for each nuclide for the range of expected enrichments. When used in the fuel handling accident radiological analysis, this activity is also reduced to account for delay time specified in the facility Technical Specifications which limits the post criticality time duration to move fuel assemblies. Additionally, a conservative radial peaking factor of 1.75 is applied to increase the activity content to ensure that the maximum power assembly is considered in the analysis.

The postulated fuel rod gap activities are taken from Regulatory Guide 1.183. These are 0.10 Kr-85, 0.08 I-131 and 0.05 for other iodines and noble gases total activity in the core.

14B.4 REACTOR COOLANT FISSION PRODUCT ACTIVITIES

The parameters used in the calculation of the reactor coolant fission product inventories, together with the pertinent information concerning the expected coolant cleanup flow rate and demineralizer effectiveness, are summarized in Table 14B-5, while the results of the calculations are presented in Table 14B-6. In these calculations, the defective fuel rods were assumed to be present at the initial core loading and were uniformly distributed throughout the core. Thus, the fission product escape rate coefficients were based upon the average fuel temperature. The calculations were performed with proper consideration of the various coolant densities in the purification stream.

The fission product activities in the reactor coolant during operation with small cladding defects (fuel rods containing pinholes or fine cracks) in 1 percent of the fuel rods were computed using the following differential equations:

1. First order nuclides:

$$\frac{dN_{w_i}}{dt} = \frac{hn\gamma_i}{V_w} N_{c_i}(t) - \left( \lambda_i + \frac{PF_{EQ_i} Q_1}{V_w} + \check{Q}_i \frac{T_1}{T_2} \right) N_{w_i}(t) \quad (14B.4.1)$$

2. Second order nuclides:

$$\frac{dN_{w_j}}{dt} = \frac{hn\gamma_j}{V_w} N_{c_j}(t) + \lambda_{i f_{ij}} N_{w_i}(t) - \left( \lambda_j + \frac{PF_{EQ_j} Q_1}{V_w} + \check{Q}_j \frac{T_1}{T_2} \right) N_{w_j}(t) \quad (14B.4.2)$$

3. Third order nuclides:

$$\begin{aligned} \frac{dN_{w_k}}{dt} = & \frac{hn\gamma_k}{V_w} N_{c_k}(t) + \lambda_{i f_{ik}} N_{w_i}(t) + \lambda_{j f_{jk}} N_{w_j}(t) \\ & - \left( \lambda_k + \frac{PF_{EQ_k} Q_1}{V_w} + \check{Q}_k \frac{T_1}{T_2} \right) N_{w_k}(t) \end{aligned} \quad (14B.4.3)$$

- where:
- i, j, k = First, second and third order nuclide parameters
  - $N_{c_i}(t)$  = Population of nuclide i per fuel region at time t (atoms per region)
  - $N_{w_i}(t)$  = Concentration of nuclide i in the main coolant at time t (atoms/cm<sup>3</sup>)
  - h = Fraction of fuel rod cladding defect
  - n = Total number of fuel regions
  - $\gamma_i$  = Escape rate coefficient (second<sup>-1</sup>)
  - $\check{Q}$  =  $\sigma_{a_i} \bar{r}_{th}$  = Burnup rate (seconds<sup>-1</sup>)

$V_w$	=	Volume of main coolant ( $\text{cm}^3$ )
$\lambda_i$	=	Decay constant for isotope i ( $\text{second}^{-1}$ )
$\text{PF}_{\text{EQ}_i}$	=	Equivalent purification factor (fraction) for i
$T_1$	=	Coolant residence time in core (seconds)
$T_2$	=	Coolant circulation time (seconds)
$f_{ij}$	=	Branching fraction from i to j
$Q_1$	=	Equivalent flow into purification stream ( $\text{cm}^3/\text{sec}$ )
	=	$Q_p \frac{k_p}{k_w}$
$Q_p$	=	Actual flow entering purification stream at coolant loop density ( $\text{cm}^3/\text{sec}$ )
$k_w$	=	Density of the main coolant ( $\text{g}/\text{cm}^3$ )
$k_p$	=	Density of the purification flow ( $\text{g}/\text{cm}^3$ )

The equivalent purification factor includes the effect of mixed bed demineralizers, periodically used cation demineralizer and noble gas stripping in the volume control tank.

#### 14B.4.1 Reactor Coolant and Secondary System Equilibrium Activities

The reactor coolant activities tabulated in Table 14B-6 are based on 1.0% failed fuel defects and a core power level of 2918 MWt. While the 1.0% fuel defects reactor coolant activities were the basis of most design basis radiological analyses performed during original licensing, current analysis practice is to base many of these analyses on the primary and secondary equilibrium activities that correspond to the specific activity limits for reactor coolant and secondary coolant provided in technical specifications. Table 14B-15 tabulates these equilibrium activities and reflects the relative nuclide abundance determined by leakage from a core with an inventory as provided in Table 14B-1A. Note that the primary and secondary coolant iodine activity limits reflected in Table 14B-15 and utilized in the DBA analyses are based on the BVPS-1 Technical Specification limit.

#### 14B.4.2 Reactor Coolant System Iodine Spiking

Two cases of iodine spiking are considered in current design basis radiological analyses. The first is the pre-incident spike which occurs such that the technical specification maximum dose equivalent I-131 concentrations are reached just prior to accident initiation. The second case is the iodine spike that is initiated by the accident transient (i.e., co-incident spike). For this case,



and except as noted, regulatory practice per Regulatory Guide 1.183 requires analyses to include an iodine spike appearance rate that is 500 times the iodine appearance rate that would result in RCS equilibrium concentrations equal to the technical specification. For the Steam Generator Tube Rupture, the iodine spike appearance rate is 335 times the iodine appearance rate that would result in RCS equilibrium concentrations equal to the technical specifications. Table 14B-16 tabulates the pre-incident spike concentrations and the methodology for calculating co-incident iodine spike release rates.

## 14B.5 TRITIUM PRODUCTION WITHIN A LIGHT WATER REACTOR (HISTORICAL)

### 14B.5.1 General - Overall Sources

Within a light water reactor, tritium is formed from several sources. The most abundant potential source in a PWR is the fissioning of the uranium within the nuclear fuel, which yields tritium as a ternary fission product. Tritium atoms are generated in the fuel at a rate of approximately  $8 \times 10^{-5}$  atoms per fission, or  $1.04 \times 10^{-2}$  curies per MWt per day. If there are any boron bearing control rods in the core, these can also be a potential source of tritium to the reactor coolant. These potential sources of tritium are only present in the reactor coolant as they would diffuse through the fuel and control rod cladding.

A direct source of tritium is the reaction of neutrons with dissolved boron in the reactor coolant. Boron is used in the reactor coolant for reactivity control in a PWR. Neutron reactions with lithium are also a direct source of tritium. Lithium is present in the reactor coolant for pH control, and as a product of boron reactions with neutrons. The amount of lithium present is carefully controlled by demineralization. An extremely small amount of tritium is also produced by neutron reactions with naturally occurring deuterium in light water.

The purpose of the following discussion is to review these sources in some detail as to their relative significance, and with respect to present operating experience.

### 14B.5.2 Specific Individual Sources of Tritium - Light Water Reactors

#### 14B.5.2.1 Ternary Fissions - Clad Diffusion

Because of the mode of operation of the PWR to minimize any liquid or gaseous discharges from the station, it has been possible to very accurately determine the buildup of tritium from various sources in the station and to identify their origin.

Such a program has been undertaken by Westinghouse to determine the source of tritium in the reactor coolant in operating stations with both stainless steel and zircaloy cladding. This program has clearly indicated that with the current generation of Westinghouse reactors with Zircaloy fuel cladding, 1 percent or less of the tritium produced in the fuel will diffuse through the cladding into the coolant. For those stations containing stainless steel cladding, operational data has shown that as high as 80 percent of the ternary tritium produced will diffuse through this type of cladding.

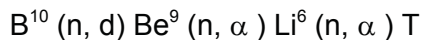
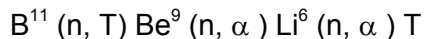
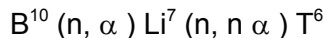
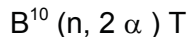
The tritium concentration in the reactor coolant (and the tritium discharged) in those stations having stainless steel and zircaloy fuel cladding has been substantially different. The tritium concentrations at Yankee-Rowe (600 MWt), which has stainless steel cladding, has shown a level of about 4.5 to 5  $\mu\text{Ci}$  per cc essentially throughout the core cycle with a total discharge from the station during the core cycle of approximately 1500 curies of tritium as reported in the monthly operating reports. In addition, with the stainless steel clad cores, there has been a continuing source of tritium to the reactor coolant during the power coastdown period after all the boric acid has been removed from the system. This information, in particular, substantiates the high tritium diffusion through the stainless steel clad.

The experience at the Ginna station has been substantially different. This station operates at 1455 MWt and has Zircaloy cladding. After approximately 8 months of operation, the tritium concentrations are less than 0.3  $\mu\text{Ci}$  per cc in the reactor coolant. The monthly discharges from the station have averaged approximately 5 curies per month. The experience at the Beznau and Jose de Cabrera plants are comparable. An extensive program to follow the generation of tritium in the Ginna reactor coolant was initiated, and the results to date indicate a potential source from the core which is 1 percent or less of the ternary fissions generated in the fuel. Based on this experience and program, Westinghouse believes the tritium sources during the operation of a PWR reactor can be very accurately predicted.

Westinghouse has in the past assumed that 30 percent of the tritium from ternary fissions would diffuse through the Zircaloy fuel, and this value was used as a basis for systems and operational design. Present experience indicates that this was clearly conservative.

#### 14B.5.2.2 Tritium Produced from Boron Reactions

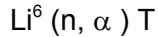
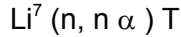
The neutron reactions with boron resulting in the production of tritium are:



Of the above reactions, only the first two contribute significantly to the tritium production in a PWR. The  $\text{B}^{11} (n, \text{T}) \text{Be}^9$  reaction has a threshold of 14 Mev and a cross section of approximately 5 mb. Since the number of neutrons available at this energy are less than  $10^9$  n/cm<sup>2</sup>-sec, the tritium produced from this reaction is negligible. The  $\text{B}^{10} (n, \text{d})$  reaction may be neglected since  $\text{Be}^9$  has been found to be unstable and thus the probability of its decay is much greater than the probability of its being converted to tritium.

### 14B.5.2.3 Tritium Produced from Lithium Reactions

The neutron reactions with lithium which produce tritium are:



In Westinghouse designed reactors, lithium is used for pH adjustment of the reactor coolant. The reactor coolant is maintained at a maximum level of 2.2 ppm lithium by the addition of  $\text{Li}^7\text{OH}$  and by a cation demineralizer included in the chemical and volume control system. This demineralizer will remove any excess of lithium produced in the  $\text{B}^{10} (n, \alpha) \text{Li}^7$  reaction.

The  $\text{Li}^6 (n, \alpha) \text{T}$  reaction is controlled by limiting the  $\text{Li}^6$  impurity in the  $\text{Li}^7\text{OH}$  used in the reactor coolant and by lithiating the demineralizers with 99.9 atom percent  $\text{Li}^7$ . This limitation has been in effect on Westinghouse designed reactors since 1962.

### 14B.5.2.4 Control Rod Sources

In a fixed burnable poison rod, there are two primary sources of tritium generation including the  $\text{B}^{10} (n, 2 \alpha) \text{T}$  and the  $\text{B}^{10} (n, \alpha) \text{Li}^7 (n, n) \text{T}$  reactions. Unlike the coolant where the  $\text{Li}^7$  level is controlled at 2 ppm, there is a buildup of  $\text{Li}^7$  in the burnable poison rod. The burnable poison rods were required during the first year of operation. During that cycle the tritium production was 72 curies per lb of  $\text{B}^{10}$ .

The control rod materials used in the Westinghouse PWR are Ag-In-Cd; there are no tritium sources in these materials.

### 14B.5.2.5 Tritium Production from Deuterium Reactions

Since the weight percent of naturally occurring deuterium in water is less than 0.015, the tritium produced from this reaction is negligible (less than 1 curie per year).

### 14B.5.2.6 Total Tritium Sources

Table 14B-7 lists the basic assumptions and station parameters used in calculating the various tritium sources. Tritium sources in the reactor coolant system of a PWR are listed in Table 14B-8, which is presented on the basis of 12 months of operation at full power (2,766 MWt) and a 0.8 load factor.

#### 14B.6 WASTE GAS SYSTEM DECAY TANK RUPTURE ACTIVITY RELEASE

The radioactivity available for release following rupture of a waste gas system decay tank was determined using the guidance of Regulatory Guide 1.24 and NUREG-0800 Branch Technical Position ETSB 11-5, that is, the noble gas is removed from the RCS as quickly as possible and collected in decay tanks. Additionally, the RCS activity concentration is conservatively based on equilibrium achieved while operating with 1% fuel rod cladding defects, since the maximum condition permitted by Technical Specifications is less than the value used. When a tank is full, it immediately ruptures and releases its entire contents directly to the environment.

Hold-up in the charcoal delay bed is considered in the radiological analysis. Because of the long hold-up time for Xe, there are no Xe isotopes assumed to be present when the tank rupture occurs. Decay of Kr isotopes during activity collection and hold-up is considered in the analysis. The collection time duration is based on the time required to fill a decay tank. During this period RCS activity is conservatively assumed to remain constant, with no credit taken for activity depletion.

#### 14B.7 WASTE GAS SYSTEM LINE RUPTURE ACTIVITY RELEASE

The radioactivity available for release following rupture of a waste gas process system component was determined using the guidance of Regulatory Guide 1.24 and NUREG-0800 Branch Technical Position ETSB 11-5. The radioactivity release consists of two source components: 1) instantaneous release of a portion of the activity collected on the charcoal delay bed following 24 hours of degassing at power plus the time period required to remove 99% of the gas following reactor shutdown and, 2) one hour continuous flow release via the rupture assuming a constant activity removal rate (no source depletion). Additionally, the RCS activity concentration is conservatively based on equilibrium achieved while operating with 1% fuel rod cladding defects, since the maximum condition permitted by Technical Specifications is less than the value used. The dose resulting from each of these two source components is summed to provide a conservative, bounding radiological consequence determination for this accident.

#### 14B.8 DOSE MODELS FOR DESIGN BASIS ACCIDENT

This section identifies the models used to calculate the offsite radiological consequences from the release of radioactivity as a result of a loss of coolant accident.

##### 14B.8.1 Assumptions

The following assumptions are basic to both the whole body dose due to immersion in a cloud of radioactivity and the thyroid dose due to inhalation of radioactivity:

- a. All radioactive releases are treated as ground level releases regardless of the point of discharge.
- b. No credit is taken for cloud depletion by ground deposition and/or radioactive decay during transport to the exclusion area boundary (EAB) or the outer boundary of the low population zone (LPZ).

- c. No credit is taken for collection and filtration of the containment or ESF leakage by the Supplementary Leak Collection and Release System (SLCRS) in the design basis case (DBA).

#### 14B.8.2 Updated Dose Calculation Models

Commencing with analyses performed in 1995, the whole body-gamma dose, beta skin dose, and thyroid dose commitments have been calculated using the dose methodologies described in the BVPS Unit 2 UFSAR Section 15A.2.

Subsequent to containment operation at atmospheric conditions and replacement steam generators, the Total Effective Dose Equivalent (TEDE) is calculated for all design basis accidents with the exception of the Waste Gas System Rupture. The calculation models for TEDE values are consistent with regulatory guidance provided in Regulatory Guide 1.183 and are described in the BVPS Unit 2 UFSAR Sections 15A.2 and 15A.3.

#### 14B.9 CONTAINMENT LEAKAGE MODEL - DBA CASE<sup>(20)</sup>

This section describes the model used to estimate the quantity of radionuclides released to the environment by leakage from the containment building, using design basis assumptions.

##### 14B.9.1 Radioiodine and Other Aerosol

Figure 14B-1 illustrates, schematically, the leakage model. The containment free volume is assumed to consist of two regions: a sprayed region and an unsprayed region. The processes acting simultaneously on the activity in the unsprayed region are:

- a. Radioactive decay
- b. Leakage from containment
- c. Thermally induced exchange with sprayed region
- d. Small removal rate of aerosols due to steam condensation

For the sprayed region, scavenging of iodine and aerosol by chemical sprays, steam condensation and plateout is added to the list above. The scavenging rate is different for elemental iodine and aerosol. The chemical removal continues until the spray terminates at 4 days after the LOCA.

The transport of radioiodines and aerosols in and between the two regions is modeled as a first order linear process. The activity in the sprayed region (subscript "s") and in the unsprayed region (subscript "u") is determined as a function of the removal processes identified above, Z, and the exchange between regions, E, by the following differential expression:

$$dA(s)/dt = E(u)xA(u) - Z(s)xA(s)$$

$$dA(u)/dt = E(s)xA(s) - Z(u)xA(u)$$

The activity released to the environment, Q, as a function of leakage, L, is given by:

$$Q = L \int_{t=0}^T A(s) dt + L \int_{t=0}^T A(u) dt$$

The solutions to these expressions are tabulated in Table 14B-12.

#### 14B.9.2 Noble Gases and Organic Iodine

Noble gases and organic iodine are not affected by the containment sprays, and therefore, the two region model used for the radioiodines and aerosols is replaced with a model which encompasses the entire containment free volume in a single region. The noble gas and organic iodine activity released to the containment, A, as a function of time, leakage, L, and radioactive decay constant, LAMBDA is given by:

$$dA/dt = -Lx A - LAMBDA x A$$

The activity released to the environment, Q, is given as a function of leakage, L, and time:

$$Q = L \int_{t=0}^T A dt$$

These expressions are solved by the following:

$$Q = \{[Lx A(0)] / [L+LAMBDA]\} \times [1 - \text{EXP}(-(L+LAMBDA)xT)]$$

Where:

A(0) = Initial noble gas or organic iodine activity released to the containment at t=0, Ci

L = Leakage constant, sec<sup>-1</sup>

LAMBDA = Radioactive decay, sec<sup>-1</sup>

In addition, the release of noble gases generated by the decay of parent halogens/noble gases in containment is included in the calculation model.

### 14B.9.3 ESF Leakage and RWST Back-leakage

The ESF leakage model assumes that there is leakage of containment sump water to areas outside of the containment via leaks in the recirculation piping. Noble gases are not assumed to be present in the sump water and therefore are not considered in the ESF leakage model. Ten percent (10%) of the radioiodine postulated to leak from the recirculation piping is assumed to go airborne and be available for release to the environment.

All of the potential ESF leakage occurs within the areas maintained at a slight vacuum by the Supplementary Leak Collection and Release System (SLCRS), and is therefore collected. This activity is released via the release point located on the containment dome. However, no credit is taken for filtration via these filter banks.

The activity released to the environment via the RWST vent due to back-leakage of the sump water into the RWST is also included in the LOCA analysis.

References to Appendix 14B

1. J. J. DiNunno, et. al, "Calculation of Distance Factors for Power and Test Reactor Sites," TID 14844, U.S. Atomic Energy Commission (March 1962).
2. M. E. Meek and B. F. Rider, "Summary of Fission Produce Yields for U-235, U-238, Pu-239, and Pu-241 at Thermal Fission Spectrum and 14 Mev Neutron Energies," APED-5398, General Electric Corporation (March 1968).
3. D. F. Toner and J. S. Scott, "Fission Product Release for UO<sub>2</sub>," Nuclear Safety, Volume III No. 2 (December 1961).
4. J. Belle, Uranium Dioxide: Properties and Nuclear Applications, Naval Reactors Division of Reactor Development, United States Atomic Energy Commission (1961).
5. A. H. Booth, "A Suggested Method for Calculating the Diffusion of Radioactive Rare Gas Fission Products From UO<sub>2</sub> Fuel Elements," DCI-27, Atomic Energy Canada, Limited (1957).
6. D. C. Kocher, "Dose Rate Conversion Factors for External Exposure to Photons and Electrons", NUREG/CR-1918 (August 1981).
7. Deleted by Revision 23.
8. Deleted by Revision 23.
9. USNRC NUREG/CR-0200, ORIGEN-S: Scale System Module to Calculate Fuel Depletion, Actinide Transmutation, Fission Product Buildup and Decay, and associated Radiation Source Terms.
10. Phone memo between C. J. Code of Stone & Webster and Malvin Tower of Virginia Electric Power Company (March 20, 1973).
11. ICRP, Recommendations of the International Commission on Radiological Protection, ICRP Publication 26 (1977).
12. ICRP, Limits for Intakes of Radionuclides by Workers, ICRP Publication 30 (1978).
13. K. G. Murphy and K. W. Campe, Nuclear Power Plant Control Room Ventilation System Design for Meeting General Criterion 19, published in proceedings of 13th AEC Air Cleaning Conference.
14. USNRC, "Standard Review Plan for the Review of Safety Analysis Reports for Nuclear Power Plants," NUREG-0800.



References to Appendix 14B (CONT'D)

15. D. C. Kocher, "External Dose-Rate Conversion Factors for Calculation of Dose to the Public," DOE/EH-0700 (1988).
16. K. F. Eckerman, et. al., "Limiting Values of Radionuclide Intake and Air Concentration and Dose Conversion Factors for Inhalation, Submersion, and Ingestion," EPA-520/1-88-020 (1988).
17. Deleted by Revision 23. |
18. Deleted by Revision 23. |
19. Deleted by Revision 23. |
20. Deleted by Revision 23. |
21. Deleted by Revision 23. |
22. Deleted by Revision 23. |

BVPS UFSAR UNIT 1

TABLES FOR APPENDIX 14B

Table 14B-1A

EQUILIBRIUM CORE INVENTORY BASED ON A CORE POWER OF 2918 MWT  
AND AN 18 MONTH FUEL CYCLE

Isotope	Parent Relationship	Parent Isotope	Activity (Curies)	Isotope	Parent Relationship	Parent Isotope	Activity (Curies)
AG-111			5.05E+06	PU-239			2.86E+04
	Parent:	AG-111M	5.06E+06		Parent:	NP-239	1.66E+09
	Grandparent:	PD-111	5.04E+06		Grandparent:	U-239	1.66E+09
AG-112			2.28E+06	PU-240			3.87E+04
	Parent:	PD-112	2.27E+06		Parent:	NP-240	4.32E+06
AM-241			1.17E+04	PU-241			1.13E+07
	Parent:	PU-241	1.13E+07	PU-242			2.01E+02
BA-137M			9.35E+06		Parent:	AM-242	7.04E+06
	Parent:	CS-137	9.81E+06	RB-86			1.69E+05
	Grandparent:	XE-137	1.46E+08	RB-88			5.57E+07
BA-139			1.41E+08		Parent:	KR-88	5.43E+07
	Parent:	CS-139	1.37E+08		Grandparent:	BR-88	2.99E+07
	Grandparent:	XE-139	1.01E+08	RB-89			7.26E+07
BA-140			1.42E+08		Parent:	KR-89	6.75E+07
	Parent:	CS-140	1.23E+08		Grandparent:	BR-89	2.08E+07
	Grandparent:	XE-140	7.06E+07	RB-90			6.69E+07
BA-142			1.21E+08		Parent:	KR-90	7.24E+07
	Parent:	CS-142	5.48E+07		Grandparent:	BR-90	1.13E+07
	Grandparent:	XE-142	1.07E+07		2nd Parent:	RB-90M	2.11E+07
BR-82			3.02E+05	RB-90M			2.11E+07
	Parent:	BR-82M	2.62E+05		Parent:	KR-90	7.24E+07
BR-83			9.37E+06		Grandparent:	BR-90	1.13E+07
	Parent:	SE-83M	4.69E+06	RH-103M			1.26E+08
	2nd Parent:	SE-83	4.42E+06		Parent:	RU-103	1.26E+08
BR-85			1.95E+07	RH-105			8.16E+07

Table 14B-1A (CONT'D)

EQUILIBRIUM CORE INVENTORY BASED ON A CORE POWER OF 2918 MWT  
AND AN 18 MONTH FUEL CYCLE

Isotope	Parent Relationship	Parent Isotope	Activity (Curies)	Isotope	Parent Relationship	Parent Isotope	Activity (Curies)
CE-141			1.30E+08		Parent:	RH-105M	2.53E+07
	Parent:	LA-141	1.29E+08		Grandparent:	RU-105	8.90E+07
	Grandparent:	BA-141	1.28E+08		2nd Parent:	RU-105	8.90E+07
CE-143			1.21E+08	RH-105M			2.53E+07
	Parent:	LA-143	1.20E+08		Parent:	RU-105	8.90E+07
CE-144			9.82E+07		Grandparent:	TC-105	8.76E+07
CM-242			4.22E+06	RH-106			5.13E+07
	Parent:	AM-242	7.04E+06		Parent:	RU-106	4.63E+07
CM-244			5.97E+05	RU-103			1.26E+08
	Parent:	AM-244	1.89E+07		Grandparent:	MO-103	1.24E+08
CS-134			1.57E+07	RU-106			4.63E+07
	Parent:	CS-134M	3.69E+06		2nd Parent:	SN-125M	1.20E+06
CS-134M			3.69E+06	SB-127			6.92E+06
CS-135M			4.39E+06		Parent:	SN-127	2.78E+06
CS-136			4.97E+06		2nd Parent:	SN-127M	3.76E+06
CS-137			9.81E+06	SB-129			2.52E+07
	Parent:	XE-137	1.46E+08		Parent:	SN-129	9.90E+06
	Grandparent:	I-137	7.47E+07		2nd Parent:	SN-129M	9.29E+06
CS-138			1.48E+08	SB-130			8.37E+06
	Parent:	XE-138	1.36E+08	SB-130M			3.47E+07
	Grandparent:	I-138	3.80E+07		Parent:	SN-130	2.61E+07
CS-139			1.37E+08	SB-131			6.09E+07
	Parent:	XE-139	1.01E+08		Parent:	SN-131	2.24E+07
	Grandparent:	I-139	1.83E+07	SB-132			3.67E+07
CS-140			1.23E+08		Parent:	SN-132	1.81E+07
	Parent:	XE-140	7.06E+07	SB-133			5.08E+07

Table 14B-1A (CONT'D)

EQUILIBRIUM CORE INVENTORY BASED ON A CORE POWER OF 2918 MWT  
AND AN 18 MONTH FUEL CYCLE

Isotope	Parent Relationship	Parent Isotope	Activity (Curies)	Isotope	Parent Relationship	Parent Isotope	Activity (Curies)
	Grandparent:	I-140	4.81E+06	SE-83			4.42E+06
	Parent:	SM-155	3.11E+06	SM-153			4.02E+07
BU-156			2.29E+07		Parent:	PM-153	7.37E+06
	Parent:	SM-156	1.93E+06	SN-127			2.78E+06
BU-157			2.41E+06	SR-89			7.61E+07
H-3			4.36E+04		Parent:	RB-89	7.26E+07
I-129			2.86E+00		Grandparent:	KR-89	6.75E+07
	Parent:	TE-129	2.40E+07	SR-90			7.21E+06
	Grandparent:	TE-129M	4.87E+06		Parent:	RB-90	6.69E+07
	2nd Parent:	TE-129M	4.87E+06		Grandparent:	KR-90	7.24E+07
I-130			2.07E+06		2nd Parent:	RB-90M	2.11E+07
	Parent:	I-130M	1.10E+06	SR-91			9.50E+07
I-131			7.78E+07		Parent:	RB-91	8.85E+07
	Parent:	TE-131	6.54E+07		Grandparent:	KR-91	4.98E+07
	Grandparent:	TE-131M	1.57E+07	SR-92			1.01E+08
	2nd Parent:	TE-131M	1.57E+07		Parent:	RB-92	7.83E+07
I-132			1.14E+08		Grandparent:	KR-92	2.66E+07
	Parent:	TE-132	1.12E+08	SR-93			1.14E+08
	Grandparent:	SB-132	3.67E+07		Grandparent:	KR-93	9.04E+06
I-133			1.60E+08	SR-94			1.14E+08
	Parent:	TE-133	8.66E+07		Grandparent:	KR-94	4.18E+06
	Grandparent:	SB-133	5.08E+07	TC-99M			1.29E+08
	2nd Parent:	TE-133M	7.12E+07		Parent:	MO-99	1.45E+08
I-134			1.77E+08		Grandparent:	NB-99	8.50E+07
	Parent:	TE-134	1.41E+08	TC-101			1.33E+08
	2nd Parent:	I-134M	1.59E+07		Parent:	MO-101	1.33E+08

Table 14B-1A (CONT'D)

EQUILIBRIUM CORE INVENTORY BASED ON A CORE POWER OF 2918 MWT  
AND AN 18 MONTH FUEL CYCLE

Isotope	Parent Relationship	Parent Isotope	Activity (Curies)	Isotope	Parent Relationship	Parent Isotope	Activity (Curies)
I-135			1.52E+08	TC-104			1.05E+08
I-136			6.99E+07		Parent:	MO-104	9.99E+07
KR-83M			9.46E+06	TC-105			8.76E+07
	Parent:	BR-83	9.37E+06		Parent:	MO-105	7.38E+07
	Grandparent:	SE-83M	4.69E+06	TE-127			6.81E+06
KR-85			8.27E+05		Parent:	TE-127M	1.13E+06
	Parent:	KR-85M	1.95E+07		Grandparent:	SB-127	6.92E+06
	Grandparent:	BR-85	1.95E+07		2nd Parent:	SB-127	6.92E+06
	2nd Parent:	BR-85	1.95E+07	TE-127M			1.13E+06
KR-85M			1.95E+07		Parent:	SB-127	6.92E+06
	Parent:	BR-85	1.95E+07		Grandparent:	SN-127	2.78E+06
KR-87			3.91E+07	TE-129			2.40E+07
	Parent:	BR-87	3.09E+07		Parent:	TE-129M	4.87E+06
KR-88			5.43E+07		Grandparent:	SB-129	2.52E+07
	Parent:	BR-88	2.99E+07		2nd Parent:	SB-129	2.52E+07
KR-89			6.75E+07	TE-129M			4.87E+06
	Parent:	BR-89	2.08E+07		Parent:	SB-129	2.52E+07
KR-90			7.24E+07		Grandparent:	SN-129	9.90E+06
	Parent:	BR-90	1.13E+07	TE-131			6.54E+07
LA-140			1.46E+08		Parent:	SB-131	6.09E+07
	Parent:	BA-140	1.42E+08		Grandparent:	SN-131	2.24E+07
	Grandparent:	CS-140	1.23E+08		2nd Parent:	TE-131M	1.57E+07
LA-141			1.29E+08	TE-131M			1.57E+07
	Parent:	BA-141	1.28E+08		Parent:	SB-131	6.09E+07
LA-142			1.26E+08		Grandparent:	SN-131	2.24E+07
	Parent:	BA-142	1.21E+08	TE-132			1.12E+08

Table 14B-1A (CONT'D)

EQUILIBRIUM CORE INVENTORY BASED ON A CORE POWER OF 2918 MWT  
AND AN 18 MONTH FUEL CYCLE

Isotope	Parent Relationship	Parent Isotope	Activity (Curies)	Isotope	Parent Relationship	Parent Isotope	Activity (Curies)
	Grandparent:	CS-142	5.48E+07		Parent:	SB-132	3.67E+07
LA-143			1.20E+08		Grandparent:	SN-132	1.81E+07
MO-99			1.45E+08	TE-133			8.66E+07
	Parent:	NB-99M	5.82E+07		Parent:	TE-133M	7.12E+07
	2nd Parent:	NB-99	8.50E+07		Grandparent:	SB-133	5.08E+07
MO-101			1.33E+08		2nd Parent:	SB-133	5.08E+07
NB-95			1.34E+08	TE-133M			7.12E+07
	Parent:	ZR-95	1.33E+08		Parent:	SB-133	5.08E+07
	Grandparent:	Y-95	1.28E+08	TE-134			1.41E+08
	2nd Parent:	NB-95M	1.52E+06	XE-131M			1.08E+06
NB-95M			1.52E+06		Parent:	I-131	7.78E+07
	Parent:	ZR-95	1.33E+08		Grandparent:	TE-131M	1.57E+07
	Grandparent:	Y-95	1.28E+08	XE-133			1.60E+08
NB-97			1.27E+08		Parent:	I-133	1.60E+08
	Parent:	NB-97M	1.19E+08		Grandparent:	TE-133M	7.12E+07
	Grandparent:	ZR-97	1.26E+08		2nd Parent:	XE-133M	5.05E+06
	2nd Parent:	ZR-97	1.26E+08	XE-133M			5.05E+06
NB-97M			1.19E+08		Parent:	I-133	1.60E+08
	Parent:	ZR-97	1.26E+08		Grandparent:	TE-133M	7.12E+07
ND-147			5.22E+07	XE-135			4.84E+07
	Parent:	PR-147	5.18E+07		Parent:	I-135	1.52E+08
	Grandparent:	CE-147	4.92E+07		2nd Parent:	XE-135M	3.36E+07
NP-239			1.66E+09	XE-135M			3.36E+07
	Grandparent:	PU-243	4.23E+07		Parent:	I-135	1.52E+08
	2nd Parent:	U-239	1.66E+09	XE-137			1.46E+08
PD-109			3.26E+07		Parent:	I-137	7.47E+07

Table 14B-1A (CONT'D)

EQUILIBRIUM CORE INVENTORY BASED ON A CORE POWER OF 2918 MWT  
AND AN 18 MONTH FUEL CYCLE

Isotope	Parent Relationship	Parent Isotope	Activity (Curies)	Isotope	Parent Relationship	Parent Isotope	Activity (Curies)
PM-147			1.38E+07	XE-138			1.36E+08
	Parent:	ND-147	5.22E+07		Parent:	I-138	3.80E+07
	Grandparent:	PR-147	5.18E+07	Y-90			7.49E+06
PM-148			1.41E+07		Parent:	SR-90	7.21E+06
	Parent:	PM-148M	2.37E+06		Grandparent:	RB-90	6.69E+07
PM-148M			2.37E+06	Y-91			9.87E+07
PM-149			4.82E+07		Parent:	SR-91	9.50E+07
	Parent:	ND-149	3.02E+07		Grandparent:	RB-91	8.85E+07
	Grandparent:	PR-149	2.80E+07		2nd Parent:	Y-91M	5.51E+07
PM-151			1.60E+07	Y-91M			5.51E+07
	Parent:	ND-151	1.58E+07		Parent:	SR-91	9.50E+07
PR-142			5.57E+06		Grandparent:	RB-91	8.85E+07
PR-143			1.18E+08	Y-92			1.02E+08
	Parent:	CE-143	1.21E+08		Parent:	SR-92	1.01E+08
	Grandparent:	LA-143	1.20E+08		Grandparent:	RB-92	7.83E+07
PR-144			9.89E+07	Y-93			7.73E+07
	Parent:	CE-144	9.82E+07		Parent:	SR-93	1.14E+08
	2nd Parent:	PR-144M	1.38E+06	Y-94			1.23E+08
PU-238			3.40E+05		Parent:	SR-94	1.14E+08
	2nd Parent:	NP-238	3.98E+07	Y-95			1.28E+08
				ZR-95			1.33E+08
					Parent:	Y-95	1.28E+08
				ZR-97			1.26E+08



Table 14B-2

## CORE TEMPERATURE DISTRIBUTION

<u>Percent of Core Fuel Within Given Temperature Range</u>	<u>Power (MWt)</u>	<u>Fuel Temperature Range, (F)</u>
0.0	0.0	>3400
0.1	2.353	3400 - 3200
0.5	13.33	3200 - 3000
1.3	35.196	3000 - 2800
2.1	58.92	2800 - 2600
3.3	92.16	2600 - 2400
4.5	124.71	2400 - 2200
5.6	153.92	2200 - 2000
82.6	2284.31	<2000

Table 14B-5

PARAMETERS USED IN THE CALCULATION OF REACTOR COOLANT ACTIVITIES

1.	Core thermal power, maximum calculated, MWt	2,918	
2.	Fraction of fuel containing clad defects	0.01	
3.	Reactor coolant liquid volume, including pressurizer, ft <sup>3</sup>	7,691	
4.	Reactor coolant density (lb/ft <sup>3</sup> )	45.46	
5.	Purification flow rate (minimum), gpm	60	
6.	Effective cation demineralizer flow, gpm	6.0	
7.	Volume control tank volumes		
	a. Vapor, ft <sup>3</sup>	183	
	b. Liquid, ft <sup>3</sup>	136	
8.	Fission product escape rate coefficients:		
	a. Noble gas isotopes, sec <sup>-1</sup>	6.5 x 10 <sup>-8</sup>	
	b. Br, Rb, I and Cs isotopes, sec <sup>-1</sup>	1.3 x 10 <sup>-8</sup>	
	c. Te isotopes, sec <sup>-1</sup>	1.0 x 10 <sup>-9</sup>	
	d. Mo isotopes, sec <sup>-1</sup>	2.0 x 10 <sup>-9</sup>	
	e. Sr and Ba isotopes, sec <sup>-1</sup>	1.0 x 10 <sup>-11</sup>	
	f. Y, La, Ce, Pr, Se, Zr, Nb, Tc, Ru, Rh, Sn, Sb, Nd, Pm, Sm isotopes, sec <sup>-1</sup>	1.6 x 10 <sup>-12</sup>	
9.	Mixed bed demineralizer decontamination factors:		
	a. Noble gases and Cs, Rb	1.0	
	b. All other isotopes	10.0	
10.	Cation bed demineralizer decontamination factor for Cs, Rb	10.0	
	Noble gases, halogens, others	1.0	

Table 14B-5 (CONT'D)

PARAMETERS USED IN THE CALCULATION OF REACTOR COOLANT ACTIVITIES

11. Volume control tank noble gas stripping fraction

<u>Isotope</u>	<u>Stripping Fraction</u>
Kr-83m	7.7E-01
Kr-85m	5.8E-01
Kr-85	6.5E-05
Kr-87	8.3E-01
Kr-88	6.8E-01
Kr-89	9.9E-01
Xe-131m	1.3E-02
Xe-133m	6.9E-02
Xe-133	3.0E-02
Xe-135m	9.4E-01
Xe-135	3.0E-01
Xe-137	9.8E-01
Xe-138	9.4E-01

12. Thermal Neutron Flux in Fuel Region (n/s-cm<sup>2</sup>) 4.86E+13 |

13. Thermal Neutron Flux in Coolant Region in Core (n/s-cm<sup>2</sup>) 5.60E+13 |

14. Circulation Time of Primary Coolant (sec) 12.2

15. Residence Time of Coolant In Core (sec) 0.808

16. Density of Purification Flow (lb/ft<sup>3</sup>) 61.29

17. Volume Control Tank

Water Volume (ft <sup>3</sup> )	136
Vapor Volume (ft <sup>3</sup> )	183
Temperature (°F)	115
Pressure (psig)	20
Purge Rate (ft <sup>3</sup> /min)	0.0

18. Reactor Operation Time (days) 900 |

Table 14B-6

DESIGN REACTOR COOLANT NOBLE GAS AND IODINE ACTIVITIES  
(Based on Parameters Given in Table 14B-5)

<u>NUCLIDE</u>	<u>ACTIVITY</u> <u>(<math>\mu</math>ci/gram)</u>	<u>NUCLIDE</u>	<u>ACTIVITY</u> <u>(<math>\mu</math>ci/gram)</u>
Kr-83m	4.10E-01	Br-84	3.73E-02
Kr-85m	1.42E+00	Rb-88	2.75E+00
Kr-85	1.25E+02	Rb-89	1.57E-01
Kr-87	9.48E-01	Sr-89	3.49E-03
Kr-88	2.65E+00	Sr-90	12.16E-04
Kr-89	7.63E-02	Sr-91	1.45E-03
		Sr-92	1.03E-03
Xe-131m	5.10E+00	Y-90	5.94E-05
Xe-133m	4.2E+00	Y-91	4.78E-04
Xe-133	3.11E+02	Y-92	8.84E-04
Xe-135m	9.56E-01	Zr-95	6.32E-04
Xe-135	9.64E+00	Nb-95	6.41E-04
Xe-137	1.98E-01	Mo-99	7.62E-01
Xe-138	6.70E-01	Te-132	3.00E-01
		Te-134	2.99E-02
I-131	2.89E+00	Cs-137	3.79E+00
I-132	1.13E+00	Cs-138	1.03E-00
I-133	4.32E+00	Ba-140	4.10E-03
I-134	6.32E-01	La-140	1.41E-03
I-135	2.48E+00	Ce-144	4.69E-04
		Pr-144	4.72E-04
Mn-54	4.80E-03		
Co-58	1.38E-02		
Co-60	1.59E-03		
Fe-59	9.00E-04		
Cr-51	9.30E-03		

Table 14B-7 - [HISTORICAL]

PARAMETERS USED IN THE CALCULATION OF TRITIUM SOURCES

Basic Assumptions and Station Parameters:

1.	Core thermal power, MWt	2,766
2.	Plant load factor	0.8
3.	Core volume, ft <sup>3</sup>	937.8
4.	Core volume fractions	
	a. UO <sub>2</sub>	0.3029
	b. Zr + SS	0.1048
	c. H <sub>2</sub> O	0.5923
5.	Initial reactor coolant boron level	
	a. Initial cycle, (hot, full power, equilibrium xenon) ppm	700
	b. Equilibrium cycle, (hot, full power, equilibrium xenon) ppm	1,000
6.	Reactor coolant volume, ft <sup>3</sup>	9,387
7.	Reactor coolant transport times	
	a. Incore, seconds	0.87
	b. Out-of-core, seconds	10.50
8.	Reactor coolant peak lithium level (99% pure Li <sup>7</sup> ), ppm	2.2
9.	Core averaged neutron fluxes, n/cm <sup>2</sup> -second	
	a. E > 6 Mev	2.91 x 10 <sup>12</sup>
	b. E > 5 Mev	7.90 x 10 <sup>12</sup>
	c. 3 Mev ≤ E ≤ 6 Mev	2.26 x 10 <sup>13</sup>
	d. 1 Mev ≤ E ≤ 5 Mev	5.31 x 10 <sup>13</sup>
	e. E < 0.625 ev	2.26 x 10 <sup>13</sup>

Table 14B-7 (CONT'D) - [HISTORICAL]

PARAMETERS USED IN THE CALCULATION OF TRITIUM SOURCES

10.	Neutron reaction cross-section, barns		
	a.	$B^{10} (n, 2 \alpha ) T: (1 \text{ MEV} \leq E \leq 5 \text{ Mev})$	= 0.0316 (spectrum weighted)
		$(E > 5 \text{ Mev})$	= 0.075
	b.	$Li^7 (n, n \alpha ) T: (3 \text{ Mev} \leq E \leq 6 \text{ Mev})$	= 0.0391 (spectrum weighted)
		$(E > 6 \text{ Mev})$	= 0.400
	c.	$Li^6 (n, \alpha ) T:$	= 945
11.	Fraction of ternary tritium diffusing through zirconium cladding		0.01

Table 14B-8 - [HISTORICAL]

TRITIUM PRODUCTION IN THE REACTOR COOLANT  
CURIES PER YEAR

(Based on Parameters Given in Table 14B-7)

<u>Tritium</u>	<u>Total Produced</u>	<u>Released to the Coolant</u>
Ternary Fissions	8,498	85
Burnable Poison <sup>(1)</sup> Rods (Initial Cycle)	408	4
Soluble Poison Boron (Initial Cycle)	285	285
(Equilibrium Cycle)	405	405
Li-7 Reaction	10	10
Li-6 Reaction	5	5
Deuterium Reaction	1	1
Total Initial Cycle	9,207	390
Total Equilibrium Cycle	8,920	506

(1) Weight of B<sub>2</sub>O<sub>3</sub> = 85 lb (B<sup>10</sup> = 5.23 lb)

Table 14B-11

THYROID DOSE CONVERSION FACTORS<sup>(1)</sup>

<u>Nuclide</u>	<u>Sv/Bq</u>
I <sup>131</sup>	2.92E-07
I <sup>132</sup>	1.74E-09
I <sup>133</sup>	4.86E-08
I <sup>134</sup>	2.88E-10
I <sup>135</sup>	8.46E-09

BREATHING RATES<sup>(2)</sup>

<u>Time Period</u>	<u>m<sup>3</sup>/sec</u>
0-8 hours	3.5 10 <sup>-4</sup>
8-24 hours	1.8 10 <sup>-4</sup>
24-duration	2.3 10 <sup>-4</sup>

Notes:

- (1) EPA 520, Federal Guidance Report No. 11  
(conversion factor, 3.7E+09 mrem-Bq/Sv-μCi)
- (2) U. S. Nuclear Regulatory Commission, Regulatory Guide 1.183



Table 14B-12

SUMMARY OF TWO-REGION SPRAY MODEL EXPRESSIONS

$w_1$  and  $w_2$  are the roots of the expression:

$$w^2 + (Z_u + Z_s)w + (Z_s Z_u - E_u E_s) = 0$$

$$A'_{2s} = \frac{A_o V_u (w_1 + Z_u) (w_2 + Z_u) - A_o V_s E_s (w_2 + Z_u)}{E_s V_t (w_1 - w_2)}$$

$$A'_{2u} = \frac{A_o V_s (w_1 + Z_s) (w_2 + Z_s) - A_o V_u E_u (w_2 + Z_s)}{E_u V_t (w_1 - w_2)}$$

$$A'_{1s} = \frac{E_s A_o V_s (w_1 + Z_u) - A_o V_u (w_2 + Z_u) (w_1 + Z_u)}{E_s V_t (w_1 - w_2)}$$

$$A'_{1u} = \frac{E_u A_o V_u (w_1 + Z_s) - A_o V_s (w_2 + Z_s) (w_1 + Z_s)}{E_u V_t (w_1 - w_2)}$$

The activity in the containment at any time =

$$A_1(t) = \sum_{i=1}^2 A'_{1s} \text{EXP}(w_i t) + \sum_{i=1}^2 A'_{1u} \text{EXP}(w_i t)$$

The activity in the environment is then:

$$A_2(t) = L_1 \sum_{i=1}^2 \frac{A'_{1u} + A'_{1s}}{w_i} (\text{EXP}(w_i t) - 1)$$

WHERE:

$A'_{i,j}$  = Integration constants for sprayed and unsprayed regions of primary containment,  $i = 1, 2$ ;  $j = s, u$

$A_{1,j}$  = Activity in sprayed and unsprayed region of primary containment (Ci)  $j = u, s$

$A_{2,j}$  = Activity to environment from leakage from sprayed and unsprayed regions of primary containment (Ci)  $j = u, s$

Table 14B-12 (CONT'D)

## SUMMARY OF TWO-REGION SPRAY MODEL EXPRESSIONS

$A_0$	=	Initial activity in containment (Ci)
$A_1(t)$	=	Activity in primary containment at time = t (Ci)
$A_2(t)$	=	Activity in environment at time = t (Ci)
$\lambda$	=	Radioactive decay constant ( $\text{sec}^{-1}$ )
$L_1$	=	Containment leak rate ( $\text{sec}^{-1}$ )
$Z_u$	=	Removal rate from unsprayed region ( $\text{sec}^{-1}$ )
$Z_s$	=	Removal rate from sprayed region ( $\text{sec}^{-1}$ )
$E$	=	Exchange rate between sprayed and unsprayed regions ( $\text{cm}^3/\text{sec}$ )
$E_u$	=	$E/V_u$ = Exchange from unsprayed to sprayed region ( $\text{sec}^{-1}$ )
$E_s$	=	$E/V_s$ = Exchange from sprayed to unsprayed region ( $\text{sec}^{-1}$ )
$V_u, V_s$	=	Volumes of unsprayed and sprayed regions ( $\text{cm}^3$ )
$w_1, w_2$	=	Roots of quadratic expression above
$V_t$	=	Volume of containment ( $\text{cm}^3$ )
	=	$V_u + V_s$

Table 14B-15

PRIMARY AND SECONDARY COOLANT TECHNICAL SPECIFICATION  
IODINE AND NOBLE GAS CONCENTRATIONS

<b><u>Nuclide</u></b>	<b>Primary Coolant<sup>(1)</sup> <u>(<math>\mu</math>Ci/gm)</u></b>	<b>Secondary Coolant<sup>(2)</sup> <u>(<math>\mu</math>Ci/gm)</u></b>
I-131	2.74E-01	8.33E-02
I-132	1.08E-01	1.40E-02
I-133	4.10E-01	9.39E-02
I-134	6.00E-02	1.95E-03
I-135	2.36E-01	3.39E-02
Kr-83m	3.89E-02	
Kr-85m	1.35E-01	
Kr-85	1.18E+01	
Kr-87	9.00E-02	
Kr-88	2.52E-01	
Xe-131m	4.84E-01	
Xe-133m	3.99E-01	
Xe-133	2.95E+01	
Xe-135m	9.09E-02	
Xe-135	9.16E-01	

**Notes:**

1. Based on 0.35  $\mu$ Ci/gm I-131 dose equivalent concentration.
2. Based on 0.1  $\mu$ Ci/gm I-131 dose equivalent concentration.

TABLE 14B-16  
RCS IODINE SPIKE ACTIVITIES

Pre-incident Concentration,  $\mu\text{Ci/g}$

Corresponding to  
21  $\mu\text{Ci/g}$  D.E. I-131

I-131	1.64E+01
I-132	6.46E+00
I-133	2.46E+01
I-134	3.60E+00
I-135	1.41E+01

Co-incident Iodine Spike Rate - Parameters, Assumptions and Model

Thyroid dose conversion factors	<u>Nuclide</u>	<u>mrem/<math>\mu\text{Ci}</math></u>
	I-131	1.08E+03
	I-132	6.44E+00
	I-133	1.80E+02
	I-134	1.07E+00
	I-135	3.13E+01

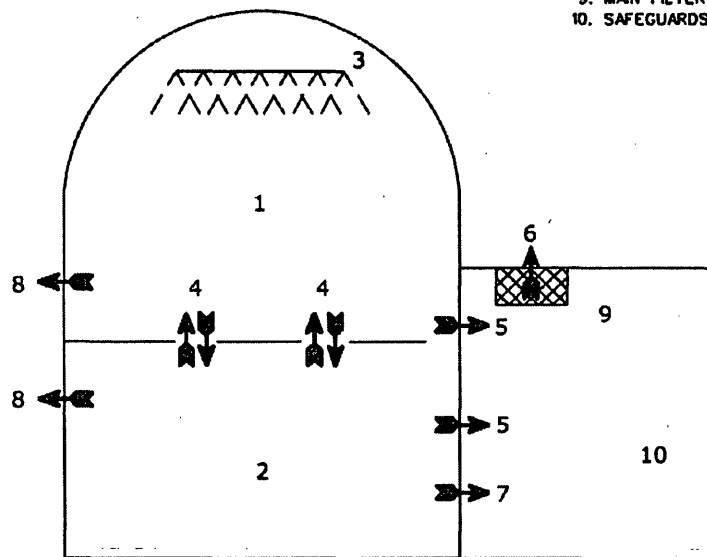
Nuclide decay constants ( $\lambda_r$ )	<u>Nuclide</u>	<u>second<sup>-1</sup></u>
	I-131	9.9783E-07
	I-132	8.3713E-05
	I-133	9.2568E-06
	I-134	2.1963E-04
	I-135	2.9129E-05

Reactor coolant system leakage (L)	Technical Specification maximum allowable value
Reactor coolant system mass (M)	Limiting value specific to the accident
Letdown purification removal (E)	1.0
Letdown purification flow rate (F)	120 gpm
RCS Equilibrium concentrations (EQ)	Table 14B-15
Formula for iodine loss constant	$\lambda_{\text{total}} = (F \cdot E / M) + (L / M) + \lambda_r$
Co-incident iodine spike release rate (RR)	$RR = EQ \cdot M \cdot \lambda_{\text{total}}$

Notes:

1. Formulas for iodine release rated from EPRI Report, "Review of Iodine Spike Data from PWR Power Plants in Relation to SGTR with MSLB, TR-103680.
2. This Table is applicable to current design basis accident analysis

1. SPRAYED REGION ( $V_s$ )
2. UNSPRAYED REGION ( $V_u$ )
3. CONTAINMENT SPRAYS
4. EXCHANGE BETWEEN REGIONS (E)
5. COLLECTED LEAKAGE
6. SLCRS RELEASE TO ENVIRONMENT, NOT CREDITED IN DBA MODEL
7. ESF LEAKAGE DURING RECIRCULATION
8. UNCOLLECTED LEAKAGE
9. MAIN FILTER BANKS
10. SAFEGUARDS AREAS



## NOTES:

- (1) FOR DBA MODEL, ALL CONTAINMENT LEAKAGE IS UNFILTERED.
- (2) WHEN RECIRCULATION SPRAYS INITIATE, CONTAINMENT IS ONLY 63% SPRAYED.
- (3) PATHWAY 7 COMMENCES AT  $t=1200$  SEC. WHEN RECIRCULATION SPRAY STARTS.

FIGURE 14B-1

LOSS OF COOLANT ACCIDENT RELEASE PATHWAYS  
 BEAVER VALLEY POWER STATION UNIT NO. 1  
 UPDATED FINAL SAFETY ANALYSIS REPORT

APPENDIX 14CHEAT TRANSFER COEFFICIENTS USED IN THE LOCTA-R2  
CORE THERMAL ANALYSIS

The heat transfer correlations used in the LOCA analyses are presented below in order of application during the accident.

## 14C.1 TIME OF BREAK UNTIL OCCURRENCE OF DNB

The time of the break until occurrence of DNB is taken conservatively to be 0.1 sec. The heat transfer regime during this period of the accident is forced convection turbulent heat transfer or fully developed nucleate boiling. The correlation for nucleate boiling is that by Jens and Lottes.<sup>(1)</sup>

$$TW - T_{sat} = \Delta T_{sat} = 1.9 * (\text{Exp}(-P/900))^* q^{**0.25} \quad (14C.1-1)$$

In the nucleate boiling regime, the wall temperature is a function of the heat flux and pressure, not coolant velocity. The Jens and Lottes correlation is independent of geometry, i.e., valid for tubes, plates, or rod bundles. It is also used for both local and bulk boiling. The correlation has been compared to subcooled water data obtained from single heated tubes having internal diameters from 0.143 inch to 0.288 inch, length from 3 inches to 24.6 inches, and pressure ranging from 500 to 2000 psia. The Dittus-Boelter correlation is used for forced convection turbulent heat transfer.

## 14C.2 FROM DNB UNTIL TIME OF UNCOVERING (STEAM COOLING PERIOD)

In the large break design calculations, DNB is assumed to occur at 0.1 sec. After DNB occurs, the mode of heat transfer is unstable with both nucleate boiling and film boiling existing for times of short duration. The heat transfer correlation used in the transition to film boiling period has been experimentally verified for post DNB heat transfer during a transient blowdown.

The initial operating conditions prior to blowdown were:

- |    |                   |                                    |
|----|-------------------|------------------------------------|
| 1. | Pressure          | 2250 psia                          |
| 2. | Mass Velocity     | 1,000,000 to 2,500,000 lb/hr-sq ft |
| 3. | Inlet Temperature | 480 to 560 F                       |
| 4. | Heat Flux         | 635,000 to 1,100,000 Btu/hr-sq ft  |

Blowdown conditions were:

- |    |                         |   |
|----|-------------------------|---|
| 1. | Initial blowdown rate   | 200 to 10,000 psi per second                |
| 2. | Average flow decay rate | 250,000 to 1,150,000 lb per hr-sq ft second |

The test section consisted of a 1/2 inch inside diameter circular tube 3 ft long. The 3 ft length is sufficient to establish fully developed flow at the exit of the test section (L/D = 72).

A total of 50 transient blowdown runs were performed. To determine the effect of flow decay, 20 runs were performed during which the flow rate was maintained as close as possible to the initial value. Thirty runs were performed in which the flow to the test section was allowed to decay in addition to the depressurization. This latter condition more nearly resembles the predicted conditions in a PWR core during the large break LOCA. For this reason the majority of the runs were performed with flow decay.

The comparison of predicted heat transfer coefficient with the measured data is shown in Figure 14C-1. It is readily apparent that the correlation is conservative with respect to the results of this test since the measured value is greater than predicted for 95 percent of the data. The degree of conservatism contained in the correlation increases with increasing values of the heat transfer coefficient.

14C.3 DURING UNCOVERING (STEAM COOLING PERIOD)

This period of the LOCA considers either turbulent or laminar forced convection to steam combined with radiation from the fuel rod surface to the steam. Radiation between fuel rods is not considered.

1. For turbulent forced convection to steam a Dittus-Boelter type equation, modified by McEligot<sup>(2)(3)</sup> to account for the variation in fluid properties near the wall due to a large temperature gradient, is used.

$$Nu = C * (Reb^{**0.8}) * (Prb^{**0.4}) * ((Tb/Tw)^{**0.5}) \tag{14C.3-1}$$

The Tb/Tw term is independent of geometry. The Dittus-Boelter type equation was developed from flow inside tubes with values of C = 0.023. Weisman<sup>(4)</sup> has shown that C is higher for rod bundle data. A value of C equal to 0.020 is presently used in the loss-of-coolant analyses. (See page 14C-6 for list of symbols.)

The McEligot correlation was compared to data with hydraulic equivalent diameter values of 0.125 inch and 0.25 inch and L/D greater than 150. Additional coolant conditions are described below.

<u>Coolant</u>	<u>Reynolds Number</u>	<u>Maximum Wall Temperature, F</u>	<u>Tw/Tb</u>
Air	1450-15000	1520	2.17
Helium	7570-13400	1050	1.56
Nitrogen	18200-45000	1620	4.78

The Prandtl number of steam is similar to those obtained with the above coolants.

2. For laminar forced convection to steam, the heat transfer correlation used is based on theoretical calculations of laminar flow in tubes made by Hausen<sup>(5)</sup> and Kays<sup>(6)</sup>:

$$\text{for } (Tw-Tb) \text{ small, } \begin{aligned} h * De / k &= 3.66 \\ h / h_{iso} &= (Tb / Tw)^{**0.25} \end{aligned}$$

These calculations indicate that the local Nusselt number is highest near the inlet

and drops until it reaches a limit corresponding to fully developed thermal conditions. For the case of constant wall temperature, the limiting Nusselt number is 3.66. For constant heat flux at the wall, the asymptote is 4.36.

Furthermore, these calculations indicate that the asymptotic values are reached for all practical purposes when  $L/D/RePr > 0.05$ . For the Reynolds numbers ranging from 100 to 1000 and a  $Pr = 1.0$  for steam, the developing length is from 2.5 inches to 25 inches.

The correlation was compared to data from laminar air flow in circular tubes where the  $L/D$  ranges from 42 to 80 and  $Re < 3000$ .

The  $[(T_b/T_w)^{0.25}]$  term is to account for variations in fluid properties near the wall due to large temperature gradients.

3. Radiation to steam is evaluated employing the empirical method of Hottel<sup>(7)</sup>.

$$h = .1713 \cdot \varepsilon \cdot [((T_w/100)^{4.0}) - ((T_{H2O}/100)^{4.0})] / (T_w - T_b) \quad (14C.3-2)$$

where:

$$\varepsilon = 1.0 / ((1.0/W) + (1.0/\alpha_{H2O}) - 1.0) \quad (14C.3-3)$$

$$\alpha_{H2O} = E_{H2O} \cdot C_{H2O} \cdot ((T_{H2O}/T_w)^{0.45}) \quad (14C.3-4)$$

The present value of the correlation factor,  $C$ , for  $\alpha_{H2O}$  at higher pressure than 0 or 1 atmosphere is 2.0.

#### 14C.4 VERIFICATION OF CORRELATIONS USED DURING STEAM COOLING PERIOD

The use of the above correlations during the steam cooling period was verified by the work performed at the University of Michigan under Westinghouse funding and direction. This was part of the Flashing Heat Transfer Program. The primary objective of this test was to determine the behavior of radiation heat transfer to steam at elevated pressure (up to 5 atm).

The heat transfer test facility consisted of an open heat transfer loop. Steam was delivered to the test section and discharged to the atmosphere through the necessary piping and control apparatus.

The test sections consisted of 1/2 inch inside diameter pipes, with an active length of three feet. The walls of the test section were heated by electrical resistance heating. Test sections having both uniform and nonuniform axial heat generation were employed.

The range of variables were representative of that in a PWR when the core is uncovered and is as follows:

Mass Velocity	$G = 4 \times 10^3$ to $4 \times 10^4$ lb/hr-sq ft
---------------	--

Temperature	$T_{in} = 300$ to $1100$ F
-------------	----------------------------



Wall Temperature	400 to 1800 F
Pressure	$P_{in} = 25$ to 75 psia
Inlet Reynolds Number	1900 to 35000

The results of the low pressure heat transfer test yield the following conclusions:

1. The McEligot et al. correlation realistically predicts the convection heat transfer coefficients in turbulent flow.
2. In turbulent flow, the radiant heat transfer contribution to the total heat transfer coefficient is adequately predicted by Hottel's technique.
3. The total heat transfer coefficient to steam in turbulent flow may be calculated by adding the convection term determined by McEligot's correlation and radiative term determined by Hottel's technique. A comparison of predicted versus measured total turbulent heat transfer coefficient is shown in Figure 14C-2 and excellent agreement can be seen.
4. In laminar flow the total heat transfer coefficient is conservatively predicted by using the correlation of Hausen and Hays for the convective contribution and the method of Hottel for the radiant contribution.
5. The prediction of laminar heat transfer coefficient can be improved by evaluating the steam properties at film conditions instead of bulk conditions.
6. The effect of a nonuniform heat flux on the heat transfer coefficient is negligible for the conditions which exist during a LOCA.

#### 14C.5 RECOVERY PHASE OF THE ACCIDENT

After entrainment has been initiated, heat transfer coefficients obtained from the FLECHT Program are used. The objective of the Pressurized Water Reactor FLECHT Program was to obtain experimental reflooding heat transfer data under simulated LOCA conditions for use in evaluating the heat transfer capabilities of the pressurized water reactor emergency core cooling system. Reference 8 summarizes the results of the Pressurized Water Reactor FLECHT Program. The test results verified the ability of a bottom flooding emergency core cooling system design to terminate the temperature increase during a LOCA. In particular, it has been shown that the effects of a variable flooding rate can be predicted, using constant flooding rate data and that complete blockage of as many as sixteen adjacent channels will not impair bottom flooding core cooling effectiveness.

NOMENCLATURESYMBOLS

- C - coefficient in Dittus-Boelter type equation
- De - equivalent diameter
- G - mass velocity
- L - length of heat source
- Nu - Nusselt number
- P - system pressure
- Pr - Prandtl number
- Re - Reynolds number
- T - temperature
- g - gravity constant
- h - heat transfer coefficient
- k - thermal conductivity
- q" - heat flux
- $\varepsilon$  - effective emissivity

SUBSCRIPTS

- b - quantities evaluated at bulk fluid temperature
- iso - evaluation of the parameter when the temperature difference ( $T_w - T_b$ ) is small
- sat - refers to saturated condition
- v - saturated vapor
- L - refers to liquid
- w - wall
- H2O - water
- in - inlet condition

References for Appendix 14C

1. W. H. Jens and P. A. Lottes, "Analyses of Heat Transfer, Burnout, Pressure Drop, and Density Data for High Pressure Water," ANL-4627, Argonne National Laboratory (1951).
2. D. M. McEligot, P. M. Magee, and G. Leppert, "Effect of Large Temperature Gradients on Convective Heat Transfer: The Downstream Region," J. of Heat Transfer, Volume 87, pp. 67-76, (1965).
3. D. M. McEligot, L. W. Ormand, and H. C. Perkins, "Internal Low Reynolds-Number Turbulent and Transitional Gas Flow with Heat Transfer", J. of Heat Transfer, Volume 88, pp. 239-245 (1965).
4. J. Weisman, "Heat Transfer to Water Flowing Parallel to Tube Bundles," Nuclear Science and Engineering, 6, p. 79, (1959).
5. H. Hausen, "Darstellung des Wärmeüberganges in Rohren durch verallgemeinerte Potenzbeziehungen," VDI Zeit., No. 4, p. 91, (1943).
6. W. M. Kays, "Numerical Solutions for Laminar-Flow heat Transfer in Circular Tubes," Trans. American Society of Mechanical Engineers, Volume 77, pp. 1265-2374, (1955).
7. H. C. Hottel, "Radiation Heat Transmission," Ch. 4 of Heat Transmission ed. W. H. McAdams, McGraw-Hill, New York (1954).
8. F. F. Cadek, et. al., "PWR FLECHT (Full Length Emergency Cooling Heat Transfer), Final Report," WCAP-7665, Westinghouse Electric Corporation (April 1971).

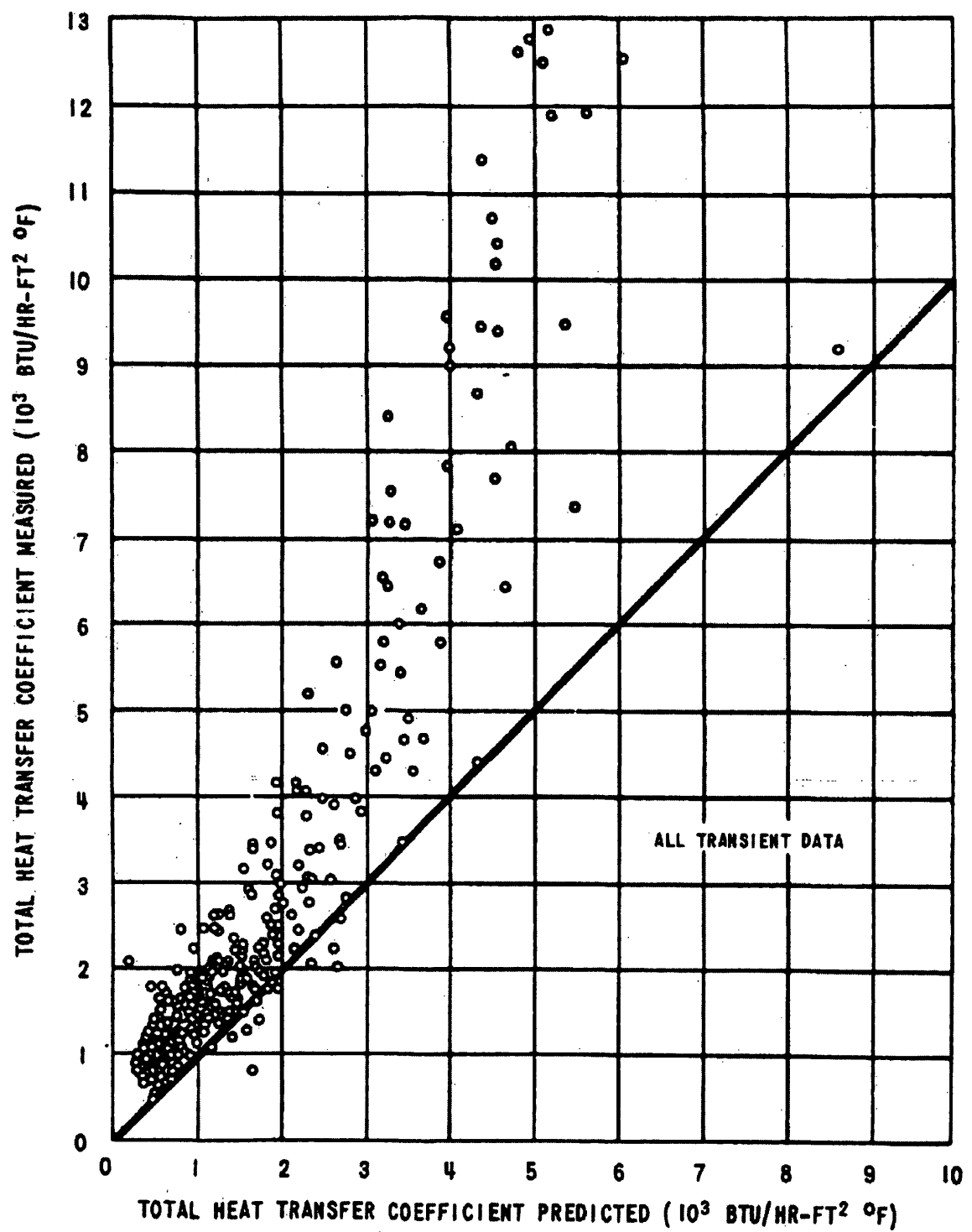


FIGURE 14C-1  
PREDICTED VERSUS MEASURED  
TOTAL HEAT TRANSFER COEFFICIENT -  
BLOWDOWN HEAT TRANSFER TEST  
BEAVER VALLEY POWER STATION UNIT NO. 1  
UPDATED FINAL SAFETY ANALYSIS REPORT

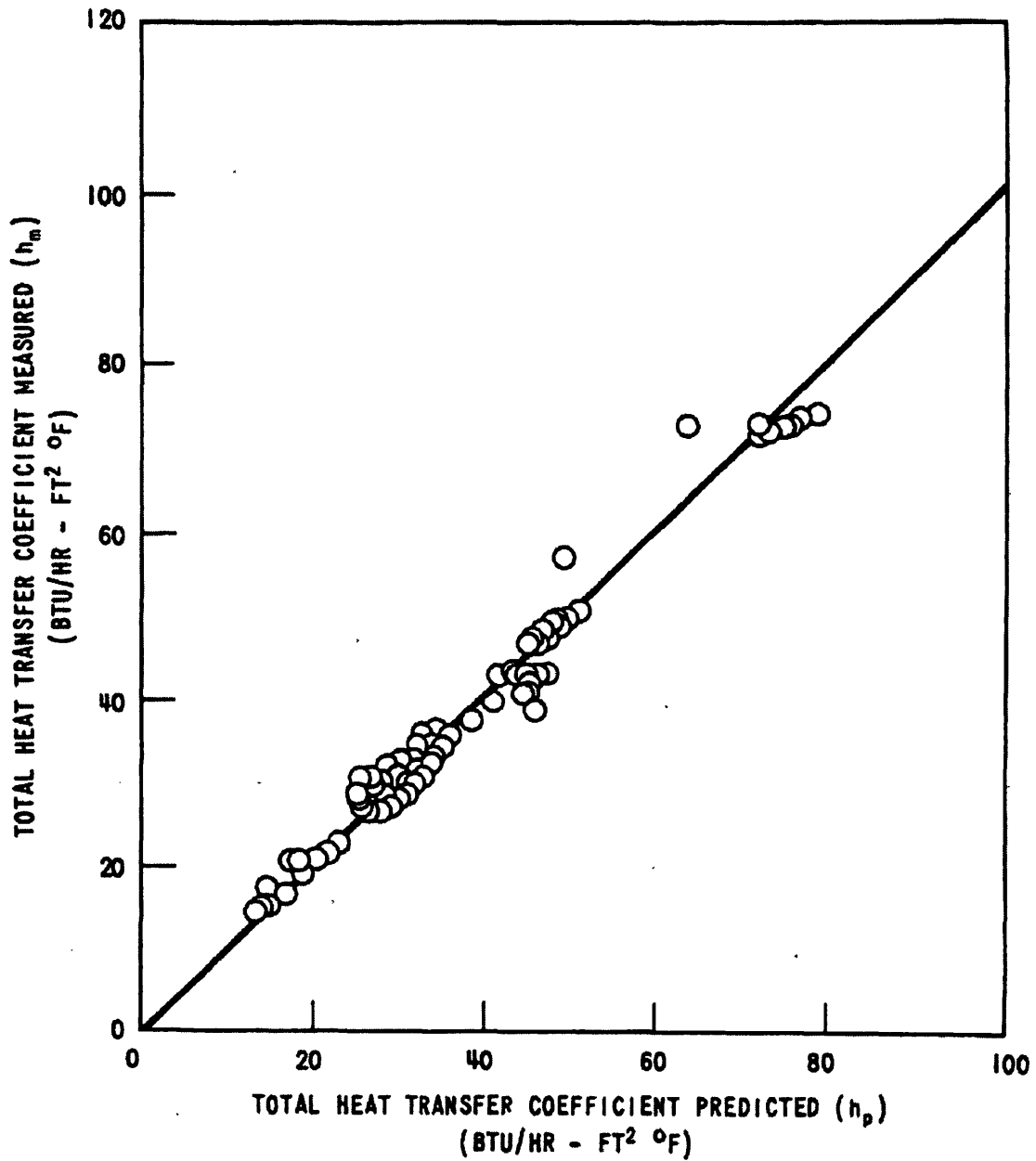


FIGURE 14C-2  
PREDICTED VERSUS MEASURED  
TOTAL HEAT TRANSFER COEFFICIENT -  
STEAM IN TURBULENT FLOW  
BEAVER VALLEY POWER STATION UNIT NO. 1  
UPDATED FINAL SAFETY ANALYSIS REPORT

APPENDIX 14DCONDITION I - NORMAL OPERATION AND OPERATIONAL TRANSIENTS

## 14D.1 DELETED

## 14D.2 OPTIMIZATION OF CONTROL SYSTEMS

A setpoint study has been performed in order to simulate performance of the reactor control and protection systems. Emphasis is placed on the development of a control system which will automatically maintain prescribed conditions in the plant even under the most conservative set of reactivity parameters with respect to both system stability and transient performance.

For each mode of plant operation, a group of optimum controller setpoints is determined. In areas where the resultant setpoints are different, compromises based on the optimum overall performance are made and verified. A consistent set of control system parameters is derived satisfying plant operational requirements throughout the core life and for power levels between 15 and 100 percent. The study comprises an analysis of the following control systems: Rod cluster control assembly control (RCCA), steam dump, steam generator level, pressurizer pressure, and pressurizer level.

## 14D.3 INITIAL POWER CONDITIONS ASSUMED IN ACCIDENT ANALYSES

14D.3.1 Power Rating

Table 14D-1 lists the Nuclear Steam Supply System thermal power output, which is the power rating values that is assumed in analyses performed in this section. This power output includes the thermal power generated by the reactor coolant pumps.

Note: The thermal power values used for each transient analyzed are given in Table 14D-2.

Where initial power operating conditions are assumed in accident analyses, the "Nuclear Steam Supply System thermal power output" plus allowance for errors in steady state power determination is assumed.

14D.3.2 Initial Conditions

For most events that are DNB limited, nominal values of initial conditions are assumed. The allowances on power, temperature and pressure are determined on a statistical basis, and are included in the limit DNBR, as described in WCAP-11397 (Reference 19). This procedure is known as the "Revised Thermal Design Procedure" (RTDP).

For accidents that are not DNB limited and for which the RTDP is not used, the initial conditions are obtained by adding the maximum steady state errors to rated values. The following steady state errors were assumed in the analyses:

- |    |                         |   |
|----|-------------------------|---|
| a. | Core Power              | $\pm 0.6$ allowance for calorimetric error                                      |
| b. | Average RCS Temperature | $\pm 4^{\circ}\text{F}$ allowance for controller deadband and measurement error |
| c. | Pressurizer Pressure    | $\pm 40$ psi allowance for steady state fluctuations and measurement error      |

Table 14D-2 summarizes initial conditions and computer codes used in the accident analyses.

The outer surface of the fuel rod at the hot spot operates at a temperature of approximately 660°F for steady state operation at rated power throughout core life due to the onset of nucleate boiling. Initially (beginning of life), this temperature is that of the cladding metal outer surface. During operation over the life of the core, the buildup of oxides and crud on the fuel rod surface causes the cladding surface temperature to increase. Allowance is made in the fuel center melt evaluation for this temperature rise. Since the thermal-hydraulic design basis limits DNB, adequate heat transfer is provided between the fuel cladding and the reactor coolant so that the core thermal output is not limited by considerations of the cladding temperature. Figure 3.4-4, shows the axial variation of average cladding temperature for a typical rod (17 x 17 fuel assembly) both at beginning and end of life. End of life is after three typical cycles of operation (approximately 20,000 effective full-power hours). These temperatures are calculated using the Westinghouse fuel rod model<sup>(1)</sup> which has been reviewed and approved by the NRC.

### 14D.3.3 Power Distribution

The transient response of the reactor system is dependent on the initial power distribution. The nuclear design of the reactor core minimizes adverse power distribution through the placement of control rods and operation instruction. The power distribution may be characterized by the radial factor  $F(\Delta H)$ , and the total peaking factor  $F(Q)$ . The peaking factor limits are given in the Technical Specifications.

For transients which may be DNB limited, the radial peaking factor is of importance. The radial peaking factor increases with decreasing power level due to rod insertion. This increase in  $F(\Delta H)$  is included in the core limits illustrated in Figure 14D-1. All transients that may be DNB limited are assumed to begin with a  $F(Q)$  consistent with the initial power level defined in the Technical Specifications.

The axial power shape used in the DNB calculation is discussed in Section 3.4.3.2.2.

For transients which may be over power limited the total peaking factor  $F(Q)$  is of importance. The value of  $F(Q)$  may increase with decreasing power level such that full power hot spot heat flux is not exceeded, i.e.  $F(Q)$  times Power = design hot spot heat flux. All transients that may be overpower limited are assumed to begin with a value of  $F(Q)$  consistent with the initial power level as defined in the Technical Specifications.

The value of peak kW/ft can be directly related to fuel temperature as illustrated on Figures 3.4-1 and 3.4-2. For transients which are slow with respect to the fuel rod thermal time constant the fuel temperatures are illustrated on Figures 3.4-1 and 3.4-2. For transients which are fast with respect to the fuel rod thermal time constant, for example, rod ejection, a detailed heat transfer calculation is made.

#### 14D.4 TRIP POINTS AND TIME DELAYS TO TRIP ASSUMED IN ACCIDENT ANALYSES

A reactor trip signal acts to open two trip breakers connected in series feeding power to the control rod drive mechanisms. The loss of power to the mechanism coils causes the mechanisms to release the RCCA which then fall by gravity into the core. There are various instrumentation delays associated with each trip function, including delays in signal actuation, in opening the trip breakers, and in the release of the rods by the mechanisms. The total delay to trip is defined as the time delay from the time that trip conditions are reached to the time the rods are free and begin to fall. Limiting trip setpoints assumed in accident analyses and the time delay assumed for each trip function are given in Table 14D-3. Reference is made in that table to the overtemperature and overpower  $\Delta T$  trip shown in Figure 14D-1.

The difference between the limiting trip point assumed for the analysis and the nominal trip point represents an allowance for instrumentation channel error and setpoint error. During preliminary startup tests, it was demonstrated that actual instrument errors and time delays are equal to or less than the assumed values.

#### 14D.5 DELETED

#### 14D.6 ROD CLUSTER CONTROL ASSEMBLY INSERTION CHARACTERISTIC

The negative reactivity insertion following a reactor trip is a function of the acceleration of the RCCA, and the variation in rod worth as a function of rod position. With respect to accident analyses, the critical parameter is the time of insertion up to the dashpot entry or approximately 85 percent of the rod cluster travel. For accident analyses and evaluations it is conservatively assumed that the insertion time to dashpot entry is 2.7 seconds. The RCCA position versus time assumed in accident analyses is shown in Figure 14D-2.

Figure 14D-3 shows the fraction of total negative reactivity insertion for a core where the axial distribution is skewed to the lower region of the core. An axial distribution which is skewed to the lower region of the core can arise from a xenon oscillation or can be considered as representing a transient axial distribution which would exist after the RCCA bank had already traveled some distance after trip. This curve is used in the analyses and evaluations of the transients which utilize point kinetics core models.

There is inherent conservatism in the use of this curve in that it is based on a skewed distribution which would exist relatively infrequently. For cases other than those associated with xenon oscillations significant negative reactivity would have been inserted due to the more favorable axial distribution existing prior to trip.

The normalized RCCA negative reactivity insertion versus time is shown in Figure 14D-4. The curves shown in this figure were obtained from Figures 14D-2 and 14D-3.



## 14D.7 REACTIVITY COEFFICIENTS

The transient response of the reactor system is dependent on reactivity feedback effects, in particular the moderator temperature coefficient and the Doppler power coefficient. These reactivity coefficients and their values are discussed in detail in Section 3.3.

In the analysis of certain events, conservatism requires the use of large reactivity coefficient values, whereas, in the analysis of other events, conservatism requires the use of small reactivity coefficient values. Some analyses, such as loss of reactor coolant from cracks or ruptures in the RCS, do not depend on reactivity feedback effects. The values used are given in Table 14D-2. Reference is made in that table to Figure 14D-5 which shows the upper and lower Doppler power coefficients as a function of power used in the transient analysis. The justification for use of conservatively large versus small reactivity coefficient values are treated on an event by event basis.

Condition II Events	<u>Section</u>
1. Uncontrolled RCCA Bank Withdrawal from a Subcritical Condition	14.1.1
2. Uncontrolled RCCA Bank Withdrawal at Power	14.1.2
3. RCCA Misalignment	14.1.3
4. Uncontrolled Boron Dilution	14.1.4
5. Partial Loss of Forced Reactor Coolant Flow	14.1.5
6. Loss of External Electrical Load and/or Turbine Trip	14.1.7
7. Loss of Normal Feedwater	14.1.8
8. Loss of All Offsite Power to the Station Auxiliaries	14.1.11
9. Excessive Heat Removal due to Feedwater System Malfunctions	14.1.9
10. Excessive Load Increase Incident	14.1.10
11. Accidental Depressurization of the RCS	14.1.15
12. Accidental Depressurization of Main Steam System	14.1.13
13. Spurious Operation of the Safety Injection System at Power	14.1.16

Condition III Events

- |    |  |         |
|----|--|---------|
| 1. | Complete Loss of Forced Reactor Coolant Flow | 14.2.9  |
| 2. | Single RCCA Withdrawal Full Power            | 14.2.10 |

Condition IV Events

- |    |  |        |
|----|--|--------|
| 1. | Major Secondary System Pipe Break                              | 14.2.5 |
| 2. | Single Reactor Coolant Pump Locked Rotor                       | 14.2.7 |
| 3. | Rupture of a Control Rod Drive Mechanism Housing RCCA Ejection | 14.2.6 |
| 4. | SGTR   | 14.2.4 |

14D.8 FISSION PRODUCT INVENTORIES

The activities in the core are presented in Appendix 14B, Section 14B.1.

Appendix 14B also presents the bases for their calculation in the following Sections:

1. Fuel Rod Gap for Non-LOCA Events (Section 14B.2)
2. Fuel Handling Sources (Section 14B.3)
3. Reactor Coolant Fission Product Activities (Section 14B.4)
4. Tritium Production in a Light Water Reactor (Section 14B.5)
5. Waste Gas System Decay Tank Rupture Activity Release (Section 14B.6)
6. Waste Gas System Line Rupture Activity Release (Section 14B.7)

14D.9 RESIDUAL DECAY HEAT

Residual heat in a subcritical core consists of:

1. Fission product decay energy
2. Decay of neutron capture products
3. Residual fissions due to the effect of delayed neutrons.

These constituents are discussed separately in the following paragraphs.

.14D.9.1 Fission Product Decay

For short times (<10<sup>3</sup> seconds) after shutdown, data on yields of short half-life isotopes is sparse. Very little experimental data is available for the gamma-ray contributions and even less for the beta-ray contribution. Several authors have compiled the available data into a conservative estimate of fission product decay energy for short times after shutdown, notably Shure<sup>(2)</sup> and Dudziak<sup>(3)</sup>, and Teage<sup>(4)</sup>. Of these three selections, Shure's curve is the highest and it is based on the data of Stehn and Clancy<sup>(5)</sup> and Obenshain and Foderaro<sup>(6)</sup>.

The fission product contribution to decay heat which has been assumed in the accident analyses is the curve of Shure increased by 20 percent for conservatism. This curve with the 20 percent factor included is shown in Figure 14D-6.

14D.9.2 Decay of U-238 Capture Products

Betas and gammas from the decay of U-239 (23.5 minute half-life) and Np-239 (2.35 day half-life) contribute significantly to the heat generation after shutdown. The cross section for production of these isotopes and their decay schemes are relatively well known. For long irradiation times their contribution can be written as:

$$P_1 / P_0 = \frac{E_{\gamma 1} + E_{\beta 1}}{200 \text{ Mev}} c (1+a) e^{-\lambda_1 t} \text{ watts/watt} \tag{14D.9-1}$$

$$P_2 / P_0 = \frac{E_{\gamma 2} + E_{\beta 2}}{200 \text{ Mev}} c (1+a) \left[ \frac{\lambda_2}{\lambda_1 - \lambda_2} (e^{-\lambda_2 t} - e^{-\lambda_1 t}) + e^{-\lambda_2 t} \right] \text{watts/watt} \tag{14D.9-2}$$

- where:
- $P_1/P_0$  = the energy from U-239 decay
  - $P_2/P_0$  = the energy from NP-239 decay
  - $t$  = the time after shutdown (seconds)
  - $c(1+\alpha)$  = the ratio of U-238 captures to total fissions = 0.6 (1 + 0.2)
  - $\lambda_1$  = the decay constant of U-239 = 4.91 x 10<sup>-4</sup> seconds<sup>-1</sup>
  - $\lambda_2$  = the decay constant of Np-239 decay = 3.41 x 10<sup>-6</sup> per seconds
  - $E_{\gamma 1}$  = total  $\gamma$ -ray energy from U-239 decay = .06 Mev
  - $E_{\gamma 2}$  = total  $\gamma$ -ray energy from Np-239 decay = 0.30 Mev
  - $E_{\beta 1}$  = total  $\beta$ -ray energy from U-239 decay = 1/3 x 1.18 Mev

$$E_{\beta_2} = \text{total } \beta\text{-ray energy from } N_p\text{-239 decay} = 1/3 \times 0.43 \text{ Mev (Two-thirds of the potential } \beta\text{-energy is assumed to escape by the accompanying neutrinos.)}$$

This expression with a margin of 10 percent is shown in Figure 14D-6. The 10 percent margin, compared to 20 percent for fission product decay, is justified by the availability of the basic data required for this analysis. The decay of other isotopes, produced by neutron reactions other than fission, is neglected.

#### 14D.9.3 Residual Fissions

The time dependence of residual fission power after shutdown depends on core properties throughout a transient under consideration. Core average conditions are more conservative for the calculation of reactivity and power level than actual local conditions as they would exist in hot areas of the core. Thus, unless otherwise stated in the text, static power shapes have been assumed in the analyses and these are factored by the time behavior of core average fission power calculated by a point model kinetics calculation with six delayed neutron groups.

For the purpose of illustration only a one delayed neutron group calculation, with a constant shutdown reactivity of -4 percent  $\Delta k$ , is shown in Figure 14D-6.

#### 14D.9.4 Distribution of Decay Heat Following Loss of Coolant Accident

During a loss-of-coolant accident the core is rapidly shut down by void formation or RCCA insertion, or both, and a large fraction of the heat generation to be considered comes from fission product decay gamma rays. This heat is not distributed in the same manner as steady state fission power. Local peaking effects which are important for the neutron dependent part of the heat generation do not apply to the gamma ray contribution. The steady state factor of 97.4 percent which represents the fraction of heat generated within the clad and pellet drops to 95 percent for the hot rod in a loss of coolant accident.

For example, consider the transient resulting from the postulated double ended break of the largest RCS pipe; 1/2 second after the rupture about 30 percent of the heat generated in the fuel rods is from gamma-ray absorption. The gamma power shape is less peaked than the steady state fission power shape, reducing the energy deposited in the hot rod at the expense of adjacent colder rods. A conservative estimate of this effect is a reduction of 10 percent of the gamma-ray contribution or 3 percent of the total. Since the water density is considerably reduced at this time, an average of 98 percent of the available heat is deposited in the fuel rods, the remaining 2 percent being absorbed by water, thimbles, sleeves, and grids. The net effect is a factor of 0.95 rather than 0.974, to be applied to the heat production in the hot rod.

#### 14D.10 COMPUTER CODES UTILIZED

Summaries of some of the principal computer codes used in transient analyses are given below. Other codes, in particular, very specialized codes in which the modeling has been developed to simulate one given accident, such as the SATAN VI Code<sup>(16)</sup> as in the analysis of the RCS pipe rupture, and which consequently have a direct bearing on the analysis of the accident itself, are summarized in their respective accident analyses sections. The codes used in the analyses of each transient have been listed in Table 14D-2.

#### 14D.10.1 FACTRAN

The FACTRAN Code<sup>(7)</sup> calculates the transient temperature distribution in a cross section of a metal clad  $\text{UO}_2$  fuel rod and the transient heat flux at the surface of the clad using as input the nuclear power and the time-dependent coolant parameters (pressure, flow, temperature, density). The code uses a fuel model which exhibits the following features simultaneously:

1. A sufficiently large number of radial space increments to handle fast transients such as rod ejection accidents.
2. Material properties which are functions of temperature and a sophisticated fuel-to-clad gap heat transfer calculation.
3. The necessary calculations to handle post-DNB transients: film boiling heat transfer correlations, Zircaloy-water reaction and partial melting of the materials.

The gap heat transfer coefficient is calculated according to an elastic pellet model (refer to Figure 14D-7). The thermal expansion of the pellet is calculated as the sum of the radial (one-dimensional) expansions of the rings. Each ring is assumed to expand freely. The cladding diameter is calculated based on thermal expansion and internal and external pressures.

If the outside radius of the expanded pellet is smaller than the inside radius of the expanded clad, there is no fuel-clad contact and the gap conductance is calculated on the basis of the thermal conductivity of the gas contained in the gap. If the pellet outside radius so calculated is larger than the clad inside radius (negative gap), the pellet and the clad are pictured as exerting upon each other a pressure sufficiently important to reduce the gap to zero by elastic deformation of both. This contact pressure determines the gap heat transfer coefficient. FACTRAN is further discussed in Reference 7.

14D.10.2 LOCTA IV is described in Section 14.3.1

14D.10.3 NOTRUMP is described in Section 14.3.1

14D.10.4 LOFTRAN

The LOFTRAN program<sup>(10)</sup> is used for studies of transient response of a pressurized water reactor system to specified perturbations in process parameters. LOFTRAN simulates a multi-loop system by a lumped parameter single loop model containing reactor vessel, hot and cold leg piping, steam generator (tube and shell sides) and the pressurizer. The pressurizer heaters, spray, relief and safety valves are also considered in the program. Point model neutron kinetics, and reactivity effects of the moderator, fuel, boron and rods are included. The secondary side of the steam generator utilizes a homogeneous, saturated mixture for the thermal transients and a water level correlation for indication and control. The reactor protection system is simulated to include reactor trips on neutron flux, overpower and overtemperature reactor coolant  $\Delta T$ , high and low pressure, low flow, and high pressurizer level. Control systems are also simulated including rod control, steam dump, feedwater control, and pressurizer pressure control. The safety injection system including the accumulators are also modeled.

LOFTRAN is a versatile program which is suited to both accident evaluation and control studies as well as parameter sizing. LOFTRAN also has the capability of calculating the transient value of DNB ratio based on the input from the core limits illustrated on Figure 14D-1. The core limits represent the minimum value of DNBR as calculated for typical or Thimble cell.

LOFTRAN is further discussed in Reference 10.

#### 14D.10.5 LEOPARD

The LEOPARD computer program<sup>(11)</sup> determines fast and thermal spectra, using only basic geometry and temperature data. The code optionally computes fuel depletion effects for a dimensionless reactor and recomputes the spectra before each discrete burnup step.

LEOPARD is further described in Reference 11.

#### 14D.10.6 TURTLE

TURTLE<sup>(12)</sup> is a two-group, two-dimensional neutron diffusion code featuring a direct treatment of the nonlinear effects of xenon, enthalpy, and Doppler. Fuel depletion is allowed.

TURTLE was written for the study of azimuthal xenon oscillations, but the code is useful for general analysis. The input is simple, fuel management is handled directly, and a boron criticality search is allowed.

TURTLE is further described in Reference 12.

##### 14D.10.6.1 Advanced Nodal Code (ANC)

ANC is a two-group, multi-dimensional nodal diffusion theory code. ANC can be used for all nuclear core design calculations, including critical boron concentrations, control rod worths, and reactivity coefficients.

ANC is further described in Reference 17.

##### 14D.10.6.2 PHOENIX-P

PHOENIX-P is a two-dimensional multigroup transport theory code used to calculate lattice physics parameters for pressurized water reactors. This code generates cross section and feedback parameters that are consistent with dimensional code requirements.

PHOENIX-P is further described in Reference 18.

##### 14D.10.6.3 NEXUS/PARAGON

PARAGON is a two-dimensional multigroup transport theory code used to calculate lattice physics parameters for pressurized water reactors. NEXUS is a cross section processing code which represents cross section and feedback parameters in terms of fitting equations. These codes generate cross section and feedback parameters that are consistent with dimensional code requirements. NEXUS and PARAGON are further described in References 21 and 22.

14D.10.7 TWINKLE

The TWINKLE program<sup>(13)</sup> is a multi-dimensional spatial neutron kinetics code, which was patterned after steady-state codes presently used for reactor core design. The code uses an implicit finite-difference method to solve the two-group transient neutron diffusion equations in one, two and three dimensions. The code uses six delayed neutron groups and contains a detailed multi-region fuel-clad-coolant heat transfer model for calculating pointwise doppler and moderator feedback effects. The code handles up to 2000 spatial points, and performs its own steady state initialization. Aside from basic cross-section data and thermal-hydraulic parameters, the code accepts as input basic driving functions such as inlet temperature, pressure, flow, boron concentration, control rod motion, and others. Various edits provide channelwise power, axial offset, enthalpy, volumetric surge pointwise power, fuel temperatures, and so on.

The TWINKLE code is used to predict the kinetic behavior of a reactor for transients which cause a major perturbation in the spatial neutron flux distribution.

TWINKLE is further described in Reference 13.

14D.10.8 W-COBRA-TRAC is described in Section 14.3.2

14D.10.9 DELETED

14D.10.10 VIPRE

The VIPRE code is described in Section 3.4.3.1, and in Reference 20.

References to Appendix 14D

1. Supplemental information on fuel design transmitted from R. Salvatori, Westinghouse, to D. Knuth, Atomic Energy Commission, as attachments to letters NS-SL-518 (12/22/72), NS-SL-521 (1/4/73), NS-SL-524 (1/4/73) and NS-SL-543 (1/12/73), (Westinghouse Proprietary); and supplemental information on fuel design transmitted from R. Salvatori, to D. Knuth, as attachments to letters NS-SL-527 (1/2/73) and NS-SL-544 (1/12/73).
2. K. Shure, "Fission Product Decay Energy" WAPD-BT-24, pp. 1-17, Westinghouse Bettis Atomic Power Laboratory (December 1961).
3. K. Shure and D. J. Dudziak, "Calculating Energy Released by Fission Products," Trans. American Nuclear Society, 4 (1) p. 30 (1961).
4. Teake, United Kingdom Atomic Energy Authority Decay Heat Standard. (Private Communication)
5. J. R. Stehn and E. F. Clancy, "Fission-Product Radioactivity and Heat Generation" in "Proceedings of the Second United Nations International Conference on the Peaceful Uses of Atomic Energy, Geneva, 1958," Volume 13, pp. 49-54, United Nations, Geneva, (1958).
6. F. E. Obenshain and A. H. Foderaro, "Energy from Fission Product Decay," WAPD-P-652, Westinghouse Bettis Atomic Power Laboratory (1955).
7. H. G. Hargrove, "FACTRAN - A FORTRAN IV Code for Thermal Transients in a UO<sub>2</sub> Fuel Rod," WCAP-7908-A, Westinghouse Electric Corporation (December 1989).
8. Deleted By Revision 8.
9. Deleted By Revision 23.
10. T. W. T. Burnett, C. J. McIntyre, J. C. Baker, R. P. Rose, "LOFTRAN Code Description," WCAP-7907-P-A, Westinghouse Electric Corporation (April 1984).
11. R. F. Barry, "LEOPARD, a Spectrum Dependent Non-Spatial Depletion Code for the IBM-7094," WCAP-3269-26, Westinghouse Electric Corporation (September 1963).
12. R. F. Barry and S. Altomare, "The TURTLE 24.0 Diffusion Depletion Code": WCAP-7213,(Westinghouse Proprietary) (June 1968); WCAP-7758 (September 1971).
13. D. H. Risher, Jr., R. F. Barry, "TWINKLE - A Multi-Dimensional Neutron Kinetics Computer Code," WCAP-7979-P-A, Westinghouse Electric Corporation (January 1975).
14. Deleted by Revision 8.
15. Deleted by Revision 8.



References to Appendix 14D (CONT'D)

16. F. M. Bordelon, et. al., "SATAN-VI Program: Comprehensive Space-Time Dependent Analysis of Loss-of-Coolant", WCAP-8306, Westinghouse Electric Corporation (June 1974).
17. Liu, Y. S., et. al., "ANC: A Westinghouse Advanced Nodal Computer Code," WCAP-10965-P-A, September 1986.
18. Nguyen, T. Q., et. al., "Qualification of the PHOENIX-P/ANC Nuclear Design System for Pressurized Water Reactor Cores," WCAP-11596-P-A, June 1988.
19. Friedland, A. J. and Ray, S., Revised Thermal Design Procedure," WCAP-11397-P-A (Proprietary) and WCAP-11398-A (non-Proprietary), April 1984.
20. Sung, Y. X., et. al., "VIPRE-01 Modeling and Qualification for Pressurized Water Reactor non-LOCA Thermal-Hydraulic Safety Analysis," WCAP-14565-P-A (Proprietary) and WCAP-15306-NP-A (non-Proprietary), October 1999.
21. Ouisloumen, M. et al., "Qualification of the Two-Dimensional Transport Code PARAGON," WCAP-16045-P-A, Westinghouse, 2004.
22. Zhang, B. et al., "Qualification of the NEXUS Nuclear Data Methodology," WCAP-16045-P-A, Addendum 1, Westinghouse 2005.

BVPS UFSAR UNIT 1

TABLES FOR APPENDIX 14D

Table 14D-1

NUCLEAR STEAM SUPPLY SYSTEM POWER RATINGS USED IN ANALYSIS		
Nuclear Steam Supply System thermal power output	2910 MWt	
Thermal power generated by the reactor coolant pumps	10 MWt	
Rated core thermal power output	2900 MWt	

Table 14D-2

SUMMARY OF INITIAL CONDITIONS AND COMPUTER CODES USED

<u>Faults</u>	<u>Computer Codes Utilized</u>	REACTIVITY COEFFICIENTS ASSUMED		<u>Doppler<sup>(2)</sup></u>	<u>Initial Core Thermal Power (MWt)</u>
		<u>Moderator<sup>(1)</sup> Temperature (pcm/°F)</u>	<u>Moderator<sup>(1)</sup> Density (<math>\Delta</math>k/gm/cc)</u>		
CONDITION II					
Uncontrolled RCC Assembly Bank Withdrawal from a Subcritical Condition	TWINKLE, FACTRAN VIPRE	+5	---	See Section 14.1.1.2	0
Uncontrolled RCC Assembly Bank Withdrawal at Power	LOFTRAN	+5	0.43	Lower and Upper	2910 <sup>(4)</sup>
RCC Assembly Misalignment	VIPRE, ANC LOFTRAN	---	0	Upper	2900 <sup>(7)</sup>
Uncontrolled Boron Dilution	NA	NA	NA	NA	NA
Partial Loss of Forced Reactor Coolant Flow	LOFTRAN VIPRE, FACTRAN	---	0	Upper	2910 <sup>(4)</sup>
Loss of External Electrical Load and/or Turbine Trip: Pressure case DNB case	LOFTRAN	---	0 <sup>(3)</sup>	Lower	2927.5 <sup>(5)</sup> 2910 <sup>(4)</sup>
Loss of Normal Feedwater	LOFTRAN	---	0 <sup>(3)</sup>	Upper	2927.5 <sup>(5)</sup>
Loss of Offsite Power to the Plant Auxiliaries	LOFTRAN	---	0 <sup>(3)</sup>	Upper	2927.5 <sup>(5)</sup>
Excessive Heat Removal Due to Feedwater System Malfunctions	LOFTRAN	---	0.43, and function of Moderator Density and Boron Concentration <sup>(8)</sup>	Lower and Note 8	0 and 2910 <sup>(4)</sup>

Table 14D-2 (CONT'D)

SUMMARY OF INITIAL CONDITIONS AND COMPUTER CODES USED

REACTIVITY COEFFICIENTS  
ASSUMED

<u>Faults</u>	<u>Computer Codes Utilized</u>	<u>Moderator<sup>(1)</sup> Temperature (pcm/°F)</u>	<u>Moderator<sup>(1)</sup> Density (<math>\Delta k/gm/cc</math>)</u>	<u>Doppler<sup>(2)</sup></u>	<u>Initial Core Thermal Power (MWT)</u>
Excessive Load Increase	LOFTRAN	---	---	---	2910 <sup>(4)</sup>
Accidental Depressurization of the Reactor Coolant System	LOFTRAN	+5	0	Lower	2910 <sup>(4)</sup>
Accidental Depressurization of the Main Steam System	LOFTRAN	---	Function of Moderator Density and Boron Concentration	(Note 8)	0 (Subcritical)
Inadvertent Operation of ECCS During Power Operation (PSV Operability Case)	LOFTRAN	---	0.43	Upper	2927.5 <sup>(5)</sup>
CONDITION III					
Loss of Reactor Coolant from Small Pipe Breaks or from Cracks in Large Pipe which Actuate Emergency Core Cooling	NOTRUMP LOCTA-IV	---	Function of Moderator Density	Function of Fuel Temperature	2705 <sup>(Note 3)</sup>
Inadvertent Loading of a Fuel Assembly into an Improper Position	LEOPARD, TURTLE	---	NA	NA	2705 <sup>(Note 3)</sup>
Complete Loss of Forced Reactor Coolant Flow	LOFTRAN VIPRE, FACTRAN	---	0	Upper	2910 <sup>(4)</sup>

Table 14D-2 (CONT'D)

SUMMARY OF INITIAL CONDITIONS AND COMPUTER CODES USED

Faults	Computer Codes Utilized	REACTIVITY COEFFICIENTS ASSUMED			Initial Core Thermal Power (MWT)
		Moderator <sup>(1)</sup> Temperature (pcm/°F)	Moderator <sup>(1)</sup> Density ( $\Delta k/gm/cc$ )	Doppler <sup>(2)</sup>	
Single RCC Assembly Withdrawal Full Power	ANC, THINC PHOENIX or NEXUS/PARAGON	---	NA	NA	2927.5
CONDITION IV					
Major break of pipes containing reactor coolant up to and including double-ended break of the largest pipe in the Reactor Coolant System (Loss of Coolant Accident)	WCOBRA-TRAC	Function of Moderator Density	---	Function of Fuel Temp. See Technical Specifications	2917.4 <sup>(6)</sup>
Major secondary system pipe break up to and including double-ended break (Rupture of a Steam Pipe)	LOFTRAN, VIPRE	---	Function of Moderator Density and Boron Concentration <sup>(8)</sup>	(Note 8)	0 (Subcritical)
Major break of a Main Feedwater Pipe	LOFTRAN	+5	0.43	Upper and Lower	
Single Reactor Coolant Pump Locked Rotor Pressure case DNB case	LOFTRAN FACTRAN, VIPRE	---	0 <sup>(3)</sup>	Upper	2917.4 <sup>(6)</sup> 2910 <sup>(4)</sup>
Rupture of a Control Rod Mechanism Housing (RCCA Ejection)	TWINKLE, FACTRAN	See Section 14.2.6.2.1	---	See Section 14.2.6.2.1	0 and 2917.4 <sup>(6)</sup>

- NOTES: (1) Only one is used in an analysis, i.e. either moderator temperature or moderator density coefficient.  
 (2) Reference Figure 14D-5.  
 (3) Analyses at hot full power with a zero MTC bound analyses at part power with a positive MTC  
 (4) Nominal NSSS Power (2910 MWt)  
 (5) 100.6% of Nominal NSSS Power (1.006 x 2910)

Table 14D-2 (CONT'D)

SUMMARY OF INITIAL CONDITIONS AND COMPUTER CODES USED

REACTIVITY COEFFICIENTS  
ASSUMED

NOTES: (Continued)

- (6) 100.6% of Nominal Core Power (1.006 x 2900)
- (7) Nominal Core Power (2900 MWt)
- (8) The reactivity model that results from the moderator density and Doppler coefficients is validated for each reload
- (9) 104.5% of nominal core power (1.045 x 2900)

Table 14D-3

## TRIP POINTS AND TIME DELAYS TO TRIP ASSUMED IN ACCIDENT ANALYSES

<u>Trip Function</u>	<u>Limiting Trip Point Assumed In Analyses</u>	<u>Time Delay (seconds)</u>
Power Range High Neutron Flux, High Setting	116%	0.5
Power Range High Neutron Flux, Low Setting	35%	0.5
Overtemperature $\Delta T$	Variable (See Technical Specifications)	2.0 <sup>(1)</sup>
Overpower $\Delta T$	Not Applicable (See Technical Specifications)	2.0 <sup>(1)</sup>
High pressurizer pressure	2,420 psig <sup>(2)</sup>	2.0
Low pressurizer pressure	1,920 psig <sup>(3)</sup>	2.0
Low reactor coolant flow (from loop flow detectors)	87% loop flow	1.0
Undervoltage Trip	75% nominal <sup>(4)</sup>	1.2 <sup>(4)</sup>
Turbine Trip	Not applicable	1.0
Low-Low steam generator level	0% of narrow range level span	2.0
High steam generator level trip of the feedwater pumps and closure of feedwater system valves, and turbine trip	100% of narrow range level span <sup>(5)</sup>	2.0



Table 14D-3 (CONT'D)

## TRIP POINTS AND TIME DELAYS TO TRIP ASSUMED IN ACCIDENT ANALYSES

- (1) The time delay given includes only channel electronics, trip logic and gripper release. Additional delays in the trip are a six second RTD response, a two second filter on the vessel Tavg signal, and a six second filter on the vessel  $\Delta T$  signal.
- (2) 2420 psig (2435 psia) is the limiting High Pressurizer Pressure reactor trip setpoint assumed in the accident analyses. Thus, 2420 psig is the Safety Analysis Setpoint Limit (SAL), and is supported by the Technical Specification setpoint of 2385 psig.
- (3) 1920 psig (1935 psia) is the limiting Low Pressurizer Pressure reactor trip setpoint assumed in the accident analyses. Thus, 1920 psig is the Safety Analysis Setpoint Limit (SAL), and is supported by the Technical Specification setpoint of 1945 psig.
- (4) This trip function is not explicitly modeled in the Loss Of Flow analyses. The Low Reactor Coolant Flow Trip provides protection for all of the Loss Of Flow events. The Undervoltage Trip acts only as a backup trip.

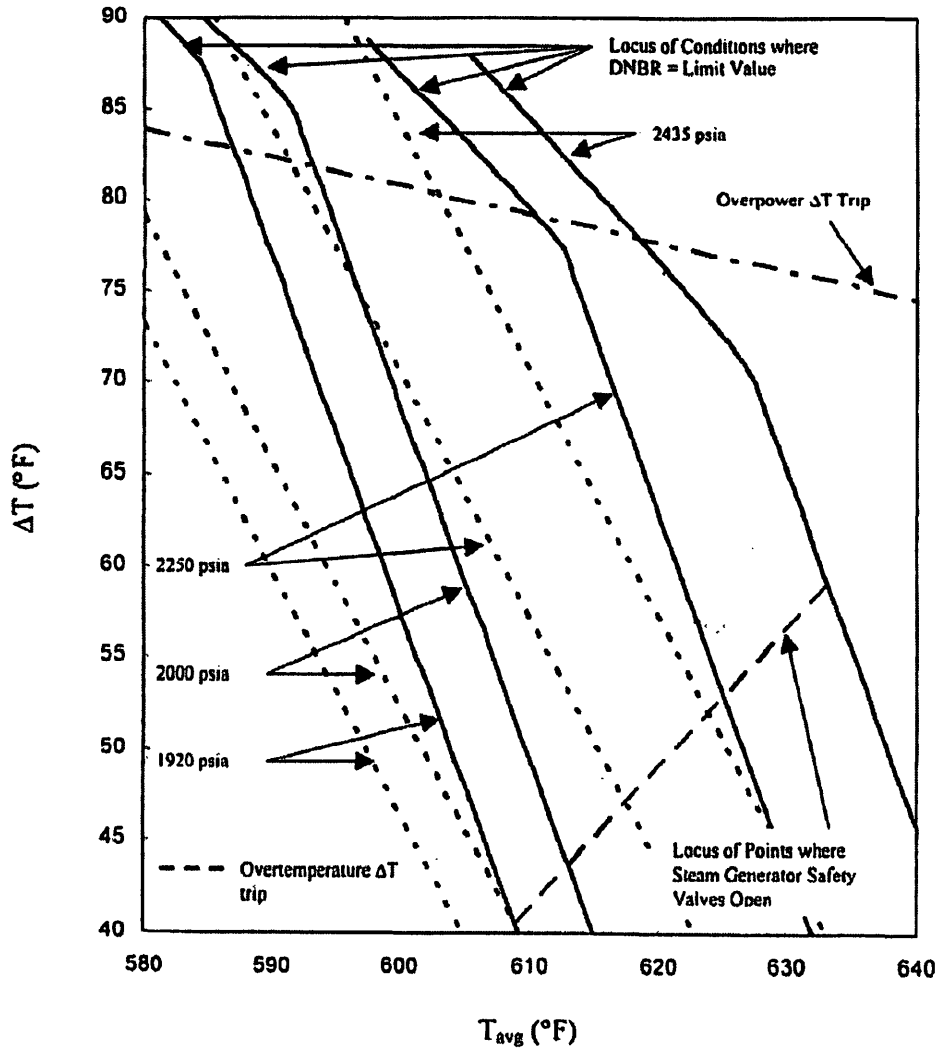


FIGURE 14D-1

ILLUSTRATION OF OVERTEMPERATURE  
AND OVERPOWER DELTA-T PROTECTION

BEAVER VALLEY POWER STATION UNIT NO. 1  
UPDATED FINAL SAFETY ANALYSIS REPORT

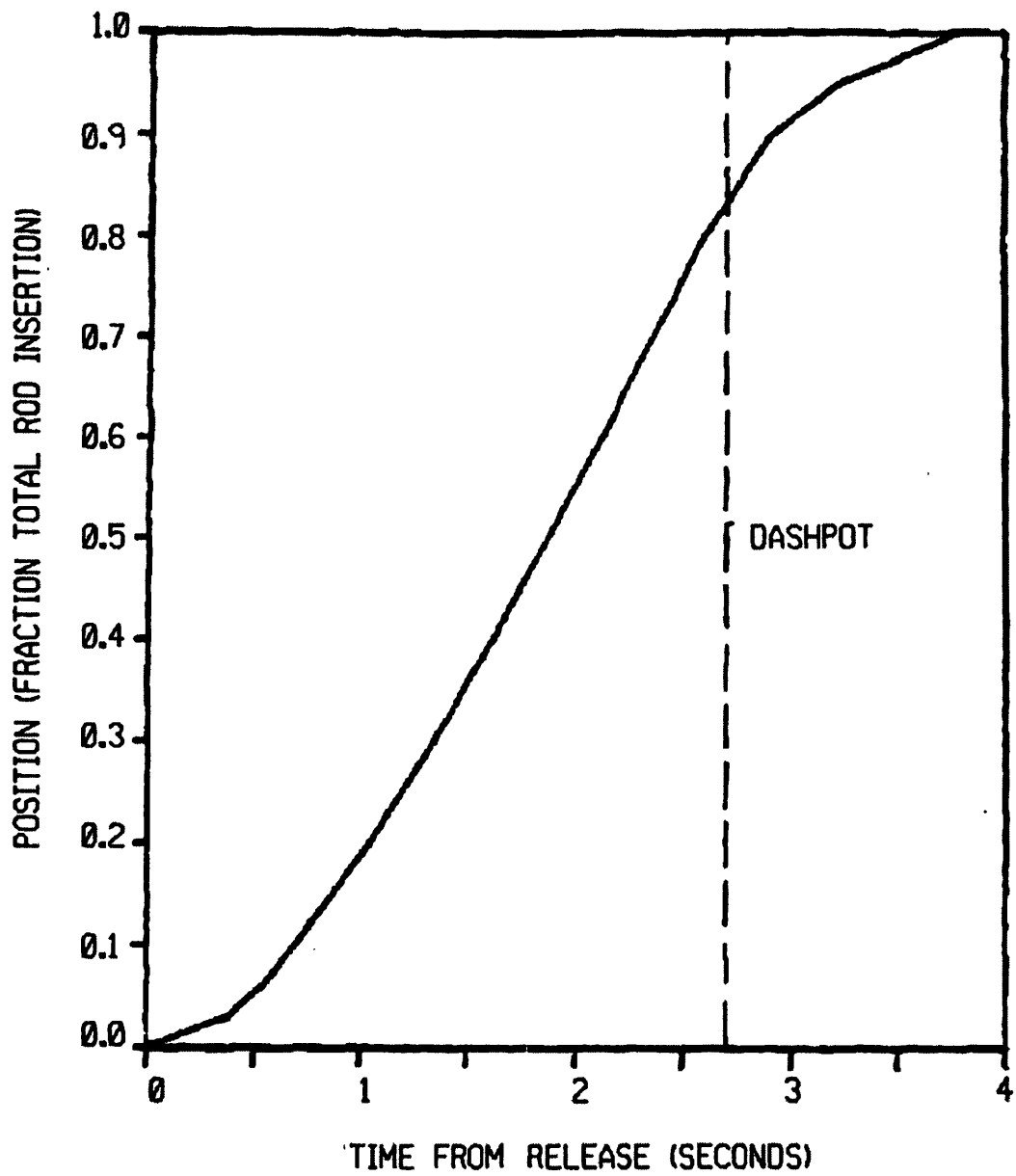


FIGURE 14D-2

NEGATIVE REACTIVITY INSERTION VS  
TIME ON REACTOR TRIP

BEAVER VALLEY POWER STATION UNIT 1  
UPDATED FINAL SAFETY ANALYSIS REPORT

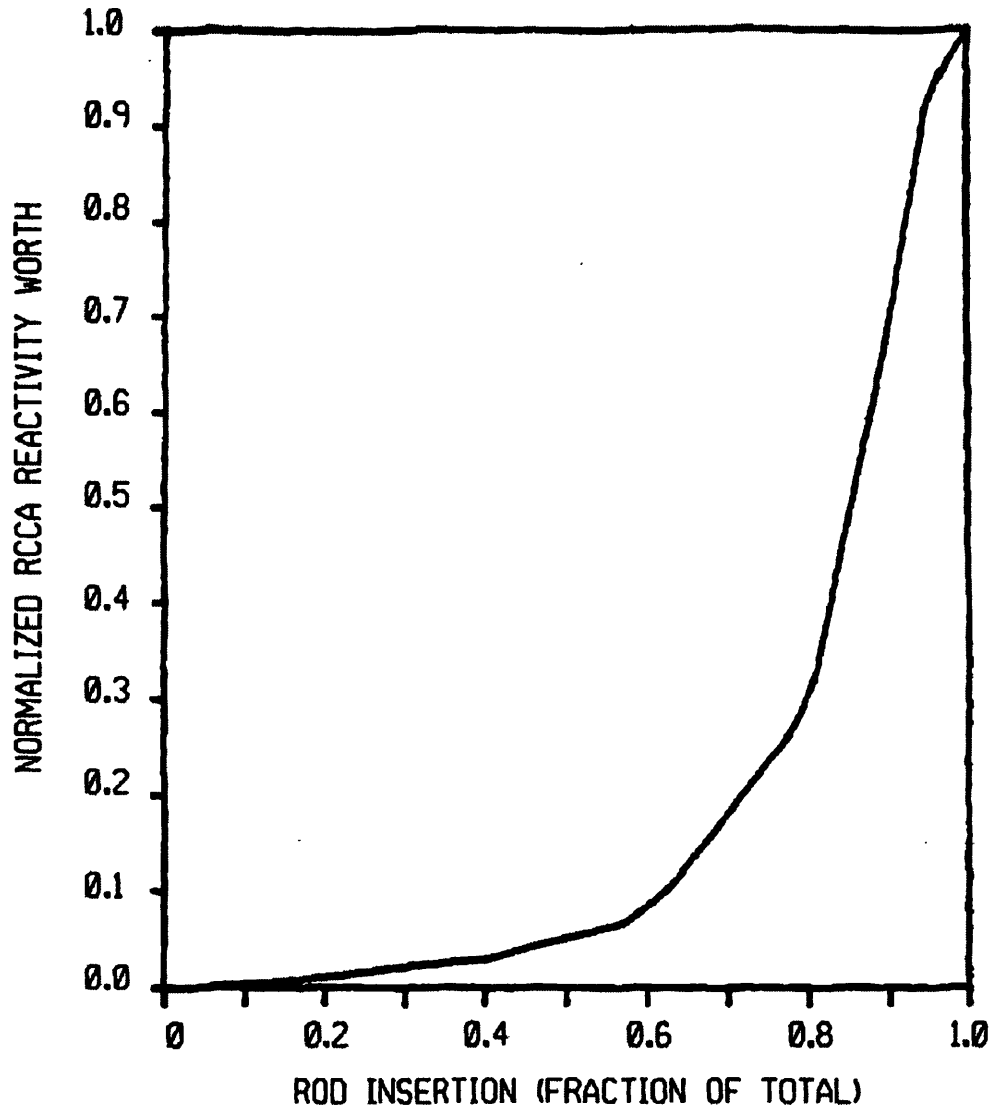


FIGURE 14D-3

NORMALIZED RCCA REACTIVITY  
WORTH VS ROD INSERTION

BEAVER VALLEY POWER STATION UNIT 1  
UPDATED FINAL SAFETY ANALYSIS REPORT

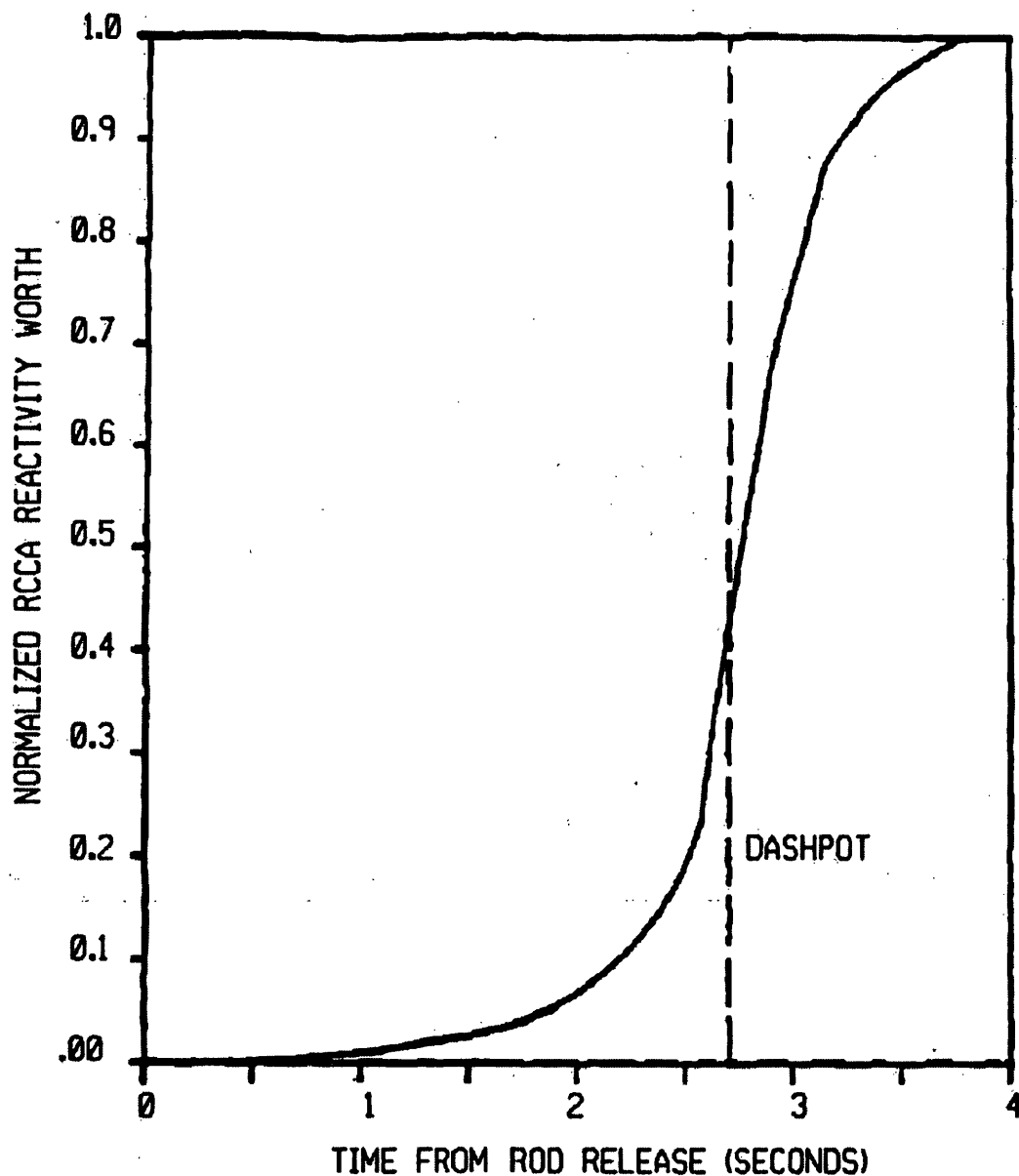


FIGURE 14D-4

NORMALIZED RCCA BANK REACTIVITY  
WORTH VS TIME AFTER TRIP

BEAVER VALLEY POWER STATION UNIT 1  
UPDATED FINAL SAFETY ANALYSIS REPORT

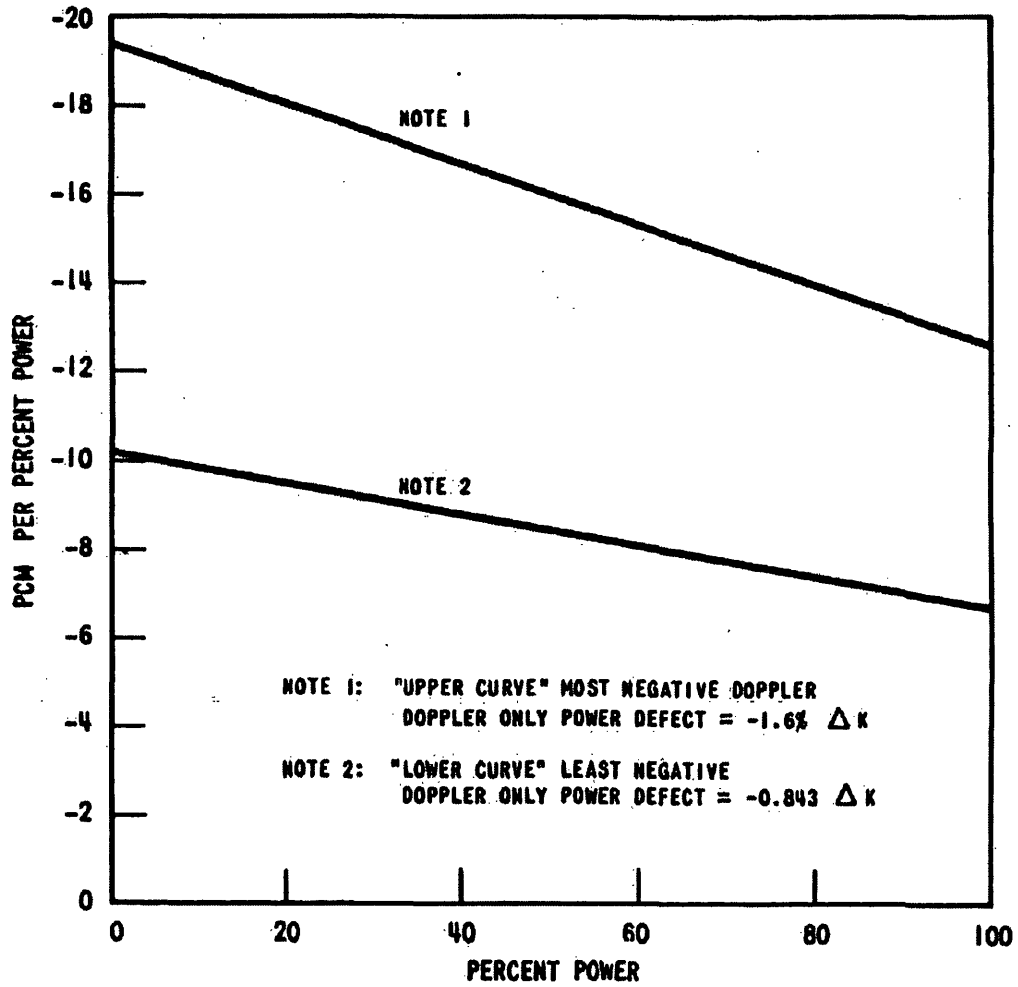


FIGURE 14D-5  
DOPPLER POWER COEFFICIENT  
USED IN ACCIDENT ANALYSIS  
BEAVER VALLEY POWER STATION UNIT NO. 1  
UPDATED FINAL SAFETY ANALYSIS REPORT

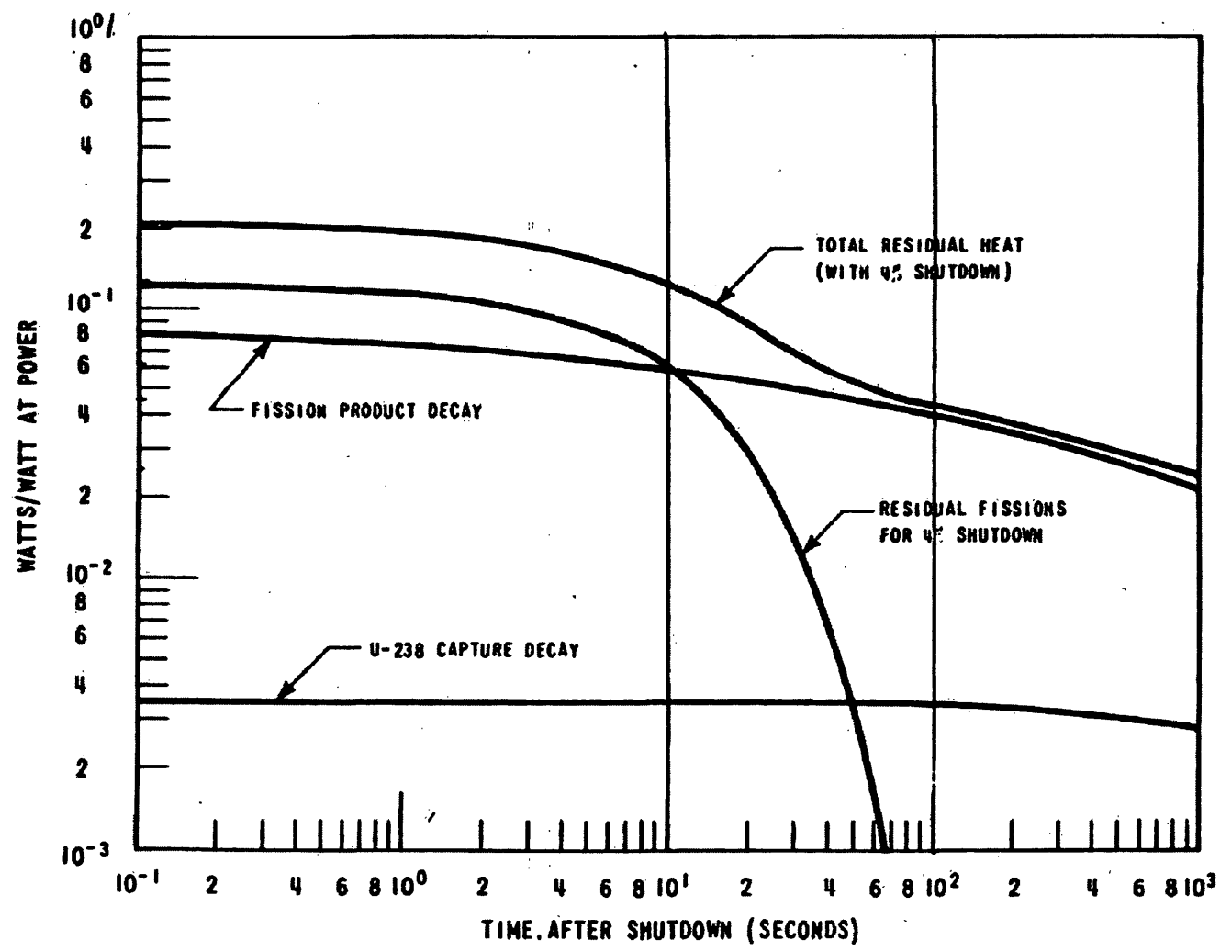


FIGURE 14D-6  
RESIDUAL DECAY HEAT  
BEAVER VALLEY POWER STATION UNIT NO. 1  
UPDATED FINAL SAFETY ANALYSIS REPORT

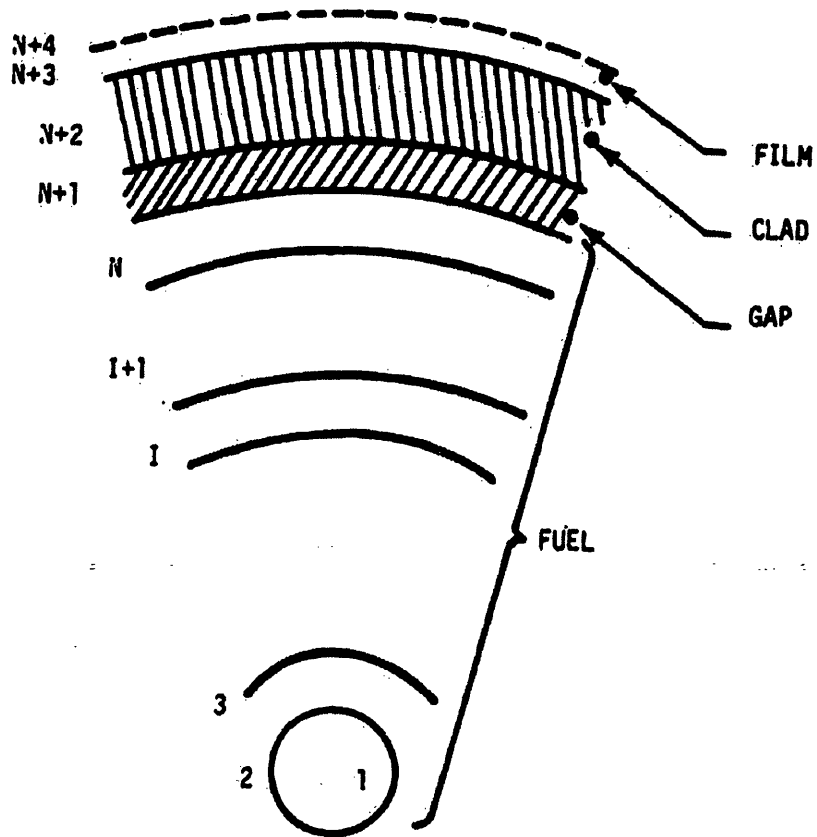


FIGURE 14D-7  
FUEL ROD CROSS SECTION  
BEAVER VALLEY POWER STATION UNIT NO. 1  
UPDATED FINAL SAFETY ANALYSIS REPORT